The regulatory effect of glucocorticoids on perineuronal nets occurs through different mechanisms: potential relationship to schizophrenia

Liang Yue

BSc.

Thesis submitted in fulfilment of the requirements for the degree of Doctor of Philosophy

School of Neuroscience and Psychology

College of Medical, Veterinary and Life Science

University of Glasgow

Glasgow, G12 8QQ

UK

September 2024

Abstract

Perineuronal nets (PNNs) are extracellular matrix structures surrounding mainly parvalbumin (Pv)-expressing γ-aminobutyric acid (GABAergic) interneurons, providing several cellular or neural functions during the brain developmental period, such as maintaining cellular or synaptic connections, regulating neural plasticity, controlling the closure of critical period and protecting neurons from being damaged by external substrates. Disrupted expression of PNNs and PNN components could result in brain dysfunction, and could be observed in various brain disorders, including schizophrenia. Schizophrenia is a psychiatric disorder, affecting approximately 1% of the population worldwide. Patients diagnosed with schizophrenia exhibit positive, negative and cognitive symptoms. With regard to the aetiology of schizophrenia, genetic and environmental risk factors are associated with schizophrenia, and prenatal maternal stress is robustly detected as an environmental risk factor, roughly doubling the likelihood of the condition in offspring. How risk factors, particularly environmental stress, are associated with schizophrenia is still unclarified.

PNN and Pv-expressing neurons are one of the neuronal systems involved in the pathology of schizophrenia, with several lines of evidence that abnormalities of PNN structure and Pv expression are observed in schizophrenia. Hence a potential pathway through which stress could increase the risk of schizophrenia is by altering PNN and Pv formation or expression. There is some evidence that stress could alter the general expression and formation of PNNs and PNN components, including chondroitin sulfate proteoglycans (CSPGs) (aggrecan, brevican, neurocan, versican and phosphacan), hyaluronan synthase (*Has*) and link proteins (*Haplns*), and tenascin R (*TnR*). Apart from PNNs, evidence demonstrated disrupted Pv expression after stress exposure, and abnormal PNN and Pv expression, with disturbed density and intensity of staining, is observed in schizophrenia patients. Additionally, glutamate decarboxylase (*Gad*), a critical factor contributing to GABA synthesis, is consistently demonstrated to be disturbed in schizophrenia subjects in previous studies, supporting disrupted GABA neurotransmission in schizophrenia.

In this case, disrupted Pv, *Gad* and PNN components influenced by external stress might be associated with the increased risk of schizophrenia, which could be a potential pathway underlying the aetiology of schizophrenia. However, the alterations of Pv and *Gad* expression by stress remained controversial, and whether the expression of PNN components is affected by stress is not fully investigated. Thus, the current study aimed to investigate the effect of glucocorticoids (GCs) – likely mediators of the effects of prenatal maternal stress on the foetus - on PNN component genes, Pv and *Gad* expression, and further to investigate whether the altered expression was associated with schizophrenia-like changes.

In primary cultured mouse cortical neurons, the data from the current study reported that GCs could alter the gene expression of specific PNN components, including, versican (*Vcan*), hyaluronan synthase 1 and hyaluronan synthase 3 (*Has1, Has3*), *Hapln4* and *TnR* and Pv. Altered gene expression was detected primarily at the mRNA level, with corresponding protein changes proving harder to detect. However, altered structural properties of PNNs in the cultures were detected following GC exposure, using Wisteria floribunda agglutinin (WFA) staining. Reduced length of PNNs covering neuronal dendrites was observed, indicating that expression and formation of PNNs were affected by GCs. These results confirmed the hypothesis that over-exposure to stress could disrupt the expression of some of PNN components and suppress the PNN structure.

GCs proved to be able to modify the expression of a number of different PNN component genes, but this was evident primarily at 7 days in vitro (DIV), and also at 14 DIV, but not at 21 DIV, suggesting a major modulatory effect early in development as PNNs are forming. Interestingly, the effects on PNN structure were detected at 21 DIV as well as 14 DIV, a time when no effects on PNN gene expression were observed, suggesting a distinct mechanisms of action.

The precise mechanisms involved in these GC actions appeared diverse, but difficult to identify. The suppressive effects of GCs on *Vcan, Hapln4* and *TnR* mRNA expression appeared to occur through a non-genomic pathway, as they were rapid (detectable within 4h) and not reproduced by the mineralocorticoid agonist aldosterone, or blocked by the GR antagonist mifepristone. The possibility of a post-transcriptional action to accelerate mRNA decay was tested, but no evidence was obtained in support of this idea. The suppressive effects on *Has1*, *Has3* and Pv were also rapid, but were sensitive to mifepristone, suggesting mediation through GRs. Mifepristone alone affected the expression of some PNN component mRNAs, including aggrecan (*Acan*), brevican (*Bcan*), neurocan (*Ncan*), and *Has1*, implying that basal (non-stressed level) GCs in the culture medium were exerting effects on these genes.

The changes in protein expression that were detected, including GC-induced deceases in the levels of *Has2* and *Gad65*, and increased levels of *Has3*, *TnR* and *Gad1* induced by mifepristone alone, appeared to occur within 4h, and in the absence of any corresponding changes in mRNA levels. The possibility that GCs might be modulating the activity of the proteasome was considered. Decreased activity was observed after GC exposure that was rapid and specific for the chymotrypsin-like activity. While this novel action cannot explain the GC-induced reduction in *Has2* protein, it could contribute to the ability of mifepristone to increase PNN component protein levels in the absence of any mRNA changes. Further work should assess the ability of mifepristone alone to affect proteasome activity in these cultures.

To examine the expression of PNNs and Pv in the brain from mouse models of aspects of schizophrenia, an overview of the distributions of PNNs and Pv in various brain regions is needed. In brain sections from mice expressing Td-tomato from the GABAergic interneuron-specific Nkx2.1 promoter, PNNs and Pv-expressing interneurons were largely distributed in cortical layers2/3 and layers 4/5, in prefrontal cortex (PFC) and retrosplenial granular cortex. No sex differences in PNN expression were detected. PFC is an important cortical region regulating executive functions and associated with various abnormal behaviours in schizophrenia. Since duplications of chr.16p11.2 are one of the strongest genetic variants associated with schizophrenia, Pv, PNN component and *Gad* expression gene expression was assessed in wild-type mice and 16p11.2 duplication mice, both without and with an environmental risk factor manipulation, specifically, maternal immune activation (MIA). Similar changes in Pv and CSPG component expression were observed in MIA-exposed adult offspring in both conditions with dams or littermates as experimental units. The expression of CSPG genes was elevated by MIA, as opposed to the decreases observed with GC exposure *in vitro*. No overt effects of the genetic manipulation were observed, nor interactions with the MIA.

Taken together, the data presented in the current study suggested that GCs could suppress expression of Pv, several PNN component genes, and PNN morphology, and the altered Pv and CSPG expression were also caused by MIA. A remarkable diversity of GC effects on PNN component gene expression were observed, acting on multiple targets, utilizing a number of different mechanisms, and with clear developmental regulation. The results indicated that external and prenatal stressors might be associated with the increased risk of schizophrenia by disrupting PNN and Pv expression. However, to fully investigate the underlying mechanisms and

their relationship to the pathology of schizophrenia, these alterations in the function of PNNs and Pv need to be further investigated.

Table of Contents

List of Tables

List of Figures

Acknowledgements

Firstly, I would like to thank my primary supervisor Professor Brian Morris for the guidance and support throughout my PhD study, and for helping me with the data analysis, fulfilling the background knowledge and making corrections on my thesis.

I would also like to thank my secondary supervisor Dr. Mick Craig for the help and support throughout my PhD study, especially the help with the animal experiments.

I'm grateful to John Craig for the technique support, helping me with the experiment procedures, making solutions and completing genotyping experiments.

I would also like to thank the work colleague Klaudia Jasionowska working in the University of Glasgow and University of Strathclyde for the maternal immune activation mouse experiments, and for showing me the experiment procedures during the start of my PhD; and thank Dr. Lilya Andrianova working in the University of Glasgow for helping me with the mouse experiments, including drug injection and brain dissection.

Last but not least, I would like to thank the constant support and love from my parents, for funding my PhD study, covering the cost of my life in the UK and giving me emotional support remotely.

Author’s declaration

I declare that the work presented in this thesis is entirely my own with all exceptions being clearly indicated or/and properly cited in the context.

Signature: ___ _____

Abbreviations

5-HT	Serotonin
7TM	7 transmembrane
11β-HSD1	11β-hydroxysteroid dehydrogenases1
11β-HSD2	11β-hydroxysteroid dehydrogenases2
ACAN/Acan	Aggrecan
ACC	Anterior cingulate cortex
Act D	Actinomycin D
ACTH	Adrenal-cortical hormone
AD	Alzheimer's disease
aGPR	Adhesion G-protein coupled receptor
AMC	7-amino-4-methylcoumarin
AMPA	α-amino-3-hydroxy-5-methyl-4-isoxazolepropionic acid
ANOVA	Analysis of variance
AP	Action potential
ATP	Adenosine 5'-triphosphate
BCAN/Bcan	Brevican
BSA	Bovine serum albumin
CA1	Cornu Ammonis area1
CA2	Cornu Ammonis area2
CA3	Cornu Ammonis area3
CBG	Corticosteroid-binding globuli
CCK	Cholecystokinin
cDNA	complimentary DNA
ChABC	Chondroitinase ABC
CNS	Central nervous system
CNV	Copy number variations
COMT	Catechol-O-methyltransferase
CS-GAG	Chondroitin-sulfate glycosaminoglycan
CGE	Caudal ganglion eminence
CSPGs	Chondroitin-sulfate peoteoglycans
Ct	Cycle threshold
CTF	C terminal fragment
ddH_2O	Double distilled water
dH_2O	Distilled water
DIV	Days in vitro
DISC1	Disruption in Schizophrenia
DMEM	Dulbecco's modified Eagle's medium
DNA	Deoxyribonucleic acid
Ds	Double strand
DSM	Diagnostic and Statistical Manual of Mental Disorders
DZ	Dizygotic
E	Embryonic day
ECM	Extracellular matrix
ECx	Entorhinal cortex

EDTA	Ethylenediaminetetraacetic acid
EPSC	Excitatory postsynaptic currents
FAAH	Fatty Acid Amide Hydrolase
Fig	Figure
FS	Fast spiking
Gad/GAD	Glutamate decarboxylase
GAPDH/Gapdh	Glyceraldehyde-3-phosphate dehydrogenase
GAT1	GABAergic transporter1
GABA	Gamma-aminobutyric acid
GC	Glucocorticoid
GMD	Glucocorticoid-mediated mRNA decay
GPCR	G-protein coupled receptor
GR	Glucocorticoid receptor
GRE	Glucocorticoid response elements
GSTT1	Gutathione S-transferase theta 1
GWAS	Genome wide association studies
HA	Hyaluronan
HAPLN	Hyaluronan link protein
HAPLN1/Hapln1	Hyaluronan link protein1
HAPLN2/Hapln2	Hyaluronan link protein2
HAPLN3/Hapln3	Hyaluronan link protein3
HAPLN4/Hapln4	Hyaluronan link protein4
HAS/Has	Hyaluronan synthase
HAS1/Has1	Hyaluronan synthase1
HAS2/Has2	Hyaluronan synthase2
HAS3/Has3	Hyaluronan synthase3
HBSS	Hanks Balanced Salt Solution
HCA	Hydrocortisone acetate
HCL	Hydrochloric acid
HEPES	Hydroxyethylpiperazine-N-2-Ethane Sulfonic Acid
HPA	Hypothalamic-pituitary-amygdala
HRP	Horseradish peroxidase
Hsp90	Heat shock protein 90
IHC	Immunohistochemistry
IL-8	Interleukin 8
IPSC	Inhibitory postsynaptic currents
KO	Knock out
LGE	Lateral ganglion eminence
LPS	Lipopolysaccharide
LTD	Long-term potential
MAM	Methylazoxymethanol acetate
$MgCl_2$	Magnesium dichloride
MGE	Medial ganglion eminence
MIA	Maternal immune activation
Mif	Mifepristone
MMP	Metallopeptidase

MOPS	4-Morpholinepropanesulfonic acid
MR	Mineralocorticoid receptor
mRNA	messenger RNA
MZ	Monozygotic
N	Number
NaCl	Sodium chloride
NaOH	Sodium hydroxide
NaH_2PO_4	Sodium dihydrogen phosphate
NaH_2PO_4 ($2H_2O$)	Sodium phosphate monobasic dihydrate
NCAN/Ncan	Neurocan
NF-kB	Nuclear factor kB
NFW	Nucleus free water
NGS	Normal goat serum
NMDA	N-methyl-D-aspartate
NPY	Neuropeptide Y
NTF	N terminal fragment
OR	Strata oriens
P	Postnatal day
PBS	Phosphate buffer saline
PD	Parkinson's disease
PFA	Paraformaldehyde
PFC	Prefrontal cortex
PGPH	Peptidylglutamyl-peptide hydrolyzing
PNN	Perineuronal net
PNS	Peripheral nervous system
Poly I:C	Polyinosinic-polycytidylic acid
PTPRZ1/Ptprz1	Phosphacan
Pv	Parvalbumin
qPCR	Quantitative polymerase chain reaction
RFW	RNase free water
RIPA	Radioimmunoprecipitation assay
RNA	Ribonucleic acid
RSC	Retrosplenial cortex
RSG	Retrosplenial granular cortex
SDS	Sodium dodecyl sulphate
Ss	Single strand
SST	Somatostatin
TBP/Tbp	TATA-binding protein
TBS	Tris buffer saline
TLR3	Toll-like recptor3
TLR4	Toll-like recptor4
TLR7	Toll-like recptor7
TLR8	Toll-like recptor8
TnC	Tenascin C
TnR	Tenascin R
TnW	Tenascin W

TnC	Tenascin X
TRN	Thalamic reticular nucleus
UT	Untranslated regions
VCAN/Vcan	Versican
Veh	Vehicle
VGLUT2	Vesicular glutamate transporter 2
VIP	Vasoactive intestinal peptide
WFA	Wisteria floribunda agglutinin
WT	Wild type

Chapter1
General introduction

1.1. Overview and general introduction

Schizophrenia is a complex, common and severe psychiatric disorder, having a profound effect on both individuals and society (Owen, Sawa & Mortensen, 2016). Exposure to early life stress or prenatal stressors are critical risk factors to the development of schizophrenia. Previous studies have showed that exposure to environmental stressors could result in increasing risk of schizophrenia in the offspring or in the individuals' later life (Khashan et al. 2008; Seckl,2001; Guo et al.,2019; Selten et al., 1999). In addition to external stress stimulations, damaged perineuronal net (PNN) structure and dysfunctional parvalbumin (Pv)-expressing GABAergic interneurons are also involved in the increased onset risk of schizophrenia. PNNs mainly develop around Pv-expressing GABAergic interneurons (Song and Dityatev, 2018), protecting the interneurons from being damaged by stressors and external harmful agents (Cabungcal et al., 2013; Morishita et al., 2015). As PNNs protect Pv neurons and contribute to neuronal plasticity, abnormalities of PNNs can result in alterations in cognitive functions in schizophrenia patients (Sorg et al., 2016). Disrupted PNN structure and expression were also reported in schizophrenia individuals, providing an association of PNNs and the onset of schizophrenia (Steullet et al., 2017; Pantazopoulos et al., 2015; Mauney et al., 2013). Furthermore, PNN structure and expression were affected by stress exposure in rodent studies (Ueno et al. 2017; Gomes et al., 2019; Lensjo et al., 2017). As increased risk of schizophrenia is found after early life stress or prenatal stress exposure, and PNN structure and expression were also shown to be disrupted by external stressors, there is a possibility that PNNs damaged by stress might be correlated with schizophrenia. However, how stress affects PNN structure and expression and whether the stress affected PNNs associated with schizophrenia remained unclear. This thesis aimed to investigate the underlying mechanism of the effect of stress on PNN expression and structure.

1.2. Background of PNN

1.2.1. PNN structure and molecular components

PNNs are extracellular matrix structures covering the somata, dendrites and proximal axon segment of distinct neuronal populations (Berretta, et al., 2015), mainly protecting Pv-expressing GABAergic interneurons from being damaged by stressors and external harmful agents (Cabungcal et al., 2013; Morishita et al., 2015). The PNN is a lattice-like structure (Fig.1) with the main components consisting chondroitin sulfate proteoglycans (CSPGs), containing aggrecan (*Acan*), brevican (*Bcan*), neurocan (*Ncan*), versican (*Vcan*) and phosphacan (*Ptprz1*), which are essential for PNN functions and structure (Deepa et al., 2006). These CSPGs molecules make up the protein with various chondroitin-sulfate glycosaminoglycan (CS-GAG) chains (Maeda, 2010). Hyaluronan is the backbone of PNNs, and is produced by hyaluronan synthase (HAS), of which there are 3 isoforms/genes - *Has1*, *Has2* and *Has3*. In addition, the link proteins, hyaluronan and proteoglycan link proteins (*Hapln*s) are necessary to stabilise CSPGs and bind CSPGs to hyaluronan. There are 4 genes: *Hapln1*, *Hapln2*, *Hapln3* and *Hapln4*; only *Hapln1*, *Hapln2* and *Hapln4* are found in CNS, but *Hapln3* is found to be expressed only in PNS (Oohashi et al., 2015). Tenascins are also part of the PNN structure, and again these can be derived from

different genes, which are Tenascin C (*TnC*), Tenascin W (*TnW*), Tenascin X (*TnX*) and Tenascin R (*TnR*), and these bind to the C-terminal domain of the CSPG lectins (Wen et al., 2018). Additionally, a lectin, wisteria fluoribunda agglutinin (WFA), is suggested to bind to the N-acetyl-d-galactosamine on the CS chains in the PNN structure, and is widely used to visualise PNNs (Kurokawa et al., 1976).

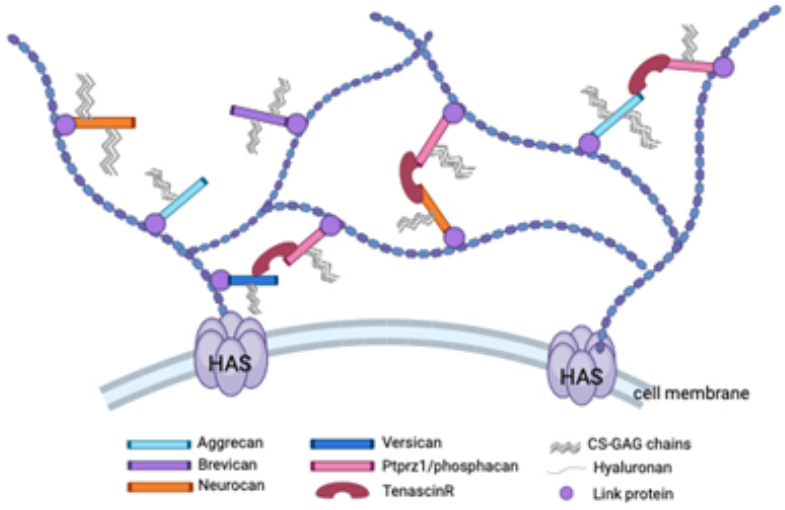

Figure 1.1: the formation of PNNs. The molecules include the CSPG family, containing aggrecan, brevican, neurocan, versican and phosphacan (*Ptprz1*), which are attached to the PNN structure by hyaluronan link proteins, and the CSPG molecules are linked to each other by *TnR.* The PNN formation is attached to the cell membrane by hyaluronan produced by hyaluronan synthase.

1.2.1.1. CSPG

CSPGs consist of a core protein and are attached with several chondroitin sulfate (CS) chains, which are the main matrix that forms PNNs in the mammalian CNS (Fawcett et al., 2019). 98% of CSPGs are present in general CNS ECM, including the perisynaptic matrix, only 2% of CSPGs are present in PNNs (Deepa, et al., 2006). While there are more than 30 types of CSPGs, 5 main components were shown to contribute to PNN structure, including *Acan*, *Bcan*, *Ncan*, *Vcan* and *Ptprz1*. *Acan*, *Bcan*, *Ncan* and *Vcan* are the members of the lectican family (Ruoslahti, 1996). *Acan* is the main component for the formation of PNN structure specifically in brain regions, as an *Acan* knock-out (KO) mouse in vivo study reported a loss of all PNN components surrounding *Pv*-expressing cells in CNS; but in peripheral system, all other CSPG components could still be detected with absence of *Acan* (Giamanco and Matthews, 2012). In addition, PNN can be detected not only by WFA lectins, but also by visualising *Acan* (Matthews et al., 2002). The antibodies used to visualise *Acan* include AB1031 and Cat-315 by detecting the *Acan*-bound domain CS-GAG chains, and the *Acan* HNK-1 carbohydrate epitope, respectively (Giamanco et al., 2010; Lendvai et al., 2013; Matthews et al., 2002; Dino et al., 2006; McRae et al., 2007). However, several studies noted above illustrated that while *Acan* was a main component in the PNN structure and could contribute to the PNN formation, WFA-labelled PNNs observed in prefrontal cortex (PFC) were not always co-localised with *Acan* expression (Ueno et al., 2017), suggesting a possibility that *Acan* might not be a necessary component for PNN formation.

With regard to other CSPG components, it has been suggested that they were not essential and necessary for PNN formation, as animals lacking these components (*Bcan*, *Ncan* or *Vcan*) still showed structured PNNs (Brakebusch et al., 2002; Zhou et al., 2001), although PNNs were

partly disrupted in cells cultured with conditional KO mice (*Bcan*/*Ncan* KO mice) (Geissler et al., 2013). For example, PNN structure was not completely disrupted in *Bcan* KO mice and could be detected with fuzzy WFA expression (Suttkus et al., 2014). In *Ncan* KO mice, WFA expression could still be detected but with a diffused and striped appearance in olfactory bulb, and the accumulation of *Acan* expression was also decreased but not fully disappeared, indicating a damaged but detectable PNN structure with the absence of *Ncan,* which in turn demonstrated *Ncan* is not an essential component for PNN stabilisation (Hunyadi et al., 2020). In addition, WFA-labelled PNNs could still be detected with a lack of *Ncan* or *Bcan (*Zhou et al., 2001, Brakebusch et al., 2002).

Ptprz1, a secreted proteoglycan, is a receptor protein tyrosine phosphatase ζ/β encoded by the *Ptprz1* gene, and is also an additional component of CSPGs extracellularly (Haunso et al., 1999). Like other CSPG components, it is attached to the CS-GAG chains (Maurel et al., 1994). It was demonstrated to play a critical role in PNN formation, as the net-like structure of PNNs was altered in *Ptprz1* KO mice, to a punctate structure on the neuronal surface in cortical areas (Eill et al., 2020). Moreover, on the cortical neuronal surface, phosphacan was also shown to bind to *Acan* and *TnR*, and the linkage among these 3 molecules contributed to the PNN structure stabilisation (Eill et al., 2020).

1.2.1.2. Tenascin R

Tenascins belong to a family of extracellular matrix glycoproteins with 4 subtypes/genes, comprising *TnC*, *TnW*, *TnX* and *TnR*). Among these subtypes of the Tenascin family, *TnR* is the main component of PNNs. In the CNS, in addition to presence in interneuron PNN, *TnR* was observed to accumulate around nodes of Ranvier during myelination (Anlar and Onzcar, 2012; Pesheva and Probstmeier, 2000; Carulli et al., 2006). *TnR* was demonstrated to stabilise the PNN structure by becoming attached to *Acan, Ptprz1* and CS-GAG chains (Morawski et al., 2014; Eill et al., 2020). No *Ptprz1* expression was observed in *TnR* KO mice (Brückner et al., 2000). The disrupted *TnR* expression was associated with an abnormal WFA-labelled PNN structure, with a granular appearance, and was accompanied by decreased *Acan, Bcan* and *Ncan* expression (Brückner et al., 2003; Sutkkus et al., 2014). In *TnR* deficient cultures, the PNN structure was abnormal with sparsely PNN-covered dendrites. Application of polyclonal antibodies to *Acan* could result in the recovery of PNN structure in *TnR* deficient cultures (Morawski et al., 2014), suggesting an interacting contribution of *TnR* and *Acan* to PNN stabilisation.

1.2.1.3. Hyaluronan and link protein

Hyaluronic acid (HA) or hyaluronan is a polysaccharide typically with around 25000 disaccharide units, and is a major component of the ECM, especially in PNN structures in the CNS. In the PNN, HA structures the form of PNNs and binds to CSPGs components. It is synthesised by *Has* enzymes, encoded by one of 3 genes: *Has1*, *Has2* and *Has3*. *Has* components are proposed to be present in the cell membrane acting as a basic structure for PNN to develop (Carulli et al.2006; Galtrey et al.2008; Kwok et al., 2010). Among the 3 *Has* genes, *Has3* was suggested to be the critical molecule for *Has* synthesis and PNN formation, in the PNN-like structure could be formed after *Has3* production (Kwok et al., 2010). Diffused HA components were suggested to be attached to *Has3*, and transferred into the PNN matrix structure when *Hapln1* and *Acan* were produced, indicating that *Has3*, *Hapln1* and *Acan* were the fundamental components for PNN formation (Kwok et al., 2010). The binding of HA and CSPGs was stabilised by the *Hapln* proteins (Kwok et al., 2010).

The *Haplns* family consists of 4 genes, which are *Hapln1*, *Hapln2*, *Hapln3* and *Hapln4* (Spicer et al., 2003). Different *Hapln* molecules were proposed to connect to different CSPG molecules, with the 4 pairs of proteins represented by *Hapln1-Vcan*, *Hapln2-Bcan*, *Hapln3-Acan*, and *Hapln4-Ncan* genes (Spicer et al., 2003). Previous studies focused more on H*apln1,* reporting *Hapln1* is the major component which could affect the WFA-labelled PNN structure, and expression of some of the CSPGs. For example, WFA-labelled PNNs were attenuated or disturbed in *Hapln1* KO mice, with no WFA staining around cells and dendrites (Carulli et al., 2010; Suttkus et al., 2014), in addition, the expression of *Acan*, *Bcan*, *Ncan* and *Ptprz1* were also decreased in *Hapln1* KO mice (Carulli et al., 2010), further indicating the association between *Haplns* and CSPGs and the role of *Haplns* in stabilising PNN structure, and that the disruption of a single component might result in damaged expression or formation of PNNs. A detailed summary of the effect of loss of individual PNN components on PNNs is described in Table 1.1.

Disrupted PNN component	**WFA- labelled PNN expression**	***Acan*-staining expression**	***Bcan*-staining expression**	***Ncan*-staining expression**	***Ptprz1*-staining expression**	**Citation**
Acan KO	No WFA immunoreactivity found	No *Acan* positive PNNs were detected				Giamanco et al. (2010); Suttkus et al. (2014)
Bcan KO	Slightly fuzzy, but WFA staining was not greatly disturbed					Suttkus et al. (2014)
Ncan KO	No detectable changes	Diffuse *Acan* accumulation				Hunyadi et al. (2020)
Ptprz1 KO	↓	↓		↓ (not significant), but the staining became granular		Eill et al. (2019)
TnR KO	The staining became granular, but not fully disturbed	↓			↓	Suttkus et al. (2014); Eill et al. (2019)
Has3 KO	No matrix structure found	Diffused expression			No detectable changes	Kwok et al. (2010)
Hapln1 KO	WFA labelled PNN were attenuated or disturbed (no staining around cells or dendrites).	↓	↓	↓	↓	Suttkus et al. (2014); Carulli et al. (2010)

Table 1.1: The structural roles and interactions of PNN components for PNN stabilisation. Impairments of some of PNN components were shown to affect other component's expression and disrupt PNN formation (mainly WFA labelled).

1.2.1.4. Neurons covered by PNN

PNNs mainly cover gamma-aminobutyric acid (GABAergic) interneurons (Härtig et al., 1992). The inhibitory GABAergic interneurons can be divided into several subtypes (DeFelipe et al.,

2013). Based on molecular properties, GABAergic interneurons could be classified into 5 groups, including Pv-, somatostatin (SST)-, neuropeptide Y (NPY)-, vasoactive intestinal peptide (VIP)-, and cholecystokinin (CCK)- expressing interneurons (DeFelipe et al., 2013). The latter 3 groups share the property of expressing 5-HT-3 receptors. Based on physiological properties, GABAergic interneurons are classified into 6 subgroups, the subgroups were listed as follows (DeFelipe et al., 2013):

a. Fast-spiking (FS) interneurons with high frequency of firing rates (more than 50 Hz).

b. Non-fast-spiking interneurons with no increased frequency of firing rates at the steady state.

c. Adapting interneurons with increased spiking intervals at burst stage and a steady rate at the continuous stage.

d. Irregular spiking interneurons with irregular spiking intervals at burst and continuous stage.

e. Intrinsic bursting interneurons with the production of 2 or more spikes in depolarisation and followed by a hyperpolarisation at the continuous stage.

f. Accelerating interneurons with decreased spiking intervals at steady-state and delayed stage.

Converging evidence reported that WFA-labelled PNNs mostly enveloped fast-spiking GABAergic inhibitory interneurons, mainly Pv-expressing neurons found widely in brain regions, including cortex, hippocampus and striatum areas (Nahar et al., 2021). Pv-expressing interneurons can be divided into 2 classes of cells, including chandelier cells which target the axons of pyramidal neurons, and basket cells which target the proximal dendrites of pyramidal neurons (DeFelipe et al., 2013). Although it is clear that PNNs mostly cover Pv-expressing GABAergic interneurons, whether PNNs surround chandelier cells or basket cells still remains unclear (Favuzzi et al., 2009). Apart from Pv-expressing interneurons, a small amount of WFA-labelled PNNs also cover the calcium-buffering protein calbindin-expressing neurons (Pantazopoulos et al., 2006), and 30% WFA-labelled PNNs were shown to cover SST-expressing neurons (Berretta et al., 2015). Among all the types of cells covered by WFA-labelled PNNs, GABAergic interneurons make up the largest proportion in most brain areas, including cortical, hippocampal, inferior colliculus, septum and amygdala regions (Pantazopoulos et al., 2006; Lee et al., 2012; Foster et al., 2014).

Although PNNs mainly cover fast spiking Pv-expressing interneurons, PNNs are also suggested to envelop non-Pv expressing neurons. For example, in rat hippocampus, PNN-like structures covered CamKII-expressing glutamatergic pyramidal neurons (Lensjø et al., 2017).

Approximately 50% of glutamatergic pyramidal neurons in the neocortex, amygdaloid nuclei, parietal and piriform cortex, and dorsal taenia tecta are surrounded by PNNs (Hu et al., 2014; Morikawa et al., 2017), and WFA labelled PNNs were found to be colocalised with vesicular glutamate transporter 2 (VGLUT2) in hypothalamic neurons (Méschizophreniaár et al., 2012). In human prefrontal cortex (PFC), some PNNs were formed around neurons with a typical pyramidal morphology, which further supported the idea that PNNs not only covered GABAergic but also glutamatergic pyramidal excitatory neurons (Enwright et al., 2016; Alcaide et al., 2019). The observation of pyramidal neurons covered by PNNs raised the possibility that PNNs could be classified into 2 different types by the morphological structure, that is pyramidal and non-pyramidal types of PNN (Wegner et al., 2003). The PNNs covering pyramidal neurons showed a faint appearance with weak intensity, whereas PNNs covering non-pyramidal neurons showed a

clear net-like structure (Wegner et al., 2003). However, the specific classification and structure of PNN surrounded excitatory interneurons remains to be addressed.

More additional studies demonstrated that WFA-labelled PNN also surround a small percentage of pyramidal cells in cortical areas, motor neurons in spinal cord and Purkinje cells in cerebellum (Hartig et al., 1992; Wegner et al., 2003; Pantazopoulos et al., 2006). In addition to neurons, glial cells can also be covered by PNNs in cortical and hippocampal regions (Bruckner et al., 1993; Patel et al., 2019; Chaunsali et al., 2021). In medial entorhinal cortex, reelin-expressing stellate cells were also demonstrated to be enwrapped by PNN (Lensjø et al., 2017). Thus, quite a diverse range of different cell types can be enveloped by PNNs.

The expression of PNNs is reported to be highly variable in hippocampus, with several distinct cell types surrounded by PNNs. For example, in hippocampus and dentate gyrus, PNNs were shown mostly to cover glutamatergic pyramidal neurons (Celio, 1993; Brückner et al., 2003). Specifically, in stratum oriens (OR) and pyramidale of the CA1 and CA3 areas, WFA-labelled PNNs covered neurons with non-pyramidal phenotypes (Brückner et al., 2003), which was in accordance with the later findings from Yamada and Jinno (2013) that more Pv positive neurons with PNNs were observed in strata oriens in Cornu Ammonis1 (CA1) and CA3. In CA2, PNNs were shown to ensheath neurons with pyramidal morphology (Brückner et al., 2003). Similar findings were reported in later research, which suggested that PNNs in CA2 area were not dominantly localised around Pv-expressing GABAergic neurons, but colocalised with CamkII-expressing pyramidal neurons (Lensjø et al., 2017). However, no PNNs were detected in hippocampal strata radiatum or lacunosum moleculare regions (Brückner et al., 2003). Compared to the expression of PNNs in cortical regions, the general density and intensity of PNNs in hippocampus were sparse and weak (Yamada and Jinno, 2013), although the structure of PNNs could still be defined clearly across different hippocampal regions, especially in CA1 (Lensjø et al., 2017).

In some other brain regions, PNNs were also found to be primarily expressed around excitatory neurons rather than inhibitory neurons, including ventromedial hypothalamus and some amygdala regions, such as, lateral amygdala, the basolateral amygdala, and the basal medial amygdala (Morikawa et al., 2017). In hypothalamus, the general intensity of PNNs was quite weak and with lower density compared to other brain regions (Morikawa et al., 2017; Zhang et al., 2021). Furthermore, in cerebellum, PNNs were reported to surround mostly excitatory neurons, 96% of excitatory neurons expressing Kv3.1b which is a marker for excitatory neurons (Weiser et al., 1994; Kelly et al. 2019) were detected to be enwrapped by WFA-labelled PNNs in cerebellum (Carulli et al., 2005).

Notably, PNNs are suggested to cover not only neurons, but also glial cells, including astrocytes, oligodendrocytes and microglial cells. Several studies illustrated that in addition to neurons, PNN structure and components are produced around glial cells (Wiese et al., 2012; Crapser et al., 2021; Ribot et al., 2021), which raised the suggestion that PNN components could originate from both neurons and glial cells. For example, although CSPGs are suggested as neuronal proteoglycans, only *Ncan* was reported to be synthesized by neurons (Margolis and Margolis, 1994), whereas *Acan*, *Bcan, Vcan, Ptprz1* originated from astrocytes (Yamada et al., 1994; Carulli et al., 2006). Furthermore, astrocytes were also suggested to synthesize hyaluronan components, including *Has* and *Hapln*s. In cultured astrocytes, hyaluronan matrix was formed, while in cultured neurons, the hyaluronan matrix was not observed (Maleski and Hockfield, 1998). In addition, *Hapln*, especially *Hapln1* expression was shown to be dependent on glial cells (Giamanco and Matthews, 2012). However, the studies observed hyaluronan immunoreactivity around Pv-expressing interneurons, and the CSPG components were shown to be present in

neurons but not glial cells, indicating the possibility that hyaluronan and CSPGs components could also be synthesised by neurons (Miyata et al., 2005; Giamanco and Matthews, 2012).

In the adult CNS, some PNN components, including *Bcan*, *Vcan* (particularly V2 isoform), *Ptprz1*, *TnR* and *Hapln2*, are predominant components in white matter ECM, and are accumulated at nodes of Ranvier (Schmalfeldt et al., 1998; Oohashi et al., 2002; Melendez-Vasquez et al., 2005). In white matter, oligodendrocytes are the predominant cell type and contribute to the function of white matter by developing myelin sheaths (Ohtomo et al., 2018). Therefore, *Bcan*, *Vcan* (particularly V2 isoform), *Ptprz1*, *TnR* and *Hapln2* could also be originating from oligodendrocytes, which is consistent in several findings (Schemalfeldt et al. 2000; Asher et al. 2000; Pesheva and Probsmeier, 2000).

To conclude, PNN structure is developed originally from hyaluronan synthesised by *Has* on the cell membrane. Hyaluronan which synthesised by Has binds to CSPGs by connecting to *Haplns*, and the terminus of different CSPG components binds to *TnR* and CS-GAG chains (Kwok et al., 2010). This complex structure forms the whole PNN in the extracellular region of cells. PNNs mostly cover fast-spiking GABAergic interneurons, including Pv-expressing and SST-expressing interneurons. Apart from GABAergic interneurons, PNNs also cover almost half of glutamatergic pyramidal cells, and other subtypes of cellular or neuronal populations, such as motor neurons and Purkinje cells. In cortical and hippocampal regions, PNNs mainly surround GABAergic interneurons (mainly Pv-expressing) and glutamatergic pyramidal neurons.

1.2.2. Distribution of PNN in different brain regions

1.2.2.1. General distribution of PNN in CNS

PNNs surround approximately 15% of neurons throughout the brain (Guimarães et al., 1990; McRae et al., 2007). In terms of the cellular structure, WFA-labelled PNNs surround somata and proximal dendrites, while no PNNs are detected around axon terminals and axons (Miyata et al., 2005; Hendry et al 1988, Brückner et al., 2000).

PNNs are distributed in various brain areas with different expression patterns or morphologies. For example, in cortical areas, PNNs present mostly in neocortex, especially motor and primary sensory cortex (Brückner et al 1993, Hausen et al 1996). In the sensory cortex, approximately 40% of Pv-expressing neurons were ensheathed by PNN mainly in layer 2/3 and layer 4/5 (Nowicka et al., 2009). Similarly, in PFC, PNN were also shown to express mostly in layer 2/3 and layer 4/5 with Pv-expressing neurons (Sultana et al., 2021), but with a more discrete and granular expression rather than a net-like structure (Ueno et al., 2017; Sultana et al., 2021). The intensity of Pv-expressing neurons was also lower in PFC compared to other cortical areas. It has been illustrated that the granular and discrete structure of PNNs might be attributed to the lack of tenascins or *Hapln* components in PFC with no *TnR* and *Hapln1* detected in mouse PFC (Ueno et al., 2017). Furthermore, PNNs also enwrapped pyramidal neurons in rat cortex (Alpár et al., 2006). For example, it has been demonstrated that more pyramidal neurons were enwrapped by PNNs in primary sensory cortex compared to other cortical regions, although the structure of PNNs around pyramidal cells was sparse and less condensed (Brückner et al., 1999).

In the entorhinal cortex (ECx), in humans, PNNs were detected in the layer 2 and layer 3 of ECx, and were observed without the presence of surrounded Pv-expressing neurons, but with glial cells being surrounded instead (Pantazopoulos et al., 2010), which was consistent with another

finding that PNNs were detected mainly in layer 2 and layer 3 of ECx in human brains (Lendvai et al., 2013). In the rodent brain, a high density of Pv-expressing neurons with PNNs was found in layer 2 and layer 3 of medial ECx (Lensjø et al., 2017), and in another study, colocalisation of Pv-positive neurons and PNNs was also detected in layer I of ECx (Uneo er al., 2017). Apart from the observation of PNNs covering Pv-expressing neurons in ECx, converging evidence further suggested that PNNs also enwrapped a part of reelin-expressed stellate cells and calbindin-expressed pyramidal cells in layer 2 of ECx (Sun et al., 2015).

Inhibitory GABAergic neurons are the main neuronal population in the thalamic reticular nucleus (TRN). In human brain, a high density of Pv- and calbindin-expressing neurons is found in TRN, and part of them (around 50% of Pv-expressing interneurons) are ensheathed by WFA-labelled PNNs (Steullet et al., 2018), just as PNNs in cortex mainly cover GABAergic Pv-expressing interneurons. Similarly, in mouse brain, higher expression of PNNs is found in thalamic reticular nucleus (TRN) compared to other subcortical regions (Ciccarelli et al., 2021).

1.2.2.2. Distribution of CSPG in CNS

Different PNN components are expressed with different density or intensity in different brain areas. CSPGs, including *Acan, Bcan, Ncan, Vcan* and *Ptprz1* were found to colocalise with WFA-labelled PNNs in mouse PFC and motor cortex, but the intensities of staining for *Ncan* in PFC and *Vcan* in motor cortex were weaker than other CSPGs (Ueno et al., 2017). However, *Acan* could not be detected by immunohistochemistry in WFA-labelled PNNs in PFC (Ueno et al., 2017). This is interesting considering the evidence noted earlier (Table 1,1) that *Acan* appears to be essential for PNN formation.

Specifically, *Acan* showed the highest immunohistochemical signal in hippocampus areas and the lowest signal in hypothalamus and amygdala (Dauth et al., 2016). In general, *Acan* expression in PNNs had the highest density in isocortex compared to other brain regions, and had the lowest density in thalamic areas (Dauth et al., 2016). Several studies used Cat301, Cat315 and Cat316 (*Acan)* antibodies to mark PNNs in primate CNS, demonstrating PNN expression of *Acan* in visual cortex, motor cortex, hippocampal regions (dentate gyrus, CA1, CA2 and CA3) (Hockfield et al., 1983; Hockfield et al., 1990; Matthews et al., 2002). In human brain, within the hippocampus region, *Acan* expression was higher in CA1 areas and colocalised mainly with GABAergic interneurons, whereas pyramidal neurons were found to be devoid of *Acan* (Lendvai et al., 2012). This suggests that PNNs with distinct functional roles may have distinct compositions.

Similarly, in rats, *Bcan* is expressed with the highest intensity in hippocampus and with lowest intensity in hypothalamus (Dauth et al., 2016). *Bcan* expression was found in all parts of brain, colocalising with pyramidal neurons in hippocampus, and with granule and Purkinje cells in cerebellum (Seidenbecher et al. 1995). Compared to *Acan,* the overall *Bcan* expression in PNNs was quite low (Dauth et al., 2016). *Ncan* was expressed widely throughout cortical areas, such as, cerebral cortex, somatosensory cortex and barrel field cortex (Watanabe et al., 1995). The expression of *Ncan* in the outer layers (layer I and II) showed higher intensity than the inner layers (layer IV and V). *Ncan* mRNA expression was also measured and was restricted to CNS; in rat brain, *Ncan* mRNA expression was most abundant in cortex, and in granule cells and Purkinje cells in cerebellum (Engel et al., 1996). *Vcan* was also expressed across all brain regions, especially around cortical and hippocampal pyramidal neurons, and cerebellar Purkinje cells (Horri-Hayashi, et al., 2008). However, *Vcan* was not detected around Pv-expressing GABAergic neurons (Horri-Hayashi, et al., 2008), while other CSPG components in PNNs were all observed to surround both glutamatergic and GABAergic neurons (Matthews et al., 2002;

Okamoto et al., 2001). *Ptprz1* was widely distributed across brain regions. *Ptprz1 was* expressed in layer 2/3 cerebral cortex with high intensity in mice, and in hippocampus, *Ptprz1* was localised in CA1 and CA3. In both cerebral cortex and hippocampus *Ptprz1* covered mainly pyramidal neurons (Hayashi et al., 2005) with levels higher in hypothalamus (Engel et al., 1996). In the cerebellum, *Ptprz1* mRNA was also detected in the cell bodies of the Bergmann glia (Engel et al., 1996).

1.2.2.3. Distribution of *TnR* in CNS

In the CNS, *TnR* colocalised with PNNs in isocortex and hippocampus in mice, with lower abundance in thalamus (Dauth et al., 2016). TnR could also be observed in cultured mouse cortical neurons (Dickens et al., 2022).

1.2.2.4. Distribution of hyaluronan and link proteins in CNS

HA is a non-sulfated glycosaminoglycan chain which is found during the earliest period of neuronal development in CNS, peaking in the embryonic stages and declining after adulthood (Margolis, et al., 1975). *Has1*, *Has2* and *Has3 are* expressed in various brain regions with different expression levels. In general, *HAS1* is expressed at lower concentrations than *HAS2* and *HAS3*, while *HAS2* is highly expressed in all cell types in humans (Nishida et al., 1999). In mouse cortical neurons, *Has* expression is observed in cortical and hippocampal neurons coinciding with PNN expression (Fowke et al., 2017); in addition, the mRNA expression of *Has2* and *Has3* is abundant throughout cortical areas, whereas *Has1* mRNA expression is very low, with no detectable *Has1* immunoreactivity in mice cultured cortical neurons (Fowke et al., 2017). The mRNA expression of *Has2* and *Has3* has been shown in rat cerebellum and visual cortex, and in cultured cortical neurons, while *Has1* mRNA was not found in these areas (Carulli et al., 2006; Carulli et al., 2007).

In human and rodents, expression of *Hapln2* and *Hapln4* is reportedly restricted to the CNS, while *Hapln3* is expressed widely throughout all tissues (Spicer et al., 2003). *Hapln1* is the most investigated *Hapln* isoform, and is suggested to be the main *Hapln* molecule in PNNs. In human brain, *HAPLN1* is expressed in neocortex and hippocampus (Long et al., 2018; Lendvai et al., 2013). Specifically, in human hippocampal regions, *HAPLN1* is less densely expressed in CA1, CA2 and CA3, with expression restricted to strata oriens and radiatum (Lendvai et al., 2013). *Hapln2* and *Hapln4* may also be necessary components in PNN formation. *Hapln2* is present in various brain regions, including olfactory bulb, hippocampus, brain stem and cerebellum with relative high intensity, while in cerebral cortex, *Hapln2* is expressed with weaker intensity (Bekku et al., 2012; Wang et al., 2016). However, in human cerebral cortex, *HAPLN4* is suggested to be the most strongly expressed member of the *HAPLN* family (Sim et al., 2009). In mice brain tissues, *Hapln4 is* expressed widely in various regions, including cerebellar cortex, inferior colliculus and deep cerebellar nuclei (Bekku et al., 2012).

Therefore, it could be seen that all the PNN components are expressed differentially across various brain regions. This may suggest some heterogeneity in PNN composition in different brain regions.

Apart from this spatial variability in expression levels, PNN component expression also shows dynamic temporal changes accompanied by the development of the neurons enwrapped by the PNNs.

1.2.2.5. Temporal expression of PNN components

PNNs are mainly expressed around Pv-expressing GABAergic interneurons (Caballero et al., 2014). In the mouse cortex, Pv expression starts to develop at postnatal day (P) 10 in sensory cortex, P13 in visual cortex and P14 in PFC (Gonchar et al., 2008; Nowicka et al., 2009; Ueno et al., 2017). At around the same time, PNNs start to occur around these neurons. The specific time of PNN development varies between brain regions, accompanied with the development of neurons they surrounded, usually between P10 to P56 in rodents, and 1 month and 20 years in humans. For example, PNNs start to develop at P10 in sensory cortex and P14 in PFC, but appeared with lattice-like or diffuse reticular-like structures (Nowicka et al., 2009; Ueno et al., 2017). At P56, PNN exhibited a condensed reticular-like structure in cortical regions (Ueno er al., 2017). PNNs develop at a similar stage in cultured neurons as *in vivo*, usually being visible after 10 days in vitro (DIV) (Miyata et al., 2005). In humans, PNNs develop at 8 weeks and became mature around 8 years (Rogers et al., 2018). The maturation of PNNs usually accompanied by the closure of critical period.

During the developmental period, the expression of PNNs increases and peaks at various time points. The peak time points vary among different PNN components (Galtrey et al., 2008; Carulli et al., 2007). For example, in rats after birth, *Acan* expression peaked at P10 to P21 (Galtrey et al., 2008). *Bcan* expression increased steadily after birth, and remained unchanged after 5 months (Milev, et al., 1998). *Ncan* expression changed quite differently; *Ncan* expression in mouse brain started at embryonic day 10 (E10), and peaked around the day of birth and decreased postnatally (Milev, et al., 1998). *Vcan* is expressed as 2 main isoforms, V1 and V2, which showed different dynamical changes. V1 expression increased from E10 and peaked at birth whereas V2 increased after birth and peaked at around 3 months (Milev, et al., 1998). *Ptprz1* also showed steadily increasing expression after birth peaking at approximately 3 weeks (Milev, et al., 1998). Thus, in the developing brain, the levels of *Vcan* and *Bcan* increase during the neuronal development period and remain stable in the adulthood, while the levels of *Ncan* peaked at the early developmental stage, decreased afterwards, becoming hardly detectable in the mature brain. This suggests that *Ncan* might be important in early brain development (Matsui, 1994).

In addition, *TnR* expression was also suggested to increase in rat brain after birth, accumulating during the first 2 weeks in interneurons surrounded by PNNs, but the expression of *TnR* started to decrease in adulthood (Fuss et al., 1993).

With regard to *Has* components, limited studies investigated the developmental changes in brain, however, in cultured cortical neurons, *Has1*, *Has2* and *Has3* mRNA expression gradually increased from 0 DIV and peaked at 21 DIV, 3 DIV and 7 DIV, respectively (Fowke et al., 2017). The expressions of *Has2* and *Has3* decreased after the peak time points (Fowke et al., 2017). *Haplns* also showed dynamic changes during brain development, Hapln1 expression increased from the embryonic period and peaked at juvenile ages; while Hapln2 and Hapln4 increased gradually after birth and remained steady after adulthood, which was more consistent with *Acan*, *Bcan* and *Vcan* (V2) development (Oohashi et al., 2015). The overview of temporal distribution of PNN component expression is shown in Table 1.2.

PNN components/PNN-covered neurons	Developing time in CNS	Peak time in CNS	Citation
Pv-expressing interneurons	P10-P14	P28	Gonchar et al. (2008); Nowicka et al. (2009); Ueno et al. (2017).
Acan	P10	P21	Galtrey et al. (2008)
Bcan	After birth	Increased steadily and then unchanged after 5 months	Milev, et al. (1998)
Ncan	E10	Around birth	Milev, et al. (1998); Matsui (1994)
Vcan (*V1*)	E10	Around birth	Milev, et al. (1998)
Vcan (*V2*)	After birth	3 months	Milev, et al. (1998)
TnR	After birth	14 DIV	Fuss et al. (1993)
Has1	After birth	21 DIV	Fowke et al. (2017)
Has2	After birth	3 DIV	Fowke et al. (2017)
Has3	After birth	P7	Fowke et al. (2017)
Hapln1	Embryonic stages	Juvenile age	Oohashi et al. (2015)
Hapln2	After birth	Adulthood	Oohashi et al. (2015)
Hapln4	After birth	Adulthood	Oohashi et al. (2015)

Table 1.2: temporal expression of PNN components and PNN-covered Pv-expressing interneurons. The temporal development of different PNN components and Pv cells were investigated in rodents or using cortical neuronal cultures from mouse brains.

To conclude, PNNs were shown to enwrap around not only neurons but also glia, which indicated the origination of PNN components, synthesising by neurons, astrocytes and oligodendrocytes; and expression of PNNs varied across brain regions in terms of density and intensity, including cortex, hippocampus, cerebellum, amygdala and spinal cord. Apart from the spatial expression differences throughout these brain regions, PNNs and their components also showed temporal differences as the brain developed, generally increasing at P10 and becoming mature around P21 in mammalians brain. Some PNN components, such as *Ncan* and *Vcan*, start to develop at embryonic periods (E10) and other components developed after birth, the peak timing was different depending on the specific components, ranging from P10 to adulthood.

1.2.3. Expression of PNN in different species and males and females

1.2.3.1. Different expression of PNN and components among species

PNNs have a wide distribution across all brain regions of mammals, from cortex to spinal cord, covering both excitatory and inhibitory neurons. Growing evidence illustrated that PNNs are present across species, including mice, rats, guineapigs, cats, sheep, monkeys (marmosets) and humans; apart from the mammals, PNNs are also present in birds and zebrafish. PNN distribution differences among species are related to whether PNNs developed around excitatory or inhibitory neurons in relative brain regions.

Most studies investigated PNNs in rodents, such as mice and rats. In general, in rodents, PNNs mainly cover Pv-expressing GABAergic interneurons in cortical regions, and mainly cover glutamatergic pyramidal neurons in hippocampus and excitatory glutamatergic neurons in

cerebellum (Celio, 1993; Brückner et al., 2003; Lensjø et al., 2017). However, the expression of PNNs was found to be different in hippocampal regions and amygdala between mice and rats. In mouse dorsal hippocampus, especially in CA1, PNNs are expressed sparsely but with clear formation and high intensity, colocalising with more Pv-expressing interneurons; on the contrary, in rat hippocampus, PNN in CA1 are expressed with lower intensity and colocalised with fewer Pv-expressing interneurons compared to mice (Lensjø et al., 2017). In amygdala, in mice, PNNs only enwrapped excitatory interneurons; while in rats, PNNs covered both GABAergic and glutamatergic interneurons (Baker et al., 2017; Morikawa et al., 2017).

In primates (humans and monkeys) PNNs mainly covered Pv-expressing interneurons and frequently express in cortical areas. For example, in human cortical areas, the cells surrounded by PNNs were interneurons, with a smaller proportion of pyramidal neurons (Mauney et al., 2013), and the PNNs were shown to be present mostly in layer 3 but not present in layer 1 (Mauney et al., 2013). Rogers et al. (2018) further supported that in PFC, PNNs were frequently observed in layer 3 in mPFC and were less densely presented in hippocampus compared to cortical regions. The 2 studies also consistently reported that in mPFC, PNNs mostly covered Pv-expressing neurons. A similar distribution was found in monkeys: in macaque, PNNs were also found to mostly enwrap Pv-expressing neurons in cortical regions. Consistent evidence demonstrated similar expression of *Acan*-labelled PNNs in visual cortex in both human and macaques, with expression primarily in layer 3 (DeYoe et al., 1990; Hockfield et al., 1990). In addition to cortical areas, the expression of PNNs showed similar patterns in other brain areas, such as basal forebrain, with similar number, intensity and size of PNNs (Adams et al., 2001).

Thus, it could be seen that human and monkey have similar PNN distribution across brain regions. PNN expression also showed similarities between rodents and primates. For example, humans and mice showed a similar PNN staining pattern in cortical and hippocampus areas, with a higher proportion of PNNs labelled in mPFC and ECx compared to hippocampus (Belliveau, et al., 2024). Moreover, in the subcortical regions, PNNs were shown to be expressed in discrete nuclei in both mice and marmosets, especially in amygdala and hypothalamic nuclei (Ciccarelli, et al., 2021). However, differences of PNN distribution were detected from rodents to primates. High expression of PNNs was found in TRN in mouse brain, but no PNNs were found in TRNs in marmosets (Ciccarelli et al., 2021). In motor and somatosensory cortex, a number of pyramidal neurons were covered by PNNs in layer 3 and layer 5, similar expression was found in cynomolgus and Japanese monkeys (Hausen et al., 1996; Hendry et al., 1988; Watanabe et al., 1989), while the pyramidal neurons covered by PNNs in somatosensory and motor cortex were less detected in rodent brain (Brückner et al 1994, Hausen et al 1996; Nowicka et al., 2009; Sultana et al., 2021). Moreover, in human hippocampus and amygdala, PNNs were observed to surround a subpopulation of GABAergic interneurons, including calretinin-expressing interneurons (Lendvai et al., 2013). Although calretinin-expressing interneurons were also found to exist in amygdala in other species, such as moneys, mice and rats, the neurons were devoid with PNNs (McDonald, 1994; Härtig et al., 1995).

PNNs are also present in other animals in addition to mammals, such as birds and fish. In zebra finch, PNNs were found in pallial (cortex), and song nuclei, including, the robust nucleus of the archistriatum, lateral magnocellular nucleus and the hyperstriatum ventrale (HVC) song nuclei, covering Pv-expressing interneurons (Balmer et al., 2009). PNNs were also demonstrated in zebrafish, with critical PNN components in pretectal brain nuclei, diencephalon (Becker and Becker, 2002; Kang et al., 2008).

Therefore, PNNs are distributed widely among different species, especially in mammalian brains, mainly covering Pv-expressing GABAergic interneurons in cortical areas and pyramidal neurons

in hippocampus and amygdala. However, in human amygdala, PNNs exclusively covered calbindin- expressing GABAergic interneurons, whereas the neurons were not found to be covered by PNNs in other mammals. In human motor and somatosensory cortex, more pyramidal neurons were enwrapped by PNNs compared to rodents. Additionally, PNN differences in rodents mainly presented in hippocampus, with less intensity of PNNs and fewer Pv-expressing neurons covered in CA1 region in rats than mice. Apart from mammals, PNNs were also present in zebrafish and zebra finch, mainly covered Pv-expressing neurons in related cortical regions. As the brain structure in birds and fish are different from mammals, it is difficult to compare PNN in specific brain regions.

1.2.3.2. Different expression of PNN components among species

In addition to the general expression similarities or differences of PNN among various species, specific molecular components of PNN were also suggested to be present differently in different species. However, limited studies were conducted to investigate specific PNN molecular components among different species. *Has* isoforms, including *Has1*, *Has2* and *Has3,* were highly enriched in humans, mouse, rats and zebrafish (Tien and Spicer, 2005). *TnR* expression was observed in the CNS of human, rodents, monkeys and zebrafish (Morawski et al., 2014; Becker et al., 2003; Dufresne et al., 2012). The expression of CSPGs was widely detected in various species, including human, mice, rats, monkeys, guinea pigs, zebra finches and zebra fish (Horri-Hayashi et al., 2015; Mukherjee et al., 2020; Becker & Becker, 2002; Kang et al., 2008; Ojima et al., 1998; DeYoe et al., 1990; Hockfield et al., 1990; Meyer et al., 2014).

1.2.3.3. Sex differences of PNN

There are some indications of sex differences in PNN expression. In hippocampal regions, more numerous and better-developed PNNs were detected in hippocampus CA1 region in adult male rats compared to female rats, while in the neocortex, no PNN distribution differences were found between male and female rats; additionally, the proportion of Pv-enveloping PNNs was similar between male and female rats in hippocampus (Griffiths et al., 2019). On the contrary, in mice, no PNN density sex differences were reported in hippocampus CA1 and CA2 regions (Rahmani et al., 2023), which was in line with the findings that no differences of the proportion of PNNs and Pv-expressing neurons were exhibited in hippocampus and retrosplenial cortex (RSC) between male and female mice (Mayne et al., 2024); however, PNNs presented with higher intensity in retrosplenial agranular (RSA) and retrosplenial granular (RSG) regions in female mice than male mice (Mayne et al., 2024). In medial amygdala, PNNs were found to be expressed with higher density and intensity around neurons in male mice than female mice (Ciccarelli et al., 2021). Additionally, in zebra finches, highly enriched, more densely CS-labelled PNNs were reported in anterior cortical basal ganglia and RA song nuclei in male zebra finches compared to females; conversely, female zebra finches expressed more Pv cells than males in HVC nuclei. (Meyer et al., 2014).

Thus, it could be concluded that PNNs can be expressed differently in males and females in particular brain regions, with mainly differences expressed in PNN intensity in cortical areas such as RSC; the sex differences of PNNs also showed a species variation that PNNs reportedly showed similar density or proportion in hippocampus regions in mice but not rats. Moreover, the sex differences of PNN were mainly expressed in terms of staining intensity, with males generally showing higher intensity than females, but with similar densities between males and females.

1.2.4. PNN functions in CNS

The complex formation of PNNs by various molecular components, and the wide but heterogenous distribution of PNNs throughout brain regions during postnatal period, leads to the suggestion that PNNs and their underlying molecular components might have varying functional roles in the CNS.

1.2.4.1. General functions of PNN

In the neuronal development period, PNNs are suggested to be involved in synaptic or neural plasticity at the end of the critical periods. Synaptic plasticity refers to the ability of synaptic connections between neurons to modulate their efficiency (Bassi et al., 2019) and neural plasticity refers to the ability of neurons to modify their functional or structural capacities (Berlucchi and Buchtel, 2009). The critical period is a postnatal time when the functional development or maturation of CNS properties is especially susceptible to alterations in the external environment (Rice and Barone, 2000). After the critical period, the plasticity becomes reduced or even absent (Pizzorusso et al., 2002). PNNs become completely formed at approximately the same time when the critical periods end accompanied with the maturation of neuronal functions and synaptic connections (~P24-P28 in mice) (McRae et al., 2007; McRae and Porter, 2012), indicating PNN maturation could be a marker of the closure of critical period. However, PNNs were suggested not only to act as a marker for the closure of critical period, but also to potentially control the closure of the critical period. This suggestion came from and was supported by the removal of the PNNs using Chondroitinase ABC (ChABC) which digests CS-GAG chains of PNNS. For example, degradation of PNNs using ChABC in the visual cortex resulted in the reactivity of ocular dominance plasticity (Pizzorusso et al., 2002), which in turn indicated the delay of critical period closure after PNN degradation. Apart from the influence of PNN removal on the plasticity in visual cortex, increased synaptic or neural plasticity has also been found across various brain regions, such as, auditory cortex (Happel et al., 2014), hippocampus (Hylin et al., 2013), and amygdala (Gogolla et al., 2009). Similarly, in cultured cells, PNN degradation by ChABC led to increased peri-synaptic and post-synaptic connections in hippocampal neurons, illustrating increased synaptic plasticity after removal of PNNs (Pyka et al., 2011). In addition to controlling neural plasticity, the PNN formation and development are dependent on neural activity, which has been supported by several studies. Monocular deprivation, by inducing cortical response plasticity in visual cortex, also resulted in reduced density and intensity of PNNs, in cats and rats (Guimaraes et al., 1990; Pizzorusso et al., 2002). Similarly, in cultured cells, blockage of action potentials (AP) by blocking sodium channels resulted in reduced number of WFA-labelled PNNs and impaired PNN structure (Dityatev et al., 2007).

PNNs surround mainly GABAergic inhibitory neurons, specifically *Pv*-expressing neurons which contribute to synchronised oscillations, especially gamma oscillations (Cabungcal et al., 2013; Morishita et al., 2015). PNNs were thought to inhibit synaptic plasticity during development or maturation stages by inhibiting lateral diffusion of receptors, such as α-amino-3-hydroxy-5-methyl-4-isoxazolepropionic acid (AMPA) receptors, to different synaptic regions (Frischknecht et al., 2009); or by inhibiting the signal pathways that occur in presynaptic or postsynaptic membranes, to prevent the formation of synaptic contacts. Pv-expressing interneurons are also suggested to be a critical regulator in plasticity (Hensch, 2005; Donato et al., 2013), so the function of PNNs in plasticity could also be associated with the functions of Pv-expressing neurons. This suggestion was proved and supported by several studies where removal of PNNs during the critical periods led to increased activities of putative Pv-expressing neurons (Balmer,

2016; Lensjø et al., 2017), and increased inhibitory GABAergic currents in rat critical period in cortical regions (Liu et al., 2013). These studies indicated that loss or disruption of PNNs was linked to the altered activities of Pv-expressing neurons, which could result in abnormal neuronal activities or plasticity.

In addition to being involved in the critical period and regulating synaptic or neural plasticity. PNNs perform other functions. At early stages of PNN development, PNNs were suggested to attract several neurotrophic substances, such as growth factors. Basic fibroblast growth factors in PNNs were shown to be responsible for neuronal survival and neurite extension, which indicated that PNNs might be involved in regulating neuronal maturation and stimulating axonal growth (Celio and Blumcke, 1994). At developed stages, the mature PNN enwraps cell bodies, proximal dendrites, and initial axons tightly, and it has been demonstrated that proteoglycans and *TnR* could inhibit adhesion between neurons, suggesting that PNNs create a barrier for neurons against the formation of new synaptic contacts (Pesheva et al., 1993). Therefore, it could be seen that PNN play a critical role in regulating and protecting synaptic functions.

Furthermore, PNNs also provide protective functions for neurons from being damaged by external or harmful substrates. For example, PNNs were shown to protect neurons from oxidative stress. Under conditions of elevated oxidative stress, a lower number of Pv-expressing neurons was detected in brain regions showing PNN degradation as compared to regions without PNN degradation (Cabungcal et al., 2013); and neurons enveloped by PNNs were less frequently affected compared to neurons devoid of PNNs (Morawski et al., 2004); moreover, with iron-induced oxidative stress, PNN-covered neurons showed a slower degeneration rate than PNN-devoid neurons (Suttkus et al., 2012). These lines of evidence demonstrated the protective effect of PNNs on neurons from being disrupted by oxidative stress. In addition, superoxide dismutase, which binds to CS-GAG chains in PNNs, may be a critical enzyme to protect neurons against oxidative stress (Karlsson et al., 1988; Antonyuk et al., 2009).

As synaptic plasticity can be regulated by PNN, and memory is dependent on short-term and long-term synaptic plasticity, PNNs may play a role of in cognitive functions. Enhanced memory extinction was observed in mice with PNN loss in amygdala, resulting in the erasure of fear memory (Gogolla et al., 2009). A similar effect of PNN degradation has been observed in auditory and visual cortex, where inhibition of auditory fear learning or consolidation and visual fear memory recall was detected in mice and rats, respectively (Thompson et al., 2018; Banerjee et al., 2017).

Therefore, PNNs are multi-functional structures, generally being a marker of critical period closure and the control of neural plasticity, also providing a neuroprotective role to prevent neurons from being damaged by external stimuli or substrates, and being involving in cognitive functions, especially enhancing fear learning and memory consolidation.

1.2.4.2. Functions of CSPGs

CSPGs fundamentally contribute to maintenance and stabilisation of PNN structure by interacting with other PNN molecules. For example, Eill et al. (2020) reported a new function of *Ptprz1* that could interact with *Acan* and *Ncan* to stabilise PNN structure by binding with *TnR*.

As PNNs play a critical role in regulating neural plasticity and the closure of the critical period, CSPGs generally exert similar functions. As a major component of PNNs, *Acan* was suggested to be a marker for the closure of critical period and a key regulator of neural plasticity, and increased expression of *Acan* was accompanied by reduced neural plasticity (McRae et al., 2007). In the perisynaptic cellular spaces, *Bcan* is one of the predominant components, which

suggests a role for *Bcan* in synaptic transmission (Blosa et al., 2015). *Bcan* interacts with AMPA receptors and potassium channels, and removal of *Bcan* compromised synaptic plasticity and excitatory connections onto the *Pv* neurons that the PNNs surrounded (Favuzzi et al., 2017). By interacting with AMPA receptors and potassium channels, high concentrations of *Bcan* molecules were shown to surround excitatory synapses of *Pv* –expressing basket cells rather than chandelier cells (Favuzzi et al., 2017; Klueva et al., 2014), indicating *Bcan* could regulate the afferent synapse signalling of Pv-expressing interneurons. *Bcan* expression was shown to be suppressed in an Alzheimer's disease (AD) mouse model, along with increased synaptic activity in the hippocampus (Scheff et al., 2006; Mufson et al., 2015). *Vcan* was also demonstrated to bind to the GluR1 subunit of the AMPA receptor, and the expression of *Vcan* and *Bcan* in rat hippocampus increased after spatial memory training, further indicating a role for *Bcan* and *Vcan* in neural plasticity related to memory recall (Saroja et al., 2014).

Additionally, the molecular components of PNN, CSPGs, act as promoters or inhibitors of neurite or axonal growth, providing a role for PNN in regulating neurite growth. Converging evidence suggests that axonal outgrowth is promoted after CSPG removal. Degrading CSPGs by ChABC in rat after spinal cord lesions resulted in axonal recovery, with regeneration of injured axons (Bradbury and Carter, 2011). After CNS injury, upregulated CSPGs were also found. For example, more CSPGs were presenting in the injured areas, with colocalisation of glial fibrillary acidic protein (GFAP)-positive astrocytes in glial scars (Fawcett et al., 1989), further supported by Dyck and Karimi-Abdolrezaee (2015). Specific CSPG molecules were investigated as contributing to the inhibitory effect on axonal or neurite growth. *Ptprz1* activated the RhoA pathway which in turn led to inhibition of axonal growth (Liu et al. 2015; Wu and Xu, 2016). In cultured rat retina ganglion cells, purified *Ncan* and *Ptprz1* inhibited neurite growth, with decreased dendritic and axonal length detected, indicating that both *Ncan* and *Ptprz1* had an inhibitory effect on neurite growth in cultured retina cells (Inatani et al., 2001).

1.2.4.3. Functions of *TnR*

TnR stabilises PNN structure mainly by binding *Acan* (Morawski et al., 2014). *TnR*-deficient mice showed damaged *Acan* labelling and altered PNN structure, with reduced WFA-labelled PNNs covering cell soma and proximal dendrites (Weber et al., 1999; Bruckner et al., 2000; Morawski et al., 2014). Pv interneurons were less covered by PNNs, and a reduction in synaptic GABAergic innervation of CA1 pyramidal neurons was observed in the *TnR* deficiency animal model (Morawski et al., 2014). Reduced levels of *Ncan* and *Ptprz1* were also detected in TnR deficient mice (Haunso et al., 2000), which further supported the concept that *TnR* could stabilise PNN structure by interacting with *Ptprz1* (Eill et al., 2020).

TnR was suggested to exert functions in synaptic and neural plasticity depending on the targeted brain regions and cell types. For example, in mice, lack of *TnR*, *TnC*, *Bcan* and *Ncan* increased hippocampal synaptic density, enhanced excitatory synaptic transmission and upregulated neural network activity, suggesting deficiency of the 4 molecules enhanced synaptic plasticity (Geissler et al. 2013; Gottschling et al. 2019). *TnR* could regulate synaptic plasticity by altering related CSPG expression. Cultured hippocampal neurons from *TnR* KO mice showed reduced *Acan* clusters and decreased association between *Acan* and hyaluronan, which in turn disrupted the PNN organisation around cell dendrites (Morawski et al., 2014). Reduced expression of *Ptprz1* was also found in *TnR* deficient mice (Eill et al., 2020). With the absence of *Acan* clusters and Ptprz1, abnormal PNN formation was observed in *TnR* deficient mice, resulting in deficits of long-term potential (LTP) and long-term depression (LTD) in hippocampus along with increased synaptic transmission (Freitag et al., 2003).

TnR, as one of the components of PNNs, is also involved in inhibiting axonal or neurite growth. In cultured retina neurons, cells with *TnR* expressed were unable to extend axons, and elevated expression of *TnR* was shown after optical nerve injury with inhibited axonal regeneration (Becker et al., 2000). A similar inhibitory effect of *TnR* was also detected in spinal cord with enhanced axonal outgrowth and regeneration caused by TnR antibody induction after spinal cord injury (You et al., 2012).

TnR not only inhibited axonal growth after injury, but could also recruit neurons and promote neural differentiation. *TnR* over-expression in stem cells could induce GABAergic interneurons differentiation (Hargus et al., 2008)

1.2.4.4. Functions of hyaluronan and link proteins

HA is required for neuronal development, playing a critical role in neocortical folding in late neurodevelopmental stages (Long et al., 2018). HA also has a role in dendrite extension and axonal sprouting, for example in axonal extension in primary visual cortex (Lin et al., 2007), and a role in cell migration and proliferation in cerebellum (Baier et al., 2007).

As HA and its synthetic enzymes *Has1*, *Has2* and *Has3* are the critical structure in PNN formation along with CSPGs and link proteins, HA function in PNN has been studied. Kwok et al. (2010) suggested HA functioned as a scaffold for PNNs, which in turn could organise other components to form a fully structured net. The *Haplns then* stabilise PNNs by binding to HA and CSPGs components (Spicer, 2003).

As critical parts of the PNN structure, HA and the link proteins were suggested to promote similar functions as other PNN components, such as synaptic plasticity. In cultured hippocampal neurons, removal of HA resulted in epileptiform activities with super bursts and spikes, leading to lateral diffusion of AMPA receptors (Vedunova et al., 2013), with decreased synaptic AMPA receptor density and increased synaptic plasticity (Frischknecht et al., 2009). Moreover, after inhibition of HA synthesis, astrocytic glutamate transporters, which remove glutamate at excitatory synapses, were depleted from synaptic regions, indicating HA might be involved in regulating excitatory synaptic signal transmission by controlling glutamate presence through glutamate transporters (Hayashi et al. 2019).

Unlike HA or *Has* components, limited functions of *Haplns* in the CNS have been reported, generally restricted to neuroprotective roles. *Hapln1* was demonstrated to protect neurons from oxidative stress, and in *Hapln1* deficient mice, more neural degeneration was found after iron-stress induction, compared to WT mice, suggesting a neuroprotective role of *Hapln1* (Suttkus et al., 2014). Furthermore, *Hapln* expression affected other PNN components. For example, mutation of *Hapln4* was accompanied by decreased expression of *Bcan* (Bekku et al., 2012); and in *Hapln1* KO mice, *Acan* labelling was disrupted (Suttkus et al., 2014).

A summary of PNN and PNN component functions and synthesis sources are listed in Table 1.3.

PNN components/PNN-covered neurons	Expression/sources	Functions	Citations
PNN	Neurons, glial cells (astrocytes and oligodendrocytes)	Marker of closure of critical period, regulating synaptic plasticity, maintaining memory learning and consolidation, neuroprotection.	Pizzorusso et al. (2002); Cabungcal et al. (2013); McRae et al. (2007); Pesheva et al. (1993); Suttkus et al., (2012); Gogolla et al., (2009).
CSPGs	Neurons, glial cells (astrocytes and oligodendrocytes)	Stabilising and maintaining PNN formation, regulating synaptic plasticity, maintaining memory learning and consolidation, neuroprotection.	Fawcett et al, (1989); Liu et al. (2015); Bradbury and Carter (2011)
Acan	Neurons, astrocytes	Stabilising and maintaining PNN formation, cell signalling, neural plasticity, neuroprotection	McRae et al. (2007)
Bcan	Neurons, astrocytes	Stabilising and maintaining PNN formation, synaptic plasticity, ion channels expression, regulating Pv-expressing interneurons	Favuzzi et al. (2017); Scheff et al. (2006); Mufson et al. (2015)
Ncan	Astrocytes	Stabilising and maintaining PNN formation, cell adhesion, regulating synaptic plasticity, inhibiting axonal growth	Oohira et al (1994) ; Mckeon et al (1999)
Vcan	Neurons, astrocytes	Stabilising and maintaining PNN formation, regulating synaptic plasticity (related to memory recall)	Saroja et al. (2014)
Phcan / Ptptz1	Neurons, astrocytes	Stabilising and maintaining PNN formation, inhibiting axonal growth, neuroprotection	Liu et al. (2015); Wu and Xu (2016)
TnR	Neurons, astrocytes, oligodendrocytes	Stabilising and maintaining PNN formation, inhibiting axonal growth, regulating synaptic plasticity, neuroprotection	Morawski et al. (2014); Haunso et al. (2000); Freitag et al. (2003); Becker et al. (2000)
Has	Neurons, astrocytes	Stabilising PNN formation, promoting axonal growth, cell migration and proliferation	Lin et al. (2007); Baier et al. (2007); Hayashi et al. (2019); Vedunova et al. (2013)
Haplns	Generally, from neurons (however, *Hapln1* is mainly expressed by astrocytes, and *Hapln2* by oligodendrocytes)	Stabilising and maintaining PNN formation, neuroprotection, regulating synaptic plasticity	Suttkus et al. (2014); Bekku et al. (2012)

Table 1.3: Functions and expression origin of PNN and PNN components.

To conclude, in general, PNNs exert multiple roles in cellular and regional functions, including controlling the closure of the critical period, regulating synaptic or neural plasticity and transmission, being involved in cognitive processes such as fear memory learning and consolidation, and protecting neurons from being damaged. The underlying components of PNNs, CSPGs, *TnR*, *Has isoforms* and *Hapln*s, also showed similar functions, particularly in synaptic plasticity, inhibiting axonal growth or regeneration and neuroprotection. Instead of promoting the functions on their own, PNN components could also maintain the whole PNN structure and regulate synaptic transmission by interacting with each other. For example, the aggregates of *TnR* and *Acan* interacting with HA were shown to stabilise PNNs and regulate synaptic contacts, and the interaction of *TnR* and *Ptprz1* also acted as a critical substrate to maintain PNN formation. Investigating the alterations of PNNs in several mouse models of brain disorders, such as Alzheimer's and epilepsy, suggested that PNN dysfunction could be associated with the onset of brain diseases. In the current study, we aimed to investigate the association of PNN expression with schizophrenia disorder as related to external stress stimulation. The overall introduction of how PNNs are related to schizophrenia and stress is presented in following sections.

1.3. Background of schizophrenia

1.3.1. Epidemiology and symptoms of schizophrenia

Schizophrenia is a complex, common and severe psychiatric disorder, affecting approximately 1% of the population worldwide and having a profound effect on both individuals and society (Owen, Sawa & Mortensen, 2016). The prevalence rate for schizophrenia over the lifetime is between 0.3% and 0.7% worldwide, with age of onset typically ranging from 15 to 35 ages (van Os and Kapur, 2009). The patients diagnosed with schizophrenia commonly exhibit symptoms throughout their lifetime, with more than 80% of patients presenting social dysfunctions and behavioural deficits (Thornicroft et al., 2004).

The onset of schizophrenia and the first episode of schizophrenia usually occurs during late adolescence or early adulthood, but a prodromal phase is often reported to precede the onset of schizophrenia. For example, cognitive impairments or disabled social functioning were suggested to appear before the onset of schizophrenia (Addington and Heinssen, 2012). Moreover, the onset of schizophrenia shows sex differences. The incidence of schizophrenia is higher in men than women, with the ratio of 1.4:1 (Li et al., 2022). The onset of schizophrenia in men is also 3 to 4 years earlier than women, which raised a perception that in the first half of life, before 40 years of age, the incidence rate is higher in males, and in the second half of life, the incidence rate is higher in females (Li et al., 2016; Li et al., 2022).

The core features of schizophrenia include positive and negative symptoms (Davey, 2014). Positive symptoms refer to psychotic symptoms which tend to reflect an excess or distortion of normal functions (Davey, 2014), including delusions, hallucinations, disorganised thinking or speech and abnormal motor behaviour (Davey, 2014). Delusions usually involve the misunderstanding of others' perceptions or experiences, which are exhibited in 75% of patients who are diagnosed with schizophrenia disorder (Masher, 2005). Hallucinations refers to an external sensory experience perceiving a thing which does not exist, among all the sensory experiences, auditory hallucinations are the most commonly experienced in patients diagnosed with schizophrenia, with 70% of patients suffering from auditory hallucinations (Cleghorn et al.,

1992). Disorganised thinking is another positive symptom, usually inferred from disorganised speech, for example speech with loose associations, no relevant answers to questions, or disorganised words or sentences (Davey, 2014). Abnormal motor behaviours are manifested in various ways, such as unpredictable behaviours or difficulty to complete goal-directed activities (Davey, 2014).

Negative symptoms refer to the characteristics of a loss or diminution of individuals' normal functions, including diminished emotional expression, affective flattening, avolition, alogia, anhedonia and asociality (Davey, 2014). Diminished emotional expression shows similar symptoms as affective flattening, which refers to the inability to show facial expression related to emotions. Avolition represents the inability to complete and follow goal-oriented tasks. Alogia is presented by individuals' simple and short speech, which lacks fluency. Anhedonia is characterised by lack of interest in usually pleasurable experiences and an inability to response to positive stimuli. Asociality shows as a lack of interest in social interactions and withdrawal from social activities. These are interconnected – for example anhedonia is likely to contribute to avolition and asociality.

Patients with schizophrenia also exhibit cognitive deficits, including impairments in working memory performance, attention and executive functioning. Deficits of attention were suggested as the primary cognitive symptoms damaged in schizophrenia patients (Cornblatt et al., 1985), with inability to focus on events/stimuli. Dysfunction of working memory is also a core impairment in cognitive functions in schizophrenia patients. Working memory is mainly characterised as the ability to process, manipulate and retain information, and schizophrenia is associated with impaired performance in tasks such as the "N-back" task. Executive functions consist of a range of cognitive processes necessary to plan and complete goal-directed tasks. In schizophrenia patients, impaired ability to perform tasks such as the Wisconsin Card Sorting Test, which probes aspects of executive function and cognitive flexibility, was reported (Gold et al., 1997; McGurk, et al., 2004)

The symptoms of schizophrenia also show some sex differences. Male patients were suggested to exhibit more severe negative symptoms, such as social withdrawal, diminished speech or lack of motivations, than female patients; while female patients exhibited more affective symptoms and emotional disturbances, such as depression or anxiety (Li et al., 2016; Li et al., 2022). These gender differences in symptoms associate with cognitive functions. For example, the negative symptoms were more linked to speech fluency and recall in male patients rather than female patients (Strauss et al., 2013). In addition to negative and positive symptoms, male and female patients presented cognitive differences. For example, male schizophrenia patients performed worse in several cognitive tests than females, such as Colour-Word Interference, and Interference/Switching tests and card sorting tests (Vaskinn et al., 2011). Moreover, in memory and language tests with schizophrenia patients, female patients performed better than male patients, indicating females tend to express less cognitive impairment (Han et al., 2012). Thus, schizophrenia symptoms were suggested to present in a gender-based format. A summary of the symptoms and the epidemiology of schizophrenia, and the gender difference, is presented in Table 1.4.

In the fifth edition of Diagnostic and Statistical Manual of Mental Disorders (DSM), schizophrenia was included with psychosis disorders, which are divided into affective psychosis and non-affective psychosis. Affective psychosis disorders contain bipolar disorder, and major depressive disorder with psychotic features; while the non-affective psychosis contains schizophreniform disorder, and psychotic disorder. Different types of psychosis are differentiated based on the diagnosis of duration of symptoms, the exhibition of somatic symptoms, co-occurrence of other

psychiatric disorders symptoms, such as depression or anxiety, and whether the pattern of symptoms is associated with substance abuse. According to DSM-5 (2013), the diagnosis of schizophrenia requires the exhibition of symptoms, presenting impairments in both social and behavioural functions, for more than 6 months.

	Schizophrenia	Gender differences	Citation
Core symptoms	**Positive**: delusions, hallucinations, grossly disorganised speech and abnormal motor behaviour. **Negative**: diminished emotional expression, affective flattening, avolition, alogia, anhedonia and asociality	Female patients express more positive symptoms, male patients express more negative symptoms.	Thornicroft et al. (2004); Li et al. (2016); Li et al. (2022); Davey, (2014).
Additional symptoms	Cognitive impairments and depressive emotions	Female patients tend to present more depressive emotions.	Thornicroft et al. (2004); Li et al. (2016); Li et al. (2022); Davey, (2014); Cornblatt et al. (1985); Han et al. (2012).
Heritability	Approximately 80%		Thornicroft et al. (2004).
Prevalence rate	Approximately 0.3% to 0.7% worldwide	The ratio of schizophrenia patients in males and females were 1.4:1.	Thornicroft et al. (2004); Li et al. (2016); Li et al. (2022); Davey, (2014).
Age of onset	Late adolescence and early adulthood, usually from the age of 15 to 36 years.	Men are 3 to 4 years earlier than women.	Addington and Heinssen (2012); Li et al. (2016); Li et al. (2022).

Table 1.4: Summary symptoms and prevalence of schizophrenia with gender differences.

1.3.2. Aetiology of schizophrenia

Risk of schizophrenia is influenced by the combination of genetic factors and external environmental factors, indicating that an individual with a significant burden of genetic risk of variants for schizophrenia might not develop schizophrenia-like symptoms unless the individual was also affected by environmental factors, particularly, environmental stressors.

1.3.2.1. Genetic factors

Based on genetic epidemiological studies, genetic factors contribute to the risk of schizophrenia, and individuals who have a family history of schizophrenia have a higher risk for schizophrenia. For example, individuals who have first-degree relatives who were diagnosed with schizophrenia were 10 times more likely to develop schizophrenia (Schneider and Deldin, 2001). In addition, consistent evidence showed that twins had a higher heritability rate for schizophrenia, of approximately 80% (Cardno and Gottesman, 2000; Sullivian et al., 2003). Monozygotic (MZ) twins who shared 100% genetic material had higher risk of developing schizophrenia than dizygotic (DZ) twins who shared 50% of genetic materials (Cardno and Gottesman, 2000; Sullivan et al., 2003). The concordance percentage of schizophrenia diagnoses in MZ twins was 44%, while the percentage in DZ twins was 12% (Gottesman et al., 1987). 16.8% of offspring of MZ twins who were diagnosed with schizophrenia were possible to develop schizophrenia, whereas 17.4% offsprings of MZ twins with schizophrenia were not diagnosed with schizophrenia or relative psychosis symptoms (Gottesman et al., 1987). This evidence demonstrated that

schizophrenia is heritable, and individuals who shared more genetic material with schizophrenia patients had higher risk of developing schizophrenia, and this genetic risk was also passed on to the offspring.

In general, no specific single gene variant could cause schizophrenia; however, the genome wide association studies (GWAS) also illustrated that multiple common genetic variants were associated with schizophrenia (Ripke et al., 2014). Currently, more than 280 loci are associated with schizophrenia risk (Trubetskoy et al., 2022), indicating that schizophrenia is a polygenic disorder. Several mutations have also been identified related to schizophrenia, in particular copy number variations (CNV), which represent deletion or duplication of usually a small number of genes. One of the most studied genes associated with schizophrenia was the deletion at chromosome 22q11.2 (Bassett and Chow, 2008). The deletion at 22q11.2 was found in 1% of patients diagnosed with schizophrenia, and people carrying the deletion are at around 30% risk of developing schizophrenia (Bassett and Chow, 2008). Other CNVs also markedly increased risk of schizophrenia. For example, the international schizophrenia consortium reported that large deletions of chromosome 1q21.1 were associated with schizophrenia, and the deletions at 15q13.3 were also significantly associated with schizophrenia (Stefansson et al., 2008). In addition, duplications at 16p11.2 increased risk of schizophrenia, whereas the deletions at 16p11.2 were linked to the increased risk of autism (McCarthy et al., 2010). Duplications at 16p11.2 increased the risk with 8 to 24 fold, while the deletions at 15q13.3 and 1q21.1 increased the risk with 7 to 18 fold (McCarthy et al., 2010), suggesting the duplications at 16p11.2 contribute to higher risk of development of schizophrenia compared to other CNVs.

1.3.2.2. Environmental factors

Genetic factors alone are not sufficient to explain the increased risk of schizophrenia. Environmental factors, including prenatal stress exposure or infection, birth complications, childhood trauma, substance addiction and social isolation, were also suggested to contribute to the increased risk of schizophrenia.

Increased risk of schizophrenia is associated with exposure to maternal stress. For example, where mothers experienced severe stressful life events during pregnancy, such as loss of relatives or serious illnesses, there was increased risk of schizophrenia in the offspring (~2x) (Khashan et al., 2008). Individuals who were exposed prenatally to natural disasters, such as the Tangshan Earthquake in 1976, or the Netherlands flood in 1953, had a higher risk of exhibiting schizophrenia symptoms (~2x), indicating that severe maternal stress has a long-lasting effect on offspring risk of schizophrenia in later life (Guo et al., 2010; Selten et al., 1999). Prenatal inflammation or virus infection has a similar effect. Various studies suggested that increased maternal immune responses after exposure to viruses or infectious agents, such as, cytomegalovirus, rubella virus or *Toxoplasma gondii* (*Toxo*), was associated with a higher risk of schizophrenia and schizophrenia spectrum disorders in offspring: roughly 5 times more likely to develop schizophrenia compared with individuals who did not experience prenatal inflammations (Babulas et al., 2006; Buka et al., 2001). Moreover, elevated expression of inflammation markers, such as interleukin 8, was observed in mothers of schizophrenia patients (Canetta et al., 2014). The studies consistently reported that the increased risk of schizophrenia was more likely to link to the maternal stress exposure during the first trimester which is a critical time for embryonic neurodevelopment and fetal brain was more vulnerable and susceptible to external stress than later periods in pregnancy (Seckl, 2001).

Apart from maternal stressors, experience of trauma and adversities in both childhood and adulthood are another potential risk factor for schizophrenia. A meta-analysis reported a strong

correlation between early childhood abuse (including bullying, neglect and parental death) and increased risk of schizophrenia or other psychosis disorders developed in adulthood (Varese et al., 2012). Several consistent findings also reported a robust association between early life adversities and higher risk of schizophrenia, for example, individuals who experienced childhood trauma were reported to express positive symptoms of schizophrenia in later life, especially auditory hallucinations and affective symptoms (Janssen et al., 2004; Bentall et al., 2014). In addition, adults who experienced adverse life events were 3 times more likely to develop psychosis (Beards et al., 2013). The time period when individuals experience life adversities or abuse was also suggested to link to the onset of schizophrenia or other psychosis disorders: a meta-analysis revealed that before the diagnosis of psychosis, elevated adverse life events occurred in patients with the time periods ranging from 3 months to 3.5 years (Beards et al., 2013).

1.3.2.3. Interaction of genetic and environmental factors

Prenatal stressors, such as prenatal infection and inflammation, are a risk factor increasing the risk of schizophrenia. Infectious agents, including cytomegalovirus, rubella virus and *Toxo*, are associated with higher risk of schizophrenia in offspring by increasing the maternal immune response (Sutterland et al., 2015). Thus, studies have investigated genetic and environmental interactions using *Toxo* induction. Expression of various genes was reported to be affected by *Toxo* in relation to the risk of schizophrenia. For example, C-reactive protein (CRP), which is elevated by *Toxo*-induced inflammation, was detected to elevate in schizophrenia patients (Dickerson et al., 2013; Avramopoulos et al., 2015). Additionally, another gene matrix metallopeptidase-9 (*MMP-9*) also responded to neuroinflammation, and a promoter allele of the *MMP-9* gene, *MMP-9 -1562C/T,* was reported to be associated with elevated MMP-9 levels in schizophrenia patients infected by *Toxo* (Mouhawess et al., 2020). Furthermore, the glutathione S-transferase theta 1 (*GSTT1)* gene is located at chromosome 22q11.2 (a risk locus for schizophrenia), and patients diagnosed with schizophrenia with signs of *Toxo* infection showed increased prevalence of *GSTT1* deletions (Ansari-Lari et al., 2021), indicating increased risk of schizophrenia was related to *GSTT1* deletion and *Toxo* infection. Therefore, several genes responded to inflammation or infection by *Toxo* induction, including CRP, *MMP-9 1562C* and *GSTT1,* are potentially involved in the increased risk of schizophrenia, suggesting the interaction of genes responsible for inflammation and prenatal infection could be a factor influencing the risk of schizophrenia.

Environmental stress and childhood abuse are associated with increased risk of schizophrenia. Several studies have investigated the relationship between candidate schizophrenia risk genes and susceptibility to environmental stress in the development of schizophrenia and related psychosis symptoms. One of the candidate genes, catechol-O-methyltransferase (*COMT*), was suggested to be involved in the development of schizophrenia and susceptible to external stressors. *COMT* is a gene located on chromosome 22q11.1, and the deletion of 22q11.1 increases risk of schizophrenia (Bassett and Chow, 2008). *COMT* plays a role in the dopaminergic system by mediating breakdown of dopamine (Chen et al., 2004). As the release of dopamine is suggested to be upregulated after exposure to environmental or psychological stress in the striatum (Pruessner et al., 2004) this could be exacerbated by deletion of *COMT,* and thus contribute to risk of schizophrenia. It has been suggested that an allele of the *COMT* gene, *Val158Met,* affected susceptibility to stress (Chen et al., 2004). Patients with psychosis homozygous for the *COMT Met*^{158} variant were suggested report more stressful life events compared to other genotypes (Winkel et al., 2008). Conversely, another study reported that homozygosity for the *COMT Met*^{158} allele was protective against the tendency of stressful events

to precipitate psychosis (Stefanis et al., 2007), which nevertheless suggests that an interaction of gene-environment factors played a role in the aetiology of psychosis. In addition to the stressful life events, *COMT* was also shown to affect vulnerability to childhood trauma or adversity. Individuals who carried *COMT Val*^{158} allele and a *MTHFR* T allele, and experienced childhood adversities were more likely to develop schizophrenia compared to those with other genotypes (Debost et al., 2017). Thus, while the data are not totally consistent, the interaction between *COMT* genes and life stress or childhood abuse could be relevant for the genetic and environmental interaction influencing the risk of schizophrenia and psychosis disorders.

To conclude, genetic and environmental risk factors were associated with the increased risk of schizophrenia and other psychosis disorders. However, no single genetic or environmental factor is sufficient to cause schizophrenia. Therefore, it has been suggested that the interaction of genetic and environmental factors is essential. The candidate genes, such as *COMT, GSTT1*and *MMP-9*, were suggested to be associated with risk of schizophrenia and psychosis by interacting with several environmental factors, such as prenatal stress, early-life adversity, childhood trauma and substance abuse. Consistent studies reported a link between schizophrenia or psychosis risks and the interactions of potential genes and prenatal stress, early-life adversity, childhood trauma factors. However, the details as to how substance abuse interacts with potential genes still remains controversial.

1.3.3. Neurobiology of schizophrenia

The underlying neurobiological changes in the CNS of schizophrenia patients includes abnormal cellular processes, dysregulated neurotransmitter system and alterations in neuroanatomy.

1.3.3.1. Abnormal cellular processes and synaptic formation

The onset of schizophrenia commonly occurs during late adolescence or early adulthood. Adolescence is a time when cognitive and behavioural functions develop dramatically (Huttenlocher et al., 1979; Blakemore and Choudhury, 2006). As synchronised neural oscillations are crucial for synaptic plasticity and cognitive processes, disrupted neural oscillations may be a fundamental pathology in the disease.

In human PFC, spatial working memory involves approximately 40Hz synchronised neural oscillations, defined as high gamma synchronisations (Alekseichuk et al., 2016). These synchronised oscillations can be detected by EEG or MEG, and can monitor brain activity while individuals are performing cognitive tasks (Alekseichuk et al., 2016; Schirner et al., 2018). In healthy subjects, the synchronised neural oscillations are related to several cognitive processes. For example, the generation of gamma oscillations is observed in various brain regions, including PFC, hippocampus, amygdala and striatum, associated with recognition, memory, and emotion regulation (Guan et al., 2022). However, in schizophrenia patients, abnormal neural oscillations are detected while processing cognitive tasks, for example a reduction of amplitude of evoked gamma oscillations in frontal regions while performing working memory tasks (Uhlhaas and Singer, 2010). Additionally, the detected amplitude of evoked gamma oscillations was correlated with the degree of positive symptoms (auditory hallucinations) (Spencer et al., 2009); whereas the reduction in gamma oscillations was associated with the negative or disorganised behaviours (Cho et al, 2006; Haenschel et al., 2009). Moreover, in image detection tasks, a longer time was required for schizophrenia patients to respond to the images compared with the healthy subjects, and this longer reaction time correlated with reduced synchrony of beta oscillations (20Hz to 30

HZ) and increased power of gamma oscillations (Uhlhaas et al., 2006); and patients with schizophrenia showed working memory deficits along with reduced amplitude of theta and gamma oscillations (Schmiedt et al., 2005; Cho et al., 2006). Therefore, disrupted neural oscillations are observed in patients with schizophrenia, especially gamma oscillations, and the disruptions are associated with schizophrenia symptoms.

The generation of synchronised neural activity, and in particular gamma oscillations, is dependent on pyramidal cells modulated by the fast-firing Pv-expressing GABAergic inhibitory interneurons (Uhlhaas and Singer, 2010). Converging evidence from post-mortem studies supports dysfunction of these neurons in schizophrenia patients, with lower dendritic spine density on pyramidal neurons, and reduced mRNA expression of Pv in PFC and hippocampus (Hashimoto et al., 2008). The mRNA and protein expression of glutamate decarboxylase 67 (*Gad67*/*GAD1*), an enzyme mediating synthesis of GABA, were also demonstrated to be decreased in schizophrenia patients (Thompson et al., 2009; Woo et al., 2004). Taken together, the reduced dendritic spines around pyramidal neurons, altered expression of Pv-expressing interneurons and *GAD67* suggest the disruption of inhibitory mechanisms in neural activities in schizophrenia patients.

Microglia were suggested to contribute to synaptic pruning which could eliminate dysfunctional synapses, and maintain fundamental neural circuits (Mordelt and Witte, 2023). Overactivation and increased density of microglia were observed in brain tissue from people with schizophrenia (Doorduin et al., 2009; Petrasch-Parwez et al., 2020; Hill et al., 2021), indicating that the hyperactivation of microglia early in development might result in overactivation of synaptic pruning, leading to reduced dendritic spine density on pyramidal neuron dendrites, which could in turn alter the firing rates of pyramidal cells in schizophrenia subjects. As pyramidal neurons are excitatory, the altered firing rates of pyramidal neurons might result in disrupted excitatory transmission in schizophrenia patients. The expression of N-methyl-D-aspartate receptors (NMDAR), a receptor which played a role in excitatory glutamatergic signalling, was found to be decreased in PFC in schizophrenia patients, with reduced expression of several NMDAR subunits, including GluN1 and GluN2C (Catts et al., 2016; Weickert et al., 2013).

Thus, based on the alterations of synaptic pruning and dendritic spines in schizophrenia patients, a hypothesis of schizophrenia aetiology has been derived, which is the synaptic hypothesis (Howes and Onwordi, 2023). The first version of the synaptic hypothesis suggested a causal role for synaptic alterations in schizophrenia, such as, reduced spine density and disorganised synaptic formation, accompanied by several abnormal neuronal transmissions, such as, deficits in synchronised oscillations and reduced synaptic plasticity (Feinberg, et al., 1984).

The second version of the hypothesis further clarified the specific region of the synaptic alterations, suggesting the elimination of the synapses or dendritic spines in cortical regions with excessive synaptic pruning, and overexpression or production of synapses in the subcortical regions with reduced synaptic pruning activities (Keshavan, et al., 1994). In addition, the brain anatomy was also included in the second version, illustrating the reduction of the grey matter volume, cortical thinning and sulcal enlargement (Keshavan, et al., 1994).

The third version of the hypothesis linked the genetic and environmental factors of schizophrenia. Several genes associated with schizophrenia risk were related to the synaptic development and formation, such as, complement component 4A (C4A) (Kim et al., 2021), indicating elevated expression of C4A was associated with the increased risk of schizophrenia, and the C4A-expressed gene was also related to the synaptic and glial pathways with the regulation of synaptic pruning activities (Kim et al., 2021). As noted in previous contents, microglia could contribute to synaptic pruning (Mordelt and Witte, 2023), thus, with elevated expression of C4A,

increased expression of microglia could occur, with overactivation of synaptic pruning leading to reduced synaptic spine density. Moreover, various environmental factors associated with schizophrenia were also suggested to relate to synaptic alterations. Social isolations and prenatal infections were demonstrated to correlate to decreased synaptic or dendritic spine densities (Ciesilk, et al., 2020; Silva et al., 2003). Additionally, genetic variants in synaptic pathway-related genes were shown to associate with abnormal brain anatomy. For example, elevated C4A expression was related to reduced cortical and hippocampal surface (Silva et al., 2021; Connell et al., 2021).

Therefore, the synaptic hypothesis of schizophrenia initially suggested the involvement of the reduction of synapses or dendritic spines in the underlying neurobiology of schizophrenia. The second version further clarified the specific location and synaptic activities, with the elimination of the synapses in cortical region, and overexpression of synapses in subcortical regions, and provided a fundamental change of neuronal anatomy, such as reduced grey matter and enlarged sulci. Furthermore, the third version provided a link between the synaptic alterations and the risk factors for schizophrenia, such as genetic and environmental factors.

Taken together, it could be concluded that the disrupted gamma oscillations, coordinated with compromised expression and functions of GABAergic and pyramidal neurons were suggested to contribute to the abnormal cellular and neural processes in schizophrenia. Gamma oscillations play a key role in cognitive functions, including information processing, attention, and cognitive flexibility (Kim et al., 2016; Cho et al., 2015), and were suggested as a fundamental impairment in schizophrenia. The alterations of synchronised oscillations have been related to different symptoms of schizophrenia, the evoked gamma oscillations with increased frequency linked to positive symptoms, such as hallucinations; and the reduced synchrony and power of beta and theta oscillations correlated with cognitive deficits, such as impaired working memory, indicating increased synchrony of oscillations might associate with positive symptoms and reduced synchrony of oscillations might relate to deficits of behaviours. The abnormal cellular activities were also related to the abnormalities of synaptic formation and dendritic spines, such as reduced dendritic spines and altered synaptic pruning ability in various brain regions of schizophrenia patients, which supported the development of the synaptic hypothesis of schizophrenia.

1.3.3.2. Dysregulated neurotransmitter system

There are more than 40 types of neurotransmitters in human CNS, and it has been suggested that 4 of them are associated with the altered neurotransmission in schizophrenia, contributing to abnormalities of neural oscillations: these are GABA, glutamate, dopamine and serotonin.

It has been noted in the previous section that neural activities are abnormal in schizophrenia patients, particularly the abnormalities in generation and synchronisation of gamma oscillations. The network of GABAergic interneurons is crucial to the generation of high frequency oscillations by transferring inhibitory postsynaptic potentials to pyramidal neurons, regulating their firing rates (Uhlhaas and Singer, 2010). Pv-expressing GABAergic interneurons are suggested to mediate the generation of gamma oscillations (Sohal et al., 2009). Thus, in order to maintain the regular neural activities, GABAergic neurotransmission is a fundamental and critical factor.

Converging evidence indicated that GABAergic neurotransmission is altered in schizophrenia subjects. For example, consistent studies reported the reduction of *GAD1* expression in various cortical regions in schizophrenia patients, illustrating that decreased mRNA levels of *GAD67* were found in PFC in schizophrenia subjects compared with healthy subjects, accompanied by

the loss of GABAergic transporter1 (*GAT1*), the GABA reuptake protein (Akbarian et al., 1995; Volk et al., 2000). The reduced expression of GAD67 was mainly located in layer 2 and layer 3 of the cortical areas (Akbarian et al., 1995; Volk et al., 2000). *GAD* is a key component for GABA synthesis, so reduced expression of GAD67 combined with the loss of reuptake suggests decreased GABA neurotransmission in schizophrenia. Among all subtypes of GABAergic interneurons, Pv-expressing interneurons are involved in the impairments in GABA neurotransmission; the immunohistochemical staining intensity and mRNA levels of Pv-expressing neurons are reduced in PFC in schizophrenia subjects, and the reduction of Pv-expressing neurons is correlated with decreased *GAD67* expression, with only 55% of Pv-expressing interneurons expressing *GAD67* in schizophrenia subjects (Hashimoto et al., 2003).

Abnormal GABA transmission in schizophrenia subjects has been proposed to be directly associated with disrupted neural oscillations. In an auditory stimuli task, schizophrenia subjects responded to lower frequency auditory stimuli than healthy subjects, presenting decreased strength of GABA synaptic transmission and reduced expression of *GAT1* (Vierling-Claassen et al., 2008). Decreased expression of Pv was shown to cause reduced gamma oscillations in PFC and ECx in schizophrenia mouse models (Lodge et a., 2009; Cunningham et al., 2006). Thus, Pv-expressing neurons are affected in schizophrenia subjects or animal models, and the altered expression seems to be linked to abnormal neural oscillations.

Thus, based on the dysregulated GABA neurotransmission found in schizophrenia subjects, a hypothesis for GABA deficits in schizophrenia has been suggested, addressing the role of GABA in schizophrenia pathology. As noted in the previous contents, the alterations of GABA neurotransmission and GABA related markers were widely reported in various brain regions of schizophrenia patients, especially in the PFC and ECx (Lewis et al., 2012; Berretta et al., 2015; Chung et al., 2016; Enwright et al., 2016; Schubert et al., 2015). The deficits of GABA neurotransmission and GABA related neurons and markers raised the importance of the GABAergic alterations in the underlying neuropathology of schizophrenia and supported the GABA hypothesis for schizophrenia.

As Pv-expressing GABAergic interneurons receive excitatory input signals via glutamatergic receptors, especially NMDARs, in this case the alterations in the glutamatergic system might associated with disrupted GABAergic neurotransmission. The inhibition of NMDAR with ketamine administration, an NMDAR antagonist, produced schizophrenia-like symptoms in healthy volunteers, and decreased Pv and *Gad1* expression, alongside suppressed inhibitory postsynaptic potentials and reduced power of gamma oscillations, in mice and rats (Krystal et al., 1994; Zhang et al., 2008). However, increased gamma oscillations were found in human auditory cortex and rat neocortex after inhibiting NMDARs, which were correlated with positive hallucination symptoms of schizophrenia (Plourde et al., 1997; Pinault et al., 2008), suggesting that the changes in glutamatergic systems could up or down regulate GABA neurotransmission depending on the specific brain regions.

Based on the abnormal glutamatergic transmission in schizophrenia, the glutamate hypothesis of schizophrenia has been suggested, indicating that the deficits of glutamatergic systems contributed to the onset of schizophrenia. For example, as noted in previous contexts, several antagonists of glutamatergic receptors, such as, phencyclidine (PCP) and ketamine have been used to induce schizophrenia-like phenotypes (Krystal et al., 1994; Zhang et al., 2008). Also, glutamate receptors, such as NMDARs, were consistently reported to be reduced in schizophrenia subjects, with both reduced mRNA and protein levels of the NMDAR subunits, including GRIN1, $GRIN_{2A}$, and $GRIN_{2C}$ in various brain regions, including PFC, occipital cortex and ACC (Benetyo et al., 2008; Weicker et al., 2013; Akabarian et al., 1996). The vesicular

glutamate transporter (VGluT) is involved in the transport of glutamate into synaptic vesicles, and the subtypes of VGluT, such as VGluT1 and VGluT2 were also demonstrated to be reduced in schizophrenia patients, especially in PFC, hippocampus and subcortical regions (Eastwood and Harrison, 2004; Oni-orishan et al., 2008). The reduced expression of glutamatergic receptors and transporters could contribute to the downregulated glutamate transmission in schizophrenia. Thus, the glutamate hypothesis was one of the vital suggestions for investigating underlying neurobiology of schizophrenia.

Apart from glutamatergic neurotransmission systems involved in the underlying mechanisms in schizophrenia, dopaminergic transmission is also suggested potentially to be dysfunctional in schizophrenia. Several studies indicated that dysregulation of the dopaminergic system contributed to the development of schizophrenia or schizophrenia-like symptoms. Amphetamine-induced dopamine hyperfunction, with more activation of dopamine D2 receptors, led to more severe positive symptoms in patients with schizophrenia (Abi-Dargham et al., 1998). In the prodromal state of schizophrenia subjects, overactivity of dopaminergic functions was detected in striatum regions (Howes et al., 2009).

As one of the main neurotransmitters affected in schizophrenia, with overactivation or over-transmission of dopamine in various brain regions and accompanied by the overactivation and expression of related receptors, such as D2 or D3 receptors (Abi-Dargham et al., 1998; Howes et al., 2009). Based on this mechanism, the dopamine hypothesis has been established.

The first version of dopamine hypothesis established a role for the overactivation of dopamine receptors, especially D2 receptors, correlated with upregulated dopamine transmission in the aetiology of schizophrenia (Howes and Kapur, 2009).

The second version of the hypothesis further clarified the specific location of changes and expanded the receptors involved in dopaminergic activity, illustrating that schizophrenia could be characterised by the hypodopaminergic activities in prefrontal cortex and hyperdopaminergic activities in the striatum and other subcortical regions, with the predominant involvement of D1 receptors in cortical regions and D2 receptors in subcortical regions (Howes and Kapur, 2009).

The third version of the hypothesis further included the risk factors of schizophrenia. As noted in previous section 1.3.2, increased risk of schizophrenia is highly associated with genetic or environmental factors, and the interaction between these 2 factors. Thus, in the third version of dopamine hypothesis of schizophrenia, the associations between abnormal dopamine activities and genetic, environmental factors or the interaction of genetic and environmental factors had been incorporated. For example, sequence variants in 4 dopaminergic genes *SLC6A3, DRD3, COMT* and *SLC18A2* were more frequently observed in schizophrenia patients compared to healthy individuals, and showed a high relationship to the risk of schizophrenia (Talkowski et al., 2007). After exposure to environmental stress, such as social isolation, adversities, and stress induction, the schizophrenia symptoms were detected alongside the over-release of dopamine (Fulford et al., 1998; Howes et al., 2000). In addition, interactions between genetic variants and environmental factors had a higher association with dopaminergic dysfunctions. For example, increased risk of schizophrenia was highly correlated with the variants of the *COMT* gene (involved in dopamine catabolism) interacting with early life adversities (Chen et al., 2004; Stefanis et al., 2007). Moreover, apart from the dysregulated dopamine acting on dopaminergic receptors, the third version of hypothesis further indicated that accumulated release of dopamine was also occurring in presynaptic terminals, with elevated presynaptic synthesis in striatal dopaminergic neurons (Meyer et al., 2002). The elevated dopamine levels were not only associated with schizophrenia, but also some other psychosis disorders, such as bipolar disorders or mania (Reith et al., 1994).

Therefore, the 3 versions of dopamine hypothesis in schizophrenia illustrated that dopaminergic systems are critical to the underlying mechanisms of schizophrenia. Initially, hyperdopaminergic activity was suggested, followed by the further clarification of hypodopaminergic activity in prefrontal regions and hyperdopaminergic activity in striatal or other subcortical regions; furthermore, the latest version links the dopaminergic activities to the risk factors for schizophrenia, and provided a suggestion that the dopamine dysfunctions were also presenting in presynaptic terminals and the release of dopamine was also related to other psychosis disorders, rather than being restricted to schizophrenia.

Furthermore, serotonergic systems are also thought to be disrupted in schizophrenia. Serotonin (5-HT) has been suggested to play a role in various behaviours and cognitive functions which are disturbed in schizophrenia.

Consistent post-mortem studies reported alterations of different subtypes of 5-HT receptors in subjects with schizophrenia. For example, in PFC, increased expression of 5-HT_{1A} receptors has been detected in schizophrenia patients, with the elevation rates ranging from 20% to 90% (Gray et al., 2006; Selvaraj et al., 2014). Conversely, decreased density of 5-HT_{2A} receptor is observed in PFC in schizophrenia patients (Dean et al., 1999; Dean and Hayes, 1996), which was consistent with a later study that 5-HT_{2A} receptor mRNA expression was also decreased in patients with schizophrenia (Cheah et al., 2017). Additionally, serotonin transporters (SERTs) were shown to be decreased in the frontal and cingulate cortex regions, but increased in striatum of schizophrenia subjects (Joyce et al., 1999; Laruelle et al., 1993). Thus, the changes of 5-HT receptors and transporters in schizophrenia are dependent on specific brain regions and receptors.

Based on the serotonin deficits in schizophrenia, another hypothesis has been developed, which is the serotonin hypothesis (Eggers, 2013), suggesting that the increased or decreased expression of different subtypes of 5-HT receptors or transporters plays an important role in disease aetiology, and indicating an imbalance in neurotransmission by serotonin in schizophrenia patients. For example, increased 5-HT_{1A} receptors and decreased 5-HT_{2A} receptors in cerebral cortex regions were widely observed in schizophrenia patients (Gray et al., 2006; Selvaraj et al., 2014; Dean et al., 1999; Dean and Hayes, 1996)

In conclusion, the alterations of 4 different neurotransmission systems were suggested to be involved in the underlying neurobiology of schizophrenia, including GABAergic, glutamatergic, dopaminergic and serotonergic systems. Different hypotheses for schizophrenia were also developed and provided several implications and insight for the further treatment, especially the medical treatment, for schizophrenia, by targeting different receptors and regulating the neurotransmission systems.

1.3.3.3. Abnormal brain anatomy

A number of brain structural abnormalities are observed in patients with schizophrenia. Alterations in neuroanatomy develop in individuals with schizophrenia or schizophrenia-like symptoms throughout the lifetime, and the alterations are observed during the first episode of schizophrenia symptoms, suggesting that neuroanatomical abnormalities might be critical factors associated with schizophrenia symptoms (Olabi et al., 2011). Schizophrenia patients exhibit 2 major deficits in brain anatomy, which are reduced volume of prefrontal or temporal cortex, and enlarged brain ventricles.

Firstly, reduction in brain volume was observed in schizophrenia patients, especially in prefrontal lobe, temporal lobe and hippocampus. For example, in MRI studies, a consistent reduction of

prefrontal cortex volume was detected in schizophrenia patients (Ho et al., 2003; Sun et al., 2008; Sun et al., 2009). Hippocampus volumes were also demonstrated to be decreased in schizophrenia patients, in both left and right sides (Steen et al., 2006). Decreased volumes of internal capsule and thalamus regions were reported in subjects diagnosed with schizophrenia compared to healthy subjects (Lang et al., 2006), the reduction in volume of thalamus correlating with total symptom severity.

Secondly, reduced volume of grey matter was found in schizophrenia in various brain regions, particularly in PFC and temporal cortex. Grey matter is a major component in CNS, present mostly in cortical layers and consisting of cell bodies, synapses, glial cells, and neuronal axons and dendrites which are mostly myelinated (Mercadante and Tadi, 2023). In general, the total volume of grey matter was found to be decreased in both first episode and chronic diagnosis of schizophrenia compared with healthy individuals (Zipursky et al., 1998; Gur et al., 2000). Consistent MRI evidence reported that reduction of grey matter was present across different brain regions in subjects who were in the first or middle episodes of schizophrenia. For example, decreased volume of grey matter was detected in temporal cortex in patients diagnosed with chronic schizophrenia, specifically in middle and inferior temporal gyrus (Sullivan et al., 1998; Onitsuka et al., 2004; Torres et al., 2016; Wright et al., 2000). Additionally, the volume of prefrontal grey matter was also shown to decline in dorsal or orbital regions of frontal cortex in schizophrenia patients in the first episode diagnosis (Gur et al., 2000; Hirayasu et al., 2001; Karlsgodt et al., 2010). Similar reductions of grey matter volume were also observed in hippocampus and amygdala by 8% and 4.5%, respectively (Nelson et al., 1998).

Reduced grey matter volume in various brain regions was suggested to relate to schizophrenia symptoms. A smaller volume of grey matter in temporal cortex (including auditory cortex) was associated with the positive symptoms of schizophrenia, such as auditory hallucinations. Schizophrenia patients with prominent auditory hallucinations showed reduced grey matter volume in superior or middle temporal gyrus compared to patients with no or less exhibitions of auditory hallucinations (Onitsuka, et al., 2004). Similar grey matter reduction in superior and middle temporal gyrus were also detected in schizophrenia patients primarily exhibiting auditory hallucinations, and the decreased volume in temporal regions was correlated with reduced activation of temporal gyrus detected by fMRI methods, which supported the link between hallucination symptoms and temporal grey matter reduction (Barta et al., 1990; McGuire et al., 1995; McCarley et al., 2002). Abnormalities in temporal cortex and connected regions, such as, limbic areas, cerebellum and basal ganglia were widely observed in schizophrenia (Gur et al., 2000).

Grey matter volume reductions are also exhibited in hippocampus (Nelson et al., 1998). Hippocampus is a critical region mediating learning, memory and emotional expression (Anand and Dhikav, 2012). Thus, reduced grey matter in hippocampus is likely to contribute to the impaired cognitive functions in schizophrenia, especially memory recall and restoration (Tamminga et al., 2010).

PFC plays a critical role in executive cognitive processes, including planning, attention, goal-oriented behaviours, speech mediation and memory. Disrupted PFC structure could lead to dysfunctional executive cognitive functions, which could be observed in schizophrenia symptoms, such as the cognitive impairments, including disorganised speech, damaged working memory processing; and negative symptoms, including abnormal motor behaviours and social withdrawal (Artiges et al., 2000; Pinkham et al., 2003). The prefrontal volume of grey matter is suggested to associated with spatial memory and attention, with larger volume in PFC correlated with better spatial memory and attention; the negative symptoms are associated with grey matter

volume reductions in PFC, with lower volume of prefrontal grey matter correlated with more severe negative symptoms, especially depressive mood and flattening emotional expression (Gur et al., 2000). In addition, another neuroimaging study showed consistent associations between grey matter reduction and degree of negative symptoms in schizophrenia (Chua et al., 1997).

Thirdly, apart from the decreased grey matter volumes, enlarged ventricles were widely and consistently detected in schizophrenia patients. Increased global ventricular volume was reported in several studies. For example, a meta-analysis reported that ventricular regions increased in schizophrenia patients with 16% larger volumes compared to healthy subjects (Wright et al., 2000). In longitudinal studies, patient ventricular volume enlarged progressively, with a rate of increase of 3.7% per year in schizophrenia patients (Ho et al., 2003). Enlarged ventricles were mostly observed in patients who suffered from chronic schizophrenia (Haijma et al., 2013; Kuo et al., 2019). As grey matter volumes were shown to decrease in schizophrenia, the enlargement of the ventricular areas was observed with accompanied by general reductions of grey matter volumes in patients with schizophrenia (Andreasen et al., 1994). With increased volume of ventricles, the cortical volume tended to decrease with frontal and temporal grey matter reduction (Horga et al., 2011). Unlike grey matter reductions which could be detected in the first episode of schizophrenia, the enlargement of ventricles was difficult to detect in the first episode (Narr et al., 2006), which could be supported by the suggestion that enlarged ventricles could only be detected in chronic patients.

Enlargement of ventricular regions was suggested to correlate with higher scores on the Brief Psychiatric Rating Scale (BPRS) - negative symptoms, including the symptoms of blunted affect, emotional withdrawal and motor retardation (Mathalon et al., 2001; Saijo et al., 2001). However, ventricular enlargement was also reported to be associated with positive symptoms along with the decline of grey matter volumes (Mathalon et al., 2001). As ventricular enlargement developed progressively in schizophrenia patients, the enlarged ventricular volume was also shown to be correlated with worsening of negative symptoms, further suggesting that changes of symptoms in schizophrenic subjects were linked to progressively increased ventricular regions over time (Saijo et al., 2008).

1.3.3.4. Sex differences of brain abnormalities in schizophrenia

As males and females with schizophrenia showed a slightly different incidence rate, onset time and symptom profile, the sex differences of schizophrenia symptoms were suggested to be attributed to different brain structure in males and females (Goldstein et al., 2001).

Converging studies illustrated the sex differences of brain anatomical disruptions in schizophrenia, suggesting that male patients presented with more severe brain structural abnormalities than females, including smaller volumes of frontal lobes, temporal gyrus and medial temporal lobe, and larger ventricular spaces (Andreasen et al.,1994; Bryant et al., 1999). Enlarged ventricular volumes with decreased frontal cortex volumes were found to be most obvious in male patients, while in female patients, less ventricular enlargement was reported (Andreasen et al.,1994). Although a reduction of several temporal regions was detected in both male and female patients, a smaller left temporal cortex was only detected only in males (Bryant et al., 1999). In a schizophrenia longitudinal study, the volume of ventricles increased more dramatically in male patients compared to females (Narr et al., 2001).

Apart from the sex differences of morphology abnormalities, regional functions were also suggested to be different in males and females. Several functional MRI studies demonstrated

that male patients presented greater regional brain activities than female patients after exposure to negative stimuli, the intense activities were observed in the regions which were found to be abnormal in schizophrenia, such as temporal cortex, cingulate cortex and cerebellum (Mendrek et al., 2007). During emotional processing, females diagnosed with schizophrenia showed more intense activity in limbic areas compared to male patients, including anterior cingulate cortex and thalamus, which were correlated with emotional processing (Wager et al., 2003). This was consistent with the symptom exhibition that schizophrenic female patients presented with more emotional deficits, with more depressive or anxious mood.

In addition to neuroanatomy sex differences, limited studies investigated sex differences in neurotransmitter systems potentially involved in schizophrenia, in either human subjects or animal models.

Compared to healthy subjects, in the anterior cingulate cortex (ACC), the expression of $GABA_A$ receptors was decreased in male patients with schizophrenia, while in female patients, the $GABA_A$ receptors tended to be increased relative to controls (Bristow et al., 2015). *GAD67* expression is generally decreased in schizophrenia subjects (Akbarian et al., 1995; Volk et al., 2000), however, Bristow et al. (2015) reported an increased expression of *GAD1* in ACC in female schizophrenia patients. Additionally, the expression of GABAergic neurons showed sex differences, in healthy rat PFC, male rats expressed higher numbers of Pv-expressing GABAergic interneurons than females (Basta-Kaim et al., 2015; Leussis et al., 2012); and healthy female rats expressed higher Gad67 expression in PFC than males (Basta-Kaim et al., 2015). In terms of glutamate transmission, in healthy rat and human PFC, males were shown to release higher levels of glutamate compared to females (Pena-Bravo et al. 2019; O'Gorman et al., 2011). The subunits of NMDARs also showed sex-based expression, for example, the $GluN_{2A}$ subunit showed higher expression in female PFC compared to male PFC; as $GluN_{2A}$-containing receptors have faster kinetics, females tended to show more rapid activation, while males showed much slower and prolonged activation of NMDARs (Wang, et al., 2015). In schizophrenia subjects, women showed higher NMDAR binding capacity than men (Nudmamud-Thanoi and Reynolds, 2004).

The dopaminergic system also showed sex differences. In healthy rats, females showed higher concentrations of D1 receptor in cortex and striatum than males (Orendain-Jaime et al., 2016); and in healthy human subjects, women showed higher D2 receptor levels than males in thalamus or frontal and temporal cortex (Kaasinen et al., 2001). Inconsistent results related to sex differences of serotonin were reported. Some studies suggested no sex differences of serotonergic systems (Arato et al., 1991; Dean et al., 1995), however, greater synthesis of serotonin in males than females throughout the brain were also suggested (Nishizawa et al., 1997).

To conclude, several neurological alterations were suggested to be related to schizophrenia, including abnormal neural or cellular processes, such as disrupted gamma, beta and theta oscillations, and the disrupted oscillations were associated with abnormal brain anatomy, such as reduced volumes of temporal or frontal cortex accompanied with reduced grey matter volumes and enlarged ventricular spaces, which were suggested as a specific marker and clinical features of schizophrenia. As male and female patients exhibited different onset time or symptoms of schizophrenia, it is possible that the neurobiology of schizophrenia might also show gender differences. Male patients showed more severe brain anatomy abnormalities with more reduction of grey matter and more ventricular enlargement, showed more responses to negative stimuli and reduced GABAergic receptors after diagnosis with schizophrenia; while female patients expressed more intense activities in limbic areas with emotional stimuli and presented increased

GABAergic receptors and more dopaminergic receptors after diagnosis with schizophrenia. These sex differences in neurobiological abnormalities might be linked to the differences in schizophrenic symptoms.

1.3.4. PNN and GABAergic related neuronal abnormalities schizophrenia

In addition to deficits in cellular processes, synaptic formation, neurotransmission and brain anatomy, another neurobiological systems had been suggested to involve in the pathology of schizophrenia, which is PNN and the neurons (mainly Pv-expressing GABAergic neurons) it covered.

Consistent evidence suggests that the schizophrenia involves disrupted synaptic contacts. Post-mortem studies in schizophrenia patients found reduced cortical synaptic and dendritic spine densities (Huttenlocher and Dabholkar, 1997; Huttenlocher, 1979). The disrupted synaptic connection related to schizophrenia could be related to the neural oscillations or neural transmission abnormalities, especially the gamma band oscillations (Alekseichuk et al., 2016; Schirner et al., 2018; Spencer et al., 2009) which could be regulated by the inhibitory neural networks containing Pv-expressing GABAergic neurons (Uhlhaas and Singer, 2010; Hashimoto et al., 2008). Additionally, Pv-expressing interneurons are a regulator of synaptic plasticity to maintain neural functional and structural capacities (Hensch, 2005; Donato et al., 2013). Thus, the damaged Pv-expressing GABAergic interneurons with abnormal gamma oscillations might contribute to the mechanisms of schizophrenia. As PNNs mainly covered GABAergic interneurons (Cabungcal et al., 2013; Morishita et al., 2015), especially Pv-expressing interneurons, and PNNs were demonstrated to play a critical role in synaptic plasticity, which is disrupted in schizophrenia patients (Pizzorusso et al., 2002; McRae et al., 2007; McRae and Porter, 2012), damaged PNNs could contribute to the underlying mechanisms of schizophrenia.

1.3.4.1. Overall disrupted expression of PNN and Pv-expressing neurons in schizophrenia

Abnormal PNN expression is observed in schizophrenia patients. Consistent evidence demonstrated a reduction of PNN expression in schizophrenia subjects. For example, a study conducted with post-mortem tissue found decreased densities of PNN in layers 3/5 of PFC by 70% and 76%, respectively, but no alterations of PNNs were found in visual cortex (Mauney et al., 2013). A post-mortem study further reported decreased density of PNNs in ECx and amygdala (Pantazopoulos er al., 2014). Additionally, in the genetic mouse model of schizophrenia with Disruption in Schizophrenia (DISC1) mutation, similar reductions of PNN density and protein expression were observed in layer2/3 and layer 4/5 of PFC in DISC1 mutation mice (Sultana et al., 2021). Although the DISC1 mutation is associated with various psychiatric disorders, such as schizophrenia, schizoaffective disorder and bipolar disorder (Hodgkinson et al., 2004), Mauney et al (2013) reported decreased PNN density only in schizophrenia subjects rather than subjects with bipolar disorder, suggesting that PNN reduction was specific to schizophrenia, which was consistent with the findings from Pantazopoulos et al (2014) that the abnormalities of PNN expression were specific to schizophrenia. However, in another study, the density of PNNs remained unchanged in schizophrenia subjects, while reduced intensity of WFA-labelled PNNs was observed in dorsal lateral PFC (Enwright et al., 2016). Furthermore, after enzymatic removal of PNNs in the mouse hippocampus region, increased dopamine neurotransmission and response to amphetamine were detected, which was

consistent with the clinical features presented by schizophrenia patients after exposure to psychomotor stimulants, and with the over-released dopamine transmission in schizophrenia (Shah and Lodge, 2013). Hence, these lines of evidence illustrated that disrupted PNN expression could be associated with schizophrenia in various brain regions, including PFC, hippocampus, amygdala and ECx, but no changes of PNNs expression were detected in visual cortex. The deficits of PNNs expression might also be associated with the underlying cellular mechanism of schizophrenia, and detailed explanations are presented in section 1.4.3.

Apart from PNN expression, Pv-containing neurons are also abnormal in schizophrenia. Fewer Pv-expressing neurons, and colocalisation of PNNs and Pv-expressing neurons were found in thalamic reticular nucleus in patients with schizophrenia compared to healthy subjects (Steullet et al., 2017). In another schizophrenia post-mortem study, reduced Pv-expressing neurons were found in several subregions of ECx; the size of Pv-expressing neurons soma were decreased in ECx1 region (Pantazopoulos et al., 2007). The mRNA levels of various GABA interneuron genes was reduced by roughly 40% in schizophrenia subjects (Purves-Tyson et al., 2021). In addition, in schizophrenia animal models treated with methylazoxymethanol acetate (MAM), reduced density of Pv-expressing interneurons was found in medial PFC and ventral subiculum of hippocampus, accompanied by abnormal behaviours in fear conditioning and decreased gamma and theta oscillations in medial PFC and ventral hippocampus, suggesting decreased Pv-expressing neurons were correlated with abnormal cognitive behaviours in animal model for schizophrenia (Lodge et al., 2009). Consistent reductions were also reported in schizophrenia animal models, for example, reduced Pv-expressing neurons expression were observed in PFC in MAM treated mice (Moore et al., 2006); decreased Pv-containing neurons were found in hippocampus in MAM administrated mice accompanied with positive schizophrenic features presented by increased locomotor activities (Penschuck et al., 2006). Moreover, schizophrenia patients also expressed lower levels of mRNA of Pv-containing neurons levels in layer 3 and 5 of PFC (Hashimoto et al., 2003), which was consistent with the findings in animal models (Moore et al., 2006). Similar reduction of Pv-expressing interneurons was reported in a meta-analysis study, demonstrating a significant decrease in Pv-expressing neurons in patients with schizophrenia, however, the mRNA expression of Pv-expressing neurons was not reported (Kaar et al., 2019).

Thus, the decreased expression of PNNs and Pv-containing neurons were found in various brain regions in schizophrenia patients and animal models, accompanied with disrupted neural oscillations, such as, synchronised theta and gamma oscillations, and impaired cognitive behaviours, such as, abnormal fear conditioning behaviours and locomotor activities, which suggested a role for Pv-containing interneurons in cognitive functions and clinical features in schizophrenia by regulating theta and gamma oscillations.

In addition to altered expression of Pv-expressing GABAergic interneurons, pyramidal neurons were also demonstrated to be disturbed in schizophrenia. As the lower dendritic spine densities and altered firing rates around pyramidal cells were reported to contribute to the neurobiology of schizophrenia (Hashimoto et al., 2008; Uhlhaas and Singer, 2010), expression of pyramidal neurons abnormalities might be involved in the underlying mechanism of schizophrenia. For example, reduced dendritic spine densities of pyramidal neurons were detected in layer 3 of PFC in schizophrenia patients (Glantz and Lewis, 2000); decreased soma size of pyramidal neurons was also observed in PFC in schizophrenia patients (Pierri et al., 2001). As noted in section 1.2, PNNs not only covered GABAergic interneurons, but also pyramidal neurons, and stabilised and maintained synaptic activities of pyramidal neurons (Celio, 1993; Brückner et al., 2003; Aplar et

al., 2006). Thus, in schizophrenia patients, the loss of PNNs around pyramidal neurons might also contribute to the underlying mechanisms of schizophrenia.

As PNNs provide several functions in CNS, abnormal expression of PNNs could lead to several cellular dysfunctions, including dysregulated gamma oscillations and disrupted synaptic plasticity, which might relate to the similar cellular dysfunctions in schizophrenia. For example, PNNs and Pv-expressing neurons contribute to maintain gamma oscillations and cortical neuronal synchrony, and enzymically removed PNNs around Pv neurons rendered decreased gamma oscillation synchrony (Cabungcal et al., 2013; Morishita et al., 2015; Wulff et al., 2009). Abnormal gamma oscillations were also observed in schizophrenia patients and suggested to correlate to deficits in executive functions or information processing (Cho et al, 2006; Haenschel et al., 2009; Guan et al., 2022; Uhlhaas and Singer, 2010). In this case, disturbed PNN formation and Pv neuron expression in schizophrenia might associate with abnormalities in gamma oscillations synchrony. Apart from neural oscillations, PNN functions in synaptic plasticity and pruning, promoting dendrite growth and regulating dendritic spines, disturbances synaptic activities and dendritic spines were detected with PNNs removal (Tran et al., 2009; Shelly et al., 2011). Similar disrupted synaptic pruning and dendritic spines were also observed in schizophrenia individuals (Bitanihirwe et al., 2016). In this regard, disturbed PNN synaptic functions might be related to schizophrenia. Although evidence suggested the dysfunctions of PNN and Pv neurons in schizophrenia, limited studies have directly investigated the abnormal functions of PNNs and Pv neurons in schizophrenia patients.

1.3.4.2. Abnormal expression of specific PNNs components

The overall expression of PNNs was decreased in various brain regions in patients with schizophrenia, including PFC, amygdala, hippocampus and ECx, with reduced density and intensity of the WFA-labelling (Mauney et al., 2013; Hodgkinson et al., 2004; Enwright et al., 2016); and the expression of PNN-covered neurons, particularly, the Pv-expressing GABAergic interneurons, were also decreased in schizophrenia subjects, with reduced mRNA levels, cell density and staining intensity along with PNNs (Steullet et al., 2017; Lodge et al., 2009; Enwright et al., 2016; Hashimoto et al., 2013). Disrupted pyramidal neurons, potentially covered by PNNs, were also observed in schizophrenia (Glantz and Lewis, 2000; Pierri et al., 2001).

As general PNN expression is affected in schizophrenia, the components which form the PNNs structure and play a role in stabilisation and maintenance of the structure are also abnormal in schizophrenia.

1.3.4.2.1. Abnormal CSPG expression in schizophrenia

Abnormal expression of specific molecules in PNNs has been shown in schizophrenia subjects. For example, in the olfactory epithelium (OE), the density of CSPGs in olfactory receptor neurons (ORN) was shown to be reduced in schizophrenia patients (Pantazopoulos et al., 2013). Disturbed expression of specific CSPG components was also reported in various studies. In a postmortem study, glial-related CSPG abnormalities in amygdala and ECx were found to be associated with schizophrenia, accompanied by reduced densities of PNNs; however, increased mRNA expression of all CSPG components was observed in schizophrenia patients compared to healthy individuals, including *ACAN*, *BCAN*, *NCAN*, *VCAN* and *PRPRZ1* (Pantazopoulos et al., 2010). As a major component in CSPGs, *ACAN* expression was also suggested to be disrupted in schizophrenia patients, for instance, *ACAN* immunoreactivity labelled by Cat-301 in glial cells decreased in amygdala of schizophrenia subjects, while on the contrary, the mRNA expression

of *ACAN* increased in amygdala of schizophrenia patients (Pantazopoulos et al., 2015). Lower intensity of *ACAN*-labelled PNNs surrounding Pv-expressing interneurons was also detected in dorsal lateral PFC of schizophrenia subjects (Enwright et al., 2016). Moreover, *PTPRZ1* gene expression was upregulated in amygdala and PFC of schizophrenia patients, and reproducing the increased expression in mice was associated with cellular, behavioural and cognitive features in schizophrenia, including neurotransmission alterations such as increased dopaminergic signalling, and suppressed GABAergic signalling, hyper-locomotor activities and working memory impairments (Takahashi et al., 2011). In addition, increased gene expression of *BCAN* was also demonstrated in schizophrenia patients (Pantazopoulos et al., 2021). However, inconsistent CSPG gene expression was reported in pyramidal neurons of schizophrenia subjects, with reduced *ACAN* and *VCAN* mRNA levels in the cerebral cortex of schizophrenia patients (Pietersen et al., 2014). Furthermore, a GWAS study illustrated a relationship of *NCAN* genetic variants and schizophrenia risk (Muhleisen et al., 2012; Trubetskoy et al., 2020), and in schizophrenia patients, the expression of *NCAN* was reported to be decreased (Pantazopoulos et al., 2021). This evidence suggests that despite the reduction of overall CSPG and PNN expression observed in various brain regions, such as ECx and amygdala, the alterations of immunoreactivity of CSPG components in schizophrenia is not always parallel with the changes of mRNA expression: the alterations of specific components is dependent on the neurons where they are located. For instance, in glial cells, although decreased density of PNNs were detected, the mRNA levels of CSPG components were reported to be increased in schizophrenia subjects; while in pyramidal neurons, lower mRNA levels of *ACAN* and *VCAN* were detected in schizophrenia patients.

1.3.4.2.2. Abnormal hyaluronan synthesis and link proteins in schizophrenia

Limited studies assessed expression of *HAS* genes and link protein genes in schizophrenia patients. Pantazopoulos et al (2021) revealed alterations of PNN components in various brain regions, including amygdala, caudate, hippocampus and putamen, in post-mortem tissue from schizophrenia patients. *HAS1* gene expression decreased in caudate and hippocampus regions, but increased in putamen, while *HAS2* only decreased in hippocampus but increased in caudate and putamen. Additionally, the gene expression of the link protein, *HAPLN1,* was also downregulated in the pyramidal neurons in temporal cortex of schizophrenia patients (Pietersen, et al., 2014). Hence, the altered gene expression of *HAS* and *HAPLNs* components seems to vary in different brain regions in schizophrenia, with both increase and decreased tendency of expression of *HAS1*, *HAS2* and *HAPLN1.*

Taken together, the expression of many PNN components, including CSPGs, *Has* and *Hapln* molecules, are altered in schizophrenia patients (Table 1.5). However, not all PNN components alterations have been investigated in schizophrenia, such as *TNR* and *HAS3,* whose deficits were demonstrated to affect PNNs formation. Therefore, whether other PNNs components are disturbed in schizophrenia subjects remains to be discovered.

PNN/*PV*-expressing neurons	Expression of PNN/Pv-expressing neurons in schizophrenia	Citation
General PNN expression	↓ density and intensity	Mauney et al. (2013); Pantazopoulos et al. (2014); Sultana et al. (2021); Enwright et al. (2016).
ACAN	↓ intensity, ↑ mRNA levels	Pantazopoulos et al. (2010); Pantazopoulos et al. (2015); Enwright et al. (2016); Pietersen et al. (2014).
BCAN	↑ mRNA levels	Pantazopoulos et al. (2010); Pantazopoulos et al. (2021).
NCAN	↑ mRNA levels	Pantazopoulos et al. (2010); Muhleisen et al. (2012); Trubetskoy et al. (2020).
VCAN	↑ mRNA levels	Pantazopoulos et al. (2010); Pietersen et al. (2014).
Phcan / PTPRZ1	↑ mRNA levels	Takahashi et al. (2011); Pantazopoulos et al. (2010).
HAS1	↓ mRNA levels in hippocampus, ↑ in putamen	Pantazopoulos et al. (2021); Pietersen, et al. (2014).
HAS2	↓ mRNA levels in hippocampus and putamen	Pantazopoulos et al. (2021); Pietersen, et al. (2014).
HAS3	Not known	
HAPLNs	↓ mRNA expression (*HAPLN1*)	Pietersen, et al. (2014).
TnR	Not known	
PV-expressing neurons	↓ mRNA levels, density, intensity and size of neurons.	Steullet et al. (2017); Pantazopoulos et al. (2007); Purves-Tyson et al. (2021); Lodge et al. (2009); Moore et al. (2006); Hashimoto et al. (2003).

Table 1.5: summary of altered expression of PNNs components in schizophrenia patients

1.3.4.3. *GAD/Gad* expression and functional abnormalities in schizophrenia

1.3.4.3.1. Altered *GAD/Gad* expression in schizophrenia

As noted in section 1.3, several lines of evidence illustrated abnormalities of inhibitory GABAergic neurotransmission networks in schizophrenia (Sohal et al., 2009; Lodge et a., 2009; Cunningham et al., 2006). The regulation of GABAergic neurotransmission is partly attributed to the glutamate decarboxylase (*Gad*) synthesis enzymes which synthesise GABA from glutamate (Akbarian and Huang, 2006). *Gad* has 2 isoforms, which are *Gad1/Gad67* (for 67 KDa) and *Gad2/Gad65* (for 65KDa), located on chromosome 2 and 10, respectively (Bu et al., 1992). *Gad1*/Gad67 and *Gad2/*Gad65 play different roles in terms of GABA neurotransmission. For example, *Gad67* is responsible for basal GABA synthesis, and can be present in non-vesicular cellular spaces, whereas *Gad65* is responsible for activity-dependent changes in GABA

synthesis and acts purely in relation to vesicular release (Kaufman et al., 1991; Tian et al., 1999). Patients diagnosed with schizophrenia were generally shown to have dysregulated *GAD67* and *GAD65* expression in various brain regions, including PFC, cerebral cortex, hippocampus and ACC (Table 1.6) (Akbarian et al., 1995; Dracheva et al., 2004; Woo et al., 2004).

GAD67 expression is more robustly found to be altered in schizophrenia. The initial finding of reduced *Gad67* expression in schizophrenia patients was from Akbarian et al. (1995), suggesting decreased *GAD67* mRNA levels in PFC of schizophrenia patients. Growing consistent results were reported in later studies, for example, decreased *GAD67* mRNA levels in layer3 and layer 5 of PFC specifically in Pv-expressing interneurons (Volk et al., 2000; Hashimoto et al., 2003; Curley et al., 2011), and reductions of *GAD67* were also observed in layer 1 and layer 2 of PFC in schizophrenia subjects (Veldic et al., 2005). Apart from PFC, decreased expression of *GAD67* in schizophrenia patients were also detected in the temporal cortex, with the protein levels of GAD67 decreased by 70% in schizophrenia patients (Impagnatiello et al., 1998); and in ACC, reduced density of *GAD67*-positive neurons was observed in cortical layer 1 and layer 5 of schizophrenia subjects (Woo et al., 2004). Moreover, in midbrain, lower mRNA levels for *GAD67* were also observed in schizophrenia subjects compared to healthy controls, with approximately 40% reduction (Purves-Tyson et al., 2021). However, in hippocampus, decreased density of *GAD67*-positive neurons was found in patients with bipolar disorder rather than schizophrenia (Heckers et al., 2002); conversely, a lower density of *GAD* immunoreactivity was reported, particularly in the CA1 region of the hippocampus of schizophrenia patients (Steiner et al., 2016). Furthermore, genetic studies illustrated that mutations or sequence variations in the *GAD1* gene are associated with risk of schizophrenia, the mutations causing decreased *GAD67* activity (Magri et al., 2018; Du et al., 2008). However, the GWAS study revealed no *GAD* genes correlated with schizophrenia (Ripke et al., 2014; Trubetskoy et al., 2022). Hence, the expression of *GAD67* was consistently decreased in PFC, ACC and temporal cortex; however, inconsistent alterations of *GAD67* in schizophrenia were reported in hippocampus, with both unaltered or decreased tendency, and any genetic association is probably only relevant in rare cases.

It has been demonstrated by various post-mortem studies that reduced *GAD67* density, mRNA or protein levels are present in several brain regions of schizophrenia subjects, and the alterations of *GAD65* expression were also investigated. However, the expression of *GAD65* was not robustly altered in schizophrenia subjects. For instance, in PFC and cerebellum, the protein expression of *GAD65* was similar between schizophrenia patients and healthy subjects (Guidotti et al., 2000). On the contrary, in primary auditory cortex, the protein levels and the intensity of *GAD65* immunostaining were reported to be reduced by 40% in schizophrenia patients (Moyer et al., 2012). Similar reductions of protein and mRNA levels were also found in hippocampus (Hecker et al., 2002), although increased GAD65 mRNA was reported in PFC and occipital cortex in one study (Dracheva et al., 2004).

Overall, it could be concluded that the general expression of *GAD67* is decreased in various brain regions of schizophrenia patients, such as PFC, hippocampus and ACC. Although most studies focused on the altered expression of *GAD67*, *GAD65* expression was also investigated in schizophrenia subjects, but with less consistent results (Table 1.6).

***GAD67* in various brain regions**	**Expression in schizophrenia**	**Citation**
PFC	↓ mRNA levels	Akbarian et al. (1995); Volk et al. (2000); Hashimoto et al. (2003); Curley et al. (2011); Veldic et al. (2005).
Temporal cortex	↓ protein expression	Impagnatiello et al. (1998)
ACC	↓ density	Woo et al. (2004)
Hippocampus	↓ density or no alterations	Heckers et al. (2002); Steiner et al. (2016)
Mid brain	↓ mRNA levels	Purves-Tyson et al. (2021)
GAD65 in various brain regions	**Expression in schizophrenia**	**Citation**
PFC	— protein expression	Guidotti et al. (2000)
Auditory cortex	↓ protein levels and intensity	Moyer et al. (2012)
Occipital cortex	↑ mRNA levels	Dracheva et al. (2004)
Hippocampus	↓ mRNA and protein levels; ↓density	Hecker et al. (2002)
Cerebellum	— protein expression	Guidotti et al. (2000)
Mid brain	—	Purves-Tyson et al. (2021)

Table 1.6: summary of *GAD67/GAD65* expression in schizophrenia patients

1.3.4.3.2. Functional deficits of *GAD/Gad* in schizophrenia

While alterations of *GAD67*, and less clearly *GAD65* are observed in schizophrenia subjects, limited studies investigated the association between underlying neurobiology of schizophrenia and dysfunctional *GAD67/65.* In *Gad1* KO animal models, several effects were observed which could also be found in schizophrenia patients. For example, *Gad1* KO mice not only showed a decreased number of Pv-expressing interneurons and reduced GABA neurotransmission (Uchida et al., 2014), but also exhibited impaired social activities, such as social withdrawal related to negative symptoms of schizophrenia (Sandu et al., 2014). Consistent negative schizophrenia-like symptoms have been found in *Gad67* deficient mice, with disrupted social interactions and increased depressive-like behaviours, such as, less time spent in swimming tests (Nullmeier et al., 2020). Increased locomotor activities were also detected in *Gad67* deficient mice, which was in line with the positive symptoms of schizophrenia (Nullmeier et al., 2020). Furthermore, upregulated immunoreactivity of tyrosine hydroxylase, used to identify the dopaminergic fibres, was observed in hippocampal CA1 area of Gad67 deficient mice, indicating increased dopaminergic neurotransmission in the hippocampus, accompanied by a reduction of Gad67*,* which is consistent with the underlying neurotransmission deficits in schizophrenia (Table 1.8) (Nullmeier et al., 2020).

In *Gad1* KO rats, similar schizophrenia-like behaviours were detected. For instance, in *Gad1 KO* mice, schizophrenia-like positive and negative symptoms were both observed, such as hypoactivities in a novel environment and reduced speed and distance of locomotor activities; and the altered behaviours were accompanied by reduced GABA neurotransmission (Fujihara et al.,2020). Moreover, cognitive deficits were presented with abnormal GABAergic

neurotransmissions, such as, spatial memory deficits, impaired fear learning and fear memory (Fujihara et al., 2020; Fujihara et al., 2021b).

Therefore, *Gad1/67* KO or deficient mice or rats showed a variety of behavioural changes, which were related to the positive or negative symptoms of schizophrenia accompanied with increased dopaminergic and decreased GABAergic neurotransmissions. Hence *Gad1/67* disruption with reduced GABA neurotransmission might contribute to the underlying dysfunctions of amygdala and medial PFC in schizophrenia (Table 1.7).

Abnormal neurobiology in schizophrenia	**Functional deficits of *GAD67/65* contributed to neurobiology of schizophrenia**	**Citation**
GABAergic neural transmission	Decreased GABAergic neural transmission in Gad67 deficient mice	Uchida et al. (2014); Fujihara et al. (2020).
Dopaminergic neural transmission	Increased Dopaminergic neural transmission in Gad67 deficient mice	Nullmeier et al. (2020)
Gamma oscillations	Less Gad67 detected in Pv-expressing interneurons	Uchida et al. (2014)

Table 1.7: disrupted *GAD67/65* functions related to neurobiology of schizophrenia

1.3.5. Animal models of schizophrenia

To study the effectiveness of different drugs to treat schizophrenia symptoms, and further clarify the underlying neurobiology and the involvement of PNNs and Pv neurons in schizophrenia, animal models need to be established. The animal models of schizophrenia are classified into 4 categories, including developmental model with environmental stimulations, drug-induced or pharmacological models to regulate the changes of neuronal activities, brain lesion models with neonatal lesions in different brain regions, and genetic models with mutations or KO of some schizophrenia-related genetic variants.

Previous section (1.3.2) mentioned that environmental factors, such as external or prenatal stress and prenatal infections, could increase the risk of schizophrenia, and individuals who experienced early environmental or prenatal stressors are more likely to develop schizophrenia in later life (Guo et al., 2010; Selten et al., 1999; Khashan et al., 2008; Varese et al., 2012; Janssen et al., 2004; Bentall et al., 2014). Thus, the animal models of schizophrenia generally used manipulation of environment or drug administration during the prenatal period to produce the alterations of neuronal development and replicate the symptoms of schizophrenia. For example, prenatal drug administration with methylazoxymethanol (MAM) could selectively affect brain development in the offspring, such as reduced cerebellum and hippocampus volume, or disruption of striatal dopaminergic neurons (Balduini et al., 1991; moore et al., 2006; Lodge et al., 2009). In addition, animals that experienced the external stressors at early stages also showed abnormal neural development. Thus, social deprivation, such as post-weaning social isolation in rats or mice could induce behavioural abnormalities, including locomotor hyperactivity, deficits in sensorimotor gating ability in pre-pulse inhibition tests (PPI) test, cognitive impairments, and increased anxiety and aggression states, which was in line with the behavioural phenotypes of schizophrenia and could also be reversed by antipsychotic drugs (Marsden et al., 2011; Fone et al., 2008; Weiss et al., 2004).

As disrupted dopamine transmission was the primary hypothesis and theory of the underlying neurobiology of schizophrenia, the predominantly used animal models with pharmacological administration were targeted on dopamine systems. In rodents, amphetamine was the drug used to model schizophrenia phenotypes, which could induce several behavioural and neuronal features of schizophrenia, such as deficits in PPI, impaired spatial working memory, hyperactivities in PFC and increased locomotor activities (Featherstone et al., 2008; Fletcher et al., 2005). PCP administration could also model schizophrenia based on the glutamatergic dysregulation hypothesis of schizophrenia. PCP or ketamine induction with blockage of glutamate receptors in humans induced positive symptoms of schizophrenia, such as delusions and hallucinations (Krystal et al., 1994). In rodents, induction of PCP could lead to locomotor hyperactivities, reduced social interactions, cognitive impairments and increased response in PPI tests (Kalinichev et al., 2007; Egerton et al., 2005; Sams-Dodd, 1995). Clozapine, one of the anti-psychotic drugs, could attenuate the schizophrenia behavioural phenotypes. Thus, with amphetamine and PCP induction, psychotic or schizophrenia-like features could be modelled by regulating dopamine and glutamate systems.

Apart from environmental or prenatal factor exposure and regulating neurotransmitter systems, brain lesions could also be used to model schizophrenia. For example, lesions in ventral hippocampus in rodents with ibotenic acid (an excitotoxin) injection resulted in behavioural abnormalities which were consistent with the schizophrenia phenotypes, including reduced social interaction and increased aggressive behaviours, and cognitive impairments, including in spatial working memory and learning ability (Tseng et al., 2009; Wood et al., 1997). The lesions in ventral hippocampus also increased dopamine activity, and reduced the length and density of dendritic spines and synapses (Brake et al., 1999), which was in line with the neuronal features in schizophrenia.

Furthermore, as several alterations of genetic variants are demonstrated to be associated with the increased risk of schizophrenia, thus, the manipulation of these genetic variants could be a model of schizophrenia. For example, one of the primary genes implicated in the underlying neurobiology of schizophrenia is *disrupted-in-schizophrenia 1* (*DISC1*), which plays a critical role in regulating synaptogenesis, synaptic plasticity and neuronal migration (Jarro-Peled, et al., 2009). *DISC1* transgenic or mutation rodents presented with enlarged ventricles and reduced brain volumes (Jarro-Peled, et al., 2010). In behavioural aspects, the *DISC1* mutation mice also showed deficits in PPI tests, with disorganised dendritic complexity and reduced dendritic densities (Li et al., 2007; Sultana, et al., 2021). The abnormal neuronal and behavioural features could be reversed by antipsychotic drugs, such as clozapine (Clapcote et al., 2007). Additionally, single copy-number variants (CNVs) also produce powerful genetic risk, and 16p11.2 duplications are of specific interest, as the carriers with high proportion of the 16p11.2 duplications are 14 to 28 times more likely to develop schizophrenia (Zhang et al., 2009). Thus, specific manipulation of CNVs could also be used as a schizophrenia model (Willis, 2022; Kwon et al., 2021).

Finally, in addition to modelling aspects of schizophrenia in animals with single drug administration, environmental stimulation or genetic manipulations, a combination of the underlying neurobiology alterations or genetic variants and environmental stimulations was suggested to induce the development of schizophrenia. These models are called dual-hit models. For example, schizophrenia phenotypes can be produced by disrupting glutamatergic transmission using PCP, also following post-weaning social isolation (Cale et al., 2024). In addition, the prenatal stimulations and genetic mutations were also used to conduct a dual hit model for schizophrenia, where the *DISC1* heterozygous mice were exposed to the MIA or neonatal immune activation (Lipina et al., 2013; Ibi et al., 2010). With the combination of

developmental or genetic risk factors and environmental stressors, a more enhanced and robust model for schizophrenia could be established compared to other models with a single manipulation.

Therefore, animal models for schizophrenia are critical and a necessary way to study the alterations in the underlying neurobiology of schizophrenia, and are widely used in studies to investigate the specific changes of targeted neuronal activities or expression, such as PNN or Pv expression.

1.3.6. Therapies for schizophrenia

Patients diagnosed with schizophrenia exhibit positive, negative and additional cognitive features, which make the patients find it difficult to cope with day-to-day living, such as social communication and holding down a job. In this case, medical treatment and psychological care are critical for patients to try to manage the schizophrenia symptoms. Antipsychotic medication therapy is the first choice for intervention, and it is more effective for treating positive symptoms. However, the positive symptoms of schizophrenia tend to relapse, with 17% to 78% chance to relapse after the first episode and 16% to 62% after later episodes of schizophrenia (AlAqeel and Margolese, 2012). In addition, after recovery from the first episode, patients were reported to relapse within the following 5 years, and approximately half of the patients who recovered from schizophrenia showed at least one remission of schizophrenic symptoms (Moilanen et al., 2013). Stopping antipsychotic medication therapy increased the risk of remission by 5 fold (Robinson et al., 1999). Thus, use of antipsychotic drugs alone is not sufficient to treat schizophrenia, and additional non-medication treatment, such as psychological therapy or care, can be beneficial in some schizophrenia patients.

1.3.6.1. Pharmacological treatment

The drugs used for schizophrenia therapy are known as antipsychotic drugs. Based on the mechanisms of antipsychotic actions, the drugs can be classified into 3 groups, which are first generation, second generation and third generation antipsychotics, targeted on different mechanisms and hypothesis of schizophrenia.

First-generation antipsychotics (also referred to as typical antipsychotics) were developed in the 1940s and 1950s, initially by Delay and Deniker (1952). The drugs can reduce the positive symptoms of schizophrenia, such as hallucinations, delusions and disorganised thinking or speech. The mechanism of the first-generation antipsychotics was based on the dopamine hypothesis of schizophrenia and targets the dopaminergic system.

As noted in section 1.3.2 and 1.3.3, the dopaminergic system is highly involved in the neurobiology of schizophrenia, suggesting over-release of dopamine and upregulated occupation of D2 receptors shown to be associated with positive symptoms in schizophrenia (Abi-Dargham et al., 1998). In this case, by blocking the D2 receptors, the neurotransmission of dopamine could be inhibited, which in turn reduces the positive symptoms in those patients who respond. Thus, to treat the positive symptoms, D2 receptor antagonists are used in schizophrenia. Several first-generation antipsychotic drugs have been developed as antagonists to D2 receptors, with core structures including phenothiazines, butyrophenones, dihydroindoles, and diphenylbutylpiperidines. The occupancy of D2 receptors is vital in the therapy of schizophrenia. It has been suggested that the antipsychotic effect of the drugs was effective with 65% to 72% occupancy of D2 receptors, but further occupancy by the first-generation of antipsychotic drugs might lead to an increased risk of extrapyramidal side effects (Kapur et al., 2000). Extrapyramidal

side effects can occur in patients with antipsychotic drug therapy, with symptoms of akathisia, akinesia and dyskinesia. Prolactin elevation can also occur, and all are caused by inhibition of D2 receptors (Souza and Hooten, 2023). To improve the limitations of first-generation antipsychotic drugs, second-generation drugs were developed.

Second-generation antipsychotic drugs (often referred to as atypical) were developed in 1980s, and included risperidone, olanzapine, quetiapine, ziprasidone, asenapine, lurasidone, iloperidone and clozapine. The mechanism of action of second antipsychotic drugs is similar to the first-generation antipsychotic drugs, that is inhibiting D2 receptors to reduce the over-release of dopamine and suppress the positive schizophrenia symptoms (Chokhawala and Stevens, 2023). In addition to inhibiting D2 receptors, second-generation drugs also target 5-HT_{1A} and 5-HT_{2A} receptors, amongst others (Chokhawala and Stevens, 2023). The serotonergic system was also suggested to be involved in the neurobiology of schizophrenia, with increased expression of 5-HT_{1A} receptors and decreased expression of 5-HT_{2A} receptors in PFC in patients with schizophrenia (Dean et al., 1999; Dean and Hayes, 1996; Cheah et al., 2017). With the combination of dopamine and serotonin hypothesis, the second-generation antipsychotic drugs can have additional effects on 5-HT receptors, in some cases acting as partial agonists of 5-HT_{1A} and antagonists of 5-HT_{2A} receptors (Willner et al., 2022). Fewer extrapyramidal side effects and less risk of remission of the symptoms were also reported with the treatment of second-generation antipsychotic drugs compared to the first-generation drugs (Csernansky and Schuchart, 2002; Leucht et al., 2003), although more previous evidence suggests that this is not the case (Naber and Lambert, 2009).

Although second-generation antipsychotic drugs may have improved on the limitations of first-generation drugs, various shortcomings have been suggested. For example, some of the drugs, such as, clozapine, could lead to unique side effects affecting immune systems, and increasing weight (Young et al., 2010; Rummel et al., 2010). Moreover, comparative studies also illustrated that no differences of effectiveness were found in schizophrenia patients after therapies with first- and second-generation drugs (Lieberman et al., 2005; Jones et al., 2006).

Following the second generation of antipsychotic drugs, the latest generation antipsychotic drugs have been developed, which are partial agonists of dopamine D2 or D3 receptors and of 5-HT receptors and are suggested to be the third generation of antipsychotic drugs (Lieberman et al., 2004). Unlike the full agonists, the partial agonists have lower intrinsic activity on particular receptors and could act as either agonists or antagonists based on the level of release of the endogenous neurotransmitters (Leiberman et al., 2004). For example, in schizophrenia, a partial D2 receptor agonist could function as an antagonist in an environment with over-released or hyperactivity of dopamine, while in a situation with hypoactivity of dopamine, the partial agonists on D2 receptors could function as an agonist (Leiberman et al., 2004). Aripiprazole, one of these partial agonists, has high affinity for dopamine D2 and D3 receptors and 5-HT_{1A} and 5-HT_{2A} receptors, occupying up to 90% of D2 receptors and a lesser effect on 5-HT receptors (Casey et al., 2017). Another partial agonist, cariprazine, is also a partial agonist of dopamine D2 or D3 receptors and 5-HT_{1A} receptors, and an antagonist at 5-HT_{2B} receptor (Laschizophrenialovschizophreniaky et al., 2021). Different from aripiprazole, though, cariprazine has greater affinity for D3 receptors, with relatively higher affinity for 5-HT_{1A} and lower affinity for 5-HT_{2A} receptors (Stahl et al., 2016). Thus, the mechanisms of the third-generation drugs are based on partial agonist activity on D2 or D3 receptors and 5-HT_{1A} receptors, and antagonism at 5-HT_{2A} receptors. Therapeutic effectiveness via activation of D3 receptors is uncertain, however, the animal studies suggested actions on D3 receptors are able to improve the cognitive, negative and depressive clinical features, with suppression of memory impairments and anti-depressant-like activities (Duman et al., 2012; Zimnisky et al., 2013). Thus, partial agonists could target the

treatment of positive or negative symptoms, and the additional cognitive impairments, although the clinical picture is not clear yet.

Despite 3 generations of antipsychotic drug therapies being effective in regulating positive, but not negative and cognitive symptoms, mainly occupying dopamine D2 or D3 receptors and 5-HT_{1A} and 5-HT_{2A} receptors; the side effects include extrapyramidal side effects, immune system deficits and weight gain. In addition, discontinuing the antipsychotic drugs therapies after recovery from the schizophrenic symptoms might result in the remission of schizophrenia in later years. The shortcomings of the pharmacological therapy of schizophrenia raised a suggestion of the non-pharmacological therapies, which could improve the ability of social communication and emotional regulation of schizophrenic patients. The list of the antipsychotic drugs and the risk of potential side effect were presented in Table 1.8.

Thus, the approved antipsychotic drugs treating schizophrenia act primarily as antagonists or partial agonists on dopamine receptors, and some also act as antagonists or partial agonists on 5-HT_{1A} or 5-HT_{2A} receptors. Among all antipsychotic drugs, the second or the newest generation drugs are predominantly used. However, these drugs are mostly effective on positive symptoms rather than negative or cognitive impairments, and some patients might be resistant or tolerate to the drugs, even after taking several different drugs, which might lead to the low efficiency of the treatment.

Apart from dopamine and 5-HT receptors, muscarinic acetylcholine receptors (mAChR) are also suggested to be involved in the pathophysiology of schizophrenia, a concept which is supported by the exacerbated cognitive impairments in schizophrenia after exposure to antagonists of mAChRs (Wagg et al., 2010; Yamamoto et al., 2011; Paul et al., 2022). In the past decades, agonists at mAChRs were reported to improve the cognitive impairments in both AD and schizophrenia (Bodick et al., 1997; Shekhar et al., 2008). One of these mAChR agonists, xanomeline, has been implicated in treatment of schizophrenia, producing an effect on cognitive impairments and diminishing the psychotic symptoms. However, xanomeline could lead to the gastrointestinal adverse effects (Shannon et al., 1994).

To avoid the side effects, trospium chloride, a peripherally-restricted muscarinic antagonist, was applied and combined to xanomeline, therefore, xanomeline–trospium (KarXT) has shown both efficacy and tolerability in recent trials, with less incidence of adverse effects than xinomiline alone. It has been demonstrated to be a safe and well tolerated drug in several clinical trials and approved in the US to treat schizophrenia recently (Correll et al., 2022; Breier et al., 2023; Dolgin, 2024). Thus, compared to other first or second-generation antipsychotic drugs, one main advantages of the KarXT compared to other antipsychotic drug is that fewer side effects were reported, and it could improve not only positive symptoms such as delusions or hallucinations, but could also improve cognitive functions in schizophrenia patients. The discovery and approvement of the KarXT could provide an alternative choice for the schizophrenia patients who showed no improvements after taking other anti-psychotic drugs or had more severe side effects.

Drugs	Weight gain	Extrapyramidal symptoms	Citations
First-generation (typical) antipsychotic drugs: work on dopamine receptors			
Chlorpromazine	Moderate risk	High risk	Kapur et al. (2000), Souza and Hooten (2023)
Fluphenazine	Low risk	High risk	
Haloperidol	Low risk	High risk	
Prochlorperazine	Low risk	High risk	
Thioridazine	Low risk	High risk	
Thiothixene	Low risk	High risk	
Second-generation (atypical) antipsychotic drugs: work on dopamine and serotonin receptors			
Asenapine	Low risk	Moderate risk	Chokhawala and Stevens (2023), Csernansky and Schuchart (2002); Leucht et al. (2003).
Clozapine	High risk	Low risk	
Iloperidone	Moderate risk	Low risk	
Lurasidone	Low risk	Low risk	
Olanzapine	High risk	Moderate risk	
Paliperidone	Moderate risk	Moderate risk	
Quetiapine	Moderate risk	Low risk	
Risperidone	Moderate risk	Moderate risk	
Ziprasidone	Low risk	Low risk	
Third-generation antipsychotic drugs: work as partial agonists of both dopamine and serotonin receptors			
Aripiprazole	Low risk	Low risk	Lieberman et al. (2005), Jones et al. (2006), Casey et al. (2017), Laschizophrenialovschizophreniaky et al. (2021)
Cariprazine	Low risk	Low risk	
Latest approved drug works as muscarinic acetylcholine receptor agonists			
Xanomeline–trospium (KarXT)	Low risk	Low risk	Shannon et al. (1994), Correll et al. (2022); Breier et al. (2023); Dolgin (2024).

Table 1.8: list of antipsychotic drugs and related risk of side effects.

1.3.6.2. Sex differences of antipsychotic medication

Schizophrenia symptoms are exhibited differently in male and female patients, with male patients exhibiting more severe symptoms in general, and more negative symptoms, while female patients exhibiting more positive and emotional symptoms. In this case, antipsychotic mediation therapy might also show sex differences.

Gender-based medication therapies have been suggested according to the differences of schizophrenic symptoms. For example, as female patients showed less severe symptoms compared to male patients, it has been demonstrated that female patients showed better consequences after antipsychotic therapies, with 50% fewer female patients experiencing hospitalisation (Smith, 2010). In addition, as male patients presented more severe schizophrenic symptoms, male patients were suggested to be treated with higher doses of antipsychotic drugs, with approximately twice higher doses than female patients (Melkersson et al., 2001). Male patients were also reported to be more likely to smoke cigarettes, which could suppress the effectiveness of antipsychotic drugs (Goff et al., 1992).

The risk and the severity of side effects after antipsychotic therapy were also shown to be different in male and female patients. Consistent studies illustrated that female patients tend to exhibit more side effects. For example, after risperidone and phenothiazine therapy which targeted 5-HT_{2A} receptors, more female patients exhibited pulmonary embolism compared to male patients (Kamijo et al., 2003). Additionally, wight gain was also found in a larger population of female patients, with 78% of female patients suffering from weight gain over 5% of starting weight after clozapine therapy (Heimburg et al., 1994). The therapy of clozapine also increase the body mass index (BMI) in female patients, from 23.2 to 29.1 kg/m^2, and the increased BMI rate also appeared to upregulate the risk of cardiovascular disease with 3.5 times more in female patients (Frankenburg et al., 1998).

1.3.6.3. Non-pharmacological therapies

As schizophrenia patients exhibit cognitive, behavioural and emotional symptoms, such as memory deficits, depressive emotions and abnormal motor behaviours, this might lead to patients withdrawal from social communities, and difficulties in maintenance of day-to-day life. The non-pharmacological therapies target improvement of schizophrenic symptoms, relapse prevention, and adaptive social functioning, which mainly aimed to help patients interaction with the social community. One major non-pharmacological therapy is psychological therapy, including therapies targeted at social skills, cognitive behaviour, personal therapy and cognitive remediation.

Social skill therapy contains several trainings in daily skills, with a combination of trials of role playing, positive reinforcement and the skill to interact appropriately to different social situations, which improve the communication skills, physical gestures and facial expression (Smith et al., 1996). Cognitive behavioural therapy tended to target the positive symptoms, such as, delusions and hallucinations, providing patients with symptom-oriented strategies to cope with the psychotic thinking or auditory hallucinations (Gould et al., 2001). Personal therapy was designed to help patients reduce the risk of relapse of schizophrenic symptoms with the identification of relapse signs, such as abnormal motor behaviour, depressive or anxious emotions, social withdrawal and cognitive or thinking biases (Hogarty et al., 1997). In order to improve the basic cognitive skills in schizophrenia patients, cognitive remediation training was suggested, with various cognitive tasks, such as computer-based tasks to improve attention and memory skills (Hogarty et al., 2004).

Therefore, apart from the pharmacological therapy targeted on the neurobiology of schizophrenia, non-pharmacological therapy, especially psychological therapies including social skills, cognitive behaviour, personal therapy and cognitive remediation training, were suggested to improve patients' cognitive and behavioural symptoms and reduce the risk of remission of schizophrenic symptoms.

The current treatment and antipsychotic drugs mentioned in previous Section 1.3.6.1 are targeted on the abnormal neurotransmitter system in schizophrenia, however, despite PNN and Pv abnormalities being consistently found in schizophrenia patients and animal models of schizophrenia (as mentioned in Section 1.3.4), only very limited studies have been targeted on the PNN or Pv deficits. Although there are some suggestions that removal of PNNs could attenuated the cognitive impairments in animal models of AD (Howell et al., 2012), and degrading CSPGs enzymically could promote axonal or neurite growth and promote axonal recovery after CNS injury (Bradbury et al. 2002; Wang et al. 2011; Azizi et al. 2020), no specific drugs were approved based on this effect. However, apart from the antipsychotic drugs, some behavioural or cognitive tasks provided a suggestion to improve PNNs abnormalities. For

example, the reduced PNNs expression could be reversed after a series of behavioural or cognitive tests in rodents with increased expression of *Bcan* and *Vcan*, which supported the complete organisation of PNN structure (Saroja et al., 2014). However, the current non-pharmacological therapies for schizophrenia do not target and focus on PNN recovery, despite there was a suggestion that PNN expression could be recovered after a series of behavioural tasks in some psychiatric disease animal models. Therefore, with further investigations of PNN alterations and the relationship to schizophrenia in the current study, more suggestions and insights of the schizophrenia treatment could be provided.

To conclude, the therapies of schizophrenia and psychosis disorders contain pharmacological and non-pharmacological therapies. Antipsychotic medications are the first choice for the recovery of schizophrenia patients, including first-, second- and third-generation of drugs, mainly targeting dopamine D2 or D3 receptors and 5-HT_{1A} and 5-HT_{2A} receptors. As male and female patients exhibited different types of schizophrenic symptoms, the consequences of antipsychotics medication were also shown to differ in males and females, suggesting males required higher doses of drugs and females showed more side effects. However, after recovery from the schizophrenic symptoms with the treatment of antipsychotic drugs, patients had high risk for schizophrenia remission. Therefore, the non-pharmacological therapies were suggested to reduce the relapse risk and improve the cognitive behaviours and social skills in schizophrenia patients.

1.4. Stress effect on PNNs and its relationship to schizophrenia symptoms

1.4.1. Stress and release of stress hormones, glucocorticoids

As external environmental stress was suggested to increase the risk of schizophrenia, understanding the underlying mechanisms of stress is vital to investigate the potential neural pathway through which stress affects neural and cellular processes in schizophrenia neurobiology.

After exposure to the stressful events, catecholamines, including adrenaline and noradrenaline, are released from the sympathetic nervous system, and the HPA axis is also activated with the secretion of corticotrophin-releasing hormone (CRH) from the hypothalamus paraventricular nucleus; subsequently, adrenal-corticotrophic hormone (ACTH) is secreted from the pituitary gland in the anterior lobe, followed by the release of glucocorticoids (GCs) from adrenal glands (Fig 1.2) (Smith and Vale, 2006). Thus, elevated GC levels are present in the brain, causing activation of GRs and MRs. GRs and MRs are expressed in glial cells and neurons across several brain regions, with the highest abundance in hippocampus and amygdala which are responsible for the emotional and cognitive activities (Lupien et al., 2007; Walker and Spencer, 2018). MRs have 10-fold higher affinity for GCs compared to GRs, and so are occupied by the basal levels of GCs in the normal situation; however, the GRs have lower affinity for GCs, thus the activation of GRs is generally based on the elevated levels of GCs in stressful situations (Lupien et al., 2007). Thus, the altered gene expression or neural activities after stress exposure is predominantly mediated by glucocorticoids receptors (GRs) activation.

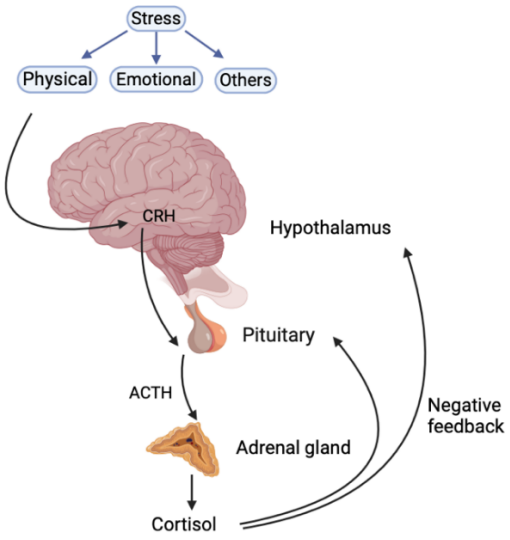

Figure 1.2: Stress and corticosterone pathways through the HPA axis (Lupien et al., 2007). After experience of stress events, CRH was released from the hypothalamus paraventricular nucleus; followed by ACTH secreted from the pituitary gland in the anterior lobe, and elevated GCs were secreted from adrenal glands and showed negative feedback to CNS regions.

1.4.1.1. GCs and GRs

In the cytoplasm, GRs and MRs bind to protein complexes without the presence of ligand. GCs are the primary hormones secreted from adrenal cortex responding to stress, mainly cortisol in humans, and corticosterone in rodents (Miller and Auchus, 2011). The release of GCs varies with the circadian rhythm, with the lowest level at midnight and peaking in the morning (Chan and Debono, 2010). The HPA-axis is the major system regulating the circadian oscillation (Walker et al., 2015). The total GC levels are maintained by adrenal synthesis, however, most of the secreted GCs bind to corticosteroid binding globulin (CBG) in the blood, accounting for 80% to 90% of the total amount of synthesised GCs levels, while approximately another 10% to 15% of secreted GCs are bound to albumin to keep the rest of the GCs an inactive state. Around 5% of secreted GCs are free in various tissues (Breuner and Orchinik, 2002). Thus, the levels of free GCs are regulated primarily by CBG.

The presence and secretion of GCs is regulated by the metabolic enzymes 11β-hydroxysteroid dehydrogenases (11β-HSDs) (Seckl, 2004). 11β-HSDs consisted of 2 subtypes, namely 11β-HSD1 and 11β-HSD2 (Seckl, 2004). 11β-HSDs have a major function in converting active cortisol to inactive cortisone, and 11β-HSD2 was suggested to prevent active cortisol from crossing into specific tissues, such as kidney and placenta (Seckl, 2004). However, 11β-HSD2 only acts on endogenous GCs after stress, and the basal levels of GCs are not regulated by 11β-HSD2 (Cooper and Stewart, 2009). In this case, 11β-HSD1 acts as the predominant metabolic enzyme in tissues which are enriched in GCs, such as, liver, brain and lung (Cooper and Stewart, 2009). Thus, the 11β-HSD1 and 11β-HSD2 target different aspects of GC function to maintain the total availability and activity of GCs.

The structures of GRs and MRs are similar, consisting of an N-terminal transactivation domain, a DNA binding domain, and a C terminal ligand binding domain without the presence of ligand, including heat shock protein 90 (hsp90), and hsp70 (Kirschke et al., 2014), while with the presence of ligand, GRs and MRs dissociate from the protein complexes and undergo nuclear

translocation (Kirschke et al., 2014). In the nucleus, the activated GRs and MRs mediate effects on gene expression by binding to GC response elements (GREs) in the promoters of targeted genes (Zalachoras et al., 2013).

1.4.1.2. Genomic action of GCs

Generally, the effects of GCs are to modify target gene transcription, which are defined as the genomic actions of GRs (Figure 3). Additionally, previous studies illustrated that the effects of GCs could also progress through non-genomic pathways (Figure 3) (Groeneweg et al., 2011).

The genomic actions of GCs are mediated via GRs, and are mediated through binding to DNA directly, or indirectly by interacting with other transcription factors (Figure 3). The genomic actions are not rapid, taking usually between 4h to 24h to complete (Escoter-Torres et al., 2020). GRs modulate target gene expression by directly binding to GREs, with both activation or repression effects (Ramamoorthy and Cidlowski, 2013). The structure of GREs contains 2 hexanucleotide sites separated by 3 nucleotides, and the GR binds to the 2 GREs sites as a dimer, each receptor occupying one of the GRE sites (Beato, 1989). After binding to GREs with a dimer formation, the coregulator or the chromatin-remodelling complexes are recruited and influence the activation of RNA polymerase, which could in turn activate gene expression (Ramamoorthy and Cidlowski, 2016). A predominant isoform of GR generated by alternative splicing, the GC receptor α (GRα), mediates the classic genomic GCs effects (De Bosscher et al., 2010). For example, most upregulation effects of GCs on anti-inflammatory genes result from transactivation mechanisms, by directly increasing the transcription of some anti-inflammatory genes, such as, interleukin-10 and the inhibitor of nuclear factor kappa B (NF-κB) (Ehrchen et al., 2007).

1.4.1.3. Non-genomic action of GCs

The non-genomic action is suggested to be mediated through activating membrane-bound receptors, cytoplasmic receptors and direct interaction with cell membranes (Figure 3). Unlike the genomic actions of GCs, the onset of non-genomic actions is much faster, usually within 4h, or even seconds to minutes, as the action does not require the interaction of transcription factors, gene transcription and the synthesis of protein complexes (Groeneweg et al., 2012).

The non-genomic effect of GCs involves 2 types of receptors, including classic GRs and non-classic GRs which are both located on or associated with the plasma membrane. The classic membrane GRs were mostly present in periphery rather than the CNS and are generally found in human monocytes and lymphocytes (Gametchu et al., 1999). The non-classic membrane GRs are expressed in the CNS, with 7 transmembrane helices, and coupled with G proteins, hence defined as members of the G-protein coupled receptor (GPCR) super-family (Lagerström and Schiöth, 2008). However, the non-classic membrane GPCRs in the CNS have higher affinity for corticosterone as compared to other stress hormones or synthetic ligands that were commonly suggested to bind to GRs, such as aldosterone or dexamethasone (Orchinik et al., 1991). Another study also reported a high affinity binding between GPCRs and GCs (Ping et al., 2021). Among the GPCRs family, Ping et al (2021) reported that GCs could activate the adhesion family GPCRs G-protein coupled receptor 97 (GPR97) and G-protein coupled receptor 56 (GPR56), affecting cellular functions or processes, such as inhibiting the intracellular cyclic adenosine monophosphate (cAMP) levels and neuronal migration.

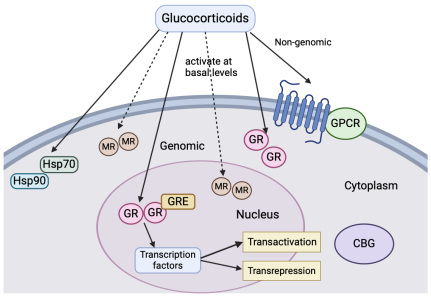

Figure 1.3: Genomic and non-genomic pathways of GCs actions (Groeneweg et al., 2011). Elevated GCs could bind to GRs in the cell nucleus and affect gene expression directly by binding to GREs located on DNA binding sites, or indirectly by interacting with transcription factors, inducing a genomic action; and GCs could also bind to receptors in the cytoplasm or located on the cell membranes, affecting signal transduction by inhibiting cAMP activities, which could further inhibit the transcription processes and affect targeted gene expression.

1.4.1.4. Cellular functions of genomic and non-genomic actions of GCs

As the genomic actions of GCs could mediate altered gene expression through interaction with transcription factors, such as AP1, NF-κB and STAT5, altered transcription of several genes after activation of GRs was detected in hippocampal neurons. For instance, in a serial analysis of gene expression study, several genes were detected that responded to corticosterone in hippocampus with changes in expression, including calcium-binding proteins, NCAMs and neurofilaments, which were suggested to play a critical role in synaptic plasticity, memory consolidation and cellular metabolism (Morsink et al., 2006; Sandi, 2004). In addition, the long-term administration of GCs through genomic actions was suggested to inhibit synaptic transmission and suppress long-term potentiationl (LTP) in hippocampus (Pavlides et al., 1993; Pavlides and McEwen, 1999). Similarly, long-term genomic effects of GCs by chronic stress suppressed LTP (Pavlides et al., 2002)

In contrast, GCs were also reported to influence the neural transmission through non-genomic actions. For example, increased synaptic AMPA receptor GluR2 subunits, were observed after exposure to corticosterone for 3h, leading to increased amplitude of glutamate transmission, and enhanced synaptic signal transmission in hippocampus (Martin et al., 2009). Similar elevated expression of both NMDA and AMPA receptors was found on the neuronal surface after activation of non-genomic GRs by acute stress induction, resulting in enhanced LTP (Yuen et al., 2009; Whitehead et al., 2013). However, suppressed LTP was reported after both genomic and non-genomic rapid actions of GCs with both chronic and long-term exposure (Pavlides et al., 2002).

1.4.1.5. Other mechanisms of GCs

Furthermore, GCs were also demonstrated to decrease mRNA stability within hours through genomic and non-genomic actions, with reduction of target mRNA half-life. For example, the mRNA stability of interleukin 8 (IL-8) and chemokine ligand 7 (CCL7) were reduced by GCs (Cho et al., 2015; Park et al., 2016). The activated GRs induced the expression of tristetraprolin (TTP) which is a protein that binds to adenylate/uridylate (ARE)-rich (AU-rich) elements in mRNA 3' untranslated regions (UT) (Frevel et al.2003; Shi et al 2014). These elements are located on the 3' UTR of most mRNAs and are vital for mRNA stability and translation (Chen et al., 1995). Apart from affecting mRNA stability by inducing TTP, GRs can also bind directly to a GR binding site

on targeted mRNA in the presence of ligand. GR bound to the 5'UTR of targeted mRNA recruits upstream frameshift 1 (UPF1) and decapping enzyme 1A (DCP1A), and also interacts with proline-rich nuclear receptor coregulatory protein2 (PNRC2). This in turn leads to mRNA degradation by a process known as GR-mediated mRNA decay (GMD).

In conclusion, external stressful environmental factors could lead to endogenous elevated levels of GCs, activating both GRs and MRs. As MRs had higher affinity than GRs, they maintain activation by basal levels of GCs. GRs are the major receptor responding to elevated levels of GCs during stress, though both short-term non-genomic actions, with activated GRs located on the plasma membrane, and long-term genomic actions with activated GRs located in cell nucleus binding to GREs in targeted genes, or interaction with transcription factors. The genomic or non-genomic actions of GCs showed various effects on several cellular processes in the CNS, including synaptic transmission and LTP. Additionally, reduced mRNA stability and mRNA half-life could also be caused by elevated levels of GCs, which represents a new mechanism reported for GCs.

1.4.2. Effect of stress on the formation of PNNs

Stressful environmental experience is a critical risk factor in the underlying aetiology of schizophrenia, and the expression and formation of PNN were demonstrated to be abnormal in schizophrenia patients, thus the combination of external stress and disrupted PNNs might be related to the underlying aetiology of schizophrenia. Additionally, it has also been illustrated that PNNs expression and formation could be altered by external stressors which in turn affect the function of PNN, such as, synaptic plasticity, regulating axonal growth and neural transmission (Table 1.9).

1.4.2.1. Effect of stress on general PNN expression and formation

PNN expression has been investigated with exposure to stressful environments (Table 1.9). For example, mice exposed to postnatal stressful environments, such as maternal separation, social isolation or social defeat were reported to show lower PNN density or staining intensity in PFC, hippocampus and basal lateral amygdala, compared to the mice with no stress exposure (Gildawie et al., 2020; Gildawie et al., 2021; Ueno et al., 2017; Klimczak et al., 2021). Conversely, increased PNN number or intensity has also been suggested in various mouse brain regions after exposure to stressful situations. Increased PNN intensity was found in basal lateral amygdala and PFC after exposure to maternal separation, however, the increased intensity was accompanied by decreased density of PNN in PFC but not basal lateral amygdala (Gildawie et al., 2021). Similar upregulation of PNNs density or intensity was also observed in hippocampus after maternal separation or social defeat (Murthy et al., 2019; Riga et al., 2017).

In addition to stressful environment exposure, other methodologies of stress induction have also been used to investigate alterations of PNN expression. For instance, random or chronic restraint stress, including dark or bright light exposure, resulted in either increased or decreased density of PNNs in PFC and reduced density of PNN in hippocampus (Yu et al., 2020; Pesarico et al., 2019). Additionally, in adolescent rats with chronic stress exposure, increased PNN density was detected after 7 days of stress induction, but decreased density after 35 days of stress induction (Folha et al., 2017). Altered expression of PNN was also found in subjects experiencing prenatal stress. Mice with maternal restraint stress presented with decreased density of WFA-labelled PNN in medial PFC at P21 (Wang et al., 2018).

Limited studies investigated the expression of PNNs with stress hormones or in disease models linked to elevated stress hormones, such as depression. The density of PNN labelled with WFA surrounding Pv neurons in hippocampus increased in a depression mouse model involving elevated corticosterone administration (Coutens et al., 2023). Therefore, it could be concluded that PNN expression, including density and intensity, can be altered in mice with stress exposure, although with both increases or decreases reported (Table 1.9). The different results could be associated with the age of mice exposed to stressful environments, or the duration of the restraint stress (which varied from 3 to 8 hours per day and lasted for 4 to 30 days).

1.4.2.2. Effect of stress on PNN components

As the general expression of PNNs is altered by stress, and PNNs consist of several components including CSPGs, tenascins, hyaluronan synthesis and link proteins, the effect of stress could also be observed in the component's expression (Table 1.9).

In a study with a social defeat, persistent stress paradigm, rats showed generally lower CSPG-coated Pv neuron density in hippocampal CA1 region 3 days after social defeat exposure in hippocampus, but density was increased 60 days post-stress exposure (Koskinen et al., 2020). Upregulated *Acan*-labelled PNNs were reported in mouse anterior cingulate cortex after early life stress (Catale et al., 2022). In mice with prenatal maternal restraint stress exposure, *Acan*-labelled PNNs were significantly reduced in medial PFC compared to mice with no maternal stress exposure (Wang et al., 2018). Similarly, after exposure to chronic stress in adulthood, *Acan* protein levels were decreased in rat prelimbic areas (Yu et al., 2020). Moreover, rats experiencing prenatal maternal stress showed increased protein expression of *Bcan*, *Ncan* and *TnR* in hippocampus (Dimatelis et al., 2013). Moreover, a reduction of *Ncan* mRNA expression and disrupted *Ncan* immunostaining, with a granular staining pattern, was found in prelimbic cortex in mice after chronic unpredictable stress, including cold temperature, water deprivation, forced cold water swim and food restriction (Yu et al., 2022). Conversely, upregulated *Ptprz1* staining intensity and protein expression was detected in Nodes of Ranvier in rat PFC after chronic unpredicted stress exposure (with no change in *Vcan*, *Bcan*, *Ncan* or *Hapln2*), and in post-mortem PFC from people with depression (with no change in *VCAN*, *NCAN* or *HAPLN2*, but with decreased *BCAN) (*Miguel-Hidalgo et al., 2023).

Although growing evidence reported altered expression of general CSPG components after exposure to stressful experiences, limited studies reported alterations in the CNS with stress mediator administration. The expression of *Acan* and *Ncan* (with no effect on *Vcan*, *Bcan* or *Ptprz1*) was suggested to be affected by stress exposure with downregulated mRNA and protein levels in CNS (Strokotova et al., 2023). Additionally, the gene expression of *Bcan* was also suggested to be reduced in hippocampus in mice exposed to elevated corticotropin-releasing factor levels (Peeters et al., 2004); on the contrary, upregulated expression of *Bcan* was observed in mice with corticosterone administration, exhibiting increased *Bcan* protein levels compared to the mice with no corticosterone exposure (Alaiyed et al., 2020). In addition to the alterations of *Acan* and *Bcan*, *Ncan* and *Vcan* showed decreased mRNA expression and synthesis in astrocytes of dorsal ganglion and cells in skeleton muscles with GCs exposure (Liu et al., 2008; McRae et al., 2017).

Unlike the alterations of CSPGs expression, not too many studies addressed hyaluronan components with stress induction in the CNS, such as hyaluronan synthase or the link proteins. Nevertheless, the study investigating the expression of *Hapln2* in the Nodes of Ranvier in the white matter of PFC after exposure to chronic unpredictable stress in rats and in human

depression, found no alterations with regards to the staining pattern and protein levels (Miguel-Hidalgo et al., 2023).

1.4.2.3. Effect of stress on Pv-expressing neurons

Consistent studies reported the protective function of PNNs on Pv-expressing interneurons from being disrupted by external stress (Table 1.9). Pv-expressing interneurons are affected by similar kinds of stress exposure, such as a stressful environment, maternal separation or deprivation, social isolation and restraint stress. Maternal separation or deprivation in the early life experience decreased Pv-expressing neurons density in medial PFC and infralimbic cortex in adulthood (Giladawei et al., 2020). Reduction of Pv-immunostaining intensity was also demonstrated in amygdala and ventral hippocampus accompanied by a decreased number of Pv-expressing interneurons in the same region (Murthy et al., 2019). Similarly, decreased density and staining intensity of Pv-expressing interneurons were also reported in cingulate cortex and ventral hippocampus of young mice (P21) after social isolation compared with the mice without isolation (Uneo et al., 2017; Deng et al., 2019). Moreover, in primates with chronic psychosocial stress (daily psychosocial conflict), a decreased total number of Pv-expressing interneurons was reported in some hippocampal regions, including dentate gyrus, CA1 and CA2 (Czeh et al., 2005). Consistent with the PNN reductions in animals with maternal stress, a reduced number of Pv-expressing interneurons was detected in medial PFC in offspring accompanied with reduced density of surrounding PNNs (Wang et al., 2018). A similar reduction, in offspring, the density of Pv-expressing interneurons was present in hippocampus and somatosensory cortex in mice with maternal restraint stress (Uchida et al., 2014), indicating a suppressive effect of prenatal stress on the total number of Pv-expressing neurons.

Apart from exposure to stressful social environments, induction of chronic restraint stress also resulted in altered Pv neuron expression in mice brains. For example, chronic restraint stress combined with foot shock in adolescent mice led to a decreased number of Pv-expressing interneurons in ventral hippocampus; however, the same stress induction in adult mice resulted in unchanged density of Pv-expressing neurons (Gomes et al., 2019). Conversely, chronic restraint stress in adult rats increased the number Pv-expressing neurons in medial PFC (Pesarico et al., 2019). However, other studies showed different results that no alterations of the number and the immunoreactivity intensity of Pv-expressing neurons were observed in hippocampus and PFC of mice and rats with chronic restraint stress (Nowak et al., 2010; Zadrozna et al., 2011).

Another study reported that chronic (21 days) stress in rats reduced the number of Pv-expressing neurons was reduced in all hippocampal neurons (Hu et al., 2010).

Therefore, exposure to external stressful environments or prenatal stress or chronic restraint stress were suggested to have an impact on the PNN intensity and density, but with both increases and decreases reported in various brain regions (Table 1.10). Similar effect of stress was also observed on some PNN components, and on PNNs covering Pv-expressing interneurons, with altered mRNA or protein levels and immunoreactivity patterns (Table 1.10), but again the direction of effect was controversial, and some studies also found no alterations of the density of PNNs and Pv-expressing neurons in animals with stress exposure. The alterations of the density and staining intensity of Pv-expressing neurons lack clarity. The inconsistent impact of stress on the expression of Pv expression might reflect the different animal strains and duration of stress induction employed in those studies, for example, the studies used Sprague–Dawley rats or Wistar rats with restraint stress lasted for 10 days or chronic stress lasted for 16 days. The study using the shorter stress induction period resulted in increased Pv expression

(Pesarico et al., 2019), while the studies that employed longer stress induction showed decreased Pv expression (Hu et al., 2010; Gomes et al., 2019; Shepard et al. 2016).

1.4.2.4. Effect of stress on *GAD/Gad*

As noted in section 1.4.3, abnormal *GAD* expression is detected in schizophrenia. As stressful environmental factors increase the risk of schizophrenia, experiencing stressful events might also be a factor influencing the expression of *GAD* components (Table 1.9), especially *GAD67* which is more prominently involved in schizophrenia.

Altered *Gad67* expression is reported in rodent studies. For instance, increased mRNA levels of *Gad67* in prelimbic and infralimbic areas and decreased in paraventricular nucleus in hypothalamus are reported in mice after chronic restraint stress (Makinson et al., 2015). However, the protein expression of *Gad65* was not altered in PFC and hippocampus of rats after chronic unpredictable stress, while reduced *Gad67* protein levels were detected (Banasr et al., 2017). Moreover, a reduced number of *Gad67*-expressing neurons was reported in mice after chronic restraint stress in medial PFC, however, the mRNA levels were not altered (Gilabert-Juan et al., 2013), whereas in another study, the protein levels of *Gad65* and *Gad67* remained unchanged after restraint stress induction (Lussier et al., 2013).

In addition to the chronic exposure to stressful environments or situations, abnormalities of *Gad* expression were detected with direct administration of corticosterone or other stress related substrates. In rat hippocampus and amygdala, reduced protein levels of *Gad65* were observed in hippocampus, while reduced protein levels of *Gad67* were detected in amygdala, with corticosterone administration (Lussier et al., 2013). Furthermore, in cortical cultured neurons, treatment with corticosterone (100nM – 10mM) or dexamethasone resulted in decreased immunoreactivity for *Gad67* (Banasr et al., 2017).

Thus, in general a reduction of *Gad65* and *Gad67* expression, including immunoreactivity and protein, and mRNA levels, was reported in various brain regions in animals exposed to restraint stress or with administration of stress-related mediators (Table 1.9); and similar decreased expression of Gad67 was also observed in primary cultured neurons.

Components	Expression after stress exposure	Citation
General PNNs	↓ or ↑ density and intensity	Gildawie et al. (2020); Gildawie et al. (2021); Ueno et al. (2017); Klimczak et al. (2021); Murthy et al. (2019); Riga et al. (2017); Yu et al. (2020); Pesarico et al. (2019)
Acan	↓ or ↑ WFA labelling, ↓ mRNA and protein levels	Catale et al. (2022); Yu et al. (2020); Strokotova et al. (2023); Liu et al. (2008); McRae et al. (2017)
Bcan	↑ protein levels, ↓ mRNA levels	Dimatelis et al. (2013); Strokotova et al. (2023); Peeters et al. (2004); Liu et al. (2008); McRae et al. (2017)
Ncan	↑ mRNA levels ↓ *Ncan* labelling	Dimatelis et al. (2013); Yu et al. (2022); Strokotova et al. (2023); Liu et al. (2008); McRae et al. (2017)
Vcan	—	Liu et al. (2008); McRae et al. (2017)
Phcan / Ptprz1	↑	Miguel-Hidalgo et al. (2023); Strokotova et al. (2023); Liu et al. (2008); McRae et al. (2017)
Has1	N/A	
Has2	N/A	
Has3	N/A	
Haplns	—	Miguel-Hidalgo et al. (2023)
TnR	↑ protein levels	Dimatelis et al. (2013)
Pv-expressing neurons	↓ or ↑ or —	Giladawei et al. (2020); Uneo et al. (2017); Deng et al. (2019); Murthy et al. (2019); Czeh et al. (2005); Uchida et al. (2014); Gomes et al. (2019); Pesarico et al. (2019); Nowak et al. (2010); Zadozna et al. (2011); Hu et al. (2010).
Gad67/65	↓ or — in mRNA levels and protein levels, ↓ labelling	Makinson et al. (2015); Banasr et al. (2017); Gilabert-Juan et al. (2013); Lussier et al. (2013).

Table 1.9: summary of dysfunctional PNN and Pv-expressing neurons after exposure to stress

1.4.3. Stress affected PNNs in relation to schizophrenia

It is possible that abnormalities of PNNs and PV neurons affected by stress are related to risk of schizophrenia. As noted in previous sections, the expression and functions of PNNs were found to be abnormal in schizophrenia patients, and exposure to environmental stress was suggested as a risk factor for schizophrenia. However, whether the abnormalities of PNNs or Pv-expressing neurons in schizophrenia patients resulted from stress exposure or elevated stress mediators remains to be clarified.

The impaired PNN and Pv-expressing neurons induced by external stressors in rodents are also accompanied by schizophrenia-like behaviours. Upregulation of PNN density or intensity were observed in hippocampus after maternal separation, and accompanied with increased anxiety-

like behaviours (Murthy er al., 2019). Similarly, schizophrenia-like behaviours were observed in stress-induced juvenile mice, presenting with increased locomotor activities and abnormalities of social behaviours, and decreased fluorescence intensity of WFA PNN around Pv neurons (Ueno et al., 2018). This suggests a potential relationship between abnormal expression of PNNs or Pv-expressing interneurons and schizophrenia-like behaviours. Another study conducted by Gomes, Zhu and Grace (2019) evaluated the influence of stress exposure on adolescent and adult mice, demonstrating that there was Pv loss in ventral hippocampus area in stressed adolescent mice, which could lead to ventral hippocampus hyperactivity.

Likewise, reductions of Pv-expressing interneurons were found in mouse ventral hippocampus regions after 2 months social isolation The isolated mice exhibited cognitive impairments, with deficits in emotional cognition and social memory (Deng et al., 2019). The duration of stress exposure was suggested to relate to the alteration of Pv-expressing neurons, in that a relatively short time of restraint stress exposure for 7 days, resulted in an increased number of Pv-expressing neurons, while relative long-term stress exposure for 35 days resulted in a decreased number of Pv-expressing cells, with reduced density of surrounding PNNs. The stress-exposed mice also presented with impaired working memory (Folha et al., 2017).

In addition, adolescence is a critical period for maturation of GABAergic transmission and PV interneurons (Caballero, Diah and Tseng, 2013). Pv neurons are highly vulnerable to stressors in critical period, and PNNs which protect Pv neurons from being damaged by stress are not mature during this period (Lensjo et al., 2017). Therefore, environmental stressors could have an impact on developing PNNs and Pv neurons, which lead to deficits of neurodevelopment and development of psychiatric disorders such as, schizophrenia.

Moreover, oxidative stress-induced Pv-expressing interneuron deficits were also observed in some schizophrenia mouse models. For instance, a metanalysis showed that mice with schizophrenia-related gene mutations, such as 22q11.2, 1q21 and 15q13.3 deletions, showed reduced density of Pv-expressing interneurons, with fewer surrounding PNNs, in PFC with oxidative stress exposure (Steullet et al., 2017). A similar reduction was also detected after oxidative stress induction in mice lacking individual genes associated with schizophrenia, including serine racemase (*SRR*) and *GRIN2A,* which were found to express fewer Pv-expressing interneurons and reduced density of WFA-labelled PNNs, indicating a relationship between reduced Pv expression and the risk of schizophrenia (Steullet et al., 2017). Rodents with deficient glutathione (GSH) synthesis and Glutamate-Cysteine Ligase Modifier (GCLM) also showed a decreased number of Pv-expressing interneurons with decreased density of WFA-labelled enwrapping PNNs, compared to wild type mice, with oxidative stress exposure (Steullet et al., 2017). Furthermore, rats with MAM prenatal administration, which show elevated dopaminergic function, were also suggested as a schizophrenia model, and showed a decreased number of Pv-expressing interneurons and WFA-labelled PNNs in ACC after oxidative stress induction (Steullet et al., 2017).

Therefore, these reports suggested that lower levels or expression of PNNs and Pv neurons resulting from genetic mutation or cellular stress or exposure were found in schizophrenia models. However, it is not clear whether the abnormalities of PNNs and their specific components, and of Pv neurons, when influenced by maternal, or early-life stressors, are related to the onset of schizophrenia.

1.5. Aims and rationale of the study

It could be concluded from the current studies that the expression of PNN, and PNN-covered Pv expressing neurons, play a critical role in several cellular or neural processes which are altered in schizophrenia. This in turn could suggest a role of PNN and PNN-covered Pv-expressing interneurons in the neurobiology of schizophrenia (reviewed in Berretta et al., 2012). Stress was also demonstrated to alter the properties of PNN; and early-life or prenatal exposure to environmental stress is a factor increasing the risk of schizophrenia development. Thus, these lines of evidence raise the possibility that the abnormal expression of PNN or Pv-expressing neurons resulting from early-life or prenatal stress is related to the risk of schizophrenia. However, limited studies investigated the effect of stress on particular PNN components. The pathways of stress affecting PNNs components or Pv-containing neurons expression and whether the altered expression relates to schizophrenia remained to be clarified. As noted in section 1.5, elevated GCs level is released after exposure to external stress, indicating that an increased release of GCs in the neural developing period could be a reflection of experiencing early-life stress.

As stress or environmental stress factors could affect PNN expression and increase the risk of schizophrenia, and reduced PNN/Pv expression are observed in schizophrenia, so we could potentially hypothesise that the stress-induced PNN alteration might be associated with the pathology of schizophrenia. And with external stress experience, elevated stress-hormones will be secreted from adrenal cortex, specifically GCs, affect the CNS by binding to related receptors. Different underlying mechanisms were reported as regards to GCs, including long-term genomic actions by binding to GRs in cell nucleus and rapid non-genomic actions by binding to GRs in cytoplasm, or to other receptors located on cell membranes.

However, previous studies mostly investigated the overall effect of stress on PNNs expression, and mainly morphological expression, but how stress affects PNN expression is still unclarified. For example, as PNN structure is stabilized by its components, so whether stress could specifically affect expression of different components, not only at the morphological level, but also at molecular levels, needs to be further investigated; and as stress could modulate expression through different pathways, the specific mechanisms that allow stress to affect PNN and Pv expression are still remained unclear.

Previous section (1.5) mentioned that prior studies showed inconsistent results as regards to the effect on the intensity of PNN labelling, and most of them used *in vivo* animal experiments and induced environmental stressors, including maternal separation, social isolation or restraint stress, foot shock or food starvation, and they used animals at various stages of development followed by several behavioural experiments. Thus, animals might develop resilience to the stress, and PNN expression might be changed by the behaviours tests. So, this might be the reason that the research showed different effects of stress on PNNs.

Therefore, our current research decided to investigate the direct effect of stress on the expression, and used the cultured cortical neurons, and treated neurons directly with elevated GC levels, to model the direct impact of stress on neurons.

Furthermore, although previous studies illustrated the reduction of PNN or Pv expression in schizophrenia and disrupted PNN and Pv in WT animals also showed schizophrenia-like phenotypes, whether reduced expression of PNN in schizophrenia is related to stress or the environmental stress factors, or whether there are any relationship between external stress-induced PNN/Pv alterations and schizophrenia is not clear.

The current study intended to investigate how stress (acting directly via elevated GC levels) affects PNNs and the components (including molecular and morphological expression), and whether stress-induced PNN and Pv alterations are associated with schizophrenia. By investigating this topic, the underlying mechanisms and actions of stress, specifically, elevated GC on PNN and Pv expression will be determined, which may also be fundamental to finding the potential underlying pathology of schizophrenia.

The general hypothesis of the study is that the elevated GCs level could alter the expression of PNNs components and Pv-expression neurons in the CNS; and the levels of PNN components, Pv-expressing neurons and *Gad* components could be abnormal in schizophrenia mouse models.

The specific aims of the study are as follows:

a. to investigate the effect of GCs on PNN components and Pv-expressing interneurons

b. to investigate the specific pathways through which GCs affect PNN components and Pv-expressing interneurons

c. to investigate the alterations of PNN components and Pv-expressing interneurons in mouse models relevant to schizophrenia

The aims a and b are addressed from Chapter 3 to 7, illustrating the effect and specific actions of GCs on PNN components; and aim c is addressed in Chapter 8 and 9, illustrating the alterations of PNN components after MIA and its potential relationship to schizophrenia.

Chapter 2
Materials and methods

2.1 In vitro experiments

2.1.1 Primary neuronal culture

The cortical brain tissues from C57Bl/6J mouse embryos (E17) were prepared for primary neuronal culture. The whole foetal brain was extracted, the meninges were removed, the cerebral cortical tissues were dissected and washed with ice-cold Hanks Balanced Salt Solution (HBSS) (ThermoFisher, 14175053). The tissues (usually from 5-8 embryos) were then transferred into 3ml 0.67% trypsin/EDTA (Gibco, 25300-054) and incubated at 37 ° C for 10 minutes. Following this, 3ml Dulbecco's modified Eagle's medium (DMEM) (Gibco, 21885025) with 10% HI (horse serum) (ThermoFisher, 26050088), 1% Penicillin Streptomycin (Sigma-Aldrich P0781), 1% Glutamax (ThermoFisher, 350500-038) was added to inactivate the trypsin, and the tissues were centrifuged at 4 ° C at 1500rpm for 5 minutes, then the supernatant was discarded. 8ml DMEM was then added, and the mixture was transferred into 30ml clean neurobasal medium (Gibco, 21103049) with 10% B27 supplement (Gibco, 17504044), 1% Glutamax and 1% Penicillin Streptomycin. Then the cell suspension was seeded onto 12 well plates precoated overnight with 4 µg/ml poly-D-lysine (SIgma-Aldrich, P6407-5MG) and 6 µg/ml laminin (1ml/well) (ThermoFisher, 23017015). Following this, clean neurobasal (0.5 ml/ well) and DMEM (1ml/well) were added to each well. The plates were incubated at 37 degrees in a tissue culture incubator (5% CO_2). After 24 hours, 50% of medium was replaced by clean neurobasal (pre-added with 10% B27 supplement, 1% Glutamine and 1% Penicillin Streptomycin); this procedure was repeated after 48 hours and then the medium was replaced by neurobasal medium/B27/Glutamax every 4 days in the culture duration. All procedure need to be performed in the fume hood.

2.1.2 Drug administration in primary cultured cells

After 7, 14, or 21 days in vitro (DIV), the cells were treated with low dose (20nM as final concentration), high dose (100nM as final concentration) hydrocortisone acetate (HCA) (20µl/well) (Sigma-Aldrich 50-03-3) or the same volume of nuclease free water (20µ/well) (Qiagen 129117) as a vehicle group.

HCA is a GC, showing the same activity mechanisms as GCs, and the concentration of HCA will be elevated after experiencing external stressors (Rafestin-Oblin et al., 1986), therefore, HCA is an appropriate GC that could be used in the current study to model the secretion of the stress hormones in both humans and animals after stress exposure. The doses of HCA were dependent on previous studies that the receptors that involved in the non-genomic actions of GCs had higher affinity for elevated GC (could bind to the elevated GC with a minimum concentration at 3nM and maximum at 50nM) (Rafestin-Oblin et al., 1986; Joels, et al., 2013; Chatterjee et al., 2014); while receptors involved in genomic actions located in cell nucleus had lower affinity to elevated GCs and could bind to higher concentration of GCs (with minimum concentration at 100nM) (Joels, et al., 2013; Lenka et al., 2015; Chatterjee et al., 2014).

Mifepristone (20nM as final concentration) (Cayman Chemical company 10006317) was also treated to cultured cells along with HCA treatment at 7, 14 and 21 DIV, respectively. Mifepristone is a GR antagonist, which binds to GRs with inhibition of the GRs activities and blockage of the

recruitment of coactivators, thus could lead to the inactivation of GRs (Rijssen, et al., 2019). Mifepristone has higher affinity to GRs, which could bind to the GRs with a minimum concentration at 0.2nM (Rafestin-Oblin et al., 1986), the current study used 20nM, which was at an adequate level to inhibiting GR activation and the concentration was also in line with previous research (Boggaram et al., 1991; Dhawan et al., 2007). The cells were treated for 4 hours or 24 hours, respectively, to detect the involvement of GRs in genomic or non-genomic actions of GCs.

Treatment of HCA and mifepristone was used to detect the involvement GRs of GCs, but in addition to GRs, GCs could also bind to other receptors, such as GPCRs and MRs (as noted in section 1.5), thus it is worth to further investigate whether these receptors are also involved in the GCs actions.

Collagen3 (75nM as final concentration) (Cell Guidance Systems M20S), a ligand of GC-bound GPCRs, was applied to the cell culture to detect the involvement of GPCR in the rapid non-genomic actions of GCs; the current study used 50nM of collagen3, which is at an adequate level to bind to GC-bound GPCR. Although a few research suggested the minimum concentration of collagen3 to bind to GC-bound GPCR, the concentration used in the current study was based on the previous research, using 50-100nM of collagen3 to bind GC-bound GPCRs (Zhu et al., 2019; Olanine, et al., 2018).

Aldosterone (100nM as final concentration) (Sigma-Aldrich A9477), a selective agonist of MRs, or fluticasone (50nM final concentration, as a comparative group for aldosterone treatment) (Sigma-Aldrich F9428), a selective agonist for GRs, are the drugs that were used to treat the cells to detect the further involvement of MRs and confirm the involvement of GRs following the initial HCA with mifepristone experiments.

Aldosterone is a mineralocorticoid that belongs to a class of corticosteroids and has similar effects as GCs, which was also shown to be secreted from adrenal glands after external stress exposure (Taves, et al., 2011), but with high affinity to bind to MRs but not GRs. The minimum concentration of aldosterone that could bind to MRs is at 0.3nM, and previous research generally used 100nM (Kino, et al., 2010; Lenka et al., 2017), so the current study chose to use 100nM being consistent with previous studies.

Fluticasone is a synthetic GC which has much higher affinity to GRs compared to MRs, with a minimum 0.2nM concentration to bind to GRs. It is generally used at a concentration 10 to 50nM to produce an efficient effect in previous studies (Ray et al., 1997; Milara et al., 2016); so the current study chose to use 50nM of fluticasone to produce a sufficient effect on GRs activation.

Following the detection of specific receptors involved in GCs action, another pathway of GCs was considered, which is GCs-mediated mRNA decay (GMD). Thus, to investigate the mRNA decay after GCs exposure, cells were treated with Actinomycin D (Act D) (5μg/ml) (Sigma-Aldrich, A4262-2MG) at 1.5h, 2h, 3h, and 4h, respectively to inhibit the mRNA synthesis after HCA treatment. Act D is widely used to prevent the transcription processes of RNA in various mRNA stability and mRNA decay assays. The most common concentration of Act D used in previous study was 5μg/ml, which suggested a proper concentration to use in the current study (Smoak et al., 2006; Muazzen et al., 2024; Shi et al., 2014).

2.2 In vivo experiments

2.2.1 Mouse model

The mice used to model schizophrenia symptoms were obtained from Jackson Laboratory expressing a hemizygous mutation equivalent to the 16p11.2 duplication and were maintained congenic on a C57BL/J background (Horev et al., 2011). The mice were housed at University of Strathclyde, with a 12h light-dark cycle at the 18°C -23°C room temperature.

12 16p11.2 duplication female mice were bred on an inbred C57BL/6J background and timed-mated with wild-type mice to generate wild-type and 16p11.2 duplication hemizygous offspring. The female mice were injected with saline, Poly IC (20mg/kg) (InvivoGen, tirl-picw) or Resiquimod (2mg/kg) (Tocris, 4536) between 9:00 am and 11:00 am at day 12.5 of pregnancy. The animals were weighed before injection and one day after injection. The mice conditions were assessed and monitored to make sure that there was not any sickness symptoms or abnormal behaviours. When pups from these colonies (genotyped by PCR) reached the adulthood, aged 8-10 weeks, they were used in the experiments. The study is reported in accordance with ARRIVE guidelines (https://arriveguidelines.org) and the updated ARRIVE guidelines (Percie du Sert et al, 2020). The animal study was performed according to home office (UK) regulations and were approved by the University of Glasgow Animal Welfare Ethical Review Board and the University of Strathclyde Animal Welfare Ethical Review Board.

2.2.2 Drug administration in mouse model

As one of the aims of the study is to detect the association between the stress-induced PNN alterations and schizophrenia with schizophrenia mouse model, the current study used Poly I:C and resiquimod to model the MIA condition, a kind of prenatal stress factors related to schizophrenia (the reason to use MIA induction was presented in Chapter 9 and Chapter 10, Section 10.1.3).

Poly I:C is a synthetic double-strand (ds) RNA virus mimetic, and can be recognised by Toll-like receptor 3 (TLR3). Although Poly I:C is a synthetic virus mimetic, it can induce an immune response and showed significant effect on several neurobiological systems, and is therefore considered as a critical drug to model MIA and was widely used to study the immune response in various psychiatric disorders (Meyer et al, 2014; Macêdo et al, 2012; Willis et al., 2021). The current study used 20mg/kg Poly I:C for the injection, which is a concentration that was commonly and widely used in the previous studies (Meyer et al, 2014; Macêdo et al, 2012; Willis et al., 2021; Kwon et al., 2023).

Resiquimod is a single strand (ss) mRNA virus mimetic, and can be recognised by TLR 7/8. Limited studies used resiquimod to model the MIA effect. However, increased risk of schizophrenia could be produced after prenatal infections with ss viruses, such as, rubella and influenza, as noted in Chapter 1, Section 1.3.2 (Babulas et al., 2006; Buka et al., 2001; Seckl, 2001). The current study used 2mg/kg resiquimoid for the injection to model MIA, the determination of the concentration was also based on previous research that consistently used 2mg/kg as a final concentration for MIA injection (Kwon et al., 2023; Willis et al., 2021).

Therefore, the current study aims to investigate the effect of MIA on PNNs and its relationship to schizophrenia, thus, to include the MIA effect with the combination of schizophrenia genetic risk, the current study used both ds and ss virus mimetics.

2.3 Quantitative Polymerase Chain Reaction (qPCR)

2.3.1 messenger RNA (mRNA) extraction from cultured neurons or mice brains

Total mRNA was then isolated from the cultured cells or dissected mouse brains using RNeasy mini kits (Qiagen 74106). Before the mRNA isolation, Buffer RLT (Qiagen, 79216) was prepared in the fume hood with 10µl of β-mercaptoethanol (Sigma-Aldrich, M3148) per 1ml of Buffer RLT.

In the primary neuronal culture, the medium was removed from the wells completely and the cells were washed with ice-cold phosphate buffered saline (2ml/well for 12 well plates) for a few seconds. PBS was removed and 200ul RLT buffer was added to each well to lyse the cells. Following this, the cells were dislodged by rubbing the surface of each well with pipette tips and the contents were then transferred into 1,5ml tubes. The lysates in the tubes were homogenised using syringes and needles. Lysate was passed through a 20-gauge needle attached to a sterile plastic syringe 5-10 times. Then 200ul 70% ethanol was added to the lysed cells.

With the brain samples, tissue was dissected and pre-weighed from mice and placed in pre-labelled tubes. For each 20/30mg brain tissue, 600ul RLT buffer with β-mercaptoethanol was added. Subsequently, the tissues in RLT buffer were ground with tissue grinding pestles (Bio echo 050 004 100). The ground samples were centrifuged for 3 minutes at room temperature at maximum speed of 13,400 rpm. the supernatant was transferred to a fresh tube and centrifuged again for 3 minutes at room temperature at maximum speed of 13,400 rpm. The supernatant was the transferred into a fresh tube containing 1 volume of 70% ethanol and mix by inverting.

The mixture from cultured cells or brain tissues was then transferred to an RNA spin column (Qiagen, 74104). The column with the mixture of cells, lysis buffer and 70% ethanol was centrifuged for 15 seconds at 10,000 rpm, the flowthrough was discarded. The column membrane was washed with 350 µl RW1 buffer (Qiagen, 1053394). DNase I stock solution was prepared with 10 µl DNase I (Qiagen, 79254) and 70 µl RDD buffer (Qiagen, 79254) for each RNeasy column, and was added on a column membrane to inhibit DNases. The column was left at room temperature for 15 minutes. After 3 times washes with 500 µl RPE buffer (Qiagen, 1053394), the column was dried for 1 minute and centrifuged at 10,000 rpm at room temperature. 50 µl RNase free water (Qiagen, 129112) was added to each column membrane to elute RNA. The extracted mRNA was collected using RNase-free consumable tubes and the mRNA samples need to be stored at -20°C for future use. The RNA quality and concentration were confirmed using spectrophotometry (Thermo Fisher Scientific) before cDNA synthesis. The mRNA with high quality with high purification and less contamination was considered for use in the further cDNA synthesis (determined by 260/280 and 260/230 ratios, if the value of the 260/280 ratio was higher than 1.8, which means the mRNA was at high purification level; if the value of 260/230 ratio was higher than 1.8, which means the mRNA sample was not contaminated, then the samples were decided to use in the further studies). During the nanodrop procedure, the mRNA samples need to be kept on ice.

2.3.2 Complementary DNA (cDNA) synthesis

First strand cDNA was synthesized from mRNA using high capacity RNA-to-cDNA kit with 10µl RT Buffer (Applied Biosystems, 4387406) and 1 µl enzyme (Applied Biosystems, 4387406) in a final volume of 20 µL with appropriate volumes of Nuclease free water (NFW), and mRNA samples based on the results of RNA spectrophotometry. The sample loading procedure needed to be performed in an RNase-free surface in a fume hood. The components and samples were

added in RNase-free consumable tubes, and during the sample loading processes, the mRNA samples used in the experiment need to be kept on ice.

The reaction was incubated at 44 ° C for 1 hour and then inactivated at 92 ° C. 80 µl Nuclease free water was finally added to dilute cDNA. The product was aliquoted and stored at -20 ° C for future use. The cDNA quality and concentration were also confirmed using spectrophotometry before qPCR method.

The specific volume of buffer and enzymes for cDNA extraction and the extraction condition were listed under the following tables (Table 2.1 and Table 2.2).

Component	**Component volume per reaction (µl)**	
	+RT	**-RT**
2X RT buffer	10	10
20X Enzyme mix	1	-
RNA Sample	9 (change according to cDNA concentration)	9
NFW	Quantity sufficient to make 20µl	Quantity sufficient to make 20µl
Total per reaction	20µl	20µl

Table2.1: cDNA synthesis buffer

Temperature	**Duration (mins)**
37° C	60
95°C	5
4°C	hold

Table2.2: cDNA synthesis conditions

2.3.3 Quantitative polymerase chain reaction (qPCR)

Master mix for qPCR was prepared with 10 µl SYBR Green master mix (Agilent, 60082), 0.6 µl forward primers, 0.6 µl reverse primers, 0.3 µl dye (diluted 1:50 with nuclease water) (Sigma-Aldrich, 60082) and 7.5 µl NFW for one well in a 96 well qPCR plate. The volumes of master mix, primers and cDNA binding dye are listed below (Table 2.3). The sample loading procedure needed to be conducted in a RNase-free surface in a fume hood and the samples needed to be kept on ice.

Master Mix	**Per Well (µl)**
SYBR	10
Forward Primer	0.6
Reverse Primer	0.6
NFW	7.5
Dye	0.3
total	19

Table 2.3: specific volume of master mix, primers, NFW and dye in 96 well plates.

The primers targeted CSPGs (*Acan*, *Bcan*, *Ncan* and *Vcan*), HAS (*Has1, Has2 and Has3*), *Hapln4*, *TnR*, *Pvalb*, *Gad1* and *Gad2* (Table 2.4). The primer used in the current study based on previous lab experience, including the primer sequences, and concentrations needed to add in each qPCR reaction, was based on the previous studies and experience in our lab (Willis et al., 2020; Willis et al., 2022). Regarding the reference gene, generally, genes used as references for qPCR are related to basic cell functions that are expressed constantly in different conditions, called "housekeeping genes" (Feritas et al., 2019). *Gapdh* was thought to be one of the most common reference genes, which could be used to normalise gene expression data as an endogenous reference in the analysis of qPCR assay (Edwards and Denhardt 1985; Winer et al. 1999). Many previous studies in the group have shown that *Gapdh* expression is stable across many diverse models of schizophrenia neurobiology. Therefore, in the present study, *Gapdh* was selected as the reference gene. However, in terms of collagen3 treated samples, expression of *Gapdh* was observed to change with the treatment, so instead of *Gapdh*, TATA-binding protein (*Tbp*) was chosen as a reference gene.

Target gene	Forward primer sequences (5'-3')	Reverse primer sequences (5'-3')	Supplier
Acan	GTTGCAGACATTGACGAGTGC	AGTCCACCCCTCCTCACATT	Merck
Bcan	GATTCCGGGGTCTATCGCTG	ACGACCCCTTTGACCTTGAC	Merck
Ncan	AGTATGGGGGCCGGATCTGT	TGGTGTCCTGTGTGTCCTGAT	Merck
Vcan	ACCTTCCAACTATCCGGTGC	GGTATGCAGATGGGTTCATG	Merck
Ptprz1	TGCCGCCTGGATAAACCTCTC	CGGTGAAGTTGGGAAGCTGA	Merck
Has1	TGTGTCCTGCATCAGTGGTC	TTGGTGAGGTGCCTGTCATC	Merck
Has2	GCCATGTGGTTTCACAAGCA	TGAGACCCACTAGCTGGACA	Merck
Has3	GCTTCTTTGTGTGGCGTAGC	AGTCCACTGAGTTGCCAAGG	Merck
Hapln4	TCTGGAAGGGGTGGTCTTCC	AAAATGCCATCCTGTTCGGC	Sigma-Aldrich
TnR	GGATATGCGGGATGGACAGG	GAGTCTCCTGCAGTGCCATT	Merck
Pvalb	CAAGCAGTCAGCGCCACTTA	GCGCAAAAGTCCTGTGTGTT	Merck
Gad1	TTTGGAGCTGTCTGACCACC	AAATCGAGGGTGACCTGTGC	Sigma-Aldrich
Gad2	TCCTCTCTTGGCTGTAGCTGA	AGAGTTGGCCCTCTCTACTCC	Sigma-Aldrich
Gapdh	AATGTGTCCGTCGTGGATCT	AGACAACCTGGTCCTCAGTG	Merck
Tbp	TGCTGTTGGTGATTGTTGGT	AACTGGCTTGTGTGGGAAAG	Sigma-Aldrich

Table 2.4 Primer sequences used for qPCR

cDNA samples were used as templates for qPCR. Reactions were performed, in triplicate, in an ABI Prism Sequence Detection System 7000 Software, with 20µl volume in each well containing 1 µl cDNA and 19 µl master mix, with cycling conditions of 1 cycle 50 degree for 2 minutes, 1 cycle 95 degree for 2 minutes, 40 cycles for 30 seconds at 95 ° C and 10 seconds at 60 ° C, followed by a melt curve. The cycle times and temperature were listed in the following Table 2.5.

Stage	Temperature	Time (mins)	Cycle
Stage 1:	50°C	2 minutes	1 cycle
Stage 2:	95°C	2 minutes	1 cycle
Stage 3:	95°C	10 seconds	40 cycles
	60°C	30 seconds	

Table 2.5: qPCR reaction cycle times and temperatures

2.3.4 Primer efficiency tests

The extracted cDNA samples from mouse cortex were diluted in dH_2O in a series dilution of 1/5, 1/25, 1/125 and 1/625. The Ct values of undiluted sample and diluted samples were detected by qPCR with targeted primers. The undiluted and diluted samples used for efficiency test were presented in Table 2.6.

Tube	Sample	Volume of sample	Added dH2O
A	undiluted stock cDNA	10µl	0µl
B	1/5	5µl (from tube A)	5µl
C	1/25	5µl (from tube B)	5µl
D	1/125	5µl (from tube C)	5µl
E	1/625	5µl (from tube D)	5µl

Table 2.6: dilution volumes of samples used in efficiency test.

Following the qPCR, a standard curve of the targeted primers was created with the log value of the dilution quantity and the Ct value of each sample. The slope and R squared values of the standard curve between the log values and the Ct values were calculated by Graphpad Prism 9. The efficiency of the primer was calculated with the slope value with the following equation: efficiency (%) = (10^(-1/The Slope Value)-1)*10. As it was difficult to get 100% primer efficiency for all of the primers, an efficiency of between 90% and 110% was defined as the desired range. Some primer pairs had been tested for amplification efficiency in previous studies in the laboratory. All the efficiencies of the new primers used in this study were presented in Chapter 3.

2.3.5 Data analysis for qPCR

The commonly used method to analyse data from qPCR is 2^-ΔΔCt method, which is a convenient way to analyse the changes in gene expression of the target gene relative to a reference gene (Livak & Schmitten, 2001). Generally, 2^-ΔΔCt values presented the fold changes in gene expression which is normalised to a reference gene. Ct values were provided from the results of qPCR assay, where ΔCt = Ct (target gene) – Ct (housekeeping gene) and ΔΔCt = ΔCt (sample) – ΔCt (control average).

2.4 Protein analysis

2.4.1 Protein extraction from primary neuronal culture

Proteins were extracted from primary neuronal cultures in 12-well plates at 7 and 14 DIV. The plates with neuronal cultures were placed on ice and the medium was removed from the wells. 1mL ice-cold PBS (PH7.4) was added to each well for about 1 minute to wash the cells. After

removing PBS from wells, 60µl RIPA buffer (made up with 50mM Tris-HCL, 150mM NaCl, 1% Triton 100, 0.15 SDS, 0.5% sodium deoxycholate and 50mL dH_2O) with 1% protease inhibitor cocktail (Sigma P-8340) and 1% Sodium orthovanadate was added to the wells for 3 minutes. The wells were then scraped with pipette tips, the contents were transferred to 1.5mL Eppendorf tubes and centrifuged for 10 minutes at 4°C, 13,000 rpm. Supernatants were collected and were stored at 20°C for further use, and the protein concentration was measured using a Bradford Protein Assay (Bradford, 1976). The buffer used in protein extraction were listed in Table 2.7

Solutions and material	Chemical components
RIPA buffer (pH 7.4)	For 500ml RIPA buffer: 0.788g Tris-HCL (Sigma-Aldrich T3038), 4.38g Sodium Chloride (VWR, 27810.295), 0.1461g EDTA anhydrous (Sigma-Aldrich, E8008), 0.5g Sodium Dodecyl Sulfate (Fisher Scientific, S/P530/53), 0.5g Sodium Deoxycholic acid (Sigma Aldrich D-6750), 2.5g Igepal CA-630 (Sigma Aldrich, I7771)

Table 2.7: protein extraction buffer.

2.4.2 Western blot

2.4.2.1 Protein quantification

Following the protein extraction from cultured cells, a Bradford protein assay was used to normalise the protein content of the protein samples. The normalisation of samples was achieved by comparing each protein sample concentration against a standard curve of known protein concentration provided by Bovine Serum Albumin (BSA) (Sigma-Aldrich, A9418-100G). BSA was dissolved in distilled H2O to obtain a concentration (mg/ml) range including 0, 0.25, 0.5, 1.0, 1.5 and 2.0. Each protein sample was diluted 1/400 in distilled H2O. The diluted BSA standard and protein samples were mixed with Bio-Rad protein assay dye reagent (diluted 1:5 in distilled H2O) (Bio-Rad laboratories, UK).

Each BSA standard and protein sample was pipetted in 2 wells in a 96 well plate. The absorbances of the BSA standard and protein sample were measured with an Opsys MR plate reader (Dynex Technologies, UK) using SkanIt software at a wavelength of 595nm. The average reading of the wells with BSA standard was plotted to a standard curve using a linear curve fit. An example of the standard curve and the absorbance reading calculation was showed in figure 2.1.

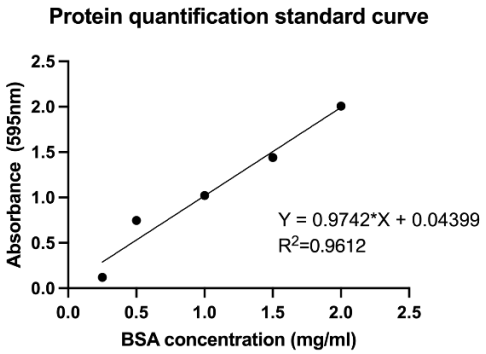

Figure 2.1: BSA curve fitting in a Bradford protein assay: an example of a Bradford standard curve used for quantifying the protein concentration. A linear regression is used to determine the line of best fit and calculate the absorbance of the unknown samples.

2.4.2.2 General method

The protein samples (-1.5μg/μl) were prepared with 4x sample buffer (NuPAGE, Novex, NP0007) and reducing reagent (NuPAGE, Novex, NP0004). Protein samples were denatured at 80°C for 10 minutes in a heating block. Protein samples were diluted in ddH2O to give roughly equal concentrations, and 25μl/lane were added to SDS-PAGE in 4%-12% Bis-Tris pre-cast gels (NuPAGE, Novex, NP0302BOX) and run at 200 volts for 1.5 hours in chilled running buffer.

The gels were then apposed to Invitrogen PVDF membranes (Invitrogen, LC2002) in transfer buffer, and run at room temperature for 1 hour at 30 volts. After the transfer procedure, membranes were then washed twice (10 minutes for each time) in ddH2O and blocked in 0.5% Tween-Tris-buffered-saline (TTBS) with 3% dried milk powder (Marvel) for 30 minutes at room temperature with slow agitation. After the blocking, membranes were incubated with targeted primary antibodies (at appropriate concentration) (table 2-6) at 4°C overnight in 1% TTBS milk with slow agitation. The following morning, membranes were washed 3 times (10 minutes for each wash) in TBS containing 0.05% Tween 20 (Sigma-Aldrich, T7949) and incubated in horseradish peroxidase (HRP) -conjugated anti-mouse/anti-rabbit (depending on the primary antibody) secondary antibodies (anti-mouse concentration: 1:10,000; anti-rabbit concentration: 1:6000 with 1% dried milk in TTBS) for 1.5-2 hours at room temperature. The antibodies that were used in western blots are listed in table2.8.

Membranes were then washed once with TTBS and washed twice with Tris-buffered-saline (TBS) after incubation of secondary antibodies. The bound antibody could be detected by adding chemiluminescent HRP Substrate (Immobilon, Millipore, WBKLS0100) using equal quantities of luminol and peroxide solution. Finally, the membranes were placed into trays and and emitted signal captured using a PXI4 (Syngene) with varying exposure times depending on the antibodies used. Solutions used in western blot were listed in Table 2.9.

Antibody	Species	Dilution	Company/supplier
Bcan	Mouse	1: 1000	Boehringer
Has1	Rabbit	1: 1000	Invitrogen
Has2	Mouse	1: 5000	Genetex
Has3	Rabbit	1: 1000	Genetex
Hapln4	Rabbit	1: 1000	St John's Laboratory
TnR	Rabbit	1: 1000	Genetex
Gad65/67	Rabbit	1:10000	Sigma-Aldrich
Gapdh-HRP conjugated	Rabbit	1:10000	Genetex
Anti-Mouse IgG HRP	Goat	1:10000	Cell Signaling
Anti-Rabbit IgG HRP	Goat	1:6000	Cell Signaling

Table2.8 table of antibodies used in western blot experiments.

Solutions and material	**Chemical components**
20x Running buffer pH7.7	For 500ml running buffer: 104.63g MOPS (Sigma, M8899), 10g Sodium Dodecyl Sulfate, 60.57g Tris-Base (Fisher Scientific BP152-1), 2.92g EDTA Anhydrous (Sigma-Aldrich, E8008).
20x Transfer buffer pH 7.2	For 500ml transfer buffer: 40.79g Bicine (Apollo Scientific, BIB1151), 52.31g Bis-Tris (Apollo Scientific, BI3932), 2.92g EDTA Anhydrous (Sigma-Aldrich, E8008).
10x Tris buffered saline (TBS)	For 1L TBS: 24.228g Tris-Base, 80.063g Sodium Chloride (VWR, 27810.295), 10mL Tween20 (Sigma-Aldrich, T7949).
Blocking solution	1% dried skimmed milk powder (Marvel) diluted in TBS.

Table 2.9: western blot solutions

2.4.2.3 Analysis

The output images from the PXI4 were quantified using ImageJ (shown in Table 2.10). The selected image was converted into grayscales and, by using the rectangular selection tool from the tool bar, a large rectangular frame was drawn around each band in turn. Subsequently, a profile plot was created for each selected band area and a straight line was drawn at the base of each signal, the bottom area which was not included in the signal area was treated as background signal. Each targeted signal was selected by the wand tracing tool, the value of the signal was expressed as a percentage of the total signal of all the signals detected from the rectangular frame section. The targeted band intensity values were measured and normalised to the signal value of *Gapdh* (a reference antibody used to get a relative intensity). Normalised data were expressed as a percentage of vehicle mean.

A	B
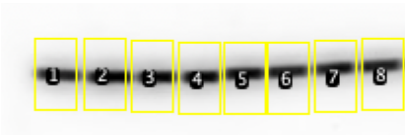	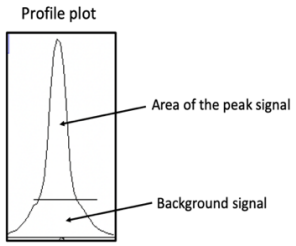

Table 2.10 analysis of western blots with image J. A: rectangular frames were drawn around the targeted bands. B: a profile plot was created for each band, a line was drawn at the base of the signal, the bottom area was background signal. The signal could be selected, and the value of the signal could be calculated.

2.5 Proteasome assay

After treatment with veh or HCA (20nM/100nM), the medium was removed and ice-cold extraction buffer was added to each well. The cells were scraped into an Eppendorf tube and were put on ice. Subsequently, the tubes were centrifuged at 13,000 rpm at 4oC for 10 minutes. The supernatants were transferred into another Eppendorf tube, and the cell samples stored at -20°C for later use.

The 20S proteasomal activity could be quantified by monitoring the accumulation of the fluorescent cleavage product 7-amino-4-methylcoumarin (AMC) (Enzo, 610-028-M010) from the synthetic proteasomal substrates Suc-Leu-Leu-Val-Tyr-AMC (Suc-LLVY-AMC) (Enzo, BML-P802-0005), Boc-Leu-Ala-Ala-AMC (Boc-LAA-AMC) (BML-BW8515-0005) or Ac-Glu-Pro-Leu-Asp-AMC (Ac-GPLD-AMC) (Cayman Chemical, 10008117), and MG132 (Enzo, ALX-092-M001) was used as a control treatment to inhibit proteasome activity. The unconjugated AMC was diluted to appropriate concentrations for a standard curve (0μM, 0.15μM, 0.31μM, 0.625μM, 1.25μM, 2.5μM, 5μM and 10μM). The substrates were diluted to 400μM.

A 96-well plate was used to load samples and unconjugated AMC, and the loading procedure was performed on ice. For each well, 80μl assay buffer, 10μl 400mM substrate, 10μl of sample supernatant and 10μl MG132 were added. The plate plan was showed in Figure 2.2.

The release of the fluorescent proteolysis product was quantified in a Fluoroskan Ascent microplate fluorometer (Thermo Labsystems). The fluorescence of the released AMC was measured every 60s for 30 minutes using excitation wavelength - 340 nm and emission

wavelength - 450 nm. Solutions and materials used in proteasome assay were listed in Table 2.11

Standard curve		Cell extracted with Suc-LLVY		Cells extracted with Boc-LAA		Cells extracted with Ac-GPLD		Cells with MG132			
0 AMC	1.25μM AMC	V1	V3	V1	V3	V1	V3	V1 + MG132	V3 + MG132		
0 AMC	1.25μM AMC	V1	V3	V1	V3	V1	V3				
0.15μM AMC	2.5μM AMC	E1	E3	E1	E3	E1	E3				
0.15μM AMC	2.5μM AMC	E1	E3	E1	E3	E1	E3				
0.31μM AMC	5μM AMC	V2	V4	V2	V4	V2	V4				
0.31μM AMC	5μM AMC	V2	V4	V2	V4	V2	V4				
0.625μM AMC	10μM AMC	E2	E4	E2	E4	E2	E4				
0.625μM AMC	10μM AMC	E2	E4	E2	E4	E2	E4				

Figure 2.2: a plate layout of proteasome assay. V1-V4: veh group samples. E1-E4: HCA treatment group samples.

Solutions and material	Chemical components
Extraction buffer	For 50ml extraction buffer: 25mM HEPES (pH 7.6) (Sigma H7006), 0.5mM EDTA (Gibco, 25300-054).
Assay buffer	For 50ml Assay buffer: 25mM HEPES (pH 7.6), 5.0mM MgCl2 (Sigma Aldrich M1028-100ML), 5mM adenosine 5'-triphosphate (ATP) (Sigma Aldrich A2383).

Table 2.11: proteasome assay solutions

2.6 Brain slice experiments

2.6.1 Slicing preparation and methods

The brains were dissected and stored in 4% paraformaldehyde (PFA) at 4°C overnight and then cryoprotected with 30% sucrose solution (Fisher Scientific S/8606/60) at 4°C. On the day of use, the brains were sectioned with a SM2010R freezing microtome (Leica, UK) into 50μm thick sections and stored in cryoprotectant in 24-well plates. The brain sections were collected from the plates using a fine brush and placed in 1x PBS.

2.7 Immunohistochemistry (IHC)

2.7.1 IHC on primary neuronal culture

The cells were cultured in 8-well chamber slides for IHC at 14 DIV and 21 DIV after HCA and HCA with or without mifepristone treatment for 4h and 24h. Following the drug treatment, the cells were fixed with 4% paraformaldehyde (PFA) at 4°C for 30 minutes. After the fixation, the cells were washed 3 times with PBS and then were stored in PBS at 4°C. On the day of use, cells were permeabilised and blocked with PBS (0.3 M NaCl)/0.25%Triton X-100/10% normal goat serum (NGS) for 1h at room temperature. Following the blocking step, cells were incubated in a humidified chamber with primary antibodies diluted in 0.3 M PBS/0.25%Triton X-100/3% NGS at 4°C overnight. To visualise PNNs, the cells were labelled with biotinylated Wisteria floribunda agglutinin (WFA, Vector Laboratories B-1355–2; 1:2000) lectin, which labelled PNNs

via preferential binding of glycans containing terminal N-acetylgalactosamine β1 residues on the chondroitin sulphate chains which were one of the components of PNNs. Following the primary antibody incubation, cells were washed three times with 0.3M PBS, each wash lasted for 5 minutes. Cells were incubated in appropriate secondary antibodies diluted in 0.3M PBS/3% NGS for 1h in the dark. The WFA was detected with streptavidin-conjugated Rhodamine Red-X (Jackson ImmunoResearch 016-290-084 1:500). After incubation in the dark, cells were washed three times in 0.3M PBS and mounted with Vectashield mounting media (Vector Laboratories, H-1200). Following the mounting step, the slides were finally covered with a coverslip.

2.7.2 IHC on brain sections

Staining was performed on glass slides. The brain sections were washed 2 times, 3 minutes for each time in PBS/Triton X-100 (PBS/TX-100), and were then blocked 15 minutes in 25μM Glycine. After the blocking, the sections were then washed 3 minutes for 2 times in PBS/TX-100. After the washes, the sections were blocked in 3% NGS in PBS for 1 hour at room temperature, followed by 2 x 3 minutes washed in PBS. The sections were then incubated in 3% NGS in PBS with lectin (WFA, 1:1000) overnight at 4°C. On the following day, the brain sections were washed 3 x 3minutes in PBS and incubated in 1% NGS in PBS with biotinylated streptavidin 488: 1/200) in the dark for 2 hours at room temperature. After the incubation, the sections were washed 3 x 3 minutes in PBS and the brain sections were dried overnight. The next day, the slides with brain sections were covered with glass coverslips with Vectashield.

Solutions and materials used in IHC were listed in Table 2.12.

Solutions and material	Chemical components
4% paraformaldehyde (PFA)	For 500ml 4% PFA: 20g of Paraformaldehyde (Fisher Scientific, P/0840/53), 300ml 0.2M phosphate buffer (PB), 200ml dH2O, and a few drops of 1M NaOH (Fluka, 72068)
Cryoprotectant	250 ml of 0.1M PB (Sigma, D5773-50L), 150ml of ethylene glycol (Sigma Aldrich A3889), 100μg sodium azide (Sigma Aldrich S2002), 150g of sucrose (Fisher Scientific S/8606/60), and finally bring the total volume up to 500 ml with 0.1M PB.
Phosphate buffer saline (PBS)	100ml 0.2M PB, 900ml dH2O, and adjust to pH7.4
0.2M phosphate buffer (PB)	Solution A: 18.72g NaH2PO4 (2H2O) (BDH 307164T) in 600ml H2O; Solution B: 42.45g NaH2PO4 (Riedel-de Haen, 04269) in 1500ml dH2O. Add 560ml solution A to 1440 ml solution B and adjust to pH7.4

Table 2.12: IHC solutions.

2.7.3 Cell quantification

The overview of the images was scanned through a confocal microscope (ZEISS, LSM900) with a 10x objective for counting and 20x objective for exhibiting. All exhibited images were captured as a Z-stack (15μM in depth) using a Z step of 0.50μM, 20X objective lens, image size 1024x1024 pixels. The images were taken using Zen blue 3.0 software and downloaded as a summed intensity zen-stack projection in the Zen black system.

Image analysis and cell counting were performed using Image J. The cell number including WFA+, td tomato+ and WFA+/td tomato+ colocalization was counted manually. A step-by-step explanation of the image J counting method was provided in Table 2.13.

Step 1 defining cell types	**Step 2** counting cells by different labels	**Step 3** summarising cell numbers
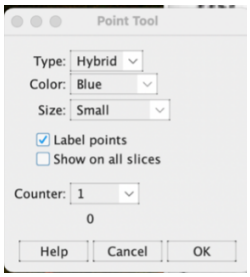 define cell identity code numbers: for example: 1 = td-tomato+; 2 = td-tomato+/WFA+; 3 = WFA+.	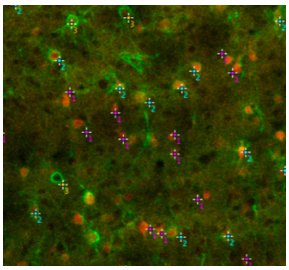 Select and count targeted cells after defining the cell types.	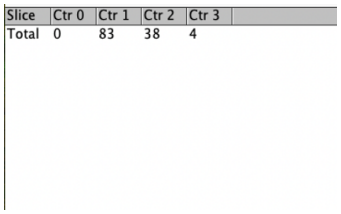 By using the “show all points” tool, the total number of different cell types could be calculated.

Table 2.13: steps involved in cell counting using image J. Three steps were highlighted which explain in general how the manually cell counting works using 3 different labels (1=td-tomato+, 2=td-tomato+/WFA+, 3=WFA+).

2.7.4 PNN measurement

The overview of the images was scanned through a confocal microscope (ZEISS, LSM900) with a 10x objective for counting and 20x objective for exhibiting. All exhibited images were captured as a Z-stack (15μM in depth) using a Z step of 0.50μM, 20X objective lens, image size 1024x1024 pixels. The images were taken using Zen blue 3.0 software and downloaded with a maximum projection size using the Zen black system.

The length of dendrites covered by PNNs and the mean intensity intensity were measured using Image J. The specific steps of Image J measurement method were provided in Table 2.14.

Step 1 set the scale	**Step 2** convert image to black/white	**Step 3** measure neurite length
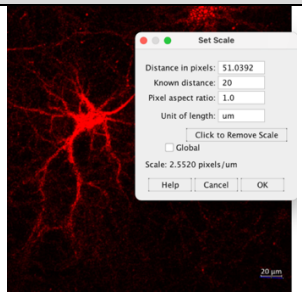 Set the scale for the image based on the scale bar, using the “line” tool in the tool bar	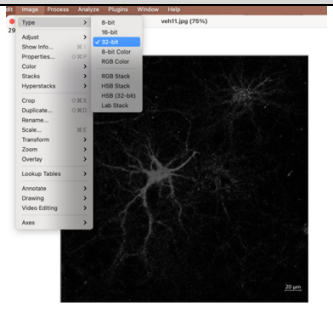 Convert image to 32 bit black and white version	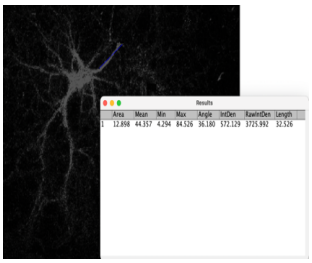 Use the “line” tool, measure the dendrite from start to the end, click measuring or tab ctrl+C+M to detect the mean intensity intensity (Mean) and length.

Table 2.14: procedure of dendritic measurement using image J.

2.8 Statistical analysis

The statistical analysis of the data was performed by Minitab Software (Minitab, USA) and IBM SPSS (version 29).

The descriptive statistics were analysed to describe the essential features of the dataset, with the output of median, mean, standard error of the mean (SEM) and standard deviation (SD).

The exclusion criteria for a data that could be treated as an outlier was set, when the value of the data was more than 2 times SD from the mean, the data was determined as an outlier and was decided to be removed. The specific removal of the outliers in each data set was further detailed in the following chapters.

The normality of the data was then assessed with Kolmogorov-Smirnov Test. The normality was depend on the p value reported from the Kolmogorov-Smirnov Test, when p value is less than 0.05, the data was not normally distributed, and when p value is more than 0.05, the data was treated as normally distributed.

Based on the outcome of normality tests, the data showing a normal distribution were analysed using Minitab Software (Minitab, USA) with ANOVA followed by Tukey's post-hoc tests; and non-normally distributed data were analysed using IBM SPSS (version 29) with Kruskal-Wallis test followed by Dunn's post-hoc tests. Statistical significance was accepted at $p<0.05$.

For the normally distributed data, the related graphs were presented as bar graphs with mean ± SEM; in terms of data which were not normally distributed, the graphs were presented as box and whisker plots with median, interquartile range (IQR) and 95% confidence intervals (CI).

2.9 Experimental consideration

The experiments described in the current study were not performed in a blind condition. In a blind experimental condition, the experimenter is not aware of the specific treatment groups, which could eliminate the subjective biases or other related biases where the experimental results could be influenced by the experimenter's own ideas. However, in the biochemical studies, such as, qPCR or western blot, the blinding condition was not as important as it would be in the behavioural or clinical trials, using animal or human participants. The results of the biochemical studies, or the results from different assays, were not easily influenced by subjective biases, and it was not easy for the experimenter alone to perform a total blind experimental condition during the sample collection and in different assay procedures. Thus, in some experiments, such as qPCR which were largely used in the current research, western blot, cell staining and proteasome assays, the experiments were not in a blind condition.

Chapter 3

Altered mRNA expression of PNN components in GCs treated cortical neurons

3.1 Introduction

Perineuronal nets (PNNs) are a structure of extracellular matrix (ECM). Most fast-spiking GABAergic interneurons, especially parvalbumin (Pv)-expressing interneurons, are fully enveloped by PNNs after maturation (Kwok et al., 2011; Morawski et al., 2004).

Emerging studies reported alterations caused by stress on PNN expression among different species. Several studies suggested that PNN formation and construction are disrupted by external stressors, with a reduction of staining intensity or density in various brain regions, such as hippocampus, PFC, or basolateral amygdala after exposure to chronic stress, in juvenile or adult rodents (Ueno et al., 2016; Santiago et al., 2018; Gomes et al, 2019).

After stress induction, GCs are secreted from the cortex of adrenal glands (Rabin, et al., 1988). As key stress hormones, GCs were demonstrated to affect expression of various target genes, such as suppressing the expression of various inflammatory genes and attenuation of inflammation (Barnes and Adcock., 2009) by inhibiting the activity of inflammatory transcription factors; and downregulating the expression of cartilage extracellular matrix-degrading matrix metalloproteinases (MMPs) 1, 13, and 16 (Pemmari et al., 2020).

In addition to inhibitory effect of GCs on inflammatory genes and extracellular MMP expression, studies also reported different effects of GCs on PNN expression. Increased aggregation of PNNs and *Bcan* mRNA levels was reported after the administration of one of the stress related hormones, corticosterone (Alaiyed et al., 2020). With the administration of GCs, downregulation of PNNs covering PV-expressing interneurons was observed in mice hippocampus and PFC (Uchida et al.,2014); and *Has2* expression was also suggested to decrease dramatically after dexamethasone injection (Pemmari et al., 2020). A similar inhibition effect was also shown in PNNs in cultured cells with methylprednisolone, a synthetic GC, with reduced CSPG expression reported in astrocytes at 14 to 18 DIV (Liu et al., 2008).

There is limited research reporting the modulatory effect of specific drugs on specific PNN components expression, for example, BDNF stimulation was demonstrated to upregulate the mRNA levels and protein expression of *Bcan*, *Vcan*, *Ncan* and a GABAergic interneuron related molecule, *Gad1* (Willis et al., 2020). Several previous studies have investigated the stress or GCs induction effects on general PNN expression, and most of the studies focused on the expression in rodent brains. Whether GCs affect specific PNNs components in cultured cells remained less clear.

Hydrocortisone acetate (HCA) is one of the GC, which binds to GRs, albeit with lower affinity compared to other corticosterone receptors, such as, MRs (Sayers et al, 2024). Therefore, the current study aimed to investigate the effect of one of the GCs, HCA, on PNN components in cortical cultured cells. As PNNs surround mainly Pv-expressing GABAergic interneurons (Cabungcal et al., 2013; Morishita et al., 2015), GABA related components, including glutamate decarboxylase (Gad) and Pv-expressing components, were also related to the stress-affected PNNs. Therefore, the mRNA alterations of Pv, Gad1 and Gad2 after HCA exposure were also measured in the current study.

3.2 Study aim

The current study aimed to investigate whether there are alterations in the expression of PNN components after exposure to GCs in the neuronal developing period. The specific research objectives in this chapter were:

a. to investigate the effect of HCA (GC) on the expression of PNN components, including mRNA expression and protein expression. This to include a short time point (4h) potentially too rapid for canonical (genomic) GC effects, as well as a more conventional time point (24h), and a low concentration (20nM) potentially too low for canonical (genomic) GC effects, as well as a more conventional concentration (100nM).

b. to investigate whether the alterations of expression were reversed by mifepristone (Mif, RU486) (antagonist of GC receptors) to determine possible pathways of how HCA affect PNNs components.

3.3 Methods

To investigate the effect of GCs on PNNs components and PNN covered GABAergic neruons (Pv, Gad) in vitro, one of the GCs, HCA, were treated into developing cultured cells at 7 DIV, 14 DIV and 21 DIV with 2 different concentrations (20nM and 100nM) and with 2 different exposure time points (4h and 24h). The vehicle group were treated with nuclease-free water. To examine whether the altered expression was reversed by mifepristone, 20nM mifepristone were treated to cultured cells prior 30 minutes before HCA treatment. The specific reason for deciding to use the specific concentration of the drugs was presented in Chapter2, section 2.1.2.

The mRNA samples were extracted from treated cultured neurons, and cDNA samples synthesised as performed in Chapter 2. The mRNA expression of PNNs components were measured by qPCR described in Chapter 2 with cDNA samples and targeted primers.

Western blotting was performed as described in Chapter 2. For the mifepristone studies, the number of samples was too great to be run on a single gel. To normalise a common measure in every blot and enable comparison of results, integrated intensities of each protein signal were divided by the average of the vehicle groups, which showed a fold change of integrated intensity relative to vehicle group as plotted in each blot. Therefore, in the mifepristone and HCA cotreated western blot analysis, vehicle groups were also presented in the blots with mifepristone treated groups.

3.4 Results

3.4.1 Efficiency tests curves for targeted primers

Before examining the mRNA expression of PNNs and GABA-related components, efficiency tests of the targeted primers were conducted to determine the quality of cDNA samples and targeted primers and avoid false calculation of fold changes of mRNA expression. The standard curve of targeted primers were analysed and the efficiency was calculated (Fig.3.1). Efficiency (%) of targeted primers ranged from 89.09% to 117.62%, which were approximately in the desired range (90% to 110%). Attempts were also made to detect *Hapln*1, *Hapln2* and *Hapln3*, but they appeared to be below the threshold for reliable detection (Ct's ~ 33 or higher)

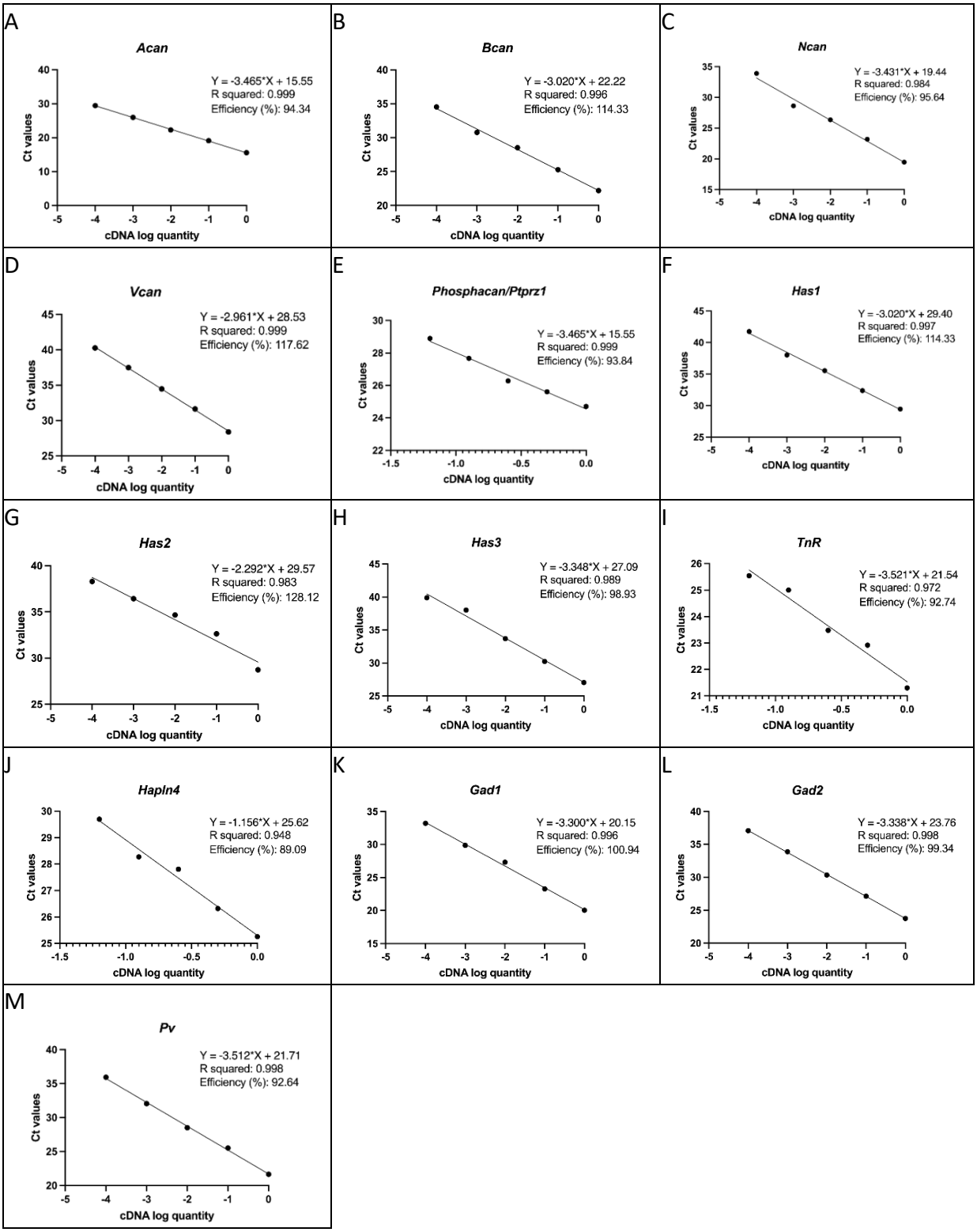

Figure 3.1: efficiency curves of targeted primers: A-J efficiency curves of PNNs-related primers; K-M: efficiency curves of GABA-related primers

3.4.2 HCA treatment altered the mRNA expression of PNN components during neuronal development period

3.4.2.1 *Gapdh*

Initial experiments established that *Gapdh* expression did not appear to be systematically and significantly affected by any of the HCA treatments (Fig.3.2)

No significant effects of HCA with or without mifepristone were reported on *Gapdh* expression (initial HCA experiment: 7 DIV: 4h: $F(2, 44)=0.49$, $p=0.616$, 24h: $F(2, 44)=0.17$, $p=0.843$; 14 DIV 4h: $F(2, 21)=0.98$, $p=0.393$, 24h: $F(2, 21)=0.47$, $p=0.630$; 21 DIV 4h: $F(2, 18)=0.10$, $p=0.909$, 24h: $F(2, 19)=0.82$, $p=0.300$; following HCA+Mif experiment: 7 DIV: 4h: $F(2, 42)=2.00$, $p=0.148$ 24h: $F(2, 42)=2.94$, $p=0.112$; 14 DIV 4h: $F(2, 42)=0.89$, $p=0.420$, 24h: $F(2, 42)=1.41$, $p=0.257$; 21 DIV: 4h: $F(2, 42)=0.03$, $p=0.974$, 24h: $F(2, 42)=0.32$, $p=0.726$).

In addition to the absence effect of HCA, mifepristone did not affect *Gapdh* expression either (7 DIV: 4h: $F(2, 42)=0.40$, $p=0.529$ 24h: $F(2, 42)=2.26$, $p=0.116$; 14 DIV 4h: $F(2, 42)=0.25$, $p=0.623$, 24h: $F(2, 42)=3.77$, $p=0.095$; 21 DIV: 4h: $F(2, 42)=0.87$, $p=0.355$, 24h: $F(2, 42)=0.04$, $p=0.837$)

No interactions of HCA*mifepristone were reported on the expression of *Gapdh* (7 DIV: 4h: $F(2, 42)=1.79$, $p=0.131$ 24h: $F(2, 42)=1.09$, $p=0.347$; 14 DIV 4h: $F(2, 42)=2.98$, $p=0.062$, 24h: $F(2, 42)=0.48$, $p=0.624$; 21 DIV: 4h: $F(2, 42)=0.09$, $p=0.910$, 24h: $F(2, 42)=0.33$, $p=0.723$)

The stability of *Gapdh* with external stimulation was consistent with previous studies in the laboratory (Willis et al., 2021).

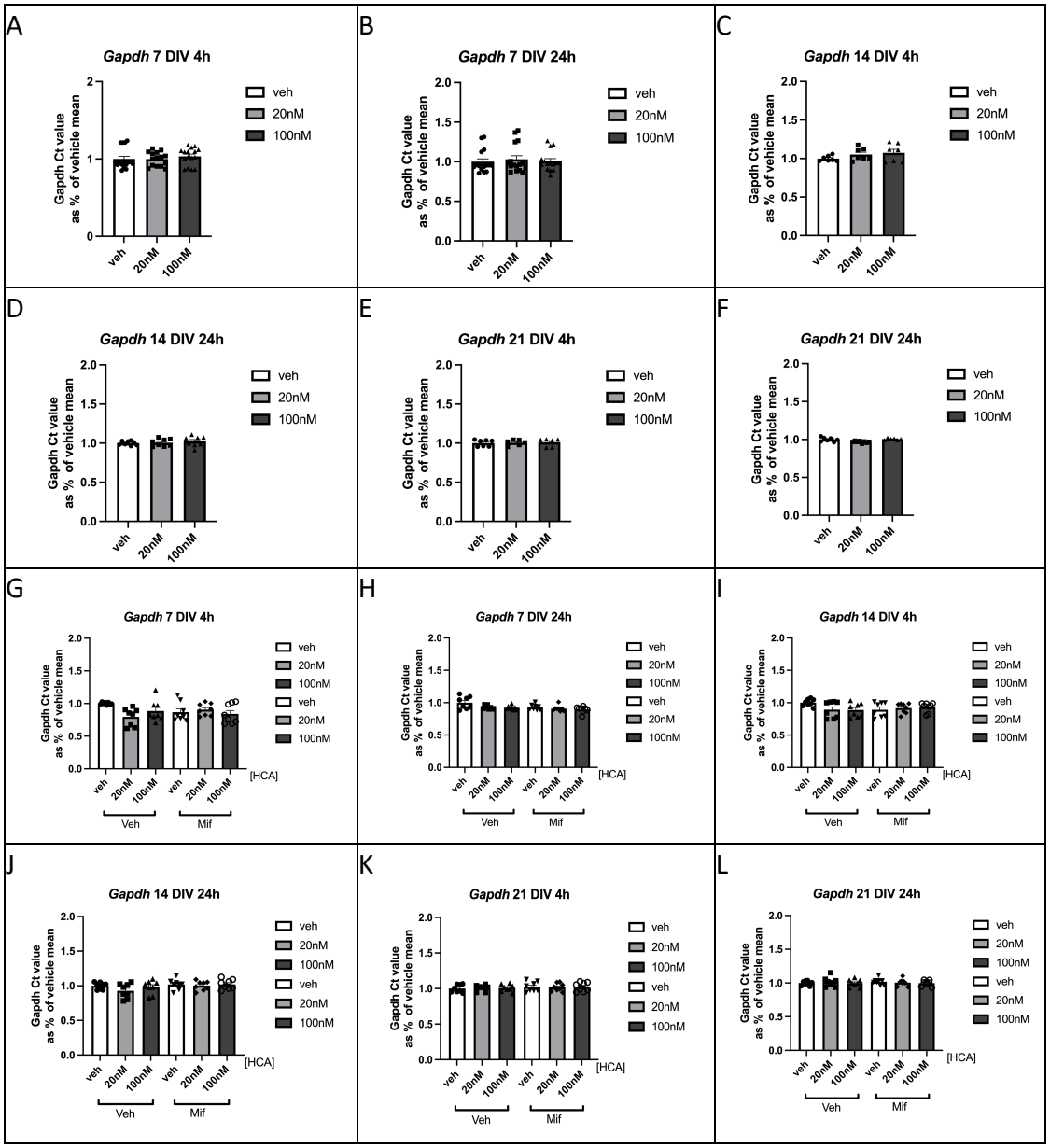

Figure 3.2. mRNA levels of *Gapdh* after exposure to low dose (20nM) and high dose (100nM) HCA for 4h and 24h with or without mifepristone. The mRNA levels remained unchanged at 7, 14 and 21 DIV with low dose (20nM) and high dose (100nM) HCA treatment for 4h and 24h A-F mRNA level of *Gapdh* without mifepristone treatment: (4h: 7 DIV: n=43 in total, veh=16, low dose=14, high dose=14; 14 DIV: n=20 in total, veh=6, low dose=8, high dose=7; 21 DIV: n=18 in total, veh=7, low dose=6, high dose=6; 24h: 7 DIV: n=48 in total, veh=16, low dose=164, high dose=16; 14 DIV: n=22 in total, veh=8, low dose=7, high dose=7; 21 DIV: n=20 in total, veh=7, low dose=7, high dose=6). G-J: mRNA levels of *Gapdh* cotreated with mifepristone at 7, 14 and 21 DIV (7 DIV 4h: n=45 in total, HCA: veh=8, low dose samples=8, high dose samples=7; HCA+Mif: veh=8, low dose samples=7, high dose samples=7, 24h: n=46 in total, HCA: veh=6, low dose samples=8, high dose samples=8; HCA+Mif: veh=8, low dose samples=8, high dose samples=8; 14 DIV: 4h: n=46 in total, HCA: veh=7, low dose samples=8, high dose samples=8; HCA+Mif: veh=7, low dose samples=8, high dose samples=8; 24h: n=46 in total, HCA: veh=7, low dose samples=8, high dose samples=8; HCA+Mif: veh=7, low dose samples=8, high dose samples=8; 21 DIV: 4h: n=45 in total, HCA: veh=7, low dose samples=8, high dose samples=8; HCA+Mif: veh=7, low dose samples=8, high dose samples=7; 24h: n=45 in total, HCA: veh=8, low dose samples=6, high dose samples=8; HCA+Mif: veh=8, low dose samples=7, high dose

samples=8). The dataset of *Gapdh* with HCA treatment at each timepoint was normally distributed as assessed with the Kolmogorov-Smirnov test, and no outliers were found. The data was analysed by ANOVA followed by Tukey's post-hoc tests. The bar graphs show mean ± SEM.

3.4.2.2 *Acan*

There was a decreasing tendency of *Acan* mRNA expression at 7 DIV with 4h HCA treatment, but the results were not significant (7 DIV 4h: Kruskal–Wallis statistic=4.68, p= 0.096) (Fig.3.3 A), and *Acan* expression showed changes after 24h HCA treatment (7 DIV 24h: Kruskal–Wallis statistic=2.82, p= 0.244) (Fig.3.3 B). No significant effects were detected at 14 or 21 DIV with both 4h and 24h HCA treatment (14 DIV 4h: Kruskal–Wallis statistic=0.62, p= 0.734, 24h: Kruskal–Wallis statistic=3.27, p=0.195; 21 DIV: 4h: Kruskal–Wallis statistic=3.00, p=0.223, 24h: Kruskal–Wallis statistic=3.91, p=0.141) (Fig.3.3 C-F).

Following detecting the effect of HCA alone, mifepristone was cotreated with HCA to detect potential mediation by GRs. At 7 DIV, although no significant mRNA expression changes of *Acan* (Fig.3.3 A) were detected, there was a decreasing tendency shown. Therefore, it was still worth testing whether the effect of HCA could be observed with and without mifepristone. As a result, no significant effect of HCA was shown with 4h exposure (Kruskal–Wallis statistic=2.89, p=0.235) (Fig.3.3 G), although there was a hint of a suppression (p=0.069 veh without mifepristone vs 20nM HCA without mifepristone, post-hoc Dunn's test). Mifepristone showed an overall tendency to increase *Acan* expression; however, the significance was at a borderline (Kruskal–Wallis statistic=3.75, p=0.053). The results suggested that there was some basal suppression of *Acan* expression by GCs, which limited the ability to detect further suppression with HCA application and showed a tendency to slightly increase with mifepristone exposure.

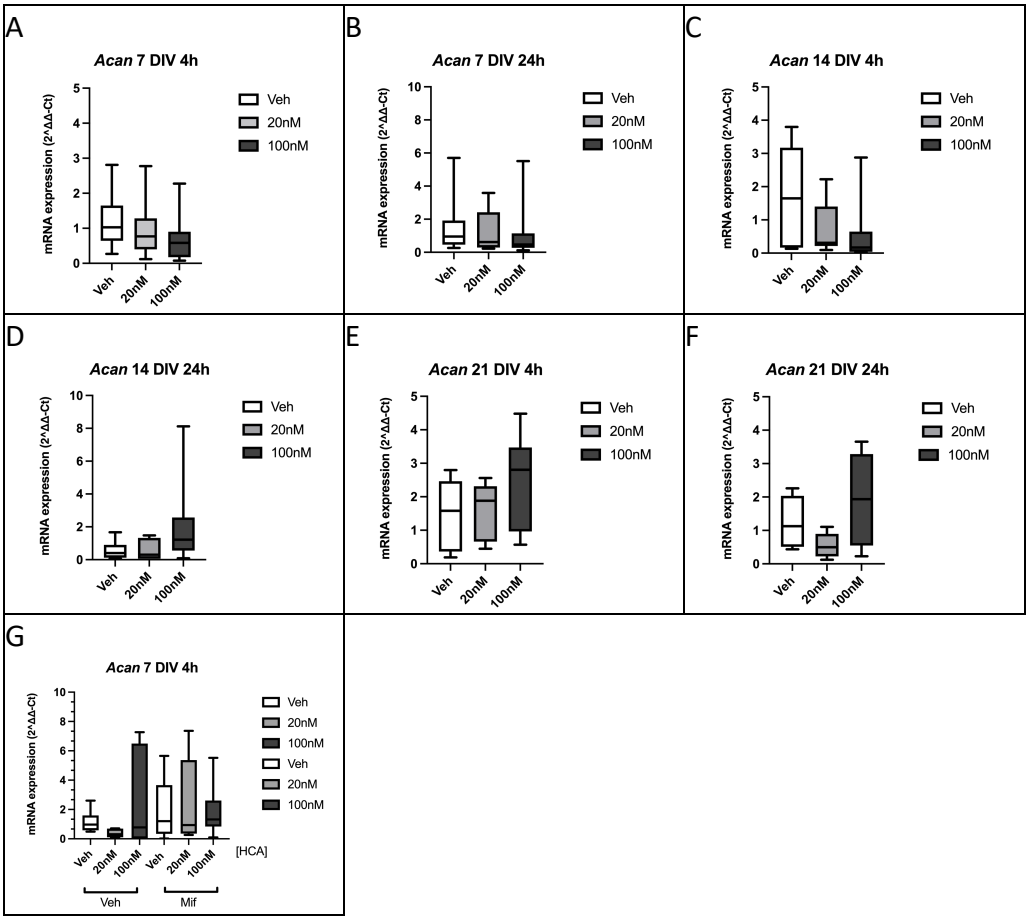

Figure 3.3: mRNA expression of *Acan*. A-F: *Acan* mRNA levels after 4h or 24h exposure to low dose HCA, high dose HCA at 7, 14 and 21 DIV, The mRNA expression tend to decrease at 7 DIV after 4h exposure, but no significant changes were observed at 14 and 21 DIV (4h: 7 DIV: n=43 in total, veh=16, low dose=14, high dose=14; 14 DIV: n=20 in total, veh=6, low dose=8, high dose=7; 21 DIV: n=18 in total, veh=7, low dose=6, high dose=6; 24h: 7 DIV: n=48 in total, veh=16, low dose=164, high dose=16; 14 DIV: n=22 in total, veh=8, low dose=7, high dose=7; 21 DIV: n=20 in total, veh=7, low dose=7, high dose=6). G: *Acan* mRNA levels with mifepristone (20nM) exposure at 7 DIV with 4h HCA treatment (n=45 in total, Veh: veh=8, low dose samples=8, high dose samples=7; Mifepristone: veh=8, low dose samples=7, high dose samples=7). The dataset of *Acan* with HCA treatment at each timepoint was generally not normally distributed based on Kolmogorov-Smirnov test results, and no outliers were found. The data were analysed by Kruskal-Wallis test followed by a Dunn's post-hoc test. Boxes show median and interquartile range, with whiskers from minimum to maximum.

3.4.2.3 *Bcan*

No significant changes in *Bcan* gene expression were detected at 7 DIV (4h: $F(2, 43) = 2.80$, $p=0.072$; 24h: $F(2, 47) = 0.85$, $p=0.436$) (Fig.3.4 A B); the expression showed a tendency to decrease after 4h exposure to low dose and high dose HCA treatment at 14 DIV, although the post-hoc test did not reach a significant level ($F(2, 19) = 3.62$, $p=0.048$; veh vs low dose: $p=0.061$, veh vs high dose $p=0.084$, Tukey's post-hoc tests), and no alterations were found after 24h HCA treatment (24h: $F(2, 21) = 0.53$, $p=0.596$) (Fig.3.4 C D). Similarly, at 21 DIV, no significant effect of HCA was shown on the *Bcan* expression with 4h HCA treatment ($F(2, 18) = 1.06$, $p=0.704$), but showed an increased effect at 24h after high dose HCA treatment, and a tendency to increase with low dose HCA treatment but it did not reach the statistical significance

level (F (2, 19) =5.07, p=0.018; veh vs low dose p=0.063, veh vs high dose p=0.020, Tukey's post-hoc tests) (Fig.3.4 E F).

In the following mifepristone experiment, at 14 DIV, no significant effect of HCA was found at 4h (F (2, 46) =1.19, p=0.316), and mifepristone did not affect the overall expression of *Bcan* either (F (2, 46)=0.29, p=0.592); although there was a significant interaction of HCA and mifepristone treatment at 4h, the post-hoc test did not show any significant differences between the mRNA levels in different treatment group with mifepristone compared to the mRNA levels in different treatment group without mifepristone (F (2, 46) =3.63, p=0.036, veh with mifepristone vs veh without mifepristone p=0.160, 20nM HCA with mifepristone vs 20nM HCA without mifepristone p=0.999, 100nM HCA with mifepristone vs 100nM HCA without mifepristone p=0.851, Tukey's post-hoc tests) (Fig.3.4 G). There was a significant effect of HCA treatment on *Bcan* mRNA expression at 14 DIV after 24h (F (2, 46) =6.85, p=0.003), although there was a decreased tendency of *Bcan* showed after low dose HCA, but the post-hoc test suggested the decreasing tendency was not significant in both group with or without mifepristone (veh without mifepristone vs low dose HCA without mifepristone p=0.147, veh without mifepristone vs high dose HCA without mifepristone p=0.999; veh with mifepristone vs low dose HCA with mifepristone p=0.106, veh with mifepristone vs high dose HCA with mifepristone p=0.588, Tukey's post-hoc tests) (Fig.3.4 H). In addition, no overall mifepristone effect was detected at 14 DIV with 24h treatment (F(2, 46)=0.97, p=0.329), and there was no significant interaction of mifepristone and HCA treatment (F(2, 46)=0.51, p=0.603).

However, at 21 DIV, the expression of *Bcan* was not affected by HCA significantly at 4h (F(2, 44)=0.59, p=0.560) (Fig.3.4 I). The effect of mifepristone was not significant either at 4h (F(1, 44)=0.01, p=0.936), no interaction of mifepristone and HCA treatment was found at 4h (F(1, 44)=1.24, P=3.000). Similarly, at 24h, no significant effect of HCA was reported (F(2, 44)=2.78, p=0.075) and there was no overall effect of mifepristone (F(1, 44)=1.58, p=0.217), the interaction of HCA and mifepristone was not reported to reach the significant level (F(1, 44)=0.78, p=0.466) (Fig.3.4 J). These complex effects suggested a rapid non-GR-mediated suppression of *Bcan* expression by HCA, although the suppression effect was not replicated in the following mifepristone experiment. The reason could be attributed to the variability between cell cultures and different biological samples.

Although several *Bcan* mRNA alterations were observed at 14 DIV, the protein expression of *Bcan* (155kDa) remained unchanged after 4h HCA exposure (F(2, 26)=1.5, p=0.227), but the 145kDa band of *Bcan* was not clearly expressed (Fig.3.4 K). With mifepristone cotreatment, no significant changes were observed on *Bcan* (155kDa/145kDa) protein levels with 4h HCA exposure (155kDa: F(2, 47)=0.97, p=0.389; 145kDa: F(2, 47)=2.64, p=0.083), and no overall mifepristone effect was shown (155kDa: F(1, 47)=1.54, p=0.221; 145kDa: F(1, 47)=0.21, p=0.652), the significant interaction of HCA and mifepristone was not detected (155kDa: F(2, 47)=0.27, p=0.765; 145kDa: F(2, 47)=0.38, p=0.686) (Fig.3.4 L). Similarly, after 24h, no effect of HCA was significantly reported in terms of the *Bcan* protein levels (155kDa: F(2, 47)=0.77, p=0.469; 145kDa: F(2, 47)=1.10 p=0.342). Moreover, there were no overall effects of mifepristone (155kDa: F(1, 47)=0.00, p=0.963; 145kDa: 24h: F(1, 47)=0.23, p=0.631) and no significant interactions of HCA and mifepristone was detected (155kDa: F(2, 47)=0.28, p=0.759; 145kDa: F(2, 47)=1.73, p=0.190) (Fig.3.4 M). In the western blot, we used *Gapdh* as a reference gene, which was quite stable with external drug treatment, such as HCA; but in the current study, some *Gapdh* protein signals showed slight differences, this differences might be attributed to the different expression of *Gapdh* protein signals with different drug treatment, or the sample loading error in western blot procedure, which will be further discussed in the discussion section (Section 3.5).

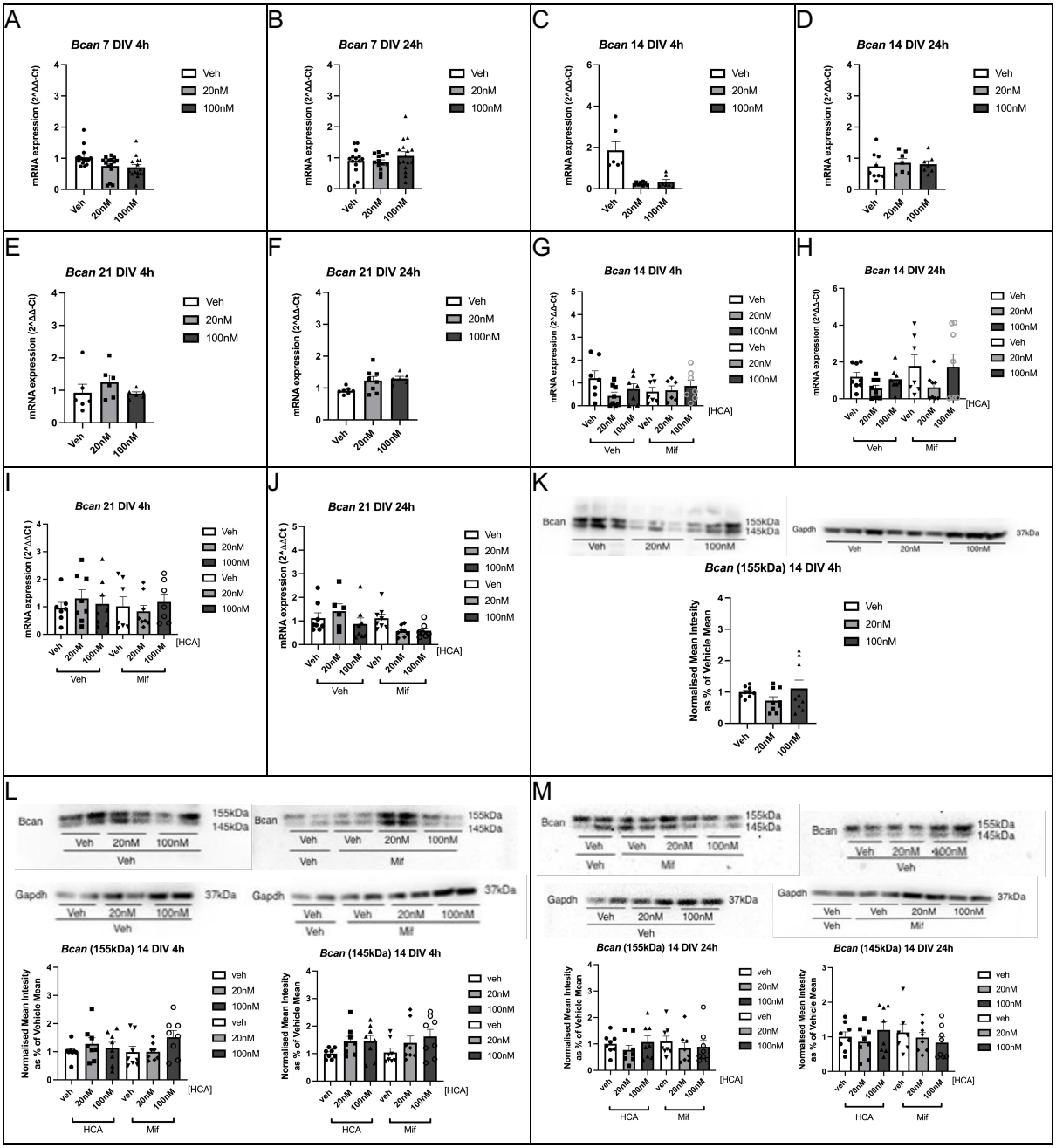

Figure 3.4: mRNA and protein expression of *Bcan* at 7, 14 and 21 DIV. A-F: mRNA expression of *Bcan* after 4h and 24h exposure to low dose (20nM) and high dose (100nM) at 7, 14 and 21 DIV (4h: 7 DIV: n=43 in total, veh=16, low dose=14, high dose=14; 14 DIV: n=20 in total, veh=6, low dose=8, high dose=7; 21 DIV: n=18 in total, veh=7, low dose=6, high dose=6; 24h: 7 DIV: n=48 in total, veh=16, low dose=164, high dose=16; 14 DIV: n=22 in total, veh=8, low dose=7, high dose=7; 21 DIV: n=20 in total, veh=7, low dose=7, high dose=6). G-J: mRNA levels of *Bcan* cotreated with mifepristone at 14 and 21 DIV (14 DIV: 4h: n=46 in total, HCA: veh=7, low dose samples=8, high dose samples=8; HCA+Mif: veh=7, low dose samples=8, high dose samples=8; 24h: n=46 in total, HCA: veh=7, low dose samples=8, high dose samples=8; HCA+Mif: veh=7, low dose samples=8, high dose samples=8; 21 DIV: 4h: n=45 in total, HCA: veh=7, low dose samples=8, high dose samples=8; HCA+Mif: veh=7, low dose samples=8, high dose samples=7; 24h: n=45 in total, HCA: veh=8, low dose samples=6, high dose samples=8; HCA+Mif: veh=8, low dose samples=7, high dose samples=8). K-M: Protein expression and related box plots with *Bcan* normalised mean intensity of the bands' signals after HCA and mifepristone exposure at 14 DIV with 4h and 24h exposure with or without mifepristone treatment (4h: HCA: n=27 in total,

veh=9, low dose=9, high dose=9; HCA+Mif: n=48 in total HCA: veh=8, low dose=8, high dose=8, Mif: veh=8, low dose=8, high dose=8; 24h: HCA: n=27 in total, veh=9, low dose=9, high dose=9; HCA+Mif: n=48 in total HCA: veh=8, low dose=8, high dose=8, Mif: veh=8, low dose=8, high dose=8). The normality of *Bcan* dataset was generally normally distributed as assessed with the Kolmogorov-Smirnov test, no outliers were detected. The data were analysed by ANOVA followed by Tukey's post-hoc tests. The bar graphs show mean ± SEM.

3.4.2.4 *Ncan*

The mRNA expression of *Ncan* at 7 DIV was decreased by high dose HCA at 4h ($F(2, 47) = 4.24$, $p=0.021$, veh vs high dose $p=0.025$ Tukey's post-hoc tests) (Fig.3.5 A); but no effect were observed at 24h HCA treatment ($F(2, 45) = 0.16$, $p=0.85$) (Fig.3.5 B). There is a suggestion of increased *Ncan* expression 4h after HCA treatment at 14 DIV, although the variability was large and this effect did not reach statistical significance ($F(2, 20) = 3.03$, $p=0.073$; low dose HCA vs veh $p=0.062$, Tukey's post-hoc test) (Fig.3.5 C). No significant changes in *Ncan* expression were detected 24h after treatment at 14 DIV ($F(2, 22) = 0.09$, $p=0.92$) (Fig.3.5 D); or at either time point at 21 DIV (4h: $F(2, 17) = 1.50$, $p=0.26$; 24h: $F(2, 20) = 1.66$, $p=0.22$) (Fig.3.5 E F).

With co-exposure of mifepristone and HCA at 7 DIV, a significant effect of HCA on *Ncan* was detected after 4h ($F(2,45)=7.66$, $p=0.002$), and the Tukey's post-hoc tests revealed that the mRNA expression decreased relative to vehicle treatment with low dose HCA treatment at 4h in the absence of mifepristone (veh without mifepristone vs low dose HCA without mifepristone $p=0.008$ Tukey's post-hoc test) (Fig.3.5 G). This partially reproduced the earlier finding that high dose HCA could suppress the *Ncan* expression (Fig.3.5 A), but the expression decreased with the low dose HCA treatment was reported here. Moreover, no significant changes were observed with 4h HCA exposure in the presence of mifepristone (veh with mifepristone vs low dose HCA with mifepristone, $p=0.869$, veh with mifepristone vs high dose HCA with mifepristone, $p=0.683$, Tukey's post-hoc tests). No overall mifepristone effect was reported in terms of the *Ncan* mRNA levels ($F(2,45)=1,06$, $p=0.310$) (Fig.3.5 G). However, the interaction of mifepristone and HCA treatment was significant after 4h ($F(2, 45)=9.79$, $p<0.001$), suggesting the level of low dose HCA treated *Ncan* without mifepristone increased after mifepristone presence (low dose HCA without mifepristone vs low dose HCA with mifepristone, $p=0.002$, Tukey's post-hoc test), indicating the presence of mifepristone with GR inhibition could potentially affect the HCA effect on *Ncan* with 4h HCA exposure.

A similar reduction of *Ncan* expression was shown after both low dose and high dose HCA at 7 DIV with 24h treatment in the absence of mifepristone ($F(2, 45)=4.96$, $p=0.012$, veh without mifepristone vs low dose HCA without mifepristone $p=0.017$, veh vs high dose HCA $p=0.036$, Tukey's post-hoc tests) (Fig.3.5 H), which was not in line with the initial HCA results (Fig.3.5 B). and the reduction was also detected in the presence of mifepristone, with a reduction of mRNA levels but only after low dose HCA treatment (veh with mifepristone vs low dose HCA with mifepristone, $p=0.023$, Tukey's post-hoc tests). Additionally, there was an overall effect of mifepristone ($F(2, 45)=12.47$, $p=0.001$), with the overall reduction of *Ncan* mRNA expression (Fig.3.5 H). But the interaction of HCA and mifepristone was not significant at 24h treatment ($F(2, 45)=2.20$, $p=0.124$). The results indicated that suppressive effect of HCA on *Ncan* was not mediated by the activation of GRs; while after the mifepristone treatment, significant decrease of *Ncan* mRNA levels was reported, suggesting a basal slow-acting elevation of *Ncan* expression by GRs in culture medium.

Although the current results on *Ncan* reported partially consistent rapid suppressive effects of HCA at 7 DIV, the initial HCA experiment suggested that high dose HCA decreased the *Ncan*

mRNA levels, and the following mifepristone experiment, it showed a suppressive effect by low dose HCA. This variability between these 2 experiments might be due to the variability between different biological samples in different culture sets, which might lead to the variations, such as variable concentration and purification of the neurons, and this might in turn lead to the different results.

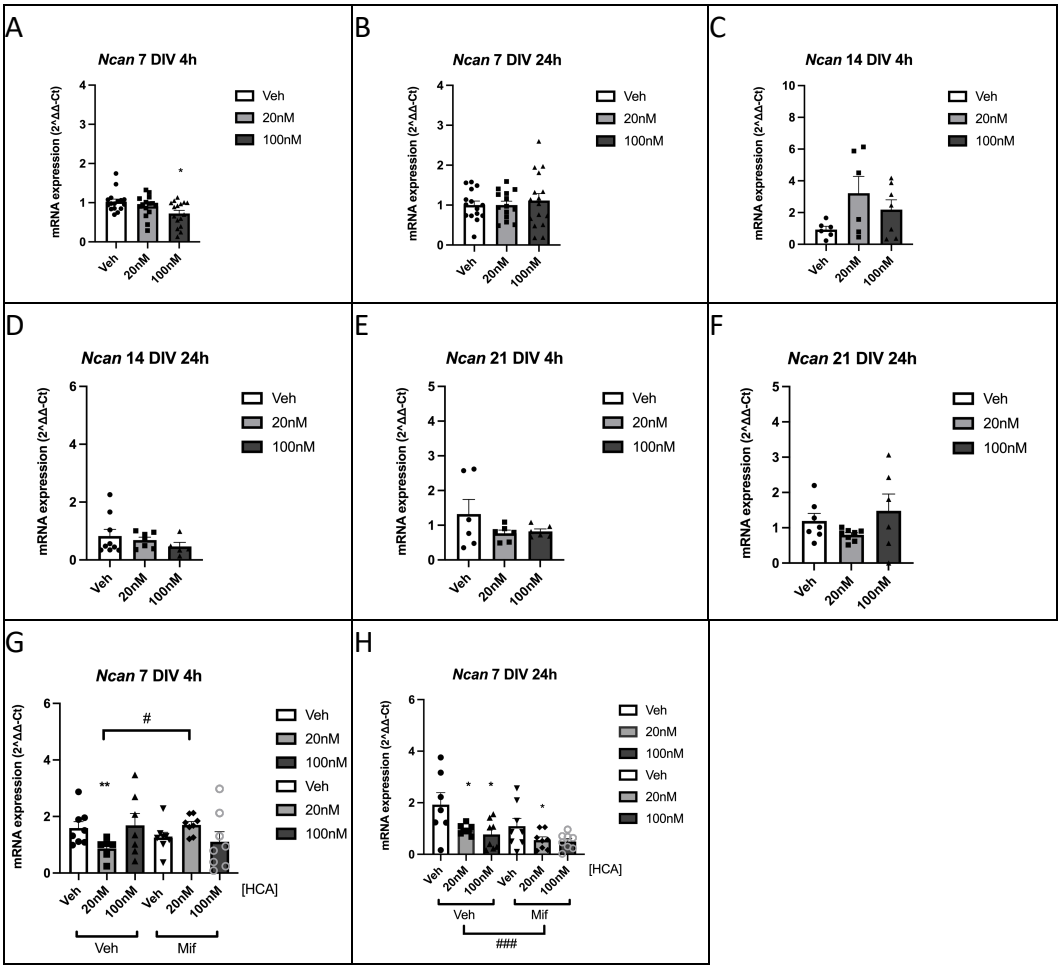

Figure 3.5: mRNA expression of *Ncan.* A-F: mRNA expression of *Ncan* after 4h and 24h exposure to low dose (20nM) and high dose (100nM) HCA, at 7, 14 and 21 DIV (4h: 7 DIV: n=43 in total, veh=16, low dose=14, high dose=14; 14 DIV: n=20 in total, veh=6, low dose=8, high dose=7; 21 DIV: n=18 in total, veh=7, low dose=6, high dose=6; 24h: 7 DIV: n=48 in total, veh=16, low dose=164, high dose=16; 14 DIV: n=22 in total, veh=8, low dose=7, high dose=7; 21 DIV: n=20 in total, veh=7, low dose=7, high dose=6). G-H: mRNA levels of *Ncan* after low dose (20nM) and high dose (100nM) HCA and cotreatment of mifepristone (20nM) at 7 DIV (4h: n=45 in total, HCA: veh=8, low dose samples=8, high dose samples=7; HCA+Mif: veh=8, low dose samples=7, high dose samples=7; 24h: n=46 in total, HCA: veh=6, low dose samples=8, high dose samples=8; HCA+Mif: veh=8, low dose samples=8, high dose samples=8). The data for *Ncan* expression was normally distributed when tested with the Kolmogorov-Smirnov test. One outlier was removed in low dose HCA group in the mifepristone experiment at 7 DIV with 4h HCA exposure (Fig.3.5 G), as the value was more than 2 times SD from the mean (Mean=1.407, SD=1.814). The data were analysed by ANOVA followed by Tukey's post-hoc tests. * $p<0.05$, *** $p<0.001$ HCA effect vs corresponding vehicle group, post-hoc Tukey's test; ### $p<0.001$ overall effect of mifepristone vs vehicle group, ANOVA, Tukey's post-hoc test. The bar graphs show mean ± SEM.

3.4.2.5 *Vcan*

The mRNA expression of *Vcan* were not significant at 7 DIV (4h: F (2, 43) =1.02, p=0.370; 24h: F (2, 42) =0.42, p=0.66) (Fig.3.6 A B). Similarly, at 14 DIV, no significant HCA effect was reported with 4h treatment (F (2, 19) =0.66, p=0.531) (Fig.3.6 C); but the expression of *Vcan* decreased significantly after 24h treatment (F (2, 21) =5.12, p=0.017, veh vs low dose p=0.028, Tukey's 'spost-hoc tests) (Fig.3.6 D). And no significant HCA effects were observed at 21 DIV (4h: F (2, 19) =3.00, p=0.085; 24h: F (2, 18) =0.11, p=0.894) after 4h and 24h HCA treatment (Fig.3.6 E F).

Following the mifepristone exposure at 14 DIV, there was a significant effect of HCA treatment at 4h (F(2, 46)=3.32, p=0.046), the post-hoc tests suggested that the expression of *Vcan* showed a decreased tendency with low dose HCA treatment, and was significantly decreased after high dose HCA treatment in the absence if mifepristone (veh without mifepristone vs low dose HCA without mifepristone p=0.069, veh without mifepristone vs high dose HCA without mifepristone p=0.007, Tukey's post-hoc test), but the suppression effect did not appear in the presence of mifepristone (veh with mifepristone vs low dose HCA with mifepristone p=1.000, veh with mifepristone vs high dose HCA with mifepristone p=0.999, Tukey's post-hoc test). The overall effect of mifepristone was not significant at 4h (F(2, 46)=2.37, p=0.131). However, the interaction of HCA and mifepristone was significant at 4h (F(2, 46)=4.63, p=0.016), suggesting a decreased expression in vehicle treated group with the presence of mifepristone (veh without mifepristone vs veh with mifepristone p=0.027 Tukey's post-hoc test) (Fig.3.6 G). And the suppressive tendency was attenuated after mifepristone treatment, suggesting there was a potential effect of mifepristone on the expression of *Vcan* and could eliminate the significant effect of HCA. Hence, just as with the regulation of *Bcan* expression, GCs seem to exert a rapid non-GR-mediated suppression of *Vcan* mRNA levels by HCA, and a basal GR-mediated enhancement by GCs in the medium, which is rapidly blocked by mifepristone.

At 24h, there was a significant effect of HCA treatment (F(2, 46)=3.92, p=0.028), however, the post-hoc test did not significantly reported the effect (veh without mifepristone vs low dose HCA without mifepristone p=0.898, veh without mifepristone vs high dose HCA without mifepristone p=0.742; veh with mifepristone vs low dose HCA with mifepristone p=0.887, veh with mifepristone vs high dose HCA with mifepristone p=0.120), which did not replicate the initial HCA effect with the same time point. The overall effect of mifepristone was not significant either (F(2, 46)=0.01, p=0.943). However, the interaction of HCA and mifepristone was still not signifiant (F(2, 46)=0.43, p=0.653). The results suggested that *Vcan* expression was not affected by long exposure of HCA and inhibition of GRs by mifepristone did not change the overall Vcan expression. Like the results in *Bcan* and *Ncan*, the inconsistent results found between the initial HCA and following mifepristone experiment might be due to the reason that samples that used in these 2 experiments were not collected from the same biological sample, which will lead to the variations of the results in these 2 experiments, resulting in different results in these 2 experiments.

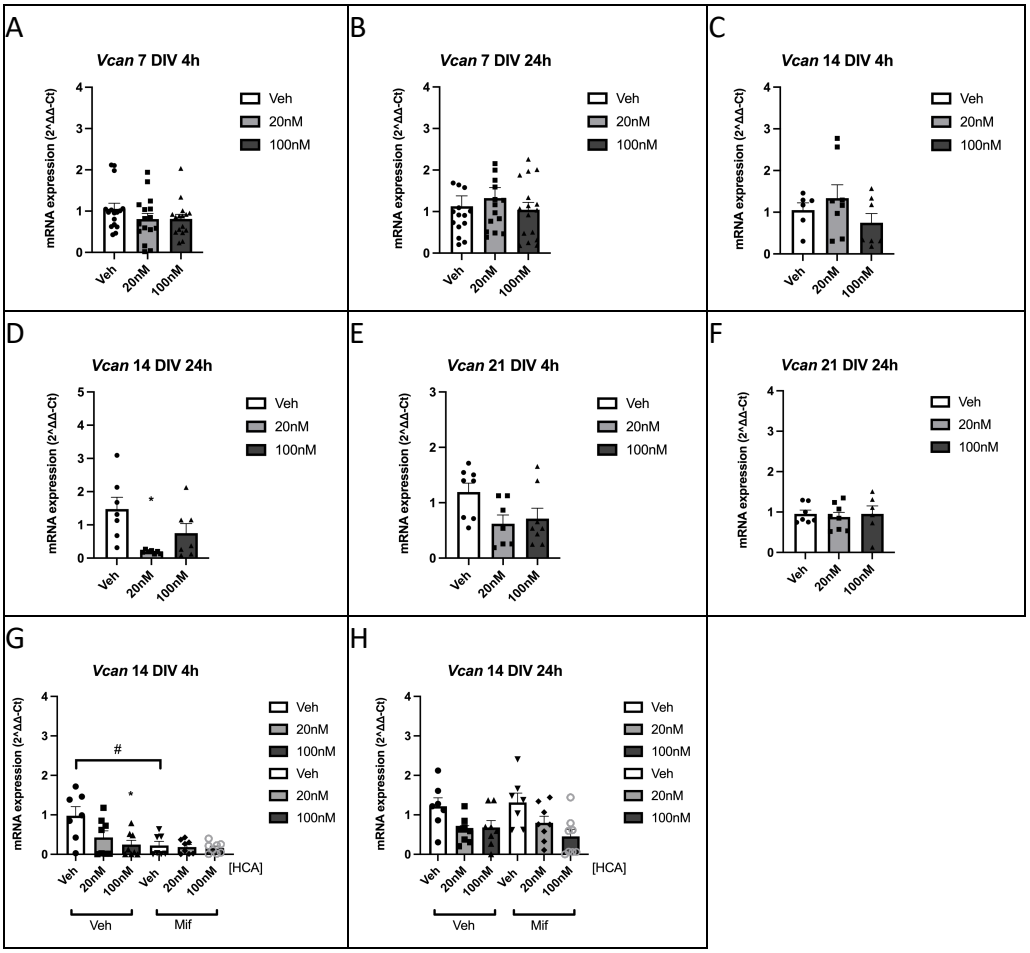

Figure 3.6: mRNA expression of *Vcan*. A-F: mRNA expression of *Vcan* after 4h and 24h exposure to low dose (20nM) and high dose (100nM) HCA at 7, 14 and 21 DIVn (4h: 7 DIV: n=43 in total, veh=16, low dose=14, high dose=14; 14 DIV: n=20 in total, veh=6, low dose=8, high dose=7; 21 DIV: n=18 in total, veh=7, low dose=6, high dose=6; 24h: 7 DIV: n=48 in total, veh=16, low dose=164, high dose=16; 14 DIV: n=22 in total, veh=8, low dose=7, high dose=7; 21 DIV: n=20 in total, veh=7, low dose=7, high dose=6). G-H: mRNA expression of *Vcan* at 14 DIV after 4h and 24h low dose (20nM) and high dose (100nM) HCA with mifepristone (20nM) treatment (4h: HCA: n=46 in total, veh=7, low dose samples=8, high dose samples=8; HCA+Mif: veh=7, low dose samples=8, high dose samples=8; 24h: n=46 in total, HCA: veh=7, low dose samples=8, high dose samples=8; HCA+Mif: veh=7, low dose samples=8, high dose samples=8). The data for *Vcan* were normally distributed as assessed with the Kolmogorov-Smirnov test. No outliers were detected in this study. The data were analysed by ANOVA followed by Tukey's post-hoc tests. *p<0.05 HCA effect vs corresponding vehicle group, Tukey's post-hoc test; # p<0.05 overall effect of mifepristone vs group without mifepristone, ANOVA, Tukey's post-hoc test. The bar graphs show mean ± SEM.

3.4.2.6 *Phcan/Ptprz1*

For *Phcan/Ptprz1*, another CSPG component, its mRNA expression was also examined after 4h and 24h HCA exposure with low and high doses at 7 DIV, 14 DIV and 21 DIV. However, the results proposed that there were no significant changes of *Ptprz1* expression after HCA exposure (7 DIV: 4h: F (2, 22)=0.63 p=0.542, 24h: F (2, 22) =1.78, p=0.66; 14 DIV: 4h: F (2, 22)=1.21 p=0.39, 24h: F (2, 18)=0.49 p=0.623; 21 DIV: 4h: F (2, 17)=0.68 p=0.219, 24h: F (2, 19)=0.55 p=0.584) (Fig 3.7). As exposure of HCA alone did not lead to the changes of *Ptprz1* mRNA

expression, GRs mediation was definitely not involved during the HCA exposure. Thus, mifepristone was not treated on *Ptprz1* mRNA.

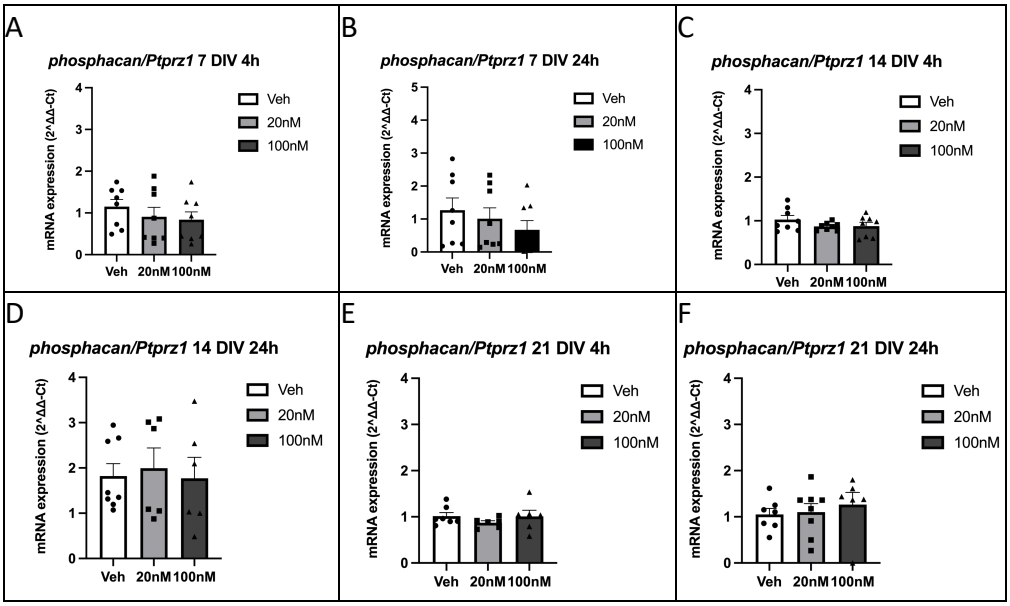

Figure 3.7: mRNA expression of *phosphacan/Ptprz1*. A-F: mRNA expression of *phosphacan/Ptprz1* after 4h and 24h exposure to low dose and high dose HCA at 7, 14 and 21 DIV (4h: 7 DIV: n=24 in total, veh=8, low dose=8, high dose=8; 14 DIV: n=24 in total, veh=8, low dose=8, high dose=8; 21 DIV: n=19 in total, veh=7, low dose=6, high dose=6; 24h: 7 DIV: n=24 in total, veh=8, low dose=8, high dose=8; 14 DIV: n=20 in total, veh=8, low dose=6, high dose=6; 21 DIV: n=21 in total, veh=7, low dose=8, high dose=6). The data for *Phcan/Ptprz1* was normally distributed as assessed with the Kolmogorov-Smirnov test, no outliers were detected in this study. The data were analysed by ANOVA followed by Tukey's post-hoc tests. The bar graphs show mean ± SEM.

3.4.2.7 *Has1*

The changes of gene expression of *Has1* were not detected significantly at 7 DIV (4h: F (2, 22) =2.02, P=0.161; 24h: F (2, 22) =2.71, p=0.360) (Fig.3.8 A B) and 14 DIV (4h: F (2, 22) =0.07, p=0.933, 24h: F (2, 18) =1.75, p=0.223) (Fig.3.8 C D). However, the expression increased significantly after 4h treatment at 21 DIV with high dose HCA (F (2, 17) =6, p=0.012, veh vs high dose, p=0.009 Tukey's post-hoc tests), but not 24h (F (2, 19) =0.65, p=0.536) (Fig.3.8 E F).

In the following mifepristone study, although no significant alterations were found at 7 DIV in both 4h and 24h treatment and 14 DIV with 24h treatment, there was a tendency towards decreased *Has1* mRNA expression shown (Fig.3.8 A B D), it was still worth to further detect the HCA effect and GR involvement in the decreasing tendency. As a result, at 7 DIV, no significant effect of HCA was shown with 4h treatment (F (2, 45) =0.204 p=0.959) (Fig.3.8 G). There was an overall effect of mifepristone (F (1, 46) =6.75, p=0.014), indicating mifepristone significantly increased the overall expression of *Has1*. However, the interaction of mifepristone and HCA treatment was not significant (F (2, 45) =1.78, p=0.183). After 24h exposure to HCA and mifepristone, the mRNA levels of *Has1* still remained unchanged (F (2, 45) =1.34, P=0.273), and no overall effect of mifepristone (F (1, 46) =1.29, p=0.263) and interactions of HCA and mifepristone (F (2, 45) =0.26, p=0.775) were found (Fig.3.8 H).

Additionally, the expression changes of *Has1* at 14 DIV were not significant after 24h HCA treatment (F(2, 45)=0.88, p=0.422) (Fig.3.8 I). However, there was an overall effect of

mifepristone after 24h (F(1, 46)=12.48, p=0.001), suggesting that the expression of *Has1* increased after being treated with mifepristone. The interaction of mifepristone and HCA treatment was not significant (F(2, 45)=0.35, p=0.708).

These results suggested that mifepristone significantly inhibited a basal suppression of *Has1* expression by GCs in the medium at 7 and 14 DIV; however, no HCA effect was detected with or without mifepristone. The results suggested that there may be a rapidly relievable effect of GCs in the culture medium to suppress *Has1* mRNA levels at 7 and 14 DIV by GR-mediation, an effect diminished by mifepristone exposure; however, the additional HCA treatment did not show an effect.

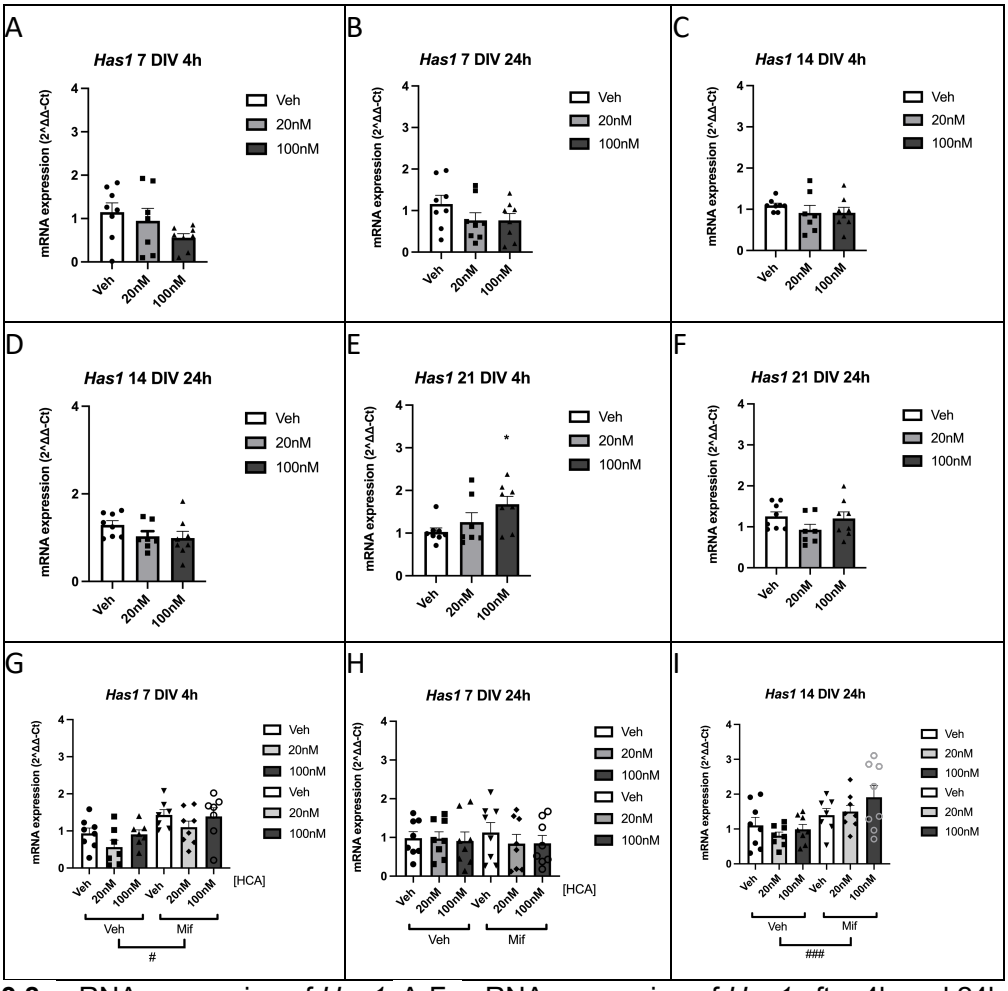

Figure 3.8: mRNA expression of *Has1.* A-F: mRNA expression of *Has1* after 4h and 24h exposure to low dose (20nM) and (100nM) high dose HCA at 7, 14 and 21 DIV (4h: 7 DIV: n=24 in total, veh=8, low dose=8, high dose=8; 14 DIV: n=24 in total, veh=8, low dose=8, high dose=8; 21 DIV: n=19 in total, veh=7, low dose=6, high dose=6; 24h: 7 DIV: n=24 in total, veh=8, low dose=8, high dose=8; 14 DIV: n=20 in total, veh=8, low dose=6, high dose=6; 21 DIV: n=21 in total, veh=7, low dose=8, high dose=6). G-I: the mRNA expression of *Has1* at 7 and 14 DIV after 4h and 24h low dose (20nM) and (100nM) high dose HCA and mifepristone (20nM) treatment. 4h: HCA: n=46 in total, veh=7, low dose samples=8, high dose samples=8; HCA+Mif: veh=7, low dose samples=8, high dose samples=8; 24h: n=46 in total, HCA: veh=7, low dose samples=8, high dose samples=8; HCA+Mif: veh=7, low dose samples=8, high dose samples=8). The data for *Has1* were normally distributed as assessed with the Kolmogorov-Smirnov test. One outlier was removed in this study in the mifepristone experiment at 7 DIV with 4h treatment within high dose treated HCA group without mifepristone (Fig.3.8. G), the data was more than 2 times SD from the mean (mean=1.003, SD=0.363). The data were analysed by ANOVA followed by

Tukey's post-hoc tests. *p<0.05 HCA effect vs corresponding vehicle group, post-hoc Tukey's test; ### p<0.001 overall effect of mifepristone vs vehicle group, ANOVA, Tukey's post-hoc tests. The bar graphs show mean ± SEM.

3.4.2.8 *Has2*

There is a suggestion that the gene expression of *Has2* decreased at 7 DIV 4h after high dose HCA treatment (Fig.3.9 A), although the effect did not reach the significance value ($F(2, 22) = 3.78$, $p=0.070$; veh vs high dose $p=0.065$, Tukey's post-hoc test). No significant expression changes were detected at 7 DIV 24h after treatment ($F(2, 122) = 0.22$, $p=0.816$) (Fig. 3.9 B). similar nonsignificant results were also showed in 14 DIV (4h: $F(2, 22) = 3.46$, $p=0.082$; 24h: $F(2, 18) = 0.66$, $p=0.537$) (Fig. 3.9 C D) and 21 DIV (4h: $F(2, 19) = 2.02$, $p=0.165$, 24h: $F(2, 17) = 3.07$, $p=0.072$) (Fig. 3.9 E F).

Previous results suggested a decreased tendency *Has2* mRNA levels at 7 DIV after 4h HCA treatment, although it was not significant, it was still worth to further investigate whether the tendency was mediated by GRs by adding mifepristone. As a result, no significant effect of HCA was found with 4h exposure ($F(2, 44) = 0.38$, $p=0.686$) (Fig.3.9 G). The overall effect of mifepristone was not significant either ($F(1, 45) = 2.50$, $P=0.123$). Additionally, no significant interaction of mifepristone and HCA treatment was detected ($F(2, 44) = 0.80$, $p=0.457$). Regards to the effect of HCA at 7 DIV with 24h treatment, no alterations of *Has2* mRNA levels were observed after ($F(2, 44) = 1.98$, $p=0.151$), and the overall effect of mifepristone was not detected either ($F(1, 45) = 1.85$, $p=0.181$) (Fig.3.9 H). No interactions of HCA and mifepristone were found ($F(1, 44) = 0.38$, $p=0.688$), suggesting that HCA has no rapid or long-term effect on *Has2* mRNA levels.

Although no significant alterations were found at 14 and 21 DIV previously with 24h HCA treatment, an upregulation or downregulation tendency was shown. Therefore, the effect of mifepristone was still investigated. At 14 DIV, the changes in *Has2* expression were not significant 24h after HCA treatment ($F(2, 44) = 0.36$, $p=0.701$) (Fig. 3.9 I), but the expression of *Has2* was significantly affected by mifepristone ($F(1, 45) = 7.20$, $p=0.011$), suggesting an increase of *Has2* expression after blocking GRs with mifepristone. The interactions of mifepristone and HCA treatment were not significant ($F(2, 44) = 1.46$, $p=0.246$), indicating that the effect of HCA was not dependent on the GRs mediation (Fig. 3.9 I). At 21 DIV, the effect of HCA was not significant at 24h ($F(2, 44) = 0.25$, $p=0.783$) (Fig. 3.9 J). Mifepristone did not have an overall effect on *Has2* expression at 24h either ($F(1, 45) = 0.11$, $p=0.738$). And there was no significant interaction of mifepristone and HCA treatment detected with 24h exposure ($F(2, 44) = 1.10$, $p=0.303$) (Fig. 3.9 J).

Following the mRNA alterations, protein expression of *Has2* was measured. At 7 DIV, there was an effect of HCA on *Has2* (59kDa) protein expression, which increased significantly at 4h with low dose and high dose HCA exposure ($F(2, 26)=3.73$, $p=0.039$, veh vs low dose $p=0.020$, veh vs high dose HCA $p=0.036$, Tukey's post-hoc tests) (Fig. 3.9 K), but the lower band of Has2 (48kDa) was not affected ($F(2, 26)=3.31$, $p=0.287$) (Fig. 3.9 K). In terms of the protein levels at 7 DIV with 24h HCA treatment, no significant changes were found on both higher band (59kDa) ($F(2, 26) = 2.09$, $p=0.146$) or lower band (48kDa) ($F(2, 26) = 2.09$, $p=0.146$) (Fig.3.9 L).

Moreover at 14 DIV, an effect of HCA on *Has2* (59KDa) protein expression was also observed, *Has2* (59KDa) protein expression was reduced significantly at 4h with both low dose and high dose HCA treatment ($F(2, 35)=9.29$, $p=0.001$, veh vs high dose $p=0.002$, Tukey's post-hoc tests), but the lower band was not significantly affected ($F(2, 35)=0.94$, $p=0.401$) (Fig 3.9 M). No

effect of HCA was found with 24h HCA treatment (59kDa: F (2, 35)=0.08, p=0.920; 48kDa: F (2, 35)=1.89, p=0.168) (Fig 3.9 N).

As noted in Bcan western blot results, the current Gapdh protein signals also showed slight differences in different treatment groups (Fig. 3.9 N). The altered Gapdh signals might be attributed to the different expression of Gapdh protein with different drug treatment, or the sample loading error in western blot procedure, which will be further discussed in the discussion section (Section 3.5).

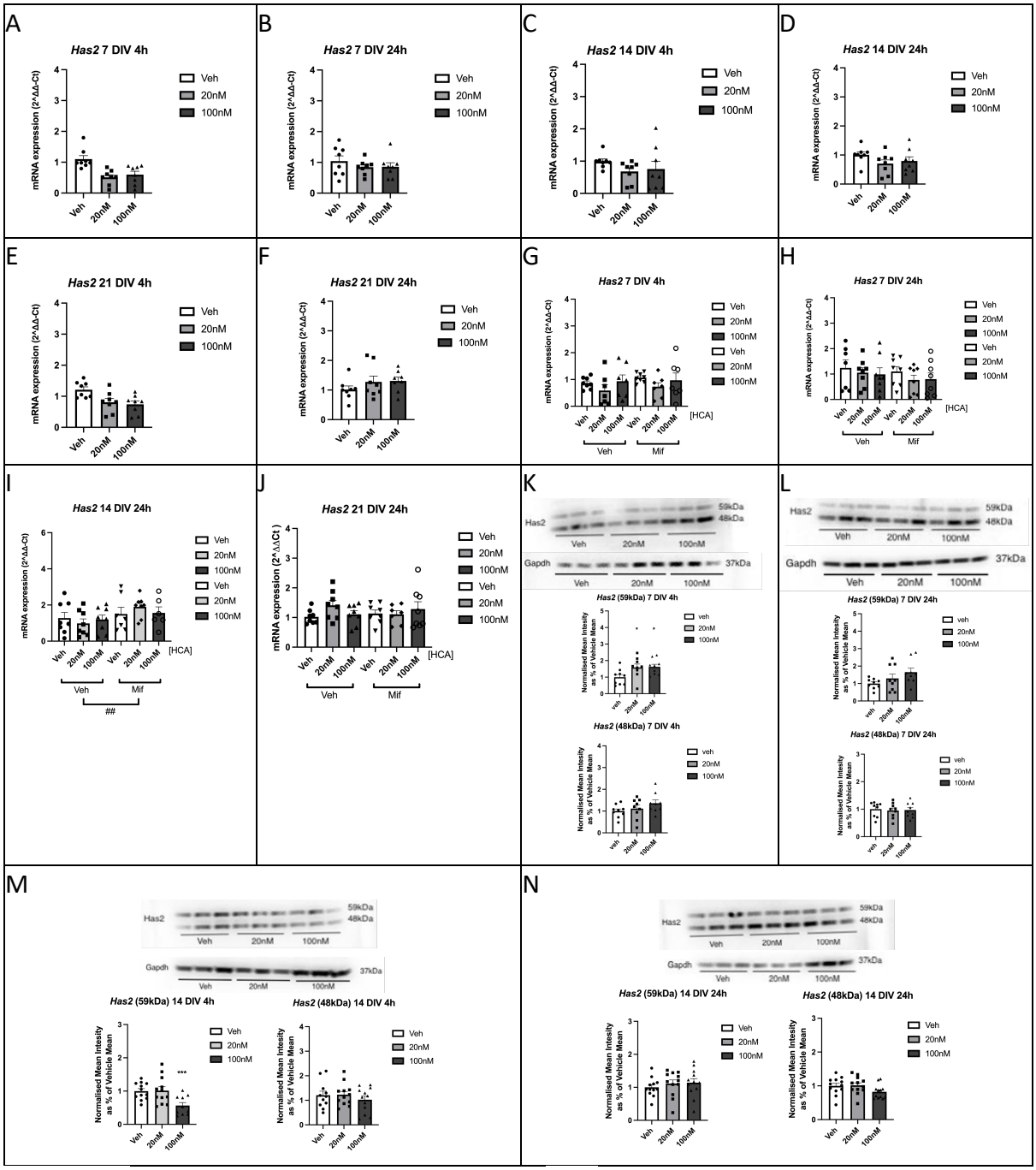

Figure 3.9: mRNA and protein expression of *Has2* A-F: mRNA expression of *Has2* after 4h and 24h exposure to low dose (20nM) and high dose (100nM) HCA at 7, 14 and 21 DIV (4h: 7 DIV: n=24 in total, veh=8, low dose=8, high dose=8; 14 DIV: n=24 in total, veh=8, low dose=8, high dose=8; 21 DIV: n=19 in total, veh=7, low dose=6, high dose=6; 24h: 7 DIV: n=24 in total, veh=8, low dose=8, high dose=8; 14 DIV: n=20 in total, veh=8, low dose=6, high dose=6; 21 DIV: n=21

in total, veh=7, low dose=8, high dose=6). G-I: the mRNA expression of *Has2* at 7, 14 and 21 DIV after 4h and 24h low dose (20nM) and (100nM) high dose HCA and mifepristone (20nM) treatment. 4h: HCA: n=46 in total, veh=7, low dose samples=8, high dose samples=8; HCA+Mif: veh=7, low dose samples=8, high dose samples=8; 24h: n=46 in total, HCA: veh=7, low dose samples=8, high dose samples=8; HCA+Mif: veh=7, low dose samples=8, high dose samples=8). K-N: Western blot analysis of Has2 protein levels exposed with low dose HCA (20nM) and high dose HCA (100nM) HCA at 7 and 14 DIV for 4h and 24h. (4h: n=34 in total, veh=12, low dose HCA=12, high dose HCA=10; 24h: n=34 in total, veh=12, low dose HCA=12, high dose HCA=10). The data for *Has2* was normally distributed as assessed with the Kolmogorov-Smirnov test. No outliers were detected in this study. The data were analysed by ANOVA followed by Tukey's post-hoc tests. * $p<0.05$, ***$p<0.001$ HCA effect vs corresponding vehicle group, Tukey's post-hoc test; ## $p<0.01$ an overall effect of mifepristone vs corresponding vehicle group, ANOVA, Tukey's post-hoc test. The bar graphs show Mean ± SEM.

3.4.2.9 *Has3*

In the initial HCA experiment, the mRNA expression of *Has3* decreased significantly at 7 DIV after 4h high dose HCA treatment ($F (2, 22) =5.40$, $p=0.038$, veh vs high dose HCA, $p=0.039$, Tukey's post-hoc test) (Fig.3.10 A), but not 24h ($F (2, 22) =2.37$, $p=0.149$) (Fig.3.10 B). No significant changes were detected at 14 DIV (4h: $F (2, 22) =0.13$, $p=0.875$; $F (2, 18) =0.99$, $p=0.406$) (Fig.3.10 C D). At 21 DIV, the *Has3* mRNA expression was reduced with both low dose and high dose HCA treatment at 4h, however the statistics did not reach the significance level in the post-hoc tests ($F (2, 19) =3.86$, $p=0.043$, veh vs low dose HCA $p=0.059$, veh vs high dose HCA $p=0.096$, Tukey's post-hoc tests) (Fig.3.10 E); but the mRNA expression was significantly reduced with low dose HCA but not high dose at 24h ($F (2, 17) =7.33$, $p=0.005$, veh vs low dose HCA $p=0.005$, veh vs high dose HCA $p=0.518$, Tukey's post-hoc tests) (Fig.3.10 F).

After exposure to mifepristone, at 7 DIV, there was no significant effect of HCA treatment at 4h, although there was a decreasing tendency showed with high dose HCA ($F (2, 45) =0.82$, $p=0.452$); the overall effect of mifepristone was not significant either ($F (2, 45)=2.04$, $P=0.163$); however, a significant interaction of HCA and mifepristone was found, suggesting a decreased tendency of *Has3* mRNA levels with exposure of high dose HCA and mifepristone (high dose HCA with mifepristone vs high dose HCA without mifepristone $p=0.045$, Tukey's post-hoc tests) (Fig.3.10 G). At 24h, no significant effect of HCA was reported on mRNA expression of *Has3* ($F (2, 45) =1.97$, $p=0.753$). The overall effect of mifepristone was not significant either ($F (2, 45)=2.45$, $P=0.126$) and no interaction was found between HCA and mifepristone ($F(2, 45)=0.05$, $p=0.955$) (Fig.3.10 H). The results indicated that, at 7 DIV, the rapid suppressive tendency of high dose HCA on *Has3* mRNA levels was significantly mediated by mifepristone, and hence this rapid suppression was mediated through GRs.

At 21 DIV, no significant effect of HCA on the expression of *Has3* mRNA levels were found at 4h ($F(2, 47)=1.79$, $p=0.179$), and mifepristone did not show an effect on overall expression of *Has3* ($F(1, 47)=0.30$, $p=0.43$), no interaction was reported either ($F(2, 47)=0.30$, $P=0.743$) (Fig.3.10 I). Moreover, similar results were reported at 24h, the *Has3* mRNA levels were not altered with HCA exposure ($F(2, 47)=0.24$, $p=0.787$), and no effect of mifepristone was found either ($F(1, 47)=2.70$, $p=0.108$). Additionally, no significant interaction of mifepristone and HCA treatment was detected ($F(2, 47)=0.57$, $P=0.568$) (Fig.3.10 J).

Regards to the mRNA level, the alteration in the followed mifepristone treatment experiments was not consistent with the initial HCA experiments, such as significant reduction of *Has3* at 7

and 21 DIV with low or high dose HCA was not replicated in the following mifepristone experiments, although a decreased tendency was shown at 7 DIV (Fig.3.10 G). Just like the results showed in *Bcan*, *Ncan* and *Vcan,* the inconsistent results might be due to the biological variation between samples collected in different cell cultures, which might lead to the different results in these 2 experiments with the same drug treatment; further explanation was presented in discussion Section 3.5.

With regard to the protein alterations after HCA exposure, at 7 DIV, Has3 protein levels decreased significantly after 4h exposure with both low dose and high dose HCA ($F(2, 17)=11.14$, $p=0.014$; veh vs low dose HCA, $p=0.001$ veh vs high dose HCA, Tukey's post-hoc tests) (Fig.3.10 K); but no significant changes of Has3 protein expression were observed after 24h HCA exposure ($F(2, 26)=0.57$, $p=0.572$) (Fig.3.10 L).

Following detecting HCA effect on Has3 protein levels at 7 DIV, the overall effect of mifepristone was examined. The results reported that no HCA effect was found with either 4h ($F (2, 47) =0.41$, $p=0.665$), but mifepristone significantly increased Has3 protein levels with 4h treatment ($F (1, 47) =8.29$, $p=0.006$), with the overall increasing protein levels of Has3 mediated by GRs, suggesting an effect of basal GCs in the cell culture medium affecting overall protein levels of Has3 during cell developmental stage by GRs pathway (Fig.3.10 M). No significant interactions of HCA and mifepristone were observed ($F (2, 47) =0.51$, $p=0.603$) (Fig.3.10 M). With 24h HCA treatment, no effect was reported ($F (2, 47) =1.21$, $p=0.309$) and the protein levels of Has3 were not altered with mifepristone exposure ($F (1, 47) =3.38$, $p=0.073$) (Fig.3.10 N). Moreover, no significant interactions of HCA and mifepristone were observed ($F (2, 47) =1.12$, $p=0.336$) (Fig.3.10 N).

Just like the Gapdh signals presented in Bcan and Has2 western blot results, the current Gapdh signals also showed slight differences in different treatment groups (Fig. 3.10 K M N). The similar reason was considered that the altered Gapdh signals might be attributed to the different expression of Gapdh protein with different drug treatment, or the sample loading error in western blot procedure, which will be further discussed in the discussion section (Section 3.5).

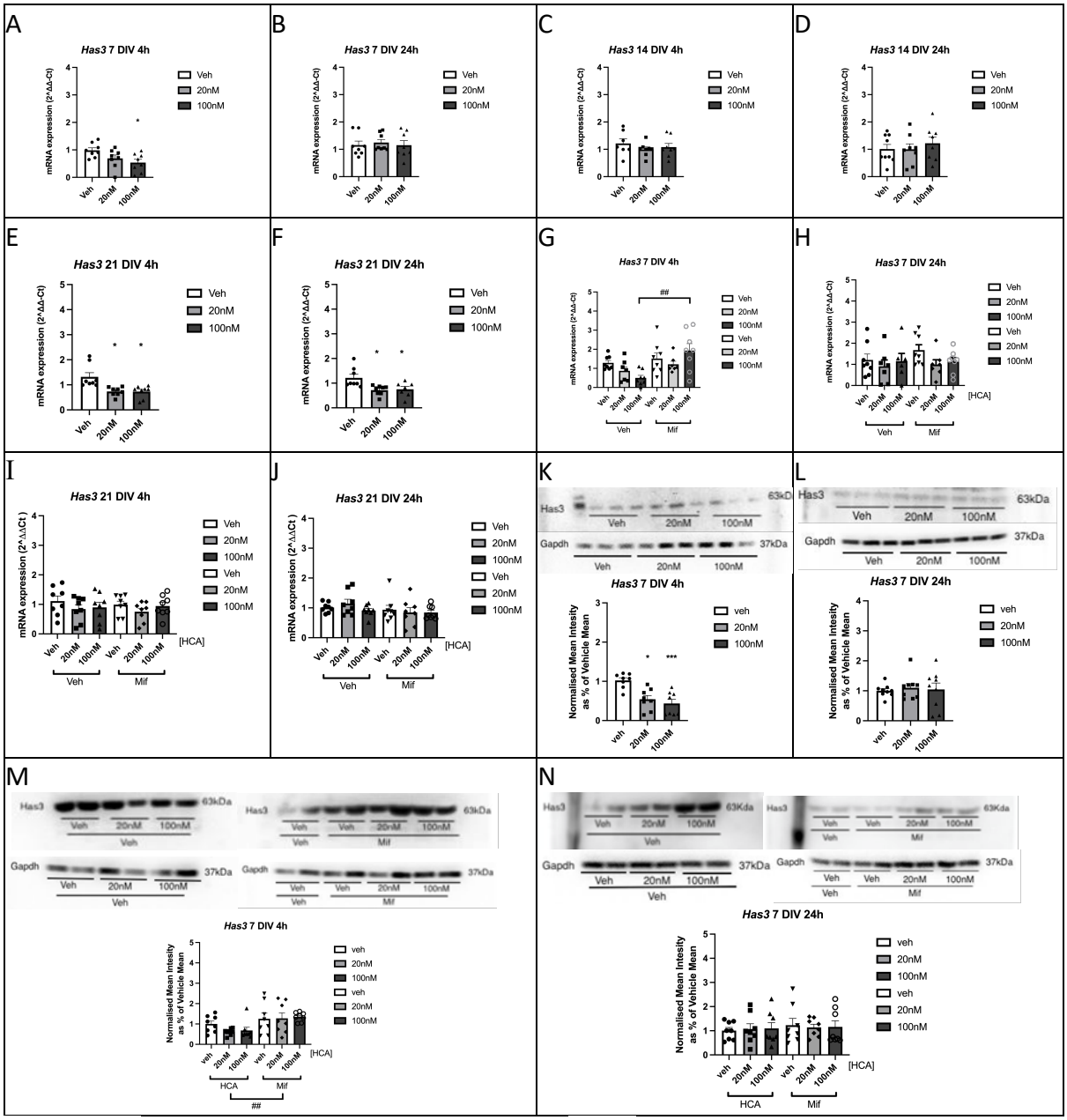

Figure 3.10: mRNA and protein expression of *Has3*. A-F: mRNA expression of *Has3* after 4h and 24h exposure to low dose (20nM) and high dose (100nM) HCA at 7, 14 and 21 DIV (4h: 7 DIV: n=24 in total, veh=8, low dose=8, high dose=8; 14 DIV: n=24 in total, veh=8, low dose=8, high dose=8; 21 DIV: n=19 in total, veh=7, low dose=6, high dose=6; 24h: 7 DIV: n=24 in total, veh=8, low dose=8, high dose=8; 14 DIV: n=20 in total, veh=8, low dose=6, high dose=6; 21 DIV: n=21 in total, veh=7, low dose=8, high dose=6). G-J: the mRNA expression of *Has3* at 7 and 21 DIV after 4h and 24h low dose (20nM) and (100nM) high dose HCA and mifepristone (20nM) treatment. 4h: HCA: n=46 in total, veh=7, low dose samples=8, high dose samples=8; HCA+Mif: veh=7, low dose samples=8, high dose samples=8; 24h: n=46 in total, HCA: veh=7, low dose samples=8, high dose samples=8; HCA+Mif: veh=7, low dose samples=8, high dose samples=8). K-l: Western blot analysis of Has3 protein levels exposed with low dose HCA (20nM) and high dose HCA (100nM) HCA at 7 DIV for 4h and 24h with or without mifepristone (4h: HCA: n=27 in total, veh=9, low dose=9, high dose=9; HCA+Mif: n=48 in total HCA: veh=8, low dose=8, high dose=8, Mif: veh=8, low dose=8, high dose=8; 24h: HCA: n=27 in total, veh=9, low dose=9, high dose=9; HCA+Mif: n=48 in total HCA: veh=8, low dose=8, high dose=8, Mif: veh=8, low dose=8, high dose=8). The data for *Has3* was normally distributed as assessed with

the Kolmogorov-Smirnov test. No outliers were detected in this study. The data were analysed by ANOVA followed by Tukey's post-hoc tests. *p<0.05, ***p<0.001 HCA effect vs corresponding vehicle groups, Tukey's post-hoc tests; ## p<0.01, overall effect of mifepristone vs corresponding veh group, ANOVA, Tukey's post-hoc test. The bar graphs show mean ± SEM.

3.4.2.10 *Hapln4*

In the initial HCA experiment, no significant changes were detected at 7 DIV with both 4h and 24h treatment (4h: F (2, 21) =2.94, p=0.104, 24h: F (2, 22) =0.82, p=0.483) (Fig.3.11 A B). However, the expression decreased significantly at 14 DIV with 4h high dose HCA treatment (F (2, 22) =3.79, p=0.050; veh vs high dose HCA, p=0.048, Tukey's post-hoc test) (Fig.3.11 C), while no changes were found with 24h HCA treatment (F (2, 18) =0.13, p=0.879) (Fig.3.11 D). At 21 DIV, the expression of *Hapln4* was not affected by HCA with 4h treatment (F (2, 17) =0.22, p=0.801) (Fig.3.11 E), but after 24h treatment, *Hapln4* expression was reduced by low dose HCA (F (2, 19) =0.44, p=0.008; veh vs low dose p=0.041, Tukey's post-hoc test) (Fig.3.11 F).

Following mifepristone treatment at 14 DIV, the effect of HCA was also significant after 4h (F (2, 46) =5.91, p=0.006), however, the following post-hoc test suggested the effect of HCA on mRNA expression of *Hapln4* did not reach the significance with both absence or presence of mifepristone (veh without mifepristone vs low dose HCA without mifepristone p=0.087, veh without mifepristone vs high dose HCA without mifepristone p=1.000, Tukey's post-hoc tests; veh with mifepristone vs low dose HCA with mifepristone p=0.882, veh with mifepristone vs low dose HCA with mifepristone p=0.965, Tukey's post-hoc tests) (Fig.3.11 G); the overall effect of mifepristone was not significant at 4h HCA treatment group (F (2, 44) =0.14, p=0.714), and no significant interactions of HCA and mifepristone was reported (F (1, 46) =0.69, p=0.506) (Fig.3.11 G). Similarly, at 14 DIV after 24h treatment, no significant effect of HCA was reported (F (2, 44) =0.18, p=0.836) and the overall expression of *Hapln4* was not altered by mifepristone (F (1, 45) =0.11, p=0.745). No interactions of HCA and mifepristone were reported (F (2, 44) =1.17, p=0.323) (Fig.3.11 H).

At 21 DIV, the effect of HCA was not significant to affect the expression of *Hapln4* at 4h (F (2, 44) =1.62, p=0.210) (Fig.3.11 I), but there was a decreasing tendency of high dose HCA showed with the absence of mifepristone (veh without mifepristone vs high dose without mifepristone p=0.066, Tukey's post-hoc test); moreover, the effect of mifepristone was not significant either (F (1, 45) =0.23, p=0.635); although an interaction was reported between HCA and mifepristone (F(2, 44)=3.71, p=0.033), the following post-hoc tests showed no specific differences between different groups (veh without mifepristone vs veh with mifepristone p=0.628, low dose HCA without mifepristone vs low dose HCA with mifepristone p=1.000, high dose HCA without mifepristone vs high dose HCA with mifepristone p=0.225, Tukey's post-hoc test) (Fig.3.11 I). After 24h treatment, *Hapln4* expression was not affected by HCA in the absence or presence of mifepristone (F (2, 44) =0.83, p=0.443); no overall effect of mifepristone was detected (F (1, 45) =0.00, p=0.959); additionally, there was no significant interaction of mifepristone and HCA treatment (F(2, 44)=1.71, p=0.194) (Fig.3.11 J).

Compared to the results in the initial HCA experiments, the following mifepristone experiment did not report any significant HCA effects, similar to the results showed for *Bcan*, *Ncan*, *Vcan* and *Has3.* The inconsistent results could be attributed to the sample collection from different biological samples, leading to the biological variability between each separate experiments.

Based on the findings of mRNA alterations, protein levels of *Hapln4* were measured with HCA and mifepristone cotreatment at 14 DIV. The protein levels of *Hapln4* remained unchanged after

4h HCA treatment (F (2, 46) =0.23, p=0.794) and mifepristone exposure (F (1, 47) =2.01, p=0.763), the interactions of HCA and mifepristone was not significantly reported (F(2, 46)=0.24, p=0.786) (Fig.3.11 K). With 24h treatment, no alterations of protein levels were affected by HCA (F (2, 46)=0.80, p=0.455) and mifepristone (F (1, 47)=0.95, p=0.336); the interaction of HCA and mifepristone was not detected either (F(2, 46)=1.38, p=0.263).

As noted in Bcan, Has2, Has3 western blot results, the Gapdh protein signals in the current experiment were also slightly different in different treatment groups (Fig. 3.11 K L). The altered Gapdh signals might be attributed to the different expression of Gapdh protein with different drug treatment, or the sample loading error in western blot procedure, which was further discussed in the discussion section (Section 3.5).

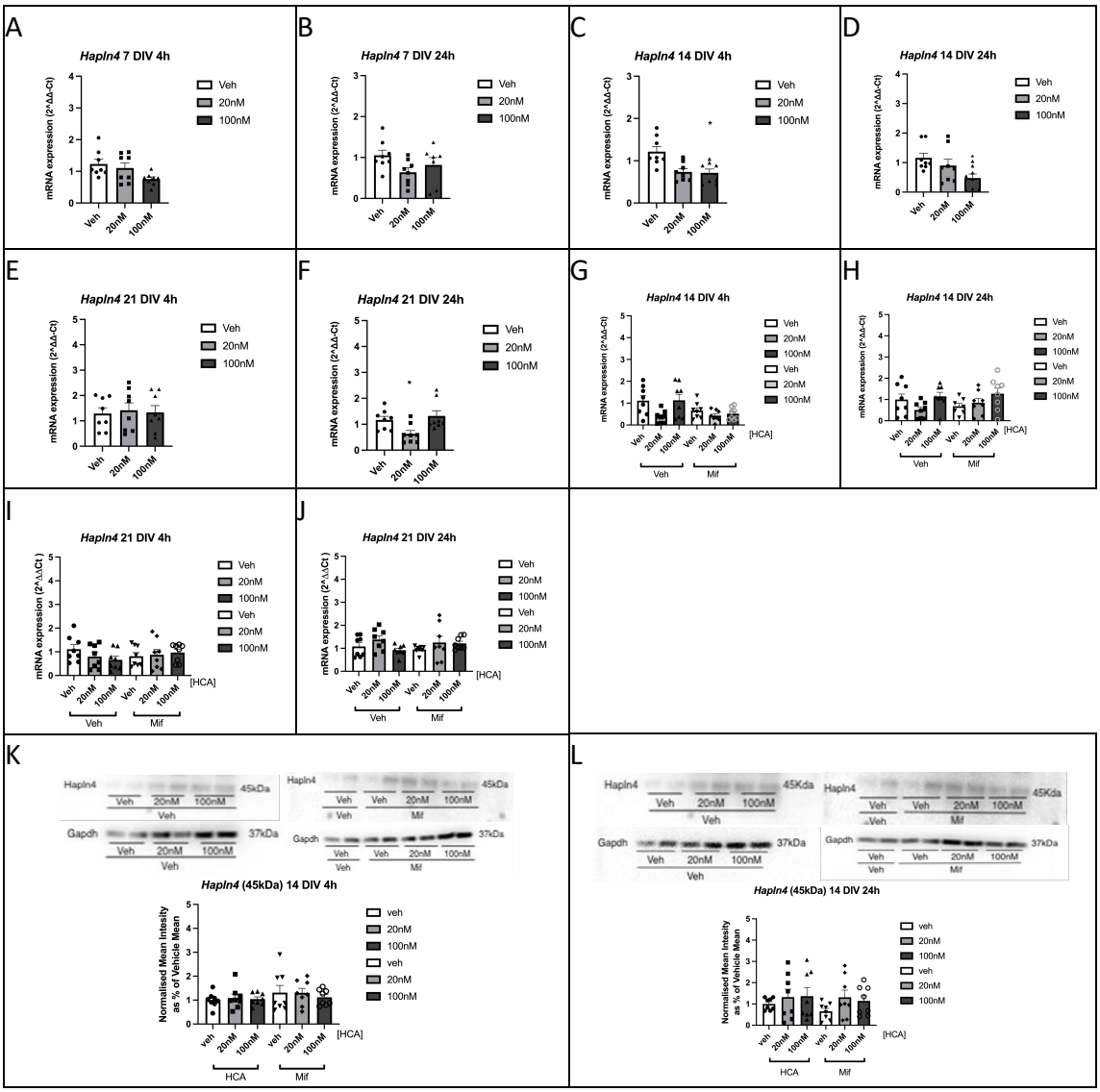

Figure 3.11: A-F: mRNA and protein expression of *Hapln4.* A-F: mRNA expression of *Hapln4* after 4h and 24h exposure to low dose (20nM) and high dose (100nM) HCA at 7, 14 and 21 DIV (4h: 7 DIV: n=24 in total, veh=8, low dose=8, high dose=8; 14 DIV: n=24 in total, veh=8, low dose=8, high dose=8; 21 DIV: n=19 in total, veh=7, low dose=6, high dose=6; 24h: 7 DIV: n=24 in total, veh=8, low dose=8, high dose=8; 14 DIV: n=20 in total, veh=8, low dose=6, high dose=6; 21 DIV: n=21 in total, veh=7, low dose=8, high dose=6). G-J: the mRNA expression of *Hapln4* at 7 and 21 DIV after 4h and 24h low dose (20nM) and (100nM) high dose HCA and mifepristone (20nM) treatment. 4h: HCA: n=46 in total, veh=7, low dose samples=8, high dose samples=8;

HCA+Mif: veh=7, low dose samples=8, high dose samples=8; 24h: n=46 in total, HCA: veh=7, low dose samples=8, high dose samples=8; HCA+Mif: veh=7, low dose samples=8, high dose samples=8). K-L: Protein expression of *Hapln4* detected by western blot after low dose (20nM) and high dose (100nM) HCA and mifepristone (20nM) exposure at 14 DIV, presenting with normalised mean intensity (HCA+Mif: 4h: n=48 in total HCA: veh=8, low dose=8, high dose=8, Mif: veh=8, low dose=8, high dose=8; 24h: n=48 in total HCA: veh=8, low dose=8, high dose=8, Mif: veh=8, low dose=8, high dose=8). The data for *Hapln4* was normally distributed as assessed with the Kolmogorov-Smirnov test. One outlier was more than 2 times of SD from the mean and was removed in this study, in the low dose HCA treatment group at 7 DIV with 4h treatment (SD=0.662, mean=0.873) (Fig 3.11 A). The data were analysed by ANOVA followed by Tukey's post-hoc tests. *p<0.05, ***p<0.001 HCA effect vs corresponding vehicle groups, Tukey's post-hoc tests; ## p<0.01, overall effect of mifepristone vs corresponding veh group, ANOVA, Tukey's post-hoc tests. The bar graphs show mean ± SEM.

3.4.2.11 *TnR*

The mRNA levels of *TnR* decreased significantly at 7 DIV after 4h low dose and high dose HCA treatment (F (2, 11) =5.01, p=0.035, veh vs low dose p=0.024, veh vs high dose p=0.021, Tukey's post-hoc tests) (Fig.3.12 A), but increased after 24h high dose HCA treatment (F (2, 11) =5.73, p=0.025, veh vs high dose p=0.038, Tukey's post-hoc tests) (Fig.3.12 B). Moreover, there were no significant changes at 14 DIV (4h: F (2, 12) =1.32, P=0.309; 24h: F (2, 11) =0.33, P=0.729) (Fig.3.12 C D) or 21 DIV (4h: F (2, 16) =0.01, P=0.990; 24h: F (2, 20) =1.65, P=0.219) (Fig.3.12 E F).

As mRNA levels of *TnR* were altered at 7 DIV by low dose and high dose HCA, mifepristone was cotreated with HCA to investigate the involvement of GRs mediation. The results suggested that at 7 DIV, there was a significant decrease of *TnR* mRNA expression after 4h low dose HCA treatment in the absence of mifepristone (F (2, 45)=3.28, p=0.049, veh without mifepristone vs low dose HCA without mifepristone, p=0.019, Tukey's post-hoc tests), but the overall effect of *TnR* was not affected by mifepristone (F(2, 45)=1.69, P=0.201); additionally, no interaction of HCA and mifepristone was detected (F(2, 45)=2.51, P=0.095) (Fig.3.12 G). After 24h treatment, no effect of HCA was reported (F(2,45)=0.49, p=0.619), but the overall expression of *TnR* was altered after mifepristone treatment (F (2, 45)=9.17, P=0.004), the level of mRNA expression with 24h mifepristone was lower than that with the absence mifepristone; and there was a significant interaction of HCA treatment and mifepristone treatment after 24h (F(2, 45)=5.42, P=0.008), suggesting a reduction of mRNA levels of veh treatment group after 24h mifepristone exposure (veh without mifepristone vs veh with mifepristone p=0.003, Tukey's post-hoc test) (Fig.3.12 H).

Similar to the results reported previously in *Bcan*, *Ncan*, *Vcan, Hapln4* and *Has3,* expression of *TnR* showed the inconsistent results between the initial HCA experiment and following mifepristone experiment, with suppression after both low and high dose HCA reported in the initial HCA experiment, but with suppression reported after only low dose HCA treatment in the following mifepristone experiment. This inconsistency, as previously mentioned, could be attributed to the variability between each separate experiments with different biological samples, resulting in results differences.

In addition to mRNA alterations at 7 DIV, *TnR*-immunoreactivity (180kDa) showed an increasing tendency after 4h high dose HCA exposure, but the tendency was not statistically significant (F (2, 26) =2.91, P=0.074), the protein expression remained unchanged at 24h (F(2, 26)=0.08, P=0.928) (Fig.3.12 I J). However, the 160kDa band of *TnR* was not clearly detected.

Following the mifepristone treatment, protein levels of *TnR* (180kDa and 160kDa) remained unchanged with 4h HCA exposure at 7 DIV (180kDa: F(2, 47)=0.32, 160kDa: 4h F(2, 47)=1.15). However, there was a significant effect of mifepristone on *TnR* (180kDa) (F(1, 47)=5.83, p=0.018), with an increasing tendency after mifepristone exposure; but no changes of *TnR* (160kDa) were detected after mifepristone (F(1, 47)=2.51, p=0.120). No interactions of HCA and mifepristone were found in *TnR* protein levels in both 180kDa and 160kDa bands (180kDa: F(2, 47)=0.02, p=0.977; 160kDa: F(2, 47)=0.45, p=0.639) (Fig.3.12 K). After 24h treatment, no HCA effect was reported on both band of *TnR* (180kDa and 160kDa) (180kDa: F(2, 47)=0.68, p=0.501; 160kDa: F(2, 46)=0.26, p=0.268). However, there was a significant effect of mifepristone on the overall levels of both band of *TnR* (180kDa and 160kDa) (180kDa: (F(1, 46)=9.92, p=0.003; 160kDa: F(1, 46)=25.30, p<0.001), with an increasing tendency after mifepristone exposure. No interactions of HCA and mifepristone were found in both bands of *TnR* (180kDa and 160kDa) protein levels (180kDa: F(2, 47)=1.11, p=0.338; 160kDa: F(2, 46)=1.44, p=0.248) (Fig.3.12 L).

Just like the results reported in Bcan, Has2, Has3 and Hapln4 western blot experiments, the Gapdh protein signals in the current experiment were slightly different in different treatment groups (Fig. 3.12 I K L). The altered Gapdh signals might be attributed to the different expression of Gapdh protein with different drug treatment, or the sample loading error in western blot procedure, which was further discussed in the discussion section (Section 3.5).

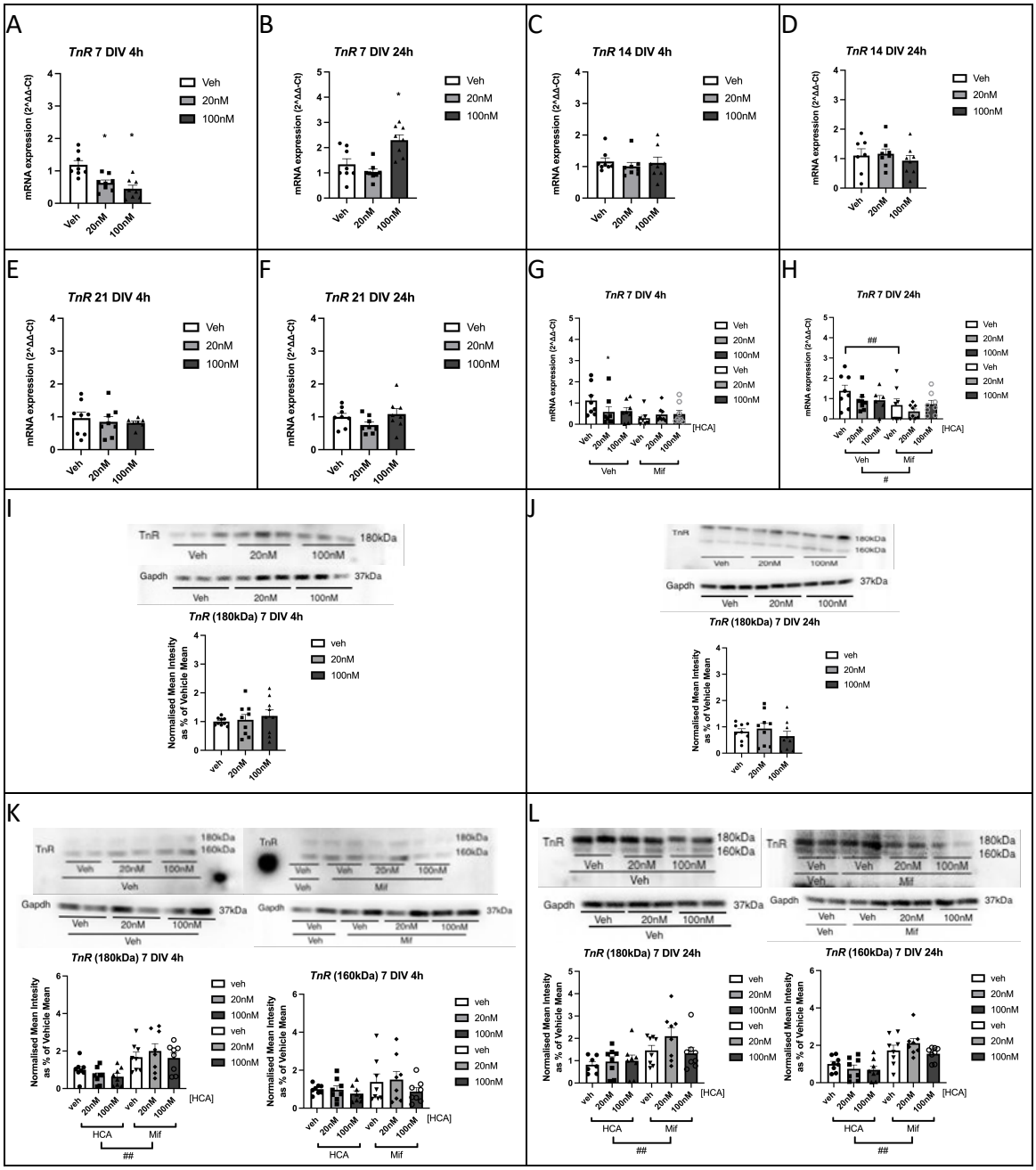

Figure 3.12: A-F: mRNA and protein expression of *TnR.* A-F: mRNA expression of *TnR* after 4h and 24h exposure to low dose (20nM) and high dose (100nM) HCA at 7, 14 and 21 DIV (4h: 7 DIV: n=24 in total, veh=8, low dose=8, high dose=8; 14 DIV: n=24 in total, veh=8, low dose=8, high dose=8; 21 DIV: n=19 in total, veh=7, low dose=6, high dose=6; 24h: 7 DIV: n=24 in total, veh=8, low dose=8, high dose=8; 14 DIV: n=20 in total, veh=8, low dose=6, high dose=6; 21 DIV: n=21 in total, veh=7, low dose=8, high dose=6). G-J: the mRNA expression of *TnR* at 7 DIV after 4h and 24h low dose (20nM) and (100nM) high dose HCA and mifepristone (20nM) treatment (4h: HCA: n=46 in total, veh=7, low dose samples=8, high dose samples=8; HCA+Mif: veh=7, low dose samples=8, high dose samples=8; 24h: n=46 in total, HCA: veh=7, low dose samples=8, high dose samples=8; HCA+Mif: veh=7, low dose samples=8, high dose samples=8). I-L: *TnR* protein expression after HCA treatment. Western blot analysis of *TnR* proteins with HCA at 7 DIV for 4h and 24h respectively, with veh, low dose HCA (20nM) and high dose HCA (100nM), presenting with normalised mean intensity of the bands signals of *TnR* (4h: HCA: n=27 in total, veh=9, low dose=9, high dose=9; HCA+Mif: n=48 in total HCA: veh=8, low dose=8, high dose=8, Mif: veh=8, low dose=8, high dose=8; 24h: HCA: n=27 in total, veh=9, low

dose=9, high dose=9; HCA+Mif: n=48 in total HCA: veh=8, low dose=8, high dose=8, Mif: veh=8, low dose=8, high dose=8). The data for *TnR* was normally distributed as assessed with the Kolmogorov-Smirnov test. No outlier was detected in this study. The data were analysed by ANOVA followed by Tukey's post-hoc tests. * p<0.05 HCA effect vs corresponding vehicle group, Tukey's post-hoc test; # p<0.05, ## p<0.01 overall effect of mifepristone vs corresponding veh group, ANOVA, Tukey's post-hoc tests. The bar graphs show mean ± SEM.

3.4.3 HCA altered expression of GABA related components

3.4.3.1 *Pv*

As a result, there were no significant changes at 7 DIV (4h: F(2, 23)=1.25, p=0.308; 24h: F(2, 22)=0.50, p=0.613) (Fig.3.13 A B) and 14 DIV (4h: F(2, 23)=0.25, p=0.785; 24h: F(2, 22)=1.31, p=0.292) after both 4h and 24h HCA treatment (Fig.3.13 C D). Similarly, at 21 DIV, no alterations were reported after 4h HCA treatment (F(2, 18)=0.26, p=0.775) (Fig.3.13 E); however, the expression of *Pv* decreased significantly after 24h high dose HCA treatment (F(2, 20)=4.72, p=0.023, veh vs high dose HCA p=0.043, Tukey's post-hoc tests) (Fig.3.13 F).

After mifepristone exposure, the results showed that, at 7 DIV, there was no significant effect of HCA on the expression of *Pv* after 4h exposure (F(2, 44)=0.89, p=0.420) (Fig.3.13 G). However, there was a significant overall effect of mifepristone (F(1, 45)=12.40, p=0.001) with an overall increase expression of *Pv*, suggesting that the mRNA levels of *Pv* increased significantly with 4h exposure of HCA and mifepristone; and the overall interaction of HCA and mifepristone was significant (F(1, 45)=11.30, p=0.002), indication the expression *Pv* with low dose HCA treatment in the absence of mifepristone increased with the presence of mifepristone (low dose HCA with mifepristone vs low dose HCA without mifepristone p=0.022, Tukey's post-hoc tests) (Fig.3.13 G), implying that there is a basal GR-mediated suppression of *Pv* mRNA at 7 DIV.

At 21 DIV, there was a significant effect of low dose and high dose HCA after 24h exposure with both presence and absence of mifepristone (F(2, 47)=8.66, p=0.001, veh without mifepristone vs high dose HCA without mifepristone p=0.048; veh with mifepristone vs low dose HCA with mifepristone p=0.035, veh with mifepristone vs high dose HCA with mifepristone p<0.001, Tukey's post-hoc test) (Fig.3.13 H). However, the overall effect of mifepristone was not significant (F(1, 47)=1.88, p=0.178). The interaction of mifepristone and HCA treatment was not detected with 24h exposure (F(2, 47)=0.88, p=0.423), suggesting that the suppressive effect was not mediated by GRs.

Similar to the results reported previously for *Bcan*, *Ncan*, *Vcan, Hapln4, Has3* and *TnR,* expression of Pv also showed the inconsistent results between the initial HCA experiment and following mifepristone experiment, with suppression after high dose HCA reported in the initial HCA experiment at 21 DIV, but with suppression reported after both low and high dose HCA treatment in the following mifepristone experiment. This inconsistency could be due to variability between each separate experiments with different biological samples.

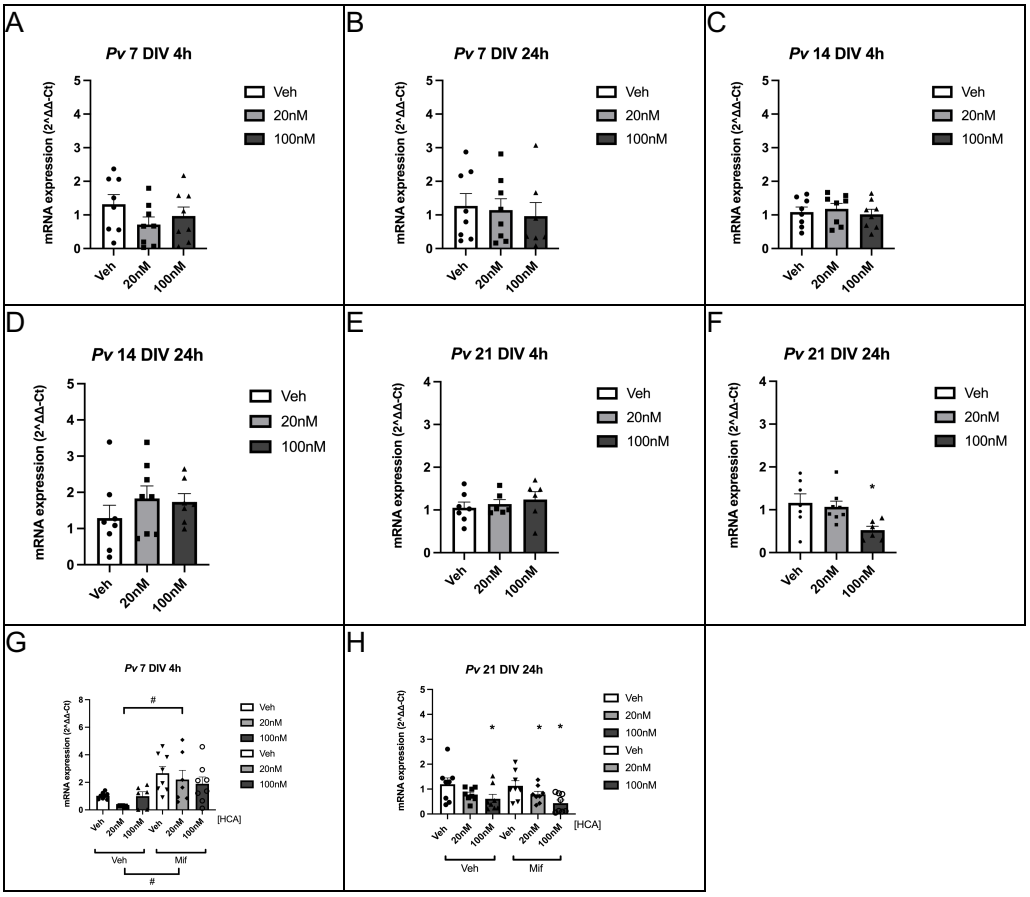

Figure 3.13: mRNA expression of *Pv.* A-F: mRNA expression of *Pv* after 4h and 24h exposure to low dose (20nM) and high dose (100nM) HCA at 7, 14 and 21 DIV (4h: 7 DIV: n=24 in total, veh=8, low dose=8, high dose=8; 14 DIV: n=24 in total, veh=8, low dose=8, high dose=8; 21 DIV: n=19 in total, veh=7, low dose=6, high dose=6; 24h: 7 DIV: n=24 in total, veh=8, low dose=8, high dose=8; 14 DIV: n=20 in total, veh=8, low dose=6, high dose=6; 21 DIV: n=21 in total, veh=7, low dose=8, high dose=6). G-H: the mRNA expression of *Pv* at 7 DIV after 4h and 24h low dose (20nM) and (100nM) high dose HCA and mifepristone (20nM) treatment (4h: HCA: n=46 in total, veh=7, low dose samples=8, high dose samples=8; HCA+Mif: veh=7, low dose samples=8, high dose samples=8; 24h: n=46 in total, HCA: veh=7, low dose samples=8, high dose samples=8; HCA+Mif: veh=7, low dose samples=8, high dose samples=8). The data for *Pv* was normally distributed as assessed with the Kolmogorov-Smirnov test. No outliers were detected in this study. The data were analysed by ANOVA followed by Tukey's post-hoc tests. * $p<0.05$ HCA effect vs corresponding vehicle group, Tukey's post-hoc test; # $p<0.05$ overall effect of mifepristone vs corresponding vehicle group, ANOVA, Tukey's post-hoc tests. The bar graphs show mean ± SEM.

3.4.3.2 *Gad1* mRNA expression

There was a decreasing tendency of the expression at 7 DIV after 4h HCA treatment ($F(2, 23)=2.92$, $p=0.076$), the changes of *Gad1* mRNA expression after 24h HCA treatment at 7 DIV were not significant ($F(2, 23)=2.24$, $p=0.132$) (Fig.3.14 A B). The expression at 14 DIV increased significantly at 4h HCA treatment ($F(2, 23)=3.78$, $p=0.040$, veh vs low dose $p=0.034$, Tukey's post-hoc tests), but not at 24h ($F(2, 17)=0.52$, $p=0.572$) (Fig.3.14 C D). At 21 DIV, no alterations were found after 4h treatment ($F(2, 18)=0.09$, $p=0.914$); after 24h, there was a decreased tendency with HCA treatment, but the post-hoc tests did not reach the significance level ($F(2,$

20)=11.20, p=0.001, veh vs low dose p=0.056, veh vs high dose p=0.088, Tukey's post-hoc tests) (Fig.3.14 E F).

After mifepristone treatment, at 7 DIV, the expression of *Gad1* was not significantly changed after HCA after 4h exposure (F (2, 40) =0.93, p=0.406) (Fig.3.14 G). The overall effect of mifepristone was approaching significance (F (1, 40) =4.01, p=0.053), suggesting a tendency of increasing *Gad1* expression in the presence of mifepristone. Additionally, the interaction of HCA treatment and mifepristone was not significant (F (1, 40) =4.01, p=0.237) (Fig.3.14 G). As there was a decreased tendency of *Gad1* mRNA expression after HCA exposure in previous results, similar tendency was shown in the current result, implying a GR-mediated suppression of *Gad1* mRNA levels that was on the borderline of detectability of the sample sizes.

At 14 DIV, no significant change in the mRNA levels after 4h HCA exposure was found (F (2, 47) =0.22, p=0.803) (Fig.3.14 H). The borderline significant increase in *Gad1* expression detected before was not reproduced. The overall effect of mifepristone was not significant either (F (1, 47) =0.19, p=0.661). There was a significant interaction of HCA and mifepristone (F (2, 47) =0.823, p=0.038), however, no specific significant changes were found in the following post-hoc tests (veh without mifepristone vs veh with mifepristone p=0.169, low dose HCA without mifepristone vs low dose HCA with mifepristone p=0.964, high dose HCA without mifepristone vs high dose HCA with mifepristone p=0.954, Tukey's post-hoc tests) (Fig.3.14 H).

Moreover, at 21 DIV, the effect of HCA treatment on *Gad1* expression was not significant after 24h exposure (F (2, 46) =0.71, p=0.496) (Fig.3.14 I). There was not a significant effect of mifepristone on *Gad1* expression at 24h (F (1, 46) =0.21, p=0.647). The interaction of mifepristone and HCA treatment was not detected with 24h (F (2, 46) =0.23, p=0.798) exposure (Fig.3.14 I).

Similar to the previous results, inconsistent findings were reported for *Gad1* between the initial HCA experiment and following mifepristone experiment, with an increase after low dose HCA reported in the initial HCA experiment at 14 DIV, but no changes reported in the following mifepristone experiment. These inconsistent results could be attributed to the different biological samples used in different experiments, leading to the results variability between each separate experiments.

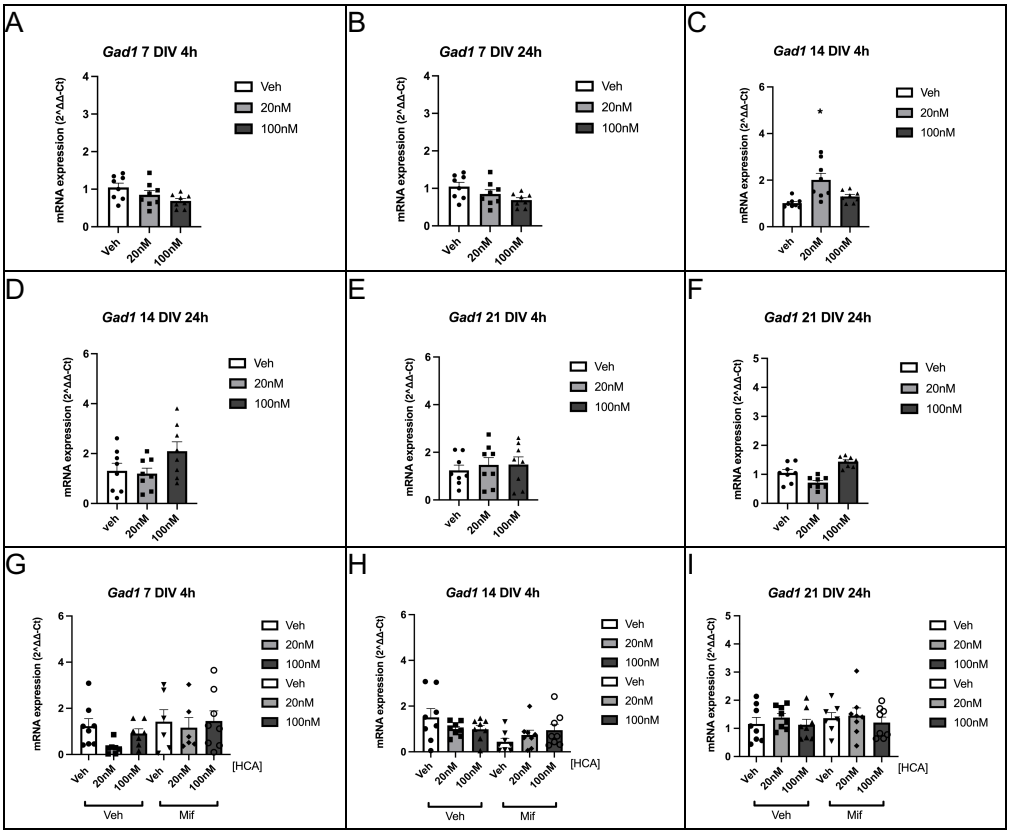

Figure 3.14: mRNA expression of *Gad1*. A-F: mRNA expression of *Gad1* after 4h and 24h exposure to low dose (20nM) and high dose (100nM) HCA at 7, 14 and 21 DIV (4h: 7 DIV: n=24 in total, veh=8, low dose=8, high dose=8; 14 DIV: n=24 in total, veh=8, low dose=8, high dose=8; 21 DIV: n=19 in total, veh=7, low dose=6, high dose=6; 24h: 7 DIV: n=24 in total, veh=8, low dose=8, high dose=8; 14 DIV: n=20 in total, veh=8, low dose=6, high dose=6; 21 DIV: n=21 in total, veh=7, low dose=8, high dose=6). G-H: the mRNA expression of *Gad1* at 7, 14 and 21 DIV after 4h or 24h low dose (20nM) and (100nM) high dose HCA and mifepristone (20nM) treatment (4h: HCA: n=46 in total, veh=7, low dose samples=8, high dose samples=8; HCA+Mif: veh=7, low dose samples=8, high dose samples=8; 24h: n=46 in total, HCA: veh=7, low dose samples=8, high dose samples=8; HCA+Mif: veh=7, low dose samples=8, high dose samples=8). The data for *Gad1* mRNA levels were normally distributed as assessed with the Kolmogorov-Smirnov test. No outliers were detected in this study. The data were analysed by ANOVA followed by Tukey's post-hoc tests. *p<0.05 HCA effect vs vehicle group, Tukey's post-hoc test. The bar graphs show mean ± SEM.

3.4.3.3 *Gad2* mRNA expression

However, the expression of *Gad2* remained unchanged at 7 DIV (4h: F(2, 23)=0.38, P=0.687; 24h: F(2, 22)=0.31, p=0.740) (Fig.3.15 A B), 14 DIV (4h: F(2, 23)=0.33, p=0.723; 24h: F(2, 23)=2.21, p=0.134) (Fig.3.15 C D), and 21 DIV (4h: F(2, 18)=0.52, P=0.604; 24h: F(2, 20)=0.73, P=0.495) (Fig.3.15 E F) after HCA treatment for 4h and 24h.

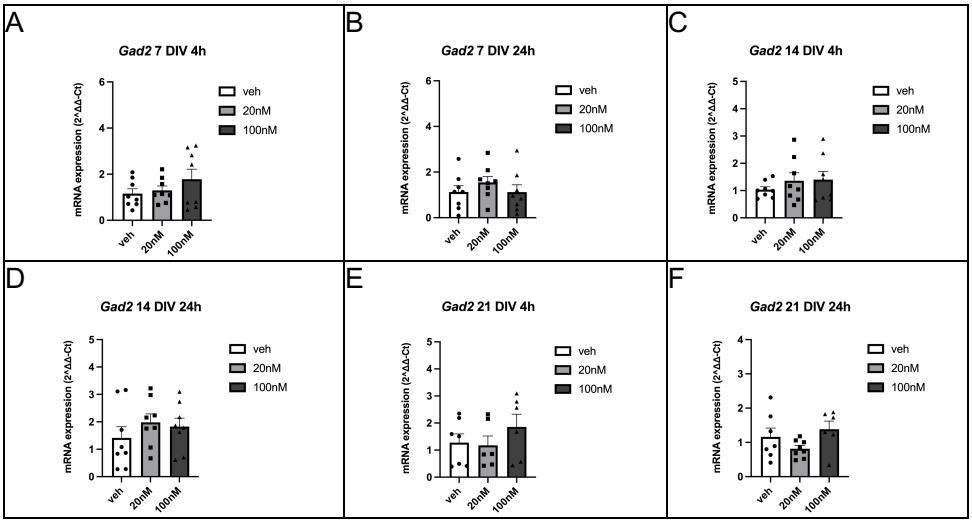

Figure 3.15: mRNA expression of *Gad2*. A-F: mRNA levels of *Gad2* after 4h and 24h exposure to low dose (20nM) and high dose (100nM) HCA at 7, 14 and 21 DIV. (7 DIV: n=20 in total, veh=8, low dose=6, high dose=7; 14 DIV: n=28 in total, veh=9, low dose=11, high dose=9; 21 DIV: n=39 in total, veh=14, low dose=14, high dose=12). The data for *Gad2* mRNA levels were normally distributed as assessed with the Kolmogorov-Smirnov test. No outliers were detected in this study. The data were analysed by ANOVA followed by Tukey's post-hoc tests. The bar graphs show mean ± SEM.

3.4.3.4 Gad67/65 protein levels

Following the measurement of *Gad* mRNA levels after HCA and mifepristone exposure, protein levels were also measured. With the initial HCA treatment, at 7 DIV, the protein levels of Gad67/65 remained unchanged after both 4h and 24h treatment (4h: Gad67: $F(2, 26)=0.60$, $p=0.555$, Gad65: $F(2, 26)=0.07$, $p=0.930$; 24h: Gad67: $F(2, 26)=0.04$, $p=0.959$, Gad65: $F(2, 26)=1,91$, $p=0.170$) (Fig.3.16 A B).

At 14 DIV, Gad67/65 protein expression remained unchanged with 4h HCA treatment (Gad67: $F(2, 26)=1.74$, $p=0.196$; Gad65: $F(2, 26)=2.01$, $p=0.156$) (Fig.3.16 C); after 24h treatment, no alterations were found in Gad67 protein levels ($F(2, 26)=2.18$, $p=0.135$), but Gad65 protein expression was reduced ($F(2, 26)=4.37$, $p=0.024$, veh vs high dose $p=0.032$, Tukey's post-hoc tests) (Fig.3.16 D).

After mifepristone exposure, at 7 DIV, there were no significant changes of Gad67/65 with 4h HCA treatment (Gad67: $F(2, 47)=0.95$, $p=0.393$; Gad65: 4h $F(2, 47)=1.47$, $p=0.241$), however, mifepristone significantly suppressed the overall protein expression (Gad67: $F(1, 47)=12.02$, $p=0.001$; Gad65: $F(1, 47)=11.55$, $p=0.001$). There were no significant interactions of HCA and mifepristone were detected for *Gad67/65* at 4h (Gad67: $F(2, 47)=0.32$, $p=0.726$; Gad65: $F(2, 47)=1.48$, $p=0.240$) (Fig.3.16 C). Similarly, after 24h, no HCA effect was reported on the protein levels of Gad67/65 (Gad67: $F(2, 47)=3.15$, $p=0.053$; Gad65: $F(2, 47)=2.61$, $p=0.085$), but the overall expression increased after mifepristone treatment (Gad67: $F(1, 47)=12.72$, $p=0.001$; Gad65: $F(1, 47)=13.68$, $p=0.001$). No significant interactions of HCA and mifepristone were detected (Gad67: $F(2, 47)=0.72$, $p=0.493$; Gad65: $F(2, 47)=2.61$, $p=0.085$) (Fig.3.16 D).

At 14 DIV, HCA had no effect on Gad67/65 with 4h treatment (Gad67: $F (2, 47) =2.14$, $p=0.130$; Gad65: $F(2, 47)=0.57$, $p=0.567$). The protein levels of Gad67 increased significantly after 4h mifepristone exposure ($F (1, 47) =7.49$, $p=0.009$), but no alterations were found in Gad65 protein band ($F (1, 47) =0.40$, $p=0.529$). No interactions of HCA and mifepristone was found in Gad67/65 (Gad67: $F (2, 47) =0.52$, $p=0.601$; Gad65: $F(2, 47)=0.84$, $p=0.439$) (Fig.3.16 G). After 24h, the

protein levels of Gad67/65 remained unchanged (Gad67: F (2, 47) =0.68, p=0.512; Gad65: F(2, 47)=0.03, p=0.861). Mifepristone had no effect on Gad65/65 (Gad67: F (1, 47) =0.03, p=0.861; Gad65: F(1, 47)=2.67, p=0.110). No interactions of HCA and mifepristone was found in Gad67/65 protein levels (Gad67: F (2, 47)=1.50, p=0.235; Gad65: F(2, 47)=1.50, p=0.235). (Fig.3.16 H). These results suggested that HCA had no effect on *Gad1*/*Gad67* protein levels through activating GRs. However, mifepristone exposure revealed a basal suppression of Gad67 protein, at this stage without a corresponding suppression of Gad65.

As with the inconsistent results reported in previous experiments with regards to the mRNA levels, Gad67/65 protein levels also showed inconsistent results in the initial HCA experiment and subsequent HCA with mifepristone experiments, suggesting an increased at 14 DIV with low dose HCA treated, but no alterations reported in the following mifepristone treatment. This could be due to the variability between different cultures with different biological samples.

Additionally, similar to the results reported in Bcan, Has2, Has3, Hapln4 and TnR western blot experiments, the Gapdh protein signals in the current experiment were also slightly different in different treatment groups (Fig. 3.16 A-H). The altered Gapdh signals might be attributed to the different expression of Gapdh protein with different drug treatment, or the sample loading error in western blot procedure, which was further discussed in the discussion section (Section 3.5).

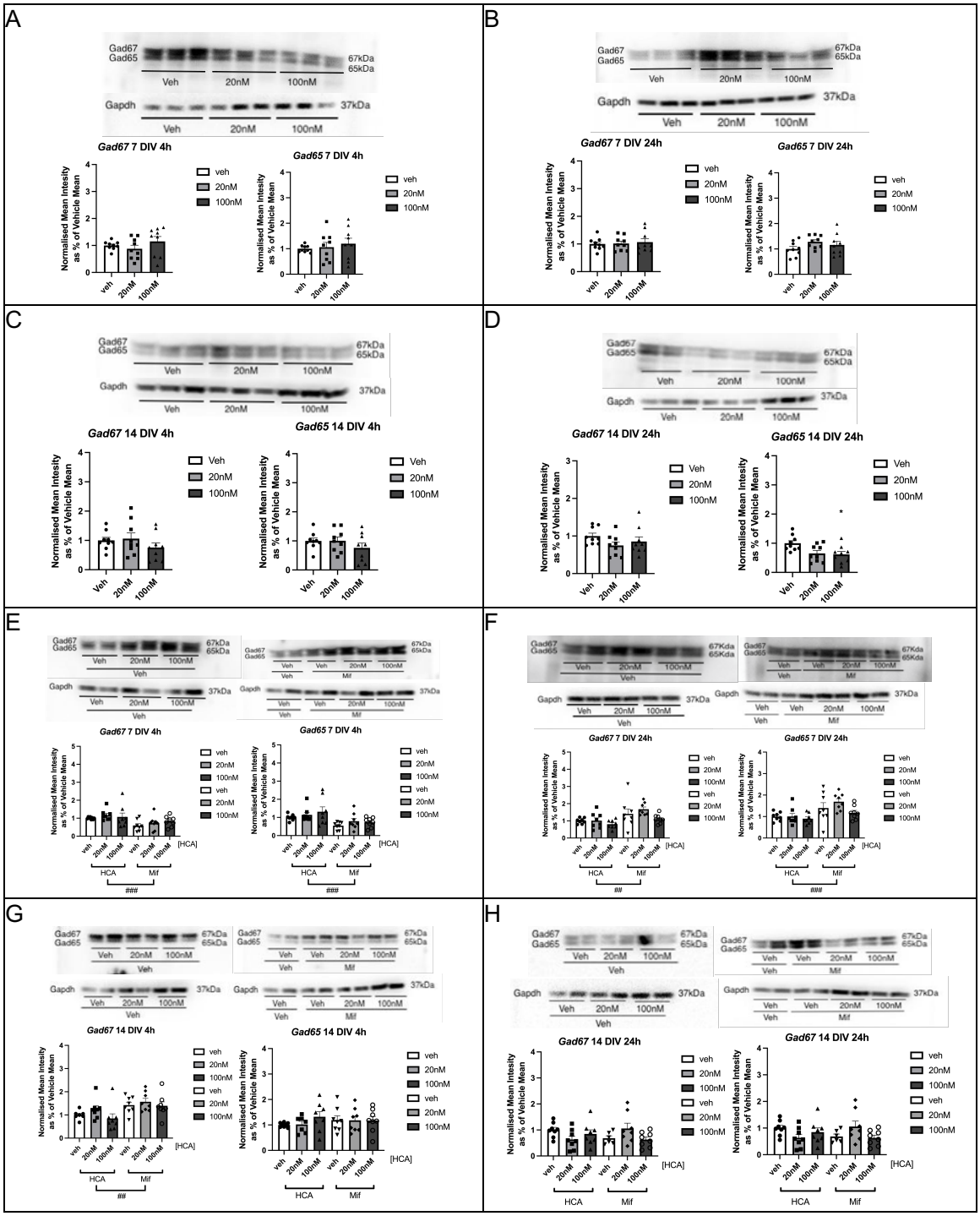

Figure 3.16: Protein expression of Gad67/65. A-D: Protein expression of Gad67/65 at 7 and14 DIV after low dose (20nM) and high dose (100nM) HCA exposure for 4h and 24h. (4h: n=34 in total, veh=12, low dose HCA=12, high dose HCA=10; 24h: n=34 in total, veh=12, low dose HCA=12, high dose HCA=10). E-H: Protein expression of Gad67/Gad65 after cotreatment with low dose (20nM) and high dose (100nM) HCA, and mifepristone (20nM) at 7 and 14 DIV (4h: n=48 in total HCA: veh=8, low dose=8, high dose=8, Mif: veh=8, low dose=8, high dose=8; 24h: n=48 in total HCA: veh=8, low dose=8, high dose=8, Mif: veh=8, low dose=8, high dose=8). The Gad67/65 protein data were normally distributed as assessed with the Kolmogorov-Smirnov test. No outliers were detected in this study. The data were analysed by ANOVA followed by Tukey's post-hoc tests. * $p<0.05$, HCA effect vs corresponding veh group, Tukey's post-hoc test; ## $p<0.01$, ### $p<0.001$ overall effect of mifepristone vs corresponding veh group, ANOVA, Tukey's

post-hoc tests. Boxes show median and interquartile range, with whiskers from minimum to maximum. The bar graphs show mean ± SEM.

Overall, numerous effects of GCs on PNN component gene expression were revealed. These encompassed more than one mechanism of action, generally suppressing the mRNA levels of Ncan, Vcan, Hapln4 and TnR without the reversible effect of mifepristone, and suppressing Has3 mRNA levels with a reversible effect of mifepristone. The overall effect of elevated HCA was summarised in the following Table 3.1.

	7 DIV						14 DIV						21 DIV					
	HCA				Mif		HCA				Mif		HCA				Mif	
	4h low	4h high	24h low	24h high	4h	24h	4h low	4h high	24h low	24h high	4h	24h	4h low	4h high	24h low	24h high	4h	24h
Acan					#													
Bcan											#							
Ncan	🡻 *					###												
Vcan								🡻 *										
Ptprz1																		
Has1					#							###		↑ *				
Has2												##						
Has3		🡻*											🡻*	🡻 *	🡻*	🡻 *		
Hapln4										🡻 *					🡻*			
TnR	🡻 *	🡻 *		↑ *		#												
Pvalb					#											🡻 *		
Gad1							↑ *								🡻*			
Gad2																		

Table 3.1: summary effect of GCs and mifepristone effects. 🡻: decreased tendency after HCA or collagen3; ↑ increased tendency after HCA or collage3; 🡻 * decreased tendency was statistically significant; ↑ * increased tendency was statistically significant; # overall significant effect of mifepristone, # $p<0.05$, ## $p<0.01$; ###$p<0.001$.

3.5 Discussion

The current study investigated the effect of GCs on mRNA and protein levels of PNN components and GABAergic related molecules including *Gad1*, *Gad2* and *Pv* in cultured neurons from neonatal mouse brains, and whether the alterations of expression were mediated by GRs.

Collectively, the results indicated primarily that mRNA levels of *Ncan* and *TnR* were reduced after both 4h exposure with low and high dose HCA at 7 DIV, and similar suppressive effect was also observed in *Has3* mRNA levels after high dose HCA exposure at 7 DIV; *Vcan* and *Hapln4* mRNA levels were downregulated by low dose HCA at 4h and high dose HCA at 24h treatment at 14 DIV, respectively. *Pv* mRNA expression were reduced by 24h exposure to high dose GCs at 21 DIV. Conversely, the mRNA levels of *TnR* and *Gad1* were upregulated by high dose HCA at 7 DIV with 24h treatment and low dose HCA at 14 DIV with 4h treatment time, respectively; and *Has1* mRNA levels were also upregulated at 21 DIV with high dose HCA exposure. These mRNA alterations were not reversed by mifepristone, suggesting the regulating effect of GCs were not activated through GRs.

However, unlike the alterations in mRNA levels, protein levels of PNNs components and GABAergic molecules did not present obvious changes with HCA treatment. Has3 protein levels decreased after low and high dose HCA with 4h treatment time at 7 DIV, and Has2 (59KDa) and Gad2/Gad65 protein levels decreased at 14 DIV after 4h and 24h high dose GCs, respectively.

For CSPG components, the mRNA expression of *Ncan* decreased with exposure to high dose HCA at 4h at 7 DIV. *Vcan* presented a significant decreased tendency at 14 DIV after 24h low dose HCA exposure. However, no significant changes were observed in *Acan*, *Bcan* and *Ptprz1* expression at 7 DIV, 14 DIV or 21 DIV after 4h and 24h HCA exposure.

The results of CSPG expression were partly consistent with the hypothesis and previous findings, with mainly suppression effect showed. In previous research, Strokotova et al. (2023) demonstrated that *Acan* was one of the most sensitive CSPGs components to long-term dexamethasone exposure, resulting in downregulation of its mRNA and protein levels in mouse brain tissues. In terms of *Bcan* expression, overexpression of corticotropin-releasing factor responding to stress was proved to suppress the extracellular matrix formation, including *Bcan* mRNA expression, indicating that elevated stress could reduce *Bcan* expression (Peeters et al., 2004). Moreover, several studies reported decreased expression of *Ncan* after rapid or chronic exposure to GCs. For example, Liu et al. (2008) demonstrated a downregulating effect of methylprednisolone on the expression *of Ncan* in astrocyte cultures with both short-term and long-term administration. Koskinen et al. (2020) and Yu et al. (2022) found reduced *Ncan* density and protein expression in brain after exposure to chronic stress. Zhong and Bellamkonda (2007) also supported the idea that intracerebral dexamethasone could lead to decreased staining intensity of expression of *Ncan*. Apart from the reduced expression of *Bcan* and *Ncan*, *Vcan* mRNA expression was proved to decrease after exposure to dexamethasone (McRae et al., 2017); and several studies also demonstrated a downregulation effect of GCs on *Vcan* mRNA expression in lungs among different species, such as, sheep and mice (Short et al., 2020; McDougall et al., 2018).

Although most of the studies were conducted in vivo and in different species, it is robustly reported that GCs could inhibit the mRNA expression of *Ncan* and *Vcan*. In the present study, decreased expression of *Ncan* and *Vcan* was detected at 7 DIV and 14 DIV, which is in line with the previous research and supported the inhibition effect of GCs on CSPGs components during neuronal developing period. The effects on *Ncan* are consistent with the presence of conserved

GC response elements (GREs) in the gene promoters, confirming the possibility of the effect of GCs on *Ncan* expression (Rauch et al., 1995; Wantanabe et al., 1995).

In addition to the inhibition effect of GCs on *Ncan* and *Vcan*, no mRNA expression changes were observed in *Ptprz1*, which was in line with Strokotova et al. (2023)'s study demonstrating no effect of dexamethasone on P*tprz1*'s mRNA expression. Although P*tprz1* was reported to be one of the CSPG components in the PNN structure in brain tissues and cultured cells (Haunso et al., 1999; Carulli et al., 2006; Miyata et al., 2005) and could stabilise PNN structure by cooperating with *TnR* (Eill et al., 2020), it showed lower intensity compared to other CSPGs components in rat cortex and hippocampus (Carulli et al., 2006), indicating that P*tprz1* might be not abundant in these areas. Therefore, the effect of GCs on P*tprz1* might not be robust and obvious.

Furthermore, no significant changes were observed in *Acan* mRNA expression, which was not consistent with most of the previous research (Berretta et al., 2015; Strokotova et al., 2023). However, this result was consistent with Ueno et al. (2018) illustrating that stress was not able to change the number and the intensity of *Acan* labelled PNNs in mouse hippocampus and cortex. The reason that the expression of aggrecan was not affected might be attributed to the complete cortical brain tissue collection for the primary neuronal culture. It has been revealed that PNNs components are expressed differently in different brain regions (Gao et al., 2018; Berretta et al., 2015; Pantazopoulos et al., 2021). *Acan* and *Bcan* are the 2 main components of CSPGs and are broadly distributed across different brain regions (Caterson, 2012; Ajmo et al., 2008). Higher levels of *Acan* were shown to be present in amygdala and hippocampus, and brevican showed high intensity levels in hippocampus (Pantazopoulos et al., 2021). As the samples were collected from the complete cortical tissues from foetal mouse brains in this study, the specific gene expression of different CSPGs components might not be detected exactly in the specific brain region.

Nevertheless, the mRNA expression of *Bcan* remained unchanged at 7 or 14 DIV and tended to increase at 21 DIV with 24h low and high doses of HCA exposure (although this effect did not reach significance when repeated in the mifepristone study). This finding was also not consistent with the reduced expression of *Bcan* in previous studies (Peeters et al., 2004). As noted above, *Bcan* had higher expression levels in hippocampal regions compared to other brain regions (Pantazopoulos et al., 2021), the current study collected samples from cultured cortical neurons. The abundance level of *Bcan* in cortical regions might not be sufficient to detect the decreases, and the alterations might not be clear enough to be detected after HCA treatment. And at 21 DIV, the neuronal structure is quite robust, and becomes mature after 21 DIV, so the expression of *Bcan* might be less susceptible to the external stressors. As *Bcan* expression was shown to increase steadily during the development period and even in the mature brain (Matsui, 1994), there is a possibility that *Bcan* expression tends to increase regardless of the external stressors' effect.

At 7 DIV, *Ncan* mRNA expression decreased rapidly with exposure to low dose HCA without mifepristone, but the mRNA levels remained unchanged with the presence of mifepristone; conversely, after long-term exposure, the downregulation effect of low dose HCA was observed even with the presence of mifepristone, suggesting that the rapid GCs downregulating effect was mediated though GRs, but a longer-lasting effect of GCs could still be detected without GR mediation. Similar effects were also found in *Vcan* at 14 DIV that the downregulation effect of high dose HCA could be observed after long term exposure with the presence of mifepristone. Culture medium with B27 supplement contains a small amount of corticosterone (Crochemore et al., 2005; Kino et al., 2010), which might suppress the mRNA levels of *Ncan* and *Vcan* through GRs during the cell growth period, resulting in rapidly reversible GR-mediated effects (although

the rapidity of reversal of the effect is surprising if it is genomic) and enhancement of the effect of added HCA.

Moreover, the results also reported that there was a significant decrease of *Has3, Hapln4* and *TnR* gene expression at 7, 14 or 21 DIV, but an increase in *Has1* expression at 21 DIV, indicating that GCs could suppress the gene expression of *Has3*, and *TnR* during early neurodevelopment (7 DIV), and suppress the gene expression of Hapln4 and upregulate *Has1* during late neurodevelopment (21 DIV).

These findings were partly consistent with the hypothesis and previous studies. There are no studies to date directly investigating GC effects on hyaluronan synthesis focusing on cells in brain tissues, but there are some equivalent studies using peripheral cells. In fibroblasts, a high concentration of GCs was demonstrated to suppress all genes encoding hyaluronan synthases (Stuhlmeier & Pollaschek, 2004) after 7h exposure. This suppressing effect of GCs on hyluronan synthesis was reproduced by Gebhardt et al. (2010) illustrating an inhibition effect of high concentrations of dexamethasone on *Has1* and *Has2* components. In human osteosarcoma cells, *Has1* and *Has2* mRNA levels were suppressed by dexamethasone with both short-term and long-term exposure (2h and 36h) (Zhang et al., 2000). This was insensitive to mifepristone (even at 100mM), whereas the effect observed here was blocked by mifepristone. GCS also down-regulated *HAS3* expression in keratinocytes and in fibroblasts after 8h of exposure (mifepristone sensitivity was not assessed) (Galgoczi et al., 2022), which is consistent with the results in current study. However, Gebhardt et al. (2010) reported no changes of *Has3* mRNA levels after dexamethasone exposure, as the study was conducted on human's fibroblast cells, it is possible that the results were different from the current study due to the cell type.

In addition to the suppressing effect, the current study reported an increasing tendency of *Has1* expression after 4h high dose (100nM) HCA exposure at 21 DIV. This result was in line with Galgoczi's et al. (2022) research demonstrating an increasing expression of *Has1* after 100nM dexamethasone exposure in fibroblasts. The upregulation could be supported by a previous suggestion that *Has1* plays a role in inflammation during cell stress, with inflammatory cytokines increased after stress induced inflammation, resulting in upregulation of *Has1* expression (Yamada et al., 2004). Upregulated expression of *Has1* was also observed in response to inflammatory diseases, such as atherosclerosis (Marzoll et al., 2009).

Thus, there is evidence from diverse peripheral cells as well as neurons, that *Has* genes are influenced by GCs. Compared to *Has3*, *Has1* is the least abundant HA, while *Has2* is the most abundant HA in brain tissues. However, *Has3* is more active than *Has1* and *Has2* and its expression is associated with early macrophage-induced inflammation (Heldin et al., 2019), which could suggest Has3 is the main HA influenced by GCs.

The results also showed that the *TnR* expression increased at 7 DIV after 24h high dose treatment, which was consistent with the hypothesis that GCs exposure could disrupt PNN components. The increased expression initially detected was not replicated in the subsequent experiment. The results might be partly attributed to the complex *TnR* recycling mechanisms (Dankovich et al., 2021). *TnR* molecules were demonstrated to be endocytosed within the initial 6h of incubation and resurfaced in 18h subsequently (Dankovich et al., 2021). Based on this mechanism, the *TnR* could be rapidly decreased by GCs treatment during the initial 4h and recycled with elevated expression later. In addition, TnR gene regulation by GCs, while not having been previously reported, is consistent with the presence of a conserved GRE in the promoter region of the gene (Putthoff et al., 2003).

In addition, to investigate the effect of GCs on PNNs components, the current study also measured the expression of *Pv*, *Gad1* and *Gad2* after exposure to HCA, as PNNs mainly surround GABAergic interneurons, mostly parvalbumin-expressing neurons (Cabungcal et al., 2013; Morishita et al., 2015). Exposure to stress and mutations in *Gad1* or *Gad2*, which encode GABA synthesizing enzyme glutamate decarboxylase (*Gad*), are the primary risk factors for psychiatric disorders associated with abnormalities in *Pv*-positive GABAergic interneurons (Wang et al., 2018). Therefore, examining the effect of GCs on the expression of Pv, *Gad1* and *Gad2* is crucial for investigating underlying mechanisms of stress and its relationship between risk genes for psychiatric disorders.

An initial elevation of *Gad1* expression by HCA was detected at 14 DIV, but this proved not to be replicable. The current study reported a downregulating effect on *Pv* with 24h HCA exposure, but no significant effect was found in *Gad2* expression. These results were consistent with the previous findings demonstrating that GCs decreased the number of *Pv* positive cells and reduced mRNA expression of *Pv* after high concentrations of corticosterone exposure (100nM-10μM) (Hu et al., 2010; Banasr et al., 2017). The increasing tendency of *Gad1* expression we observed in the initial experiment was also detected in previous research suggesting that cells treated with 100nM dexamethasone showed a 10-fold increase in the expression of *Gad1* mRNA levels after 6h (Kim et al., 2002) and high-level corticosterone upregulated *Gad1* expression in mice hippocampus. Conversely, Banasr et al. (2017) argued that in the in vitro study, *Gad1* expression decreased after long term (72 hours) high concentration dexamethasone exposure at 10 DIV. These converse results may be related to the exposure time to corticosterone or GCs, suggesting that short-term exposure might lead to upregulation of *Gad1*, and long-term exposure might lead to downregulation of *Gad1* expression, which is consistent with the current study where *Gad1* mRNA was possibly upregulated with rapid (4h) HCA exposure but was potentially suppressed with long-term (24h) HCA exposure.

The effects of HCA were observed in some targeted genes, such as *Ncan, Vcan, Has1, Has3, Hapln4, TnR* and *Pv*, however, the effects were not replicated in the experiments with absence or presence of mifepristone. As noted in the results section, the primary HCA treatment resulted in several alterations of mRNA levels of different PNN components and GABAergic neurons, however, these primary alterations up or downregulated by HCA were not replicated in the following mifepristone experiment, although some similar regulated tendencies toward changes were shown, such as with *Ncan, Vcan, Has1,* and *Has3.* These trends towards alterations did not reach the statistical significance level; or the significant alterations in the initial HCA experiments were not replicated in the same dose of HCA treatment group in the subsequent mifepristone experiments, such as with *TnR* and *Pv.* The inconsistent results, as noted in each results section, might be due to the biological variability. As the samples in the initial HCA study and the following mifepristone with HCA experiments were collected from different sets of cultures with different biological samples with slightly different cell growth conditions, different sample purification efficiencies and different mRNA abundance or concentrations. Apart from the sample variability, the results of the mRNA levels might vary between each qPCR runs (Hellemans et al., 2007; Neuberger et al.,2021). For example, as the samples used in the initial HCA treatment study and following HCA and mifepristone treatment study were collected from different biological samples, and the total number of samples that was loaded in each qPCR reaction plate was different, with more samples in the subsequent mifepristone treated experiment loaded in the qPCR plate. The use of different samples and the loading of a different total number of samples might lead to the variation between different qPCR runs, with the variability of the setting of the threshold line and cycle number processing after qPCR quantification, resulting slight differences in the report of the final mRNA levels.

In addition to the various effects of GCs, mifepristone alone also tends to influence the overall mRNA expression on CSPGs components. For example, the overall mRNA expression of *Ncan*, *TnR*, *Has1*, *Has2*, *Pv* and *Gad*1 was altered with exposure to mifepristone. The altered expression by mifepristone might be attributed to the corticosterone levels in culture medium.

The cultured cells were grown in medium consisting of B27 supplement (details were shown Chapter 2), which contains low amounts of hydrocortisone and corticosterone in the B27 serum of approximately 15 to 30 ng/ml (37nM-75nM) (Crochemore et al., 2005). Not only the B27 supplement, but the neurobasal medium also contains low amounts of corticosterone of 20ng/ml (50nM) (Chen et al., 2009). Therefore, the cultured medium consists of neurobasal medium and B27 supplement contains approximately 87nM to 125nM corticosterone, which is a basal concentration of corticosterone that might affect PNNs and GABA-related components during the cell growth period.

The concentration of basal corticosterone in the cultured medium is similar to the concentration in the human and mouse brain in non-stressed conditions. Due to the dynamic circadian changes of cortisol level, previous studies illustrated that the basal levels of human cortisol levels ranged from 152nM to 598nM (Hagg et al., 1987) which was consistent with the Oster et al. (2017) findings that normal human cortisol levels ranged from 60nM to 600nM approximately; and in human plasma, the basal levels of cortisol are around 275.9nM (10 ug/dl) (Taylor et al., 1983). In human foetal plasma, the cortisol levels were suggested to range from 40nM to 100nM. In mouse plasma, basal cortisone levels ranged from 120nM to 240nM (Gong et al., 2015), however, after restraint stress induction, the cortisone levels were upregulated to approximately 3000nM (Gong et al., 2015).

Corticosteroid-binding globulin (CBG) transports and binds GCs and progesterone in plasma, being able to bind approximately 80% to 90% of cortisol or corticosterone in plasma, with only 10% to 20% free cortisol or corticosterone left in plasma (Siiteri et al., 1982). In this case, free cortisol or cortisone levels in human and mouse ranged approximately from 30nM to 120nM, and 24nM to 48nM, respectively.

Corticosterone in the culture medium could cross the cell plasma membrane and rapidly activate receptors intracellularly, such as MRs and GRs, thus, the amount of corticosterone in the B27 supplement and neurobasal medium seems to provide a basal suppression effect on PNN component and GABA-related genes through both GRs or potentially MRs. As MRs have high affinity for corticosterone and HCA, the corticosterone in the culture medium will essentially activate MRs, which might result in the suppression of mRNA levels. Therefore, the downregulation effect regardless of the presence of mifepristone might be regulated by MRs. Furthermore, the overall mRNA levels reduced after long-term exposure to mifepristone, suggests an effect of GCs, through GRs mediation, in the basal culture medium.

In addition to the alterations of mRNA expression, not too many changes were observed in protein expression with HCA exposure except from Has2. The protein expression of Has2 increased at 7 DIV and decreased at 14 DIV after 4h treatment. The changes were not in line with the changes in mRNA, which decrease at 4h and was unchanged at 24h. A general correspondence between mRNA and protein levels is predicted, although there are many known exceptions (Liu et al., 2016). At the very least, this suggests separate control mechanisms for mRNA and protein.

Limited studies reported the functions of the 2 isoforms (represented by the 2 protein bands on the gels) of Has2 in CNS. However, in general, in embryo stem cells, Has2 is critical for muscle cell differentiation (Russell et al., 2016). In the current study, Has2 from the cultured cortical cells

exhibited 2 different protein bands with 59KDa and 48KDa molecular weight. Different protein bands of Has2 were reported in human fibroblast cells, with 63KDa and 53KDa molecular weight (Zhang et al., 2009). Since Has2 might be expressed differently in different cell types, it is possible that the molecular weight of Has2 protein varied between cell types.

Compared to the expression of Has2 and Has3, Has1 exhibited lower mRNA levels, thus, the protein levels of Has1 might not be as abundant as Has2 and Has3. In the current study, protein signals were not detected on western blots due to the low levels of Has1 protein. The undetectable Has1 protein expression was also reported previously which further supported the current results (Fowke et al., 2017).

Like Has1, the protein expression of Bcan (145kDa) was not clearly presented on all blots. Similar result was also reported in previous study that the lower band of Bcan protein was not clearly detected in western blot experiments (Lubbers et al., 2016).

Gad1/Gad67 and Gad2/Gad65 protein expression was bidirectionally regulated with mifepristone exposure. The overall protein levels were reversibly upregulated by the presence of mifepristone after 24h long-lasting exposure, indicating that the upregulation of Gad1/Gad67 and Gad2/Gad65 might be mediated by the inhibition of GR pathways, and suppressing the effect of GCs increases the protein levels. On the contrary, the protein levels of Gad1/Gad67 and Gad2/Gad65 were downregulated after short-term mifepristone exposure. The mechanisms whereby 4h antagonism of GRs suppresses expression, but a longer period of antagonism enhances expression, are not clear. It is possible that GAD regulation is tightly controlled, and a compensatory mechanism comes into operation after a few hours of reduced protein levels.

The effects on protein (present within 4h) are also surprisingly rapid, and suggestive of post-transcriptional actions. The fast effects might be attributed to altered proteasome activities. Proteasomes are protein complexes and are responsible for degradation of unhealthy or damaged proteins to maintain intracellular homeostasis (Schipper-Krom et al., 2019). They also mediate the regulation of cellular processes such as transcription and cell cycle control (Geng et al., 2002). Therefore, with the increasing tendency of *Has2* mRNA expression at 14 DIV, decreased Has2 protein levels might be the result of increased proteasome activities. There is some limited evidence suggesting that GCs might either activate or inhibit proteasomal degradation pathways (Sun et al., 2008: Kassel et al., 2001; Sundberg et al., 2006). In this case, proteasome activities were also tested with samples collected from cultured cells at 14 DIV with HCA and mifepristone exposure. The results are presented in Chapter 7.

In contrast to the sparsity of HCA effects on protein levels, a number of PNN-related genes showed altered expression at the protein level after mifepristone exposure. For example, TnR and Has3 protein levels were upregulated significantly after mifepristone exposure at 7 DIV, but with no regulation effect of HCA. The up-regulating effect of mifepristone suggested a GR-mediated influence on protein levels, due to the corticosterone in the culture medium. Thus, with inhibition of GRs by mifepristone, the overall protein levels tend to increase. As protein levels can be more susceptible to external stimulation (Cheng et al., 2016), protein expression was already regulated by corticosterone in the culture medium, resulting in no obvious additional changes with HCA exposure.

In some experiments for protein detection, the protein signal of the reference gene Gapdh seems to be slightly changed with the HCA treatment, such as, at 7 or 14 DIV, and the signal of Gapdh was lower in the veh group than HCA treated groups (Fig 3.4 L M; Fig 3.9 L M; Fig 3.9 M N; Fig 3.10 K M N; Fig 3.11 K L; Gig. 3.12 I K L; Fig 3.16 A-H). The altered signal detected for Gapdh might be firstly due to the drug treatment, as it has been shown in previous research that in some

drug-treated cells or samples, slightly different signals of Gapdh could be detected (Willis et al., 2022; Willis et al., 2020; Kwon et al., 2021). Secondly, the variable protein signals shown for Gapdh might also be attributed to the sample loading error and the limitations of western blotting, despite the protein concentration being quantified before proceeding to the procedure, the highly concentrated protein can make the samples viscous, which can then stick on pipette tips and result in sample loading error (Hong et al., 2018).

In the current study, two time points have been employed – 4h and 24h of GC exposure. The canonical GC mechanism of action involves binding to an intracellular receptor, and nuclear translocation of the complex, resulting in repression or activation of gene expression. These transcriptional effects are not rapid – a typical time-course would have an onset of altered mRNA levels 8-12h after GC exposure (Luca et al., 2013; Escoter-Torres et al., 2020), although occasionally more rapid effects can be observed. The altered levels would then be maintained for more than 24h after the original exposure. It is noteworthy that we do not see any changes in PNN component gene expression, either with HCA or mifepristone, that are present at 24h but not 4h, and hence would have been consistent with these genomic actions of GCs. However, we also see a number of effects at 4h exposure, that may or may not still be present after 24h. The non-genomic effects of GCs, which are thought to involve membrane receptor-mediated actions, not necessarily involving alterations in gene transcription, occur much more rapidly (Hynes & Harvey, 2019; Joels, 2018; Joels, Pasricha & Karst, 2013). While there is evidence for non-genomic actions mediated by the GR (and hence sensitive to mifepristone) (Panettieri et al., 2019, Groeneweg et al., 2011), there is also evidence that many non-genomic effects of GCs do not involve the canonical GRs; rather GCs can bind other receptors such as GPR97 (Ping et al., 2021). The affinity of GCs for these non-canonical receptors appears to be higher than the conventional receptor, and thus effects are seen at lower agonist concentrations. The altered mRNA levels that we observe 4h after exposure, with the lower concentration of HCA, may therefore be due to non-genomic actions. If so, they are likely to reflect post-transcriptional modulation of mRNA levels. Therefore, to test whether the effect was mediated through GRs, the GR antagonist, mifepristone was co-treated with HCA. It is intriguing that most of the HCA actions at 7 DIV were mifepristone reversible, whereas none of those at 14 or 21 DIV were. It may be that during maturation of the neurons and circuits, there is a switch from GR involvement to other receptor actions. Equally, this suggests that neurons may be especially sensitive to GC effects early in development.

As there are 2 genomic receptors for corticosterone, one is the MR, and another is the GR, both receptors can be involved in the mechanism of GCs. Corticosterone has higher affinity to MRs compared to GRs. As it has different binding affinity to different types of receptors, with lower concentrations of corticosterone exposure, it might bind to MRs only to maintain corticosterone responses for daily life, such as circadian rhythms; while at higher concentrations of corticosterone, it binds to GRs, resulting in the activation of GRs which could represent the stress response. This corticosterone mechanism is critical to maintain the secretion of ACTH and also important for homeostatic mechanisms: too much or too little corticosterone could lead to adverse results in the regulation of different components. Therefore, the level of corticosterone exposure is relevant to different pathways of the underlying mechanisms. In the current study, the effect of HCA occurred not only with high dose (100nM) treatment but also with low dose (20nM) treatment in different components with different time exposures. These results might be caused through binding to different receptors. Therefore, except from the GRs, MRs could also be a potential pathway for HCA effect. Mifepristone, at the concentration used, will be selective for GRs and not prevent GC actions at MRs. Therefore, some of the mifepristone-resistant actions of HCA may be MR-mediated. In this case, aldosterone, an MRs agonist, was used to tests whether the HCA effect is through MRs. The results are presented in Chapter 4. In addition,

collagen3, an activating ligand of GC-sensitive GPCRs (Huang and Lin, 2018; Leon et al., 2020; Krishnan et al., 2016), was also used to test if HCA could regulate PNNs components through GPCRs. The results for collagen3 are presented in Chapter 4.

The effect of GCs on CSPG components varied at different DIVs. This finding might be due to the reason that the temporal development of PNN components is expressed differently, suggesting that *Acan* and *Bcan* showed upregulated expression across this whole developmental period, *Ncan* developed rapidly at approximately 10 days, and *Vcan*, however, showed a downregulated expression after 10 days (Gao et al., 2018). In this case, there are clearly other regulatory factors operating, and GCs could affect CSPG gene expression differently at different development stages, which in turn leads to the changes of expression at different days in vitro.

Overall, numerous effects of GCs on PNN component gene expression were revealed. These encompassed more than one mechanism of action (summarised in table 3.1). The mechanisms and the receptors involved will be investigated further in the next Chapters.

Chapter 4

Effect of collagen3 and aldosterone on the expression of PNN components

4.1 Introduction

Results in Chapter 3 suggested an effect of HCA on expression of some of the PNN components at different development stages, including a suppressive effect on *Ncan*, *Has3* and *TnR* at 7 DIV, and *Vcan*, *Hapln4* and *Gad1* at 14 DIV. Although the effect of HCA on *Bcan* at 14 DIV did not reach statistical significance, there was an obvious tendency towards a change at 14 DIV with both low and high dose HCA treatment. Among the altered PNN components, the suppressive effect of HCA on *Has3* was diminished by mifepristone, although the effect of HCA was not significantly replicated in the following HCA and mifepristone treated experiment, the tendency towards suppression was observed, and this tendency was inhibited after mifepristone exposure, suggesting a possible GR-mediated action of GCs in regulating *Has3* expression. However, for other alterations, such as *Ncan*, *Vcan*, *TnR* and *Hapln4,* although still not significantly replicated in the subsequent HCA cotreated with mifepristone treatment experiment, trends towards decreased expression were observed, and these trends were not inhibited or diminished after mifepristone treatment inhibiting GRs, indicating that any effect of GCs on these components was not mediated by GRs. As the suppression effect of HCA acted in a rapid (4h) non-genomic way, with this consideration, other specific receptors could be suggested to be involved in the rapid non-genomic actions of GCs. As mentioned in Chapter 3 discussion section (section 3.5), 2 kinds of receptors were considered: one is GC-binding GPCR, and another is MR.

The GPCR family is one of the largest membrane protein families. The GPCR families participate in various physiological functions and are major targets of pharmaceutical drugs (Sriram and Insel, 2018). The whole GPCR family consists of 5 subgroups, comprising glutamate, rhodopsin, adhesion, frizzled and secretin receptors (Lagerström and Schiöth, 2008). Adhesion GPCRs (ADGRs/aGPCRs) contain several subfamilies, including ADGRL, ADGRE, ADGRA, ADGRC, ADGRD, ADGRF, ADGRB, ADGRG and ADGRV (Hamann et al., 2015), which consist of 2 fragments, the N terminal fragment (NTF) and C terminal fragment (CTF). The NTF comprises a protein extracellular domain (ECD), an autoproteolysis-inducing (GAIN) domain and glycosylated N-terminal region which varies between the different types of GPCRs; the CTF contains a 7 transmembrane (7TM) bundle and an intracellular C-terminal tail. The extracellular GAIN domain contains the GPCR proteolysis site (GPS). In many aGPCRs, the new N-terminus of the CTF after autoproteolysis acts as a tethered agonist to activate the receptor (Hamann et al., 2015).

In the previous years, aGPCRs were demonstrated to interact with other related ligands for several cellular responses (Lagerström and Schiöth, 2008), including brain development, cell adhesion, cell migration, ion-water homeostasis and inflammation (Piao et al.,2004; Monk et al., 2009). Although several cellular processes were discovered relating to aGPCRs suggesting novel roles of aGPCRs, the structural basis of aGPCRs activation, is still under investigation and the specific ligand for the activation mechanisms of different aGPCRs subtypes is still unclarified.

As aGPCRs function in cell-to-cell adhesion, receptors were found to be located on the cell membrane (Stacey et al., 2003). GPR97 (*ADGRG3*), a member of the aGPCRs family, was identified originally in mouse intestinal lymphatic endothelium, regulating endothelium cell migration (Valtcheva et al., 2013). Ping et al. (2020) discovered a new pathway for the effect of

stress hormones, demonstrating that the GCs could inhibit intracellular cyclic adenosine monophosphate (cAMP) levels via the activation of GPR97. GPR97 could bind to 2 GCs, the anti-inflammatory drug beclomethasone (BCM) and cortisol (Ping et al., 2020). Other GCs were suggested to interact with and activate GPR97.

Several studies also demonstrated that collagen 3 is a potential ligand for GPR56 (Huang and Lin, 2018; Leon et al., 2020; Krishnan et al., 2016). GPR56 (*ADGRG1*) is another subtype of aGPCRs, sharing a highly similar structure with GPR97. Collagen 3 is encoded by the *Col3a1* gene, mostly presenting in blood vessels and skin, and involved in the development of blood and skin tissues (Kim et al., 2005). Luo et al, (2014) discovered that collagen 3 expressed in the meninges and blood vessels interacted with GPR56 NTF specifically during mouse embryonic development stages. The activation by collagen 3 of GPR56 could activate RhoA pathways and inhibit neuronal migration in cultured cells (Luo et al., 2014). Similar phenotypes were found in collagen 3 KO mice and GPR56 mutation mice with over migration of neurons and cobblestone like brain appearance (Luo et al., 2014), which further proved that collagen 3 is a ligand of GPR56. As GPR56 and GPR97 share a highly similar structure, it is possible that these 2 receptors might have the same ligand, collagen 3. The cellular functions of GPR97 might be mediated by interacting with collagen 3 through the cell surface or extracellular matrix. In this case, the effect of GCs might work through the same mechanism as collagen 3, by activating GPR97 on the cell membrane, resulting in rapid or short-term alterations in the expression of targeted components.

In addition to GPR97, another receptor which should also be considered to potentially mediate the effect of corticosterone is the MR. Corticosterone binds to 2 receptors, MRs and GRs (Reul and de Kloet, 1985; Evans and Arriza, 1989), which are present in both CNS and PNS. MRs have 10-fold higher affinity for corticosterone than GRs, being substantially activated by lower levels of corticosterone; conversely, GRs could be activated by higher levels of corticosterone (Munck et al., 1984; Reul and de Kloet, 1985).

Both MR and GR are nuclear transcription factors. Corticosterone could bind to these intracellular localised receptors and start to initiate and participate in the regulation of gene transcription by recruiting transcription factors and binding to DNA-binding sites, which results in long lasting genomic effects. The intracellular GR and MR activation by corticosterone may have different effect on brain functions. Activation of GRs was suggested to increase glutamate transmission, but suppress long-term potentiation (Shors et al., 1990; Pavlides et al., 1993; Joels and Krugers, 2007; Joels et al., 2012); as MRs have higher affinity than GRs and they are substantially activated by normal levels of corticosterone, activation of MRs was reported to stabilise neuronal networks (Joels et al., 2012). The long-lasting genomic way that corticosterone activates MRs and GRs was investigated over the last several decades, however, it is suggested that corticosterone could also activate MRs through a rapid signalling pathway.

Electrophysiology studies showed that a rapid, non-genomic action played a role in different brain structures, including hippocampus, PFC and amygdala (Karst et al.,2005; Musazzi et al., 2010). The selective MR agonist, aldosterone, increased miniature excitatory postsynaptic currents (mEPSCs) frequency in principal neurons in hippocampus, dentate gyrus and basal amygdala within minutes (Karst et al.,2005). Prager et al. (2010) detected MRs at postsynaptic membrane densities of excitatory synapses, further proving that MRs could be located on the cell membranes and is possible to involve in the rapid non-genomic pathway.

The previous results reported that some PNNs components mRNA levels were affected by HCA, but not reversed by mifepristone, and with rapid (4h) exposure. As HCA could bind to both GR and MR, it is possible that this effect might be mediated through MRs or through GPR97.

4.2 Study aims

In this study, the aim was to investigate the effect of collagen 3 (a ligand of GPR97), aldosterone (selective agonist of mineralocorticoid receptors with low affinity for GRs) and fluticasone (selective agonist of GRs with low affinity for mineralocorticoid receptors) in order to determine whether GCs could regulate PNN components through other cellular pathways apart from via GRs. The specific aims were to:

a. to investigate whether GCs might regulate PNN components expression through GPR97 with short term exposure in cultured cortical neurons, in which case the effect might be reproduced by exposure to collagen 3.

b. to determine whether PNN components mRNA expression might be regulated through mineralocorticoid receptors in cultured cortical neurons.

4.3 Methods

The primary cultured cortical neurons were treated with collagen 3 (75nM final concentration), a ligand of GPR56 or GPR97 (considering the similarity between GPR97 and GPR56, they are likely to share the same ligands); aldosterone (100nM final concentration), an MR agonist, with little activity on GRs, and compared with fluticasone (50nM final concentration), a selective GR agonist that should reproduce effects of HCA mediated via GRs, but had little activity on MRs. The vehicle group were treated with nuclease-free water with 0.33% ethanol.

The cells were treated at 7 DIV and 14 DIV with 4h exposure time. Concentrations were selected based on literature values for robust agonist effects (Piechota et al., 2017; Dong et al., 2012). The reason for specific use of concentrations was presented in Chapter 2, Section 2.1.2,

The mRNA expression of PNN components were measured by qPCR with cDNA samples synthesised from treated cultured cells. the targeted primers include *Bcan*, *Vcan, Ncan*, *TnR*, *Hapln4* and *Gad1*.

4.4 Results

4.4.1 Collagen 3 effects on *Ncan* and *TnR* mRNA levels at 7 DIV with 4h exposure time

The mRNA expression of *TnR* was significantly upregulated by collagen 3 treatment for 4h at 7 DIV ($F(1, 23) = 6.33$, $p = 0.020$) (Fig 4.1 A). *Ncan* mRNA expression was downregulated by collagen 3 treatment for 4h ($F(1, 23) = 9.29$, $P = 0.006$) (Fig. 4.1 B) at 7 DIV.

The results indicated that collagen 3 could increase *TnR* mRNA expression and suppress *Ncan* mRNA expression rapidly. The former effect is opposite to the effect of HCA, but the effect on *Ncan* expression is similar, raising the possibility that both collagen 3 and GCs could be acting via the same (non-genomic) mechanism in this case.

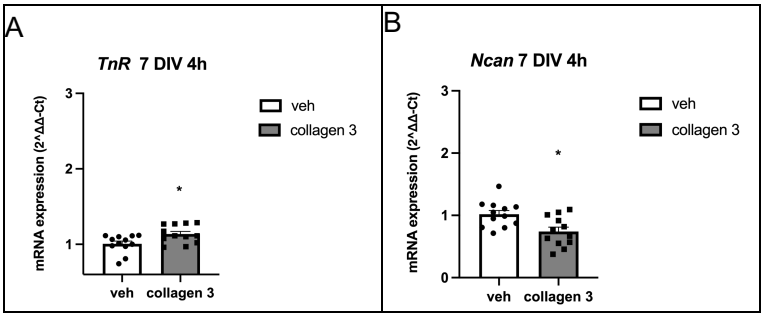

Figure 4.1: mRNA expression of *TnR* and *Ncan* at 7 DIV after collagen 3 treatment. A. mRNA expression of *TnR* at 7 DIV after 4h collagen 3 treatment (75nM); B. mRNA expression of *Ncan* at 7 DIV after 4h collagen 3 treatment treatment (75nM). (n=23 in total, veh=12, collagen 3 treated samples=11). The data for *TnR* and *Ncan* in the current study was normally distributed as assessed with the Kolmogorov-Smirnov test. No outliers were detected in this study. The data were analysed by ANOVA with Tukey's post-hoc test. * $p<0.05$ alterations after collagen3 treatment vs vehicle group, ANOVA followed by Tukey's post-hoc test. The bar graphs show mean ± SEM.

In addition, the mRNA levels of *Bcan* showed a tendency to increase after collagen3 treatment, suggesting an opposite effect of HCA, but the statistical results did not reach the significance level ($F(1, 10)=4.20$, $p=0.071$) (Fig. 4.2 A). Moreover, the mRNA levels of *Vcan* ($F(1, 10)=0.00$, $p=0.985$) (Fig. 4.2 B), *Hapln4* ($F(1, 10)=0.43$, $p=0.528$) (Fig. 4.2 C) and *Gad1* ($F(1, 10)=0.67$, $p=0.434$) (Fig. 4.2 D) were not affected by collagen 3 at 14 DIV, suggesting that mRNA levels of *Bcan*, *Vcan, Hapln4* and *Gad1* were not affected through an action of GCs bound to GPR56/97.

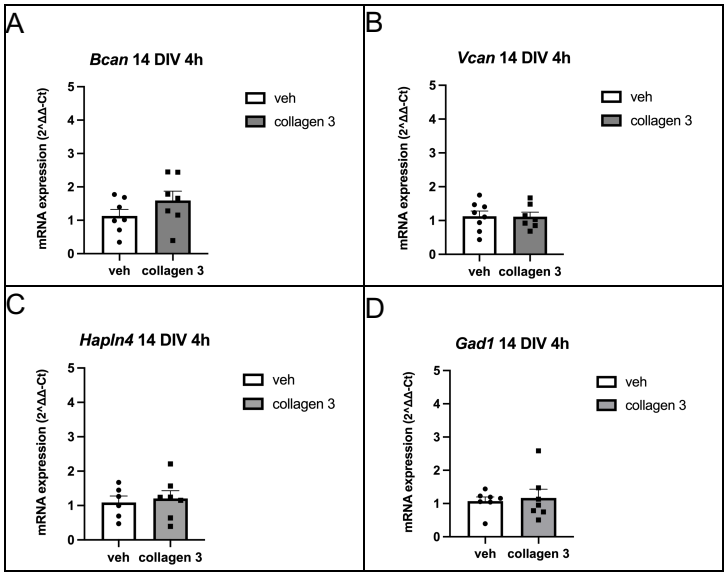

Figure 4.2: mRNA expression of *Bcan*, *Vcan*, *Hapln4* and *Gad1* at 14 DIV after collagen 3 treatment. A: mRNA expression of *Bcan* at 14 DIV after 4h collagen 3 treatment (75nM); B: mRNA expression of *Vcan* at 14 DIV after 4h collagen 3 treatment (75nM); C: mRNA expression of *Hapln4* at 14 DIV after 4h collagen 3 treatment (75nM); D: mRNA expression of *Gad1* at 14 DIV after 4h collagen 3 treatment (75nM). (n=23 in total, veh=12, collagen 3 treated samples=11). The data for *Bcan*, *Vcan, Hapln4* and *Gad1* in the current study was normally distributed as assessed with the Kolmogorov-Smirnov test. No outliers were detected in this study. The data were analysed by ANOVA with Tukey's post-hoc tests. The bar graphs show mean ± SEM.

4.4.2 Aldosterone had no effect on mRNA levels of PNNs components

The mRNA expression of *Bcan* (F(2,22)=1.77; p=0.197, veh vs aldosterone: p=0.938, veh vs fluticasone: p=0.201, Tukey's post-hoc tests) (Fig. 4.3 A), *Vcan* (F(2,22)=1.02, P=0.378, veh vs aldosterone: p=0.440, veh vs fluticasone: p=0.460, Tukey's post-hoc tests) (Fig 4.3 B), *Hapln4* (F(2,22)=3.30, P=0.058, veh vs aldosterone: p=0.887, veh vs fluticasone: p=0.060, Tukey's post-hoc tests) (Fig. 4.3 C) and *Gad1* (F(2,22)=0.68, P=0.517, veh vs aldosterone: p=0.981, veh vs fluticasone: p=0.636, Tukey's post-hoc tests) (Fig 4.3 D) remained unchanged after exposure to aldosterone and fluticasone at 14 DIV for 4h treatment. These results indicated that MRs were probably not the mediator of the effects of HCA on the expression of these genes. Further, the lack of effect of fluticasone provided additional evidence that GRs are also not involved in these effects.

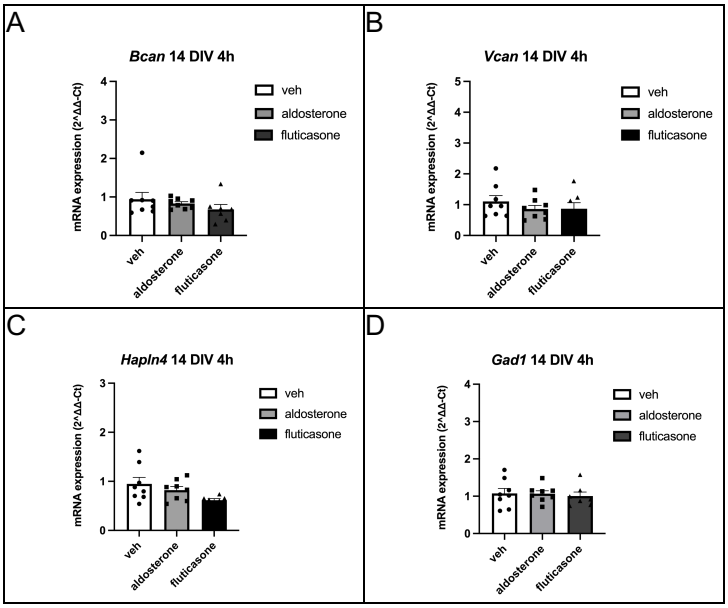

Figure 4.3: mRNA expression after 4h exposure to aldosterone (100nM) or fluticasone (50nM) at 14 DIV. A: mRNA levels of *Bcan.* B: mRNA levels of *Vcan*. C: mRNA levels of *Hapln4*. D: mRNA levels of *Gad1*. (n=22 in total, Veh=6, aldosterone treated samples=8, fluticasone treated samples=8). The data for *Bcan*, *Vcan, Hapln4* and *Gad1* in the current study was normally distributed as assessed with the Kolmogorov-Smirnov test. No outliers were detected in this study. The data were analysed by ANOVA followed by Tukey's post-hoc tests. The bar graphs show mean ± SEM.

4.5 Discussion

The data showed that the mRNA expression of *TnR* was significantly upregulated by collagen 3, while on the contrary, *Ncan* mRNA expression was downregulated by collagen 3 with 4h exposure at 7 DIV. However, the mRNA levels of *Bcan*, *Vcan, Hapln4*, *Gad*1 and *Pv* remained unchanged.

The previous results of the current study showed an up or downregulated effect of GCs and the antagonist of GCs, mifepristone, on some of PNN or PNN-related components, including *Ncan*, *Vcan*, *Has3*, *TnR, Gad*1 and an obvious decreased tendency of *Bcan*, at different neuronal development stages in a rapid non-genomic action. However, the rapid effects of GCs were also observed with no overall influence of mifepristone, which indicated that the effect of GCs was not mediated by GR. In this case, other GC-mediating pathways were considered to affect the mRNA

expression of PNNs or PNNs-related components. Therefore, another 2 receptors were considered to mediate the mRNA expression, which were GPR56/97 and MRs.

There are no previous studies investigating regulation of PNN component gene expression through GPR97. The current study measured the mRNA expression of *Bcan*, *Ncan*, *Vcan*, *TnR, Hapln4*, and *Gad1*, and reported that the altered expression of *TnR* and *Ncan* after 4h HCA exposure could be a non-genomic GC effect activity, as, in the case of *Ncan*, it was reproduced by collagen 3. This raises the possibility that both agents are acting via GPR56/97 or a closely related receptor, through the cell surface or extracellular region, and not involving changes in gene transcription through intracellular receptors, and hence occurring much more rapidly, usually less than 4 hours (Hynes & Harvey, 2019; Joels, 2018; Joels, Pasricha & Karst, 2013).

However, the changes of mRNA levels of *TnR* and *Ncan* were opposite, increasing for *TnR* but decreasing for *Ncan*. The mRNA levels of *TnR* and its relationship with collagen 3 has not been fully investigated in CNS, but in the periphery, members of the tenascin family were proved to bind directly to different types of collagens, with evidence that tenascin X could bind to collagen1 and collagen 4 (Minamitani et al., 2004), and tenascin C could bind to collagen1 in the fibroblast (Ehrismann and Tucker, 2011). The interaction of tenascin proteins and collagen contributed to the immune response and modified cell adhesion (Ehrismann and Tucker, 2011), which suggest a similar role of collagen 3 and TnR in the developing nervous system. Although limited studies showed the relationship of tenascin family members and collagen 3 in the CNS, it is possible that there might be a relationship of *TnR* and collagen 3 at the protein level, and not involving adhesion GPCRs. Collagen 3 might bind to *TnR*, which in turn lead to altered turnover of *TnR* molecules around the cell membrane and increase *TnR* mRNA levels.

As with *TnR*, no previous studies investigated the relationship of *Ncan* expression and collagen 3. However, the decreased mRNA expression of *Ncan* after rapid exposure to collagen 3 could be attributed to the interaction of collagen 3 and GC-bound GPR56/97, this downregulating effect and the activation were consistent with the hypothesis that either GCs or collagen 3 interacted with GPR56/97 and activated GPR56/97, leading to suppression of the mRNA expression of *Ncan*. This suppression effect of GCs was in line with previous studies illustrating rapidly decreased expression of *Ncan* after exposure to GCs (Liu et al., 2008), although involvement of GRs was suggested in the former study. Definitive evidence that ADGRGs mediate the action of corticosteroids on *Ncan* expression will require the development of a selective GPR56/97 antagonist acting at the same binding site.

The current results reported that the mRNA expression of *Ncan* could be affected by HCA through GPR97/ADGRG3 at 7 DIV after 4h exposure. *TnR* expression could be decreased by HCA via an unknown mechanism. Apart from affecting PNN components through GRs and GPR56/97, GCs also affected mRNA levels of *Bcan*, *Vcan*, *Hapln4* and *Gad1* at 14 DIV with 4h exposure. These altered mRNA levels were not significantly influenced by mifepristone and not collagen 3. Thus, the altered expression of *Bcan, Vcan*, *Hapln4* and *Gad1* were not mediated by GPCR. As HCA could act on both GRs and MRs, these altered expression levels might be transduced by MRs.

Aldosterone is an endogenous MRs agonist, with little activity on GRs. Therefore, in order to investigate whether HCA was able to affect the expression PNN components through MRs, the cultured cells were treated with aldosterone and compared with the GR-selective agonist fluticasone. The mRNA levels of mRNA levels of *Bcan*, *Vcan, Hapln4* and *Gad1* were measured at 14 DIV.

The results showed that the mRNA levels of mRNA levels of *Bcan*, *Vcan*, and *Gad1* remained unchanged after aldosterone and fluticasone exposure, indicating that HCA could not affect mRNA levels of *Bcan*, *Vcan*, and *Gad1* through MRs or GRs. However, the expression of Hapln4 showed suppression tendency after fluticasone with a p value reached the significance borderline, suggesting a potential inhibition effect of fluticasone mediated by GRs.

Corticosterone binds to MRs and GRs (Reul and de Kloet, 1985; Evans and Arriza, 1989), both being present in the CNS and PNS. As MRs, which are present predominantly in brain limbic areas (Krezt et al., 2001), have a high affinity for corticosterone, lower concentrations of corticosterone are sufficient to occupy MRs (Munck et al., 1984; Reul and de Kloet, 1985). On the contrary, GRs, which are present throughout the rat brain, have a 10-fold lower affinity compared to MRs (Munck et al., 1984; Reul and de Kloet, 1985). In this case, MRs were suggested to be in a constantly active state with low concentrations of corticosterone. Previous studies suggested that MRs and GRs were found in the cell's nucleus rather than cytoplasm or cell membranes, indicating necessary genomic actions while activating GRs or MRs (Gesing et al., 2001). However, previous studies proved that MRs were also present in the cell membrane (Karst et al., 2005; Musazzi et al., 2010), which could be activated by related corticosterone via rapid non-genomic actions. Hence, related to our previous results, low dose HCA could affect PNNs components through MRs via rapid non-genomic actions. However, with the exposure to aldosterone, an MRs agonist, mRNA levels remained unchanged, which is inconsistent with the hypothesis that MRs are involved. Aldosterone generally shows maximal activation of MRs at around 5nM to 100nM (Queisser et al., 2014; Rupprecht et al., 1993), so the concentration used should be adequate to see any effects of the drug. The power calculation based on the aldosterone treatment group suggested that the sample size has 65%, 50% and 23% power to detect the alterations of *Bcan*, *Vcan* and *Gad1*, respectively, suggesting that the sample size used had lower power to detect the change. However, in terms of Hapln4, the power analysis showed that the sample size had 92% chance to detect the changes. Therefore, we are not confident as to whether or not the MRs were involved in the corticosterone mechanisms on the components other than *Hapln4*.

Hapln4 mRNA levels tended to be decreased with 4h fluticasone exposure, indicating a potential rapid suppression effect of fluticasone mediated by GR, however, the HCA effect on Hapln4 at 14 DIV was not reversed by mifepristone in Chapter 3 and the downregulating effect of fluticasone did not reach statistical significance level. The lack of significant changes with fluticasone suggested that GRs are not involved in these actions. Fluticasone has high affinity for GRs, generally producing maximal effects at around 10-100nM (Ray et al., 1997; Milara et al., 2016). As noted above, a power calculation based on the initial findings suggests that the sample size used had insufficient power to detect any change reliably. Thus, it remains possible that GRs were involved in the corticosterone effect on the expression of the components. As non-genomic actions are not that well-characterised, there are likely to be mechanisms of corticosteroid action not involving GRs, MRs or GPR56/97.

To conclude, the mRNA levels of *Bcan*, *Vcan*, *Hapln4* and *Gad1* remained unchanged after aldosterone or collagen3 exposure, indicating the alterations after elevated GCs levels reported in Chapter 3 were not mediated by GPCRs or MRs. Thus, these alterations presented in Chapter 3 might be mediated through other GC actions. The GR-mediated mRNA decay mechanism was then taken into consideration. The following measurements of GR-mediated mRNA decay on *Bcan*, *Vcan*, *Hapln4*, and *Gad1* are presented in Chapter 5.

Chapter 5

Rapid effect of GCs through GCs receptor mediated mRNA decay (GMD) pathway

5.1 Introduction

Based on the results reported by previous chapters, GCs were suggested to reduce *Has3* and *Ncan* mRNA levels through GRs and GPCRs in a rapid non-genomic action, respectively. However, there were some other components which were reported to be suppressed by GCs, such as *Vcan*, *Hapln4* and *Gad1*; and others showed an obvious tendency to decrease after GCs exposure, such as *Bcan.* The alterations in these PNN components were not reversed by mifepristone, and were not reproduced by collagen3, aldosterone or fluticasone administration, indicating the GC effect on these components were not mediated by GRs, GPCRs or MRs. Therefore, another pathway was considered, which is GR-mediated mRNA decay (GMD) pathway.

GCs bound to GRs alter gene expression as a transcription factor through direct DNA binding with the necessary presence of ligand (Weikum et al., 2017 Rousseau et al., 1973; Muzikar et al., 2009; Dahlman-wright et al., 1991). However, previous studies demonstrated that GRs could also affect gene expression by binding to mRNAs (Ishmael et al., 2010; Dhawan e al., 2012; Cho et al., 2015; Par et al., 2015).

Based on the binding of GRs and mRNAs, a new GR-mediated mRNA pathway has been demonstrated, which is the GR-mediated mRNA decay (GMD) pathway (Cho et al., 2015). In the absence of ligand, GR binds to a GR-binding site (5'untranslated region (UTR)) of targeted mRNA; when GCs are induced, they bind to GR which is preloaded on the mRNA GR binding site (Cho et al., 2015), recruiting proline-rich nuclear receptor coregulatory protein 2 (PNRC2), upstream frameshift 1 (UPF1) and decapping enzyme 1a (DCP1A). UPF1 is a key factor of GMD as well as other mRNA decay pathways, such as nonsense-mediated mRNA decay (NMD) and staufen-mediated mRNA decay (SMD). In the NMD pathway, a premature translation termination codon (PTC) is recognised by UPF1, then UPF1 recruits PNCR2, resulting in the degradation of mRNAs that contains PTC to prevent the accumulation of truncated proteins (Kwon et al., 2007). In the SMD pathway, the RNA binding protein, staufen 1 (STAU1) interacts directly with UPF1 tethered to 3' UTRs of mRNA binding sites, and the recruited UPF1 on mRNA binding sites interacts with PNCR2 to trigger mRNA degradation (Kim et al., 2005).

Unlike the GR-mediated effect in the cell nucleus that takes a longer action time, GR-mediated mRNA decay could occur rapidly in the cytoplasm. For example, dexamethasone induces GMD detected within 2h (Park et al., 2016; Boggaram et al. 1991) or 3h (Cho et al., 2015; Dhawan et al., 2007). Although the GMD actions occur in cytoplasm within hours, they could still be reversed by GR antagonism. For example, mifepristone (RU486) inhibited GMD, with increased mRNA expression following the cotreatment of dexamethasone and RU486, compared to without RU486 presence (Boggaram et al. 1991; Dhawan et al., 2007). Thus, GR antagonists were also not only able to inhibit GRs in the cell nucleus but also in the cytoplasm, and the mRNA degradation could be mediated by GRs at a rapid speed.

It could be concluded that GMD could lead to the downregulation of mRNA levels within hours by directly binding to mRNAs, and the effect could be inhibited by GR antagonists. Therefore, the GMD pathway could mediate decreased mRNA levels of targeted PNN components which the

previous studies showed to be suppressed by GCs but not through MRs or GPCRs, including *Bcan, Vcan*, *Gad1* and *Hapln4*. In this case, whether the suppressed mRNA levels of these PNN components were mediated through GMD pathway needs to be investigated.

Actinomycin D (Act D) is widely used to inhibit new mRNA synthesis in mRNA stability or mRNA decay examination assays (Avendano et al., 2008). Act D is an inhibitor of transcription, and is a DNA intercalator, binding to DNA guanine residues, preventing the double-stranded DNA from unwinding, and in turn inhibiting the RNA polymerase (Avendano et al., 2008). Converging studies have used Act D to detect the mRNA decay of different genes mediated by GRs in several cell types. For example, with Act D administration to inhibit mRNA synthesis, mRNA decay of TNF-α was observed within 8 hours after dexamethasone treatment in human A594 cells (Smoak and Codlowski t al., 2006); and various adenosine and uridine (AU)-rich element-containing mRNAs showed decreased stability in human A594 cells after Act D administration and dexamethasone treatment (Muazzen et al., 2024). Similar accelerated mRNA decay after dexamethasone exposure with Act D administration was also detected in human pulmonary microvascular endothelial cells, with downregulated interleukin 8 mRNA stability and expression (Shi et al., 2014).

Therefore, to investigate whether the effect of GCs on PNN components mRNA expression was mediated by the GMD pathway, Act D was used to inhibit new mRNA synthesis, and the rate of mRNA decay with HCA treatment was measured. As the GMD pathway could be inhibited by GR antagonists, mifepristone (RU486) has also been co-treated with HCA to detect whether the mRNA decay effect is mediated by GRs.

5.2 Study aims

The aim of the current study is to investigate whether the rapid effect of HCA on the targeted genes, including, *Bcan, Vcan, Hapln4* and *Gad1*, was though GMD pathway by binding directly to the RNA binding site. The specific aims included:

a. to investigate whether the mRNA degradation of targeted genes was mediated by HCA within 4h

b. to investigate whether the HCA-mediated mRNA degradation was inhibited by the presence of mifepristone.

5.3 Methods

The cells were cultured in 24-well plates, the detailed procedure of cell culture was as presented in Chapter 2. At 14 DIV, the cells were treated with 20nM HCA, in the presence or absence of 20nM mifepristone, the mifepristone was added 30 minutes prior HCA treatment.

After exposure to HCA with or without mifepristone for 30 minutes to 1h, the cells were treated with 5μg/ml Act D to inhibit mRNA synthesis. Subsequently, the mRNA samples were collected at 0,1.5, 2, 3 and 4h in presence of Act D, followed by mRNA extraction. The detailed processes of mRNA collection from cultured cells and cDNA synthesis were presented in Chapter 2. The consideration of using specific drugs and concentrations were also presented in Chapter 2.

The qPCR was performed with targeted primers, including, *Bcan, Vcan, Hapln4* and *Gad1*, to measure the mRNA levels at each time point after Act D exposure. The samples were distributed in different plates for each qPCR run, based on the Act D exposure time point, and the interplate calibrated samples were added to each plate to eliminate the plate-to-plate variation.

The mRNA levels for each targeted gene were calculated by Ct values, the detailed procedure was presented in Chapter2. In the current experiment, as the interplate calibrated samples were added to each plate to eliminate the plate-to-plate variation, the Ct values for each sample were normalised to the mean Ct values of calibrated samples in each plate for analysis.

5.4 Results

The mRNA stability of *Bcan* was not significantly affected by GCs compared to the control groups. The half-life of *Bcan* mRNA level was approximately 1.5h, and the stability was not affected by HCA and mifepristone (Fig 5.1 A). Additionally, at each time points, the mRNA levels of *Bcan* were not altered by the HCA exposure, and the overall expression was not changed after mifepristone, and no further interaction was found at 0h and 1.5h of Act D presence (0h: HCA: $F(1, 19)=0.85$, $p=0.371$, Mif: $F(1, 19)=0.99$, $p=0.334$, HCA*Mif: $F(1, 19)=0.45$, $p=0.514$; 1.5h: HCA: $F(1, 14)=0.95$, $p=0.351$: Mif: $F(1, 14)=0.18$, $p=0.618$; HCA*Mif: $F(1, 19)=0.08$, $p=0.916$) (Fig 5.1 B C). Similarly, at 2h, no HCA effect was found, but the overall mRNA levels increased after mifepristone exposure, the interaction of HCA and mifepristone was not significantly reported (HCA: $F(1, 19)=2.26$, $p=0.152$; Mif: $F(1, 19)=18.06$, $p=0.001$; HCA*Mif: $F(1, 19)=0.40$, $p=0.535$) (Fig 5.1 D). At 3h and 4h, the mRNA levels of *Bcan* remained unchanged with both HCA and mifepristone treatment, no interactions were found either (3h: HCA: $F(1, 19)=1.76$, $p=0.204$, Mif: $F(1, 19)=0.78$, $p=0.390$, HCA*Mif: $F(1, 19)=1.84$, $p=0.193$; 4h: HCA: $F(1, 19)=1.33$, $p=0.265$, Mif: $F(1, 19)=1.03$, $p=0.324$, HCA*Mif: $F(1, 19)=1.14$, $p=0.301$) (Fig. 5.1 E F).

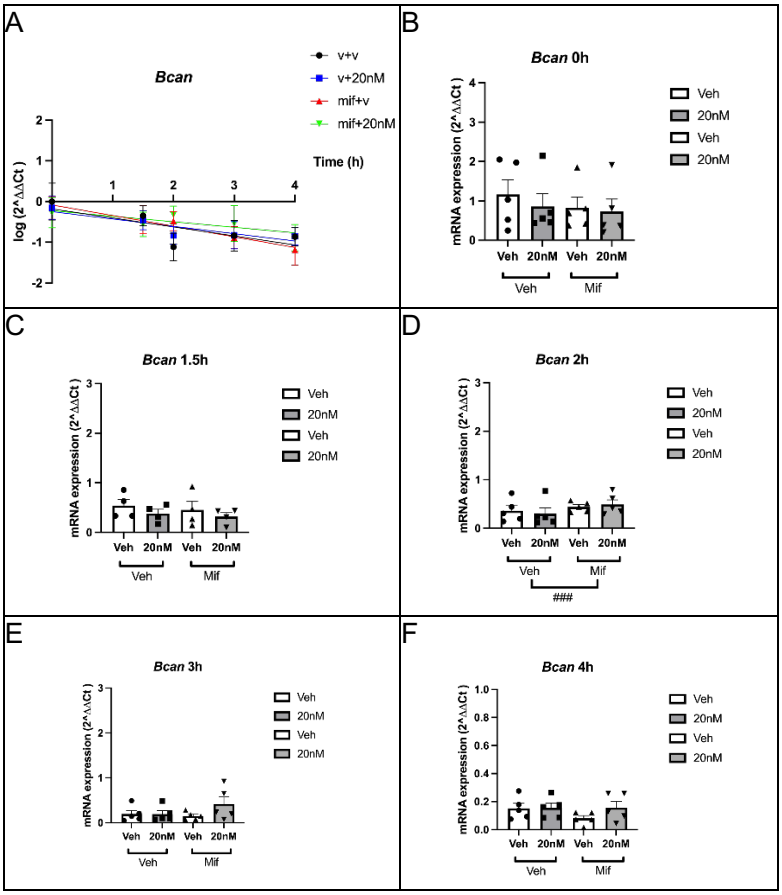

Figure 5.1: measurement of *Bcan* mRNA decay with HCA and mifepristone. **A:** measurement of *Bcan* mRNA decay with HCA (20nM) and mifepristone (20nM), the mRNA synthesis was inhibited by Act D (5µg/ml) for 0h, 1.5h, 2h, 3h and 4h. **B-F**: mRNA levels of *Bcan* with HCA and mifepristone exposure at different time points of mRNA synthesis inhibition (Veh: veh: n=5, HCA: n=5; Mif: n=5, HCA: n=5). The data for *Bcan* in the current study was normally distributed as assessed with the Kolmogorov-Smirnov test. No outliers were detected in this study. The data were analysed by ANOVA with Tukey's post-hoc test. ### p<0.001 overall effect of mifepristone vs corresponding to relative veh groups, ANOVA, Tukey's post-hoc tests. The bar graphs show mean ± SEM.

After HCA exposure, no significant alterations were detected in mRNA stability of *Vcan*. The half-life of *Vcan* mRNA was longer than *Bcan* mRNA, at around 4h, however, the stability was not affected by external HCA and mifepristone treatment (Fig 5.2 A). The specific mRNA levels of *Vcan* remained unchanged at each time points of Act D presence after both HCA and Mif treatment, with no significant interactions of HCA and mifepristone were reported at each time points (0h: HCA: $F(1, 19)=0.00$, $p=0.982$, Mif: $F(1, 19)=1.59$, $p=0.229$, HCA*Mif : $F(1, 19)=0.24$, $p=0.630$; 1.5h: HCA: $F(1, 14)=2.33$, $p=0.153$, Mif: $F(1, 14)=0.19$, $p=0.269$, HCA*Mif $F(1, 19)=0.60$, $p=0.455$; 2h: HCA: $F(1, 19)=1.06$, $p=0.319$, Mif: $F(1, 19)=2.95$, $p=0.105$, HCA*Mif: $F(1, 19)=0.12$, $p=0.306$; 3h: HCA: $F(1, 19)=0.86$, $p=0.367$, Mif: $F(1, 19)=0.41$, $p=0.532$, HCA*Mif: $F(1, 19)=0.301$, $p=0.102$; 4h: HCA: $F(1, 19)=1.23$, $p=0.284$, Mif: $F(1, 19)=0.10$, $p=0.965$: HCA*Mif: $F(1, 19)=0.77$, $p=0.393$) (Fig. 5.2 B-F).

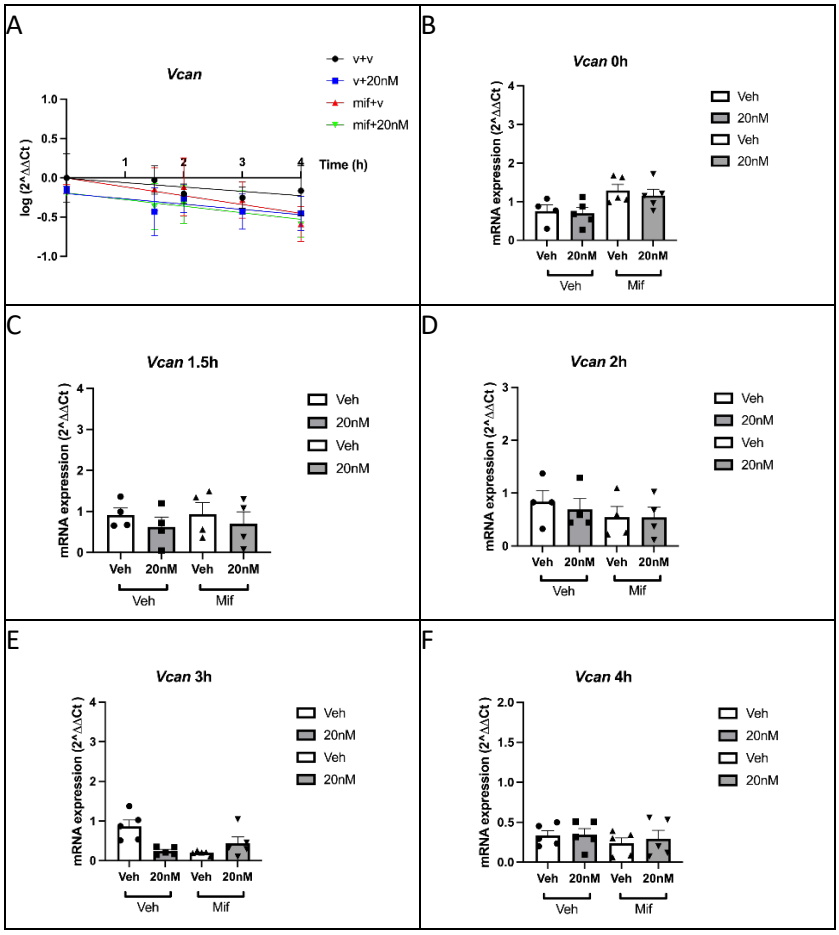

Figure 5.2: measurement of *Vcan* mRNA decay with HCA and mifepristone. **A:** measurement of *Vcan* mRNA decay with HCA (20nM) and mifepristone (20nM), the mRNA synthesis was inhibited by Act D (5μg/ml) for 0h, 1.5h, 2h, 3h and 4h. **B-F**: mRNA levels of *Vcan* with HCA and mifepristone exposure at different time points of mRNA synthesis inhibition (Veh: veh: n=5, HCA: n=5; Mif: n=5, HCA: n=5). The data for *Vcan* in the current study was also normally distributed as assessed with the Kolmogorov-Smirnov test. No outliers were detected in this study. The data was analysed by ANOVA with Tukey's post-hoc test. The bar graphs show mean ± SEM.

The results showed that HCA had no effect on the mRNA stability of *Hapln4*. The half-life of *Hapln4* was shown at 1.5h, and the overall mRNA stability of *Hapln4* was not affected by CHA and mifepristone (Fig 5.3 A). At 0h of Act D presence, the mRNA levels were not altered by HCA, but decreased with mifepristone treatment, no interactions between HCA and mifepristone was detected (HCA: F (1, 19)=3.72, p=0.072 Mif: F (1, 19)=6.43, p=0.023; HCA*Mif: F (1, 19)=0.21, p=0.650) (Fig 5.3 A). At 1.5h and 2h, the mRNA levels of Hapln4 was not affected by HCA and mifepristone treatment, no interactions of the 2 treatment groups were detected (1.5h: HCA: F (1, 14)=0.53, p=0.481, Mif: F (1, 14)=0.13, p=0.721, HCA*Mif: F (1, 19)=0.22, p=0.649; 2h: HCA: F (1, 19)=2.51, p=0.133, Mif: F (1, 19)=0.83, p=0.375, HCA*Mif: F (1, 19)=0.50, p=0.491) (Fig 5.3 C D). Although HCA did not affect the *Hapln4* expression at 3h, the overall expression increased by mifepristone, but the interaction was still not detected (HCA: F (1, 19)=1.46, p=0.244, Mif: F (1, 19)=5.72, p=0.029, HCA*Mif: F (1, 19)=0.11, p=0.749) (Fig 5.3 E). Furthermore, no HCA and mifepristone effect were reported at 4h, no significant interaction was reported at this time point (HCA: F (1, 19)=0.89, p=0.359, Mif: F (1, 19)=0.16, p=0.695, HCA*Mif: F (1, 19)=0.001, p=0.986) (5.3 F).

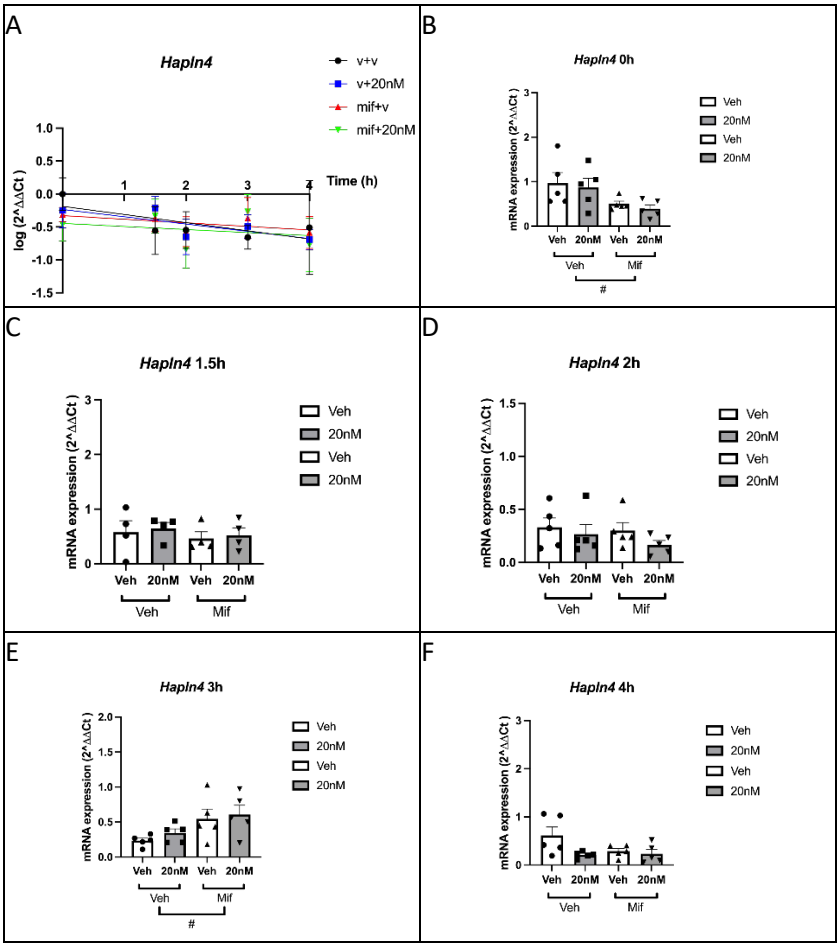

Figure 5.3: measurement of *Hapln4* mRNA decay with HCA and mifepristone. **A:** measurement of *Hapln4* mRNA decay with HCA (20nM) and mifepristone (20nM), the mRNA synthesis was inhibited by Act D (5μg/ml) for 0h, 1.5h, 2h, 3h and 4h. **B-F**: mRNA levels of *Hapln4* with HCA and mifepristone exposure at different time points of mRNA synthesis inhibition (Veh: veh: n=5, HCA: n=5; Mif: n=5, HCA: n=5). The data for *Hapln4* in the current study was also normally distributed as assessed with the Kolmogorov-Smirnov test. No outliers were detected in this study. The data was analysed by ANOVA with Tukey's post-hoc test, # $p<0.05$, overall effect of mifepristone vs corresponding to relative veh groups, ANOVA, Tukey's post-hoc tests. The bar graphs show mean ± SEM.

The mRNA stability and expression of *Gad1* with HCA exposure, the mRNA stability was not affected, and the half-life of *Gad1* was around 2h (Fig 5.4 A). The mRNA levels of *Gad1* were unchanged at 0, 1.5, 2 and 3h with both HCA and mifepristone exposure, and no interactions of HCA and mifepristone were detected (0h: HCA: $F(1, 19)=1.48$, $p=0.241$, Mif: $F(1, 19)=0.05$, $p=0.818$, HCA*Mif: $F(1, 19)=0.01$, $p=0.908$; 1.5h: HCA: $F(1, 14)=0.54$, $p=0.476$, Mif: $F(1, 14)=0.06$, $p=0.813$, HCA*Mif: $F(1, 19)=0.01$, $p=0.991$; 2h: HCA: $F(1, 19)=0.13$, $p=0.720$, Mif: $F(1, 19)=2.90$, $p=0.109$, HCA*Mif: $F(1, 19)=1.70$, $p=0.212$; 3h: HCA: $F(1, 19)=0.27$, $p=0.611$, Mif: $F(1, 19)=3.22$, $p=0.096$, HCA*Mif: $F(1, 19)=2.11$, $p=0.170$) (Fig 5.4 B-E). Moreover, the *Gad1* mRNA level was upregulated at 4h after exposure to HCA, however, the upregulation was only observed with the presence of mifepristone, and the overall expression of *Gad1* also increased with the presence of mifepristone, but no interaction of HCA and mifepristone treatment was reported (4h: HCA: $F(1, 19)=13.04$, $p=0.007$, Veh with mifepristone vs HCA with mifepristone Tukey's post-hoc test, Mif: $F(1, 19)=4.69$, $p=0.046$, HCA*Mif: $F(1, 19)=0.96$, $p=0.341$) (Fig 5.4 F).

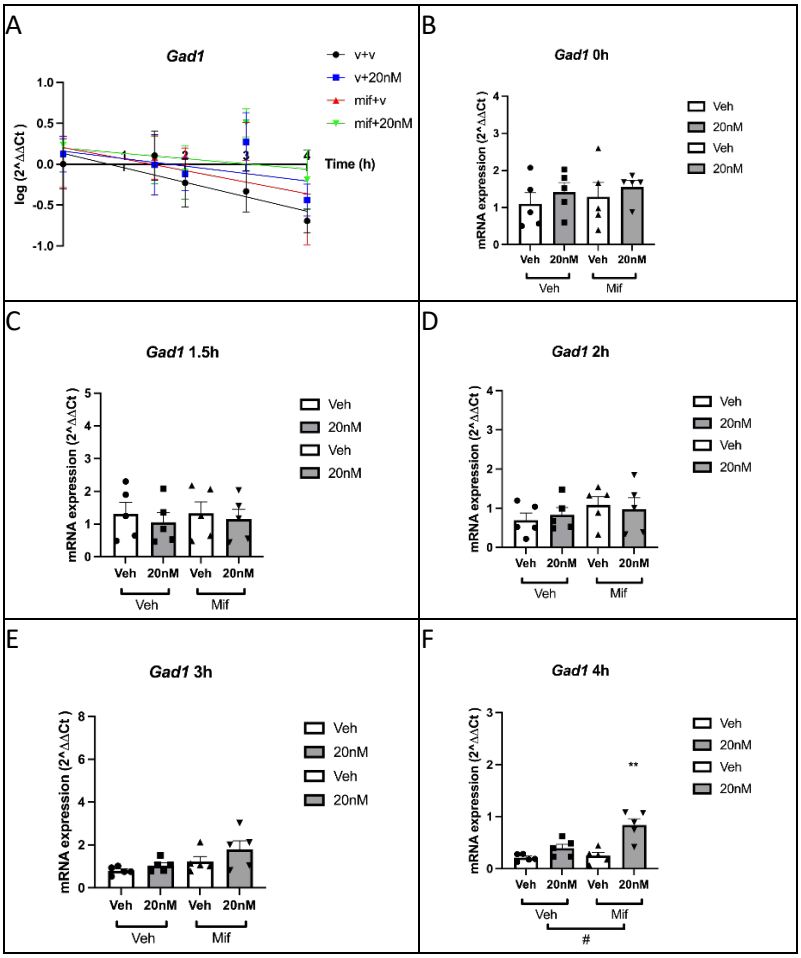

Figure 5.4: measurement of *Gad1* mRNA decay with HCA and mifepristone. **A:** measurement of *Gad1* mRNA decay with HCA (20nM) and mifepristone (20nM), the mRNA synthesis was inhibited by Act D (5μg/ml) for 0h, 1.5h, 2h, 3h and 4h. **B-F**: mRNA levels of *Gad1* with HCA and mifepristone exposure at different time points of mRNA synthesis inhibition (Veh: veh: n=5, HCA: n=5; Mif: n=5, HCA: n=5). The data for *Gad1* was normally distributed as assessed with the Kolmogorov-Smirnov test. No outliers were removed in this study. The data was analysed by ANOVA followed by Tukey's post-hoc tests. **p<0.01 HCA effect vs veh group, ANOVA, Tukey's post-hoc test; # p<0.05 overall effect of mifepristone vs corresponding to relative veh groups, ANOVA, Tukey's post-hoc tests. The bar graphs show mean ± SEM.

Therefore, the results suggested that the mRNA stability and degradation *of Bcan, Vcan, Hapln4* and *Gad1* were not affected by GCs. The mRNA levels *of Bcan, Vcan, Hapln4* and *Gad1* were not altered by GCs exposure after inhibition of mRNA synthesis by Act D at different time points, apart from *Gad1*, with increased mRNA levels with co-treatment of GCs and mifepristone. In addition, the upregulated overall effect of mifepristone was only observed in mRNA levels of *Hapln4* and *Gad1* with 3h and 4h exposure of GCs, respectively.

5.5 Discussion

Previous results illustrated the altered expression of *Bcan, Vcan, Gad1* and *Hapln4* mRNAs after 4h HCA exposure, suggesting a non-genomic effect of HCA. However, the alterations were not observed to be mediated by the rapid effect of MRs or GPCRs. Thus, the current experiment investigated whether the rapid alterations of *Bcan, Vcan, Gad1* and *Hapln4* expression by HCA exposure could have occurred via the GMD pathway. The results showed that the mRNA decay

of *Bcan, Vcan, Gad1* and *Hapln4* were not affected by GCs, with no differences of mRNA half-life observed between vehicle groups and HCA treated groups.

With the inhibition of mRNA synthesis by Act D for 0, 1.5, 2, 3, and 4h, the mRNA levels of *Bcan, Vcan, Gad1* and *Hapln4* were not altered by HCA exposure at different time points. However, an overall effect of mifepristone was detected for *Bcan, Hapln4* and *Gad1*, mRNAs, suggesting an increased overall effect of mifepristone on mRNA levels of *Bcan*, *Hapln4* and *Gad1*, with 2h, 3h and 4h mRNA synthesis inhibition, respectively, but a decreased effect on *Hapln4* mRNA levels with 0h mRNA synthesis inhibition. As these effects of mifepristone were not detected previously, these may be isolated occurrences of p values less than 0.05, but without any underlying biological significance. The only highly significant mifepristone effect was on *Bcan* mRNA at 2h, but even this was very clearly not observed at the 1.5h time point, and so seems unlikely to be a genuine effect.

No previous research has been conducted to investigate the contribution of GMD to PNN component gene regulation in the CNS. However, some studies illustrated increased mRNA degradation of *Vcan* mRNA in monkey muscle cells and human macrophages with elevated inflammation. For example, *Vcan* mRNA expression and stability was suppressed by interleukin-b in monkey arterial smooth muscle cells, with reduced *Vcan* mRNA half-life from 6h to 2h (Lemire et al., 2006). On the contrary, in human macrophages, the expression of *Vcan* mRNA stability and degradation rates were not changed after exposure to hypoxia, and the half-life of *Vcan* remained at around 10h (Sotoodehnejadnematalahi et al., 2015).

The initial results presented in Chapter3 showed that the mRNA levels of *Bcan* were suppressed by HCA exposure within 4h at 14 DIV, which was also replicated in the presence of mifepristone (n=6-8/group). However, the current results (n=5/group) showed no alterations of *Bcan* mRNA levels and mRNA stability after GCs exposure, indicating the suppressed effect of GCs on *Bcan* might not be through the GMD pathway. The lack of significant suppression effect of GCs on *Bcan* in this study might be attributed to lower sample sizes, with only 4 samples per group, which might lead to false negative results.

Although a significant rapid suppressive effect of GCs was detected on *Vcan* and *Hapln4* mRNA levels after HCA exposure at 14 DIV in the presence of mifepristone (as shown in Chapter 3), the initial GCs effect without mifepristone presence was also not detected here. Similar inconsistent results were also shown for *Gad1* mRNA levels. These inconsistent results might be due to a lack of statistical power in the current experiment.

Although limited studies have investigated the effect of GCs on the mRNA decay of *Bcan* and *Hapln4*, the half-life of the mRNAs for *Vcan* and *Gad1* were previously reported. For example, *Gad1* mRNA, which contains AU-rich elements, was suggested to have a half-life of around 2h, which is consistent with the current findings that the half-life of *Gad1* mRNA levels were around 2h (Frevel et al., 2003). As mentioned previously, the mRNA half-life of *Vcan* was between 6h and 10h in monkey muscle cells and human macrophages, while the current study estimated the half-life of *Vcan* mRNA levels at around 4h, which was partially consistent with the previous study that *Vcan* had a longer mRNA half-life compared to other components, such as, *Gad1*. As the current study only detected the mRNA expression in the first 4h of the degradation process in mouse CNS, it is possible that the differences of *Vcan* mRNA half-life could be attributed to the species and cell types where the targeted gene is located. In addition, no studies have investigated the half-life of *Hapln* mRNAs in the CNS, however, the half-life of hyaluronan in the PNS system was reported, ranging from minutes to days among different PNS tissues, illustrating that the half-life of hyaluronan was dependent on the specific region (Laurent and Reed, 1997).

As mRNA synthesis was inhibited by Act D for 0h, 1.5h, 2h, 3h and 4h, the mRNA levels of the reference gene are also possibly decreasing. However, various studies illustrated that the expression of *Gapdh* remained steady in the first 12h of mRNA decay, indicating that the half-life of *Gapdh* mRNA was much longer than most other mRNAs, and was not altered by external stimulation. For instance, the mRNA stability of *Gapdh* remained unchanged after exposure to Act D for 2h, 4h and 6h (Kang et al., 2014). In addition, Sinn and Sigmund (1999) indicated that the inhibitory effect of Act D on *Gapdh* expression was negligible in the first 12 hours, which was consistent with later findings that *Gapdh* mRNA has a long half-life of more than 12 hours (Mfossa et al., 2019). In this case, although mRNA synthesis was inhibited by Act D, *Gapdh* mRNA was still stable in the first 12 hours, suggesting that degraded mRNA levels could be observed here in targeted genes, rather than *Gapdh*. Thus, *Gapdh* could be a suitable reference gene in the current study.

The current study investigated the effect of GCs on mRNA levels with Act D inhibition at different time points. Therefore, the samples were divided into different plates for qPCR, based on the different time points, leading to a possibility that the plate variation might be a factor influencing the mRNA levels detected by qPCR. As the threshold used for Ct determination in each qPCR run is dependent on the number of samples and the fluorescent intensity, which is likely to vary between different plates. In this case, to eliminate the plate variation factor, calibrated reference samples were used in each plate. Hellemans et al. (2007) developed a system of inter-run calibration samples to remove the between plate/run variations in PCR methods, suggesting that the plate-to-plate variation could be removed by measuring the normalised relative quantity between the inter plate calibration values in each run. A similar method has also been used in other research to remove the plate-to-plate variation in each qPCR run. Neuberger et al (2021) used interplate reference samples for the interplate corrections, and Kochmanski et al. (2018) also used the interplate calibration samples to calculate the relative mRNA expression across multiple plates. Hence, apart from using housekeeping genes, calibrated referencing samples were also used in each plate to eliminate the plate-to-plate variation, to get a more accurate relative gene expression across different qPCR plates.

In conclusion, the current study found no effect of GCs on the rapid mRNA degradation of *Bcan, Vcan, Hapln4* and *Gad1* mRNAs in cortical cultured neurons, and the mRNA levels were not altered by GCs at different time points after transcription inhibition. The current results of the GC effects were not consistent with the initial findings presented in Chapter3, but this could be attributed to smaller sample sizes, reducing statistical power.

Chapter 6

Altered structural and dendritic formation of PNNs labelled by WFA

6.1 Introduction

Some of the PNN components, such as the CSPG molecules, could be affected by stress or stress related hormones such as corticosterone (Peeters et al., 2004; Liu et al. 2008; McRae et al., 2017; Bellamkonda et al., 2007). CSPGs are the main components to form the PNN structures, and so if these components are affected, this could lead to disrupted PNN organisation. Converging evidence has demonstrated that alterations in PNN formation were observed due to the lack of these main components. In some CSPG KO mice models, loss of PNNs was detected in different brain areas. As noted in Section 1.2.1 in Chapter 1, loss of some of the CSPGs or HA components, such as loss of *Acan*, *Ncan* and *Hapln1,* resulting in PNNs disorganisation, with faint, attenuated or distinct WFA-labelled PNNs presenting in various brain regions (Giamanco et al., 2010; Hunyadi et al., 2020; Carulli et al., 2010; Suttkus et al., 2014)

As PNNs not only enwrap the cell soma, but also proximal neuronal dendrites, in addition to the intensity or intensity expression of WFA labelling as an indication of PNN density, the length of dendrites covered by PNNs is also a factor reflecting PNN structural formation. Decreased length of proximal dendrites covered by PNNs was also reported with disturbed PNN main components. In *TnR* deficient mice, in addition to an atypical granular appearance of WFA-labelled PNNs, a reduction of dendritic length covered by PNNs was observed, and the number of cells' dendrites covered by PNNs was also decreased in both cortex and hippocampus areas (Weber, et al., 1999). In addition, lack of *Ptprz1* was also shown to affect PNN-covered dendrites, with the loss of net-like PNNs surrounding cell soma and dendrites (Eill et al., 2020); and similar PNN disruption around cells and dendrites were also detected in *Halpn1* KO mice, indicating lack of *Hapln1* was accompanied by attenuated WFA-labelled PNNs around cells, and no PNNs were found to be present around dendrites (Suttkus et al., 2014; Carulli et al., 2010). These results raised a suggestion that altered PNN morphology could not only be observed as alterations of PNN expression, such as intensity or intensity, but also by the length and the number of cell dendrites covered by PNNs.

Stress is an important factor influencing PNN development, including affecting specific components' expression, which may result in alterations of PNN morphology, such as disrupted intensity, the dendritic length and number of dendrites covered proximally by PNN. Consistent evidence illustrated the reduction of PNN intensity with stress exposure or stress hormone administration. However, whether stress affects the dendritic length covered by PNNs remained less clear. Therefore, in the current study, the experiments aimed to investigate the effect of the stress hormone, HCA, on PNN morphology, including intensity, dendritic length and number covered by PNNs, in cultured cells at 14 DIV and 21 DIV.

6.2 Study aims

In this study, the aim was to investigate the effect of GCs on PNN morphology, including alterations of intensity, the length of dendrites covered by PNNs, and the number of dendrites covered by PNNs, in cultured cortical neurons. The specific aims were:

a. to investigate the effect of GCs on the length of dendrites covered by PNNs.

b. to investigate the effect of GCs on the intensity of PNNs.

c. to investigate the effect of GCs on the number of dendrites covered by PNNs.

6.3 Methods

Cortical neurons were cultured from C57BL/6 embryonic mice at E17 in chamber slides and treated with HCA, and cotreatment with HCA and mifepristone at 14 DIV and 21 DIV for 4h and 24h, respectively. The detailed procedure of cell culture was presented in Chapter 2.

The cultured neurons were fixed by 4% paraformaldehyde (PFA) for 30 minutes and stored in PBS at 4°C and ready for immunohistochemistry. The procedure was performed as described in Chapter 2, whereby the cultured neurons underwent a blocking step before incubation with biotinylated Wisteria floribunda agglutinin (WFA) (1:1000) overnight. Afterward, streptavidin-conjugated Rhodamine Red-X (1:500) was added to the cultured cells in the dark for 2 hours. Subsequently, the cultured slides were mounted with vectashield mounting media and covered with coverslips.

The overview of PNNs surrounding cultured neurons was detected through a confocal microscope (Zeiss, LSM900) with a 10x objective for counting and 20x objective for exhibiting, and the images were captured through the Zen Blue system. All exhibited images were captured as a Z-stack (15μm in depth) using a Z step of 0.50μm, 20X objective lens, image size 1024x1024 pixels. The images were taken using Zen blue 3.0 software and downloaded with a maximum projection size using the Zen black system. The dendritic length and mean intensity intensity covered by PNNs were measured by Image J as stated in Chapter 2.

6.4 Results

6.4.1 HCA downregulated length and mean intensity of dendrites covered by PNNs at 14 DIV and 21 DIV

At 14 DIV, exposure to both 20nM and 100nM HCA lead to decreased length of PNN covering dendrites after 4h (Kruskal–Wallis statistic=124.4, $p<0.001$) (Fig 6.1 A B) with mean length of PNN surrounding dendrites reduced from 25.6μm to 19.9μm after 100nM (Dunn's post-hoc test, $p<0.001$) HCA exposure and 18.6μm after 20nM HCA exposure (Dunn's post-hoc test, $p<0.001$). Additionally, the intensity of PNNs surrounding dendrites remained unchanged after 4h exposure to HCA treatment (Kruskal–Wallis statistic=4.19, $p=0.123$) (Fig 6.1 A B).

After 24h, 20nM or 100nM HCA exposure (Kruskal–Wallis statistic=38.80, $p<0.001$) reduced the mean length of PNNs covering dendrites significantly from 26.9μm to 24.3μm with 20nM HCA (Dunn's post-hoc test, veh vs 20nM HCA $p<0.001$) and 19.3μm with 100nM HCA (Dunn's post-hoc test, veh vs 100nM HCA $p<0.001$) (Fig 6.1 C D). On the contrary, after 24h HCA exposure, the intensity of PNNs covering dendrites showed a significant increasing tendency (Kruskal–Wallis statistic=50.69, $p<0.001$) from 15.18 a.u. to 19.22 a.u. and 24.8 a.u. with 20nM HCA (Dunn's post-hoc test, veh vs 20nM HCA $p<0.001$) and 100nM HCA exposure (Dunn's post-hoc test, veh vs 100nM HCA $p<0.001$), respectively (Fig 6.1 C D).

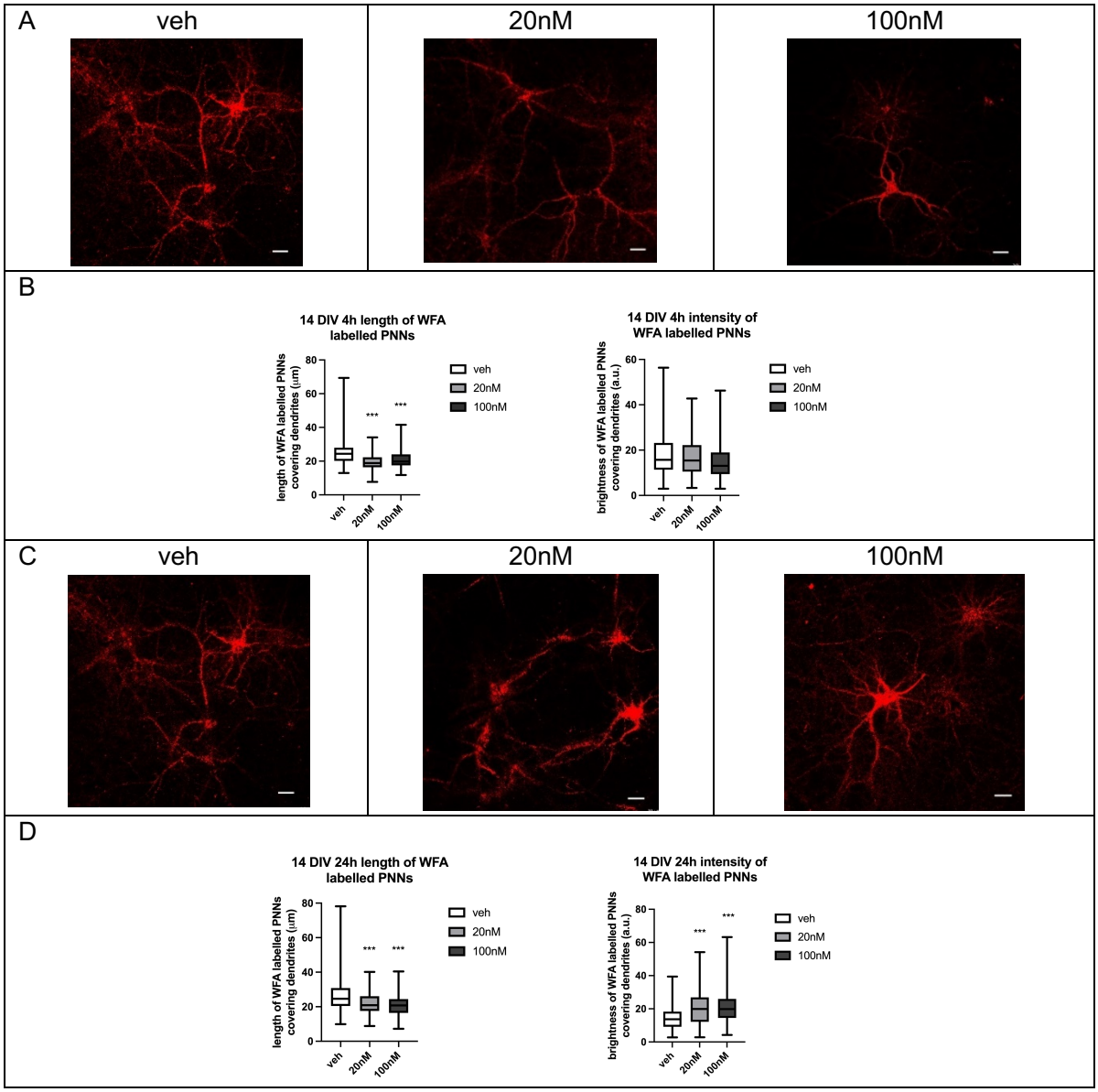

Figure 6.1. Fluorescent detection of WFA-labelled PNNs in cultured cells at 14 DIV A: representative immunofluorescence images of WFA labelled PNNs around cultured cells after 4h treated with vehicle, 20nM and 100nM HCA. B: length and intensity intensity of dendrites covered by WFA labelled PNNs after 4h treatment (Veh: 270 dendrites in 20 cells nested in 3 different slides with 2 cultures, 20nM: 166 dendrites in 20 cells nested in 3 different slides with 2 cultures, 100nM: 199 dendrites in 16 cells nested in 3 different slides with 2 cultures). C: representative immunofluorescence images of WFA labelled PNNs around cultured cells after 24h treated with vehicle, 20nM and 100nM HCA. D: length and intensity intensity of dendrites covered by WFA labelled PNNs after 24h treatment (Veh: 153 dendrites in 17 cells nested in 3 different slides with 2 cultures, 20nM: 164 dendrites in 17 cells nested in 3 different slides with 2 cultures, 100nM: 196 dendrites in 19 cells nested in 3 different slides with 2 cultures). Scale bar: 20µM. The data for length and intensity of PNNs surrounding dendrites were not normally distributed at 14 DIV with 4h and 24h HCA as assessed with the Kolmogorov-Smirnov test. No outliers were detected. The data were analysed by Kruskal–Wallis test followed by Dunn's post-hoc tests, *** $p<0.001$ HCA effect vs corresponding veh group, Kruskal-Wallis test with Dunn's post-hoc test. Boxes show median and interquartile range, with whiskers from minimum to maximum.

The length and intensity of PNNs surrounding dendrites in cultured cells were also measured at 21 DIV (a time when GC-induced changes in PNN constituent gene expression are no longer evident), again based on WFA staining after HCA treatment.

As a result, exposure to 20nM and 100nM HCA resulted in decreased length of PNNs covering dendrites after 4h (Kruskal–Wallis statistic=239.16, $p<0.001$), with reduction of mean length from 29.3μm to 23.4μm with 20nM HCA (Dunn's post-hoc test, veh vs 20nM HCA, $p<0.001$) and to 21.7μm with 100nM HCA exposure (Dunn's post-hoc test, veh vs 100nM HCA, $p<0.001$) (Fig 6.2 A B). However, no significant changes of PNN's intensity were found (Kruskal–Wallis statistic=4.25, $p=0.119$) treatment (Fig 6.2 A B).

Length of PNNs covering dendrites also decreased after 24h HCA exposure (Kruskal–Wallis statistic=34.64, $p<0.001$) (Fig 6.2 C D), with reduction of mean length from 25.3μm to 21.0μm with 20nM HCA (Dunn's post-hoc tests, $p<0.001$) and to 23.4μm with 100nM HCA exposure (Dunn's post-hoc test, $p<0.001$). Similarly, the intensity of WFA-labelled PNNs covering dendrites also decreased after 24h (Kruskal–Wallis statistic=59.59, $p<0.001$) with both 20nM and 100nM HCA treatment, from 23.09 a.u. to 20.13 a.u. and 16.9 a.u., respectively ($p<0.001$ veh vs 20nM Dunn's post-hoc test; $p<0.001$, veh vs high dose, Dunn's post-hoc test) (Fig 6.2 C D).

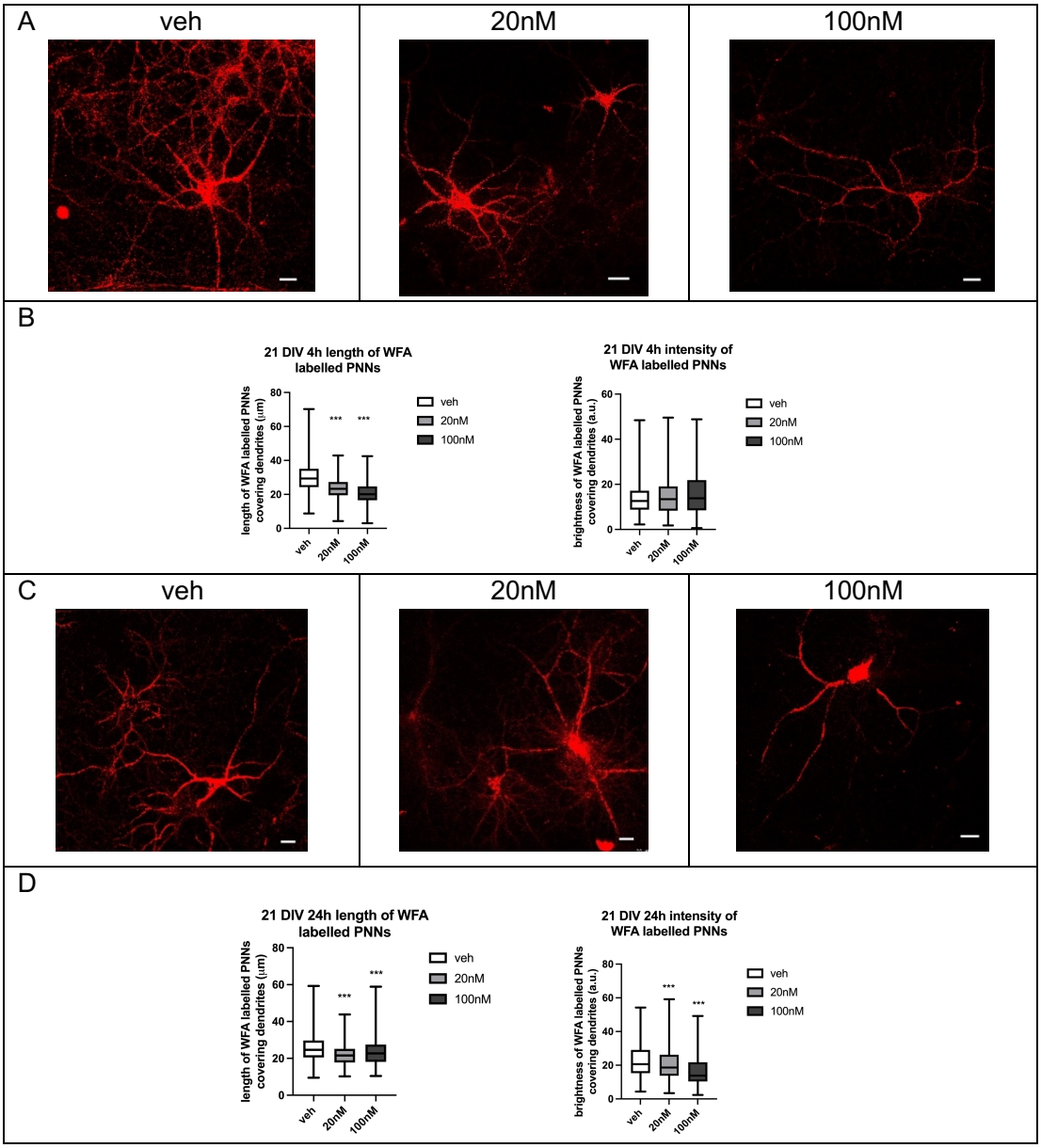

Figure 6.2. Fluorescent detection of WFA-labelled PNNs in cultured cells at 21 DIV. A: representative immunofluorescence images of WFA labelled PNNs around cultured cells after 4h treated with vehicle, 20nM and 100nM HCA. B: length and intensity intensity of dendrites covered by WFA labelled PNNs after 4h treatment (Veh: 326 dendrites in 26 cells nested in 3 different slides with 2 cultures, 20nM: 352 dendrites in 24 cells nested in 3 different slides with 2 cultures 100nM: 323 dendrites in 23 cells nested in 3 different slides with 2 cultures). C: representative immunofluorescence images of WFA labelled PNNs around cultured cells after 24h treated with vehicle, 20nM and 100nM HCA. D: length and intensity intensity of dendrites covered by WFA labelled PNNs after 24h treatment (Veh: 338 dendrites in 34 cells nested in 3 different slides with 2 cultures, 20nM: 224 dendrites in 20 cells nested in 3 different slides with 2 cultures, 100nM: 163 dendrites nested in 21 cells with 2 cultures). Scale bar: 20µM. The data for length and intensity of PNNs surrounding dendrites were not normally distributed at 21 DIV with 4h and 24h HCA as assessed with the Kolmogorov-Smirnov test. No outliers were detected. The data were analysed by Kruskal–Wallis test followed by Dunn's post-hoc tests, *** p<0.001 HCA effect vs corresponding veh group, Kruskal-Wallis test with Dunn's post-hoc test. Boxes show median and interquartile range, with whiskers from minimum to maximum.

Following treatment with HCA alone, mifepristone was co-treated with HCA, to assess the role of GRs. As a result, the earlier observation of HCA decreasing length of PNN surrounding dendrites at 14 DIV with 4h HCA treatment was not reproduced (Kruskal–Wallis statistic=1.54, p=0.208), which might be attributed to the different biological samples used for the sample collection, as noted in Chapter 3. However, there was a significant overall effect of mifepristone on the length of PNNs covering dendrites after 4h HCA exposure (Kruskal–Wallis statistic=133.84, p<0.001), suggesting the length of PNNs covering dendrites decreased with the presence of mifepristone (Fig 6.3 A B). However, no significant effect of HCA (Kruskal–Wallis statistic=0.69, p=0.708) and mifepristone treatment effect (Kruskal–Wallis statistic=6.27, p=0.102) were found on the intensity of PNNS surrounding dendrites (Fig 6.3 A B). The results potentially suggested the basal effect of GCs in the culture medium affecting the length of PNNs covering dendrites by GRs, and thus, the total length of PNNs in all treatment groups could be altered by mifepristone with blockage of GRs action.

Moreover, after 24h, there was a significant effect of HCA treatment (Kruskal–Wallis statistic=36.59, p<0.001), with the decreasing tendency of length of PNNs from a mean value of 25.7μm to 22.16μm and 19.089μm after 20nM and 100nM HCA treatment, respectively, in the absence of mifepristone (veh without mifepristone vs low dose HCA without mifepristone p<0.001, veh without mifepristone vs high dose HCA without mifepristone p<0.001, Dunn's post-hoc tests) (Fig 6.3 C D). This reproduces the finding observed previously in the study with initial HCA treatment. However, the effect of HCA was not significantly reported in the presence of mifepristone (veh with mifepristone vs low dose HCA with mifepristone p=0.254, veh with mifepristone vs high dose HCA with mifepristone p=0.765, Dunn's post-hoc tests). No overall effect of mifepristone on the length of PNNs covering dendrites was found at 14 DIV after 24h HCA and mifepristone co-treatment (Kruskal–Wallis statistic=2.39, p=0.122) (Fig 6.3 C D).

Regarding the intensity of WFA-labelled PNNs covering dendrites with 24h treatment, the intensity was not significantly affected by HCA treatment (Kruskal–Wallis statistic=5.48, p=0.064), but there was a slightly increasing tendency with both low and high dose HCA treatment in the absence of mifepristone, which was partially in line with the initial HCA effect; additionally, mifepristone affected the overall intensity expression (Kruskal–Wallis statistic=5.28, p=0.022), suggesting mifepristone could attenuate the increasing tendency presented in the absence of mifepristone. Although the upregulated intensity of PNNs by HCA treatment was not significant, the p value almost reached the borderline, and mifepristone was demonstrated to diminish the upregulated tendency by inhibiting GRs, which could potentially suggest that upregulated HCA effect on the intensity of PNNs was mediated through GRs.

The results suggested a slow genomic GR-mediated suppressive effect of GCs on the length of PNNs covering neuronal dendrites at 14 DIV, and also potentially showed an enhancing effect on the intensity of PNNs covering neuronal dendrites with slow genomic GR mediation.

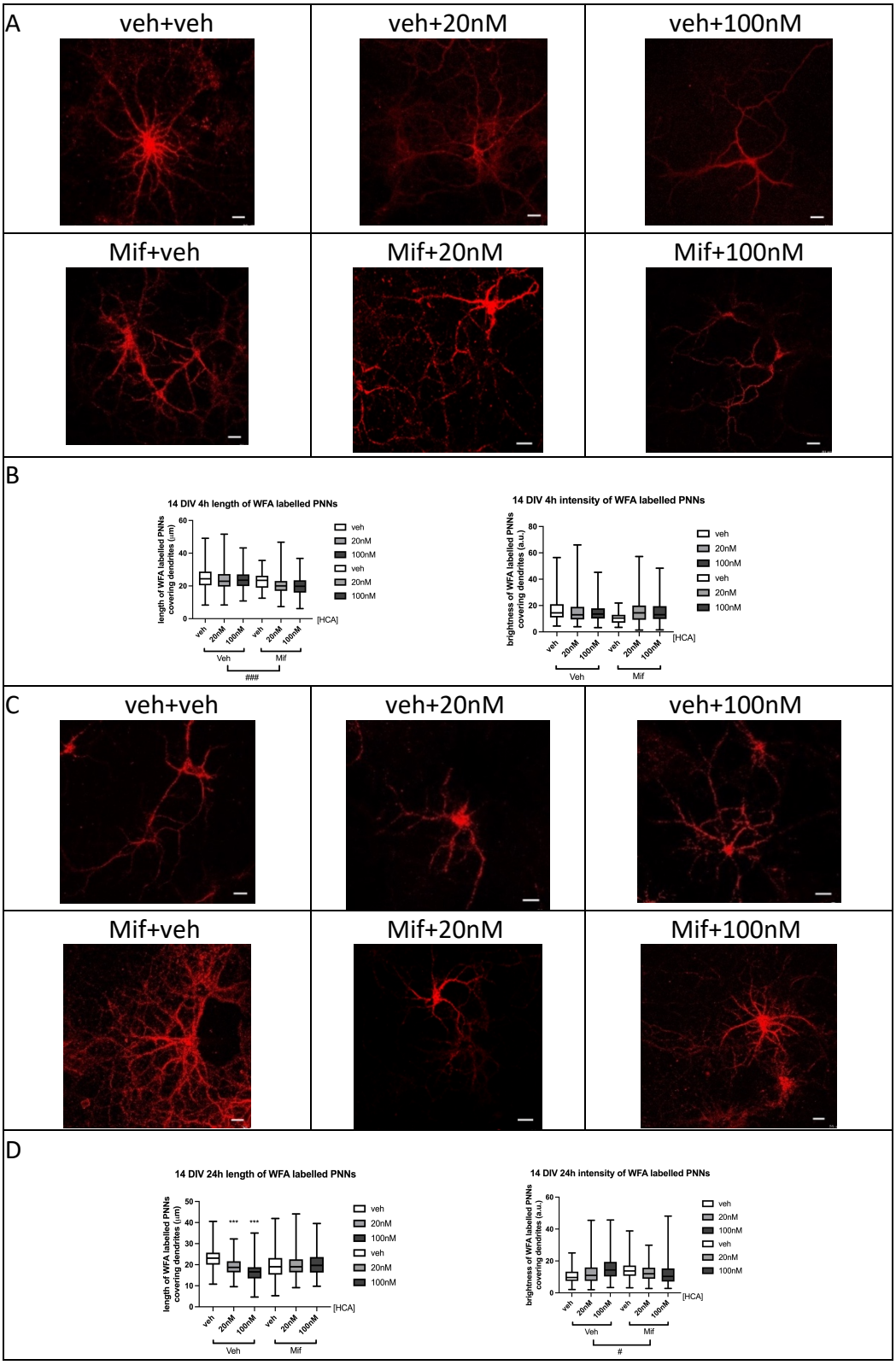

Figure 6.3. Fluorescent detection of WFA-labelled PNNs in cultured cells at 14 DIV. A: representative immunofluorescence images of WFA labelled PNNs around cultured cells after 4h treated with vehicle, 20nM and 100nM HCA; and mifepristone cotreated with vehicle, 20nM and 100nM HCA. B: length and intensity intensity of dendrites covered by WFA labelled PNNs after 4h treatment (Veh: veh: 351 dendrites in 25 cells nested in 3 different slides with 2 cultures, 20nM: 186 dendrites in 17 cells nested in 3 different slides with 2 cultures, 100nM: 112 dendrites in 20 cells nested in 3 different slides with 2 cultures; Mif: 176 dendrites in 19 cells nested in 3

different slides with 2 cultures, 20nM: 346 dendrites in 31 cells nested in 3 different slides with 2 cultures, 100nM: 283 dendrites in 21 cells nested in 3 different slides with 2 cultures). C: representative immunofluorescence images of WFA labelled PNNs around cultured cells after 24h treated with vehicle, 20nM and 100nM HCA; and mifepristone cotreated with vehicle, 20nM and 100nM HCA. D: length and intensity intensity of dendrites covered by WFA labelled PNNs after 4h treatment (Veh: veh: 139 dendrites in 13 cells nested in 3 different slides with 2 cultures, 20nM: 275 dendrites in 17 cells nested in 3 different slides with 2 cultures, 100nM: 164 dendrites in 15 cells nested in 3 different slides with 2 cultures; Mif: 290 dendrites in 21 cells nested in 3 different slides with 2 cultures, 20nM: 182 dendrites in 16 cells nested in 3 different slides with 2 cultures, 100nM: 177 dendrites in 14 cells nested in 3 different slides with 2 cultures). Scale bar: 20μM. The data for length and intensity of PNNs surrounding dendrites were not normally distributed at 14 DIV with 4h and 24h HCA or mifepristone as assessed with the Kolmogorov-Smirnov test. No outliers were removed. The data were analysed by Kruskal–Wallis test followed by Dunn's post-hoc tests, *** p<0.001 HCA effect vs corresponding veh group, Kruskal-Wallis test with Dunn's post-hoc test. # p<0.05, overall mifepristone effect vs corresponding veh group, Kruskal-Wallis test, Dunn's post-hoc tests. Boxes show median and interquartile range, with whiskers from minimum to maximum.

At 21 DIV, the decreased length of PNN covering dendrites observed previously with HCA exposure was confirmed at 4h (Kruskal–Wallis statistic=0.79, p<0.001), with the length of PNNs surrounding dendrites decreased from 25.94 μm to 22.39 μm and 19.26 μm with both low dose and high dose HCA in the absence of mifepristone, respectively (veh without mifepristone vs low dose HCA without mifepristone p<0.001, veh without mifepristone vs high dose HCA without mifepristone p<0.001, Dunn's post-hoc tests); and decreased from 24.67 μm to 23.38 μm and 19.63 μm with both low dose and high dose HCA in the presence of mifepristone, respectively (veh with mifepristone vs low dose HCA with mifepristone p<0.001, veh with mifepristone vs high dose HCA with mifepristone p<0.001, Dunn's post-hoc tests). The results also showed that there was no overall effect of mifepristone on length of PNNs after 4h HCA treatment at 21 DIV (Kruskal–Wallis statistic=0.79, p=0.374) (Fig 6.4 A B).

The overall intensity of PNNs was not affected by HCA treatment (Kruskal–Wallis statistic=1.13, p=0.596), which reproduced the results in the previous initial experiment with only HCA treated. The intensity increased slightly after 4h mifepristone treatment (Kruskal–Wallis statistic=4.47, p=0.029) (Fig 6.4 A B), suggesting the intensity of PNNs was affected by the basal effect of GCs in the cell culture medium during cell development.

Moreover, after 24h, the prior observation of decreased length of PNNs covering dendrites after HCA exposure was confirmed (Kruskal–Wallis statistic=201.62, p<0.001), with the length of PNNs surrounding dendrites decreased from 24.74μm to 20.45μm and 19.91μm with both low dose and high dose HCA in the absence of mifepristone, respectively (veh without mifepristone vs low dose HCA without mifepristone p<0.001, veh without mifepristone vs high dose HCA without mifepristone p<0.001, Dunn's post-hoc tests); and decreased from 22.43μm to 20.44μm and 19.23μm with both low dose and high dose HCA in the presence of mifepristone, respectively (veh with mifepristone vs low dose HCA with mifepristone p<0.001, veh with mifepristone vs high dose HCA with mifepristone p<0.001, Dunn's post-hoc tests) (Fig 6.4 C D). Moreover, there was an overall effect of mifepristone on the length of PNNs covering cell dendrites after 24h HCA and mifepristone treatment (Kruskal–Wallis statistic=38.56, p<0.001).

Regards to the intensity of PNNs with 24h treatment, the alterations was detected after HCA treatment (Kruskal–Wallis statistic=25.70, p<0.001), which reproduced the results from the initial HCA experiment, with increased intensity from 14.73 a.u. to 17.45 a.u. and decreased to 13.91

a.u. with both low dose and high dose HCA in the absence of mifepristone, respectively (veh without mifepristone vs low dose HCA without mifepristone $p<0.001$, veh without mifepristone vs high dose HCA without mifepristone $p<0.001$, Dunn's post-hoc tests); and slightly increased from 15.42 a.u. to 15.44 a.u. and decreased to 13.29 a.u. with both low dose and high dose HCA in the presence of mifepristone, respectively (veh with mifepristone vs low dose HCA with mifepristone $p=0.004$, veh with mifepristone vs high dose HCA with mifepristone, $p<0.001$ Dunn's post-hoc tests,) (Fig 6.4 C D). Moreover, an overall effect of mifepristone on the intensity of WFA-labelled PNNs covered dendrites was found after 24h HCA and mifepristone treatment (Kruskal–Wallis statistic=25.70, $p<0.001$) (Fig 6.4 C D), suggesting the intensity of PNNs was slightly increased with mifepristone exposure and a basal effect of GCs presented in the cultured medium.

The results indicated that at 21 DIV, the length of PNNs surrounding cell dendrites could be suppressed by GCs in a non-GR mediated pathways in both rapid genomic and long-term non-genomic actions. However, the intensity was not obviously affected by GCs, with both up or down regulation of GCs, upregulated the intensity with low dose HCA, but downregulated the intensity with a high dose HCA after long-term GCs exposure via a non-GR mediated way.

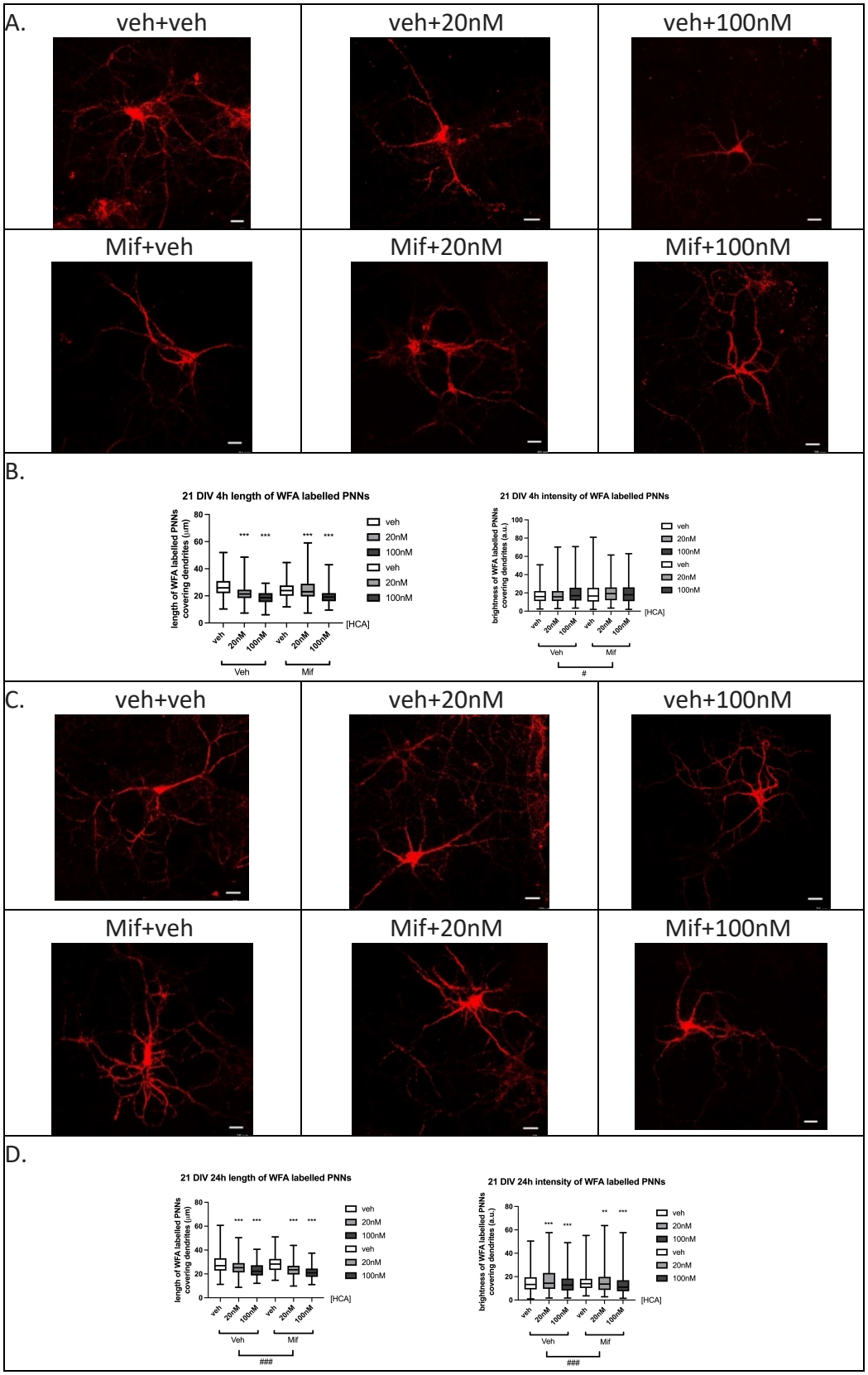

Figure 6.4. Fluorescent detection of WFA-labelled PNNs in cultured cells at 21 DIV. A: representative immunofluorescence images of WFA labelled PNNs around cultured cells after 4h treated with vehicle, 20nM and 100nM HCA; and mifepristone cotreated with vehicle, 20nM and 100nM HCA. B: length and intensity of dendrites covered by WFA labelled PNNs after 4h treatment (Veh: veh: 273 dendrites in 22 cells nested in 3 different slides with 2 cultures, 20nM:

397 dendrites in 27 cells nested in 3 different slides with 2 cultures, 100nM: 94 dendrites in 20 cells nested in 3 different slides with 2 cultures; Mif: 173 dendrites in 24 cells nested in 3 different slides with 2 cultures, 20nM: 172 dendrites in 27 cells nested in 3 different slides with 2 cultures, 100nM: 150 dendrites in 20 cells nested in 3 different slides with 2 cultures). C: representative immunofluorescence images of WFA labelled PNNs around cultured cells after 24h treated with vehicle, 20nM and 100nM HCA. D: length and intensity intensity of dendrites covered by WFA labelled PNNs after 24h treatment (Veh: veh: 360 dendrites in 32 cells nested in 3 different slides with 2 cultures, 20nM: 263 dendrites in 20 cells nested in 3 different slides with 2 cultures, 100nM: 265 dendrites in 20 cells nested in 3 different slides with 2 cultures; Mif: 165 dendrites in 20 cells nested in 3 different slides with 2 cultures, 20nM: 297 dendrites in 18 cells nested in 3 different slides with 2 cultures, 100nM: 291 dendrites in 19 cells nested in 3 different slides with 2 cultures). Scale bar: 20μM. The data for length and intensity of PNNs surrounding dendrites were not normally distributed with 4h and 24h HCA or mifepristone treatment as assessed with the Kolmogorov-Smirnov test. No outliers were detected. The data were analysed by Kruskal–Wallis test followed by Dunn's post-hoc tests. ** p<0.01, *** p<0.001 HCA effect vs corresponding veh group, Kruskal-Wallis test with Dunn's post-hoc test; # p<0.05, ### p<0.001, overall effect of mifepristone vs vehicle group, Kruskal–Wallis test with Dunn's post-hoc tests. Boxes show median and interquartile range, with whiskers from minimum to maximum.

6.4.2 Dendritic number covered by PNNs remained unchanged after HCA exposure

Mice lacking *TnR* reportedly showed a substantial reduction (~50%) in the number of dendrites per cell covered by PNNs, in both cortex and hippocampus areas (Weber, et al., 1999). Hence, after measuring the length and intensity intensity of neuronal dendrites covered by WFA labelled PNNs, the number of dendrites covered by PNNs has been measured after exposure to HCA, and HCA with mifepristone.

There were no significant differences in the number of neuronal dendrites covered by WFA-labelled PNNs after exposure to HCA at 14 DIV after 4h (fig 6.5 A) and 24h (Fig 6.5 B) (4h: (Kruskal–Wallis statistic=3.15, p=0.270; 24h: F (2, 55) =1.52, P=0.230).

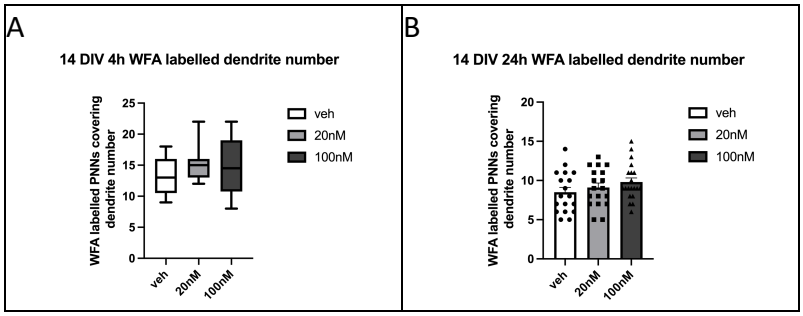

Figure 6.5: effect of HCA on the number of neuronal dendrites per cell covered by PNNs labelled by WFA at 14 DIV. A: the number of dendrites covered by PNNs quantified after 4h treatment with veh (distilled water), 20nM HCA and 100nM HCA. (Veh: 270 dendrites in 20 cells nested in 3 different slides with 2 cultures, 20nM: 166 dendrites in 20 cells nested in 3 different slides with 2 cultures, 100nM: 199 dendrites in 16 cells nested in 3 different slides with 2 cultures). B: the number of dendrites covered by PNNs quantified after 24h treatment with veh (distilled water), 20nM HCA and 100nM HCA. (Veh: 153 dendrites in 17 cells nested in 3 different slides with 2 cultures, 20nM: 164 dendrites in 17 cells nested in 3 different slides with 2 cultures, 100nM: 196 dendrites in 19 cells nested in 3 different slides with 2 cultures). The data for number of PNNs surrounding dendrites were not normally distributed with 4h HCA, but the data for number of

PNNs surrounding dendrites were normally distributed with 24h HCA, as assessed with the Kolmogorov-Smirnov test. No outliers were removed. The data were analysed by Kruskal–Wallis test at 4h with Dunn's post-hoc test and ANOVA at 24h with Tukey's post-hoc test. Boxes show median and interquartile range, with whiskers from minimum to maximum, and the bar graph shows mean ± SEM.

There were no differences in number of dendrites covered by PNNs after 4h and 24 HCA and Mif treatment. There was no effect of HCA on the number of PNN-covered dendrites after 4h HCA and mifepristone treatment (HCA: Kruskal–Wallis statistic=0.17, p=0.917, Mif: Kruskal–Wallis statistic=4.08, p=0.403) (Fig 6.6 A). similar effect was shown in 24h treatment, suggesting no effect of HCA on the number of PNN-covered dendrites after 24h HCA and mifepristone treatment (HCA: Kruskal–Wallis statistic=4.18, p=0.124, Mif: Kruskal–Wallis statistic=0.81, p=0.369) (Fig 6.6 B).

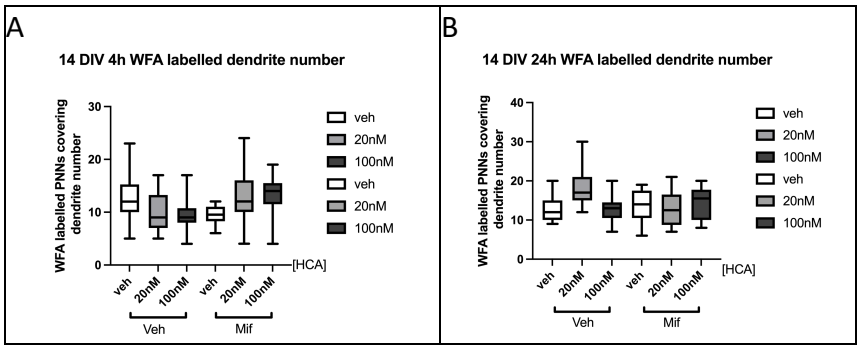

Figure 6.6: effect of HCA and mifepristone on the number of neuronal dendrites per cell covered by PNNs labelled by WFA at 14 DIV. A: the number of dendrites covered by PNNs quantified after 4h treatment with veh+veh (distilled water), veh+20nM HCA and veh+100nM HCA, and Mif+veh, Mif+20nM HCA and Mif+100nM HCA. (Veh: veh: 351 dendrites in 25 cells nested in 3 different slides with 2 cultures, 20nM: 186 dendrites in 17 cells nested in 3 different slides with 2 cultures, 100nM: 112 dendrites in 20 cells nested in 3 different slides with 2 cultures; Mif: 176 dendrites in 19 cells nested in 3 different slides with 2 cultures, 20nM: 346 dendrites in 31 cells nested in 3 different slides with 2 cultures, 100nM: 283 dendrites in 21 cells nested in 3 different slides with 2 cultures). B: the number of dendrites covered by PNNs quantified after 4h treatment with veh+veh (distilled water), veh+20nM HCA and veh+100nM HCA, and Mif+veh, Mif+20nM HCA and Mif+100nM HCA. (Veh: veh: 139 dendrites in 13 cells nested in 3 different slides with 2 cultures, 20nM: 275 dendrites in 17 cells nested in 3 different slides with 2 cultures, 100nM: 164 dendrites in 15 cells nested in 3 different slides with 2 cultures; Mif: 290 dendrites in 21 cells nested in 3 different slides with 2 cultures, 20nM: 182 dendrites in 16 cells nested in 3 different slides with 2 cultures, 100nM: 177 dendrites in 14 cells nested in 3 different slides with 2 cultures). The data for number of PNNs surrounding dendrites were not normally distributed with 4h and 24h HCA cotreated with mifepristone as assessed with the Kolmogorov-Smirnov test. No outliers were detected. The data were analysed by Kruskal–Wallis test followed by Dunn's post-hoc test. Boxes show median and interquartile range, with whiskers from minimum to maximum.

At 21 DIV, there was no significant differences in neuronal PNN-covered dendrite numbers after exposure to HCA after 4h ($F(2, 71)=1.31$, $P=0.279$) (Fig 6.7 A) and after 24h HCA exposure (Kruskal–Wallis statistic=5.45, p=0.065) (Fig 6.7 B).

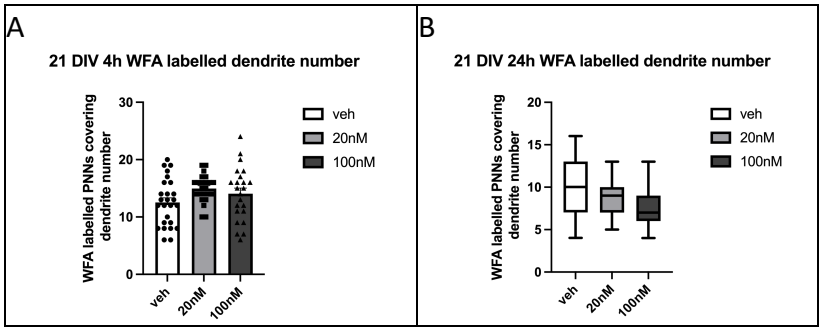

Figure 6.7: effect of HCA on the number of neuronal dendrites covered by PNNs labelled by WFA at 21 DIV. A: the number of dendrites covered by PNNs quantified after 4h treatment with veh (distilled water), 20nM HCA and 100nM HCA. (326 dendrites in 26 cells nested in 3 different slides with 2 cultures, 20nM: 352 dendrites in 24 cells nested in 3 different slides with 2 cultures 100nM: 323 dendrites in 23 cells nested in 3 different slides with 2 cultures). B: the number of dendrites covered by PNNs quantified after 24h treatment with veh (distilled water), Veh: 338 dendrites in 34 cells nested in 3 different slides with 2 cultures, 20nM: 224 dendrites in 20 cells nested in 3 different slides with 2 cultures, 100nM: 163 dendrites nested in 21 cells with 2 cultures. The data for number of PNNs surrounding dendrites were normally distributed with 4h HCA, but not normally distributed with 24h HCA treatment, as assessed with the Kolmogorov-Smirnov test. No outliers were detected. The data were analysed by ANOVA at 4h with Tukey's post-hoc test and Kruskal–Wallis test with Dunn's post-hoc test at 24. Boxes show median and interquartile range, with whiskers from minimum to maximum, and the bar graph shows mean ± SEM.

After 4h HCA and mifepristone treatment, no differences of number of PNNs covered dendrites were found after HCA treatment (Kruskal–Wallis statistic=1.18, p=0.554) (Fig 6.8 A). And the overall effects of mifepristone did not significantly affected the number of PNNs (Kruskal–Wallis statistic=1.62, p=0.203) (Fig 6.8 A).

After 24h HCA and mifepristone treatment, the number of PNNs was significantly affected by HCA treatment ($F(2, 108) = 3.67$, $P=0.029$) (Fig 6.8 B), however, no significant post-hoc tests suggested the specific alterations between each treatment groups (veh without mifepristone vs low dose without mifepristone p=0.208, Tukey's post-hoc test; veh without mifepristone vs high dose without mifepristone p=0.165, Tukey's post-hoc test; veh with mifepristone vs low dose with mifepristone p=0.861, Tukey's post-hoc test; veh with mifepristone vs high dose with mifepristone p=0.902, Tukey's post-hoc test) (Fig 6.8 B). The number of dendrites was not affected by mifepristone either ($F(1, 108) = 2.05$, $P=0.155$).

These results indicated that the number of PNNs covering cell dendrites were not affected by HCA or mifepristone, suggesting GCs showed no effect on numbers of PNNs at 14 and 21 DIV.

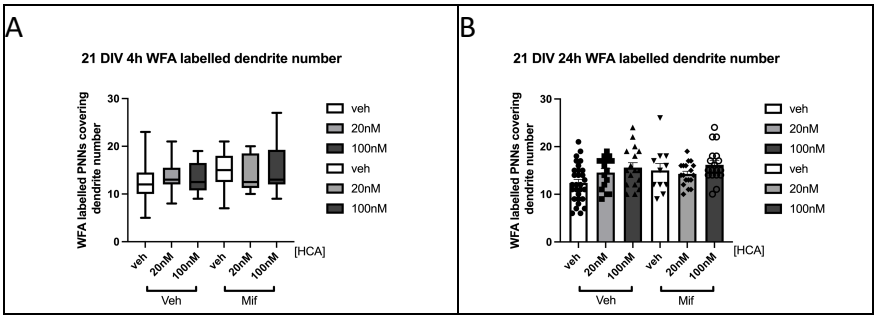

Figure 6.8: effect of HCA and mifepristone on the number of neuronal dendrites covered by PNNs labelled by WFA at 21 DIV. A: the number of dendrites covered by PNNs quantified after 4h treatment with veh+veh (distilled water), veh+20nM HCA and veh+100nM HCA, and Mif+veh, Mif+20nM HCA and Mif+100nM HCA. (Veh: veh: 273 dendrites in 22 cells nested in 3 different slides with 2 cultures, 20nM: 397 dendrites in 27 cells nested in 3 different slides with 2 cultures, 100nM: 94 dendrites in 20 cells nested in 3 different slides with 2 cultures; Mif: 173 dendrites in 24 cells nested in 3 different slides with 2 cultures, 20nM: 172 dendrites in 27 cells nested in 3 different slides with 2 cultures, 100nM: 150 dendrites in 20 cells nested in 3 different slides with 2 cultures). B: the number of dendrites covered by PNNs quantified after 4h treatment with veh+veh (distilled water), veh+20nM HCA and veh+100nM HCA, and Mif+veh, Mif+20nM HCA and Mif+100nM HCA. (Veh: veh: 360 dendrites in 32 cells nested in 3 different slides with 2 cultures, 20nM: 263 dendrites in 20 cells nested in 3 different slides with 2 cultures, 100nM: 265 dendrites in 20 cells nested in 3 different slides with 2 cultures; Mif: 165 dendrites in 20 cells nested in 3 different slides with 2 cultures, 20nM: 297 dendrites in 18 cells nested in 3 different slides with 2 cultures, 100nM: 291 dendrites in 19 cells nested in 3 different slides with 2 culture). The data for number of PNNs surrounding dendrites were not normally distributed with 4h HCA but were normally distributed with 24h HCA treatment, as assessed with the Kolmogorov-Smirnov test. No outliers were detected. The data were analysed by Kruskal–Wallis test at 4h with Dunn's post-hoc test and ANOVA at 24h with Tukey's post-hoc test. Boxes show median and interquartile range, with whiskers from minimum to maximum, and the bar graph shows mean ± SEM.

6.5 Discussion

The current study measured the length and intensity of PNNs covering dendrites in cultured cells at 14 DIV and 21 DIV (PNNs are too incomplete to be assessed at 7 DIV). There was little obvious difference in PNN morphology between 14 and 21 DIV. The mean length of dendrite covered by PNN tended to be slightly longer at 21 DIV versus 14 DIV, but the difference was marginal. Previous studies showed various PNNs morphology in cultured neurons at 14 and 21 DIV. Most studies suggested that at 14 DIV, PNNs were almost mature and presented a net-like structure covering cell soma and proximal dendrites, and showed similar morphology as 21 DIV (Geisser et al, 2013; Dityatev et al, 2006; Fowke et al., 2017). However, PNNs were also shown to express granular-like structures at 14 DIV, and more widely cover cells and dendrites at 21 DIV (Dickens et al., 2002; Miyata et al., 2005). The various patterns of PNNs morphology from different studies might be associated with the phenomenon that PNN structure is activity dependent, as a reduced number of WFA-binding neurons and impaired PNN formation (attenuated WFA labelling) were observed after blockage of action potentials (Dityatev et al, 2006). Similar results were also shown in an in vivo study where monocular deprivation, inducing cortical response plasticity in visual cortex, also resulted in reduced density and intensity of PNNs, in cats and rats (Guimaraes et al., 1990; Pizzorusso et al., 2002). As increased excitatory

neuronal transmissions were shown in cultured neurons supplied with Brain Phys medium (Miyata et al., 2005), the neurons will show increased neuronal activities with late maturation time occurred in PNNs compared to the neurons cultured in other medium. Thus, in cultured cells, the spatial density and temporal development of cultured cells will vary in different sets of experiments, thus PNN morphology in cell cultures might vary between experiments, which might lead to different PNN morphologies at 14 DIV in different studies.

6.5.1 Alterations of dendritic length and intensity covered by PNNs with comparison to previous studies

The length of the PNN-covered dendrites decreased significantly after 4h and 24h HCA exposure at both 14 DIV and 21 DIV. This appeared to be a highly robust observation. Apart from the unaltered length of PNNs after 4h treatment at 14 DIV in the subsequent mifepristone experiment, similar decrease in length of PNNs were replicated at 14 and 21 DIV. It appeared that the downregulating effects of HCA on length of PNNs covering dendrites were also shown in the presence of mifepristone at 14 DIV and at 21 DIV, although no overall reversible effect of mifepristone was detected at 14 DIV and 21 DIV in both 4h and 24h treatment with regards to the length of PNNs. This implies a mechanism not involving GR mediation at 14 DIV and 21 DIV.

In fact, this appears to be the first demonstration that GCs may act directly to modify PNN structure, and hence may be the mediators of the effects of stress reported in the literature.

Changes in the intensity of PNNs covering dendrites were also partially consistent. Initial observations suggested PNN intensity remained unchanged at 4h but increased after 24h at 14 DIV; and at 21 DIV, no changes were reported at 4h treatment, but the intensity decreased after 24h treatment. Similar alterations were found at 14 DIV in the following mifepristone experiment, however, at 21 DIV, in addition to the consistent changes at 4h, the intensity appeared to increase with low dose HCA but decreased with high dose HCA at 24h. These alterations at 14 or 21 DIV could still be observed after mifepristone treatment, indicating the altered intensity after HCA exposure were not involving GRs; however, at 14 DIV with 24h HCA and mifepristone treatment, the increasing tendency of PNN intensity was diminished after mifepristone exposure, although the tendency and the effect of mifepristone did not reach the statistical significance level, it provided a possibility for GR-mediated enhancing effect of HCA on PNNs intensity.

Limited research about the effect of GCs on the morphology of PNNs or PNN-covered dendrites were conducted previously in cultured cells, but similar results on neuronal dendrites were observed in rodents' brains with stress induction or with stress related neuroinflammation induction. Acute or chronic stress was reported to induce atrophy of neurons with shortening of the dendrites and decreases in dendritic number in different brain regions (Watanabe et al., 1992). Administration of GCs could reproduce these effects. Reduced dendritic length was also observed in rat PFC and hippocampus after chronic stress exposure (Eiland et al., 2012). Pawley et al. (2020) reported a reduced neurogenesis in rat hippocampus at the age of 4 to 5 weeks with reduced neuronal dendritic branching after chronic neuronal inflammation by over expressing interleukin-1β. These studies demonstrated that stress or the induction of stress hormones could affect neuronal morphology. Hence it is possible that the decreased length of PNN-covered dendrite could reflect a general shortening of dendrites after HCA exposure, rather than a specific action on PNN architecture.

In addition to the direct effect of stress on neuronal dendrites, one of the main components of PNNs, *TnR*, was demonstrated to influence dendritic PNN length, as detected by WFA-labelled dendrites (Weber et al., 1991). The study suggested decreased dendritic length labelled by WFA

in both cortex and hippocampus in *TnR* KO mice, the mean length decreased from 22.26 μm to 14.22 μm in cortex and from 28.15μm to 18.96μm in hippocampus (Weber et al., 1991). The changes and the average length of WFA labelled dendrites are consistent with the results in current study. Morawski et al. (2014) further supported that PNN-covered dendrite length appeared to decrease at 15 DIV in cultured cells from *TnR* deficient mice, indicating that PNNs which surround somata or cover neuronal dendrites were less developed with disrupted *TnR* expression. In the previous results, mRNA expression of *TnR* decreased significantly after HCA exposure at 7 DIV and 14 DIV, which might raise a possibility that alterations or abnormal structures of PNNs observed at 14 DIV might occur due to reduced levels of *TnR* during the neuronal development period. TnR shows high affinity binding to Ptprz1 (Phosphacan) in the PNN structure (Barnea et al., 1994). It has been shown that the PNNs in *TnR* KO mice had similar morphologies to those in *Ptprz1 KO* mice (Werber et al., 1999; Brückner et al. 2000; Eill et al., 2020). In *Ptprz1 KO* mice, disrupted PNN structure was detected, and presented with loss of the PNN reticular, lattice-like structure around neurons and dendrites (Eill et al., 2020). Damaged dendritic-PNN structure was also found in *Hapln1* KO mice. Mice lacking *Hapln1* showed attenuated WFA-labelled PNNs around the cell soma, and no PNNs present around dendrites (Suttkus et al., 2014; Carulli et al., 2010).

Several studies suggested that changes in PNNs could occur through changes in neuronal activity during the developmental period and adulthood, for example, blockage of action potentials and restricting the window of neural plasticity decreased the accumulation of PNN components (Dityatev et al., 2007; Carstens et al., 2021; Devienne et al., 2021). Therefore, in the current study, the reduced length of dendrites covered by PNNs might be attributed to altered network activity in response to HCA administration, for example, long-term potentiation is suppressed by acute or chronic stress, which might restrict the accumulation of PNN components around cell soma or dendrites, resulting in disrupted dendritic PNNs structure (Pavlides et al., 2002; Yuen et al., 2009; Whitehead et al., 2013).

Although there is limited research focusing on the effect of stress or stress related hormones, such as, GCs, on the intensity of PNNs which covered neuronal dendrites, PNN morphology was suggested to be affected by stress or stress related hormones, as detected by WFA staining or levels of the main PNN components surrounding neurons. Several lines of evidence reported that reduced intensity of WFA-labelled PNNs was found in chronically stressed mice and rats (Ueno et al., 2016; Ganes, Zhu and Grace, 2019), which is not really consistent with the current results, raising the possibility that GCs are not involved in this action. The alterations in the intensity of PNNs after stress exposure were also controversial in previous studies. Reduced PNN staining intensity was detected in basolateral amygdala after postnatal stress (Santiago et al., 2018). Conversely, other studies found increased PNN staining intensities in PFC, hippocampus or amygdala with early postnatal developmental stress in mice or rats (Murthy et al., 2019) or with chronic stress in adult rats (Pesarico et al., 2019). Others showed no effects with early postnatal developmental stress in rats (Richardson et al., 2021) or chronic stress in adult mice (Page et al., 2018), although both these studies suffered from weak statistical power (n=3=6/group). These inconsistent results might be due to the stress exposure time, as lower PNN intensity was observed after 4 days stress exposure, while increased PNN intensities were detected with 6 to 18 days exposure, suggesting PNN intensity changes might be dependent on the stress induction time points.

The most consistent finding with stress exposure is probably an increase in PNN staining intensity, and in the current study, increased intensity of WFA labelled PNNs was detected with long-lasting 24h GCs exposure at 14 DIV, the results were also replicated in the following mifepristone co-treatment experiments. In cultured cells, PNNs reached maturation at 21 DIV

(Miyata et al., 2005), but are still developing around 14 DIV, thus developing PNNs might be more susceptible to disruption than matured PNNs. Our data suggested that these effects of stress on PNNs may not be mediated by GRs.

As these studies used different stress models with different exposures and induction time points, along with various methods, it is more difficult to determine whether the time points could be a factor influencing the intensity of WFA labelled PNNs. The detection methods in these studies varied as well. WFA is a common labelling marker for PNNs visualisation, PNNs were well-detected by WFA in cortex and hippocampus in mouse brain tissues but not rats. Some of the studies using rat models often used Cat-301, a marker for *Acan*, to visualise PNNs (Riga et al., 2017). PNN visualisation depends on the brain regions and species, which is susceptible to detection methods, including the antibodies used for visualising PNNs. In this case, different results of PNN intensity or intensity could be reported. Additionally, increased PNN intensity might be due to the aggregation of immunoreactive PNNs components detected by WFA, suggesting the maturation pf PNNs (Gildawei e al., 2020).

However, a number of studies raised a phenomenon that the suppression effect of stress could be observed at first immediately after stress induction and then followed by a rebound upregulating effect of stress after long term exposure (Koskinen et al., 2020; Spijker et al., 2020), which is in line with the PNN remodelling theory, involving a stress-induced effect that PNN expression, including density and intensity, would be suppressed first after stress exposure but then followed by a rebound.This neuronal activity could lead to different changes in PNNs intensity tendency within a cell population.

In terms of the effect on HCA on the number of PNNs covering dendrites, the number of PNNs remained unchanged at 14 and 21 DIV with both 4h and 24h HCA exposure. The results were consistent and replicated in the following experiments with HCA and mifepristone. Our results were not in line with previous research where decreased number of PNNs surrounding dendrites was detected in mice lacking *TnR*, with the disruption in both cortex and hippocampus regions (Weber et al. 1999). The main reason for the inconsistent results might be attributed to the experimental manipulation that we applied. The current study treated the cells with elevated GC concentrations which might have a subtle effect on the total PNNs structure, but the previous research used the *TnR* KO animals to directly disrupt PNNs formation. Our previous results reported in Chapter 3 showed *TnR* mRNA expression was suppressed by GCs during early neuronal development stages, and it's possible that the downregulated *TnR* expression could lead to a decreased number of PNN-covered dendrites. However, no consistent changes were detected.

6.5.2 Relationship to mRNA and protein changes

Effects of HCA on PNN-covered dendrite length and intensity of WFA staining appeared to be sensitive to mifepristone at 14 DIV bit not at 21 DIV. This is reminiscent (although with 7 days' time dislocation) of the changes in PNN component gene expression detected previously, where GRs seemed to be involved early in development (7 DIV), with other mechanisms of HCA action coming into play later in development (14 DIV). It sems unlikely though that the observed alterations in PNN component gene expression underly the changes in WFA staining. No changes in PNN component gene expression were detected when HCA was applied at 21 DIV, yet altered WFA staining characteristics are observed. Similarly, changes in PNN component gene expression detected when HCA was applied at 14 DIV were not attenuated by mifepristone, whereas alterations in WFA staining characteristics at 14 DIV were sensitive to mifepristone. The precise mechanisms involved in PNN modification by GCs are elusive. It is proposed the matrix

metalloprotease enzymes may rapidly degrade PNNs (Wen et al., 2018; Gray et al., 2008). GCs are generally associated with a slow, genomic reduction in metalloprotease expression, rather than a rapid activation of these enzymes, but maybe there could be some fast GC action not involving changes in gene expression.

6.5.3 Limitations

The results reported from the current study could be interpreted with several limitations and future considerations. Firstly, a number of initially highly-significant observations were not successfully replicated. This did not appear to reflect a lack of statistical power. The inconsistent results in the initial and follow-on experiments might be due to the nature of manually counting of the neurons and dendrites. Therefore, the measuring might not be highly accurate. The cells were cultured from cortical areas in mice brains, however, the expression of PNNs might be heterogeneous in different layers of the cortex areas (Lupori et al., 2023). PNNs are enriched in layer 4 in primary sensory cortices (Lupori et al., 2023), but in primary visual cortex, strong expression of PNNs is present across all layers except for layer 1 (Lensjo et al., 2017). In addition, different types of cells are surrounded by PNNs, and might be affected differently by stress or GCs. For example, decreased density and intensity of Pv-expressing neurons was found after stress (Page et al., 2019), but another cell type sometimes covered by PNNs, somatostatin-expressing neurons, was reported to increase after responding to stress (Nageava et al., 2023). WFA-labelled PNNs are present mostly around Pv expressing interneurons (Miyata et al., 2005). Therefore, WFA-labelled PNN measurements might be focused on a restricted cell type, but with the heterogenous population of cells varying between cultures, with slight variations in tissue dissection or neuronal survival during culture preparation. Finally, as noted in the discussion part 6.5.1, the decreased length of PNNs might be accompanied by or due to the decreased dendritic length of neurons, so the reduction in the length of PNNs might be dependent on the underlying neuronal structure. With this consideration, in the future study, double staining of PNNs and neuronal structure could be used, such as labelling cells with tubulin-1 and WFA, to further detect whether there are any simultaneous changes of PNNs and neuronal dendrites.

6.5.4 Conclusions

The current study examined the effect of GCs on PNNs morphology, by measuring the PNN-covered dendritic length, intensity and number. The results illustrated that GCs downregulated the length of PNNs covered dendrites at 14 DIV and 21 DIV with both short- and long-term HCA exposure. The alterations of PNN intensity influenced by GCs was somewhat inconsistent, but robustly increasing with long-term exposure at 14 DIV. The increasing tendency of intensity was in line with the PNNs remodelling theory. The data add to the complexity of regulation of PNNs by GCs and raise the possibility of parallel actions to affect the existing PNN structure while simultaneously altering component gene expression.

Chapter 7

Proteasome activities in cortical cultured neurons

7.1 Introduction

In the previous Chapter 3, the mRNA levels of some PNNs components were downregulated by elevated GCs. The alterations of mRNA were also accompanied by some related protein level changes, such as consistent downregulated protein levels of Has3 and TnR. However, there were downregulated protein levels for Has2 and Gad65 at 14 DIV, but the downregulation was not in line with the mRNA changes after HCA treatment (*Has2* and *Gad2* mRNA levels remained unchanged at 14 DIV). Thus, the inconsistent downregulation might be due to altered proteasome activities degrading ubiquitinated and wasted proteins during the cell developmental stages, and without any change in the related mRNA levels.

The proteasome is a ubiquitous complex structure with multi-catalytic activities which is involved in several cellular processes, such as cell differentiation and proliferation (Ichihara and Tanaka, 1995), response to immune or oxidative stress (Zong et al., 1999), maintaining proteostasis (Ramachandran and Margolis, 2017), and protein degradation (Davies et al., 2001). The structure of the proteasome complex consists of the 20S proteasome, which is defined as the core proteasomal complex, and the 19S proteasome, which is defined as a regulator part of the structure (Coux et al., 1996). The 20S core structure is bound at each terminus to 19S regulatory particles, the tethered 20S and 19S structures forming the complete 26S complex structure (Yoshimura et al., 1996). The 19S proteasome was demonstrated to recognise damaged proteins, and the 20S core structure mainly functioned to degrade the proteins recognised by the 19S regulatory structure (Yoshimura et al., 1996).

The 20S proteasome, demonstrated to be the most abundant proteasome structure in cell plasma and nucleus (Baumeister et al., 1998), is formed as a cylinder-like structure, in eukaryotic cells containing 2 subunit classes known as α subunits and β subunits (Baumeister et al., 1998). Each subunit class comprises seven similar proteins: α1 to α7 and β1 to β7 (Baumeister et al., 1998). The α subunits act as a gate allowing different lengths of substrates to enter the structure, which could determine the degradation rate of the 20S proteasomes (Groll et al., 2000). Among the β subunits, 3 of the β subunits (β1, β2 and β5) contain catalytic threonine residues at the N terminus, and the subunits cleave the substrate peptides at the C terminal side of acidic, basic and hydrophobic amino acid residues (Coux et al., 1996). These 3 β subunits are catalytically active and provide the 3 different proteasomal activities, β1 linked to caspase-like/PGPH (peptidylglutamyl-peptide hydrolyzing) activity, β2 linked to trypsin-like activity and β5 linked to chymotrypsin-like activity (Borissenko and Groll, 2007).

The critical and main function of proteasome is degrading damaged proteins, which could proceed through either a 20S or 26S proteasome pathway (Coux et al., 1996; Sitte et al., 1998). The 26S proteasome degrades proteins in a ubiquitin-dependent pathway while the 20S proteasome degrades proteins in a ubiquitin-independent pathway (Raynes et al., 2017). Ubiquitin is a protein that could be found in mostly eukaryotic cells, which contains several lysine residues, including K6, K11, K29, K33, K48 and K63 (Goldstein et al., 1975). K48 is a residue that is involved in the process of proteolysis (Komander, 2009). The ubiquitin-dependent degradation is activated by a ubiquitin-activating enzyme, the activated ubiquitin can then be transferred to a ubiquitin-conjugating enzyme, which can transfer ubiquitin to targeted protein substrates (Ciechanover, 1995). A polyubiquitin chain can be formed attached to targeted protein substrates, and the proteins can then be recognised by the 19S proteasomal regulator and

degraded by the 26S complex (Ciechanover, 1995). In addition, ubiquitin-independent degradation by the 20S proteasome structure is often focused on unfolded or damaged proteins which are not fully structured, due to denaturing stressors, including external toxins, oxidative stress and harmful agents (Raynes et al., 2017). Oxidative stress was suggested to play a critical role in separating the whole 26S proteasome complex into 20S core particle and two 19S regulator particles, resulting in the ubiquitin-independent degradation of misfolded proteins with unstable structures (Raynes et al., 2017). The unfolded or misfolded proteins expose hydrophobic areas which can be recognised and degraded by 20S proteasome structure (Raynes et al., 2017).

Although the ubiquitinated, unfolded or misfolded proteins could be degraded by both ubiquitin-dependent (26S) and ubiquitin-independent (20S) pathways, several studies have demonstrated that the 20S proteasome was more critical to general proteolysis. For example, proteasomes degrade oxidative stress-damaged proteins, and here too, the 26S proteasome was suggested to degrade ubiquitinated proteins, while the 20S proteasome degrades oxidised proteins without a ubiquitin tag (Voges et al., 1999). More efficient protein degradation was promoted by 20S proteasome compared to 26S proteasome (Pacifici, et al., 1989; Salo et al., 1990; Pacifici et al., 1993). It has also been reported that 20S proteasomes were more resistant to oxidative stress, whereas 26S proteasomes were more vulnerable compared to 20S proteasomes (Reinheckel et al., 1998). Thus, it can be concluded that 20S proteasomes are the more important structure in proteolytic systems involved in degradation of not only oxidised proteins, but also misfolded or unfolded proteins caused by denaturing stressors or external stimulants.

As a channel gating access to the 20S proteasome, the opening of α subunits initiated degradation by enabling entrance of protein substrates (Baumeister et al., 1998), and rapid opening of α subunits is observed in the immune response (Kisselve et al., 1999), which suggests new roles of 20S proteasome in addition to protein degradation. For example, in the immune response, proteasomes could mediate removal of the transcription factor inhibitor IκBα in response to immune stimuli, and proteolytic processes could also activate the NF-κB factor (Palombella et al., 1994; Zong et al., 1999). Moreover, proteasomes were also demonstrated to contribute to cell growth, with higher expression in immature cells, inhibited by cell differentiation agents (Ichihara and Tanka, 1995).

During aging, the degradation rate of proteasomes was suggested to decrease, with accumulation of oxidised and ubiquitinated proteins, and the proteasomes became more vulnerable to oxidative stress (Reinheckel et al., 1998). The proteasome's activities were impaired by exposure to elevated oxidative stress and were suppressed in aged cells. For example, the caspase-like/PGPH activity of 20S proteasome declined in aged human fibroblasts accompanied with oxidised protein accumulation (Sitte et al., 2000); in mice liver tissues, decreased activation of caspase-like/PGPH activity has also been reported (Conconi et al., 1996); and multi-catalytic proteasome activities decreased with age and were suppressed after oxidative stress in several regions of CNS, including cortex, hippocampus, cerebellum and spinal cord (Keller et al., 2000). Disruption of proteasome functions was also observed in the age-related neurodegenerative diseases, such as Alzheimer's disease (AD) and Parkinson's disease (PD) (McNaught and Jenner, 2001; Keller et al., 2000; Lopez-salon et al., 2000). In patients with PD, damaged functions of proteasomes were found in substantia nigra, and disrupted 20S proteasome structure without α subunits was observed in PD patients (McNaught et al., 2003). In AD patients, proteasome activities were reported to be decreased in hippocampus. Therefore, proteasome activities play a critical role in several cellular functions, but activities become suppressed and dysfunctional with increasing age, and could be inhibited by oxidative stress, accompanied with accumulation of damaged proteins.

In the previous results of the study, protein levels of *Has2* and *Gad2* decreased significantly after GC exposure at 14 DIV, but without any corresponding mRNA alteration tendency. The decreased protein levels after exposure to stress-related hormones raised a possibility that proteasome activities might contribute to the protein degradation of *Has2* and *Gad2* following GC exposure. As we treated the cells with elevated level of HCA in the cultured cells, the current understanding of whether GCs could affect proteasome activities in the cultured cells is unclear. Therefore, the current experiment aimed to investigate the effect of GCs on proteasome activities, focusing on the multi-catalytic activities of 20S proteasomes.

7.2 Study aims

The current study aimed to investigate possible alterations of 20S catalytic proteasome activities after exposure to GCs, by measuring proteasome catalytic activities in cultured cortical neurons, including chymotrypsin-, trypsin- and caspase-like activities. The specific aims were:

a. to investigate proteasome activities in cultured mouse cortical neurons.

b. to investigate whether GCs could affect proteasome activities in cultured cortical neurons.

7.3 Methods

Following 4h treatment with vehicle (nucleus-free water) or HCA (20nM/100nM), protein samples were extracted from the cultured cortical cells at 14 DIV. The detailed extraction procedures were presented in Chapter 2.

To test whether the GCs affect proteasome activities, cells treated with GCs were measured with fluorogenic proteasome assay with 3 different proteasome substrates related to the 3 proteasome activities, including chymotrypsin-like activity, caspase-like activity, and trypsin-like activity.

Subsequently, all 3 catalytic 20S proteasome activities were measured by detecting the 7-amino-4-methylcoumarin (AMC) fluorescence liberated from the synthetic proteasomal substrates,: Suc-Leu-Leu-Val-Tyr-AMC (Suc-LLVY-AMC) for chymotrypsin-like activity, Boc-Leu-Ala-Ala-AMC (Boc-LAA-AMC) for trypsin-like activity and Ac-Glu-Pro-Leu-Asp-AMC (Ac-GPLD-AMC) for caspase-like activity. To recognise whether the activities were related to the proteasome, MG132 was used as an inhibitor for all 3 activities of the 20S proteasome. Unconjugated AMC was diluted into appropriate concentrations to create a standard curve which allowed the fluorescence signal to be converted to units of AMC.

A proteasome assay was conducted to detect the accumulation of released fluorescence from proteasome substrates. The released fluorescence was measured every 60s for 30 minutes by using excitation wavelength 340 nm and emission wavelength 450 nm.

7.4 Results

7.4.1 AMC standard curve

The AMC standard curves showed a linear relationship between fluorescence and AMC concentrations. The linear standard curve could be used to determine proteolytic activity from proteasome substrates (Fig 7.1).

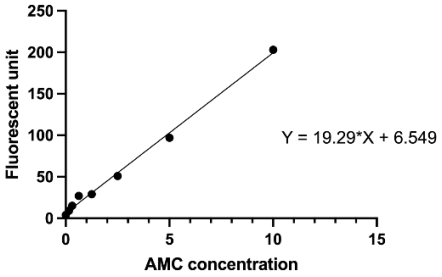

Figure 7.1: The AMC standard curve.

7.4.2 Proteasome activities after GCs exposure

The results of the proteasome assays showed that low and high doses of HCA tended to inhibit the proteasome activities. The chymotrypsin-like activity could be inhibited by both low dose and high dose HCA compared to the vehicle group (Fig 7.2 A B), however, only the inhibition by high dose HCA was statistically significant ($F(2, 11) = 7.18$, $p=0.011$ veh vs high dose HCA; $p=0.144$ veh vs low dose HCA, Tukey's post-hoc test). However, no apparent effect of low or high dose HCA on caspase-like activity was observed ($F(2, 11) = 0.32$, $p=0.910$ veh vs low dose HCA; $p=0.923$ veh vs high dose HCA, Tukey's post-hoc test) (Fig 7.2 C D). Moreover, only very low activity was observed using the substrate which detected the trypsin-like activity (Fig 7.2 E F). Although an inhibition tendency was shown with high dose HCA exposure, the inhibition was not significant ($F(2, 11) = 2.65$, $p=0.947$ veh vs low dose HCA; $p=0.219$ veh vs high dose HCA, Tukey's post-hoc test).

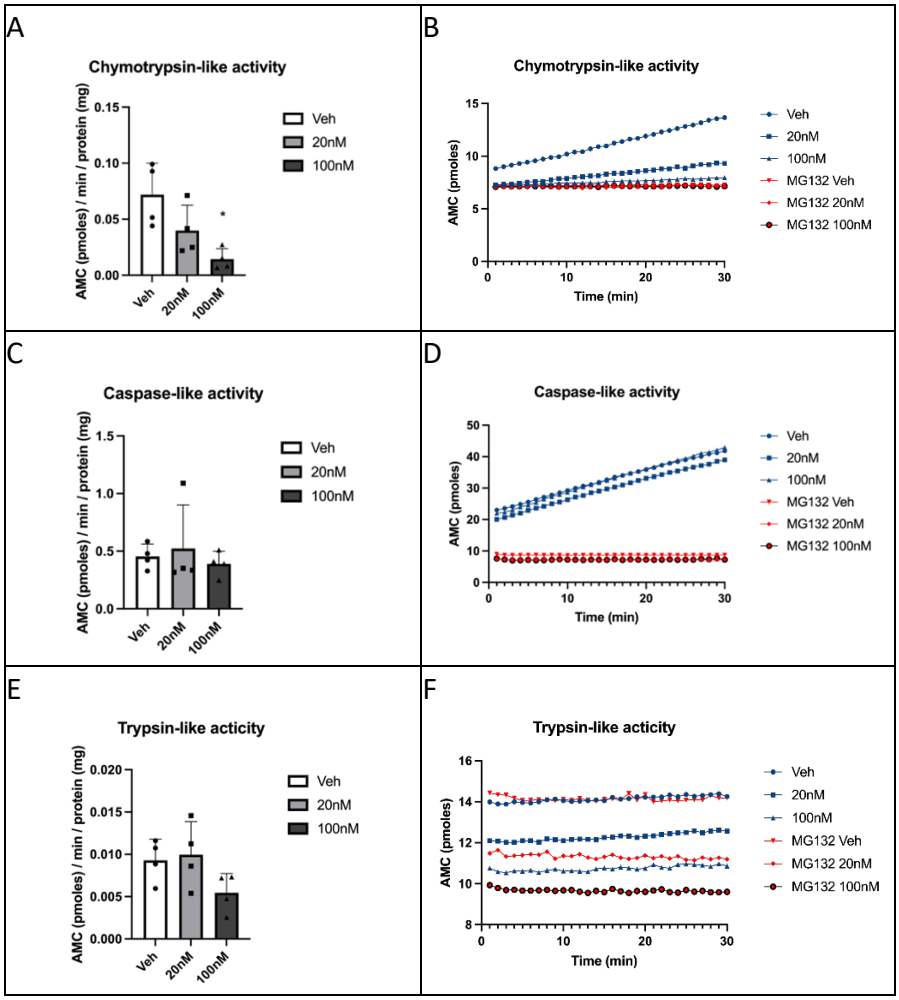

Figure 7.2: proteasome activities from cells treated with veh (distilled water), 20nM and 100nM HCA for 4h. A B: chymotrypsin-like activity and the activity inhibited by MG132 (10μM) from cells at 14 DIV treated with veh, 20nM and 100nM HCA (n=4). C D: caspase-like activity and the activity inhibited by MG132 (10μM) from cells at 14 DIV treated with veh, 20nM and 100nM HCA (n=4). E F: trypsin-like activity and the activity inhibited by MG132 (10μM) from cells at 14 DIV treated with veh, 20nM and 100nM HCA (n=4). The data for the effect of HCA on the 3 catalytic proteasome activities were normally distributed as assessed with the Kolmogorov-Smirnov test. No outliers were detected in the current study. The data were analysed by ANOVA followed by Tukey's post-hoc test, * $p<0.05$ effect of HCA vs corresponding veh group, Tukey's post-hoc tests, the bar graphs show mean ± SEM.

7.5 Discussion

Chymotrypsin-like proteasome activity was decreased by GCs with high dose (100nM) exposure; and for trypsin-like activities, the high dose-treated activity tended to be lower than vehicle and low dose treated activities, but with no statistical significance. The caspase-like activity remained unchanged after HCA exposure.

Chymotrypsin-like and caspase-like activities showed a constant rate of release of AMC from the substrates over time. Both activities were inhibited by MG132, as expected (Mitani et al., 2005; Alexandrova et al., 2008; Rodgers & Dean, 2003). However, trypsin-like activity appeared to be very low, with only marginal release of AMC over the time of the assay, and too little activity to

reliably detect inhibition by MG132. This implies that it would also be difficult to detect any potential inhibition by GCs for this activity, and the tendency towards suppression with 100nM HCA could be a genuine effect that failed to reach significance due to the low basal activity and low statistical power.

In the CNS, caspase-like proteasomal activity could be detected in both cortex and hippocampus areas in mice (Dash et al., 2000; Stepanichev et al., 2005). Trypsin-like activity is expressed the most in striatum, substantia nigra and cerebellum, whereas chymotrypsin-like activity is expressed and altered dynamically with age mainly in cerebral cortex and hippocampus (Zeng et al., 2005). Therefore, in the current study with measurements of proteasome activities in cultured cortex and hippocampus neurons, the chymotrypsin- and caspase-like activities could be detected with proteasome AMC substrates, but trypsin-like proteasomal activity was not shown in cortex and hippocampal neurons. Moreover, in mouse and rat brain regions, especially in cortex areas, the caspase/PGPH-like activities were the highest, followed by similar expression of chymotrypsin- and trypsin-like activities (Zeng et al., 2005), which is consistent with the current findings that caspase-like activities showed higher levels of fluorescent AMC production compared to chymotrypsin- and trypsin- like activities.

There is little evidence to support a direct effect of GCs on the proteasome. Previously, studies reported that oxidative stress could be a critical factor disrupting proteasome functions and activation. For example, decreased proteasome activities by exposure to stress has been demonstrated by several studies. In mouse CNS, downregulation of chymotrypsin-like activity was reported after oxidative stress induction in hippocampus and cerebral cortex (Keller et al., 2001). Impairment of chymotrypsin-, trypsin- and caspase/PGPH-like activities were suggested to correlate to the degree of cerebral oxidative stress (Keller et al., 2000). 4-hydroxynonenal (HNE), a peroxidation product involved in oxidative stress, modified the α subunits of the 20S proteasome, which was associated with inhibition of the 3 20S proteasome activities (chymotrypsin-, trypsin- and PGPH-like activities) (Bulteau et al., 2001). As GCs could directly induce neuronal oxidative stress (Du et al., 2009; You et al., 2009), exposure to an elevated amount of GCs might result in suppressed activity of proteasome activities with increased neuronal oxidative stress.

Once the proteasome activity is inhibited, the ability to degrade waste proteins is also disrupted, thus, the misfolded or oxidized proteins start to accumulate, resulting in increased overall protein levels. Therefore, the increased Has2 protein levels at 7 DIV shown previously in Chapter 3 after GC exposure might be attributed to proteasome activity disruption. However, the data showed a suppressive effect of GCs on chymotrypsin-like activity at 14 DIV after HCA exposure, thus, the decreased tendency of Has2 protein levels at 14 DIV is not related to elevated proteasome activities. Although limited studies investigated the role of proteasome activities in Has2 protein degradation in CNS neurons, consistent previous evidence demonstrated that the protein levels of Has2 could be suppressed by proteasome activities. For instance, the protein degradation of HAS2 was inhibited by MG132 after the blockage of new protein synthesis in human aortic smooth muscle cells, suggesting the involvement of proteasome activities in HAS2 protein degradation (Vigetti et al., 2012). In human kidney cells, HAS2 protein levels were also shown to be mediated by proteasome activities by regulating the ubiquitination of HAS2 (Karousou et al., 2010; Mehić et al., 2017). Hence, these lines of evidence suggest the involvement of proteasome activities in Has2 protein degradation.

Considering the scarcity of evidence for modulation of proteasome degradation activity by GCs, this would represent a novel mechanism of GC action. However, it should be noted that this suppression of chymotrypsin-like activity by HCA was demonstrated at 14 DIV, while at this stage

HCA decreased Has2 protein levels, rather than the increase detected at 7 DIV. It seems likely that a similar action of GCs on the proteasome occurs at 7 DIV, but additional experiments would be needed to formally demonstrate this, potentially implicating suppression of proteasome activity in the *Has2* protein increase. In any case, it is not easy to reconcile the decrease in proteasome activity caused by HCA at 14 DIV with its simultaneous action to decrease Has2 protein levels.

Although the increased protein levels could be supported by the evidence of proteasome inhibition, possibly via stress induction, controversial findings suggested increased protein degradation after GC administration. In hepatocytes, dexamethasone was demonstrated to stimulate protein degradation within 4h, which could last for several hours after the removal of dexamethasone (Hopgood et al, 1980). The same results were also reported in human muscle cells - that GCs could accelerate protein degradation regulated by proteasomal ubiquitin pathways (Sun et al., 2008). These lines of evidence suggest that the effect of GCs is to stimulate protein degradation, which implies an enhancement of proteasome activities. However, another study illustrated that in human fibroblasts, a suppressive effect of GCs on protein levels did not involve proteasomal pathways (Mi et al., 2017). Equally, there is also a report of physiologically relevant concentrations of dexamethasone in thymocytes suppressing chymotrypsin-like and caspase-like, but not trypsin-like, proteasome activity within 3h (Beyette et al., 1998). Therefore, various effects of GCs on proteasomal activities have been reported although the number of studies is small, and this may be the first evidence for effects in neurons.

In the current study, only chymotrypsin-like activity was suppressed by GCs. This decline was supported by previous studies that chymotrypsin-like activity was found to decrease only in hippocampus and cerebral cortex in old rats, and the declined activity might be attributed to oxidative stress damage (Kelle et al., 2000). While not decreasing in cortex and hippocampus, trypsin-like activity was suggested to decrease in striatum and cerebellum regions (Zeng et al., 2005). Unlike chymotrypsin- and trypsin-like activities, restricted studies have demonstrated dynamic changes of caspase-like proteasomal activities in CNS with or without external stimulations. However, with proteasome inhibitor induction in rat brain, caspase-like activity was found to be significantly suppressed in fronto-parietal cortex, with a similar decreasing tendency in hippocampus (Stepanichev et al., 2005), indicating that caspase-like activity might be mainly altered in specific cortex regions. Therefore, it is possible that decreased proteasome activities in cortical and hippocampal hippocampus by GCs could be only observed in chymotrypsin activity.

The purpose of the current experiment was to investigate whether the reduction of protein levels in Has2 at 14 DIV was attributed to an effect on proteasome activities. Current results reported only chymotrypsin-like activity decreased after GCs exposure at 14 DIV, therefore, the decreased protein levels of Has2 protein expression at 14 DIV are not mediated by altered proteasome activities; on the contrary, Has2 protein levels increased at 7 DIV, in this case, the increased protein levels might be regulated by inhibited proteasome activities, especially suppressed chymotrypsin activity, which might also occur at 7 DIV.

In addition, decreased protein levels of Gad65/Gad2 were also detected at 14 DIV after HCA exposure but with no related reduction of mRNA levels, thus a possibility that the decreased protein might be regulated by proteasome activities has been considered. Like Has2, Gad67/65 protein expression were also demonstrated to be downregulated by proteasome activities, the proteasome inhibitor MG132 was shown to prevent the cleavage of *Gad67/65* proteins in hippocampal cultured neurons (Baptista et al., 2010). However, suppressed chymotrypsin activities by HCA exposure were reported in the current study, indicating the reduction of

Gad65/Gad2 protein levels could not be attributed to altered proteasome activities, particularly chymotrypsin activity.

Among all 3 types of proteasome activities, chymotrypsin-like activity is the most critical activity in protein degradation. Chymotrypsin-like activity was suggested mainly to determine the protein degradation processes among all 3 proteasomal activities (Wilk et al., 1980). For example, dramatically decreased proteolysis rate was shown with specific inhibition of chymotrypsin-like activity in cultured neurons and lymphoblasts (Rock et al., 1994; Chen and Hochstrasser, 1996; Craiu et al., 1997). However, inhibition of trypsin-like activity resulted in little effect on the overall proteolysis rate, with minor deficits in intracellular proteasomal degradation (Arendt and Hochstrasser, 1997). As reported by previous studies, caspase-like activity was not mainly involved in degradation processes for cellular proteins, and caspases were suggested to play a role as degradation enzymes, but functioning more in cell signaling rather than through specific proteasomal proteolysis (Fadeel et al., 2000; Perfettini and Kroemer, 2003); for example, caspase-like activity could modulate cell differentiation in human muscle cells (Fernando et al., 2002), and cell cycling processes in B cells (Woo et al., 2003). Therefore, chymotrypsin-like activity is arguably the main proteasomal activity mediating proteolysis functions.

Several physiological processes were affected by proteasomal activities, for example, cell differentiation and proliferation (Ichihara and Tanaka, 1995), maintaining proteostasis (Ramachandran and Margolis, 2017), and more primarily and importantly, degrading oxidised, ubiquitinated and misfolded proteins (Davies et al., 2001). Reduced proteasomal activities could lead to the impairment of protein degradation processes, resulting in waste protein accumulation in the cells. Although trypsin- and caspase-like activity function less in the degradation processes, chymotrypsin-like activity is suggested to play a critical role in proteolysis. In the current study, chymotrypsin-like activity was significantly inhibited by high dose GCs, which could result in the accumulation of protein levels. The result was partially correlated to the initial results of GC experiments in Chapter 3, with increase protein levels after both low and high dose HCA of *Has2* at 7 DIV. Although a tendency towards decreased chymotrypsin activity was detected after low dose HCA exposure, a non-significant statistical output was found, which might be attributed to the low sample sizes (n=4 per group) in this study.

Despite various studies illustrating the involvement of proteasome activities in the protein degradation of Has2 and Gad67/65 protein levels (Vigetti et al., 2012; Karousou et al., 2010; Mehić et al., 2017; Baptista et al., 2010), the tendency towards decreased protein levels after HCA exposure in the previous experiments could not be related to increased proteasome activities, since inhibited chymotrypsin activities were observed after high dose HCA exposure. As chymotrypsin activity is suggested to be the major catalytic activity among all 3 proteasome activities functioning in protein degradation, decreased chymotrypsin activity caused by HCA exposure should inhibit the major protein degradation functions. Caspase-like activity was not affected by HCA but is not a major factor in protein degradation.

Conversely, significantly increased *Has2* protein levels were observed at 7 DIV after 4h HCA exposure, which could be possibly regulated by chymotrypsin-like proteasome activities. As 20S proteasome complex subunits are located on the cell plasma membrane and exposed to extracellular structures (Ramachandran and Margolis, 2017), thus this rapid increased effect might occur through the rapid non-genomic GC-mediated inhibition at the cell membrane and lead to the accumulation of protein expression within a short time.

To conclude, followed by the inconsistent increased alterations of *Has2* and *Gad2/Gad65* protein levels reported at 7 DIV and 14 DIV after rapid GCs exposure in previous results, the current study investigated whether this inconsistent alteration was attributed to the regulation of

proteasome activity by GCs. The current results showed that proteasomal chymotrypsin-like activity was suppressed after high-dose GC treatment within 4h exposure, with disrupted protein degradation ability of the activity, which might lead to the accumulation of oxidised or misfolded waste proteins and increase the overall protein levels.

Chapter 8

Distribution of PNNs expression in mouse brain tissues

8.1 Introduction

The distribution of PNNs was demonstrated to be different in various brain regions. As introduced in Chapter 1, in mouse cortical layers, PNNs were shown to be present mostly in layer 2/3 and layer 4/5 enwrapping Pv-expressing GABAergic interneurons (Nowicka et al., 2009; Sultana et al., 2021; Lensjø et al., 2017). Similar findings were also reported in humans (Pantazopoulos et al., 2010; Lendvai et al., 2013). In hippocampus, PNNs were found to be expressed highly in CA1 and CA3 covering Pv-expressing neurons, while in CA2, a lower density of PNNs was found and most of them covered glutamatergic pyramidal neurons (Brückner et al., 2003; Yamada and Jinno, 2013; Lensjø et al., 2017). Approximately half of GABAergic neurons in TRN were ensheathed by PNNs, and TRN was suggested to present the largest density of PNNs and GABAergic neurons (Steullet et al., 2018; Ciccarelli et al., 2021). Hence, apart from cortex and hippocampus, TRN is also an important region with PNNs expression.

GABAergic interneurons throughout the cortex and hippocampus are characterised by Nkx2.1 expression early in development (Anderson et al., 2002; Marín, 2012). These GABAergic interneurons are derived from the ganglion eminence in the basal telencephalon at the embryonic stage, usually emerging between E12 to E15, which then disperse widely across the brain in the later development period (Butt et al., 2005). In the forebrain, the subtypes of GABAergic neurons are related to the specific ganglion eminence sub-regions they are derived from, including medial, caudal and lateral ganglion eminence. The medial ganglion eminence (MGE) produces Pv- and SST- expressing GABAergic interneurons, and the neurons migrate to cortex and hippocampus; the caudal ganglion eminence (CGE) produces VIP- and CR-expressing GABAergic interneurons which migrate to the superficial layers of cortex; additionally, lateral ganglion eminence (LGE) produces interneurons migrating to olfactory bulb and striatum (Butt et al., 2005). The GABAergic neurons surrounded by PNNs originate from MGE.

Nkx2.1 is a transcription factor expressed in MGE rather than CGE and LGE (Bandler et al., 2018), thus, the Pv-and SST- expressing GABAergic interneurons derived from MGE are characterised by the expression of Nkx2.1. Nkx2.1 is a critical factor for the expression of GABAergic interneurons in MGE, as in the absence of Nkx2.1, the interneurons in MGE were shown to switch to the neuronal types in CGE, with an increased number of VIP- and CR-expressing neurons in CGE and the loss of Pv- and SST- expressing neurons derived from MGE (Butt et al., 2008). Hence, Nkx2.1 transcription factor is a critical regulator for the production of Pv- and SST- GABAergic interneurons derived from MGE.

As noted previously in Chapter 1, converging evidence illustrated the distribution of PNNs in different brain regions of different species, with consistent results reporting that the distribution of PNNs was tightly correlated with the expression pf Pv-expressing neurons. However, instead of the overall expression of PNNs in cortex and hippocampus regions, the studies only investigated the distribution of PNNs in a limited number of brain regions, and the proportion of GABAergic neurons surrounded by PNNs were not measured. Furthermore, controversial results showed some sex differences of PNNs distribution. Therefore, the current study aimed to investigate the overall distribution of PNNs in cortical regions (mainly layer 2/3 and 4/5), hippocampal regions (CA1, CA2 and CA3) and TRN; and whether PNN expression was different in male and female animals.

8.2 Study aims

The aims of the current study were to investigate the general distribution of WFA-labelled PNNs, and td tomato-expressing GABAergic interneurons in cortex and hippocampus, including PFC, restroplenial cortex, auditory cortex, visual cortex, CA1, CA2 and CA3 regions. The specific aims were:

a. to investigate the expression of WFA-labelled PNNs, td tomato-expressing GABAergic interneurons and the colocalisation of PNNs and GABAergic interneurons, in cortex, hippocampus and TRN.

b. to investigate the proportion of PNNs covering GABAergic interneurons, and the proportion of GABAergic interneurons covered by PNNs in cortex, hippocampus and TRN.

8.3 Methods

3 male and 3 female C57BL/6 adult mice expressing the td Tomato reporter driven by the promotor of Nkx2.1 were used for the study at the age of 5 weeks.

The brains were dissected and stored in 4% paraformaldehyde (PFA) at 4°C overnight and the brains were then stored in NaCl the next day at 4°C. On the day of use, the brains were sectioned with a freezing microtome in 50μm thick sections and stored in cryoprotectant in 24-well plates. The brain sections were collected from the plates using a fine brush and placed in 1x PBS.

Following the sectioning, the WFA-staining was performed on glass slides. The detailed procedure was presented in Chapter 2.

The overview of the images was scanned through a confocal microscope (ZEISS, LSM900) with a 10x objective for counting and 20x objective for illustrations. The images were taken and downloaded using Zen blue 3.0 software.

Image analysis and cell counting were performed using Image J. The cell number including WFA+, td tomato+ and WFA+/td tomato+ colocalisation was counted manually, the counting procedure was shown in Chapter 2.

8.4 Results

8.4.1 General distribution and sex differences of GABAergic interneurons and PNNs in cortical and hippocampal regions

A similar proportion of GABAergic interneurons which were not surrounded by WFA-labelled PNNs, and of those showing colocalization with WFA-labelled PNNs, were found in cortical regions and hippocampus, accounting for approximately around 60% to 80%, and 20% to 40%, respectively (Fig 8.1 A-D). Moreover, the td tomato-negative WFA-labelled PNNs were observed more frequently in hippocampus compared to cortical regions, with around 10% to 20% diffused PNNs expressing in hippocampus, but 5% to 10% expressing in cortical regions (Fig 8.1 E-G). However, no td tomato expressing GABAergic neurons were detected in TRN (Fig 8.1 H).

The proportion of PNN distribution in terms of sex differences was studied. The results revealed no significant sex differences of td tomato +ve, WFA -ve cells, td tomato -ve WFA +ve cells, or colocalised td tomato-expressing neurons with PNNs, were found in either cortex or hippocampus (Fig 8.1 A-G; Fig 8.3) (PFC: $F(2,152)=0.00$, only td tomato+ $p=0.460$; only WFA+

p=0.121; colocalisation p=0.999 male vs female, Tukey's post-hoc tests; RSC: F(2, 63)=0.00, only td tomato+ p=0.986; only WFA+ p=0.855; colocalisation p=0.996 male vs female, Tukey's post-hoc tests; auditory cortex (F(2, 99)=0.00, only td tomato+ p=1.00; only WFA+ p=0.764; colocalisation p=0.773 male vs female, Tukey's post-hoc tests; visual cortex: F(2, 114)=0.00, only td tomato+ p=0.081; only WFA+ p=0.137; colocalisation p=1.000 male vs female, Tukey's post-hoc tests; CA1: F(2, 51) =0.00, only td tomato+ p=1.000; only WFA+ p=0.170; colocalisation p=0.596 male vs female, Tukey's post-hoc tests; CA2 F(2, 69)=129.97, only td tomato+ p=0.985; only WFA+ p=0.876; colocalisation p=0.373 male vs female, Tukey's post-hoc tests; CA3 F(2, 63)=0.00, only td tomato+ p=0.886; only WFA+ p=0.763; colocalisation p=1.000 male vs female, Tukey's post-hoc tests).

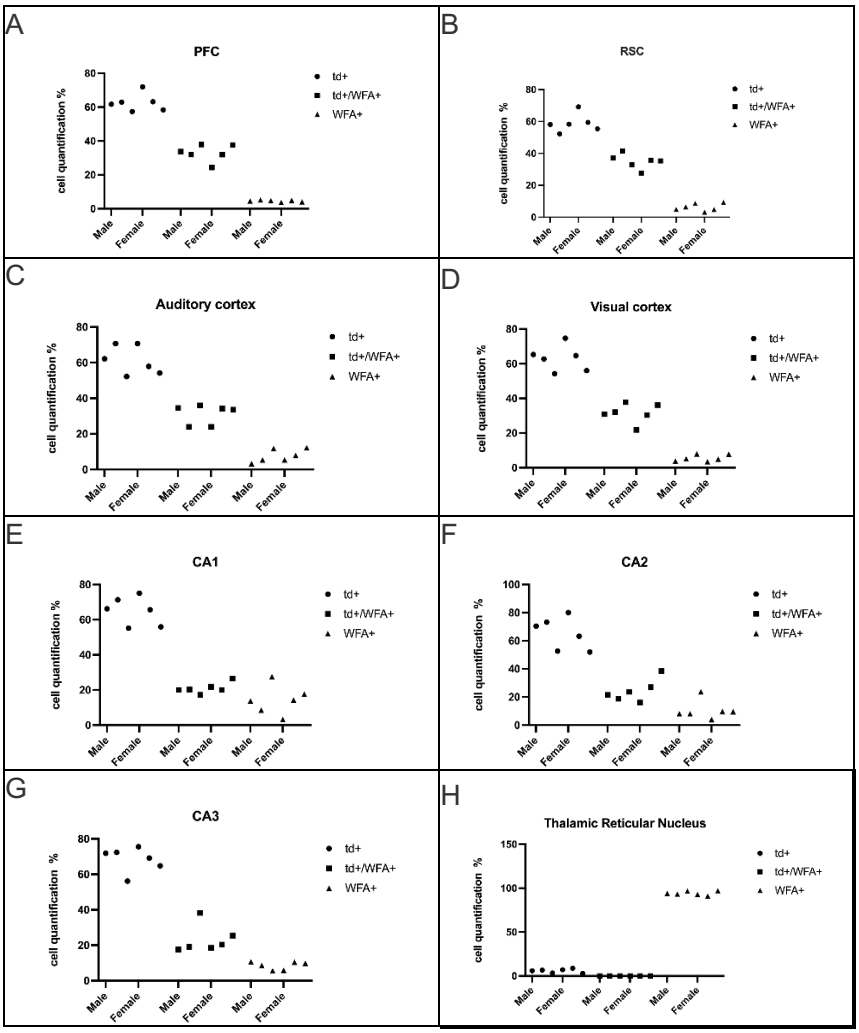

Figure 8.1: proportion of GABAergic neurons, PNNs, and GABAergic neurons with PNN in different brain regions. **A-D**: proportion of td tomato expressed GABAergic interneurons (no WFA staining), WFA-labelled PNNs (no td tomato staining), and colocalisation of td tomato +ve neurons and WFA-labelled PNNs, in cortex (male: n=3; female n=3). E-G: proportion of td tomato expressed GABAergic interneurons (no WFA staining), WFA-labelled PNNs (no td tomato staining), and colocalisation of td tomato +ve neurons and WFA-labelled PNNs in hippocampus (male: n=3; female n=3). H: amount of td tomato expressed GABAergic interneurons (no WFA staining), WFA-labelled PNNs (no td tomato staining), and colocalisation of td tomato +ve neurons and WFA-labelled PNNs in TRN (male: n=3; female n=3). The data for the proportion of each type cells labelled with WFA, td-tomato and co-labelled with WFA/td-tom are normally distributed in each brain regions as assessed with the Kolmogorov-Smirnov test. No outliers

were detected in the current study. The data were analysed by ANOVA followed by Tukey's post-hoc tests. Symbols represent the mean values in that region for individual mice.

8.4.2 The distribution and sex differences of PNNs covering GABAergic interneurons in cortical and hippocampal regions

The data were reconfigured to examine the proportion of each class of labelled cell (td tomato-+ve or WFA-+ve) that were double-labelled. The results showed that in the cortical regions including PFC, restroplenial cortex, auditory cortex, and visual cortex, most of td tomato-expressing GABAergic interneurons were enwrapped by PNNs, accounting for 60% to 80% (Fig 8.2 A-D); additionally, 70% to 90% of WFA-labelled PNNs were shown to covering GABAergic interneurons. In the hippocampal regions, including CA1, CA2 and CA3, less proportion with approximately 60% to 80% of Pv-expressing GABAergic interneurons covered by WFA-labelled PNNs were observed (Fig 8.2 E-G), and around 70% to 90% WFA-labelled PNNs were found to cover GABAergic interneurons. However, no td tomato expressing GABAergic interneurons were detected in TRN.

In terms of the sex differences, the proportion differences of GABAergic interneurons surrounded by WFA-labelled PNNs were not detected in both cortical and hippocampus regions in male and female mice (Fig 8.2 A-G; Fig. 8.3) (PFC: $F(1,100) = 2.76$, $p=0.056$ male vs female, Tukey's post-hoc tests, RSC: $F(1, 79) = 0.22$, $p=0.461$ male vs female, Tukey's post-hoc tests; auditory cortex: $F(1, 69)=2.270$, $p=0.445$ male vs female, Tukey's post-hoc tests; visual cortex: $F(1, 79)=1.89$, $p=0.057$ male vs female, Tukey's post-hoc tests; CA1: $F(1, 33)=1.14$, $p=0.960$ male vs female, Tukey's post-hoc tests; CA2: $F(1,49)=8.03$, $p=0.725$ male vs female, Tukey's post-hoc tests; CA3: $F(1, 45)=1.53$, $p=0.833$ male vs female, Tukey's post-hoc tests).

With regards to the sex differences of the proportion of PNNs covering GABAergic interneurons, in the auditory cortex, more PNNs were observed to surround GABAergic interneurons in male mice compared to female mice with around 85% of PNNs surrounding GABAergic interneurons in males but 75% in females (Fig 8.3 C K) ($F(1, 69) =2.27$, $p<0.01$, male vs female, Tukey's post-hoc tests); conversely, in the CA2 hippocampal region, more PNNs in female mice covered GABAergic interneurons than PNNs in male mice with around 77% of PNNs surrounding GABAergic interneurons in females but 60% in males (Fig 8.3 F N) ($F(1,49)=8.03$, $p<0.05$ male vs female, Tukey's post-hoc tests). However, in addition to auditory cortex and CA2, no significant sex differences were found in other cortical and hippocampal regions (Fig 8.3 A B D E G I J L M) (PFC: $F(1,100) = 2.76$, $p=0.997$ male vs female, Tukey's post-hoc tests; RSC: $F(1, 79) = 0.22$, $p=0.160$ male vs female, Tukey's post-hoc tests; visual cortex: $F(1, 79)=1.89$, $p=0.922$ male vs female, Tukey's post-hoc tests; CA1: $F(1, 33)=1.14$, $p=0.211$ male vs female, Tukey's post-hoc tests; CA3: $F(1, 45)=1.53$, $p=0.811$ male vs female, Tukey's post-hoc tests)

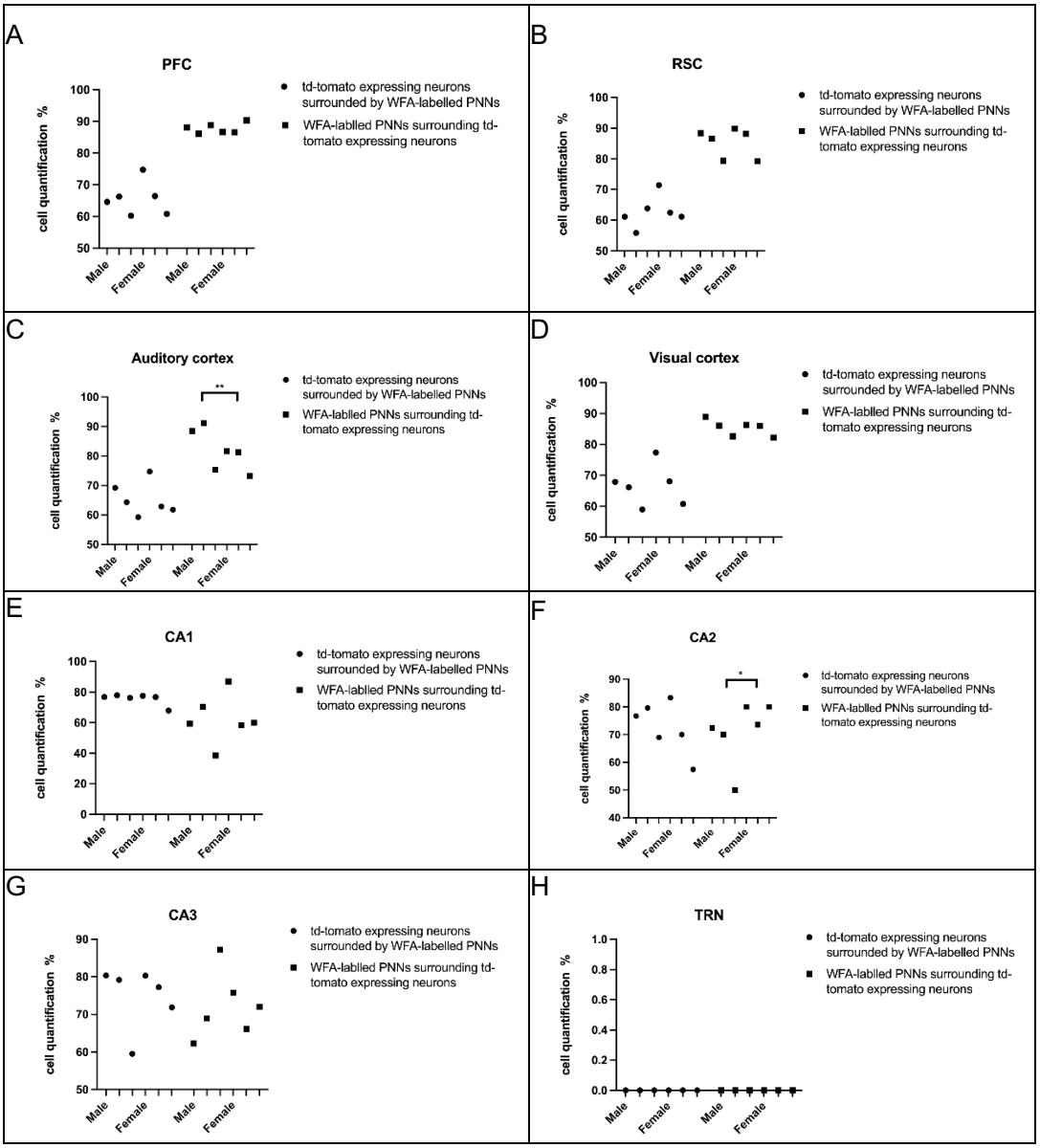

Figure 8.2: proportion of GABAergic interneurons covered by PNNs and proportion of PNNs covering GABAergic neurons in different brain regions. A-D: proportion of GABAergic neurons covered by PNNs and proportion of PNNs covering GABAergic neurons in cortex (male: n=3; female n=3). E-G: proportion of GABAergic interneurons covered by PNNs and proportion of PNNs covering GABAergic neurons in hippocampus (male: n=3; female n=3). H: proportion of GABAergic interneurons covered by PNNs and proportion of PNNs covering GABAergic neurons in TRN (male: n=3; female n=3). The data for the proportion of each type cells labelled with WFA, td-tomato and co-labelled with WFA/td-tom are normally distributed in each brain regions as assessed with the Kolmogorov-Smirnov test. No outliers were detected in the current study. The data were analysed by ANOVA followed by Tukey's post-hoc tests, * $p<0.05$ vs corresponding veh group, Tukey's post-hoc tests. Symbols represent the mean values in that region for individual mice.

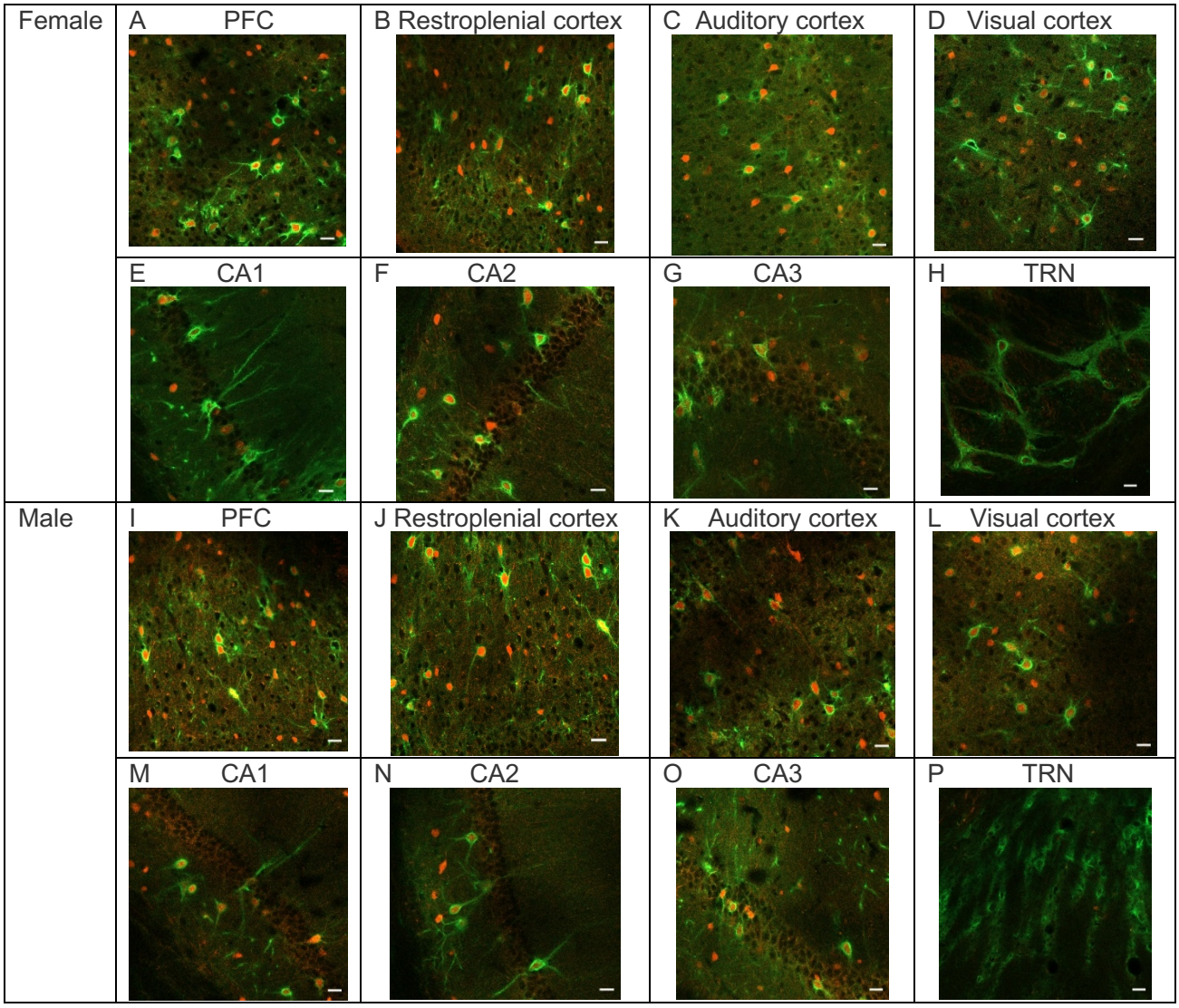

Figure 8.3: Representative images of WFA-labelled PNNs and td tomato-expressing GABAergic neurons in male and female mouse brain tissues, the images were taken from a confocal microscope with 20μm scale. A-H: WFA labelled-PNNs with td tomato-expressed GABAergic interneurons in female brain regions; I-P: WFA labelled-PNNs with td tomato-expressed GABAergic interneurons in male brain regions.

8.5 Discussion

The study investigated the distribution of PNNs across brain regions in both male and female mice, mainly focused on cortical layer2/3 and layer4/5. The results showed that PNNs mostly covered inhibitory GABAergic interneurons, with few WFA+ve, td tomato-ve cells, but in the hippocampus, more PNNs were detected that did not cover GABAergic interneurons, especially in CA1 and CA2 regions, compared to the cortical layers investigated. No sex differences of td tomato+ve cell or PNN distribution were detected in cortex and hippocampus; but in the auditory cortex, more PNNs were shown to cover GABAergic interneurons in male mice, while in the CA2 region, female mice presented more PNNs surrounding GABAergic interneurons than male mice.

The current results reported the largest proportion of PNNs covering GABAergic interneurons in RSC and PFC, followed by auditory cortex, visual cortex and hippocampus region, and there were no Nkx2.1 td tomato expressing GABAergic neurons in TRN surrounded by PNNs. The

distribution differences across brain regions were in line with the finding that PNNs are distributed differently in different brain areas. For example, it has been revealed that approximately 40% of Pv-expressing GABAergic interneurons were ensheathed by PNNs, mainly in layer 2/3 and layer 4/5 cortex (Nowicka et al., 2009).

In the cortical layer2/3 and 4/5, 60% to 80% of td tomato+ve interneurons were enwrapped by PNNs, which was consistent with the previous finding that around 75% of Pv-expressing neurons in the RSC were ensheathed by PNNs in the normal condition and around 60% to 70% of Pv-expressing td tomato+ve GABAergic interneurons covered by PNNs in RSC after social isolation stress induction (Klimczak et al., 2021). Moreover, the study also confirmed that most PNNs, approximately 80% to 90%, covered GABAergic interneurons in cortical layer 2/3 and 4/5, which was in line with the findings that PNNs express mostly in layer 2/3 and layer 4/5 of PFC surrounding Pv-expressing neurons (Sultana et al., 2021). In the retrosplenial cortex, previous results illustrated that almost all PNNs were found to cover Pv-expressing GABAergic interneurons, while the current results showed that approximately 90% of PNNs covered GABAergic interneurons in RSC (Klimczak et al., 2021).

Instead of a fully net-like structure, PNNs were also detected in discrete and granular, rather than reticular structures (Ueno et al., 2017; Sultana et al., 2021), which was partially consistent with the current findings that in the cortical areas, some of the PNNs presented in a more discrete but still net-like structure manner.

In the hippocampus, the proportion of td tomato expressing neurons without PNNs was similar to the cortical regions, moreover, the proportion of GABAergic neurons covered by PNNs was also found to be similar with the cortical regions, accounting for 60% to 80%. This result was in line with the previous findings that unlike the PNNs covering mostly GABA interneurons in the retroplenial cortex, only around 80% of PNNs surrounded presumed Pv-expressing neurons in the hippocampus; while around 80% of Pv-expressing neurons in the hippocampus were covered by PNNs, the percentage was similar to the restrosplenial cortex (Klimczak et al., 2021). Additionally, more diffuse WFA-labelled PNNs were detected in hippocampus compared to the cortical areas, accounting for approximately 20%, which was consistent with the following findings that a smaller proportion of PNNs was covering GABAergic interneurons in hippocampus than in cortical regions. Instead of GABAergic interneurons, PNNs are most likely covering glutamatergic-expressing pyramidal neurons in hippocampus, especially in the CA2 region (Celio, 1993; Brückner et al., 2003). Conversely, in CA1 and CA3 areas, WFA-labelled PNNs were detected to cover neurons with non-pyramidal phenotypes (Brückner et al., 2003), which was in line with later and current results that more Pv-positive neurons were observed in CA1 and CA3 with surrounding PNNs compared to CA2 (Yamada and Jinno, 2013).

The study also illustrated a large proportion of PNNs present in TRN. Similar results were also reported in a previous study that, in mouse brain, higher expression of PNNs was found in TRN compared to other subcortical regions (Ciccarelli et al., 2021); and PNNs were found to be present in TRN with high density and high WFA staining intensity. GABAergic neurons represent the vast majority of neurons in TRN, but reportedly only a proportion of them are covered by PNNs (Fader et al., 2016). However, the current results showed no td tomato expressing neurons in TRN. This is expected, as the current study used Nkx2.1-td tomato mice, and it is known that the TRN is not derived from MGE, but from prethalamus, which does not express Nkx2,1, and hence td tomato expressed in Nkx2.1-reporter mice was not detected in TRN (Abecassis et al., 2020; Altman and Bayer, 1988).

Pv-expression defines one of the subtypes of GABAergic interneurons, and Nkx2.1 is required for the development of 2 subgroups of GABAergic interneurons: Pv- and SST-expressing

interneurons (Du et al., 2008), it is possible that GABAergic neurons in cortex and hippocampus with surrounding PNNs might include SST-expressing interneurons as well as Pv neurons. However, consistent studies illustrated that PNNs only ensheathed Pv-expressing neurons but not SST-expressing neurons (Rossier et al., 2015; Oohira et al., 2013; Yamada et al., 2015). Thus, it can be assumed that in the current study, the neurons covered by WFA-labelled PNNs were Pv-expressing GABAergic interneurons. The numerous td tomato+ve, WFA-ve cells are most likely these SST cells, which are generally reported as more numerous the Pv cells in mouse cortex (Nassar et al., 2015; Vogt et al., 2015).

With regards to the sex differences of PNN distribution in different brain areas, the current results indicated that PNNs took up similar proportions surrounding GABAergic interneurons in male and female mice, and the percentage of td tomato-expressing GABAergic neurons covered by PNNs was also similar in male and female mice. However, in the auditory cortex, a larger proportion of PNNs surrounding presumed Pv-expressing GABAergic interneurons was found in male mice compared to female mice; conversely, in CA2, female mice showed more PNNs covering Pv-expressing GABAergic neurons. These findings were opposite to the previous studies that the distribution of PNNs was different between male and female animals across various brain regions. For example, adult male mice showed more PNNs covering Pv-expressing neurons in hippocampus, and PNNs were found to be expressed with higher density and intensity around Pv-expressing neurons in male mice than female mice (Ciccarelli et al., 2021). Additionally, other results also reported no differences of PNN expression with Pv-expressing neurons between male and female animals. For example, in the neocortex, no PNN distribution differences were found between male and female rats; and the proportion of PNNs covering Pv-expressing neurons was similar between male and female rats in both hippocampus and neocortex (Griffiths et al., 2019); furthermore, in mouse hippocampus, similar densities of PNN expression were reported in CA1 and CA2 regions in both male and female mice (Rahmani et al., 2023). Thus, it could be seen that the sex differences of PNNs expression throughout brain regions still remained controversial.

Furthermore, there were no sex differences in cortical and hippocampal regions reported by the current results, in terms of the general distribution of td tomato expressing GABAergic interneurons, td tomato-ve WFA-labelled neurons, and colocalisation of td tomato-expressing neurons and WFA-labelled PNNs. The results were partially in accordance with previous findings. For example, the quantity of Pv-expressing GABAergic neurons was similar in male and female mice in medial PFC (Woodward et al., 2023), and the proportion of Pv-expressing neurons was similar between male and female rats in both hippocampus and neocortex (Griffiths et al., 2019). However, another study reported that female rats expressed more Pv-expressing neurons in infralimbic and prelimbic cortex than male rats (Binette et al., 2023). Apart from Pv-expressing GABAergic neurons, no PNN expression differences between sexes were reported in hippocampus and cortex (Rahmani et al., 2023; Mayne et al., 2024). Additionally, in zebra finches, highly enriched PNNs were reported in anterior cortical basal ganglia and song nuclei in male zebra finches as compared to females (Meyer et al., 2014). Thus, the sex differences of Pv-expressing GABAergic interneurons and WFA-labelled PNNs also remained controversial.

Although the current results were largely consistent with the previous findings, several limitations also need to be considered. Firstly, previous studies and the current experiment used WFA to detect and visualise PNNs, however, not all PNNs would be observed by WFA labelling. For example, *Acan*-labelled PNNs were found to be distributed more in subcortical regions compared to WFA-labelled PNNs (Morawski et al., 2010). These studies indicated that WFA-labelling could not visualise all PNNs throughout the brain regions, which might result in an overall low accuracy of PNN quantifying. Secondly, the quantification of the labelled PNNs and GABAergic

interneurons was counted manually with Image J, which was similar to the methods used in previous studies (Lensjo et al., 2017; Sultana et al., 2021; Nowicka et al., 2009). As manual counting is highly dependent on human visualisation, perception and interpretation, which might influence the overall quantities of the cell number; additionally, distinguishing different types of labelled cells, including td tomato expressed GABAergic interneurons, WFA-labelled PNNs and colocalisation of GABAergic neurons and PNNs, was highly dependent on personal rather than standard criteria. In this case, the quantification of the same type of cells could vary between different experiments and researchers, which might be a reason that an inconsistent proportion of WFA-labelled PNNs covering Pv expressing GABAergic interneurons could be reported in the same brain region of the same type of animals. Finally, only 3 mice of each sex were analysed, which is likely to be insufficient to detect subtle sex differences.

To conclude, the current study investigated the general distribution of Nkx2.1-expressing GABAergic neurons, cells with PNNs and colocalisation of PNNs and Nkx2.1-expressing neurons, in cortex and hippocampus. In the cortex and hippocampus, a similar percentage of Nkx2.1-expressing GABAergic interneurons, and colocalised PNNs and Nkx2.1-expression were observed; while more cells with PNNs lacking Nkx2.1 expression were detected in hippocampus. The study also confirmed that PNNs mostly covered Nkx2.1-expressing GABAergic neurons expressed in cortical layer2/3 and layer4/5 surrounding GABAergic neurons, but a smaller proportion of PNNs were found to cover GABAergic neurons in hippocampus. In terms of the td tomato expressing GABAergic neurons, around 60% to 80% of GABAergic neurons in cortical layer 2/3 and layer 4/5 were enwrapped by PNNs, a similar proportion were found in hippocampus. The distribution of PNNs in cortex and hippocampus were largely consistent with previous findings. By further confirming the distribution of PNNs and GABAergic neurons surrounded by PNNs in cortex and hippocampus, the current results gave an overview of cortical and hippocampal PNN expression, and provided a region-specific suggestion for further study to examine the alterations of PNN and Pv expression in schizophrenia mouse models.

However, the study reported that few sex differences were observed in terms of PNN distribution, which is partially consistent with previous findings. The different results reported between studies might be attributed to the limitation of the methods, including using WFA for PNNs visualization, quantifying cell numbers with manually counting, and the small sample size. In this case, improvement of cell counting method would be necessary in the future studies, such as using automatic counting software; and antibodies to detect PNNs, such as an *Acan* antibody (Cat-301) combined with WFA to visualise PNNs.

Chapter 9

Differences of mRNA levels of PNNs components in schizophrenia MIA mice model and in WT mice

9.1 Introduction

Prenatal maternal immune activation (MIA) is one of the risk factors, as with prenatal stress, resulting in increasing incidence of schizophrenia (Beydoun et al., 2008; de Kloet et al., 2004; Weinstock et al., 2008). To study whether MIA linked to schizophrenia or schizophrenia-like symptoms, MIA animal models were established with different reagents to induce an immune response during the animals' pregnancy. In viral or bacterial infection, double-stranded RNA (dsRNA) viruses could be recognised by Toll-like recptor3 (*TLR3*) and bacteria by Toll-like receptor 4 (T*LR4*), resulting in increased pro-inflammatory cytokine expression (Meyer et al, 2014; Macêdo et al, 2012). Polyinosinic-polycytidylic acid (Poly I:C) and lipopolysaccharide (LPS) are the 2 agents that could activate *TLR3* and *TLR4* to mimic dsRNA viral or bacterial infection. Thus, Poly I:C and LPS are most commonly used in MIA animal models. Apart from ds-viruses, TLRs could also respond to single strand (ss) viral infections by binding to *TLR7* and *TLR8*. Resiquimod is an infectious agent activating *TLR7* and *TLR8* and used to mimic ssRNA virus infection.

MIA animal studies demonstrated that offspring exhibited hyperfunction in dopaminergic systems and disrupted cognitive function with maternal Poly I:C induction; these impairments were in line with schizophrenia-like phenotypes, representing a neurodevelopmental aetiology of schizophrenia (Ozawa et al. 2006). Prenatal exposure to Poly I:C was also reported to produce effects related to the behavioural changes in schizophrenia. For example, deficient social interaction, impaired object recognition memory, prepulse inhibition and increased anxiety-like behaviours were observed in adult offspring exposed to maternal Poly I:C injection (Shi et al., 2003; Ibi et al., 2009; Ito et al., 2010). Furthermore, genome wide studies reported the association between MIA and downregulated expression of schizophrenia-related genes in the foetal brains (Lahiru et al., 2021), including the genes from cadherin family and protocadherin family. This evidence supported the concept that MIA during pregnancy increases the risk of schizophrenia, and behavioural and cognitive impairments induced by MIA are consistent with clinical schizophrenia-like symptoms.

As potentially a critical factor involved in the development of schizophrenia, PNN formation and component gene expression can be disrupted by MIA. The density of PNNs was reported to decrease in medial PFC in offspring with prenatal maternal Poly I:C exposure. The time when PNN reduction was observed was consistent with the onset time of schizophrenia (Paylor et al., 2016), which supported the link of MIA-disrupted PNNs to schizophrenia. A similar decrease of (WFA-labelled) PNN areas and intensities was reported, and the complexity of axons covered by PNNs was reduced, in hippocampal neurons after prenatal MIA (Wegrzyn et al., 2020). Collectively, these studies suggested that MIA could increase the risk of schizophrenia in offspring by affecting the expression and formation of PNNs. As the previous results in the current study illustrated the effect of stress on component gene expression and formation of PNNs, the study in this chapter mainly focused on investigating the effect of MIA on PNN component gene expression. General PNN structure was demonstrated to be altered by MIA, however, how different components are affected by MIA remained less clear. Poly I:C is commonly and widely used as an agent for MIA in mouse models, reproducing in the effects of dsRNA virus infection, but ssRNA virus infection models are less frequently used to examine the

effects of MIA. As PFC was suggested to play a critical role in cognitive deficits and is disrupted in schizophrenia patients, and the previous study in Chapter 8 illustrated that PNN and Pv neurons were largely expressed in PFC, PFC was selected as the specific region to be investigated. Therefore, the current study aimed to investigate the effect of MIA on expression of PNN component mRNA in offspring with either Poly I:C or resiquimod administration, in both WT mice and mice reproducing the 16p11.2 microduplication associated with schizophrenia risk.

9.2 Study aims

In the current study, the aim was to investigate the effect of MIA on the expression of PNN components associated with schizophrenia phenotypes. The specific aims were to:

a. Investigate the changes of PNN component mRNA expression following MIA induction

b. Compare the expression differences of PNN component mRNAs between WT mice and 16p11.2 duplication mice before and after MIA induction

9.3 Methods

6 female hemizygous 16p11.2 duplication (Dup.) mice and 6 female WT mice were injected subcutaneously with saline (2ml/kg), resiquimod (2mg/kg) or Poly I:C (20mg/kg) at day 12.5 of pregnancy (saline: 2 WT mice, 2 Dup. mice; poly I:C: 2 WT mice, 2 Dup. mice; resiquimod: 2 WT mice, 2 Dup. mice). After dams had littered, the total number of pups was 73, comprising 23 pups from saline injected mice (WT mice: 10 Dup mice: 13), 27 pups from resiquimod injected mice (WT mice: 10 Dup mice: 17) and 23 pups from Poly I:C injected mice (WT mice: 16 Dup mice: 7). When the pups reached adulthood (8 weeks), the brain tissues from different brain regions were extracted, including left PFC, right PFC, left hippocampus and right hippocampus. PFC was used in the current study for the mRNA expression measurement. The study is reported in accordance with ARRIVE guidelines (https://arriveguidelines.org) and the updated ARRIVE guidelines (Percie du Sert et al, 2020). The animal study was performed according to home office (UK) regulations and were approved by the University of Glasgow Animal Welfare Ethical Review Board and University of Strathclyde Animal Welfare Ethical Review Board. The housing condition was mentioned in Chapter 2.

mRNA samples were extracted from the right PFC tissues and cDNA produced by reverse transcription: the detailed methods were presented in Chapter 2. qPCR was performed to measure the mRNA expression in right PFC brain tissues with targeted primers, including *Acan*, *Bcan*, *Ncan*, *Vcan*, *Ptprz1*, *Has1*, *Has2*, *Has3*, *Hapln4*, *TnR*, *Pv*, *Gad1* and *Gad2*. The current study used 2 kinds of experimental unit, one is using littermates as experimental unit, but this might include pseudo-replication and artificially inflated sample sizes; another method is using dams as experimental units. Using 2 kinds of experimental units was to investigate the effect of MIA on PNN components with and without the consideration of the similarities between different littermates. As pups littered from the same dam might share similar utero or postnatal environmental conditions, resulting in limited variations regards to the physiology and behavioural activities between each pup (Kentner et al., 2019). Thus, to improve the rigour and reproducibility of the animal experiment, and to eliminate the similarities between each littermates, the mRNA values reported from the qPCR assay for all littermates of the same genotype from the same dam were averaged to give a mean value for the dam.

9.4 Results

9.4.1 Alterations of PNNs and *Gad* components after MIA induction using littermates as experimental unit

Firstly, the results were reported and analysed based on the experimental units with different littermates.

After prenatal maternal Poly I:C or resiquimod exposure, mRNA levels of CSPG components increased compared to maternal saline (vehicle) exposure except for *Acan*. Among all CSPG components, *Acan* mRNA levels decreased after resiquimod administration but remained unchanged after polu I:C induction (Fig 9.1 A) ($F(2, 70)=3.12$, $P =0.051$; saline vs resiquimod: $P=0.042$; saline vs Poly I:C: $P=0.302$ Tukey's post-hoc tests), and mRNA levels of *Bcan* ($F(2, 66)=6.49$, $P =0.003$, saline vs Poly I:C Tukey's post-hoc tests: $P=0.022$) and *Ncan* ($F(2, 70)=6.16$, $P =0.004$, saline vs Poly I:C $P=0.024$, Tukey's post-hoc tests:) increased significantly with Poly I:C administration, while mRNA levels of *Vcan* ($F(2, 61)=18.37$, $P<0.001$; saline vs resiquimod $P=0.001$, Tukey's post-hoc tests; saline vs Poly I:C: $P<0.001$, Tukey's post-hoc tests) and *Ptprz1* ($F(2, 64)=8.51$, $P =0.001$; saline vs resiquimod: Tukey's post-hoc tests $P=0.002$, saline vs Poly I:C: Tukey's post-hoc tests $P=0.006$) increased with both resiquimod and Poly I:C administration (Fig 9.1 D E.). Among all the alterations in CSPG components, *Vcan* mRNA levels were the most clearly affected by MIA induction.

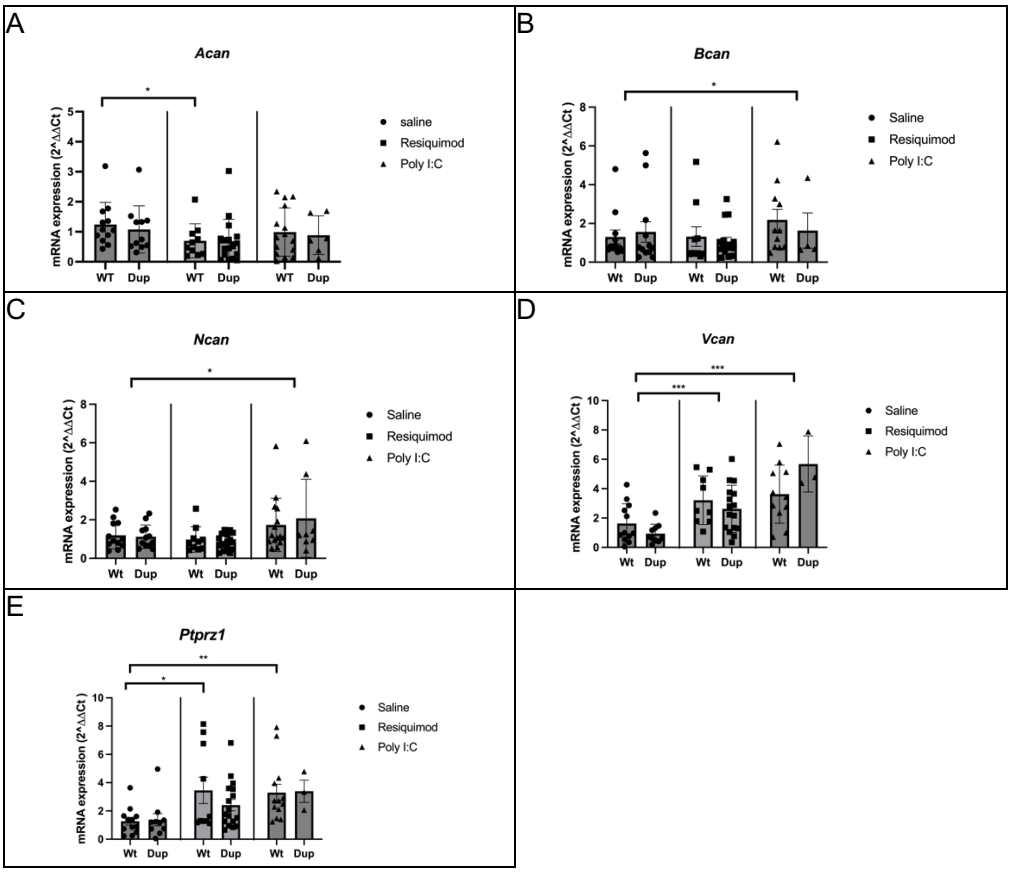

Figure 9.1: mRNA level of CSPG components changes after prenatal maternal vehicle, resiquimod or Poly I:C administration in WT or 16p11.2 duplication offspring mice. Following the administration of vehicle, resiquimod or Poly I:C, altered mRNA levels of CSPG components of PNNs were found in both WT and 16p11.2 dup mice compared to the control (saline) group. A. *Acan* mRNA levels were downregulated by resiquimod administration. B C. The mRNA levels for

Bcan and *Ncan* were upregulated by Poly I:C in both WT and 16p11.2 duplication mice compared to control (saline). E F. The mRNA levels of *Vcan* and *Ptprz1* were upregulated by both resiquimod and Poly I:C administration (Saline: WT=13, 16p11.2 duplication duplication=10; Resiquimod: WT=10, 16p11.2 duplication=17; Poly I:C: WT=16, 16p11.2 duplication=7). The data were normally distributed as assessed with the Kolmogorov-Smirnov test, no outliers were found. The data were analysed by ANOVA followed by Tukey's post-hoc tests, * p<0.05, ** p<0.01, *** p<0.001 MIA effect vs corresponding vehicle group, Tukey's post-hoc tests. The bar graphs show mean ± SEM.

There were no significant alterations of mRNA levels observed in hyaluronan (*Has1*: F (2, 68) =0.07, P =0.936; *Has2*: F(2, 65)=1.72, P =0.189; *Has3*: F (2, 66) =1.29, P=0.284) (Fig 9.2 A-C) and hyaluronan link proteins (*Hapln4*: F (2, 70) =1.16, P =0.321) after either resiquimod or Poly I:C administration (Fig 9.2 D).

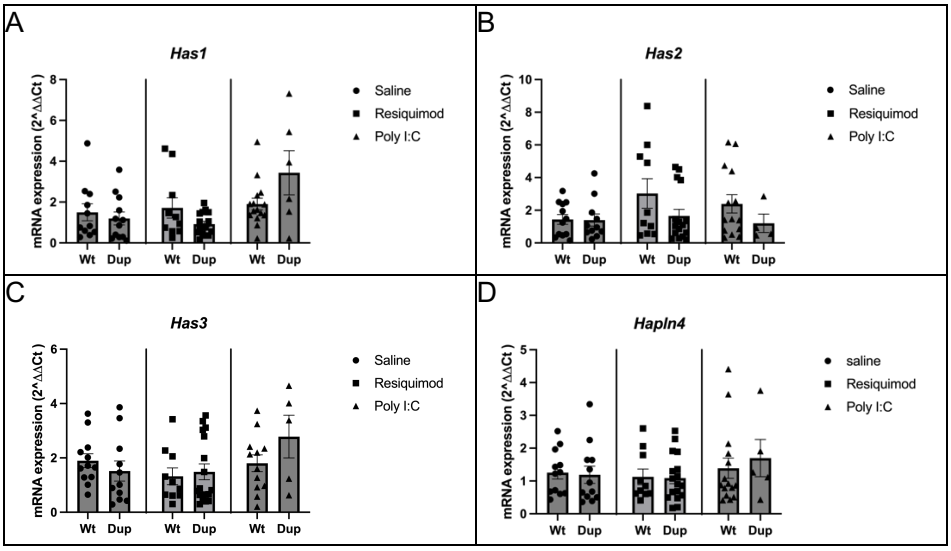

Figure 9.2: mRNA levels of hyaluronan and link protein components after Poly I:C and resiquimoid induction. A-C. the mRNA expression of *Has* components. The results showed that there were no changes of *Has* mRNA levels in either WT or 16p11.2 duplication mice compared to control (saline). D. No changes were detected in *Hapln4* mRNA expression levels after resiquimod or poly I:C treatment in either WT or 16p11.2 duplication mice compared to control (saline) (Saline: WT=13, 16p11.2 duplication=10; Resiquimod: WT=10, 16p11.2 duplication=17; Poly I:C: WT=16, 16p11.2 duplication=7). The data were normally distributed as assessed with the Kolmogorov-Smirnov test no outliers were found. The data were analysed by ANOVA followed by Tukey's post-hoc test. The bar graphs show mean ± SEM.

In terms of *TnR* and *Pv* mRNA expression (Fig 9.3), no changes were observed in mRNA levels of *TnR* after resiquimod or Poly I:C administration (Fig 9.3 A) (F (2, 70) =2.56, p =0.085). Although *Pv* mRNA expression was downregulated tendency following resiquimod administration, the post-hoc test showed it did not reach the significance level (F (2, 71) =3.27, p =0.045; saline vs resiquimod p=0.070 Tukey's post-hoc tests), however, the alterations detected after Poly I:C administration failed to reach the threshold for significance (F (2, 71) =3.27, p =0.696, saline vs poly I:C Tukey's post-hoc tests).

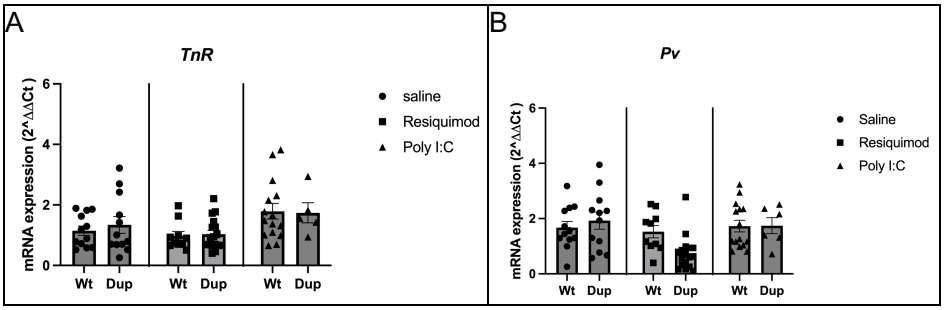

Figure 9.3: mRNA expression of Pv and *TnR* after Poly I:C and resiquimoid induction**.** A. No changes of *TnR* mRNA levels after resiquimod or poly I:C treatment in either WT or 16p11.2 duplicate mice compared to control (saline). B. Resiquimod could reduce the expression of *Pv* in both WT and 16p11.2 Dup mice compared to saline treated group. In addition, the mRNA levels tended to remain the same after Poly I:C treatment (Saline: WT=13, 16p11.2 duplication=10; Resiquimod: WT=10, 16p11.2 duplication=17; Poly I:C: WT=16, 16p11.2 duplication=7). The data were normally distributed as assessed with the Kolmogorov-Smirnov test no outliers were found. The data were analysed by ANOVA followed by Tukey's post-hoc tests. The bar graphs show mean ± SEM.

There were no alterations of mRNA levels detected for *Gad1* (Fig 9.4 A) or *Gad2* (Fig 9.4 B) following MIA induction with either resiquimod or Poly I:C (*Gad1*: F (2, 62) =0.10, P=0.908; *Gad2* F (2, 62) =0.97, P=0.385).

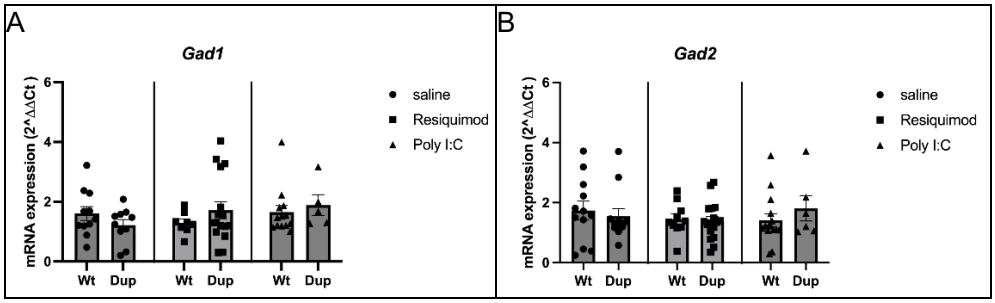

Figure 9.4: Gad1 and Gad2 mRNA expression after resiquimod or Poly I:C treatment. The mRNA levels of both *Gad1* (A) and *Gad2* (B) remained unchanged after resiquimod and Poly I:C treatment in WT and 16p11.2 dup mice (Saline: WT=13, 16p11.2 duplication=10; Resiquimod: WT=10, 16p11.2 duplication=17; Poly I:C: WT=16, 16p11.2 duplication=7). The data was normally distributed as assessed with the Kolmogorov-Smirnov test no outliers were found. The data were analysed by ANOVA with Tukey's post-hoc test. The bar graphs show mean ± SEM.

9.4.2 No differences of PNN components and *Gad* mRNA levels between WT and 16p11.2 duplication mice using littermates as experimental unit

In the condition that the littermates were treated as experimental units, no differences in mRNA levels between WT mice and 16p11.2 duplication mice were observed, before or after MIA induction, in any component measured. For example, no significant differences of mRNA levels between mice genotype were found in all CSPGs components (Fig. 9.1) (*Acan*: F(2, 70)=0.26, P =0.613; *Bcan*: F(2, 66)=1.23, P =0.272; *Ncan*: F(2, 70)=0.59, P =0.447; Vcan: F(2, 61)=1.49, P =0.228; *Ptprz1*: F(2, 64)=8.51, P =0.664). Additionally, no significant differences of mRNA levels between mouse genotype were found in hyaluronan and hyaluronan link protein components (Fig. 9.2) (*Has1*: F (2, 68) =1.35, P =0.249; *Has2*: F (2, 65) =2.42, P =0.126; *Has3*: F (2, 66)

=0.64, P=0.427; *Hapln4*: (F (2, 70) =0.66, P =0.421). *TnR* (F (2, 70) =0.69, P =0.408) and *Pv* (F (2, 71) =0.03, P =0.872); expression levels were not between different mouse genotype in different MIA treatment groups (Fig. 9.3). Moreover, no significant differences were detected in *Gad* components (Fig. 9.4) between the 2 mice genotypes (*Gad1*: F(2, 62)=2.93, P=0.093; *Gad2* F(2, 62)=0.05, P=0.815). Although there was a tendency that *Gad2* was expressed at lower mRNA levels in saline treated 16p11.2 duplication mice, no statistically significant differences were observed.

9.4.3 Alterations of PNNs and *Gad* components after MIA induction using dams as experimental unit

In the condition that the dams were treated as experimental unit, the number of dams in each treatment groups was not adequate for the data analysis (n=2 / group). However, similar tendencies were observed after MIA compared to the results reported from the analysis using littermates as experimental unit. The mRNA levels of CSPG components increased compared to maternal saline (vehicle) exposure after prenatal maternal Poly I:C or resiquimod exposure, except from *Acan*. Among all CSPG components, *Acan* mRNA levels showed a slight tendency to decrease after resiquimod administration but remained unchanged after Poly I:C induction (Fig 9.5 A), and mRNA levels of *Bcan* tended to increase with both Poly I:C and resiquimod administration, and *Ncan* showed a tendency to increase with Poly I:C administration (Fig 9.5 B C), while mRNA levels of *Vcan* and *Ptprz1* reported a trend towards increase with both resiquimod and Poly I:C administration (Fig 9.5 D E).

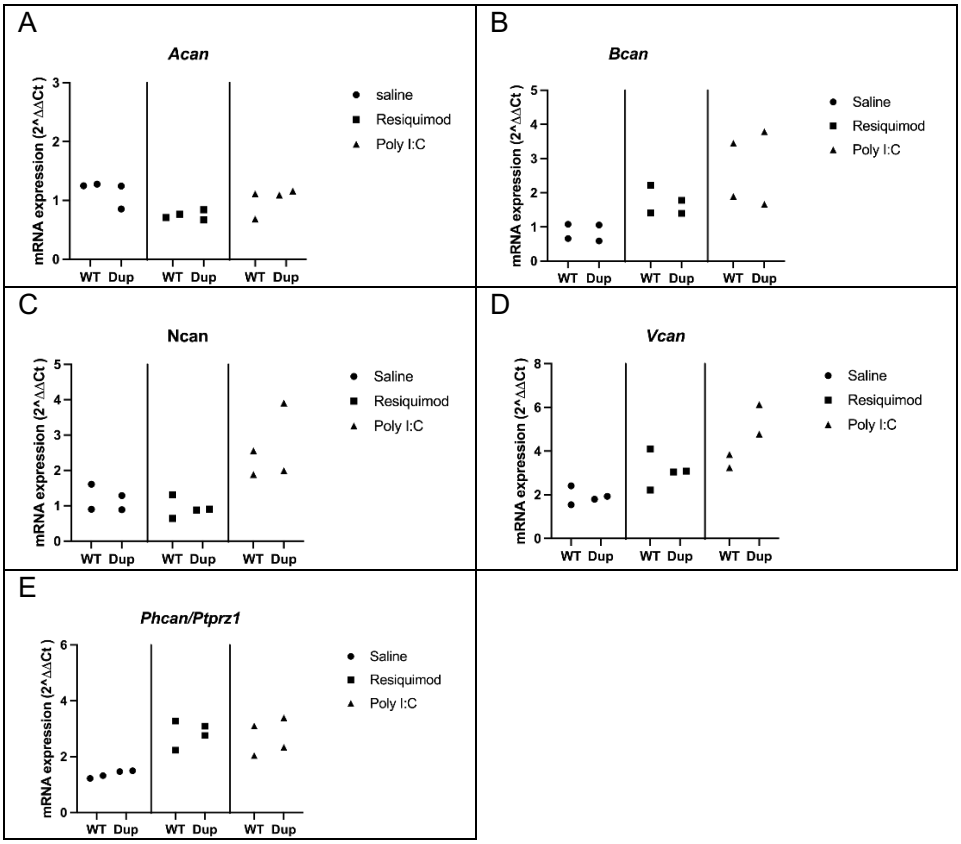

Figure 9.5: mRNA level of CSPG components changes after prenatal maternal vehicle, resiquimod or Poly I:C administration in WT or 16p11.2 duplication offspring mice. Following the administration of vehicle, resiquimod or Poly I:C, altered mRNA levels of CSPG components of PNNs were found in both WT and 16p11.2 dup mice compared to the control (saline) group. A. *Acan* mRNA levels were downregulated by resiquimod administration. B C. The mRNA levels for

Bcan and *Ncan* were upregulated by Poly I:C in both WT and 16p11.2 duplication mice compared to control (saline). E F. The mRNA levels of *Vcan* and *Ptprz1* were upregulated by both resiquimod and Poly I:C administration (Saline: WT: n=2, 16p11.2 duplication: n=2; Resiquimod: WT: n=2, 16p11.2 duplication: n=2; Poly I:C: WT: n=2, 16p11.2 duplication: n=2). Symbols represent the mean values of the littermates for each individual dam.

There were no alteration tendencies of mRNA levels observed in hyaluronan synthase (Fig 9.6 A-C) and hyaluronan link proteins after either resiquimod or Poly I:C administration (Fig 9.6 D).

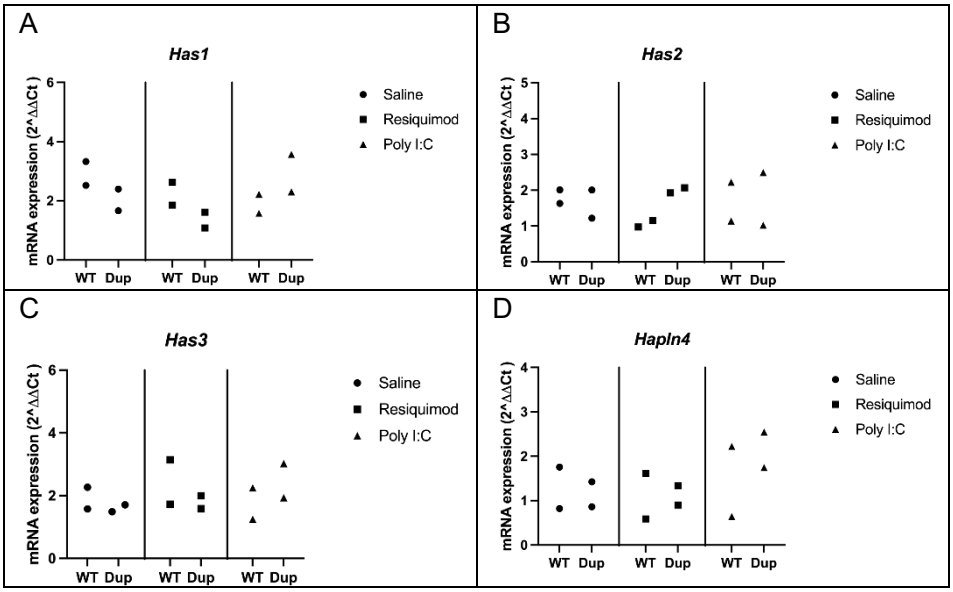

Figure 9.6: mRNA levels of hyaluronan and link protein components after Poly I:C and resiquimoid induction. A-C. the mRNA expression of *Has* components. The results showed that there were no changes of *Has* mRNA levels in either WT or 16p11.2 duplication mice compared to control (saline). D. No changes were detected in *Hapln4* mRNA expression levels after resiquimod or poly I:C treatment in either WT or 16p11.2 duplication mice compared to control (saline). (Saline: WT: n=2, 16p11.2 duplication: n=2; Resiquimod: WT: n=2, 16p11.2 duplication: n=2; Poly I:C: WT: n=2, 16p11.2 duplication: n=2). Symbols represent the mean values of the littermates for each individual dam.

In terms of *TnR* and *Pv* mRNA expression (Fig 9.7), no obvious changes were observed in mRNA levels of *TnR* and *Pv* after resiquimod or Poly I:C administration (Fig 9.7 A B).

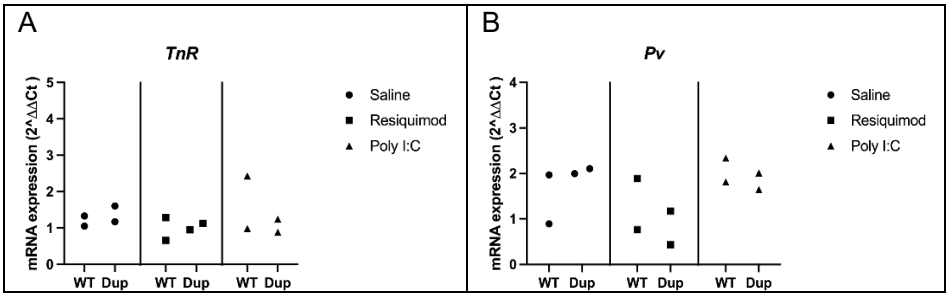

Figure 9.7: mRNA expression of Pv and *TnR* after Poly I:C and resiquimoid induction**.** A. No changes of *TnR* mRNA levels after resiquimod or poly I:C treatment in either WT or 16p11.2 duplicate mice compared to control (saline). B. Resiquimod could reduce the expression of *Pv* in both WT and 16p11.2 Dup mice compared to saline treated group. In addition, the mRNA levels tended to remain the same after Poly I:C treatment. (Saline: WT: n=2, 16p11.2 duplication: n=2;

Resiquimod: WT: n=2, 16p11.2 duplication: n=2; Poly I:C: WT: n=2, 16p11.2 duplication: n=2). Symbols represent the mean values of the littermates for each individual dam.

There were no trends for altered mRNA levels detected for *Gad1* (Fig 9.8 A) or *Gad2* (Fig 9.8 B) following MIA induction with either resiquimod or Poly I:C.

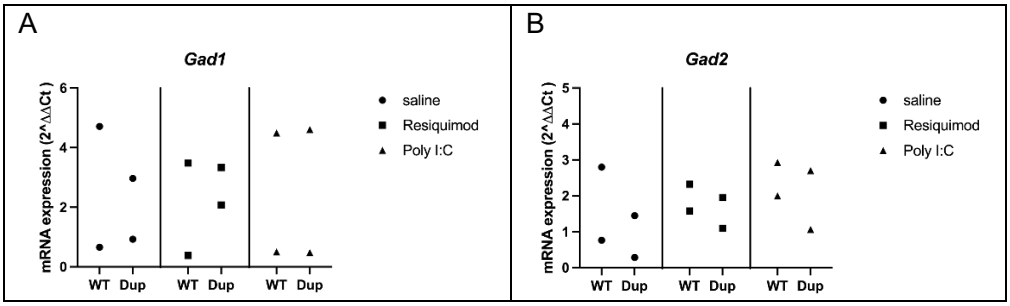

Figure 9.8: Gad1 and Gad2 mRNA expression after resiquimod or Poly I:C treatment. The mRNA levels of both *Gad1* (A) and *Gad2* (B) remained unchanged after resiquimod and Poly I:C treatment in WT and 16p11.2 dup mice (Saline: WT: n=2, 16p11.2 duplication: n=2; Resiquimod: WT: n=2, 16p11.2 duplication: n=2; Poly I:C: WT: n=2, 16p11.2 duplication: n=2). Symbols represent the mean values of the littermates for each individual dam.

9.4.4 No differences of PNN components and *Gad* mRNA levels between WT and 16p11.2 duplication mice using dams as experimental unit

In the condition that the dams were treated as experimental units, similar results were reported, no differences in mRNA levels between WT mice and 16p11.2 duplication mice were detected, before or after MIA induction, in any component measured. For example, no obvious differences of mRNA levels between mouse genotype were found for all the CSPGs components (Fig 9.5). Additionally, no differences of mRNA levels between mouse genotype were found in hyaluronan synthase and hyaluronan link protein components (Fig 9.6). *TnR* and *Pv* expression levels were not altered between different mouse genotype in the different MIA treatment groups (Fig 9.7). Moreover, no differences were detected in *Gad* components (Fig 9.8) between the 2 mouse genotypes.

9.5 Discussion

The current study reported that mRNA levels of CSPG components changed after resiquimod and Poly I:C administration in both 16p11.2 duplicate mice and WT mice. In the condition that the littermates were treated as experimental units, *Acan* and *Pv* mRNA expression were suppressed after resiquimod administration. Conversely, mRNA levels of *Ncan* and *Bcan* were slightly upregulated after by Poly I:C administration. *Vcan* and *Ptprz1* mRNA level mRNA levels were also upregulated after both resiquimod and Poly I:C administration. Similarly, in the condition that the dams were treated as the experimental unit, the results showed that *Acan* mRNA expression were tended to be suppressed after resiquimod administration. On the contrary, mRNA levels of *Ncan* showed a trend to be slightly upregulated after by Poly I:C administration. *Bcan, Vcan* and *Ptprz1* mRNA levels also showed a tendency to be upregulated after both resiquimod and Poly I:C administration. The results suggested that MIA altered PNN component expression, especially CSPG mRNA levels, which might in turn disrupt neuronal activities and neurons' susceptibility to external stimulation during the developmental period. Moreover, the increased alterations of CSPG components, including *Bcan*, *Ncan*, *Vcan* and *Ptprz1* were suggested to further supported the role of CSPGs in immune responses.

The mRNA level of one key component of PNNs, *Acan*, showed a trend to be decreased in the offsprings' brain tissue after resiquimod administration. Similar results were reported by Wegrzyn's et al. (2020) finding that the area of PNNs labelled with *Acan* decreased after Poly I:C exposure in cultured hippocampus neurons.

Conversely, a tendency for *Bcan* expression to be upregulated was detected after Poly I:C induction in the current study, suggesting that *Bcan* could respond to immune stimulation. In previous research, a few studies investigated *Bcan*'s expression with immune activation by drug administration, such as, Poly I:C or LPS. For example, depletion of microglia has been reported to increase the density and intensity of perineuronal nets in several brain regions along with increased expression of peri-synaptic *Bcan* (Basilico et al., 2021; Liu et al., 2021; Strackeljan et al., 2021). This appears to be an opposite effect to that observed here, where the early developmental inflammation elevates *Bcan* expression.

Ncan mRNA levels also tend to increase after Poly I:C induced MIA. The increase might be related to the upregulation of *Ncan* after CNS injury and glial scar (Asher et al., 1999). The glial scar develops after CNS injury, containing astrocytes, oligodendrocytes, microglia and meningeal cells (Fawcett et al., 1999). Li et al (2015) also supported that astrogliosis, a process to activate astrocytes, which was associated with overexpression of *Ncan*. In this case, expression of *Ncan* could be upregulated by production of a glial scar containing microglia. Microglial cells were demonstrated to be activated by MIA (Wegrzyn et al., 2020), which might lead to an increased tendency of *Ncan* expression.

Like *Ncan*, *Ptprz1* mRNA also showed a tendency to be upregulated after MIA induction with both Poly I:C and resiquimod treatment. The upregulation was consistent with a previous study, suggesting increased expression of *Ptprz1* both by early developmental MIA in these experiments, and after CNS injury, with both elevated mRNA levels and protein expression (Mckeon et al., 1999). After injury to cerebral cortex, both *Ncan* and *Ptprz1* were expressed with reactivation of astrocytes (Mckeon et al., 1999). After Poly I:C induction, subtypes of glial cells, including microglia and astrocytes, are activated (He et al., 2021), which could promote the development of *Ncan* and *Ptprz1* resulting in upregulated expression.

In addition to the tendency towards upregulation of *Bcan*, *Ncan* and *Ptprz1*, mRNA levels of *Vcan* also showed a similar tendency with both resiquimod and Poly I:C exposure prenatally. Although there are limited studies examining the influence of immune activation on *Vcan* expression in CNS cells, several studies investigated the association of *Vcan* and Poly I:C treatment in human fibroblasts, reporting consistent results with the current study that mRNA expression and localisation of *Vcan* increased after Poly I:C treatment by reducing *Vcan* degradation (Perigo et al., 2010), and Poly I:C-induced immune stimulation also lead to the accumulation of *Vcan* (Kang et al., 2017). The overall upregulation of *Vcan* might be due to the increases in one of the *Vcan* isoforms, *V1* (Beggah et al., 2002), while other studies reported decreased *Vcan V2* following CNS injury (Tang et al., 2003).

Thus, while the experiments here may be the first to identify altered PNN component gene expression in adult offspring following prenatal MIA, there were still a number of reports in the literature of altered expression of these genes following either acute exposure to infectious agents, or as part of an injury-associated inflammatory response. Growing evidence proved that MIA altered PNN gene expression and disrupted PNN formation and structure in the offspring, however, the specific alterations of PNNs components were less clarified.

The current results supported an effect of MIA on PNN gene expression and further demonstrated that CSPGs were the main components affected by MIA. Consistent studies

illustrated altered CSPGs components following an immune response. Instead of administration of immune stimulants, such as LPS, Poly I:C or resiquimod, most studies tested CSPG expression following diverse types of brain or spinal cord injury. In general, studies found upregulated expression of *Bcan* after cortical and thalamic stab wound (Jaworiski, et al., 1999), *Ncan* after entorhinal cortex lesion and nigrostriatal transection (Haas et al., 1999; Moon et al., 2002), *Vcan* after unilateral cortical lesion (Asher et al., 2002), but downregulated expression of *Acan*.

Among all the CSPG components, *Vcan* was a critical factor regulating and responding to immune stimulation (Wight et al., 2014). The results suggested a larger impact of MIA on *Vcan* mRNA expression compared to most other CSPG components. Although limited studies investigated *Vcan*'s role in immune responses in the CNS, several studies illustrated the accumulation of *Vcan* in fibroblasts at the early stage of human diseases as a part of the immune response. For example, *Vcan* was observed to accumulate in human lung inflammation (Kang et al., 2016) and vascular diseases (Wight, 2018). The exaggerated *Vcan* expression in these diseases was associated with equivalent changes in hyaluronan or hyaluronan link proteins (Kang et al., 2016; Joshua et al., 2020). In the PNN structure, *Vcan* is linked with hyaluronan components; this binding structure might result in an interaction of *Vcan* and hyaluronan while responding to immune stimulation. Indeed, *Vcan* was found to be colocalised with hyaluronan after inflammatory stimulation (Kang et al., 2016; Joshua et al., 2020; Gaucherand et al., 2017), and in a *Vcan-/-* mouse model, no increase in hyaluronan expression was detected with immune stimulation with Poly I:C induction (Kang et al., 2016), which further supported the interaction of *Vcan* and hyaluronan. Hyaluronan was also suggested to be a regulator with both pro- and anti-inflammatory functions. For example, hyaluronan components could activate macrophages (Taylor et al., 2007) and stimulate inflammation-related molecules, such as TNFα and interleukin β (Do et al., 2004). However, whether *Vcan* or hyaluronan could respond to immune activation independently still remains to be clarified. In the current study, only *Vcan* expression was elevated after Poly I:C and resiquimod induction and expression of hyaluronan components remained unchanged, which might suggest the possibility that *Vcan* could respond to immune stimulation independently.

In addition to the changes in PNN component gene expression, mainly CSPGs, no differences were found between WT and 16p11.2 duplicate mice, indicating no interaction of MIA and 16p11.2 duplication genotype variation for schizophrenia. However, altered expression of PNN component genes was sometimes demonstrated in previous studies in rodent schizophrenia models, which was not consistent with the current results. Although the expression of most PNN component genes was not altered, increased *Ncan* expression was detected in adult prefrontal cortical tissue from 16p11.2 mice (Willis et al., 2020). A possible explanation for this discrepancy is that the tissue used in the present study was obtained from substantially older mice, which had been employed previously in a number of behavioural experiments. The increased *Ncan* expression may not endure for a sufficiently long period to be detected in these experiments. Indeed, complex time-dependent effects of prenatal MIA with Poly I:C on WFA staining in offspring brain have been reported, with changes (decreases) at 7 weeks but not 12 weeks of age in amygdala, but conversely decreases at 12 weeks but not 7 weeks in PFC (Paylor et al., 2016). Otherwise, there seems to be a lack of studies of PNN component gene expression in rodent models of aspects of schizophrenia.

Reduced densities and intensities of PNNs, were found in schizophrenia patients in various brain regions, including amygdala, entorhinal cortex and prefrontal cortex (Pantazopoulos, et al., 2010; Mauney et al., 2013). Unlike the reduction of PNNs in schizophrenia, the number of Pv-expressing interneurons in cortical regions and amygdala in schizophrenia subjects was the

same as those in healthy subjects, and the number of PNNs enwrapping Pv-expressing interneurons also remained unchanged (Pantazopoulos et al., 2007, Pantazopoulos et al., 2010), suggesting that reductions of PNNs were not accompanied by Pv neuron loss.

The unchanged *Pv* expression is consistent with the current results that no different expression of *Pv* expression was detected between WT and 16p11.2 duplication mice. CSPGs, as the main structures in PNNs, were also found to be disrupted in schizophrenia subjects. A robust decrease of *Acan* expression was detected with abnormal WFA-labelled PNNs in schizophrenia subjects (Pantazopoulos, et al., 2015). Downregulated expression of *Ncan* and *Vcan* was also suggested in schizophrenia subjects (Pietersen et al., 2014). Notably, various alteration tendencies of *Ptprz1* in schizophrenia subjects were reported previously, with both increased and decreased expression in PFC in patients with schizophrenia (Takahashi et al., 2011; Buxbaum et al., 2008). The study also detected no changes of *Gad1*, hyaluronan and hyaluronan link proteins after MIA induction. However, previous studies suggested *Gad1*, hyaluronan and hyaluronan link proteins tend to decrease in schizophrenia. Reduced mRNA expression and protein levels of *Gad1*/*Gad67* were found in PFC (Veldic et al., 2005; Ruzicka et al., 2007; Tsubomoto et al., 2019), temporal cortex (Impagnatiello et al., 1998) and hippocampus (Heckers et al., 2002).

The unaltered gene expression of PNN components between WT and 16p11.2 duplication mice could possibly be attributed to the divergent expression changes of the molecules in neurons and glial cells. PNN components (especially CSPGs) in glial cells tend to increase, but in neurons, their expression tends to decrease. Therefore, in the 16p11.2 duplication mice model, the total expression of PNNs components might remained unchanged in the whole PFC. Converging evidence suggested a key role for astrocytes in regulating ECM structures, including synthesising CSPGs components and building PNNs structure (Faissner et al., 2010, Gundelfinger et al., 2010). CSPG molecule expression was reported to increase dramatically in glial cells in amygdala and entorhinal cortex in patients with schizophrenia (Pantazopoulos et al., 2010), which is in line with the results reported from Berrata (2012) that the expression levels of the main 5 molecules in CSPGs, including *Acan*, *Bcan*, *Ncan*, *Vcan* and *Ptprz1*, were upregulated by 1.3 to 2.3 fold in amygdala in schizophrenia subjects. Co-localisation of WFA-labelled CSPGs and glial fibrillary acidic protein (GFAP) was exclusively detected in human amygdala (Pantazopoulos et al., 2008), which further supported the role of astrocytes in CSPG expression. Furthermore, the increase of CSPGs in glial cells was accompanied by the reduction of CSPG-labelled PNNs in schizophrenia patients (Pantazopoulos et al., 2010). Therefore, no differences of PNNs components' expression detected between genotypes in the current study could be explained by increased expression of CSPGs in glial cells and decreased expression in neurons in 16p11.2 duplication mice, resulting in unchanged expression compared to WT mice.

The current study also compared the inflammation effect of ds viruses and ss viruses. Except for *Acan* and *Pv* expression levels, which were only reduced by the ss virus infection mimetic resiquimod, the other CSPGs were upregulated by ds virus infection mimetic Poly I:C alone (*Bcan*, *Ncan*), or by both agents, which illustrated that the consequences of different types of immune infections could vary among different components. Therefore, the results raised a possibility that PNN structure and PNN-covered *Pv* GABAergic interneurons could be disrupted and attenuated by stimulating TLR7/8, whereas glial cells were activated by *TLR3/4* stimulation resulting in increased expression levels of *Bcan*, *Ncan Vcan* and *Ptprz1*. This possibility could be supported by previous research that ss-virus infection activating *TLR7/8* only leads to a short duration of immune response, such as up-regulation of proinflammatory cytokines and chemokines or astrocyte activation compared to *TLR3/4* stimulation (Niranjan er al., 2008).

In animal studies, how to determine the experimental unit optimally is essential, particularly when

studying animals with different genotypes. Since littermates from the same dam or litter experience the same prenatal environment and similar postnatal circumstances, they tend to share more similarities than animals from separate litters. The similarities in littermates imply that litter-related factors can substantially impact the results of experiments. If these litter effects are not considered, it may result in conclusions with low accuracy.

Thus, following the data analysis with littermates as experimental unit, the current study then averaged the data in different littermates from the same dam to avoid the similarities between littermates potentially confounding the analysis. However, the statistical analysis was then not able to be conducted due to the low sample size (only 2 dams of each genotype per treatment group). Thus, in future studies, to confirm the effect of MIA on PNN components with the support of statistical analysis, more dams (n=8 of each genotype per treatment group, based on the power analysis and the previous lab experience) need to be housed and treated with MIA using Poly I:C or resiquimod to provide an adequate sample size and address a more statistically powerful result.

Although enough sample size and statistical power could be provided using littermates as experimental unit, it could include the similarities across littermates from the same dam or litter. Thus, apart from averaging the data of the littermates, to make the best use of the littermates effectively, several strategies could be employed in the future. For example, selecting a random animal from each litter when animals reached the adulthood, and at the relevant endpoints after immune activation, when monitoring increased cytokine levels and immune cell populations. Additionally, littermates could be housed separately to avoid confounding factors related to shared postnatal environment.

To conclude, the results suggested that both Poly I:C and resiquimod exposure prenatally can contribute to PNN disturbances in PFC in adulthood, in both WT and 16p11.2 duplication mice. These results further supported the MIA effect on PNNs with specific alterations on mainly CSPG components. The reduced expression of one of the markers of PNNs (*Acan*) and *Pv*-expressing neurons after prenatal resiquimod exposure shows similarities with alterations in schizophrenia patients observed in previous studies, which identified PNN and *Pv* expression abnormalities as potential contributors in PFC to schizophrenia. Unfortunately, tissue was not available to compare directly the effects of prenatal MIA on PNN component gene expression with effects on PNN structure, as assessed by WFA staining. However, the functional changes of PNNs and *Pv*-expressing neurons need to be further clarified in future studies to establish a better understanding of functional disturbances in the pathology of schizophrenia.

Chapter10

General discussion

10.1 Major and novel findings

The general aim of the project was to examine how GCs influence the expression of PNN components and the formation of PNNs, and whether the altered expression of PNN components is related to the changes observed in schizophrenia model animals. Whilst some of the results were negative, the current study still showed many novel findings and insights into several areas. The general results were summarised in the following Table 10.1 and 10.2:

GCs effects on PNN components and formation						
	GR (rapid non-genomic)	GR (slow genomic)	Non-GR (rapid non-genomic)	Non-GR (slow genomic)	GPCR56/97 (rapid non-genomic)	No specific action detected
Acan						
Bcan						
Ncan					↓ (7 DIV)	
Vcan						↓ (14 DIV)
Phcan / Ptprz1						
Has1						↑ (21 DIV)
Has2						
Has3	↓ (7 DIV)					
Hapln4						↓ (14 DIV)
TnR						↓ (7 DIV 4h) ↑ (7 DIV 24h)
Pv				↓ (21 DIV)		
Gad1						↓ (14 DIV)
Gad2						
Length		↓ (14 DIV)	↓ (21 DIV)	↓ (21 DIV)		
Intensity		↑ (14 DIV)		↑ (21 DIV, with low dose HCA) ↓ (21 DIV, with high dose HCA)		
Number						

Table 10.1: Summary of the effect of GCs on PNN components and formation with different actions: elevated GCs suppressed expression of *Ncan* through GPCR56/97-mediated, and suppress *Has3* through GR-mediated pathways in a rapid non-genomic action; elevated GCs levels decreased length of PNN covering dendrites by GR-mediation and non-GR-mediated pathways in both genomic and non-genomic actions.

MIA effects on PNN components and relationship to schizophrenia		
	MIA effect	Differences between WT and 16p11.2 Dup. mice
Acan	↓	—
Bcan	↑	—
Ncan	↑	—
Vcan	↑	—
Phcan/Ptprz1	↑	—
Has1	—	—
Has2	—	—
Has3	—	—
Hapln4	—	—
TnR	—	—
Pv	—	—
Gad1	—	—
Gad2	—	—

Table 10.2: Summary of the effect of MIA on PNN components and the relationship to schizophrenia: after MIA induction, CSPGs showed obvious alterations, with increased *Bcan*, *Ncan*, *Vcan* and *Ptprz1* mRNA levels and decreased *Acan* mRNA levels.

10.1.1 GC exposure led to altered expression of PNN components in cultured cells via genomic and non-genomic pathways

The major and novel findings in Chapter3 reported initial significant reductions of several PNN components in cultured cortical neurons with either rapid or long-term GC exposure, including reduced mRNA expression of *Acan*, *Has1*, *Has3, TnR* and *Ncan* at 7 DIV, *Vcan* and *Hapln4* at 14 DIV, and Pv at 21 DIV; conversely, increased expression of *Has1* was observed at 7 DIV. Among the downregulation effects, rapid suppressive effects were found in *Acan* and *Has1* with reversal by mifepristone, suggesting a rapid non-genomic GR-mediated effect, but the rapid suppression of *Ncan*, *Has3* and *TnR* at 7 DIV, *Vcan* and *Hapln4* at 14 DIV were not reversed by mifepristone, indicating a rapid non-genomic and non-GR mediated effect. Moreover, the downregulation of Pv expression at 21 DIV was detected after long-term GC exposure with no overall mifepristone effect, suggesting a slow non-GR mediated effect. However, a consistent effect on protein expression was not observed, although in some cases (e.g. *Has3*, *TnR*), an effect of mifepristone was detected, which further indicated the mediation of GRs after short-term exposure to GCs.

The downregulation of CSPG components, including *Acan*, *Bcan, Ncan* and *Vcan* by stress-related hormones was also demonstrated by a previous study. As discussed in Chapter3, *Acan* and *Vcan* mRNA levels were decreased after dexamethasone induction (Strokotova et al. 2023; McRae et al., 2017), overexpression of CRF responding to stress in mice was proved to suppress the extracellular matrix formation, including *Bcan* mRNA expression, indicating that elevated stress could reduce *Bcan* expression (Peeters et al., 2004); Ncan density and mRNA levels were shown to reduce with methylprednisolone administration (Liu et al., 2008). The current study further confirmed the suppressive effect of stress hormones, specifically, GCs, on the expression of CSPG components with a short-time exposure. The suppressive effect of corticosterone on CSPGs was observed in mice with *in vivo* administration, while the current

study confirmed reduced expression using mouse cultured cortical neurons with GC exposure, which likely mediates a more direct impact of external stressors on *Bcan* expression.

Similar downregulation of *TnR* and *Has3* expression were also detected after GC exposure. Unlike *Bcan*, the expression of *TnR* and *Has3* were not largely investigated by previous studies in brain regions. However, as discussed in Chapter 3, equivalent studies on hyaluronan components in human peripheral cells have been conducted, suggesting GCs could inhibit the induction of mRNA accumulation of all genes encoding hyaluronan synthases. *HAS3* expression was also downregulated by GCs, the reduction all occurring within a few hours (Stuhlmeier & Pollaschek, 2004; Galgoczi et al., 2022). Despite the fact that the studies were conducted with fibroblasts and keratinocytes from human patients with diseases that need to be treated with GCs, the suppressive effect of GCs on *Has3* was consistent with the current findings. Therefore, the reduced expression of *Has3* in mice cortical cultured neurons was quite convincing.

Moreover, no previous studies reported the regulation by GCs of *TnR* expression, but the rapidity of the effect is consistent with the rapid recycling mechanisms of *TnR* in neurons, with decreased expression of labelled molecules within 4-6 hours (Dankovich et al., 2021). As a GRE is present in the *TnR* promoter region, an effect of GCs via genomic actions through the GR is likely (Chiovaro et al., 2015). However, this illustrates the complexity of the GC actions that we have identified. The suppressive effect of elevating HCA concentrations at 7 DIV was still observed in the presence of mifepristone, indicating a non-GR mechanism of action. This was not replicated by collagen3, suggesting an action also independent of GPR56/97. However, mifepristone alone decreased *TnR* mRNA levels, while increasing *TnR* protein levels, suggesting that basal GCs in the culture medium (equivalent to basal physiological levels, as in a non-stressed condition) are elevating *TnR* mRNA while suppressing *TnR* protein expression. The functional significance of this complex control is unclear. This regulation was only observed at 7 DIV, and so presumably contributes specifically to the development of the PNNs. It has been proposed that mRNA expression is equivalent to a permissive switch, so when mRNA is present at significant levels, protein expression can then be modified rapidly when required, via fine-tuning (Vogel and Marcotte, 2012).

In addition to the suppressive effect, an increased expression of *Has1* was detected at 21 DIV, which was in line with the finding that Has1 developed around 20 DIV, usually accompanied with a dramatic increased expression during this period (Fowke et al., 2017). Hence, although there might be downregulation effect of GCs, an increases tendency of Has1 could be still observed.

Further experiments investigated the specific rapid non-genomic mediated pathways that GCs affecting PNNs expression. However, in Chapter 4 and 5, the results showed the altered expression was in general not mediated through MR or GPCR located on cell membranes, or through the GMD pathways. The single exception to this was the rapid suppression of *Ncan* expression at 7 DIV, where collagen 3 appeared to reproduce the actions of HCA. This confirms the impression that multiple mechanisms are operating in the GCs control of gene expression at this key point in neuronal development.

The possibility that the rapid, non-GR-mediated decreases in *Bcan*, *Vcan* and *Hapln4* mRNAs might be mediated by a post-transcriptional action was considered, especially in the context of the process of GMD (Chapter 6). However, no evidence was obtained in favour of this hypothesis. Thus, while it is clear that the regulation of PNN gene expression by GCs is complex and multi-layered, the precise mechanisms involved in many cases remain unclear.

In addition to the rapid suppressive effect on *Bcan*, *Vcan, TnR* and *Hapln4*, Pv expression was shown to decrease with long-term GC exposure at 21 DIV. The reduction was replicated in a

later experiment, and the effect was still observed in the presence of mifepristone, indicating that the GCs did not downregulate the expression of Pv through GRs. The complexity of GC effects is further illustrated by the fact that mifepristone alone elevated Pv expression at 7 DIV, implying a suppression of Pv mRNA levels by basal GCs, via the GR. Consistent previous results were reported, suggesting reduced mRNA levels of Pv with corticosterone exposure (Hu et al., 2010; Banasr et al., 2017). These studies were conducted with chronic-stressed mice (Hu et al., 2010) and primary cortical neuronal culture at 10 DIV (Banasr et al., 2017), although the latter study used very high corticosterone concentrations (in the same culture medium used here) and reported an effect not reaching statistical significance. Thus, the suppression of Pv expression by GCs in the current study is broadly consistent with previous work.

Furthermore, altered protein expression of some PNN components was detected where mRNA levels remained unchanged, including *Has2* and *Gad2*/*Gad65*. The discrepant protein and mRNA alterations were postulated to be due to elevated proteasomal activities. In this case, the components with no altered mRNA levels could still show reduced protein levels. In Chapter 7, the current results reported that the GCs could inhibit the chymotrypsin-like proteasomal activity, raising the possibility that stress might rapidly increase the levels of some proteins through this action, but also indicating that the altered *Has2* and *Gad2/Gad67* protein levels were not mediated by proteasome activation. Hence, the inconsistent protein and mRNA levels could be attributed to the shortcomings of Western Blot as a technique, which were presented in section 10.3, or to some as yet uncharacterized post-transcriptional action of GCs.

The current study investigated the effect of GCs on the gene expression of PNN components. Based on was found to be altered by chronic stress induction lasting for several days, or long-term corticosterone administration lasting for several days or months (McRae et al., 2017; Strokotova et al., 2024; Yu et al., 2020). Hence, the starting expectation of the current study was that expression of a small number of PNN component genes might be affected directly by GCs, and that these would be mainly long-term genomic actions in mechanism. However, the results reported a large number of changes, with most of the PNN components affecting by GCs, and the mechanisms of the effects were a mixture of genomic, GR-mediated and non-genomic, non-GR-mediated, transcriptional and post-transcriptional.

Among the expression alterations caused by GC treatment at different neuronal development stages, the majority of changes were at 7 DIV, fewer at 14 DIV and almost none at 21 DIV. As PNNs develop during the critical period and are completely formed at the closure of critical period, being involving in the reduction of neuronal plasticity at the end of critical period (Pizzorusso et al., 2002; McRae et al., 2007; McRae and Porter, 2012), more expression changes at 7 DIV suggests that GC regulation of PNN components becomes less important as the critical period for plasticity passes. In the cultured neurons, PNNs and their components start to develop at 0 DIV and become fully structured with a net-like structure around 21 DIV (Geisser et al, 2013; Dityatev et al, 2006; Fowke et al., 2017). At the development stages of PNN (7 DIV/14 DIV), the coordination of several PNN components is required to complete the formation processes, which needs fine tuning of the components. In this case, the PNN is vulnerable to external stimulation (GCs) during development, but at 21 DIV, the fully formed PNN is more stable and might be less affected by GCs.

The current results also reported a majority of downregulated expression of PNN components, either by basal GCs in medium or by additional GC supplementation. The downregulation effect of basal GCs in culturing medium was observed on *TnR* and *Ncan* at 7 DIV, and *Acan*, *Bcan*, *Vcan* at 14 DIV, with decreased expression after mifepristone treatment. This indicated that the basal GCs in the medium started to suppress the Ncan expression at 7 DIV and other CSPG

components at 14 DIV, illustrating that, the main part of PNN formation occurred around 14 DIV in the cultured neurons, which was in line with the previous finding that PNN could be visible and detected around 10 DIV by WFA- or *Acan*-labelling (Miyata et al., 2005).

In conclusion, the current study found rapid non-GR-mediated effects of GCs on the mRNA expression of *Bcan*, *Vcan, Has3* and *TnR* at 14 DIV, and of *TnR* at 7 DIV; rapid GR-mediated effects of GCs on the mRNA expression of *Acan*, *Has1-3* and *Gad1* at 7 DIV, and slower non-GR-mediated effects of GCs on the mRNA expression of Pv, with general downregulation of the expression. These data are for the most part completely novel, although in some cases they are consistent either with effects reported in peripheral cell types, or, for PV, with related previous findings in neurons. Therefore, the current results further confirmed the suppressive effect of external stressors or overexpression of stress-related hormones responding to stressful stimuli on several PNN components and Pv-expressing interneurons.

10.1.2 GCs altered the overall formation of PNNs in cortical cultured neurons

In chapter 6, the current results demonstrated decreased length of dendrites covered by PNNs at both 14 and 21 DIV after 24h GC exposure, and the reductions were replicated in the following experiments with the presence of mifepristone, indicating the GCs could inhibit and suppress PNN morphology, especially the length of PNNs covered dendrites. The results also reported decreased intensity of PNNs covering dendrites at 21 DIV with long-term GCs exposure, which was mediated by GRs.

No previous results were found to examine the direct effect of stress or stress-related hormones on the length of PNNs covering cell dendrites. However, similar decreased length of PNNs around dendrites was observed in mice with *TnR* KO (Weber et al., 1991; Morawski et al. 2014).

Although the results reported a suppressive effect of GCs on the PNN covering neuronal dendrites, the changes in PNN structure at 14 and 21 DIV were not apparently caused by altered expression of those PNN components which were thought to most profoundly affect PNN structure, including, *Acan*, *Ptprz1*, *Hapln4* and *TnR* (Giamanco et al., 2010; Suttkus et al.,2014; Eill et al., 2019; Weber et al., 1991; Morawski et al. 2014), as no corresponding mRNA changes were detected after GC treatment at 14 and 21 DIV in previous results presented in Chapter3. Although *Bcan* expression was suppressed by GCs at 14 DIV, the disruption of *Bcan* reportedly has little effect on WFA-labelled PNN formation (Suttkus et al., 2014).

However, at 21 DIV, a dramatic increased expression of Has1 was observed after GC treatment in Chapter 3, which might be related to the dramatic development of *Has1* during this period (Fowke et al., 2017). As discussed in Chapter 6, PNN structural formation and expression is activity-dependent during development and adulthood (Dityatev et al., 2007; Devienne et al., 2021). Similarly, *Has1* expression is also activity-dependent, with increased *Has1* expression found after inhibiting synaptic activities by blocking AP (Willis et al., 2022). GCs were demonstrated to have a profound effect on neuronal activity, such as LTP and AP (Pavlides et al., 2002; Yuen et al., 2009; Whitehead et al., 2013). Thus, in the current study, it is likely that increased activity-dependent *Has1* expression after GC treatment is correlated with WFA-labelled PNN formation, further suggesting the inhibition of synaptic activity at 21 DIV by GCs increases *Has1* expression and suppresses PNN formation (Willis et al., 2022; Dityatev et al., 2007; Devienne et al., 2021).

In addition to the disruption of *Has1*, another possibility is that the length of PNNs surrounding dendrites is due to cell dendritic disruption caused by external stressful stimuli. As PNNs were

suggested to be dependent on neural activity, impaired neuronal dendrites could influence the length of surrounded PNNs. Several previous studies illustrated the shortening of neuronal dendrites in mouse cortex and hippocampus after exposure to chronic or restraint stress (Watanabe et al., 1992; Eiland et al., 2012; Pawley et al., 2020). With the decreased branching of neuronal dendrites present after stress stimuli, the length of dendrites surrounded PNNs could potentially also be observed.

In addition to length of PNNs, the intensity or intensity of PNNs was reduced at 21 DIV with long-term GC exposure. Whether external stress or stress hormone release downregulates PNNs intensity or intensity remains controversial. In PFC, hippocampus or amygdala, increased PNN staining intensities were detected in rodents (Murthy et al., 2019; Guadagno et al. 2020; Gildawei et al., 2020; Riga et al., 2017); while reduced intensities of WFA-labelled PNNs were also found in chronically stressed rodents (Ueno et al., 2016; Gomes et al, 2019). Despite the current study observing robust reduction of PNNs intensity by GCs at 21 DIV in cultured cortical neurons from mice, increased PNN intensity was also detected with GCs exposure, but the increase was not replicated in the following mifepristone experiments. Thus, the downregulating effect of GCs on intensity of PNN staining by WFA was the significant novel finding.

The current study was the first to document altered PNN morphology regulated directly by GCs, suggesting that the over exposure to external stressors or over-release of stress hormones, such as, GCs, could have a direct negative effect on PNN morphology, presenting with reduced length and compromised structure (reduced strength of staining by WFA) surrounding dendrites.

10.1.3 MIA resulted in altered expression of PNNs components in PFC related to schizophrenia

In Chapter 8 and 9, the results reported the general distribution of PNNs throughout the mouse brain regions and demonstrated the alterations of specific PNN components in a schizophrenia mouse model incorporating genetic and environmental risk components.

In Chapter 8, the study demonstrated the distribution of PNNs surrounding Pv-expressing neurons in layer2/3 and 4/5 cortex regions, and compared to cortical regions, a smaller proportion of PNNs surrounding Pv-expressing GABAergic neurons was detected in hippocampus. Similar results were also reported by previous studies, illustrating PNNs expressed mostly in layer 2/3 and layer 4/5 of PFC surrounding Pv-expressing neurons (Nowicka et al., 2009; Sultana et al., 2021), but a lower percentage of PNNs covering td-tomato expressed GABAergic neurons in hippocampus (Yamada and Jinno, 2013; Klimczak et al., 2021). As PNNs provide several supports for cellular functions, such as neural or synaptic plasticity, synaptic transmission and connections, regulating axonal growth and protecting neurons from being damaged by external stimuli (Hensch, 2005; Frischknecht et al., 2009; Lensjø et al., 2017; Celio and Blumcke, 1994; Pesheva et al., 1993; Cabungcal et al., 2013), the distribution of PNNs located in cortical areas suggested a critical role of PNNs involved in and maintained several cortical functions, such as, attention, memory, language processing and comprehension (Neulinger et al., 2016; Flinker et al., 2015).

Among all cortical regions, PFC was demonstrated to play a critical role in several cognitive and executive functions, including attention, memory, planning and controlling goal-directed behaviours, and the lateral part of PFC was shown to be interconnected to motor and sensory cortex, further suggesting sensory learning and motor behavioural roles of PFC (Snyder et al., 2015; McTeague et al., 2016; Watanabe et al., 1990; Parker et al., 1998). In addition, in schizophrenia patients or animal models, impaired neuroanatomy, cellular expression and

connectivity, and neurotransmission were detected, accompanied by alterations in various cognitive functions and motor behaviours (Alekseichuk et al., 2016; Guan et al., 2022; Volk et al., 2000; Prasanna and Tadi, 2023; Artiges et al., 2000; Pinkham et al., 2003). The disrupted cognitive and motor behaviours were defined as critical clinical features in schizophrenia patients. Hence, PNN contributions in PFC might be a critical factor to maintain major cognitive and motor functions, and disrupted PNN expression in PFC might also be considered as a factor influencing schizophrenia.

Environmental stressors, including postnatal and prenatal stressful events and infections, are risk factors involved in the aetiology of schizophrenia, and whether prenatal external stress or infection altered PNN expression in PFC, in relation to the onset of schizophrenia, remained to be discovered. Therefore, in Chapter 9, alterations of PNN component expression induced by prenatal MIA, combined with a genetic risk factor, in mouse PFC were examined. The intention was to then compare these results with the effects of prenatal maternal GC administration, using maternal HCA doses shown in the literature to elevate foetal GC levels. However, a series of problems and delays were encountered, most prominently the loss of a number of litters, from both vehicle and HCA-injected dams. As a result, it was unfortunately not possible to complete these studies.

The study in Chapter 9 used 2 kinds of experimental unit, one is using littermates which contains adequate sample size for the statistical analysis; and another is using dams as experimental unit to avoid the similarities of the littermates from the same dam, but contains low sample size so that the statistical analysis was not able to perform. The results reported from the 2 different experimental conditions showed similar results. The results suggested a downregulated trendency of *Acan* mRNA expression after resiquimod administration. Conversely, upregulated tendency of *Ncan* and *Bcan* expression were detected after Poly I:C administration. *Vcan* and *Ptprz1* expression were also showed a trend to be upregulated after both resiquimod and Poly I:C administration. However, the alterations tended to be evident in both WT and 16p11.2 DUP mice, indicating prenatal MIA affected the CSPGs and Pv expression in PFC, but the alterations were not particularly impacted by the genotype.

As discussed in Chapter 9, a similar altered tendency was reported in previous studies with MIA exposure using prenatal Poly I:C and LPS administration. However, the initial results in Chapter 3 demonstrated the external stress exposure tend to suppress the expression of PNNs components and Pv-expressing interneurons, but the current results reported upregulated expression of *Bcan*, *Ncan*, *Vcan*, and *Ptprz1* after MIA exposure. The inconsistency might be attributed to the different neuronal types, and different mechanisms in stress mediation as opposed to infection, in these 2 studies. The effect of stress on PNN expression in Chapter 3 was conducted with primary neuronal culture which mainly contained neurons; while in Chapter 9, the expression of PNN was detected in mice brain tissues with all types of neurons, including neurons and glial cells. Converging evidence and current results consistently illustrating that exposure to stress with over-release of stress hormones suppressed the expression of PNN components in both cultured neurons and rodent brain tissues (Strokotova et al., 2023; Peeters et al., 2004; Liu et al., 2008; McRae et al., 2017). Despite the reduced PNN expression detected in rodent experiments, the specific cell types were not distinguished, with decreased PNN expression probably occurring in not only neurons, but also glial cells. In this case, the method of external stress induction was considered. In Chapter 3, over-expression of stress hormones, GCs, was used to mimic the stress exposure; in Chapter 9, MIA was used. Glial cells will respond to immune infections, as glial cells, including microglia and astrocytes, are activated after MIA (He et al., 2021). As mentioned in Chapter 1.1, PNN components were reported to

originate from both neurons and glial cells. Thus, with activation of glial cells after MIA exposure, PNN component expression could be increased.

Additionally, similar alterations of CSPG component expression were also observed in schizophrenia patients. In schizophrenia patients, decreased mRNA levels of *ACAN* were reported in cerebral cortex (Pietersen et al., 2014), up-regulated *BCAN and NCAN* expression were found across brain regions (Pantazopoulos et al., 2021), and increased *PTPRZ1* expression was also found in PFC (Takahashi et al., 2011). The changes of CSPG components were largely consistent with the findings reported after MIA. Thus, it is likely that MIA might be associated with the onset of schizophrenia by altering CSPGs expression in cortical regions, with increased *BCAN*, *NCAN* and *PTPRZ1* expression, and reduced *ACAN* expression.

The current project firstly reported the suppressive effect of stress, specifically, GCs, on the expression and morphology of PNNs in cultured neurons, though both genomic and non-genomic pathways. Furthermore, in animal experiments, PNN gene expression in PFC was also demonstrated to be altered by MIA. However, the altered expression of PNN genes induced by MIA was not affected by the genetic manipulation in the schizophrenia mouse model. Therefore, the results suggested that, in relation to schizophrenia, PNN dysfunction may be more related to the mechanisms of environmental risk than to those of genetic risk.

10.2 Significance and implications of the study

The current experiments were significant because the suppressive effect of GCs on specific PNN components *in vitro* and *in vivo* could be beneficial to understand the molecular mechanisms of stress, which could be contribute to the molecular pathways of the aetiology of various stress-affected diseases, such as, schizophrenia, depression and anxiety. Combined with previous findings, the disruption of PNN components or Pv-expressing GABAergic interneurons could result in impaired cellular or neurotransmission functions which could be related to clinical features of schizophrenia. For example, abnormal gamma oscillations are found in schizophrenia patients (Spencer et al., 2009; Cho et al et al., 2006; Haenschel et al., 2009), and PNNs help maintain gamma oscillations by regulating AMPA glutamate receptor diffusion (Frischknecht et al., 2009). Moreover, various PNN components interact with AMPARs, including *Bcan* and Hyaluronan (Vedunova et al., 2013; Favuzzi et al., 2017). Furthermore, gamma oscillations are dependent on the plasticity of Pv-expressing interneurons, requiring calcium-permeable AMPARs (Hadler et al., 2024); the plasticity of Pv-expressing interneurons is regulated by PNNs. Thus, abnormal Pv-expressing neurons together with PNN expression, specifically, reduced expression of *Bcan* induced by external stressors could lead to abnormal gamma oscillations mediated by AMPARs, which might contribute to the impaired gamma oscillations in relation to schizophrenia.

In addition to regulating and maintaining gamma oscillations, PNNs also function in synaptic pruning, promoting dendrite growth and regulating dendritic spines (Tran et al., 2009; Shelly et al., 2011), and disrupted synaptic pruning and dendritic spines are observed in schizophrenia individuals (Bitanihirwe et al., 2016). As illustrated in Chapter 6, the length of PNNs covering dendrites was decreased by over-exposure to stress hormone (GCs), and the disturbed PNN formation surrounding cell dendrites induced by stress might result in inhibition of dendrite growth and spines, and in turn lead to reduced synaptic connections. Hence, disturbed PNN formation around cell dendrites might contribute to the suppressed dendritic growth and synaptic dysfunctions in schizophrenia.

Furthermore, the novel findings of altered expression of PNN components by GCs may have implications for future findings to test novel pharmacological and molecular approach therapies, in diseases which needed to be treated by corticosteroids. Supressed CSPG expression could also be a novel therapy in various diseases.

Previous findings have investigated novel approaches to treat various diseases by suppression of PNNs or PNN components. As CSPGs were shown to inhibit axonal growth (Tan et al., 2006; Bradbury and Carter, 2011), degrading CSPGs enzymically could promote axonal or neurite growth and promote axonal recovery after CNS injury. For example, several studies targeted the potential recovery strategy after spinal cord injury using enzymically removal of CSPGs, accompanied with axonal regeneration (Bradbury et al. 2002; Wang et al. 2011; Azizi et al. 2020). Moreover, removal of CSPGs in the early stages of AD led to increased neural plasticity, and could delay occurrence of the cognitive impairments (Howell et al., 2015). In the current study, CSPG expression was reported to be decreased by GCs, thus, it could be suggested that suppression of CSPGs by GCs could be characterised as a therapeutic target for CNS or spinal cord injury and neurobiological disorders, such as, AD, by stabilising the synaptic structure and promoting axonal genesis. However, our results could also be interpreted as suggesting that GC effects on CSPG expression are only observed early in development.

The current findings also confirmed that GCs could suppress chymotrypsin-like proteasomal activities, suggesting over-exposure to external stress might also lead to impaired function of protein degradation by proteasome activities with accumulation of waste, ubiquitinated and oxidised proteins. Inhibition of proteasome activities is consistently demonstrated in schizophrenia and neurodegenerative diseases, including, Alzheimer's, Parkinson's and Huntingdon's diseases (Scott and Meador-Woodruff, 2019; reviewed in Davidson and Pickering, 2023). The contribution of dysfunctional proteasome activities to the brain disorders suggests that external stress could increase the risk of schizophrenia not only by suppressing PNN components, but also by inhibiting proteasome activities, which might be considered as a new stress-related aetiology of schizophrenia.

The last significance and implication of the current results is associated with the diagnosis of PNNs in schizophrenia and other brain disorders. Although no alterations were found in PNN expression from the schizophrenia-related genetic mutation in mice after MIA, the lack of change might be due to the limitations of the experiments presented in Chapter 9, and consistent previous results illustrated reduced expression of PNNs and their components in schizophrenia patients (Steullet et al., 2017; Lodge et al., 2009; Enwright et al., 2016; Hashimoto et al., 2013). Stress, as an important risk factor of schizophrenia and other brain disorders, was demonstrated to reduce the structural formation of PNNs, and the expression of PNN components and Pv-expressing GABAergic interneurons in the early stages of neuron development period. In this case, PNNs and Pv-expressing interneurons could be a marker of brain disorders affected by environmental stress, by detecting the abnormal expression of PNNs and Pv-expressing neurons in the early developmental stages, the risk of brain disorders could be predicted. With early prediction, effective therapies or the interventions could be conducted to prevent the worsen symptoms of the disorders in the later stages.

10.3 Technical consideration and future directions

Several technical considerations and limitations were addressed in the current experiments, which could be addressed in future studies. Firstly, the current studies were conducted mostly with primary cultured neurons. The development of PNNs in primary cultured neurons seems to replicate PNN development in animals and human brain (Dickens et al., 2022). A similar net-like

structure of PNNs could be detected in primary neuronal culture, and investigation with cultured neurons has high precision and resolution to manipulate genetic expression and structural formation (Geissler et al., 2013; Giamanco et al., 2012; Dityatev et al 2007). However, limitations of using primary neuronal cultures should also be considered. For example, behavioural effects could not be examined; the cell types were restricted; and different cell development time *in vitro* might be varied between experiments due to the culturing method. In the cultured neurons with only neurobasal medium and B27 supplement, the cell types were mainly neurons with small proportions of astrocytes or microglia (Goshi et al., 2020), which is not equivalent to mammalian brains. Co-culture of neurons, astrocytes and microglia may be optimal to support the cell growth (Goshi et al., 2022; Chen et al., 2016). Despite the tri-culture media being used to culture all 3 types of cells, the number of neurons still represented the largest proportion of the cultured cells, followed by astrocytes and microglia, the ratio was 5:2:1 (Luchena et al., 2022). Previous studies illustrated that an equal or greater proportion of glial cells is present in human or mammalian cortical areas compared to neurons (Azevedo et al., 2009; Andrade-Moraes et al., 2013). Thus, effects of GCs reported in cultured cortical neurons are likely to be mainly restricted to neurons. However, as mentioned in Section 1.2.1, PNNs were suggested to surround mainly neurons in various brain regions, and the expression of PNNs was quite abundant around neurons (Bruckner et al., 2006; Pantazopoulos et al., 2006; Lee et al., 2012; Foster et al., 2014). Thus, although there are restrictions using neuronal cultures, with a higher proportion of neurons as compared to other cell types, it is still reasonable to use primary neuronal culture to study the PNN expression with more abundant PNN expressed in the cultured neurons.

Moreover, different use of culture medium and supplements might lead to varying speed of development of neurons, resulting in varying formation and expression of PNNs between experiments. For example, instead of detecting fully structured PNNs at 14 DIV and 21 DIV in the current experiments, punctuated WFA-labelled PNNs at 14 DIV and the reticular structure of PNNs were detected from 21 DIV (Dickens et al., 2022); additionally, weak expression of PNNs with faint WFA-labelling were detected at 14 DIV, while stronger expression was shown at 21 DIV (Miyata et al., 2005). These studies used different culture medium from the current experiments, with a combination of neurobasal and BrainPhys medium with astrocyte-conditioned medium, or with additional cytosine arabinoside for glial cell elimination, which are different from the culturing procedure in the current study (presented in Chapter 2). Hence, using cultured cells for investigation will affect cell development with different usage of different cell medium. Hence, in future studies, the investigations of the effect of GCs should be conducted in tri-cultured cells with neurons, astrocytes and microglia; in addition to investigation in cultured neurons, the effect on PNN expression needs to be examined in animals with stress induction.

Secondly, to detect the PNN structural expression in cultured neurons, WFA was used to for PNN labelling and visualisation. However, as discussed in Chapter 8, despite WFA being widely used as a marker for PNNs, previous studies suggested that WFA only labels the majority of PNNs in the CNS (Fader et al., 2016; Morawski et al., 2010). Thus, the measurement and quantification of WFA-labelled PNNs in Chapter 6 and 8 did not include all PNNs, which might result in lower accuracy. In future studies, a combination of PNN labelling methods should be used, such as, Acan antibody (Cat-301) and WFA.

Thirdly, western blotting was used to investigate protein expression in the current experiments in Chapter 3. Although it was considered as the most essential and extensively used method for protein analysis, the results suffer from poor sensitivity and reproducibility, potentially due to various uncontrollable factors, and the multiple steps in the procedure. For example, the immunoblotting results were highly dependent on protein quality and concentration. Despite the protein concentration being quantified before proceeding to the procedure, the highly

concentrated protein can make the samples viscous (reviewed in Hong et al., 2018), which can then stick on pipette tips and result in sample loading error. Additionally, the time of electrophoresis was suggested to affect the results. The traditional running time for electrophoresis is 90 minutes, however, proteins with low molecular weight will not then be presented, as they run too far. For example, Pv protein has a particularly low molecular weight, around 10 KDa, and so is difficult to show on a western blot. Moreover, the time for protein transfer is also suggested as a factor influencing the results (reviewed in Liu et al., 2023). The time for protein transfer is 60 minutes with 30 volts in the current experiments; however, the efficiency of protein transfer might not be optimal for all proteins at 60 minutes. It has been suggested that proteins with relatively low molecular weight are transferred with a much faster speed compared to the proteins with high molecular weight (reviewed in Liu et al., 2023). Thus, the signal of the samples on each membrane from different proteins might be varied. As the current study (in Chapter 3) used 10-well precast gels to load enough samples in each well, not all groups of samples could be loaded in one gel, leading to signal variation from different membranes. Although reference protein samples were applied, false results could still be caused by the sample loading error. In future studies, to minimise the sample loading error, reduction of viscosity could be generated by dilution of RIPA buffer and replication of grinding during the protein sample collection.

10.4 Directions for the aims of future research

Apart from the technical considerations and the directions with regard to the methods that could be improved in future research, more considerations of the aims for further investigation can also been suggested, based on the current research.

Firstly, the current study investigated the effect of stress, specifically the elevated GC levels, on the expression of PNNs in cultured cortical neurons, and clarified the specific pathways of GC actions. However, the current research mainly focused on cultured cortical neurons. Although the cultured neurons could model the similar cell growth period in the brains and could show an alteration after direct exposure to elevated GC levels, the cells were supplied with enough cell cultured medium with adequate nutrient and growth factors, providing a stable and constant development environment, which could not mimic the complex environment with various cell connections and ongoing neural transmission in the real animal brain. Thus, in the future study, it would be worth further investigating the effect of stress on the expression of PNNs in animal experiments, with either GC injections or stress inductions, such as foot shock, food deprivation or tail pinch. In addition, it would also be useful to compare whether the stress had a similar effect on PNN expression in animal brains and cultured cells.

Secondly, our current results suggested altered PNN component gene expression after stress, however, how stress affect the functions of PNNs and the components remained to be further clarified. Therefore, in future research, in addition to gene expression, the research needs to further investigate the functional effect of stress on PNNs in animal experiments, with behavioural tests or electrophysiology studies, to detect the effect of stress-induced PNN alterations on behaviour and neuronal activities.

Thirdly, the current study clarified the specific actions of GCs on PNN components, such as non-genomic GR-mediated and GPCR-mediated pathways. To further confirm these actions, a future study could use the antagonists of the relevant receptors, such as one of the antagonists for GPR56/97 (hexahydroquinoline derivatives), to inhibit the GPR56/97 activation; or use some receptor KO animals, such as GR or GPR56/97 KO animals, to further investigate whether

elevated GCs could still show the same effect with the blockage or deficiency of the targeted receptors.

Finally, the current results reported some reduction of the specific PNN components, such as *Ncan*, *Has3*, *TnR* and *Pv,* after GC exposure. As noted in Chapter 1, different PNN components were suggested to provide several functions involved in neuronal activities, such as interacting with glutamatergic receptors, protecting neurons from being damaged, supporting neuronal growth, regulate synaptic plasticity and marking the closure of the critical period (Pizzorusso et al., 2002; Happel et al., 2014; Gogolla et al., 2009; McRae et al., 2007; McRae and Porter, 2012). Thus, with the altered expression of specific components reported here, the neuronal activities or functions could also be affected. In the future research, specific functions of these GC-affected PNN components could be further studied, with specific PNN component KO animals tested in behavioural or electrophysiology tests to clarify the behavioural and neuronal functions of these components. In addition to studying a KO condition, over-expression of specific PNN components could be induced in animals to further confirm the specific functions, with the electrophysiology / behavioural tests assessed.

10.5 Summary

The current findings reported the suppressive effect of GC on PNN components in cultured neurons, including, *Ncan*, *Has3* and *TnR*, and Pv-expressing GABAergic neurons, and could also suppress the formation of PNN, such as decreased length and intensity after HCA exposure; in the following MIA experiments, CSPGs were confirmed to play a critical role in immune response, and MIA-induced PNN alterations were potentially suggested to relate to environmental stress rather than genetic variants. However, in addition to the expression, the behavioural effect of GCs on the function of specific PNN components need to be further investigated. In future studies, behavioural tests in mice with loss of the components induced by stress could be studied, to test whether alterations of behaviours could be observed, and whether the alterations were related to the schizophrenia-like symptoms. Furthermore, the study illustrated a genomic or non-genomic pathway for GCs-mediated reduction of specific PNN components expression through GRs or non-GRs mediation. To further confirm the pathway of GCs effect, future studies should suppress GR or GPCR expression in animal studies, and then measure the expression of PNN components with GCs exposure to investigate whether elevated GCs could still show the same effect.

References

Abecassis, Z. A., Berceau, B. L., Win, P. H., García, D., Xenias, H. S., Cui, Q., Pamukcu, A., Cherian, S., et al. (2020). Npas1+-Nkx2.1+ Neurons Are an Integral Part of the Cortico-pallido-cortical Loop. *The Journal of neuroscience : the official journal of the Society for Neuroscience*, *40*(4), 743–768.

Abi-Dargham, A., Gil, R., Krystal, J., Baldwin, R. M., Seibyl, J. P., Bowers, M., van Dyck, C. H., Charney, D. S., Innis, R. B., & Laruelle, M. (1998). Increased striatal dopamine transmission in schizophrenia: confirmation in a second cohort. *The American journal of psychiatry*, *155*(6), 761–767.

Adams I, Brauer K, Arélin C, Härtig W, Fine A, Mäder M, Arendt T, Brückner G. (2001). Perineuronal nets in the rhesus monkey and human basal forebrain including basal ganglia. *Neuroscience*;108(2):285-98.

Addington, J., & Heinssen, R. (2012). Prediction and prevention of psychosis in youth at clinical high risk. *Annual review of clinical psychology*, *8*, 269–289.

Ajmo, J. M., Eakin, A. K., Hamel, M. G., & Gottschall, P. E. (2008). Discordant localization of WFA reactivity and brevican/ADAMTS-derived fragment in rodent brain. *BMC neuroscience*, *9*, 14.

Akbarian, S., & Huang, H. S. (2006). Molecular and cellular mechanisms of altered GAD1/GAD67 expression in schizophrenia and related disorders. *Brain research reviews*, *52*(2), 293–304.

Akbarian, S., Kim, J. J., Potkin, S. G., Hagman, J. O., Tafazzoli, A., Bunney, W. E., Jr, & Jones, E. G. (1995). Gene expression for glutamic acid decarboxylase is reduced without loss of neurons in prefrontal cortex of schizophrenics. *Archives of general psychiatry*, *52*(4), 258–266.

AlAqeel, B., & Margolese, H. C. (2012). Remission in schizophrenia: critical and systematic review. *Harvard review of psychiatry*, *20*(6), 281–297.

Alcaide, J., Guirado, R., Crespo, C., Blasco-Ibáñez, J. M., Varea, E., Sanjuan, J., & Nacher, J. (2019). Alterations of perineuronal nets in the dorsolateral prefrontal cortex of neuropsychiatric patients. *International journal of bipolar disorders*, *7*(1), 24.

Alekseichuk, I., Turi, Z., Amador de Lara, G., Antal, A., & Paulus, W. (2016). Spatial Working Memory in Humans Depends on Theta and High Gamma Synchronization in the Prefrontal Cortex. *Current biology : CB*, *26*(12), 1513–1521.

Alpár, A., Gärtner, U., Härtig, W., & Brückner, G. (2006). Distribution of pyramidal cells associated with perineuronal nets in the neocortex of rat. *Brain research*, *1120*(1), 13–22.

Altman, J., & Bayer, S. A. (1988). Development of the rat thalamus: III. Time and site of origin and settling pattern of neurons of the reticular nucleus. *The Journal of comparative neurology*, *275*(3), 406–428.

Alaiyed, S., McCann, M., Mahajan, G., Rajkowska, G., Stockmeier, C. A., Kellar, K. J., Wu, J. Y., & Conant, K. (2020). Venlafaxine Stimulates an MMP-9-Dependent Increase in Excitatory/Inhibitory Balance in a Stress Model of Depression. *The Journal of neuroscience : the official journal of the Society for Neuroscience*, *40*(22), 4418–4431.

Alexandrova, A., Petrov, L., Georgieva, A., Kirkova, M., & Kukan, M. (2008). Effects of proteasome inhibitor, MG132, on proteasome activity and oxidative status of rat liver. *Cell biochemistry and function*, *26*(3), 392–398.

American Psychiatric Association. Arlington, VA: American Psychiatric Association; 2013. Diagnostic and statistical manual of mental disorders, fifth edition.

Amilhon B, Huh CY, Manseau F, Ducharme G, Nichol H, Adamantidis A, Williams S. (2015). Parvalbumin Interneurons of Hippocampus Tune Population Activity at Theta Frequency. *Neuron,* 86(5):1277-89.

Anand, K. S., & Dhikav, V. (2012). Hippocampus in health and disease: An overview. *Annals of Indian Academy of Neurology*, *15*(4), 239–246.

Anderson, S. A., Kaznowski, C. E., Horn, C., Rubenstein, J. L., & McConnell, S. K. (2002). Distinct origins of neocortical projection neurons and interneurons in vivo. *Cerebral cortex (New York, N.Y. : 1991)*, *12*(7), 702–709.

Andrade-Moraes, C. H., Oliveira-Pinto, A. V., Castro-Fonseca, E., da Silva, C. G., Guimarães, D. M., Schizophreniaczupak, D., Parente-Bruno, D. R., Carvalho, L. R.,et al. (2013). Cell number changes in Alzheimer's disease relate to dementia, not to plaques and tangles. *Brain : a journal of neurology*, *136*(Pt 12), 3738–3752.

Andreasen NC, Flashman L, Flaum M, Arndt S, Swayze V 2nd, O'Leary DS, Ehrhardt JC, Yuh WT (1994). Regional brain abnormalities in schizophrenia measured with magnetic resonance imaging. *JAMA* ;272(22):1763-9.

Antonyuk, S. V., Strange, R. W., Marklund, S. L., & Hasnain, S. S. (2009). The structure of human extracellular copper-zinc superoxide dismutase at 1.7 A resolution: insights into heparin and collagen binding. *Journal of molecular biology*, *388*(2), 310–326.

Ansari-Lari, M., Zendehboodi, Z., Masoudian, M., & Mohammadi, F. (2021). Additive effect of glutathione S-transferase T1 active genotype and infection with *Toxoplasma gondii* for increasing the risk of schizophrenia. *Nordic journal of psychiatry*, *75*(4), 275–280.

Anlar, B., & Gunel-Ozcan, A. (2012). Tenascin-R: role in the central nervous system. *The international journal of biochemistry & cell biology*, *44*(9), 1385–1389.

Arato, M., Frecska, E., Maccrimmon, D. J., Guscott, R., Saxena, B., Tekes, K., & Tothfalusi, L. (1991). Serotonergic interhemispheric asymmetry: neurochemical and pharmaco-EEG evidence. *Progress in neuro-psychopharmacology & biological psychiatry*, *15*(6), 759–764.

Artiges E, Martinot JL, Verdys M, Attar-Levy D, Mazoyer B, Tzourio N, Giraud MJ, Paillère-Martinot ML (2000). Altered hemispheric functional dominance during word generation in negative schizophrenia. *Schizophrenia Bulletin*. ;26(3):709-21.

Asher RA, Morgenstern DA, Shearer MC, Adcock KH, Pesheva P, Fawcett JW (2002). Versican is upregulated in CNS injury and is a product of oligodendrocyte lineage cells. J*ournal of Neuroscience*;22(6):2225-36.

Asher, R. A., Morgenstern, D. A., Fidler, P. S., Adcock, K. H., Oohira, A., Braistead, J. E., Levine, J. M., Margolis, R. U., Rogers, J. H., & Fawcett, J. W. (2000). Neurocan is upregulated in injured brain and in cytokine-treated astrocytes. *The Journal of neuroscience : the official journal of the Society for Neuroscience*, *20*(7), 2427–2438.

Athilingam JC, Ben-Shalom R, Keeshen CM, Sohal VS, Bender KJ (2017). Serotonin enhances excitability and gamma frequency temporal integration in mouse prefrontal fast-spiking interneurons. *Elife*;6:e31991.

Avramopoulos D., Pearce B.D., McGrath J., Wolyniec P., Wang R., Eckart N., Hatzimanolis A., Goes F.S., Nestadt G., Mulle J., et al. (2015) Infection and inflammation in schizophrenia and bipolar disorder: A genome wide study for interactions with genetic variation. *PLoS ONE*;10: e0116696

Azevedo, F. A., Carvalho, L. R., Grinberg, L. T., Farfel, J. M., Ferretti, R. E., Leite, R. E., Jacob Filho, W., Lent, R., & Herculano-Houzel, S. (2009). Equal numbers of neuronal and nonneuronal cells make the human brain an isometrically scaled-up primate brain. *The Journal of comparative neurology*, *513*(5), 532–541.

Azizi, M., Farahmandghavi, F., Joghataei, M. T., Zandi, M., Imani, M., Bakhtiari, M., & Omidian, H. (2020). ChABC-loaded PLGA nanoparticles: A comprehensive study on biocompatibility, functional recovery, and axonal regeneration in animal model of spinal cord injury. *International journal of pharmaceutics*, *577*, 119037.

Babulas, V., Factor-Litvak, P., Goetz, R., Schaefer, C. A., & Brown, A. S. (2006). Prenatal exposure to maternal genital and reproductive infections and adult schizophrenia. *The American journal of psychiatry*, *163*(5), 927–929.

Baier, C., Baader, S. L., Jankowski, J., Gieselmann, V., Schilling, K., Rauch, U., & Kappler, J. (2007). Hyaluronan is organized into fiber-like structures along migratory pathways in the developing mouse cerebellum. *Matrix biology: journal of the International Society for Matrix Biology*, *26*(5), 348–358.

Baker, K. D., Gray, A. R., & Richardson, R. (2017). The development of perineuronal nets around parvalbumin gabaergic neurons in the medial prefrontal cortex and basolateral amygdala of rats. *Behavioral neuroscience*, *131*(4), 289–303.

Balashova, A., Pershin, V., Zaborskaya, O., Tkachenko, N., Mironov, A., Guryev, E., Kurbatov, L., Gainullin, M., & Mukhina, I. (2019). Enzymatic Digestion of Hyaluronan-Based Brain Extracellular Matrix *in vivo* Can Induce Seizures in Neonatal Mice. *Frontiers in neuroscience*, *13*, 1033.

Balduini, W., Elsner, J., Lombardelli, G., Peruzzi, G., & Cattabeni, F. (1991). Treatment with methylazoxymethanol at different gestational days: two-way shuttle box avoidance and residential maze activity in rat offspring. *Neurotoxicology*, 12(4), 677–686.

Bamberger, C. M., Bamberger, A. M., de Castro, M., & Chrousos, G. P. (1995). GR beta, a potential endogenous inhibitor of GC action in humans. *The Journal of clinical investigation*, *95*(6), 2435–2441.

Balmer, T. S., Carels, V. M., Frisch, J. L., & Nick, T. A. (2009). Modulation of perineuronal nets and parvalbumin with developmental song learning. *The Journal of neuroscience : the official journal of the Society for Neuroscience*, *29*(41), 12878–12885.

Barnea, G., Grumet, M., Milev, P., Silvennoinen, O., Levy, J. B., Sap, J., & Schlessinger, J. (1994). Receptor tyrosine phosphatase beta is expressed in the form of proteoglycan and binds to the extracellular matrix protein tenascin. *The Journal of biological chemistry*, *269*(20), 14349–14352.

Banasr, M., Lepack, A., Fee, C., Duric, V., Maldonado-Aviles, J., DiLeone, R., Sibille, E., Duman, R. S., & Sanacora, G. (2017). Characterization of GABAergic marker expression in the chronic unpredictable stress model of depression. *Chronic stress (Thousand Oaks, Calif.)*, *1*, 2470547017720459.

Bandler, R. C., Mayer, C., & Fishell, G. (2017). Cortical interneuron specification: the juncture of genes, time and geometry. *Current opinion in neurobiology*, *42*, 17–24.

Banerjee SB, Gutzeit VA, Baman J, Aoued HS, Doshi NK, Liu RC, Ressler KJ (2017). Perineuronal Nets in the Adult Sensory Cortex Are Necessary for Fear Learning. *Neuron*; 95(1):169-179.

Barnett, J. H., Werners, U., Secher, S. M., Hill, K. E., Brazil, R., Masson, K., Pernet, D. E., Kirkbride, J. B., Murray, G. K., Bullmore, E. T., & Jones, P. B. (2007). Substance use in a population-based clinic sample of people with first-episode psychosis. *The British journal of psychiatry : the journal of mental science*, *190*, 515–520.

Baptista MS, Melo CV, Armelão M, Herrmann D, Pimentel DO, Leal G, Caldeira MV, Bahr BA, Bengtson M, Almeida RD, Duarte CB (2010). Role of the proteasome in excitotoxicity-induced cleavage of glutamic acid decarboxylase in cultured hippocampal neurons. *PLoS One*;5(4):e10139.

Barnes, P. J., & Adcock, I. M. (2009). GC resistance in inflammatory diseases. *Lancet (London, England)*, *373*(9678), 1905–1917.

Barta, P. E., Pearlson, G. D., Powers, R. E., Richards, S. S., & Tune, L. E. (1990). Auditory hallucinations and smaller superior temporal gyral volume in schizophrenia. *The American journal of psychiatry*, *147*(11), 1457–1462.

Bassett, A. S., & Chow, E. W. (2008). Schizophrenia and 22q11.2 deletion syndrome. *Current psychiatry reports*, *10*(2), 148–157.

Basilico, B., Ferrucci, L., Ratano, P., Golia, M. T., Grimaldi, A., Rosito, M., et al. (2022). Microglia control glutamatergic synapses in the adult mouse hippocampus. *Glia*. 70(1):173-195.

Basta-Kaim A, Fijał K, Ślusarczyk J, Trojan E, Głombik K, Budzischizophreniaewska B, Leśkiewicz M, Regulska M, et al (2015). Prenatal administration of lipopolysaccharide induces sex-dependent changes in glutamic acid decarboxylase and parvalbumin in the adult rat brain. *Neuroscience*;287:78-92.

Baumeister W, Walz J, Zühl F, Seemüller E (1998). The proteasome: paradigm of a self-compartmentalizing protease. *Cell*; 92(3):367-80.

Beggah AT, Dours-Zimmermann MT, Barras FM, Brosius A, Zimmermann DR, Zurn AD (2005). Lesion-induced differential expression and cell association of Neurocan, Brevican, Versican V1 and V2 in the mouse dorsal root entry zone. *Neuroscience*. 133(3):749-62

Beyette, J., Mason, G. G., Murray, R. Z., Cohen, G. M., & Rivett, A. J. (1998). Proteasome activities decrease during dexamethasone-induced apoptosis of thymocytes. *The Biochemical journal*, *332 (Pt 2) (*Pt 2), 315–320.

Beards S, Gayer-Anderson C, Borges S, Dewey ME, Fisher HL, Morgan C (2013). Life events and psychosis: a review and meta-analysis. *Schizophrenia Bulletin.*;39(4):740–7.

Beato M (1989). Gene regulation by steroid hormones. *Cell;* 56(3):335-44.

Becker, C. G., & Becker, T. (2002). Repellent guidance of regenerating optic axons by chondroitin sulfate glycosaminoglycans in zebrafish. *The Journal of neuroscience : the official journal of the Society for Neuroscience*, *22*(3), 842–853.

Becker, C. G., Schweitzer, J., Feldner, J., Becker, T., & Schachner, M. (2003). Tenascin-R as a repellent guidance molecule for developing optic axons in zebrafish. *The Journal of neuroscience : the official journal of the Society for Neuroscience*, *23*(15), 6232–6237.

Becker T, Anliker B, Becker CG, Taylor J, Schachner M, Meyer RL, Bartsch U (2000). Tenascin-R inhibits regrowth of optic fibers in vitro and persists in the optic nerve of mice after injury. *Glia*;29(4):330-46

Bekku, Y., Saito, M., Moser, M., Fuchigami, M., Maehara, A., Nakayama, M., Kusachi, S., Ninomiya, Y., & Oohashi, T. (2012). Bral2 is indispensable for the proper localization of brevican and the structural integrity of the perineuronal net in the brainstem and cerebellum. *The Journal of comparative neurology*, *520*(8), 1721–1736.

Belliveau, C., Théberge, S., Netto, S., Rahimian, R., Fakhfouri, G., Hosdey, C., Davoli, M. A., Hendrickson, A., Hao, K., Giros, B., Turecki, G., Alonge, K. M., & Mechawar, N. (2024). Chondroitin sulfate glycan sulfation patterns influence histochemical labeling of perineuronal nets: a comparative study of interregional distribution in human and mouse brain. *Glycobiology*, *34*(8), cwae049

Benes FM, Berretta S (2001). GABAergic interneurons: implications for understanding schizophrenia and bipolar disorder. *Neuropsychopharmacology,* 25(1):1-27.

Benes F. M. (2000). Emerging principles of altered neural circuitry in schizophrenia. *Brain research. Brain research reviews*, *31*(2-3), 251–269.

Beneyto, M., & Meador-Woodruff, J. H. (2008). Lamina-specific abnormalities of NMDA receptor-associated postsynaptic protein transcripts in the prefrontal cortex in schizophrenia and bipolar disorder. *Neuropsychopharmacology*: *official publication of the American College of Neuropsychopharmacology,* 33(9), 2175–2186.

Benson, D. L., Isackson, P. J., Hendry, S. H., & Jones, E. G. (1991). Differential gene expression for glutamic acid decarboxylase and type II calcium-calmodulin-dependent protein kinase in basal ganglia, thalamus, and hypothalamus of the monkey. *The Journal of neuroscience : the official journal of the Society for Neuroscience*, *11*(6), 1540–1564.

Bentall, R. P., de Sousa, P., Varese, F., Wickham, S., Sitko, K., Haarmans, M., & Read, J. (2014). From adversity to psychosis: pathways and mechanisms from specific adversities to specific symptoms. *Social psychiatry and psychiatric epidemiology*, *49*(7), 1011–1022.

Berlucchi, G., & Buchtel, H. A. (2009). Neuronal plasticity: historical roots and evolution of meaning. *Experimental brain research*, *192*(3), 307–319.

Berretta S. (2012) Extracellular matrix abnormalities in schizophrenia. *Neuropharmacology*. 62(3):1584-97.

Berretta, S., Pantazopoulos, H., Markota, M., Brown, C., & Batzianouli, E. T. (2015). Losing the sugar coating: potential impact of perineuronal net abnormalities on interneurons in schizophrenia. *Schizophrenia research*, *167*(1-3), 18–27.

Beydoun, H., & Saftlas, A. F. (2008). Physical and mental health outcomes of prenatal maternal stress in human and animal studies: a review of recent evidence. *Paediatric and perinatal epidemiology*, *22*(5), 438–466

Binette, A. N., Liu, J., Bayer, H., Crayton, K. L., Melissari, L., Sweck, S. O., & Maren, S. (2023). Parvalbumin-Positive Interneurons in the Medial Prefrontal Cortex Regulate Stress-Induced Fear Extinction Impairments in Male and Female Rats. *The Journal of neuroscience : the official journal of the Society for Neuroscience*, *43*(22), 4162–4173.

Bioque, M., Mas, S., Costanzo, M. C., Cabrera, B., Lobo, A., González-Pinto, A., Rodriguez-Toscano, E., Corripio et al. (2019). Gene-environment interaction between an endocannabinoid system genetic polymorphism and cannabis use in first episode of psychosis. *European neuropsychopharmacology: the journal of the European College of Neuropsychopharmacology*, *29*(6), 786–794.

Bitanihirwe, B. K., Mauney, S. A., & Woo, T. U. (2016). Weaving a Net of Neurobiological Mechanisms in Schizophrenia and Unraveling the Underlying Pathophysiology. *Biological psychiatry*, *80*(8), 589–598.

Blakemore, S. J., & Choudhury, S. (2006). Development of the adolescent brain: implications for executive function and social cognition. *Journal of child psychology and psychiatry, and allied disciplines*, *47*(3-4), 296–312.

Bodick, N. C., Offen, W. W., Levey, A. I., Cutler, N. R., Gauthier, S. G., Satlin, A., Shannon, H. E., Tollefson, G. D., Rasmussen, K., Bymaster, F. P., Hurley, D. J., Potter, W. Z., & Paul, S. M. (1997). Effects of xanomeline, a selective muscarinic receptor agonist, on cognitive function and behavioral symptoms in Alzheimer disease. *Archives of neurology*, 54(4), 465–473.

Boggaram, V., Smith, M. E., & Mendelson, C. R. (1991). Posttranscriptional regulation of surfactant protein-A messenger RNA in human fetal lung in vitro by GCs. *Molecular endocrinology (Baltimore, Md.)*, *5*(3), 414–423.

Bonet-Costa, V., Sun, P. Y., & Davies, K. J. A. (2019). Measuring redox effects on the activities of intracellular proteases such as the 20S Proteasome and the Immuno-Proteasome with fluorogenic peptides. *Free radical biology & medicine*, *143*, 16–24.

Boumpas, D. T., Chrousos, G. P., Wilder, R. L., Cupps, T. R., & Balow, J. E. (1993). GC therapy for immune-mediated diseases: basic and clinical correlates. *Annals of internal medicine*, *119*(12), 1198–1208.

Blosa, M., Sonntag, M., Jäger, C., Weigel, S., Seeger, J., Frischknecht, R., Seidenbecher, C. I., Matthews, R. T., Arendt, T., Rübsamen, R., & Morawski, M. (2015). The extracellular matrix molecule brevican is an integral component of the machinery mediating fast synaptic transmission at the calyx of Held. *The Journal of physiology*, *593*(19), 4341–4360.

Bouvier, M. L., Fehsel, K., Schmitt, A., Meisenzahl-Lechner, E., Gaebel, W., & von Wilmsdorff, M. (2020). Sex-dependent alterations of dopamine receptor and glucose transporter density in rat hypothalamus under long-term clozapine and haloperidol medication. *Brain and behavior*, *10*(8), e01694.

Bradbury, E. J., & Carter, L. M. (2011). Manipulating the glial scar: chondroitinase ABC as a therapy for spinal cord injury. *Brain research bulletin*, *84*(4-5), 306–316.

Bradbury, E. J., Moon, L. D., Popat, R. J., King, V. R., Bennett, G. S., Patel, P. N., Fawcett, J. W., & McMahon, S. B. (2002). Chondroitinase ABC promotes functional recovery after spinal cord injury. *Nature*, *416*(6881), 636–640.

Brake, W. G., Sullivan, R. M., Flores, G., Srivastava, L. K., & Gratton, A. (1999). Neonatal ventral hippocampal lesions attenuate the nucleus accumbens dopamine response to stress: an electrochemical study in the adult rat. *Brain research*, 831(1-2), 25–32.

Brakebusch C, Seidenbecher CI, Aschizophreniately F, Rauch U, Matthies H, Meyer H, Krug M, Böckers TM, Zhou X, Kreutz MR, Montag D, Gundelfinger ED, Fässler R (2002). Brevican-deficient mice display impaired hippocampal CA1 long-term potentiation but show no obvious deficits in learning and memory. *Molecular Cell Biology*;22(21):7417-27.

Breier, A., Brannan, S. K., Paul, S. M., & Miller, A. C. (2023). Evidence of trospium's ability to mitigate cholinergic adverse events related to xanomeline: phase 1 study results. *Psychopharmacology*, 240(5), 1191–1198.

Breuner, C. W., & Orchinik, M. (2002). Plasma binding proteins as mediators of corticosteroid action in vertebrates. *The Journal of endocrinology*, *175*(1), 99–112

Bristow, G. C., Bostrom, J. A., Haroutunian, V., & Sodhi, M. S. (2015). Sex differences in GABAergic gene expression occur in the anterior cingulate cortex in schizophrenia. *Schizophrenia research*, *167*(1-3), 57–63.

Brown P, Oliviero A, Mazzone P, Insola A, Tonali P, Di Lazzaro V (2001). Dopamine dependency of oscillations between subthalamic nucleus and pallidum in Parkinson's disease. *Journal of Neuroscience*; 21(3):1033-8.

Bryant, N. L., Buchanan, R. W., Vladar, K., Breier, A., & Rothman, M. (1999). Gender differences in temporal lobe structures of patients with schizophrenia: a volumetric MRI study. *The American journal of psychiatry*, *156*(4), 603–609.

Brückner G, Hausen D, Härtig W, Drlicek M, Arendt T, Brauer K (1999). Cortical areas abundant in extracellular matrix chondroitin sulphate proteoglycans are less affected by cytoskeletal changes in Alzheimer's disease. *Neuroscience;* 92(3):791-805.

Brückner G, Brauer K, Härtig W, Wolff JR, Rickmann MJ, Derouiche A, Delpech B, Girard N, Oertel WH, Reichenbach A (1993). Perineuronal nets provide a polyanionic, glia-associated form of microenvironment around certain neurons in many parts of the rat brain. *Glia,* 8(3):183-200.

Brückner, G., Grosche, J., Schmidt, S., Härtig, W., Margolis, R. U., Delpech, B., Seidenbecher, C. I., Czaniera, R., & Schachner, M. (2000). Postnatal development of perineuronal nets in wild-type mice and in a mutant deficient in tenascin-R. *The Journal of comparative neurology*, *428*(4), 616–629.

Brückner, G., Grosche, J., Hartlage-Rübsamen, M., Schmidt, S., & Schachner, M. (2003). Region and lamina-specific distribution of extracellular matrix proteoglycans, hyaluronan and tenascin-R in the mouse hippocampal formation. *Journal of chemical neuroanatomy*, *26*(1), 37–50.

Brückner G, Schizophreniaeöke S, Pavlica S, Grosche J, Kacza J (2006). Axon initial segment ensheathed by extracellular matrix in perineuronal nets. *Neuroscience* ;138(2):365-75.

Bu, D. F., Erlander, M. G., Hitz, B. C., Tillakaratne, N. J., Kaufman, D. L., Wagner-McPherson, C. B., Evans, G. A., & Tobin, A. J. (1992). Two human glutamate decarboxylases, 65-kDa GAD and

67-kDa GAD, are each encoded by a single gene. *Proceedings of the National Academy of Sciences of the United States of America*, *89*(6), 2115–2119.

Buka, S. L., Tsuang, M. T., Torrey, E. F., Klebanoff, M. A., Bernstein, D., & Yolken, R. H. (2001). Maternal infections and subsequent psychosis among offspring. *Archives of general psychiatry*, *58*(11), 1032–1037.

Butchi, N. B., Pourciau, S., Du, M., Morgan, T. W., & Peterson, K. E. (2008). Analysis of the neuroinflammatory response to TLR7 stimulation in the brain: comparison of multiple TLR7 and/or TLR8 agonists. *Journal of immunology (Baltimore, Md.: 1950)*, *180*(11), 7604–7612.

Butt SJ, Fuccillo M, Nery S, Noctor S, Kriegstein A, Corbin JG, Fishell G (2005). The temporal and spatial origins of cortical interneurons predict their physiological subtype. *Neuron,* 48(4):591-604.

Butt SJ, Sousa VH, Fuccillo MV, Hjerling-Leffler J, Miyoshi G, Kimura S, Fishell G (2008). The requirement of Nkx2-1 in the temporal specification of cortical interneuron subtypes. *Neuron*; 59(5):722-32.

Buret, L., & van den Buuse, M. (2014). Corticosterone treatment during adolescence induces down-regulation of reelin and NMDA receptor subunit GLUN2C expression only in male mice: implications for schizophrenia. *The international journal of neuropsychopharmacology*, *17*(8), 1221–1232.

Bustini, M., Stratta, P., Daneluzzo, E., Pollice, R., Prosperini, P., & Rossi, A. (1999). Tower of Hanoi and WCST performance in schizophrenia: problem-solving capacity and clinical correlates. *Journal of psychiatric research*, *33*(3), 285–290.

Buxbaum, J. D., Georgieva, L., Young, J. J., Plescia, C., Kajiwara, Y., Jiang, Y., Moskvina, V., Norton, N., et al. (2008). Molecular dissection of NRG1-ERBB4 signaling implicates PTPRZ1 as a potential schizophrenia susceptibility gene. *Molecular psychiatry*, *13*(2), 162–172.

Caballero A, Diah KC, Tseng KY (2013). Region-specific upregulation of parvalbumin-, but not calretinin-positive cells in the ventral hippocampus during adolescence. *Hippocampus*, 23(12)23(12):1331-6.

Caballero, A., Flores-Barrera, E., Cass, D. K., & Tseng, K. Y. (2014). Differential regulation of parvalbumin and calretinin interneurons in the prefrontal cortex during adolescence. *Brain structure & function*, *219*(1), 395–406.

Cabungcal, J. H., Steullet, P., Morishita, H., Kraftsik, R., Cuenod, M., Hensch, T. K., & Do, K. Q. (2013). Perineuronal nets protect fast-spiking interneurons against oxidative stress. *Proceedings of the National Academy of Sciences of the United States of America*, *110*(22), 9130–9135.

Cale, J. A., Chauhan, E. J., Cleaver, J. J., Fusciardi, A. R., McCann, S., Waters, H. C., Žavbi, J., & King, M. V. (2024). GABAergic and inflammatory changes in the frontal cortex following neonatal PCP plus isolation rearing, as a dual-hit neurodevelopmental model for schizophrenia. *Molecular neurobiology*, 61(9), 6968–6983.

Canetta, S., Sourander, A., Surcel, H. M., Hinkka-Yli-Salomäki, S., Leiviskä, J., Kellendonk, C., McKeague, I. W., & Brown, A. S. (2014). Elevated maternal C-reactive protein and increased risk of schizophrenia in a national birth cohort. *The American journal of psychiatry*, *171*(9), 960–968.

Cannon, T. D., Cadenhead, K., Cornblatt, B., Woods, S. W., Addington, J., Walker, E., Seidman, L. J., Perkins, D., Tsuang, M., McGlashan, T., & Heinssen, R. (2008). Prediction of psychosis in

youth at high clinical risk: a multisite longitudinal study in North America. *Archives of general psychiatry*, *65*(1), 28–37.

Cardno, A. G., & Gottesman, I. I. (2000). Twin studies of schizophrenia: from bow-and-arrow concordances to star wars Mx and functional genomics. *American journal of medical genetics*, *97*(1), 12–17.

Carstens, K. E., Lustberg, D. J., Shaughnessy, E. K., McCann, K. E., Alexander, G. M., & Dudek, S. M. (2021). Perineuronal net degradation rescues CA2 plasticity in a mouse model of Rett syndrome. *The Journal of clinical investigation*, *131*(16), e137221.

Carulli, D., Rhodes, K. E., Brown, D. J., Bonnert, T. P., Pollack, S. J., Oliver, K., Strata, P., & Fawcett, J. W. (2006). Composition of perineuronal nets in the adult rat cerebellum and the cellular origin of their components. *The Journal of comparative neurology*, *494*(4), 559–577.

Carulli, D., Pizzorusso, T., Kwok, J. C., Putignano, E., Poli, A., Forostyak, S., Andrews, M. R., Deepa, S. S., Glant, T. T., & Fawcett, J. W. (2010). Animals lacking link protein have attenuated perineuronal nets and persistent plasticity. *Brain: a journal of neurology*, *133*(Pt 8), 2331–2347.

Caterson B. (2012). Fell-Muir Lecture: chondroitin sulphate glycosaminoglycans: fun for some and confusion for others. *International journal of experimental pathology*, *93*(1), 1–10.

Casquero-Veiga, M., Lamanna-Rama, N., Romero-Miguel, D., Rojas-Marquez, H., Alcaide, J., Beltran, M., Nacher, J., Desco, M., & Soto-Montenegro, M. L. (2023). The Poly I:C maternal immune stimulation model shows unique patterns of brain metabolism, morphometry, and plasticity in female rats. *Frontiers in behavioral neuroscience*, *16*, 1022622.

Catale, C., Martini, A., Piscitelli, R. M., Senzasono, B., Iacono, L. L., Mercuri, N. B., Guatteo, E., & Carola, V. (2022). Early-life social stress induces permanent alterations in plasticity and perineuronal nets in the mouse anterior cingulate cortex. *The European journal of neuroscience*, *56*(10), 5763–5783.

Catts, V. S., Lai, Y. L., Weickert, C. S., Weickert, T. W., & Catts, S. V. (2016). A quantitative review of the postmortem evidence for decreased cortical N-methyl-D-aspartate receptor expression levels in schizophrenia: How can we link molecular abnormalities to mismatch negativity deficits?. *Biological psychology*, *116*, 57–67.

Casey, A. B., & Canal, C. E. (2017). Classics in Chemical Neuroscience: Aripiprazole. *ACS chemical neuroscience*, *8*(6), 1135–1146.

Celio MR (1993). Perineuronal nets of extracellular matrix around parvalbumin-containing neurons of the hippocampus. *Hippocampus,* No:55-60.

Celio, M. R., & Blümcke, I. (1994). Perineuronal nets--a specialized form of extracellular matrix in the adult nervous system. *Brain research. Brain research reviews*, *19*(1), 128–145.

Chan, S., & Debono, M. (2010). Replication of cortisol circadian rhythm: new advances in hydrocortisone replacement therapy. *Therapeutic advances in endocrinology and metabolism*, *1*(3), 129–138.

Chaunsali, L., Tewari, B. P., & Sontheimer, H. (2021). Perineuronal Net Dynamics in the Pathophysiology of Epilepsy. *Epilepsy currents*, *21*(4), 273–281.

Chen, C. Y., & Shyu, A. B. (1995). AU-rich elements: characterization and importance in mRNA degradation. *Trends in biochemical sciences*, *20*(11), 465–470.

Chen, J., Lipska, B. K., Halim, N., Ma, Q. D., Matsumoto, M., Melhem, S., Kolachana, B. S., Hyde, T. M., Herman, M. M., Apud, J., Egan, M. F., Kleinman, J. E., & Weinberger, D. R. (2004). Functional analysis of genetic variation in catechol-O-methyltransferase (COMT): effects on mRNA, protein, and enzyme activity in postmortem human brain. *American journal of human genetics*, *75*(5), 807–821.

Chen, S. H., Oyarzabal, E. A., & Hong, J. S. (2016). Critical role of the Mac1/NOX2 pathway in mediating reactive microgliosis-generated chronic neuroinflammation and progressive neurodegeneration. *Current opinion in pharmacology*, *26*, 54–60.

Chen P, Hochstrasser M (1996). Autocatalytic subunit processing couples active site formation in the 20S proteasome to completion of assembly. *Cell*; 86(6):961-72.

Cheah SY, Lawford BR, Young RM, Morris CP, Voisey J (2017). mRNA Expression and DNA Methylation Analysis of Serotonin Receptor 2A (HTR2A) in the Human Schizophrenic Brain. *Genes (Basel)*; 8(1):14.

Cheng, Z., Teo, G., Krueger, S., Rock, T. M., Koh, H. W., Choi, H., & Vogel, C. (2016). Differential dynamics of the mammalian mRNA and protein expression response to misfolding stress. *Molecular systems biology*, *12*(1), 855.

Cheung, J., & Smith, D. F. (2000). Molecular chaperone interactions with steroid receptors: an update. *Molecular endocrinology (Baltimore, Md.)*, *14*(7), 939–946.

Chiovaro, F., Chiquet-Ehrismann, R., & Chiquet, M. (2015). Transcriptional regulation of tenascin genes. *Cell adhesion & migration*, *9*(1-2), 34–47.

Chiquet-Ehrismann, R., & Tucker, R. P. (2011). Tenascins and the importance of adhesion modulation. *Cold Spring Harbor perspectives in biology*, *3*(5), a004960.

Cho KK, Hoch R, Lee AT, Patel T, Rubenstein JL, Sohal VS (2015). Gamma rhythms link prefrontal interneuron dysfunction with cognitive inflexibility in Dlx5/6(+/-) mice. *Neuron*; 85:1332–1343.

Cho, H., Park, O. H., Park, J., Ryu, I., Kim, J., Ko, J., & Kim, Y. K. (2015). GR interacts with PNRC2 in a ligand-dependent manner to recruit UPF1 for rapid mRNA degradation. *Proceedings of the National Academy of Sciences of the United States of America*, *112*(13), E1540–E1549.

Cho, R. Y., Konecky, R. O., & Carter, C. S. (2006). Impairments in frontal cortical gamma synchrony and cognitive control in schizophrenia. *Proceedings of the National Academy of Sciences of the United States of America*, *103*(52), 19878–19883.

Chokhawala K, Stevens L (2024). Antipsychotic Medications. [Updated 2023 Feb 26]. In: StatPearls [Internet]. Treasure Island (FL): *StatPearls Publishing*.

Chua, S. E., Wright, I. C., Poline, J. B., Liddle, P. F., Murray, R. M., Frackowiak, R. S., Friston, K. J., & McGuire, P. K. (1997). Grey matter correlates of syndromes in schizophrenia. A semi-automated analysis of structural magnetic resonance images. *The British journal of psychiatry : the journal of mental science*, *170*, 406–410.

Ciccarelli, A., Weijers, D., Kwan, W., Warner, C., Bourne, J., & Gross, C. T. (2021). Sexually dimorphic perineuronal nets in the rodent and primate reproductive circuit. *The Journal of comparative neurology*, *529*(13), 3274–3291.

Ciechanover A (1994). The ubiquitin-proteasome proteolytic pathway. *Cell*; 79(1):13-21.

Cieślik, M., Gąssowska-Dobrowolska, M., Jęśko, H., Czapski, G. A., Wilkaniec, A., Zawadzka, A., Dominiak, A., Polowy, R., Filipkowski, R. K., Boguszewski, P. M., Gewartowska, M., Frontczak-Baniewicz, M., Sun, G. Y., Beversdorf, D. Q., & Adamczyk, A. (2020). Maternal Immune Activation Induces Neuroinflammation and Cortical Synaptic Deficits in the Adolescent Rat Offspring. *International journal of molecular sciences*, 21(11), 4097.

Clapcote, S. J., Lipina, T. V., Millar, J. K., Mackie, S., Christie, S., Ogawa, F., Lerch, J. P., Trimble, K., Uchiyama, M., Sakuraba, Y., Kaneda, H., Shiroishi, T., Houslay, M. D., Henkelman, R. M., Sled, J. G., Gondo, Y., Porteous, D. J., & Roder, J. C. (2007). Behavioral phenotypes of Disc1 missense mutations in mice. *Neuron*, 54(3), 387–402.

Cleghorn, J. M., Franco, S., Schizophreniaechtman, B., Kaplan, R. D., Schizophreniaechtman, H., Brown, G. M., Nahmias, C., & Garnett, E. S. (1992). Toward a brain map of auditory hallucinations. *The American journal of psychiatry*, *149*(8), 1062–1069.

Conconi, M., Schizophreniaweda, L. I., Levine, R. L., Stadtman, E. R., & Friguet, B. (1996). Age-related decline of rat liver multicatalytic proteinase activity and protection from oxidative inactivation by heat-shock protein 90. *Archives of biochemistry and biophysics*, *331*(2), 232–240

Cornblatt, B. A., & Erlenmeyer-Kimling, L. (1985). Global attentional deviance as a marker of risk for schizophrenia: specificity and predictive validity. *Journal of abnormal psychology*, *94*(4), 470–486.

Cooper, M. S., & Stewart, P. M. (2009). 11Beta-hydroxysteroid dehydrogenase type 1 and its role in the hypothalamus-pituitary-adrenal axis, metabolic syndrome, and inflammation. *The Journal of clinical endocrinology and metabolism*, *94*(12), 4645–4654.

Correll, C. U., Angelov, A. S., Miller, A. C., Weiden, P. J., & Brannan, S. K. (2022). Safety and tolerability of KarXT (xanomeline-trospium) in a phase 2, randomized, double-blind, placebo-controlled study in patients with schizophrenia. *Schizophrenia (Heidelberg, Germany)*, 8(1), 109.

Coutens, B., Lejards, C., Bouisset, G., Verret, L., Rampon, C., & Guiard, B. P. (2023). Enriched environmental exposure reduces the onset of action of the serotonin norepinephrin reuptake inhibitor venlafaxine through its effect on parvalbumin interneurons plasticity in mice. *Translational psychiatry*, *13*(1), 227.

Coux, O., Tanaka, K., & Goldberg, A. L. (1996). Structure and functions of the 20S and 26S proteasomes. *Annual review of biochemistry*, *65*, 801–847.

Craiu, A., Gaczynska, M., Akopian, T., Gramm, C. F., Fenteany, G., Goldberg, A. L., & Rock, K. L. (1997). Lactacystin and clasto-lactacystin beta-lactone modify multiple proteasome beta-subunits and inhibit intracellular protein degradation and major histocompatibility complex class I antigen presentation. *The Journal of biological chemistry*, *272*(20), 13437–13445.

Crapser, J. D., Arreola, M. A., Tsourmas, K. I., & Green, K. N. (2021). Microglia as hackers of the matrix: sculpting synapses and the extracellular space. *Cellular & molecular immunology*, *18*(11), 2472–2488.

Crapser, J. D., Ochaba, J., Soni, N., Reidling, J. C., Thompson, L. M., & Green, K. N. (2020). Microglial depletion prevents extracellular matrix changes and striatal volume reduction in a model of Huntington's disease. *Brain : a journal of neurology*, *143*(1), 266–288.

Crapser, J. D., Spangenberg, E. E., Barahona, R. A., Arreola, M. A., Hohsfield, L. A., & Green, K. N. (2020). Microglia facilitate loss of perineuronal nets in the Alzheimer's disease brain. *EBioMedicine*, *58*, 102919.

Crochemore, C., Lu, J., Wu, Y., Liposits, Z., Sousa, N., Holsboer, F., & Almeida, O. F. (2005). Direct targeting of hippocampal neurons for apoptosis by GCs is reversible by mineralocorticoid receptor activation. *Molecular psychiatry*, *10*(8), 790–798.

Csernansky JG, Schuchart EK (2002). Relapse and rehospitalisation rates in patients with schizophrenia: effects of second-generation antipsychotics. *CNS Drugs*; 16(7):473-84.

Cunningham, M. O., Hunt, J., Middleton, S., LeBeau, F. E., Gillies, M. J., Davies, C. H., Maycox, P. R., Whittington, M. A., & Racca, C. (2006). Region-specific reduction in entorhinal gamma oscillations and parvalbumin-immunoreactive neurons in animal models of psychiatric illness. *The Journal of neuroscience: the official journal of the Society for Neuroscience*, *26*(10), 2767–2776.

Curley, A. A., Arion, D., Volk, D. W., Asafu-Adjei, J. K., Sampson, A. R., Fish, K. N., & Lewis, D. A. (2011). Cortical deficits of glutamic acid decarboxylase 67 expression in schizophrenia: clinical, protein, and cell type-specific features. *The American journal of psychiatry*, *168*(9), 921–929.

Czeh B, Simon M, van der Hart MG, Schmelting B, Hesselink MB, Fuchs E (2005). Chronic stress decreases the number of parvalbumin-immunoreactive interneurons in the hippocampus: prevention by treatment with a substance P receptor (NK1) antagonist. *Neuropsychopharmacology*; 30(1):67-79.

D'Souza, R. S., & Hooten, W. M. (2023). Extrapyramidal Symptoms. In *StatPearls*. StatPearls Publishing.

Da Silva, T., Guma, E., Hafizi, S., Koppel, A., Rusjan, P., Kennedy, J. L., Chakravarty, M. M., & Mizrahi, R. (2021). Genetically Predicted Brain C4A Expression Is Associated With TSPO and Hippocampal Morphology. *Biological psychiatry*, 90(9), 652–660.

Dankovich, T. M., Kaushik, R., Olsthoorn, L. H. M., Petersen, G. C., Giro, P. E., Kluever, V., Agüi-Gonzalez, P., Grewe, K., Bao, G., Beuermann, S., Hadi, H. A., Doeren, J., Klöppner, S., Cooper, B. H., Dityatev, A., & Rizzoli, S. O. (2021). Extracellular matrix remodeling through endocytosis and resurfacing of Tenascin-R. *Nature communications*, *12*(1), 7129.

Dash, P. K., Blum, S., & Moore, A. N. (2000). Caspase activity plays an essential role in long-term memory. *Neuroreport*, *11*(12), 2811–2816.

Dauth, S., Grevesse, T., Pantazopoulos, H., Campbell, P. H., Maoz, B. M., Berretta, S., & Parker, K. K. (2016). Extracellular matrix protein expression is brain region dependent. *The Journal of comparative neurology*, *524*(7), 1309–1336.

Dahlman-Wright, K., Wright, A., Gustafsson, J. A., & Carlstedt-Duke, J. (1991). Interaction of the GR DNA-binding domain with DNA as a dimer is mediated by a short segment of five amino acids. *The Journal of biological chemistry*, *266*(5), 3107–3112.

Davey, G. (2015). *Psychopathology*. London: The British Psychological Society.

Davidson, K., & Pickering, A. M. (2023). The proteasome: A key modulator of nervous system function, brain aging, and neurodegenerative disease. *Frontiers in cell and developmental biology*, *11*, 1124907.

Dhawan, L., Liu, B., Pytlak, A., Kulshrestha, S., Blaxall, B. C., & Taubman, M. B. (2012). Y-box binding protein 1 and RNase UK114 mediate monocyte chemoattractant protein 1 mRNA stability in vascular smooth muscle cells. *Molecular and cellular biology*, *32*(18), 3768–3775.

de Araújo Costa Folha, O. A., Bahia, C. P., de Aguiar, G. P. S., Herculano, A. M., Coelho, N. L. G., de Sousa, M. B. C., Shiramizu, V. K. M., et al. (2017). Effect of chronic stress during adolescence in prefrontal cortex structure and function. *Behavioural brain research*, *326*, 44–51.

de Kloet, E. R., Sibug, R. M., Helmerhorst, F. M., & Schmidt, M. V. (2005). Stress, genes and the mechanism of programming the brain for later life. *Neuroscience and biobehavioral reviews*, *29*(2), 271–281.

Dean, B., & Hayes, W. (1996). Decreased frontal cortical serotonin2A receptors in schizophrenia. *Schizophrenia research*, *21*(3), 133–139.

Dean, B., Opeskin, K., Pavey, G., Naylor, L., Hill, C., Keks, N., & Copolov, D. L. (1995). [3H] paroxetine binding is altered in the hippocampus but not the frontal cortex or caudate nucleus from subjects with schizophrenia. *Journal of neurochemistry*, *64*(3), 1197–1202.

Dean, B., Hussain, T., Hayes, W., Scarr, E., Kitsoulis, S., Hill, C., Opeskin, K., & Copolov, D. L. (1999). Changes in serotonin2A and GABA(A) receptors in schizophrenia: studies on the human dorsolateral prefrontal cortex. *Journal of neurochemistry*, *72*(4), 1593–1599.

De Bosscher, K., Haegeman, G., & Elewaut, D. (2010). Targeting inflammation using selective GR modulators. *Current opinion in pharmacology*, *10*(4), 497–504.

Debost, J. C., Debost, M., Grove, J., Mors, O., Hougaard, D. M., Børglum, A. D., Mortensen, P. B., & Petersen, L. (2017). COMT Val158Met and MTHFR C677T moderate risk of schizophrenia in response to childhood adversity. *Acta psychiatrica Scandinavica*, *136*(1), 85–95.

Deepa, S. S., Carulli, D., Galtrey, C., Rhodes, K., Fukuda, J., Mikami, T., Sugahara, K., & Fawcett, J. W. (2006). Composition of perineuronal net extracellular matrix in rat brain: a different disaccharide composition for the net-associated proteoglycans. *The Journal of biological chemistry*, *281*(26), 17789–17800.

DeFelipe, J., López-Cruz, P. L., Benavides-Piccione, R., Bielza, C., Larrañaga, P., Anderson, S., Burkhalter, A., Cauli, B.,et al. (2013). New insights into the classification and nomenclature of cortical GABAergic interneurons. *Nature reviews. Neuroscience*, *14*(3), 202–216.

Deng, X., Gu, L., Sui, N., Guo, J., & Liang, J. (2019). Parvalbumin interneuron in the ventral hippocampus functions as a discriminator in social memory. *Proceedings of the National Academy of Sciences of the United States of America*, *116*(33), 16583–16592.

Desai, P. R., Lawson, K. A., Barner, J. C., & Rascati, K. L. (2013). Identifying patient characteristics associated with high schizophrenia-related direct medical costs in community-dwelling patients. *Journal of managed care pharmacy : JMCP*, *19*(6), 468–477.

Deyoe, E. A., Hockfield, S., Garren, H., & Van Essen, D. C. (1990). Antibody labeling of functional subdivisions in visual cortex: Cat-301 immunoreactivity in striate and extrastriate cortex of the macaque monkey. *Visual neuroscience*, *5*(1), 67–81.

Devienne, G., Picaud, S., Cohen, I., Piquet, J., Tricoire, L., Testa, D., Di Nardo, A. A., Rossier, J., Cauli, B., & Lambolez, B. (2021). Regulation of Perineuronal Nets in the Adult Cortex by the Activity of the Cortical Network. *The Journal of neuroscience : the official journal of the Society for Neuroscience*, *41*(27), 5779–5790.

Dick, G., Tan, C. L., Alves, J. N., Ehlert, E. M. E., Miller, G. M., Hsieh-Wilson, L. C., Sugahara, K., Oosterhof, A., van Kuppevelt, T. H., Verhaagen, J., Fawcett, J. W., & Kwok, J. C. F. (2013).

Semaphorin 3A binds to the perineuronal nets via chondroitin sulfate type E motifs in rodent brains. *The Journal of biological chemistry*, *288*(38), 27384–27395.

Dickens, Stuart & Goodenough, Ashleigh & Kwok, Jessica. (2022). An in vitro neuronal model replicating the in vivo maturation and heterogeneity of perineuronal nets.

Dickerson, F., Stallings, C., Origoni, A., Vaughan, C., Khushalani, S., Yang, S., & Yolken, R. (2013). C-reactive protein is elevated in schizophrenia. *Schizophrenia research*, *143*(1), 198–202.

Dimatelis, J. J., Hendricks, S., Hsieh, J., Vlok, N. M., Bugarith, K., Daniels, W. M., & Russell, V. A. (2013). Exercise partly reverses the effect of maternal separation on hippocampal proteins in 6-hydroxydopamine-lesioned rat brain. *Experimental physiology*, *98*(1), 233–244.

Dino, M. R., Harroch, S., Hockfield, S., & Matthews, R. T. (2006). Monoclonal antibody Cat-315 detects a glycoform of receptor protein tyrosine phosphatase beta/phosphacan early in CNS development that localizes to extrasynaptic sites prior to synapse formation. *Neuroscience*, *142*(4), 1055–1069.

Dityatev, A., Brückner, G., Dityateva, G., Grosche, J., Kleene, R., & Schachner, M. (2007). Activity-dependent formation and functions of chondroitin sulfate-rich extracellular matrix of perineuronal nets. *Developmental neurobiology*, *67*(5), 570–588.

Do, Y., Nagarkatti, P. S., & Nagarkatti, M. (2004). Role of CD44 and hyaluronic acid (HA) in activation of alloreactive and antigen-specific T cells by bone marrow-derived dendritic cells. *Journal of immunotherapy*, *27*(1), 1–12.

Dolgin E. (2024). Revolutionary drug for schizophrenia wins US approval. *Nature*, 634(8033), 276–277.

Donato F, Rompani SB, Caroni P (2013). Parvalbumin-expressing basket-cell network plasticity induced by experience regulates adult learning. *Nature*; 504(7479):272-6.

Dong F, Xie W, Strong JA, Zhang JM (2012). Mineralocorticoid receptor blocker eplerenone reduces pain behaviors in vivo and decreases excitability in small-diameter sensory neurons from local inflamed dorsal root ganglia in vitro. *Anesthesiology*. Nov;117(5):1102-12.

Doorduin, J., de Vries, E. F., Willemsen, A. T., de Groot, J. C., Dierckx, R. A., & Klein, H. C. (2009). Neuroinflammation in schizophrenia-related psychosis: a PET study. *Journal of nuclear medicine : official publication, Society of Nuclear Medicine*, *50*(11), 1801–1807.

Dracheva, S., Elhakem, S. L., McGurk, S. R., Davis, K. L., & Haroutunian, V. (2004). GAD67 and GAD65 mRNA and protein expression in cerebrocortical regions of elderly patients with schizophrenia. *Journal of neuroscience research*, *76*(4), 581–592.

Du, J., Duan, S., Wang, H., Chen, W., Zhao, X., Zhang, A., Wang, L., Xuan, J., et al. (2008). Comprehensive analysis of polymorphisms throughout GAD1 gene: a family-based association study in schizophrenia. *Journal of neural transmission (Vienna, Austria : 1996)*, *115*(3), 513–519.

Du, J., Wang, Y., Hunter, R., Wei, Y., Blumenthal, R., Falke, C., Khairova, R., Zhou, R., Yuan, P., Machado-Vieira, R., McEwen, B. S., & Manji, H. K. (2009). Dynamic regulation of mitochondrial function by GCs. *Proceedings of the National Academy of Sciences of the United States of America*, *106*(9), 3543–3548.

Du T, Xu Q, Ocbina PJ, Anderson SA (2008). NKX2.1 specifies cortical interneuron fate by activating Lhx6. *Development*; 135(8):1559-67.

Dufresne, D., Hamdan, F. F., Rosenfeld, J. A., Torchia, B., Rosenblatt, B., Michaud, J. L., & Srour, M. (2012). Homozygous deletion of Tenascin-R in a patient with intellectual disability. *Journal of medical genetics*, *49*(7), 451–454.

Duman, RS, Duric, V, Banasr, M, et al (2012). Cariprazine exhibits dopamine D3 receptor-dependent antidepressant-like activity in the chronic unpredictable stress model of anhedonia. *Neuropsychopharmacology*; 38

Dyck, S. M., & Karimi-Abdolrezaee, S. (2015). Chondroitin sulfate proteoglycans: Key modulators in the developing and pathologic central nervous system. *Experimental neurology*, *269*, 169–187.

e Araújo Costa Folha, O. A., Bahia, C. P., de Aguiar, G. P. S., Herculano, A. M., Coelho, N. L. G., de Sousa, M. B. C., Shiramizu, V. K. M., de Menezes Galvão, A. C., de Carvalho, W. A., & Pereira, A. (2017). Effect of chronic stress during adolescence in prefrontal cortex structure and function. *Behavioural brain research*, *326*, 44–51.

Eastwood, S. L., & Harrison, P. J. (2005). Decreased expression of vesicular glutamate transporter 1 and complexin II mRNAs in schizophrenia: further evidence for a synaptic pathology affecting glutamate neurons. *Schizophrenia research*, 73(2-3), 159–172.

Eastwood, S. L., Law, A. J., Everall, I. P., & Harrison, P. J. (2003). The axonal chemorepellant semaphorin 3A is increased in the cerebellum in schizophrenia and may contribute to its synaptic pathology. *Molecular psychiatry*, *8*(2), 148–155.

Egerton, A., Reid, L., McKerchar, C. E., Morris, B. J., & Pratt, J. A. (2005). Impairment in perceptual attentional set-shifting following PCP administration: a rodent model of set-shifting deficits in schizophrenia. *Psychopharmacology*, 179(1), 77–84.

El Mouhawess A., Hammoud A., Zoghbi M., Hallit S., Haddad C., El Haddad K., El Khoury S., Tannous J., Obeid S., Halabi M.A., et al (2020). Relationship between *Toxoplasma gondii* seropositivity and schizophrenia in the Lebanese population: Potential implication of genetic polymorphism of MMP-9. *BMC Psychiatry; 20:264*.

Ehrchen J, Steinmüller L, Barczyk K, Tenbrock K, Nacken W, Eisenacher M, Nordhues U, Sorg C, Sunderkötter C, Roth J (2007). GCs induce differentiation of a specifically activated, anti-inflammatory subtype of human monocytes. *Blood*; 109(3):1265-74.

Eiland L, Ramroop J, Hill MN, Manley J, McEwen BS (2012). Chronic juvenile stress produces corticolimbic dendritic architectural remodeling and modulates emotional behavior in male and female rats. *Psychoneuroendocrinology*. Jan;37(1):39-47

Eill, G. J., Sinha, A., Morawski, M., Viapiano, M. S., & Matthews, R. T. (2020). The protein tyrosine phosphatase RPTPζ/phosphacan is critical for perineuronal net structure. *The Journal of biological chemistry*, *295*(4), 955–968.

Elizalde N, García-García AL, Totterdell S, Gendive N, Venzala E, Ramirez MJ, Del Rio J, Tordera RM (2010). Sustained stress-induced changes in mice as a model for chronic depression. *Psychopharmacology* (Berl). Jun;210(3):393-406.

Elizalde N, Gil-Bea FJ, Ramírez MJ, Aisa B, Lasheras B, Del Rio J, Tordera RM (2008). Long-lasting behavioral effects and recognition memory deficit induced by chronic mild stress in mice: effect of antidepressant treatment. *Psychopharmacology* (Berl); 199(1):1-14.

Engel, M., Maurel, P., Margolis, R. U., & Margolis, R. K. (1996). Chondroitin sulfate proteoglycans in the developing central nervous system. I. cellular sites of synthesis of neurocan and phosphacan. *The Journal of comparative neurology*, *366*(1), 34–43.

Enwright JF, Sanapala S, Foglio A, Berry R, Fish KN, Lewis DA (2016). Reduced Labeling of Parvalbumin Neurons and Perineuronal Nets in the Dorsolateral Prefrontal Cortex of Subjects with Schizophrenia. *Neuropsychopharmacology*; 41(9):2206-14.

Escoter-Torres, L., Greulich, F., Quagliarini, F., Wierer, M., & Uhlenhaut, N. H. (2020). Anti-inflammatory functions of the GR require DNA binding. *Nucleic acids research*, *48*(15), 8393–8407.

Evans RM, Arriza JL (1989). A molecular framework for the actions of GC hormones in the nervous system. *Neuron*; 2(2):1105-12.

Fadeel B, Orrenius S, Zhivotovsky B (2000). The most unkindest cut of all: on the multiple roles of mammalian caspases. *Leukemia*;14(8):1514-25.

Fader, S. M., Imaizumi, K., Yanagawa, Y., & Lee, C. C. (2016). Wisteria Floribunda Agglutinin-Labeled Perineuronal Nets in the Mouse Inferior Colliculus, Thalamic Reticular Nucleus and Auditory Cortex. *Brain sciences*, *6*(2), 13.

Faissner, A., Clement, A., Lochter, A., Streit, A., Mandl, C., & Schachner, M. (1994). Isolation of a neural chondroitin sulfate proteoglycan with neurite outgrowth promoting properties. *The Journal of cell biology*, *126*(3), 783–799.

Feinberg I. (1982). Schizophrenia: caused by a fault in programmed synaptic elimination during adolescence? *Journal of psychiatric research*, 17(4), 319–334.

Faissner, A., Pyka, M., Geissler, M., Sobik, T., Frischknecht, R., Gundelfinger, E. D., & Seidenbecher, C. (2010). Contributions of astrocytes to synapse formation and maturation - Potential functions of the perisynaptic extracellular matrix. *Brain research reviews*, *63*(1-2), 26–38.

Fang, A., Li, D., Hao, Z., Wang, L., Pan, B., Gao, L., Qu, X., & He, J. (2019). Effects of astrocyte on neuronal outgrowth in a layered 3D structure. *Biomedical engineering online*, *18*(1), 74.

Fang, W., Wang, Z., Li, Q., Wang, X., Zhang, Y., Sun, Y., Tang, W., Ma, C., Sun, J., Li, N., & Yi, F. (2018). Gpr97 Exacerbates AKI by Mediating Sema3A Signaling. *Journal of the American Society of Nephrology : JASN*, *29*(5), 1475–1489.

Fatemi, S. H., Halt, A. R., Stary, J. M., Kanodia, R., Schulz, S. C., & Realmuto, G. R. (2002). Glutamic acid decarboxylase 65 and 67 kDa proteins are reduced in autistic parietal and cerebellar cortices. *Biological psychiatry*, *52*(8), 805–810.

Favuzzi E, Deogracias R, Marques-Smith A, Maeso P, Jezequel J, Exposito-Alonso D, Balia M, Kroon T, Hinojosa AJ, F Maraver E, Rico B (2019). Distinct molecular programs regulate synapse specificity in cortical inhibitory circuits. *Science*;363(6425):413-417.

Favuzzi, E., Marques-Smith, A., Deogracias, R., Winterflood, C. M., Sánchez-Aguilera, A., Mantoan, L., Maeso, P., Fernandes, C., Ewers, H., & Rico, B. (2017). Activity-Dependent Gating of Parvalbumin Interneuron Function by the Perineuronal Net Protein Brevican. *Neuron*, *95*(3), 639–655.e10.

Fawcett, J. W., & Asher, R. A. (1999). The glial scar and central nervous system repair. *Brain research bulletin*, *49*(6), 377–391.

Fawcett, J. W., Oohashi, T., & Pizzorusso, T. (2019). The roles of perineuronal nets and the perinodal extracellular matrix in neuronal function. *Nature reviews. Neuroscience*, *20*(8), 451–465.

Featherstone, R. E., Rizos, Z., Kapur, S., & Fletcher, P. J. (2008). A sensitizing regimen of amphetamine that disrupts attentional set-shifting does not disrupt working or long-term memory. *Behavioural brain research*, 189(1), 170–179.

Fernando, P., Kelly, J. F., Balazsi, K., Slack, R. S., & Megeney, L. A. (2002). Caspase 3 activity is required for skeletal muscle differentiation. *Proceedings of the National Academy of Sciences of the United States of America*, *99*(17), 11025–11030.

Fletcher, P. J., Tenn, C. C., Rizos, Z., Lovic, V., & Kapur, S. (2005). Sensitization to amphetamine, but not PCP, impairs attentional set shifting: reversal by a D1 receptor agonist injected into the medial prefrontal cortex. *Psychopharmacology*, 183(2), 190–200.

Flinker, A., Korzeniewska, A., Shestyuk, A. Y., Franaschizophreniaczuk, P. J., Dronkers, N. F., Knight, R. T., & Crone, N. E. (2015). Redefining the role of Broca's area in speech. *Proceedings of the National Academy of Sciences of the United States of America*, *112*(9), 2871–2875.

Frankenburg, F. R., Zanarini, M. C., Kando, J., & Centorrino, F. (1998). Clozapine and body mass change. *Biological psychiatry*, *43*(7), 520–524.

Frischknecht, R., Heine, M., Perrais, D., Seidenbecher, C. I., Choquet, D., & Gundelfinger, E. D. (2009). Brain extracellular matrix affects AMPA receptor lateral mobility and short-term synaptic plasticity. *Nature neuroscience*, *12*(7), 897–904.

Fone, K. C., & Porkess, M. V. (2008). Behavioural and neurochemical effects of post-weaning social isolation in rodents-relevance to developmental neuropsychiatric disorders. *Neuroscience and biobehavioral reviews*, 32(6), 1087–1102.

Fowke, T. M., Karunasinghe, R. N., Bai, J. Z., Jordan, S., Gunn, A. J., & Dean, J. M. (2017). Hyaluronan synthesis by developing cortical neurons in vitro. *Scientific reports*, *7*, 44135.

Foster, N. L., Mellott, J. G., & Schofield, B. R. (2014). Perineuronal nets and GABAergic cells in the inferior colliculus of guinea pigs. *Frontiers in neuroanatomy*, *7*, 53.

Freitag, S., Schachner, M., & Morellini, F. (2003). Behavioral alterations in mice deficient for the extracellular matrix glycoprotein tenascin-R. *Behavioural brain research*, *145*(1-2), 189–207.

Freyberg Z, Ferrando SJ, Javitch JA (2010). Roles of the Akt/GSK-3 and Wnt signaling pathways in schizophrenia and antipsychotic drug action. *Am J Psychiatry*; **167**:388–396

Frevel, M. A., Bakheet, T., Silva, A. M., Hissong, J. G., Khabar, K. S., & Williams, B. R. (2003). p38 Mitogen-activated protein kinase-dependent and -independent signaling of mRNA stability of AU-rich element-containing transcripts. *Molecular and cellular biology*, *23*(2), 425–436.

Frischknecht, R., Heine, M., Perrais, D., Seidenbecher, C. I., Choquet, D., & Gundelfinger, E. D. (2009). Brain extracellular matrix affects AMPA receptor lateral mobility and short-term synaptic plasticity. *Nature neuroscience*, *12*(7), 897–904

Fujii, T., Uchiyama, H., Yamamoto, N., Hori, H., Tatsumi, M., Ishikawa, M., Arima, K., Higuchi, T., & Kunugi, H. (2011). Possible association of the semaphorin 3D gene (SEMA3D) with schizophrenia. *Journal of psychiatric research*, *45*(1), 47–53.

Fujihara, K., Sato, T., Miyasaka, Y., Mashimo, T., & Yanagawa, Y. (2021). Genetic deletion of the 67-kDa isoform of glutamate decarboxylase alters conditioned fear behavior in rats. *FEBS open bio*, *11*(2), 340–353.

Fulford, A. J., & Marsden, C. A. (1998). Effect of isolation-rearing on conditioned dopamine release in vivo in the nucleus accumbens of the rat. *Journal of neurochemistry*, 70(1), 384–390.

Fuss, B., Wintergerst, E. S., Bartsch, U., & Schachner, M. (1993). Molecular characterization and in situ mRNA localization of the neural recognition molecule J1-160/180: a modular structure similar to tenascin. *The Journal of cell biology*, *120*(5), 1237–1249.

Gabbott, P. L., Dickie, B. G., Vaid, R. R., Headlam, A. J., & Bacon, S. J. (1997). Local-circuit neurones in the medial prefrontal cortex (areas 25, 32 and 24b) in the rat: morphology and quantitative distribution. *The Journal of comparative neurology*, *377*(4), 465–499.

Galgoczi, E., Katko, M., Papp, F. R., Csiki, R., Csiha, S., Erdei, A., Bodor, M., Ujhelyi, B., Steiber, Z., Gyory, F., & Nagy, E. V. (2022). GCs Directly Affect Hyaluronan Production of Orbital Fibroblasts; A Potential Pleiotropic Effect in Graves' Orbitopathy. *Molecules (Basel, Switzerland)*, *28*(1), 15.

Galtrey, C. M., Kwok, J. C., Carulli, D., Rhodes, K. E., & Fawcett, J. W. (2008). Distribution and synthesis of extracellular matrix proteoglycans, hyaluronan, link proteins and tenascin-R in the rat spinal cord. *The European journal of neuroscience*, *27*(6), 1373–1390.

Gametchu B, Chen F, Sackey F, Powell C, Watson CS (1999). Plasma membrane-resident GRs in rodent lymphoma and human leukemia models. *Steroids*. ;64(1-2):107-19.

Gao, R., Wang, M., Lin, J., Hu, L., Li, Z., Chen, C., & Yuan, L. (2018). Spatiotemporal expression patterns of chondroitin sulfate proteoglycan mRNAs in the developing rat brain. *Neuroreport*, *29*(7), 517–523.

Garey, L. J., Ong, W. Y., Patel, T. S., Kanani, M., Davis, A., Mortimer, A. M., Barnes, T. R., & Hirsch, S. R. (1998). Reduced dendritic spine density on cerebral cortical pyramidal neurons in schizophrenia. *Journal of neurology, neurosurgery, and psychiatry*, *65*(4), 446–453.

Gaucherand, L., Falk, B. A., Evanko, S. P., Workman, G., Chan, C. K., & Wight, T. N. (2017). Crosstalk Between T Lymphocytes and Lung Fibroblasts: Generation of a Hyaluronan-Enriched Extracellular Matrix Adhesive for Monocytes. *Journal of cellular biochemistry*, *118*(8), 2118–2130.

Gebhardt, C., Averbeck, M., Diedenhofen, N., Willenberg, A., Anderegg, U., Sleeman, J. P., & Simon, J. C. (2010). Dermal hyaluronan is rapidly reduced by topical treatment with GCs. *The Journal of investigative dermatology*, *130*(1), 141–149.

Geng, F., Wenzel, S., & Tansey, W. P. (2012). Ubiquitin and proteasomes in transcription. *Annual review of biochemistry*, *81*, 177–201.

Gesing, A., Bilang-Bleuel, A., Droste, S. K., Linthorst, A. C., Holsboer, F., & Reul, J. M. (2001). Psychological stress increases hippocampal mineralocorticoid receptor levels: involvement of corticotropin-releasing hormone. *The Journal of neuroscience : the official journal of the Society for Neuroscience*, *21*(13), 4822–4829.

Geissler, M., Gottschling, C., Aguado, A., Rauch, U., Wetzel, C. H., Hatt, H., & Faissner, A. (2013). Primary hippocampal neurons, which lack four crucial extracellular matrix molecules, display abnormalities of synaptic structure and function and severe deficits in perineuronal net

formation. *The Journal of neuroscience : the official journal of the Society for Neuroscience*, *33*(18), 7742–7755.

Giamanco, K. A., Morawski, M., & Matthews, R. T. (2010). Perineuronal net formation and structure in aggrecan knockout mice. *Neuroscience*, *170*(4), 1314–1327.

Giamanco, K. A., & Matthews, R. T. (2012). Deconstructing the perineuronal net: cellular contributions and molecular composition of the neuronal extracellular matrix. *Neuroscience*, *218*, 367–384.

Gildawie KR, Honeycutt JA, Brenhouse HC (2020). Region-specific Effects of Maternal Separation on Perineuronal Net and Parvalbumin-expressing Interneuron Formation in Male and Female Rats. *Neuroscience*.21(428):23-37.

Gildawie, K. R., Ryll, L. M., Hexter, J. C., Peterzell, S., Valentine, A. A., & Brenhouse, H. C. (2021). A two-hit adversity model in developing rats reveals sex-specific impacts on prefrontal cortex structure and behavior. *Developmental cognitive neuroscience*, *48*, 100924.

Gilabert-Juan, J., Castillo-Gomez, E., Guirado, R., Moltó, M. D., & Nacher, J. (2013). Chronic stress alters inhibitory networks in the medial prefrontal cortex of adult mice. *Brain structure & function*, *218*(6), 1591–1605.

Gilda, J. E., Ghosh, R., Cheah, J. X., West, T. M., Bodine, S. C., & Gomes, A. V. (2015). Western Blotting Inaccuracies with Unverified Antibodies: Need for a Western Blotting Minimal Reporting Standard (WBMRS). *PloS one*, *10*(8), e0135392.

Glantz, L. A., & Lewis, D. A. (2000). Decreased dendritic spine density on prefrontal cortical pyramidal neurons in schizophrenia. *Archives of general psychiatry*, *57*(1), 65–73.

Goff, D. C., Henderson, D. C., & Amico, E. (1992). Cigarette smoking in schizophrenia: relationship to psychopathology and medication side effects. *The American journal of psychiatry*, *149*(9), 1189–1194.

Gogolla N, Caroni P, Lüthi A, Herry C (2009). Perineuronal nets protect fear memories from erasure. *Science*;325(5945):1258-61.

Gold JM, Carpenter C, Randolph C, Goldberg TE, Weinberger DR (1997). Auditory working memory and Wisconsin Card Sorting Test performance in schizophrenia. *Archives of general psychiatry*; 54(2):159-65.

Goldstein, G., Scheid, M., Hammerling, U., Schlesinger, D. H., Niall, H. D., & Boyse, E. A. (1975). Isolation of a polypeptide that has lymphocyte-differentiating properties and is probably represented universally in living cells. *Proceedings of the National Academy of Sciences of the United States of America*, *72*(1), 11–15.

Goldstein JM, Seidman LJ, Horton NJ, Makris N, Kennedy DN, Caviness VS Jr, Faraone SV, Tsuang MT (2001). Normal sexual dimorphism of the adult human brain assessed by in vivo magnetic resonance imaging. *Cerebral Cortex*;11(6):490-7.

Gomes, F. V., Zhu, X., & Grace, A. A. (2019). The pathophysiological impact of stress on the dopamine system is dependent on the state of the critical period of vulnerability. *Molecular psychiatry*, *25*(12), 3278–3291.

Gonchar, Y., Wang, Q., & Burkhalter, A. (2008). Multiple distinct subtypes of GABAergic neurons in mouse visual cortex identified by triple immunostaining. *Frontiers in neuroanatomy*, *1*, 3.

Gong S, Miao YL, Jiao GZ, Sun MJ, Li H, Lin J, Luo MJ, Tan JH (2015). Dynamics and correlation of serum cortisol and corticosterone under different physiological or stressful conditions in mice. *PLoS One*;10(2):e0117503.

Gonzalez-Burgos G, Lewis DA (2008). GABA neurons and the mechanisms of network oscillations: implications for understanding cortical dysfunction in schizophrenia. *Schizophrenia Bulletin*;34(5):944-61.

Goshi, N., Morgan, R. K., Lein, P. J., & Seker, E. (2020). A primary neural cell culture model to study neuron, astrocyte, and microglia interactions in neuroinflammation. *Journal of neuroinflammation*, *17*(1), 155.

Gottesman II, McGuffin P, Farmer AE (1987). Clinical genetics as clues to the "real" genetics of schizophrenia (a decade of modest gains while playing for time). Schizophrenia Bulletin;13(1):23-47.

Gottschling, C., Wegrzyn, D., Denecke, B., & Faissner, A. (2019). Elimination of the four extracellular matrix molecules tenascin-C, tenascin-R, brevican and neurocan alters the ratio of excitatory and inhibitory synapses. *Scientific reports*, *9*(1), 13939.

Gray, L., Scarr, E., & Dean, B. (2006). Serotonin 1a receptor and associated G-protein activation in schizophrenia and bipolar disorder. *Psychiatry research*, *143*(2-3), 111–120.

Grechuk, K., Azizi, H., Sharma, V., Khan, T., & Jolayemi, A. (2021). Cannabis, Schizophrenia Risk and Genetics: A Case Report of a Patient With Homozygous Valine Catechol-O-Methyltransferase Polymorphism. *Cureus*, *13*(6), e15740.

Griffiths, B. B., Madden, A. M. K., Edwards, K. A., Zup, S. L., & Stary, C. M. (2019). Age-dependent sexual dimorphism in hippocampal cornu ammonis-1 perineuronal net expression in rats. *Brain and behavior*, *9*(5), e01265.

Groettrup, M., Kirk, C. J., & Basler, M. (2010). Proteasomes in immune cells: more than peptide producers?. *Nature reviews. Immunology*, *10*(1), 73–78.

Groeneweg, F. L., Karst, H., de Kloet, E. R., & Joëls, M. (2011). Rapid non-genomic effects of corticosteroids and their role in the central stress response. *The Journal of endocrinology*, *209*(2), 153–167.

Groeneweg, F. L., Karst, H., de Kloet, E. R., & Joëls, M. (2012). Mineralocorticoid and GRs at the neuronal membrane, regulators of nongenomic corticosteroid signalling. *Molecular and cellular endocrinology*, *350*(2), 299–309.

Groll, M., Bajorek, M., Köhler, A., Moroder, L., Rubin, D. M., Huber, R., Glickman, M. H., & Finley, D. (2000). A gated channel into the proteasome core particle. *Nature structural biology*, *7*(11), 1062–1067.

Guan, A., Wang, S., Huang, A., Qiu, C., Li, Y., Li, X., Wang, J., Wang, Q., & Deng, B. (2022). The role of gamma oscillations in central nervous system diseases: Mechanism and treatment. *Frontiers in cellular neuroscience*, *16*, 962957.

Guadagno, A., Verlezza, S., Long, H., Wong, T. P., & Walker, C. D. (2020). It Is All in the Right Amygdala: Increased Synaptic Plasticity and Perineuronal Nets in Male, But Not Female, Juvenile Rat Pups after Exposure to Early-Life Stress. *The Journal of neuroscience : the official journal of the Society for Neuroscience*, *40*(43), 8276–8291.

Guidotti, A., Auta, J., Davis, J. M., Di-Giorgi-Gerevini, V., Dwivedi, Y., Grayson, D. R., Impagnatiello, F., Pandey, G., Pesold, C., Sharma, R., Uzunov, D., & Costa, E. (2000). Decrease in reelin and glutamic acid decarboxylase67 (GAD67) expression in schizophrenia and bipolar disorder: a postmortem brain study. *Archives of general psychiatry*, *57*(11), 1061–1069.

Guimarães, A., Zaremba, S., & Hockfield, S. (1990). Molecular and morphological changes in the cat lateral geniculate nucleus and visual cortex induced by visual deprivation are revealed by monoclonal antibodies Cat-304 and Cat-301. *The Journal of neuroscience : the official journal of the Society for Neuroscience*, *10*(9), 3014–3024.

Guimaraes A, Zaremba S, Hockfield S (1990) Molecular and morphological changes in the cat lateral geniculate nucleus and visual cortex induced by visual deprivation are revealed by monoclonal antibodies Cat-304 and Cat-301. *J Neurosci* 10:3014–3024

Gundelfinger, E. D., Frischknecht, R., Choquet, D., & Heine, M. (2010). Converting juvenile into adult plasticity: a role for the brain's extracellular matrix. *The European journal of neuroscience*, *31*(12), 2156–2165.

Guo, C., He, P., Song, X., & Zheng, X. (2019). Long-term effects of prenatal exposure to earthquake on adult schizophrenia. *The British journal of psychiatry : the journal of mental science*, *215*(6), 730–735.

Gur, R. E., Cowell, P. E., Latshaw, A., Turetsky, B. I., Grossman, R. I., Arnold, S. E., Bilker, W. B., & Gur, R. C. (2000). Reduced dorsal and orbital prefrontal gray matter volumes in schizophrenia. *Archives of general psychiatry*, *57*(8), 761–768.

Gur RE, Turetsky BI, Cowell PE, Finkelman C, Maany V, Grossman RI, Arnold SE, Bilker WB, Gur RC (2000). Temporolimbic volume reductions in schizophrenia. *Archives of general psychiatry*;57(8):769-75.

Gould, R. A., Mueser, K. T., Bolton, E., Mays, V., & Goff, D. (2001). Cognitive therapy for psychosis in schizophrenia: an effect size analysis. *Schizophrenia research*, *48*(2-3), 335–342.

Gurevicius, K., Gureviciene, I., Valjakka, A., Schachner, M., & Tanila, H. (2004). Enhanced cortical and hippocampal neuronal excitability in mice deficient in the extracellular matrix glycoprotein tenascin-R. *Molecular and cellular neurosciences*, *25*(3), 515–523.

Hägg, E., Asplund, K., & Lithner, F. (1987). Value of basal plasma cortisol assays in the assessment of pituitary-adrenal insufficiency. *Clinical endocrinology*, *26*(2), 221–226.

Härtig, W., Brückner, G., Brauer, K., Schmidt, C., & Bigl, V. (1995). Allocation of perineuronal nets and parvalbumin-, calbindin-D28k- and glutamic acid decarboxylase-immunoreactivity in the amygdala of the rhesus monkey. *Brain research*, *698*(1-2), 265–269.

Haas, C. A., Rauch, U., Thon, N., Merten, T., & Deller, T. (1999). Entorhinal cortex lesion in adult rats induces the expression of the neuronal chondroitin sulfate proteoglycan neurocan in reactive astrocytes. *The Journal of neuroscience : the official journal of the Society for Neuroscience*, *19*(22), 9953–9963.

Haenschel, C., Bittner, R. A., Waltz, J., Haertling, F., Wibral, M., Singer, W., Linden, D. E., & Rodriguez, E. (2009). Cortical oscillatory activity is critical for working memory as revealed by deficits in early-onset schizophrenia. *The Journal of neuroscience : the official journal of the Society for Neuroscience*, *29*(30), 9481–9489.

Hadler, M. D., Tzilivaki, A., Schmitz, D., Alle, H., & Geiger, J. R. P. (2024). Gamma oscillation plasticity is mediated via parvalbumin interneurons. *Science advances*, *10*(5), eadj7427.

Haijma SV, Van Haren N, Cahn W, Koolschijn PC, Hulshoff Pol HE, Kahn RS (2013). Brain volumes in schizophrenia: a meta-analysis in over 18 000 subjects. *Schizophrenia Bulletin*;39(5):1129-38.

Hamann, J., Aust, G., Araç, D., Engel, F. B., Formstone, C., Fredriksson, R., Hall, R. A., Harty, B. L., et al. (2015). International Union of Basic and Clinical Pharmacology. XCIV. Adhesion G protein-coupled receptors. *Pharmacological reviews*, *67*(2), 338–367.

Han, M., Huang, X. F., Chen, D. C., Xiu, M. H., Hui, L., Liu, H., Kosten, T. R., & Zhang, X. Y. (2012). Gender differences in cognitive function of patients with chronic schizophrenia. *Progress in neuro-psychopharmacology & biological psychiatry*, *39*(2), 358–363.

Handunnetthi, L., Saatci, D., Hamley, J. C., & Knight, J. C. (2021). Maternal immune activation downregulates schizophrenia genes in the foetal mouse brain. *Brain communications*, *3*(4), fcab275.

Hanno-Iijima Y, Tanaka M, Iijima T (2015). Activity-Dependent Bidirectional Regulation of GAD Expression in a Homeostatic Fashion Is Mediated by BDNF-Dependent and Independent Pathways. *PLoS One*;10(8):e0134296.

Hausen, D., Brückner, G., Drlicek, M., Härtig, W., Brauer, K., & Bigl, V. (1996). Pyramidal cells ensheathed by perineuronal nets in human motor and somatosensory cortex. *Neuroreport*, *7*(11), 1725–1729.

Haunso, A., Celio, M. R., Margolis, R. K., & Menoud, P. A. (1999). Phosphacan immunoreactivity is associated with perineuronal nets around parvalbumin-expressing neurones. *Brain research*, *834*(1-2), 219–222.

Happel, M. F., Niekisch, H., Castiblanco Rivera, L. L., Ohl, F. W., Deliano, M., & Frischknecht, R. (2014). Enhanced cognitive flexibility in reversal learning induced by removal of the extracellular matrix in auditory cortex. *Proceedings of the National Academy of Sciences of the United States of America*, *111*(7), 2800–2805.

Hayashi, M. K., Nishioka, T., Shimizu, H., Takahashi, K., Kakegawa, W., Mikami, T., Hirayama, Y., Koizumi, S., Yoshida, S., Yuzaki, M., Tammi, M., Sekino, Y., Kaibuchi, K., Shigemoto-Mogami, Y., Yasui, M., & Sato, K. (2019). Hyaluronan synthesis supports glutamate transporter activity. *Journal of neurochemistry*, *150*(3), 249–263.

Hargus G, Cui Y, Schmid JS, Xu J, Glatzel M, Schachner M, Bernreuther C (2008). Tenascin-R promotes neuronal differentiation of embryonic stem cells and recruitment of host-derived neural precursor cells after excitotoxic lesion of the mouse striatum. *Stem Cells*;26(8):1973-84.

Harrison P. J. (1999). The neuropathology of schizophrenia. A critical review of the data and their interpretation. *Brain : a journal of neurology*, *122 (Pt 4)*, 593–624.

Härtig, W., Brauer, K., & Brückner, G. (1992). Wisteria floribunda agglutinin-labelled nets surround parvalbumin-containing neurons. *Neuroreport*, *3*(10), 869–872.

Hashimoto, T., Bazmi, H. H., Mirnics, K., Wu, Q., Sampson, A. R., & Lewis, D. A. (2008). Conserved regional patterns of GABA-related transcript expression in the neocortex of subjects with schizophrenia. *The American journal of psychiatry*, *165*(4), 479–489.

Hashimoto, T., Volk, D. W., Eggan, S. M., Mirnics, K., Pierri, J. N., Sun, Z., Sampson, A. R., & Lewis, D. A. (2003). Gene expression deficits in a subclass of GABA neurons in the prefrontal cortex of subjects with schizophrenia. *The Journal of neuroscience : the official journal of the Society for Neuroscience*, *23*(15), 6315–6326.

He, Y., Taylor, N., Yao, X., & Bhattacharya, A. (2021). Mouse primary microglia respond differently to LPS and poly(I:C) in vitro. *Scientific reports*, *11*(1), 10447.

Heckers, S., Stone, D., Walsh, J., Shick, J., Koul, P., & Benes, F. M. (2002). Differential hippocampal expression of glutamic acid decarboxylase 65 and 67 messenger RNA in bipolar disorder and schizophrenia. *Archives of general psychiatry*, *59*(6), 521–529.

Heimberg, Carolyn & Gallacher, Fiona & Gur, Ruben & Gur, Raquel. (1994). Diet and Gender Moderate Clozapine-Related Weight Gain. *Neuropsychopharmacology* : official publication of the American College of Neuropsychopharmacology. 11. 272.

Heldin, P., Lin, C. Y., Kolliopoulos, C., Chen, Y. H., & Skandalis, S. S. (2019). Regulation of hyaluronan biosynthesis and clinical impact of excessive hyaluronan production. *Matrix biology: journal of the International Society for Matrix Biology*, *78-79*, 100–117

Hendry, S. H., Jones, E. G., Hockfield, S., & McKay, R. D. (1988). Neuronal populations stained with the monoclonal antibody Cat-301 in the mammalian cerebral cortex and thalamus. *The Journal of neuroscience : the official journal of the Society for Neuroscience*, *8*(2), 518–542.

Henquet C., Rosa A., Krabbendam L., Papiol S., Fananas L., Drukker M., Ramaekers J.G., van Os J (2006). An experimental study of catechol-o-methyltransferase Val158Met moderation of delta-9-tetrahydrocannabinol-induced effects on psychosis and cognition. *Neuropsychopharmacology*;31:2748–2757.

Hensch T. K. (2005). Critical period plasticity in local cortical circuits. *Nature reviews. Neuroscience*, *6*(11), 877–888.

Herman, J. P., & Larson, B. R. (2001). Differential regulation of forebrain glutamic acid decarboxylase mRNA expression by aging and stress. *Brain research*, *912*(1), 60–66.

Hernandez, I., & Sokolov, B. P. (2000). Abnormalities in 5-HT_{2A} receptor mRNA expression in frontal cortex of chronic elderly schizophrenics with varying histories of neuroleptic treatment. *Journal of neuroscience research*, *59*(2), 218–225.

Hindocha, C., Freeman, T. P., Schafer, G., Gardner, C., Bloomfield, M. A. P., Bramon, E., Morgan, C. J. A., & Curran, H. V. (2020). Acute effects of cannabinoids on addiction endophenotypes are moderated by genes encoding the CB1 receptor and FAAH enzyme. *Addiction biology*, *25*(3), e12762.

Hill, S. L., Shao, L., & Beasley, C. L. (2021). Diminished levels of the chemokine fractalkine in post-mortem prefrontal cortex in schizophrenia but not bipolar disorder. *The world journal of biological psychiatry : the official journal of the World Federation of Societies of Biological Psychiatry*, *22*(2), 94–103.

Hirayasu Y, Tanaka S, Shenton ME, Salisbury DF, DeSantis MA, Levitt JJ, Wible C, Yurgelun-Todd D, Kikinis R, Joleschizophrenia FA, McCarley RW (2001). Prefrontal gray matter volume reduction in first episode schizophrenia. *Cerebral Cortex,*11(4):374-81.

Ho, B. C., Andreasen, N. C., Nopoulos, P., Arndt, S., Magnotta, V., & Flaum, M. (2003). Progressive structural brain abnormalities and their relationship to clinical outcome: a longitudinal

magnetic resonance imaging study early in schizophrenia. *Archives of general psychiatry*, *60*(6), 585–594.

Hockfield, S., Tootell, R. B., & Zaremba, S. (1990). Molecular differences among neurons reveal an organization of human visual cortex. *Proceedings of the National Academy of Sciences of the United States of America*, *87*(8), 3027–3031.

Hockfield, S., & McKay, R. D. (1983). A surface antigen expressed by a subset of neurons in the vertebrate central nervous system. *Proceedings of the National Academy of Sciences of the United States of America*, *80*(18), 5758–5761.

Hodgkinson, C. A., Goldman, D., Jaeger, J., Persaud, S., Kane, J. M., Lipsky, R. H., & Malhotra, A. K. (2004). Disrupted in schizophrenia 1 (DISC1): association with schizophrenia, schizoaffective disorder, and bipolar disorder. *American journal of human genetics*, *75*(5), 862–872.

Hogarty GE, Flesher S, Ulrich R, Carter M, Greenwald D, Pogue-Geile M, Kechavan M, Cooley S, DiBarry AL, Garrett A, Parepally H, Zoretich R (2004). Cognitive enhancement therapy for schizophrenia: effects of a 2-year randomized trial on cognition and behavior. *Archives of general psychiatry*;61(9):866-76.

Hogarty, G. E., Kornblith, S. J., Greenwald, D., DiBarry, A. L., Cooley, S., Ulrich, R. F., Carter, M., & Flesher, S. (1997). Three-year trials of personal therapy among schizophrenic patients living with or independent of family, I: Description of study and effects on relapse rates. *The American journal of psychiatry*, *154*(11), 1504–1513.

Holt, D. J., Coombs, G., Zeidan, M. A., Goff, D. C., & Milad, M. R. (2012). Failure of neural responses to safety cues in schizophrenia. *Archives of general psychiatry*, *69*(9), 893–903.

Hong, T., Iwashita, K., & Shiraki, K. (2018). Viscosity Control of Protein Solution by Small Solutes: A Review. *Current protein & peptide science*, *19*(8), 746–758.

Hopgood, M. F., Clark, M. G., & Ballard, F. J. (1981). Stimulation by GCs of protein degradation in hepatocyte monolayers. *The Biochemical journal*, *196*(1), 33–40.

Horev, G., Ellegood, J., Lerch, J. P., Son, Y. E., Muthuswamy, L., Vogel, H., Krieger, A. M., Buja, A., Henkelman, R. M., Wigler, M., & Mills, A. A. (2011). Dosage-dependent phenotypes in models of 16p11.2 lesions found in autism. *Proceedings of the National Academy of Sciences of the United States of America*, *108*(41), 17076–17081.

Horga, G., Maia, T. V., Wang, P., Wang, Z., Marsh, R., & Peterson, B. S. (2011). Adaptation to conflict via context-driven anticipatory signals in the dorsomedial prefrontal cortex. *The Journal of neuroscience : the official journal of the Society for Neuroscience*, *31*(45), 16208–16216.

Horri-Hayashi, N., Sasagawa, T., Matsunaga, W., & Nishi, M. (2015). Development and Structural Variety of the Chondroitin Sulfate Proteoglycans-Contained Extracellular Matrix in the Mouse Brain. *Neural plasticity*, *2015*, 256389.

Horri-Hayashi, N., Okuda, H., Tatsumi, K., Ishizaka, S., Yoshikawa, M., & Wanaka, A. (2008). Localization of chondroitin sulfate proteoglycan versican in adult brain with special reference to large projection neurons. *Cell and tissue research*, *334*(2), 163–177.

Howell, M. D., Bailey, L. A., Cozart, M. A., Gannon, B. M., & Gottschall, P. E. (2015). Hippocampal administration of chondroitinase ABC increases plaque-adjacent synaptic marker

and diminishes amyloid burden in aged APPswe/PS1dE9 mice. *Acta neuropathological communications*, *3*, 54.

Howes, S. R., Dalley, J. W., Morrison, C. H., Robbins, T. W., & Everitt, B. J. (2000). Leftward shift in the acquisition of cocaine self-administration in isolation-reared rats: relationship to extracellular levels of dopamine, serotonin and glutamate in the nucleus accumbens and amygdala-striatal FOS expression. *Psychopharmacology*, 151(1), 55–63.

Howes, O. D., Montgomery, A. J., Asselin, M. C., Murray, R. M., Valli, I., Tabraham, P., Bramon-Bosch, E., Valmaggia, L., Johns, L., Broome, M., McGuire, P. K., & Grasby, P. M. (2009). Elevated striatal dopamine function linked to prodromal signs of schizophrenia. *Archives of general psychiatry*, *66*(1), 13–20.

Howes, O. D., & Onwordi, E. C. (2023). The synaptic hypothesis of schizophrenia version III: a master mechanism. *Molecular psychiatry*, 28(5), 1843–1856.

Hu H, Gan J, Jonas P (2014). Interneurons. Fast-spiking, parvalbumin^{+} GABAergic interneurons: from cellular design to microcircuit function. *Science* 1;345(6196):1255263.

Hu W, Zhang M, Czéh B, Flügge G, Zhang W (2010). Stress impairs GABAergic network function in the hippocampus by activating nongenomic GRs and affecting the integrity of the parvalbumin-expressing neuronal network. *Neuropsychopharmacology*;35(8):1693-707.

Huang, K. Y., & Lin, H. H. (2018). The Activation and Signaling Mechanisms of GPR56/ADGRG1 in Melanoma Cell. *Frontiers in oncology*, *8*, 304.

Huttenlocher, P. R., & Dabholkar, A. S. (1997). Regional differences in synaptogenesis in human cerebral cortex. *The Journal of comparative neurology*, *387*(2), 167–178.

Hunyadi, A., Gaál, B., Mateschizophrenia, C., Meschizophreniaar, Z., Morawski, M., Reimann, K., Lendvai, D., Alpar, A., Wéber, I., & Rácz, É. (2020). Distribution and classification of the extracellular matrix in the olfactory bulb. *Brain structure & function*, *225*(1), 321–344.

Huttenlocher P. R. (1979). Synaptic density in human frontal cortex - developmental changes and effects of aging. *Brain research*, *163*(2), 195–205.

Hynes, D., & Harvey, B. J. (2019). Dexamethasone reduces airway epithelial Cl- secretion by rapid non-genomic inhibition of KCNQ1, KCNN4 and KATP K+channels. *Steroids*, *151*, 108459.

Hylin, M. J., Orsi, S. A., Moore, A. N., & Dash, P. K. (2013). Disruption of the perineuronal net in the hippocampus or medial prefrontal cortex impairs fear conditioning. *Learning & memory (Cold Spring Harbor, N.Y.)*, *20*(5), 267–273.

Ibi, D., Nagai, T., Kitahara, Y., Mizoguchi, H., Koike, H., Shiraki, A., Takuma, K., Kamei, H., Noda, Y., Nitta, A., Nabeshima, T., Yoneda, Y., & Yamada, K. (2009). Neonatal polyI:C treatment in mice results in schizophrenia-like behavioral and neurochemical abnormalities in adulthood. *Neuroscience research*, *64*(3), 297–305.

Ichihara, A., & Tanaka, K. (1995). Roles of proteasomes in cell growth. *Molecular biology reports*, *21*(1), 49–52.

Impagnatiello, F., Guidotti, A. R., Pesold, C., Dwivedi, Y., Caruncho, H., Pisu, M. G., Uzunov, D. P., Smalheiser, N. R., Davis, J. M., Pandey, G. N., Pappas, G. D., Tueting, P., Sharma, R. P., & Costa, E. (1998). A decrease of reelin expression as a putative vulnerability factor in schizophrenia. *Proceedings of the National Academy of Sciences of the United States of America*, *95*(26), 15718–15723.

Inatani, M., Honjo, M., Otori, Y., Oohira, A., Kido, N., Tano, Y., Honda, Y., & Tanihara, H. (2001). Inhibitory effects of neurocan and phosphacan on neurite outgrowth from retinal ganglion cells in culture. *Investigative ophthalmology & visual science*, *42*(8), 1930–1938.

International Schizophrenia Consortium (2008). Rare chromosomal deletions and duplications increase risk of schizophrenia. *Nature*; 455(7210):237-41.

Ishmael, F. T., Fang, X., Houser, K. R., Pearce, K., Abdelmohsen, K., Zhan, M., Gorospe, M., & Stellato, C. (2011). The human GR as an RNA-binding protein: global analysis of GR-associated transcripts and identification of a target RNA motif. *Journal of immunology (Baltimore, Md. : 1950)*, *186*(2), 1189–1198.

Ito, H. T., Smith, S. E., Hsiao, E., & Patterson, P. H. (2010). Maternal immune activation alters nonspatial information processing in the hippocampus of the adult offspring. *Brain, behavior, and immunity*, *24*(6), 930–941.

Jaaro-Peled H. (2009). Gene models of schizophrenia: DISC1 mouse models. *Progress in brain research*, 179, 75–86.

Jaaro-Peled, H., Ayhan, Y., Pletnikov, M. V., & Sawa, A. (2010). Review of pathological hallmarks of schizophrenia: comparison of genetic models with patients and nongenetic models. *Schizophrenia bulletin*, 36(2), 301–313.

Jager P, Moore G, Calpin P, Durmishi X, Salgarella I, Menage L, Kita Y, Wang Y (2021). Dual midbrain and forebrain origins of thalamic inhibitory interneurons. *Elife*. Feb 1;10: e59272.

Janssen, I., Krabbendam, L., Bak, M., Hanssen, M., Vollebergh, W., de Graaf, R., & van Os, J. (2004). Childhood abuse as a risk factor for psychotic experiences. *Acta psychiatrica Scandinavica*, *109*(1), 38–45.

Jaworski, D. M., Kelly, G. M., & Hockfield, S. (1999). Intracranial injury acutely induces the expression of the secreted isoform of the CNS-specific hyaluronan-binding protein BEHAB/brevican. *Experimental neurology*, *157*(2), 327–337.

Joëls M. (2018). Corticosteroids and the brain. *The Journal of endocrinology*, *238*(3), R121–R130.

Joëls, M., & Krugers, H. J. (2007). LTP after stress: up or down?. *Neural plasticity*, *2007*, 93202.

Joëls, M., Pasricha, N., & Karst, H. (2013). The interplay between rapid and slow corticosteroid actions in brain. *European journal of pharmacology*, *719*(1-3), 44–52.

Joëls, M., Sarabdjitsingh, R. A., & Karst, H. (2012). Unraveling the time domains of corticosteroid hormone influences on brain activity: rapid, slow, and chronic modes. *Pharmacological reviews*, *64*(4), 901–938.

John, N., Krügel, H., Frischknecht, R., Smalla, K. H., Schultz, C., Kreutz, M. R., Gundelfinger, E. D., & Seidenbecher, C. I. (2006). Brevican-containing perineuronal nets of extracellular matrix in dissociated hippocampal primary cultures. *Molecular and cellular neurosciences*, *31*(4), 774–784.

Jones, P. B., Barnes, T. R., Davies, L., Dunn, G., Lloyd, H., Hayhurst, K. P., Murray, R. M., Markwick, A., & Lewis, S. W. (2006). Randomized controlled trial of the effect on Quality of Life of second- vs first-generation antipsychotic drugs in schizophrenia: Cost Utility of the Latest Antipsychotic Drugs in Schizophrenia Study (CUtLASS 1). *Archives of general psychiatry*, *63*(10), 1079–1087.

Joyce JN, Shane A, Lexow N, Winokur A, Casanova MF, Kleinman JE (1999). Serotonin uptake sites and serotonin receptors are altered in the limbic system of schizophrenics. *Neuropsychopharmacology*; 8(4):315-36.

Jung-Testas, I., & Baulieu, E. E. (1983). Inhibition of glucocorticosteroid action in cultured L-929 mouse fibroblasts by RU 486, a new anti-glucocorticosteroid of high affinity for the glucocorticosteroid receptor. *Experimental cell research*, *147*(1), 177–182.

Kähler, A. K., Djurovic, S., Rimol, L. M., Brown, A. A., Athanasiu, L., Jönsson, E. G., Hansen, T., Gústafsson, O., et al. (2011). Candidate gene analysis of the human natural killer-1 carbohydrate pathway and perineuronal nets in schizophrenia: B3GAT2 is associated with disease risk and cortical surface area. *Biological psychiatry*, *69*(1), 90–96.

Kaasinen, V., Någren, K., Hietala, J., Farde, L., & Rinne, J. O. (2001). Sex differences in extrastriatal dopamine d(2)-like receptors in the human brain. *The American journal of psychiatry*, *158*(2), 308–311.

Kaar, S. J., Angelescu, I., Marques, T. R., & Howes, O. D. (2019). Pre-frontal parvalbumin interneurons in schizophrenia: a meta-analysis of post-mortem studies. *Journal of neural transmission (Vienna, Austria : 1996)*, *126*(12), 1637–1651.

Kalinichev, M., Robbins, M. J., Hartfield, E. M., Maycox, P. R., Moore, S. H., Savage, K. M., Austin, N. E., & Jones, D. N. (2008). Comparison between intraperitoneal and subcutaneous phencyclidine administration in Sprague-Dawley rats: a locomotor activity and gene induction study. *Progress in neuro-psychopharmacology & biological psychiatry*, 32(2), 414–422.

Kang, M. J., Abdelmohsen, K., Hutchison, E. R., Mitchell, S. J., Grammatikakis, I., Guo, R., Noh, J. H., Martindale, J. L, et al. (2014). HuD regulates coding and noncoding RNA to induce APP→Aβ processing. *Cell reports*, *7*(5), 1401–1409

Kang, I., Harten, I. A., Chang, M. Y., Braun, K. R., Sheih, A., Nivison, M. P., Johnson, P. Y., Workman, G. et al. (2017). Versican Deficiency Significantly Reduces Lung Inflammatory Response Induced by Polyinosine-Polycytidylic Acid Stimulation. *The Journal of biological chemistry*, *292*(1), 51–63.

Kang, J. S., Kawakami, Y., Bekku, Y., Ninomiya, Y., Izpisúa Belmonte, J. C., & Oohashi, T. (2008). Molecular cloning and developmental expression of a hyaluronan and proteoglycan link protein gene, crtl1/hapln1, in zebrafish. *Zoological science*, *25*(9), 912–918.

Kamijo, Y., Soma, K., Nagai, T., Kurihara, K., & Ohwada, T. (2003). Acute massive pulmonary thromboembolism associated with risperidone and conventional phenothiazines. *Circulation journal : official journal of the Japanese Circulation Society*, *67*(1), 46–48.

Kano, M., & Hashimoto, K. (2009). Synapse elimination in the central nervous system. *Current opinion in neurobiology*, *19*(2), 154–161.

Karlsgodt, K. H., Sun, D., & Cannon, T. D. (2010). Structural and Functional Brain Abnormalities in Schizophrenia. *Current directions in psychological science*, *19*(4), 226–231.

Karin M (1998). New twists in gene regulation by GR: is DNA binding dispensable? *Cell*; 93(4):487-90.

Karst, H., Berger, S., Turiault, M., Tronche, F., Schütz, G., & Joëls, M. (2005). Mineralocorticoid receptors are indispensable for nongenomic modulation of hippocampal glutamate transmission

by corticosterone. *Proceedings of the National Academy of Sciences of the United States of America*, *102*(52), 19204–19207.

Karst, H., Karten, Y. J., Reichardt, H. M., de Kloet, E. R., Schütz, G., & Joëls, M. (2000). Corticosteroid actions in hippocampus require DNA binding of GR homodimers. *Nature neuroscience*, *3*(10), 977–978.

Karousou, E., Kamiryo, M., Skandalis, S. S., Ruusala, A., Asteriou, T., Passi, A., Yamashita, H., Hellman, U., Heldin, C. H., & Heldin, P. (2010). The activity of hyaluronan synthase 2 is regulated by dimerization and ubiquitination. *The Journal of biological chemistry*, *285*(31), 23647–23654.

Kassel, O., Sancono, A., Krätzschmar, J., Kreft, B., Stassen, M., & Cato, A. C. (2001). GCs inhibit MAP kinase via increased expression and decreased degradation of MKP-1. *The EMBO journal*, *20*(24), 7108–7116.

Karlsson, K., Lindahl, U., & Marklund, S. L. (1988). Binding of human extracellular superoxide dismutase C to sulphated glycosaminoglycans. *The Biochemical journal*, *256*(1), 29–33.

Kapur, S., Zipursky, R., Jones, C., Remington, G., & Houle, S. (2000). Relationship between dopamine D(2) occupancy, clinical response, and side effects: a double-blind PET study of first-episode schizophrenia. *The American journal of psychiatry*, *157*(4), 514–520.

Kaufman, D. L., Houser, C. R., & Tobin, A. J. (1991). Two forms of the gamma-aminobutyric acid synthetic enzyme glutamate decarboxylase have distinct intraneuronal distributions and cofactor interactions. *Journal of neurochemistry*, *56*(2), 720–723.

Keller, J. N., Hanni, K. B., & Markesbery, W. R. (2000). Impaired proteasome function in Alzheimer's disease. *Journal of neurochemistry*, *75*(1), 436–439.

Keller, J. N., Hanni, K. B., & Markesbery, W. R. (2000). Possible involvement of proteasome inhibition in aging: implications for oxidative stress. *Mechanisms of ageing and development*, *113*(1), 61–70.

Keller, J. N., Huang, F. F., Zhu, H., Yu, J., Ho, Y. S., & Kindy, T. S. (2000). Oxidative stress-associated impairment of proteasome activity during ischemia-reperfusion injury. *Journal of cerebral blood flow and metabolism : official journal of the International Society of Cerebral Blood Flow and Metabolism*, *20*(10), 1467–1473.

Kelly, J. G., García-Marín, V., Rudy, B., & Hawken, M. J. (2019). Densities and Laminar Distributions of Kv3.1b-, PV-, GABA-, and SMI-32-Immunoreactive Neurons in Macaque Area V1. *Cerebral cortex*,*29*(5), 1921–1937.

Keshavan, M. S., Anderson, S., & Pettegrew, J. W. (1994). Is schizophrenia due to excessive synaptic pruning in the prefrontal cortex? The Feinberg hypothesis revisited. *Journal of psychiatric research*, 28(3), 239–265.

Khashan, A. S., Abel, K. M., McNamee, R., Pedersen, M. G., Webb, R. T., Baker, P. N., Kenny, L. C., & Mortensen, P. B. (2008). Higher risk of offspring schizophrenia following antenatal maternal exposure to severe adverse life events. *Archives of general psychiatry*, *65*(2), 146–152.

Kim H, Ährlund-Richter S, Wang X, Deisseroth K, Carlén M (2016). Prefrontal Parvalbumin Neurons in Control of Attention. *Cell*; 164(1-2):208-218.

Kim YK, Furic L, Desgroseillers L, Maquat LE (2005). Mammalian Staufen1 recruits Upf1 to specific mRNA 3'UTRs so as to elicit mRNA decay. *Cell*;120(2):195-208.

Kim, M., Haney, J. R., Zhang, P., Hernandez, L. M., Wang, L. K., Perez-Cano, L., Loohuis, L. M. O., de la Torre-Ubieta, L., & Gandal, M. J. (2021). Brain gene co-expression networks link complement signaling with convergent synaptic pathology in schizophrenia. *Nature neuroscience*, 24(6), 799–809.

Kim KS, Kang Y, Choi SE, Kim JH, Kim HM, Sun B, Jun HS, Yoon JW (2002). Modulation of GC-induced GAD expression in pancreatic beta-cells by transcriptional activation of the GAD67 promoter and its possible effect on the development of diabetes. *Diabetes*;51(9):2764-72.

Kim, J. K., Xu, Y., Xu, X., Keene, D. R., Gurusiddappa, S., Liang, X., Wary, K. K., & Höök, M. (2005). A novel binding site in collagen type III for integrins alpha1beta1 and alpha2beta1. *The Journal of biological chemistry*, *280*(37), 32512–32520.

Kirschke E, Goswami D, Southworth D, Griffin PR, Agard DA (2014). GR function regulated by coordinated action of the Hsp90 and Hsp70 chaperone cycles. *Cell*;157(7):1685-97.

Kisselev, A. F., Akopian, T. N., Woo, K. M., & Goldberg, A. L. (1999). The sizes of peptides generated from protein by mammalian 26 and 20 S proteasomes. Implications for understanding the degradative mechanism and antigen presentation. *The Journal of biological chemistry*, *274*(6), 3363–3371.

Klimczak, P., Rizzo, A., Castillo-Gómez, E., Perez-Rando, M., Gramuntell, Y., Beltran, M., & Nacher, J. (2021). Parvalbumin Interneurons and Perineuronal Nets in the Hippocampus and Retrosplenial Cortex of Adult Male Mice After Early Social Isolation Stress and Perinatal NMDA Receptor Antagonist Treatment. *Frontiers in synaptic neuroscience*, *13*, 733989.

Klueva, J., Gundelfinger, E. D., Frischknecht, R. R., & Heine, M. (2014). Intracellular Ca^{2+} and not the extracellular matrix determines surface dynamics of AMPA-type glutamate receptors on aspiny neurons. *Philosophical transactions of the Royal Society of London. Series B, Biological sciences*, *369*(1654), 20130605.

Koren D, Seidman LJ, Harrison RH, Lyons MJ, Kremen WS, Caplan B, Goldstein JM, Faraone SV, Tsuang MT (1998). Factor structure of the Wisconsin Card Sorting Test: dimensions of deficit in schizophrenia. *Neuropsychology*;12(2):28

Komander D. (2009). The emerging complexity of protein ubiquitination. *Biochemical Society transactions*, *37*(Pt 5), 937–953.

Köppe, G., Brückner, G., Brauer, K., Härtig, W., & Bigl, V. (1997). Developmental patterns of proteoglycan-containing extracellular matrix in perineuronal nets and neuropil of the postnatal rat brain. *Cell and tissue research*, *288*(1), 33–41.

Korotkova T, Fuchs EC, Ponomarenko A, von Engelhardt J, Monyer H (2010). NMDA receptor ablation on parvalbumin-positive interneurons impairs hippocampal synchrony, spatial representations, and working memory. *Neuron*;68(3):557-69.

Koskinen, M. K., van Mourik, Y., Smit, A. B., Riga, D., & Spijker, S. (2020). From stress to depression: development of extracellular matrix-dependent cognitive impairment following social stress. *Scientific reports*, *10*(1), 17308.

Kretz, O., Schmid, W., Berger, S., & Gass, P. (2001). The mineralocorticoid receptor expression in the mouse CNS is conserved during development. *Neuroreport*, *12*(6), 1133–1137.

Krishnan, A., Nijmeijer, S., de Graaf, C., & Schiöth, H. B. (2016). Classification, Nomenclature, and Structural Aspects of Adhesion GPCRs. *Handbook of experimental pharmacology*, *234*, 15–41.

Krystal, J. H., Karper, L. P., Seibyl, J. P., Freeman, G. K., Delaney, R., Bremner, J. D., Heninger, G. R., Bowers, M. B., Jr, & Charney, D. S. (1994). Subanesthetic effects of the noncompetitive NMDA antagonist, ketamine, in humans. Psychotomimetic, perceptual, cognitive, and neuroendocrine responses. *Archives of general psychiatry*, *51*(3), 199–214.

Kuo, S. S., & Pogue-Geile, M. F. (2019). Variation in fourteen brain structure volumes in schizophrenia: A comprehensive meta-analysis of 246 studies. *Neuroscience and biobehavioral reviews*, *98*, 85–94.

Kwok, J. C., Carulli, D., & Fawcett, J. W. (2010). In vitro modeling of perineuronal nets: hyaluronan synthase and link protein are necessary for their formation and integrity. *Journal of neurochemistry*, *114*(5), 1447–1459

Kurokawa, T., Tsuda, M., & Sugino, Y. (1976). Purification and characterization of a lectin from Wistaria floribunda seeds. *The Journal of biological chemistry*, *251*(18), 5686–5693.

Kwok, J. C., Dick, G., Wang, D., & Fawcett, J. W. (2011). Extracellular matrix and perineuronal nets in CNS repair. *Developmental neurobiology*, *71*(11), 1073–1089.

Lang, D. J., Khorram, B., Goghari, V. M., Kopala, L. C., Vandorpe, R. A., Rui, Q., Smith, G. N., & Honer, W. G. (2006). Reduced anterior internal capsule and thalamic volumes in first-episode psychosis. *Schizophrenia research*, *87*(1-3), 89–99.

Lagerström, M. C., & Schiöth, H. B. (2008). Structural diversity of G protein-coupled receptors and significance for drug discovery. *Nature reviews. Drug discovery*, *7*(4), 339–357.

Laurent, U.B., Reed, R.K (1991). Turnover of hyaluronan in the tissues. *Advanced Drug Delivery Reviews*,7, 237-256.

Laruelle, M., Abi-Dargham, A., Casanova, M. F., Toti, R., Weinberger, D. R., & Kleinman, J. E. (1993). Selective abnormalities of prefrontal serotonergic receptors in schizophrenia. A postmortem study. *Archives of general psychiatry*, *50*(10), 810–818.

Laschizophrenialovschizophreniaky, I., Barabássy, Á., & Németh, G. (2021). Cariprazine, A Broad-Spectrum Antipsychotic for the Treatment of Schizophrenia: Pharmacology, Efficacy, and Safety. *Advances in therapy*, *38*(7), 3652–3673.

Lee H, Leamey CA, Sawatari A. Perineuronal nets play a role in regulating striatal function in the mouse. *PLoS One*. 2012;7(3):e32747.

Lee, J., & Lee, K. (2021). Parvalbumin-expressing GABAergic interneurons and perineuronal nets in the prelimbic and orbitofrontal cortices in association with basal anxiety-like behaviors in adult mice. *Behavioural brain research*, *398*, 112915.

Lendvai, D., Morawski, M., Négyessy, L., Gáti, G., Jäger, C., Baksa, G., Glaschizophrenia, T., Attems, J., Tanila, H., Arendt, T., Harkany, T., & Alpár, A. (2013). Neurochemical mapping of the human hippocampus reveals perisynaptic matrix around functional synapses in Alzheimer's disease. *Acta neuropathologica*, *125*(2), 215–229.

Lensjø KK, Christensen AC, Tennøe S, Fyhn M, Hafting T (2017). Differential Expression and Cell-Type Specificity of Perineuronal Nets in Hippocampus, Medial Entorhinal Cortex, and Visual Cortex Examined in the Rat and Mouse. *eNeuro* ;4(3): ENEURO.0379-16.2017.

Lemire, J. M., Chan, C. K., Bressler, S., Miller, J., LeBaron, R. G., & Wight, T. N. (2007). Interleukin-1beta selectively decreases the synthesis of versican by arterial smooth muscle cells. *Journal of cellular biochemistry*, *101*(3), 753–766.

Lensjø, K. K., Lepperød, M. E., Dick, G., Hafting, T., & Fyhn, M. (2017). Removal of Perineuronal Nets Unlocks Juvenile Plasticity Through Network Mechanisms of Decreased Inhibition and Increased Gamma Activity. *The Journal of neuroscience : the official journal of the Society for Neuroscience*, *37*(5), 1269–1283.

Leon, K., Cunningham, R. L., Riback, J. A., Feldman, E., Li, J., Sosnick, T. R., Zhao, M., Monk, K. R., & Araç, D. (2020). Structural basis for adhesion G protein-coupled receptor Gpr126 function. *Nature communications*, *11*(1), 194.

Leucht, S., Barnes, T. R., Kissling, W., Engel, R. R., Correll, C., & Kane, J. M. (2003). Relapse prevention in schizophrenia with new-generation antipsychotics: a systematic review and exploratory meta-analysis of randomized, controlled trials. *The American journal of psychiatry*, *160*(7), 1209–1222.

Leussis, M. P., Freund, N., Brenhouse, H. C., Thompson, B. S., & Andersen, S. L. (2012). Depressive-like behavior in adolescents after maternal separation: sex differences, controllability, and GABA. *Developmental neuroscience*, *34*(2-3), 210–217.

Leweke, F. M., Piomelli, D., Pahlisch, F., Muhl, D., Gerth, C. W., Hoyer, C., Klosterkötter, J., Hellmich, M., & Koethe, D. (2012). Cannabidiol enhances anandamide signaling and alleviates psychotic symptoms of schizophrenia. *Translational psychiatry*, *2*(3), e94

Lewis, D. A., Curley, A. A., Glausier, J. R., & Volk, D. W. (2012). Cortical parvalbumin interneurons and cognitive dysfunction in schizophrenia. *Trends in neurosciences*, *35*(1), 57–67.

Lubbers, B. R., Matos, M. R., Horn, A., Visser, E., Van der Loo, R. C., Gouwenberg, Y., Meerhoff, G. F., Frischknecht, R., Seidenbecher, C. I., Smit, A. B., Spijker, S., & van den Oever, M. C. (2016). The Extracellular Matrix Protein Brevican Limits Time-Dependent Enhancement of Cocaine Conditioned Place Preference. *Neuropsychopharmacology* : official publication of the American College of Neuropsychopharmacology, 41(7), 1907–1916.

Luo R, Jeong SJ, Yang A, Wen M, Saslowsky DE, Lencer WI, Araç D, Piao X (2014). Mechanism for adhesion G protein-coupled receptor GPR56-mediated RhoA activation induced by collagen III stimulation. *PLoS One*;9(6):e100043.

Li, R., Ma, X., Wang, G., Yang, J., & Wang, C. (2016). Why sex differences in schizophrenia?. *Journal of translational neuroscience*, *1*(1), 37–42.

Li, X., Zhou, W., & Yi, Z. (2022). A glimpse of gender differences in schizophrenia. *General psychiatry*, *35*(4), e100823.

Lieberman, J. A., Stroup, T. S., McEvoy, J. P., Swartz, M. S., Rosenheck, R. A., Perkins, D. O., Keefe, R. S., Davis, S. M., Davis, C. E., Lebowitz, B. D., Severe, J., Hsiao, J. K., & Clinical Antipsychotic Trials of Intervention Effectiveness (CATIE) Investigators (2005). Effectiveness of antipsychotic drugs in patients with chronic schizophrenia. *The New England journal of medicine*, *353*(12), 1209–1223.

Lin, L., Wang, J., Chan, C. K., & Chan, S. O. (2007). Localization of hyaluronan in the optic pathway of mouse embryos. *Neuroreport*, *18*(4), 355–358.

Lipina, T. V., Zai, C., Hlousek, D., Roder, J. C., & Wong, A. H. (2013). Maternal immune activation during gestation interacts with Disc1 point mutation to exacerbate schizophrenia-related behaviors in mice. *The Journal of neuroscience : the official journal of the Society for Neuroscience,* 33(18), 7654–7666.

Liu, D., Wu, H., Cui, S., & Zhao, Q. (2023). Comprehensive Optimization of Western Blotting. *Gels (Basel, Switzerland)*, *9*(8), 652.

Liu Y, Beyer A, Aebersold R (2016). On the Dependency of Cellular Protein Levels on mRNA Abundance. Cell. Apr 21;165(3):535-50.

Liu, J., Gao, H. Y., & Wang, X. F. (2015). The role of the Rho/ROCK signaling pathway in inhibiting axonal regeneration in the central nervous system. *Neural regeneration research*, *10*(11), 1892–1896.

Liu, H., Gao, P. F., Xu, H. W., Liu, M. M., Yu, T., Yao, J. P., & Yin, Z. Q. (2013). Perineuronal nets increase inhibitory GABAergic currents during the critical period in rats. *International journal of ophthalmology*, *6*(2), 120–125.

Liu WL, Lee YH, Tsai SY, Hsu CY, Sun YY, Yang LY, Tsai SH, Yang WC (2008). Methylprednisolone inhibits the expression of glial fibrillary acidic protein and chondroitin sulfate proteoglycans in reactivated astrocytes. *Glia*;56(13):1390-400.

Livak, K. J., & Schmittgen, T. D. (2001). Analysis of relative gene expression data using real-time quantitative PCR and the 2(-Delta Delta C(T)) Method. *Methods (San Diego, Calif.)*, *25*(4), 402–408.

Lodge, D. J., Behrens, M. M., & Grace, A. A. (2009). A loss of parvalbumin-containing interneurons is associated with diminished oscillatory activity in an animal model of schizophrenia. *The Journal of neuroscience : the official journal of the Society for Neuroscience*, *29*(8), 2344–2354.

Long KR, Newland B, Florio M, Kalebic N, Langen B, Kolterer A, Wimberger P, Huttner WB (2018). Extracellular Matrix Components HAPLN1, Lumican, and Collagen I Cause Hyaluronic Acid-Dependent Folding of the Developing Human Neocortex. *Neuron*; 99(4):702-719.e6.

Lu, N. Z., Wardell, S. E., Burnstein, K. L., Defranco, D., Fuller, P. J., Giguere, V., Hochberg, R. B., McKay, L., Renoir, J. M., Weigel, N. L., Wilson, E. M., McDonnell, D. P., & Cidlowski, J. A. (2006). International Union of Pharmacology. LXV. The pharmacology and classification of the nuclear receptor superfamily: GC, mineralocorticoid, progesterone, and androgen receptors. *Pharmacological reviews*, *58*(4), 782–797.

Luca, F., Maranville, J. C., Richards, A. L., Witonsky, D. B., Stephens, M., & Di Rienzo, A. (2013). Genetic, functional and molecular features of GR binding. *PloS one*, *8*(4), e61654.

Luchena, C., Zuazo-Ibarra, J., Valero, J., Matute, C., Alberdi, E., & Capetillo-Zarate, E. (2022). A Neuron, Microglia, and Astrocyte Triple Co-culture Model to Study Alzheimer's Disease. *Frontiers in aging neuroscience*, *14*, 844534.

Lupori, L., Totaro, V., Cornuti, S., Ciampi, L., Carrara, F., Grilli, E., Viglione, A., Tozzi, F., Putignano, E., Mazziotti, R., Amato, G., Gennaro, C., Tognini, P., & Pizzorusso, T. (2023). A comprehensive atlas of perineuronal net distribution and colocalization with parvalbumin in the adult mouse brain. *Cell reports*, *42*(7), 112788.

Lupien, S. J., Maheu, F., Tu, M., Fiocco, A., & Schramek, T. E. (2007). The effects of stress and stress hormones on human cognition: Implications for the field of brain and cognition. *Brain and cognition*, *65*(3), 209–237.

Lussier AL, Romay-Tallón R, Caruncho HJ, Kalynchuk LE (2013). Altered GABAergic and glutamatergic activity within the rat hippocampus and amygdala in rats subjected to repeated corticosterone administration but not restraint stress. *Neuroscience; 231:38*-48.

Macêdo, D. S., Araújo, D. P., Sampaio, L. R., Vasconcelos, S. M., Sales, P. M., Sousa, F. C., Hallak, J. E., Crippa, J. A., & Carvalho, A. F. (2012). Animal models of prenatal immune challenge and their contribution to the study of schizophrenia: a systematic review. *Brazilian journal of medical and biological research = Revista brasileira de pesquisas medicas e biologicas*, *45*(3), 179–186.

Marsden, C. A., King, M. V., & Fone, K. C. (2011). Influence of social isolation in the rat on serotonergic function and memory--relevance to models of schizophrenia and the role of 5-HT_6 receptors. *Neuropharmacology*, 61(3), 400–407.

Marín O. (2012). Interneuron dysfunction in psychiatric disorders. *Nature reviews. Neuroscience*, *13*(2), 107–120

Martin S, Henley JM, Holman D, Zhou M, Wiegert O, van Spronsen M, Joëls M, Hoogenraad CC, Krugers HJ (2009). Corticosterone alters AMPAR mobility and facilitates bidirectional synaptic plasticity. *PLoS One*; 4(3):e4714.

Maeda N. (2010). Structural variation of chondroitin sulfate and its roles in the central nervous system. *Central nervous system agents in medicinal chemistry*, *10*(1), 22–31.

Makinson, R., Lundgren, K. H., Seroogy, K. B., & Herman, J. P. (2015). Chronic social subordination stress modulates glutamic acid decarboxylase (GAD) 67 mRNA expression in central stress circuits. *Physiology & behavior*, *146*, 7–15.

Maleski M, Hockfield S (1997). Glial cells assemble hyaluronan-based pericellular matrices in vitro. *Glia*;20(3):193-202.

Mao, M. J., Yu, H. L., Wen, Y. Z., Sun, X. Y., Xu, C. Y., Gao, Y. Z., Jiang, M., Yuan, H. M., & Feng, S. W. (2022). Deficit of perineuronal net induced by maternal immune activation mediates the cognitive impairment in offspring during adolescence. *Behavioural brain research*, *434*, 114027.

Margolis RU, Margolis RK, Chang LB, Preti C (1975). Glycosaminoglycans of brain during development. Biochemistry. Jan 14;14(1):85-8.

Margolis, R. K., & Margolis, R. U. (1994). Nervous tissue proteoglycans. *EXS*, *70*, 145–177.

Magri, C., Giacopuzzi, E., La Via, L., Bonini, D., Ravasio, V., Elhussiny, M. E. A., Orizio, F., Gangemi, F., Valsecchi, P., Bresciani, R., Barbon, A., Vita, A., & Gennarelli, M. (2018). A novel homozygous mutation in GAD1 gene described in a schizophrenic patient impairs activity and dimerization of GAD67 enzyme. *Scientific reports*, *8*(1), 15470.

Marzoll, A., Nagy, N., Wördehoff, L., Dai, G., Fries, S., Lindner, V., Grosser, T., & Fischer, J. W. (2009). Cyclooxygenase inhibitors repress vascular hyaluronan-synthesis in murine atherosclerosis and neointimal thickening. *Journal of cellular and molecular medicine*, *13*(9B), 3713–3719.

Maher B. (2005). Delusional thinking and cognitive disorder. *Integrative physiological and behavioral science: the official journal of the Pavlovian Society*, *40*(3), 136–146.

Matsui, F., Watanabe, E., & Oohira, A. (1994). Immunological identification of two proteoglycan fragments derived from neurocan, a brain-specific chondroitin sulfate proteoglycan. *Neurochemistry international*, *25*(5), 425–431.

Maurel, P., Rauch, U., Flad, M., Margolis, R. K., & Margolis, R. U. (1994). Phosphacan, a chondroitin sulfate proteoglycan of brain that interacts with neurons and neural cell-adhesion molecules, is an extracellular variant of a receptor-type protein tyrosine phosphatase. *Proceedings of the National Academy of Sciences of the United States of America*, *91*(7), 2512–2516.

Mathalon, D. H., Sullivan, E. V., Lim, K. O., & Pfefferbaum, A. (2001). Progressive brain volume changes and the clinical course of schizophrenia in men: a longitudinal magnetic resonance imaging study. *Archives of general psychiatry*, *58*(2), 148–157.

Mauney, S. A., Athanas, K. M., Pantazopoulos, H., Shaskan, N., Passeri, E., Berretta, S., & Woo, T. U. (2013). Developmental pattern of perineuronal nets in the human prefrontal cortex and their deficit in schizophrenia. *Biological psychiatry*, *74*(6), 427–435.

Mayne, P., Das, J., Zou, S., Sullivan, R. K. P., & Burne, T. H. J. (2024). Perineuronal nets are associated with decision making under conditions of uncertainty in female but not male mice. *Behavioural brain research*, *461*, 114845.

Matthews, R. T., Kelly, G. M., Zerillo, C. A., Gray, G., Tiemeyer, M., & Hockfield, S. (2002). Aggrecan glycoforms contribute to the molecular heterogeneity of perineuronal nets. *The Journal of neuroscience: the official journal of the Society for Neuroscience*, *22*(17), 7536–7547.

Mazzoncini, R., Donoghue, K., Hart, J., Morgan, C., Doody, G. A., Dazzan, P., Jones, P. B., Morgan, K., Murray, R. M., & Fearon, P. (2010). Illicit substance use and its correlates in first episode psychosis. *Acta psychiatrica Scandinavica*, *121*(5), 351–358.

McCarley, R. W., Salisbury, D. F., Hirayasu, Y., Yurgelun-Todd, D. A., Tohen, M., Zarate, C., Kikinis, R., Joleschizophrenia, F. A., & Shenton, M. E. (2002). Association between smaller left posterior superior temporal gyrus volume on magnetic resonance imaging and smaller left temporal P300 amplitude in first-episode schizophrenia. *Archives of general psychiatry*, *59*(4), 321–331.

McCarthy, S. E., Makarov, V., Kirov, G., Addington, A. M., McClellan, J., Yoon, S., Perkins, D. O., Dickel, D. E., et al. (2009). Microduplications of 16p11.2 are associated with schizophrenia. *Nature genetics*, *41*(11), 1223–1227.

McDonald A. J. (1994). Calretinin immunoreactive neurons in the basolateral amygdala of the rat and monkey. *Brain research*, *667*(2), 238–242.

McDougall, A. R. A., Fosang, A. J., Faggian, J., Wallace, M. J., Crossley, K. J., Cole, T. J., & Hooper, S. B. (2018). GCs influence versican and chondroitin sulphate proteoglycan levels in the fetal sheep lung. *Respiratory research*, *19*(1), 155.

McEwen, B. S., Bowles, N. P., Gray, J. D., Hill, M. N., Hunter, R. G., Karatsoreos, I. N., & Nasca, C. (2015). Mechanisms of stress in the brain. *Nature neuroscience*, *18*(10), 1353–1363.

McGrath, J., Saha, S., Chant, D., & Welham, J. (2008). Schizophrenia: a concise overview of incidence, prevalence, and mortality. *Epidemiologic reviews*, *30*, 67–76.

McGlashan, T. H., & Hoffman, R. E. (2000). Schizophrenia as a disorder of developmentally reduced synaptic connectivity. *Archives of general psychiatry*, *57*(7), 637–648.

McGuire, P. K., Silbersweig, D. A., Wright, I., Murray, R. M., David, A. S., Frackowiak, R. S., & Frith, C. D. (1995). Abnormal monitoring of inner speech: a physiological basis for auditory hallucinations. *Lancet (London, England)*, *346*(8975), 596–600.

McGurk, S. R., Coleman, T., Harvey, P. D., Reichenberg, A., White, L., Friedman, J., Parrella, M., & Davis, K. L. (2004). Working memory performance in poor outcome schizophrenia: relationship to age and executive functioning. *Journal of clinical and experimental neuropsychology*, *26*(2), 153–160.

McKeon, R. J., Jurynec, M. J., & Buck, C. R. (1999). The chondroitin sulfate proteoglycans neurocan and phosphacan are expressed by reactive astrocytes in the chronic CNS glial scar. *The Journal of neuroscience : the official journal of the Society for Neuroscience*, *19*(24), 10778–10788.

McNaught, K. S., Belizaire, R., Isacson, O., Jenner, P., & Olanow, C. W. (2003). Altered proteasomal function in sporadic Parkinson's disease. *Experimental neurology*, *179*(1), 38–46.

McNaught, K. S., & Jenner, P. (2001). Proteasomal function is impaired in substantia nigra in Parkinson's disease. *Neuroscience letters*, *297*(3), 191–194.

McIntyre, C. K., McGaugh, J. L., & Williams, C. L. (2012). Interacting brain systems modulate memory consolidation. *Neuroscience and biobehavioral reviews*, *36*(7), 1750–1762.

McRae, P. A., & Porter, B. E. (2012). The perineuronal net component of the extracellular matrix in plasticity and epilepsy. *Neurochemistry international*, *61*(7), 963–972.

McRae, P. A., Rocco, M. M., Kelly, G., Brumberg, J. C., & Matthews, R. T. (2007). Sensory deprivation alters aggrecan and perineuronal net expression in the mouse barrel cortex. *The Journal of neuroscience : the official journal of the Society for Neuroscience*, *27*(20), 5405–5413.

McRae, N., Forgan, L., McNeill, B., Addinsall, A., McCulloch, D., Van der Poel, C., & Stupka, N. (2017). GCs Improve Myogenic Differentiation In Vitro by Suppressing the Synthesis of Versican, a Transitional Matrix Protein Overexpressed in Dystrophic Skeletal Muscles. *International journal of molecular sciences*, *18*(12), 2629.

McTeague, L. M., Goodkind, M. S., & Etkin, A. (2016). Transdiagnostic impairment of cognitive control in mental illness. *Journal of psychiatric research*, *83*, 37–46.

Meijer, O. C., Buurstede, J. C., & Schaaf, M. J. M. (2019). Corticosteroid Receptors in the Brain: Transcriptional Mechanisms for Specificity and Context-Dependent Effects. *Cellular and molecular neurobiology*, *39*(4), 539–549.

Melendez-Vasquez C, Carey DJ, Zanazzi G, Reizes O, Maurel P, Salzer JL (2005). Differential expression of proteoglycans at central and peripheral nodes of Ranvier. *Glia*;52(4):301-8.

Melkersson, K. I., Hulting, A. L., & Rane, A. J. (2001). Dose requirement and prolactin elevation of antipsychotics in male and female patients with schizophrenia or related psychoses. *British journal of clinical pharmacology*, *51*(4), 317–324.

Mendrek, A., Mancini-Marië, A., Fahim, C., & Stip, E. (2007). Sex differences in the cerebral function associated with processing of aversive stimuli by schizophrenia patients. *The Australian and New Zealand journal of psychiatry*, *41*(2), 136–141.

Mercadante AA, Tadi P (2023). Neuroanatomy, Gray Matter. In: StatPearls. Treasure Island (FL): StatPearls Publishing.

Mehić M, de Sa VK, Hebestreit S, Heldin CH, Heldin P (2017). The deubiquitinating enzymes USP4 and USP17 target hyaluronan synthase 2 and differentially affect its function. *Oncogenesis*;6(6):e348.

Meyer, C.E., Boroda, E. and Nick, T.A (2014). Sexually dimorphic perineuronal net expression in the songbird, Basal Ganglia,3(4), 229–237.

Meyer-Lindenberg, A., Miletich, R. S., Kohn, P. D., Esposito, G., Carson, R. E., Quarantelli, M., Weinberger, D. R., & Berman, K. F. (2002). Reduced prefrontal activity predicts exaggerated striatal dopaminergic function in schizophrenia*. Nature neuroscience*, 5(3), 267–271.

Meyer U. (2014). Prenatal poly(i:C) exposure and other developmental immune activation models in rodent systems. *Biological psychiatry*, *75*(4), 307–315.

Méschizophreniaár, Z., Girard, F., Saper, C. B., & Celio, M. R. (2012). The lateral hypothalamic parvalbumin-immunoreactive (PV1) nucleus in rodents. *The Journal of comparative neurology*, *520*(4), 798–815.

Miguel-Hidalgo, J. J., Hearn, E., Moulana, M., Saleem, K., Clark, A., Holmes, M., Wadhwa, K., Kelly, I., Stockmeier, C. A., & Rajkowska, G. (2023). Reduced length of nodes of Ranvier and altered proteoglycan immunoreactivity in prefrontal white matter in major depressive disorder and chronically stressed rats. *Scientific reports*, *13*(1), 16419.

Milara, J., Cervera, A., de Diego, A., Sanz, C., Juan, G., Gavaldà, A., Miralpeix, M., Morcillo, E., & Cortijo, J. (2016). Non-neuronal cholinergic system contributes to corticosteroid resistance in chronic obstructive pulmonary disease patients. *Respiratory research*, *17*(1), 145.

Milev, P., Maurel, P., Chiba, A., Mevissen, M., Popp, S., Yamaguchi, Y., Margolis, R. K., & Margolis, R. U. (1998). Differential regulation of expression of hyaluronan-binding proteoglycans in developing brain: aggrecan, versican, neurocan, and brevican. *Biochemical and biophysical research communications*, *247*(2), 207–212.

Miller, W. L., & Auchus, R. J. (2011). The molecular biology, biochemistry, and physiology of human steroidogenesis and its disorders. *Endocrine reviews*, *32*(1), 81–151

Mitani, T., Terashima, M., Yoshimura, H., Nariai, Y., & Tanigawa, Y. (2005). TGF-beta1 enhances degradation of IFN-gamma-induced iNOS protein via proteasomes in RAW 264.7 cells. *Nitric oxide : biology and chemistry*, *13*(1), 78–87.

Mi Y, Wang W, Zhang C, Liu C, Lu J, Li W, Zuo R, Myatt L, Sun K (2017). Autophagic Degradation of Collagen 1A1 by Cortisol in Human Amnion Fibroblasts. *Endocrinology*;158(4):1005-1014.

Minamitani, T., Ikuta, T., Saito, Y., Takebe, G., Sato, M., Sawa, H., Nishimura, T., Nakamura, F., Takahashi, K., Ariga, H., & Matsumoto, K. (2004). Modulation of collagen fibrillogenesis by tenascin-X and type VI collagen. *Experimental cell research*, *298*(1), 305–315.

Mishra, P., Pandey, C. M., Singh, U., Gupta, A., Sahu, C., & Keshri, A. (2019). Descriptive statistics and normality tests for statistical data. Annals of cardiac anaesthesia, 22(1), 67–72.

Miyata S, Nishimura Y, Hayashi N, Oohira A (2005). Construction of perineuronal net-like structure by cortical neurons in culture. *Neuroscience*;136(1):95-104.

Mohan, V., Wyatt, E. V., Gotthard, I., Phend, K. D., Diestel, S., Duncan, B. W., Weinberg, R. J., Tripathy, A., & Maness, P. F. (2018). Neurocan Inhibits Semaphorin 3F Induced Dendritic Spine Remodeling Through NrCAM in Cortical Neurons. *Frontiers in cellular neuroscience*, *12*, 346.

Moilanen, J., Haapea, M., Miettunen, J., Jääskeläinen, E., Veijola, J., Isohanni, M., & Koponen, H. (2013). Characteristics of subjects with schizophrenia spectrum disorder with and without antipsychotic medication - a 10-year follow-up of the Northern Finland 1966 Birth Cohort study. *European psychiatry : the journal of the Association of European Psychiatrists*, *28*(1), 53–58.

Monk KR, Naylor SG, Glenn TD, Mercurio S, Perlin JR, Dominguez C, Moens CB, Talbot WS (2009). A G protein-coupled receptor is essential for Schwann cells to initiate myelination. *Science*;325(5946):1402-5.

Moon, L. D., Asher, R. A., Rhodes, K. E., & Fawcett, J. W. (2002). Relationship between sprouting axons, proteoglycans and glial cells following unilateral nigrostriatal axotomy in the adult rat. *Neuroscience*, *109*(1), 101–117.

Moore, H., Jentsch, J. D., Ghajarnia, M., Geyer, M. A., & Grace, A. A. (2006). A neurobehavioral systems analysis of adult rats exposed to methylazoxymethanol acetate on E17: implications for the neuropathology of schizophrenia. *Biological psychiatry*, *60*(3), 253–264.

Morikawa, S., Ikegaya, Y., Narita, M., & Tamura, H. (2017). Activation of perineuronal net-expressing excitatory neurons during associative memory encoding and retrieval. *Scientific reports*, *7*, 46024.

Morishita, H., Cabungcal, J. H., Chen, Y., Do, K. Q., & Hensch, T. K. (2015). Prolonged Period of Cortical Plasticity upon Redox Dysregulation in Fast-Spiking Interneurons. *Biological psychiatry*, *78*(6), 396–402.

Morawski, M., Brückner, M. K., Riederer, P., Brückner, G., & Arendt, T. (2004). Perineuronal nets potentially protect against oxidative stress. *Experimental neurology*, *188*(2), 309–315.

Morawski, M., Dityatev, A., Hartlage-Rübsamen, M., Blosa, M., Holzer, M., Flach, K., Pavlica, S., Dityateva, G., Grosche, J., Brückner, G., & Schachner, M. (2014). Tenascin-R promotes assembly of the extracellular matrix of perineuronal nets via clustering of aggrecan. *Philosophical transactions of the Royal Society of London. Series B, Biological sciences*, *369*(1654), 20140046.

Mordelt, A., & de Witte, L. D. (2023). Microglia-mediated synaptic pruning as a key deficit in neurodevelopmental disorders: Hype or hope?. *Current opinion in neurobiology*, *79*, 102674.

Morsink, M. C., Steenbergen, P. J., Vos, J. B., Karst, H., Joëls, M., De Kloet, E. R., & Datson, N. A. (2006). Acute activation of hippocampal GRs results in different waves of gene expression throughout time. *Journal of neuroendocrinology*, *18*(4), 239–252

Moyer, C. E., Delevich, K. M., Fish, K. N., Asafu-Adjei, J. K., Sampson, A. R., Dorph-Petersen, K. A., Lewis, D. A., & Sweet, R. A. (2012). Reduced glutamate decarboxylase 65 protein within primary auditory cortex inhibitory boutons in schizophrenia. *Biological psychiatry*, *72*(9), 734–743.

Mühleisen, T. W., Mattheisen, M., Strohmaier, J., Degenhardt, F., Priebe, L., Schultz, C. C., Breuer, R., Meier, S., et al. (2012). Association between schizophrenia and common variation in neurocan (NCAN), a genetic risk factor for bipolar disorder. *Schizophrenia research*, *138*(1), 69–73.

Muazzen, Z., Moghrabi, W., Bakheet, T., Mahmoud, L., Al-Saif, M., Khabar, K. S. A., & Hitti, E. G. (2024). Global analysis of the abundance of AU-rich mRNAs in response to GC treatment. *Scientific reports*, *14*(1), 913.

Mueller, A. L., Davis, A., Sovich, S., Carlson, S. S., & Robinson, F. R. (2016). Distribution of N-Acetylgalactosamine-Positive Perineuronal Nets in the Macaque Brain: Anatomy and Implications. *Neural plasticity*, *2016*, 6021428.

Mufson EJ, Mahady L, Waters D, Counts SE, Perez SE, DeKosky ST, Ginsberg SD, Ikonomovic MD, Scheff SW, Binder LI (2015). Hippocampal plasticity during the progression of Alzheimer's disease. *Neuroscience*; 309:51-67.

Mühleisen, T. W., Mattheisen, M., Strohmaier, J., Degenhardt, F., Priebe, L., Schultz, C. C., Breuer, R., Meier, S., Hoffmann, P., GROUP Investigators, Rivandeneira, F., Hofman, A., Uitterlinden, A. G., Moebus, S., Gieger, C., Emeny, R., Ladwig, K. H., Wichmann, H. E., Schwarz, M., Kammerer-Ciernioch, J., … Cichon, S. (2012). Association between schizophrenia and common variation in neurocan (NCAN), a genetic risk factor for bipolar disorder. *Schizophrenia research*, *138*(1), 69–73.

Muzikar, K. A., Nickols, N. G., & Dervan, P. B. (2009). Repression of DNA-binding dependent GR-mediated gene expression. *Proceedings of the National Academy of Sciences of the United States of America*, *106*(39), 16598–16603.

Mukherjee, N., Nandi, S., Garg, S., Ghosh, S., Ghosh, S., Samat, R., & Ghosh, S. (2020). Targeting Chondroitin Sulfate Proteoglycans: An Emerging Therapeutic Strategy to Treat CNS Injury. *ACS chemical neuroscience*, *11*(3), 231–232.

Munck, A., Guyre, P. M., & Holbrook, N. J. (1984). Physiological functions of GCs in stress and their relation to pharmacological actions. *Endocrine reviews*, *5*(1), 25–44.

Murthy, S., Kane, G. A., Katchur, N. J., Lara Mejia, P. S., Obiofuma, G., Buschman, T. J., McEwen, B. S., & Gould, E. (2019). Perineuronal Nets, Inhibitory Interneurons, and Anxiety-Related Ventral Hippocampal Neuronal Oscillations Are Altered by Early Life Adversity. *Biological psychiatry*, *85*(12), 1011–1020.

Musazzi L, Milanese M, Farisello P, Zappettini S, Tardito D, Barbiero VS, Bonifacino T, Mallei A, et al (2010). Acute stress increases depolarization-evoked glutamate release in the rat prefrontal/frontal cortex: the dampening action of antidepressants. *PLoS One*; 5(1): e8566.

Naber D, Lambert M (2009). The CATIE and CUtLASS studies in schizophrenia: results and implications for clinicians. *CNS Drugs*; 23(8):649-59

Nahar, L., Delacroix, B. M., & Nam, H. W. (2021). The Role of Parvalbumin Interneurons in Neurotransmitter Balance and Neurological Disease. *Frontiers in psychiatry*, *12*, 679960.

Narr, K. L., Bilder, R. M., Woods, R. P., Thompson, P. M., Robinson, D., Ballmaier, M., Messenger, B., Wang, Y., & Toga, A. W. (2006). Regional specificity of cerebrospinal fluid abnormalities in first episode schizophrenia. *Psychiatry research*, *146*(1), 21–33.

Narr, K., Thompson, P., Sharma, T., Moussai, J., Zoumalan, C., Rayman, J., & Toga, A. (2001). Three-dimensional mapping of gyral shape and cortical surface asymmetries in schizophrenia: gender effects. *The American journal of psychiatry*, *158*(2), 244–255.

Nassar, M., Simonnet, J., Lofredi, R., Cohen, I., Savary, E., Yanagawa, Y., Miles, R., & Fricker, D. (2015). Diversity and overlap of parvalbumin and somatostatin expressing interneurons in mouse presubiculum. *Frontiers in neural circuits*, *9*, 20.

National Center for Biotechnology Information (2024). PubChem Compound Summary for CID 5744, Hydrocortisone Acetate.

Necela, B. M., & Cidlowski, J. A. (2004). Mechanisms of GR action in noninflammatory and inflammatory cells. *Proceedings of the American Thoracic Society*, *1*(3), 239–246.

Nelson, M. D., Saykin, A. J., Flashman, L. A., & Riordan, H. J. (1998). Hippocampal volume reduction in schizophrenia as assessed by magnetic resonance imaging: a meta-analytic study. *Archives of general psychiatry*, *55*(5), 433–440.

Neulinger, K., Oram, J., Tinson, H., O'Gorman, J., & Shum, D. H. (2016). Prospective memory and frontal lobe function. *Neuropsychology, development, and cognition. Section B, Aging, neuropsychology and cognition*, *23*(2), 171–183.

Nishida, Y., Knudson, C. B., Nietfeld, J. J., Margulis, A., & Knudson, W. (1999). Antisense inhibition of hyaluronan synthase-2 in human articular chondrocytes inhibits proteoglycan retention and matrix assembly. *The Journal of biological chemistry*, *274*(31), 21893–21899.

Nishizawa, S., Benkelfat, C., Young, S. N., Leyton, M., Mzengeza, S., de Montigny, C., Blier, P., & Diksic, M. (1997). Differences between males and females in rates of serotonin synthesis in human brain. *Proceedings of the National Academy of Sciences of the United States of America*, *94*(10), 5308–5313.

Niu, L., Matsui, M., Zhou, S. Y., Hagino, H., Takahashi, T., Yoneyama, E., Kawasaki, Y., Suzuki, M., Seto, H., Ono, T., & Kurachi, M. (2004). Volume reduction of the amygdala in patients with schizophrenia: a magnetic resonance imaging study. *Psychiatry research*, *132*(1), 41–51.

Nowak, B., Zadrożna, M., Ossowska, G., Sowa-Kućma, M., Gruca, P., Papp, M., Dybała, M., Pilc, A., & Nowak, G. (2010). Alterations in hippocampal calcium-binding neurons induced by stress models of depression: a preliminary assessment. *Pharmacological reports : PR*, *62*(6), 1204–1210.

Nowicka, D., Soulsby, S., Skangiel-Kramska, J., & Glazewski, S. (2009). Parvalbumin-containing neurons, perineuronal nets and experience-dependent plasticity in murine barrel cortex. *The European journal of neuroscience*, *30*(11), 2053–2063.

Nudmamud-Thanoi, S., & Reynolds, G. P. (2004). The NR1 subunit of the glutamate/NMDA receptor in the superior temporal cortex in schizophrenia and affective disorders. *Neuroscience letters*, *372*(1-2), 173–177.

Nullmeier, S., Elmers, C., D'Hanis, W., Sandhu, K. V. K., Stork, O., Yanagawa, Y., Panther, P., & Schwegler, H. (2020). Glutamic acid decarboxylase 67 haplodeficiency in mice: consequences of postweaning social isolation on behavior and changes in brain neurochemical systems. *Brain structure & function*, *225*(6), 1719–1742.

O'Connell, K. S., Sønderby, I. E., Frei, O., van der Meer, D., Athanasiu, L., Smeland, O. B., Alnæs, D., Kaufmann, T., Westlye, L. T., Steen, V. M., Andreassen, O. A., Hughes, T., & Djurovic, S. (2021). Association between complement component 4A expression, cognitive performance and brain imaging measures in UK Biobank. *Psychological medicine*, 52(15), 1–11.

Obata K. (2013). Synaptic inhibition and γ-aminobutyric acid in the mammalian central nervous system. *Proceedings of the Japan Academy. Series B, Physical and biological sciences*, *89*(4), 139–156.

O'Gorman, R. L., Michels, L., Edden, R. A., Murdoch, J. B., & Martin, E. (2011). In vivo detection of GABA and glutamate with MEGA-PRESS: reproducibility and gender effects. *Journal of magnetic resonance imaging: JMRI*, *33*(5), 1262–1267.

Ohtomo, R., Iwata, A., & Arai, K. (2018). Molecular Mechanisms of Oligodendrocyte Regeneration in White Matter-Related Diseases. *International journal of molecular sciences*, *19*(6), 1743.

Ojima, H., Sakai, M., & Ohyama, J. (1998). Molecular heterogeneity of Vicia villosa-recognized perineuronal nets surrounding pyramidal and nonpyramidal neurons in the guinea pig cerebral cortex. *Brain research*, *786*(1-2), 274–280.

Okamoto, M., Sakiyama, J., Kurazono, S., Mori, S., Nakata, Y., Nakaya, N., & Oohira, A. (2001). Developmentally regulated expression of brain-specific chondroitin sulfate proteoglycans, neurocan and phosphacan, in the postnatal rat hippocampus. *Cell and tissue research*, *306*(2), 217–229.

Olabi, B., Ellison-Wright, I., McIntosh, A. M., Wood, S. J., Bullmore, E., & Lawrie, S. M. (2011). Are there progressive brain changes in schizophrenia? A meta-analysis of structural magnetic resonance imaging studies. *Biological psychiatry*, *70*(1), 88–96.

Onitsuka, T., Shenton, M. E., Salisbury, D. F., Dickey, C. C., Kasai, K., Toner, S. K., Frumin, M., Kikinis, R., Joleschizophrenia, F. A., & McCarley, R. W. (2004). Middle and inferior temporal gyrus gray matter volume abnormalities in chronic schizophrenia: an MRI study. *The American journal of psychiatry*, *161*(9), 1603–1611.

Oni-Orisan, A., Kristiansen, L. V., Haroutunian, V., Meador-Woodruff, J. H., & McCullumsmith, R. E. (2008). Altered vesicular glutamate transporter expression in the anterior cingulate cortex in schizophrenia. *Biological psychiatry*, 63(8), 766–775.

Oohashi, T., Edamatsu, M., Bekku, Y., & Carulli, D. (2015). The hyaluronan and proteoglycan link proteins: Organizers of the brain extracellular matrix and key molecules for neuronal function and plasticity. *Experimental neurology*, *274*(Pt B), 134–144.

Oohashi, T., Hirakawa, S., Bekku, Y., Rauch, U., Zimmermann, D. R., Su, W. D., Ohtsuka, A., Murakami, T., & Ninomiya, Y. (2002). Bral1, a brain-specific link protein, colocalizing with the versican V2 isoform at the nodes of Ranvier in developing and adult mouse central nervous systems. *Molecular and cellular neurosciences*, *19*(1), 43–57.

Ohira, K., Takeuchi, R., Iwanaga, T., & Miyakawa, T. (2013). Chronic fluoxetine treatment reduces parvalbumin expression and perineuronal nets in gamma-aminobutyric acidergic interneurons of the frontal cortex in adult mice. *Molecular brain*, *6*, 43.

Oohira A, Matsui F, Watanabe E, Kushima Y, Maeda N (1994). Developmentally regulated expression of a brain specific species of chondroitin sulfate proteoglycan, neurocan, identified with a monoclonal antibody IG2 in the rat cerebrum. *Neuroscience*;60(1):145-57.

Orchinik M, Murray TF, Moore FL (1991). A corticosteroid receptor in neuronal membranes. *Science*;252(5014):1848-51.

Orlando, C., Ster, J., Gerber, U., Fawcett, J. W., & Raineteau, O. (2012). Perisynaptic chondroitin sulfate proteoglycans restrict structural plasticity in an integrin-dependent manner. *The Journal of neuroscience : the official journal of the Society for Neuroscience*, *32*(50), 18009–18017a.

Orendain-Jaime, E. N., Ortega-Ibarra, J. M., & López-Pérez, S. J. (2016). Evidence of sexual dimorphism in D1 and D2 dopaminergic receptors expression in frontal cortex and striatum of young rats. *Neurochemistry international*, *100*, 62–66.

Oster, H., Challet, E., Ott, V., Arvat, E., de Kloet, E. R., Dijk, D. J., Lightman, S., Vgontzas, A., & Van Cauter, E. (2017). The Functional and Clinical Significance of the 24-Hour Rhythm of Circulating GCs. *Endocrine reviews*, *38*(1), 3–45.

Owen, M. J., Sawa, A., & Mortensen, P. B. (2016). Schizophrenia. *Lancet (London, England)*, *388*(10039), 86–97.

Ozawa, K., Hashimoto, K., Kishimoto, T., Shimizu, E., Ishikura, H., & Iyo, M. (2006). Immune activation during pregnancy in mice leads to dopaminergic hyperfunction and cognitive impairment in the offspring: a neurodevelopmental animal model of schizophrenia. *Biological psychiatry*, *59*(6), 546–554.

Pacifici, R. E., Kono, Y., & Davies, K. J. (1993). Hydrophobicity as the signal for selective degradation of hydroxyl radical-modified hemoglobin by the multicatalytic proteinase complex, proteasome. *The Journal of biological chemistry*, *268*(21), 15405–15411.

Pacifici, R. E., Salo, D. C., & Davies, K. J. (1989). Macroxyproteinase (M.O.P.): a 670 kDa proteinase complex that degrades oxidatively denatured proteins in red blood cells. *Free radical biology & medicine*, *7*(5), 521–536.

Page CE, Coutellier L (2018). Adolescent Stress Disrupts the Maturation of Anxiety-related Behaviors and Alters the Developmental Trajectory of the Prefrontal Cortex in a Sex- and Age-specific Manner. Neuroscience;390:265-277.

Park, O. H., Park, J., Yu, M., An, H. T., Ko, J., & Kim, Y. K. (2016). Identification and molecular characterization of cellular factors required for GR-mediated mRNA decay. *Genes & development*, *30*(18), 2093–2105.

Parker, A., & Gaffan, D. (1998). Memory after frontal/temporal disconnection in monkeys: conditional and non-conditional tasks, unilateral and bilateral frontal lesions. *Neuropsychologia*, *36*(3), 259–271.

Patel, D. C., Tewari, B. P., Chaunsali, L., & Sontheimer, H. (2019). Neuron-glia interactions in the pathophysiology of epilepsy. *Nature reviews. Neuroscience*, *20*(5), 282–297.

Patel, K. R., Cherian, J., Gohil, K., & Atkinson, D. (2014). Schizophrenia: overview and treatment options. *P & T : a peer-reviewed journal for formulary management*, *39*(9), 638–645.

Panettieri, R. A., Schaafsma, D., Amrani, Y., Koziol-White, C., Ostrom, R., & Tliba, O. (2019). Non-genomic Effects of GCs: An Updated View. *Trends in pharmacological sciences*, *40*(1), 38–49.

Pantazopoulos, H., & Berretta, S. (2016). In Sickness and in Health: Perineuronal Nets and Synaptic Plasticity in Psychiatric Disorders. *Neural plasticity*, *2016*, 9847696.

Pantazopoulos, H., Lange, N., Hassinger, L., & Berretta, S. (2006). Subpopulations of neurons expressing parvalbumin in the human amygdala. *The Journal of comparative neurology*, *496*(5), 706–722.

Pantazopoulos, H., Boyer-Boiteau, A., Holbrook, E. H., Jang, W., Hahn, C. G., Arnold, S. E., & Berretta, S. (2013). Proteoglycan abnormalities in olfactory epithelium tissue from subjects diagnosed with schizophrenia. *Schizophrenia research*, *150*(2-3), 366–372.

Pantazopoulos, H., Lange, N., Baldessarini, R. J., & Berretta, S. (2007). Parvalbumin neurons in the entorhinal cortex of subjects diagnosed with bipolar disorder or schizophrenia. *Biological psychiatry*, *61*(5), 640–652.

Pantazopoulos, H., Katsel, P., Haroutunian, V., Chelini, G., Klengel, T., & Berretta, S. (2021). Molecular signature of extracellular matrix pathology in schizophrenia. *The European journal of neuroscience*, *53*(12), 3960–3987.

Pantazopoulos, H., Markota, M., Jaquet, F., Ghosh, D., Wallin, A., Santos, A., Caterson, B., & Berretta, S. (2015). Aggrecan and chondroitin-6-sulfate abnormalities in schizophrenia and bipolar disorder: a postmortem study on the amygdala. *Translational psychiatry*, *5*(1), e496.

Pantazopoulos, H., Murray, E. A., & Berretta, S. (2008). Total number, distribution, and phenotype of cells expressing chondroitin sulfate proteoglycans in the normal human amygdala. *Brain research*, *1207*, 84–95.

Pantazopoulos, H., Woo, T. U., Lim, M. P., Lange, N., & Berretta, S. (2010). Extracellular matrix-glial abnormalities in the amygdala and entorhinal cortex of subjects diagnosed with schizophrenia. *Archives of general psychiatry*, *67*(2), 155–166.

Pavlides C, Nivón LG, McEwen BS (2002). Effects of chronic stress on hippocampal long-term potentiation. *Hippocampus,* 12(2):245-57.

Pavlides, C., & McEwen, B. S. (1999). Effects of mineralocorticoid and GRs on long-term potentiation in the CA3 hippocampal field. *Brain research*, *851*(1-2), 204–214.

Paul, S. M., Yohn, S. E., Popiolek, M., Miller, A. C., & Felder, C. C. (2022). Muscarinic Acetylcholine Receptor Agonists as Novel Treatments for Schizophrenia. *The American journal of psychiatry*, 179(9), 611–627.

Pawley, L. C., Hueston, C. M., O'Leary, J. D., Kozareva, D. A., Cryan, J. F., O'Leary, O. F., & Nolan, Y. M. (2020). Chronic intrahippocampal interleukin-1β overexpression in adolescence impairs hippocampal neurogenesis but not neurogenesis-associated cognition. *Brain, behavior, and immunity*, *83*, 172–179.

Peeters, P. J., Fierens, F. L., van den Wyngaert, I., Goehlmann, H. W., Swagemakers, S. M., Kass, S. U., Langlois, X., Pullan, S., Stenzel-Poore, M. P., & Steckler, T. (2004). Gene expression profiles highlight adaptive brain mechanisms in corticotropin releasing factor overexpressing mice. *Brain research. Molecular brain research*, *129*(1-2), 135–150.

Pemmari, A., Leppänen, T., Hämäläinen, M., Moilanen, T., Vuolteenaho, K., & Moilanen, E. (2020). Widespread regulation of gene expression by GCs in chondrocytes from patients with osteoarthritis as determined by RNA-Seq. *Arthritis research & therapy*, *22*(1), 271.

Penschuck, S., Flagstad, P., Didriksen, M., Leist, M., & Michael-Titus, A. T. (2006). Decrease in parvalbumin-expressing neurons in the hippocampus and increased phencyclidine-induced locomotor activity in the rat methylazoxymethanol (MAM) model of schizophrenia. *The European journal of neuroscience*, *23*(1), 279–284.

Pena-Bravo J. I., Penrod R., Reichel C. M., Lavin A. (2019). Methamphetamine Self-Administration Elicits Sex-Related Changes in Postsynaptic Glutamate Transmission in the Prefrontal Cortex. eneuro, 6, (1), *ENEURO*.0401–18.201

Pesarico, A. P., Bueno-Fernandez, C., Guirado, R., Gómez-Climent, M. Á., Curto, Y., Carceller, H., & Nacher, J. (2019). Chronic Stress Modulates Interneuronal Plasticity: Effects on PSA-NCAM and Perineuronal Nets in Cortical and Extracortical Regions. *Frontiers in cellular neuroscience*, *13*, 197.

Petrasch-Parwez, E., Schöbel, A., Benali, A., Moinfar, Z., Förster, E., Brüne, M., & Juckel, G. (2020). Lateralization of increased density of Iba1-immunopositive microglial cells in the anterior midcingulate cortex of schizophrenia and bipolar disorder. *European archives of psychiatry and clinical neuroscience*, *270*(7), 819–828.

Pesheva, P., & Probstmeier, R. (2000). The yin and yang of tenascin-R in CNS development and pathology. *Progress in neurobiology*, *61*(5), 465–493.

Pesheva, P., Probstmeier, R., Skubitz, A. P., McCarthy, J. B., Furcht, L. T., & Schachner, M. (1994). Tenascin-R (J1 160/180 inhibits fibronectin-mediated cell adhesion--functional relatedness to tenascin-C. *Journal of cell science*, *107 (Pt 8)*, 2323–2333.

Pepi, C., Mercier, M., Salimbene, L., Galati, C., Specchio, N., & de Palma, L. (2024). Post-Traumatic Stress-Disorder in Epilepsy: Meta-analysis of current evidence. *Epilepsy & behavior : E&B*, *157*, 109833.

Piao X, Hill RS, Bodell A, Chang BS, Basel-Vanagaite L, Straussberg R, Dobyns WB, Qasrawi B, et al (2004). G protein-coupled receptor-dependent development of human frontal cortex. *Science*; 303(5666):2033-6.

Piechota, M., Korostynski, M., Golda, S., Ficek, J., Jantas, D., Barbara, Z., & Przewlocki, R. (2017). Transcriptional signatures of steroid hormones in the striatal neurons and astrocytes. *BMC neuroscience*, *18*(1), 37.

Pierri, J. N., Volk, C. L., Auh, S., Sampson, A., & Lewis, D. A. (2001). Decreased somal size of deep layer 3 pyramidal neurons in the prefrontal cortex of subjects with schizophrenia. *Archives of general psychiatry*, *58*(5), 466–473.

Pietersen, C. Y., Mauney, S. A., Kim, S. S., Lim, M. P., Rooney, R. J., Goldstein, J. M., Petryshen, T. L., Seidman, L. J., Shenton, M. E., McCarley, R. W., Sonntag, K. C., & Woo, T. U. (2014). Molecular profiles of pyramidal neurons in the superior temporal cortex in schizophrenia. *Journal of neurogenetics*, *28*(1-2), 53–69.

Pinault D. (2008). N-methyl d-aspartate receptor antagonists ketamine and MK-801 induce wake-related aberrant gamma oscillations in the rat neocortex. *Biological psychiatry*, *63*(8), 730–735.

Pinkham, A. E., Penn, D. L., Perkins, D. O., & Lieberman, J. (2003). Implications for the neural basis of social cognition for the study of schizophrenia. *The American journal of psychiatry*, *160*(5), 815–824.

Ping YQ, Mao C, Xiao P, Zhao RJ, Jiang Y, Yang Z, An WT, Shen DD et al (2021). Structures of the GC-bound adhesion receptor GPR97-Go complex. *Nature*;589(7843):620-626.

Pizzorusso T, Medini P, Berardi N, Chierzi S, Fawcett JW, Maffei L (2002). Reactivation of ocular dominance plasticity in the adult visual cortex. *Science*;298(5596):1248-51.

Plourde, G., Baribeau, J., & Bonhomme, V. (1997). Ketamine increases the amplitude of the 40-Hz auditory steady-state response in humans. *British journal of anaesthesia*, *78*(5), 524–529.

Potter-Perigo, S., Johnson, P. Y., Evanko, S. P., Chan, C. K., Braun, K. R., Wilkinson, T. S., Altman, L. C., & Wight, T. N. (2010). Polyinosine-polycytidylic acid stimulates versican accumulation in the extracellular matrix promoting monocyte adhesion. *American journal of respiratory cell and molecular biology*, *43*(1), 109–120.

Prager EM, Brielmaier J, Bergstrom HC, McGuire J, Johnson LR (2010). Localization of mineralocorticoid receptors at mammalian synapses. *PLoS One*;5(12):e14344.

Pruessner, J. C., Champagne, F., Meaney, M. J., & Dagher, A. (2004). Dopamine release in response to a psychological stress in humans and its relationship to early life maternal care: a positron emission tomography study using [11C]raclopride. *The Journal of neuroscience : the official journal of the Society for Neuroscience*, *24*(11), 2825–2831.

Puig, M. V., Watakabe, A., Ushimaru, M., Yamamori, T., & Kawaguchi, Y. (2010). Serotonin modulates fast-spiking interneuron and synchronous activity in the rat prefrontal cortex through 5-HT_{1A} and 5-HT_{2A} receptors. *The Journal of neuroscience : the official journal of the Society for Neuroscience*, *30*(6), 2211–2222.

Purves-Tyson, T. D., Brown, A. M., Weissleder, C., Rothmond, D. A., & Shannon Weickert, C. (2021). Reductions in midbrain GABAergic and dopamine neuron markers are linked in schizophrenia. *Molecular brain*, *14*(1), 96.

Putthoff, P., Akyüz, N., Kutsche, M., Zardi, L., Borgmeyer, U., & Schachner, M. (2003). Structure of the murine tenascin-R gene and functional characterisation of the promoter. *Biochemical and biophysical research communications*, *308*(4), 940–949.

Pyka, M., Wetzel, C., Aguado, A., Geissler, M., Hatt, H., & Faissner, A. (2011). Chondroitin sulfate proteoglycans regulate astrocyte-dependent synaptogenesis and modulate synaptic activity in primary embryonic hippocampal neurons. *The European journal of neuroscience*, *33*(12), 2187–2202.

Queisser, N., Oteiza, P. I., Link, S., Hey, V., Stopper, H., & Schupp, N. (2014). Aldosterone activates transcription factor Nrf2 in kidney cells both in vitro and in vivo. *Antioxidants & redox signaling*, *21*(15), 2126–2142.

Rabin, D., Gold, P. W., Margioris, A. N., & Chrousos, G. P. (1988). Stress and reproduction: physiologic and pathophysiologic interactions between the stress and reproductive axes. *Advances in experimental medicine and biology*, *245*, 377–387.

Rafestin-Oblin, M. E., Lombes, M., Lustenberger, P., Blanchardie, P., Michaud, A., Cornu, G., & Claire, M. (1986). Affinity of corticosteroids for mineralocorticoid and GRs of the rabbit kidney: effect of steroid substitution. *Journal of steroid biochemistry*, 25(4), 527–534.

Ramamoorthy, S., & Cidlowski, J. A. (2016). Corticosteroids: Mechanisms of Action in Health and Disease. *Rheumatic diseases clinics of North America*, *42*(1), 15–vii.

Ramachandran, K. V., & Margolis, S. S. (2017). A mammalian nervous-system-specific plasma membrane proteasome complex that modulates neuronal function. *Nature structural & molecular biology*, *24*(4), 419–430.

Ramamoorthy, S., & Cidlowski, J. A. (2013). Exploring the molecular mechanisms of GR action from sensitivity to resistance. *Endocrine development*, *24*, 41–56.

Rahmani, R., Rambarack, N., Singh, J., Constanti, A., & Ali, A. B. (2023). Age-Dependent Sex Differences in Perineuronal Nets in an *APP* Mouse Model of Alzheimer's Disease Are Brain Region-Specific. *International journal of molecular sciences*, *24*(19), 14917.

Rauch, U., Grimpe, B., Kulbe, G., Arnold-Ammer, I., Beier, D. R., & Fässler, R. (1995). Structure and chromosomal localization of the mouse neurocan gene. *Genomics*, *28*(3), 405–410.

Ray, K. P., Farrow, S., Daly, M., Talabot, F., & Searle, N. (1997). Induction of the E-selectin promoter by interleukin 1 and tumour necrosis factor alpha, and inhibition by GCs. *The Biochemical journal*, *328 (Pt 2)*(Pt 2), 707–715.

Raynes, R., Pomatto, L. C., & Davies, K. J. (2016). Degradation of oxidized proteins by the proteasome: Distinguishing between the 20S, 26S, and immunoproteasome proteolytic pathways. *Molecular aspects of medicine*, *50*, 41–55.

Reinheckel, T., Sitte, N., Ullrich, O., Kuckelkorn, U., Davies, K. J., & Grune, T. (1998). Comparative resistance of the 20S and 26S proteasome to oxidative stress. *The Biochemical journal*, *335 (Pt 3)*(Pt 3), 637–642

Reith, J., Benkelfat, C., Sherwin, A., Yasuhara, Y., Kuwabara, H., Andermann, F., Bachneff, S., Cumming, P., Diksic, M., Dyve, S. E., Etienne, P., Evans, A. C., Lal, S., Shevell, M., Savard, G., Wong, D. F., Chouinard, G., & Gjedde, A. (1994). Elevated dopa decarboxylase activity in living brain of patients with psychosis. *Proceedings of the National Academy of Sciences of the United States of America*, 91(24), 11651–11654.

Reul JM, de Kloet ER (1985). Two receptor systems for corticosterone in rat brain: microdistribution and differential occupation. *Endocrinology*, 117(6):2505-11.

Revollo, J. R., & Cidlowski, J. A. (2009). Mechanisms generating diversity in GR signaling. *Annals of the New York Academy of Sciences*, *1179*, 167–178.

Rhen, T., & Cidlowski, J. A. (2005). Antiinflammatory action of GCs--new mechanisms for old drugs. *The New England journal of medicine*, *353*(16), 1711–1723.

Rhodes, K. E., & Fawcett, J. W. (2004). Chondroitin sulphate proteoglycans: preventing plasticity or protecting the CNS? *Journal of anatomy*, *204*(1), 33–48.

Ribot J, Breton R, Calvo CF, Moulard J, Ezan P, Zapata J, Samama K, Moreau M, Beme lmans AP, Sabatet V, Dingli F, Loew D, Milleret C, Billuart P, Dallérac G, Rouach N (2021). Astrocytes close the mouse critical period for visual plasticity. *Science*; 373(6550):77-81.

Rice, D., & Barone, S., Jr (2000). Critical periods of vulnerability for the developing nervous system: evidence from humans and animal models. *Environmental health perspectives*, *108 Suppl 3*(Suppl 3), 511–533.

Riga, D., Kramvis, I., Koskinen, M. K., van Bokhoven, P., van der Harst, J. E., Heistek, T. S., Jaap Timmerman, A., van Nierop, P., et al. (2017). Hippocampal extracellular matrix alterations contribute to cognitive impairment associated with a chronic depressive-like state in rats. *Science translational medicine*, *9*(421), eaai8753.

Ripke, S., Neale, B. M., Corvin, A., Walters, J. T. R., Farh, K. H., Holmans, P. A., et al. (2014). Biological insights from 108 schizophrenia-associated genetic loci. *Nature* 511, 421–427

Robinson, D., Woerner, M. G., Alvir, J. M., Bilder, R., Goldman, R., Geisler, S., Koreen, A., Sheitman, B., Chakos, M., Mayerhoff, D., & Lieberman, J. A. (1999). Predictors of relapse

following response from a first episode of schizophrenia or schizoaffective disorder. *Archives of general psychiatry*, *56*(3), 241–247.

Rock KL, Gramm C, Rothstein L, Clark K, Stein R, Dick L, Hwang D, Goldberg AL (1994). Inhibitors of the proteasome block the degradation of most cell proteins and the generation of peptides presented on MHC class I molecules. *Cell*;78(5):761-71.

Rodgers, K. J., & Dean, R. T. (2003). Assessment of proteasome activity in cell lysates and tissue homogenates using peptide substrates. *The international journal of biochemistry & cell biology*, *35*(5), 716–727.

Rogers SL, Rankin-Gee E, Risbud RM, Porter BE, Marsh ED (2018). Normal Development of the Perineuronal Net in Humans; In Patients with and without Epilepsy. *Neuroscience*;384:350-360.

Rossier, J., Bernard, A., Cabungcal, J. H., Perrenoud, Q., Savoye, A., Gallopin, T., Hawrylycz, M., Cuénod, M., Do, K., Urban, A., & Lein, E. S. (2015). Cortical fast-spiking parvalbumin interneurons enwrapped in the perineuronal net express the metallopeptidases Adamts8, Adamts15 and Neprilysin. *Molecular psychiatry*, *20*(2), 154–161.

Rousseau, G. G., Higgins, S. J., Baxter, J. D., Gelfand, D., & Tomkins, G. M. (1975). Binding of GRs to DNA. *The Journal of biological chemistry*, *250*(15), 6015–6021.

Rummel-Kluge, C., Komossa, K., Schwarz, S., Hunger, H., Schmid, F., Lobos, C. A., Kissling, W., Davis, J. M., & Leucht, S. (2010). Head-to-head comparisons of metabolic side effects of second generation antipsychotics in the treatment of schizophrenia: a systematic review and meta-analysis. *Schizophrenia research*, *123*(2-3), 225–233.

Rupprecht, R., Reul, J. M., van Steensel, B., Spengler, D., Söder, M., Berning, B., Holsboer, F., & Damm, K. (1993). Pharmacological and functional characterization of human mineralocorticoid and GR ligands. *European journal of pharmacology*, *247*(2), 145–154.

Ruoslahti E (1996). Brain extracellular matrix. *Glycobiology*;6(5):489-92.

Ruzicka, W. B., Zhubi, A., Veldic, M., Grayson, D. R., Costa, E., & Guidotti, A. (2007). Selective epigenetic alteration of layer I GABAergic neurons isolated from prefrontal cortex of schizophrenia patients using laser-assisted microdissection. *Molecular psychiatry*, *12*(4), 385–397.

Saijo, T., Abe, T., Someya, Y., Sassa, T., Sudo, Y., Suhara, T., Shuno, T., Asai, K., & Okubo, Y. (2001). Ten year progressive ventricular enlargement in schizophrenia: an MRI morphometrical study. *Psychiatry and clinical neurosciences*, *55*(1), 41–47.

Salo, D. C., Pacifici, R. E., Lin, S. W., Giulivi, C., & Davies, K. J. (1990). Superoxide dismutase undergoes proteolysis and fragmentation following oxidative modification and inactivation. *The Journal of biological chemistry*, *265*(20), 11919–11927.

Sams-Dodd F. (1995). Distinct effects of d-amphetamine and phencyclidine on the social behaviour of rats. *Behavioural pharmacology*, 6(1), 55–65.

Samarasinghe RA, Witchell SF, DeFranco DB (2012). Cooperativity and complementarity: synergies in non-classical and classical GC signaling. *Cell Cycle*;11(15):2819-27.

Sandi C. (2004). Stress, cognitive impairment and cell adhesion molecules. *Nature reviews. Neuroscience*, *5*(12), 917–930.

Sandi, C., & Loscertales, M. (1999). Opposite effects on NCAM expression in the rat frontal cortex induced by acute vs. chronic corticosterone treatments. *Brain research*, *828*(1-2), 127–134.

Sango, K., Oohira, A., Ajiki, K., Tokashiki, A., Horie, M., & Kawano, H. (2003). Phosphacan and neurocan are repulsive substrata for adhesion and neurite extension of adult rat dorsal root ganglion neurons in vitro. *Experimental neurology*, *182*(1), 1–11.

Santiago, A. N., Lim, K. Y., Opendak, M., Sullivan, R. M., & Aoki, C. (2018). Early life trauma increases threat response of peri-weaning rats, reduction of axo-somatic synapses formed by parvalbumin cells and perineuronal net in the basolateral nucleus of amygdala. *The Journal of comparative neurology*, *526*(16), 2647–2664.

Santos-Silva, T., Dos Santos Fabris, D., de Oliveira, C. L., Guimarães, F. S., & Gomes, F. V. (2024). Prefrontal and Hippocampal Parvalbumin Interneurons in Animal Models for Schizophrenia: A Systematic Review and Meta-analysis. *Schizophrenia bulletin*, *50*(1), 210–223.

Saroja, S. R., Sase, A., Kircher, S. G., Wan, J., Berger, J., Höger, H., Pollak, A., & Lubec, G. (2014). Hippocampal proteoglycans brevican and versican are linked to spatial memory of Sprague-Dawley rats in the morris water maze. *Journal of neurochemistry*, *130*(6), 797–804.

Sayers, E. W., Beck, J., Bolton, E. E., Brister, J. R., Chan, J., Comeau, D. C., Connor, R., DiCuccio, M., Farrell, C. M., Feldgarden, M., Fine, A. M., Funk, K., Hatcher, E., Hoeppner, M., Kane, M., Kannan, S., Katz, K. S., Kelly, C., Klimke, W., Kim, S., … Sherry, S. T. (2024). Database resources of the National Center for Biotechnology Information. *Nucleic acids research*, *52*(D1), D33–D43.

Scheff, S. W., Price, D. A., Schmitt, F. A., & Mufson, E. J. (2006). Hippocampal synaptic loss in early Alzheimer's disease and mild cognitive impairment. *Neurobiology of aging*, *27*(10), 1372–1384.

Schmid, W., Cole, T. J., Blendy, J. A., & Schütz, G. (1995). Molecular genetic analysis of GC signalling in development. *The Journal of steroid biochemistry and molecular biology*, *53*(1-6), 33–35.

Schmiedt, C., Brand, A., Hildebrandt, H., & Basar-Eroglu, C. (2005). Event-related theta oscillations during working memory tasks in patients with schizophrenia and healthy controls. *Brain research. Cognitive brain research*, *25*(3), 936–947.

Schipper-Krom, S., Sanz, A. S., van Bodegraven, E. J., Speijer, D., Florea, B. I., Ovaa, H., & Reits, E. A. (2019). Visualizing Proteasome Activity and Intracellular Localization Using Fluorescent Proteins and Activity-Based Probes. *Frontiers in molecular biosciences*, *6*, 56.

Schirner M, McIntosh AR, Jirsa V, Deco G, Ritter P (2018). Inferring multi-scale neural mechanisms with brain network modelling. *Elife*;7:e28927.

Schizophrenia Working Group of the Psychiatric Genomics Consortium (2014). Biological insights from 108 schizophrenia-associated genetic loci. *Nature*; 511(7510):421-7.

Schmalfeldt, M., Dours-Zimmermann, M. T., Winterhalter, K. H., & Zimmermann, D. R. (1998). Versican V2 is a major extracellular matrix component of the mature bovine brain. *The Journal of biological chemistry*, *273*(25), 15758–15764.

Schmalfeldt, M., Bandtlow, C. E., Dours-Zimmermann, M. T., Winterhalter, K. H., & Zimmermann, D. R. (2000). Brain derived versican V2 is a potent inhibitor of axonal growth. *Journal of cell science*, *113 (Pt 5)*, 807–816.

Schneider, F. & Deldin, P. J. (2001). Genetics and schizophrenia. Comprehensive handbook of psychopathology (3rd ed.) New York: Kluwer Academic/Plenum

Scott, M. R., & Meador-Woodruff, J. H. (2020). Intracellular compartment-specific proteasome dysfunction in postmortem cortex in schizophrenia subjects. *Molecular psychiatry*, *25*(4), 776–790.

Schwab, S. G., Hoefgen, B., Hanses, C., Hassenbach, M. B., Albus, M., Lerer, B., Trixler, M., Maier, W., & Wildenauer, D. B. (2005). Further evidence for association of variants in the AKT1 gene with schizophrenia in a sample of European sib-pair families. *Biological psychiatry*, *58*(6), 446–450.

Seckl J. R. (2001). GC programming of the fetus; adult phenotypes and molecular mechanisms. *Molecular and cellular endocrinology*, *185*(1-2), 61–71.

Seckl J. R. (2004). 11beta-hydroxysteroid dehydrogenases: changing GC action. *Current opinion in pharmacology*, *4*(6), 597–602.

Seidenbecher, C. I., Richter, K., Rauch, U., Fässler, R., Garner, C. C., & Gundelfinger, E. D. (1995). Brevican, a chondroitin sulfate proteoglycan of rat brain, occurs as secreted and cell surface glycosylphosphatidylinositol-anchored isoforms. *The Journal of biological chemistry*, *270*(45), 27206–27212.

Sellgren, C. M., Gracias, J., Watmuff, B., Biag, J. D., Thanos, J. M., Whittredge, P. B., Fu, T., Worringer, K., Brown, H. E., et al. (2019). Increased synapse elimination by microglia in schizophrenia patient-derived models of synaptic pruning. *Nature neuroscience*, *22*(3), 374–385.

Selten JP, Frissen A, Lensvelt-Mulders G, Morgan VA (2010). Schizophrenia and 1957 pandemic of influenza: meta-analysis. *Schizophrenia Bulletin*; 36(2):219-28.

Selten, J. P., van der Graaf, Y., van Duursen, R., Gispen-de Wied, C. C., & Kahn, R. S. (1999). Psychotic illness after prenatal exposure to the 1953 Dutch Flood Disaster. *Schizophrenia research*, *35*(3), 243–245.

Selvaraj, S., Arnone, D., Cappai, A., & Howes, O. (2014). Alterations in the serotonin system in schizophrenia: a systematic review and meta-analysis of postmortem and molecular imaging studies. *Neuroscience and biobehavioral reviews*, *45*, 233–245.

Shah, A., & Lodge, D. J. (2013). A loss of hippocampal perineuronal nets produces deficits in dopamine system function: relevance to the positive symptoms of schizophrenia. *Translational psychiatry*, *3*(1), e215.

Shang, F., & Taylor, A. (2011). Ubiquitin-proteasome pathway and cellular responses to oxidative stress. *Free radical biology & medicine*, *51*(1), 5–16.

Shannon, H. E., Bymaster, F. P., Calligaro, D. O., Greenwood, B., Mitch, C. H., Sawyer, B. D., Ward, J. S., Wong, D. T., Olesen, P. H., Sheardown, M. J., Swedberg, M. D., Suzdak, P. D., & Sauerberg, P. (1994). Xanomeline: a novel muscarinic receptor agonist with functional selectivity for M1 receptors. *The Journal of pharmacology and experimental therapeutics*, 269(1), 271–281.

Shepard R., Page C. E., Coutellier L. (2016). Sensitivity of the prefrontal GABAergic system to chronic stress in male and female mice: relevance for sex differences in stress-related disorders. *Neuroscience* 332 1–12.

Shekhar, A., Potter, W. Z., Lightfoot, J., Lienemann, J., Dubé, S., Mallinckrodt, C., Bymaster, F. P., McKinzie, D. L., & Felder, C. C. (2008). Selective muscarinic receptor agonist xanomeline as a novel treatment approach for schizophrenia. *The American journal of psychiatry*, 165(8), 1033–1039.

Shelly M, Cancedda L, Lim BK, Popescu AT, Cheng PL, Gao H, Poo MM (2011). Semaphorin3A regulates neuronal polarization by suppressing axon formation and promoting dendrite growth. *Neuron*; 71(3):433-46.

Shi, J. X., Li, J. S., Hu, R., Shi, Y., Su, X., Guo, X. J., & Li, X. M. (2014). Tristetraprolin is involved in the GC-mediated interleukin 8 repression. *International immunopharmacology*, *22*(2), 480–485.

Shi, L., Fatemi, S. H., Sidwell, R. W., & Patterson, P. H. (2003). Maternal influenza infection causes marked behavioral and pharmacological changes in the offspring. *The Journal of neuroscience : the official journal of the Society for Neuroscience*, *23*(1), 297–302.

Shonkoff JP, Boyce WT, McEwen BS (2009). Neuroscience, molecular biology, and the childhood roots of health disparities: building a new framework for health promotion and disease prevention. *JAMA*; 301(21):2252-9.

Shors, T. J., Foy, M. R., Levine, S., & Thompson, R. F. (1990). Unpredictable and uncontrollable stress impairs neuronal plasticity in the rat hippocampus. *Brain research bulletin*, *24*(5), 663–667.

Short, K. L., Bird, A. D., Seow, B. K. L., Ng, J., McDougall, A. R. A., Wallace, M. J., Hooper, S. B., & Cole, T. J. (2020). GC signalling drives reduced versican levels in the fetal mouse lung. *Journal of molecular endocrinology*, *64*(3), 155–164.

Silva-Gómez, A. B., Rojas, D., Juárez, I., & Flores, G. (2003). Decreased dendritic spine density on prefrontal cortical and hippocampal pyramidal neurons in postweaning social isolation rats. *Brain research*, 983(1-2), 128–136.

Sim, H., Hu, B., & Viapiano, M. S. (2009). Reduced expression of the hyaluronan and proteoglycan link proteins in malignant gliomas. *The Journal of biological chemistry*, *284*(39), 26547–26556.

Sinn PL, Sigmund CD (1999). Human renin mRNA stability is increased in response to cAMP in Calu-6 cells. *Hypertension*; 33(3):900-5.

Siiteri, P. K., Murai, J. T., Hammond, G. L., Nisker, J. A., Raymoure, W. J., & Kuhn, R. W. (1982). The serum transport of steroid hormones. *Recent progress in hormone research*, *38*, 457–510.

Sitte, N., Merker, K., Von Zglinicki, T., Davies, K. J., & Grune, T. (2000). Protein oxidation and degradation during cellular senescence of human BJ fibroblasts: part II--aging of nondividing cells. *FASEB journal : official publication of the Federation of American Societies for Experimental Biology*, *14*(15), 2503–2510.

Smith, S. M., & Vale, W. W. (2006). The role of the hypothalamic-pituitary-adrenal axis in neuroendocrine responses to stress. *Dialogues in clinical neuroscience*, *8*(4), 383–395.

Smith T E, Bellack A S, Liberman R P (1996). Social skills training for schizophrenia: Review and future directions, *Clinical Psychology Review*, 16(7), 599-617.

Smoak, K., & Cidlowski, J. A. (2006). GCs regulate tristetraprolin synthesis and posttranscriptionally regulate tumor necrosis factor alpha inflammatory signaling. *Molecular and cellular biology*, *26*(23), 9126–9135.

Snyder, H. R., Miyake, A., & Hankin, B. L. (2015). Advancing understanding of executive function impairments and psychopathology: bridging the gap between clinical and cognitive approaches. *Frontiers in psychology*, *6*, 328.

Soares, A. R., Gildawie, K. R., Honeycutt, J. A., & Brenhouse, H. C. (2020). Region-specific effects of maternal separation on oxidative stress accumulation in parvalbumin neurons of male and female rats. *Behavioural brain research*, *388*, 112658.

Soghomonian, J. J., & Martin, D. L. (1998). Two isoforms of glutamate decarboxylase: why?. *Trends in pharmacological sciences*, *19*(12), 500–505.

Sohal VS, Zhang F, Yizhar O, Deisseroth K (2009). Parvalbumin neurons and gamma rhythms enhance cortical circuit performance. *Nature*; 459(7247):698-702.

Song, I., & Dityatev, A. (2018). Crosstalk between glia, extracellular matrix and neurons. *Brain research bulletin*, *136*, 101–108.

Sorg, B. A., Berretta, S., Blacktop, J. M., Fawcett, J. W., Kitagawa, H., Kwok, J. C., & Miquel, M. (2016). Casting a Wide Net: Role of Perineuronal Nets in Neural Plasticity. *The Journal of neuroscience : the official journal of the Society for Neuroscience*, *36*(45), 11459–11468.

Sotoodehnejadnematalahi F, Staples KJ, Chrysanthou E, Pearson H, Ziegler-Heitbrock L, Burke B (2015). Mechanisms of Hypoxic Up-Regulation of Versican Gene Expression in Macrophages. *PLoS One*;10(6):e0125799

Spencer, K. M., Niznikiewicz, M. A., Nestor, P. G., Shenton, M. E., & McCarley, R. W. (2009). Left auditory cortex gamma synchronization and auditory hallucination symptoms in schizophrenia. *BMC neuroscience*, *10*, 85

Spicer, A. P., Joo, A., & Bowling, R. A., Jr (2003). A hyaluronan binding link protein gene family whose members are physically linked adjacent to chondroitin sulfate proteoglycan core protein genes: the missing links. *The Journal of biological chemistry*, *278*(23), 21083–21091.

Sriram, K., & Insel, P. A. (2018). G Protein-Coupled Receptors as Targets for Approved Drugs: How Many Targets and How Many Drugs?. *Molecular pharmacology*, *93*(4), 251–258.

Stahl S. M. (2016). Mechanism of action of cariprazine. *CNS spectrums*, *21*(2), 123–127.

Stacey M, Chang GW, Davies JQ, Kwakkenbos MJ, Sanderson RD, Hamann J, Gordon S, Lin HH (2003). The epidermal growth factor-like domains of the human EMR2 receptor mediate cell attachment through chondroitin sulfate glycosaminoglycans. *Blood*;102(8):2916-24.

Stampanoni Bassi, M., Iezzi, E., Gilio, L., Centonze, D., & Buttari, F. (2019). Synaptic Plasticity Shapes Brain Connectivity: Implications for Network Topology. *International journal of molecular sciences*, *20*(24), 6193

Stefansson H., Rujescu D., Cichon S., Pietiläinen O.P., Ingason A., Steinberg S., Fossdal R., Sigurdsson E., Sigmundsson T., Buizer-Voskamp J.E., et al (2008). Large recurrent microdeletions associated with schizophrenia. *Nature*;455(7210):232-6.

Steen, R. G., Mull, C., McClure, R., Hamer, R. M., & Lieberman, J. A. (2006). Brain volume in first-episode schizophrenia: systematic review and meta-analysis of magnetic resonance imaging studies. *The British journal of psychiatry : the journal of mental science*, *188*, 510–518.

Stefanis, N. C., Henquet, C., Avramopoulos, D., Smyrnis, N., Evdokimidis, I., Myin-Germeys, I., Stefanis, C. N., & Van Os, J. (2007). COMT Val158Met moderation of stress-induced psychosis. *Psychological medicine*, *37*(11), 1651–1656.

Steiner, J., Brisch, R., Schiltz, K., Dobrowolny, H., Mawrin, C., Krzyżanowska, M., Bernstein, H. G., Jankowski, Z., Braun, K., Schmitt, A., Bogerts, B., & Gos, T. (2016). GABAergic system impairment in the hippocampus and superior temporal gyrus of patients with paranoid schizophrenia: A post-mortem study. *Schizophrenia research*, *177*(1-3), 10–17.

Steullet, P., Cabungcal, J. H., Bukhari, S. A., Ardelt, M. I., Pantazopoulos, H., Hamati, F., Salt, T. E., Cuenod, M., Do, K. Q., & Berretta, S. (2018). The thalamic reticular nucleus in schizophrenia and bipolar disorder: role of parvalbumin-expressing neuron networks and oxidative stress. *Molecular psychiatry*, *23*(10), 2057–2065.

Steullet, P., Cabungcal, J. H., Coyle, J., Didriksen, M., Gill, K., Grace, A. A., Hensch, T. K., LaMantia, A. S., Lindemann, L., Maynard, T. M., Meyer, U., Morishita, H., O'Donnell, P., Puhl, M., Cuenod, M., & Do, K. Q. (2017). Oxidative stress-driven parvalbumin interneuron impairment as a common mechanism in models of schizophrenia. *Molecular psychiatry*, *22*(7), 936–943.

Stepanichev MY, Kudryashova IV, Yakovlev AA, Onufriev MV, Khaspekov LG, Lyzhin AA, Lazareva NA, Gulyaeva NV (2005). Central administration of a caspase inhibitor impairs shuttle-box performance in rats. *Neuroscience*.;136(2):579-91.

Stilo, S. A., Gayer-Anderson, C., Beards, S., Hubbard, K., Onyejiaka, A., Keraite, A., Borges, S., Mondelli, V., Dazzan, P., Pariante, C., Di Forti, M., Murray, R. M., & Morgan, C. (2017). Further evidence of a cumulative effect of social disadvantage on risk of psychosis. *Psychological medicine*, *47*(5), 913–924.

Stuhlmeier, K. M., & Pollaschek, C. (2004). GCs inhibit induced and non-induced mRNA accumulation of genes encoding hyaluronan synthases (HAS): hydrocortisone inhibits HAS1 activation by blocking the p38 mitogen-activated protein kinase signalling pathway. *Rheumatology (Oxford, England)*, *43*(2), 164–169.

Strackeljan, L., Baczynska, E., Cangalaya, C., Baidoe-Ansah, D., Wlodarczyk, J., Kaushik, R., & Dityatev, A. (2021). Microglia Depletion-Induced Remodeling of Extracellular Matrix and Excitatory Synapses in the Hippocampus of Adult Mice. *Cells*, *10*(8), 1862.

Strauss, G. P., Horan, W. P., Kirkpatrick, B., Fischer, B. A., Keller, W. R., Miski, P., Buchanan, R. W., Green, M. F., & Carpenter, W. T., Jr (2013). Deconstructing negative symptoms of schizophrenia: avolition-apathy and diminished expression clusters predict clinical presentation and functional outcome. *Journal of psychiatric research*, *47*(6), 783–790.

Strokotova, A. V., Sokolov, D. K., Molodykh, O. P., Koldysheva, E. V., Kliver, E. E., Ushakov, V. S., Politko, M. O., Mikhnevich, N. V., Kazanskaya, G. M., Aidagulova, S. V., & Grigorieva, E. V. (2023). Prolonged use of temozolomide leads to increased anxiety and decreased content of aggrecan and chondroitin sulfate in brain tissues of aged rats. *Biomedical reports*, *20*(1), 7.

Stone, J. M., Howes, O. D., Egerton, A., Kambeitz, J., Allen, P., Lythgoe, D. J., O'Gorman, R. L., McLean, M. A., Barker, G. J., & McGuire, P. (2010). Altered relationship between hippocampal

glutamate levels and striatal dopamine function in subjects at ultra high risk of psychosis. *Biological psychiatry*, *68*(7), 599–602.

Sultana, R., Brooks, C. B., Shrestha, A., Ogundele, O. M., & Lee, C. C. (2021). Perineuronal Nets in the Prefrontal Cortex of a Schizophrenia Mouse Model: Assessment of Neuroanatomical, Electrophysiological, and Behavioral Contributions. *International journal of molecular sciences*, *22*(20), 11140.

Sun, C., Kitamura, T., Yamamoto, J., Martin, J., Pignatelli, M., Kitch, L. J., Schnitzer, M. J., & Tonegawa, S. (2015). Distinct speed dependence of entorhinal island and ocean cells, including respective grid cells. *Proceedings of the National Academy of Sciences of the United States of America*, *112*(30), 9466–9471.

Sun, D., Phillips, L., Velakoulis, D., Yung, A., McGorry, P. D., Wood, S. J., van Erp, T. G., Thompson, P. M., Toga, A. W., Cannon, T. D., & Pantelis, C. (2009). Progressive brain structural changes mapped as psychosis develops in 'at risk' individuals. *Schizophrenia research*, *108*(1-3), 85–92.

Sun, D., Stuart, G. W., Jenkinson, M., Wood, S. J., McGorry, P. D., Velakoulis, D., van Erp, T. G., Thompson, P. M., Toga, A. W., Smith, D. J., Cannon, T. D., & Pantelis, C. (2009). Brain surface contraction mapped in first-episode schizophrenia: a longitudinal magnetic resonance imaging study. *Molecular psychiatry*, *14*(10), 976–986.

Sun, L., Trausch-Azar, J. S., Muglia, L. J., & Schwartz, A. L. (2008). GCs differentially regulate degradation of MyoD and Id1 by N-terminal ubiquitination to promote muscle protein catabolism. *Proceedings of the National Academy of Sciences of the United States of America*, *105*(9), 3339–3344.

Sundberg, M., Savola, S., Hienola, A., Korhonen, L., & Lindholm, D. (2006). GC hormones decrease proliferation of embryonic neural stem cells through ubiquitin-mediated degradation of cyclin D1. *The Journal of neuroscience : the official journal of the Society for Neuroscience*, *26*(20), 5402–5410.

Suttkus, A., Rohn, S., Weigel, S., Glöckner, P., Arendt, T., & Morawski, M. (2014). Aggrecan, link protein and tenascin-R are essential components of the perineuronal net to protect neurons against iron-induced oxidative stress. *Cell death & disease*, *5*(3), e1119.

Sutterland, A. L., Fond, G., Kuin, A., Koeter, M. W., Lutter, R., van Gool, T., Yolken, R., Schizophreniaoke, A., Leboyer, M., & de Haan, L. (2015). Beyond the association. Toxoplasma gondii in schizophrenia, bipolar disorder, and addiction: systematic review and meta-analysis. *Acta psychiatrica Scandinavica*, *132*(3), 161–179.

Sullivan EV, Lim KO, Mathalon D, Marsh L, Beal DM, Harris D, Hoff AL, Faustman WO, Pfefferbaum A (1998). A profile of cortical gray matter volume deficits characteristic of schizophrenia. *Cerebral Cortex*; 8(2):117-24.

Sullivan, P. F., Kendler, K. S., & Neale, M. C. (2003). Schizophrenia as a complex trait: evidence from a meta-analysis of twin studies. *Archives of general psychiatry*, *60*(12), 1187–1192.

Sultana, R., Brooks, C. B., Shrestha, A., Ogundele, O. M., & Lee, C. C. (2021). Perineuronal Nets in the Prefrontal Cortex of a Schizophrenia Mouse Model: Assessment of Neuroanatomical, Electrophysiological, and Behavioral Contributions. *International journal of molecular sciences*, *22*(20), 11140.

Takahashi, N., Sakurai, T., Bozdagi-Gunal, O., Dorr, N. P., Moy, J., Krug, L., Gama-Sosa, M., Elder, G. A., Koch, R. J., Walker, R. H., Hof, P. R., Davis, K. L., & Buxbaum, J. D. (2011). Increased expression of receptor phosphotyrosine phosphatase-β/ζ is associated with molecular, cellular, behavioral and cognitive schizophrenia phenotypes. *Translational psychiatry*, *1*(5), e8.

Talkowski, M. E., Kirov, G., Bamne, M., Georgieva, L., Torres, G., Mansour, H., Chowdari, K. V., Milanova, V., Wood, J., McClain, L., Prasad, K., Shirts, B., Zhang, J., O'Donovan, M. C., Owen, M. J., Devlin, B., & Nimgaonkar, V. L. (2008). A network of dopaminergic gene variations implicated as risk factors for schizophrenia. *Human molecular genetics*, 17(5), 747–758.

Tan, A. M., Colletti, M., Rorai, A. T., Skene, J. H., & Levine, J. M. (2006). Antibodies against the NG2 proteoglycan promote the regeneration of sensory axons within the dorsal columns of the spinal cord. *The Journal of neuroscience : the official journal of the Society for Neuroscience*, *26*(18), 4729–4739.

Tang, X., Davies, J. E., & Davies, S. J. (2003). Changes in distribution, cell associations, and protein expression levels of NG2, neurocan, phosphacan, brevican, versican V2, and tenascin-C during acute to chronic maturation of spinal cord scar tissue. *Journal of neuroscience research*, *71*(3), 427–444.

Tamminga, C. A., Stan, A. D., & Wagner, A. D. (2010). The hippocampal formation in schizophrenia. *The American journal of psychiatry*, *167*(10), 1178–1193.

Taylor, T., Dluhy, R. G., & Williams, G. H. (1983). beta-endorphin suppresses adrenocorticotropin and cortisol levels in normal human subjects. *The Journal of clinical endocrinology and metabolism*, *57*(3), 592–596.

Taylor, K. R., Yamasaki, K., Radek, K. A., Nardo, A. D., Goodarzi, H., Golenbock, D., Beutler, B., & Gallo, R. L. (2007). Recognition of hyaluronan released in sterile injury involves a unique receptor complex dependent on Toll-like receptor 4, CD44, and MD-2. *The Journal of biological chemistry*, *282*(25), 18265–18275.

Tian, N., Petersen, C., Kash, S., Baekkeskov, S., Copenhagen, D., & Nicoll, R. (1999). The role of the synthetic enzyme GAD65 in the control of neuronal gamma-aminobutyric acid release. *Proceedings of the National Academy of Sciences of the United States of America*, *96*(22), 12911–12916.

Tien, J. Y., & Spicer, A. P. (2005). Three vertebrate hyaluronan synthases are expressed during mouse development in distinct spatial and temporal patterns. *Developmental dynamics : an official publication of the American Association of Anatomists*, *233*(1), 130–141.

Thompson, E. H., Lensjø, K. K., Wigestrand, M. B., Malthe-Sørenssen, A., Hafting, T., & Fyhn, M. (2018). Removal of perineuronal nets disrupts recall of a remote fear memory. *Proceedings of the National Academy of Sciences of the United States of America*, *115*(3), 607–612.

Thompson, M., Weickert, C. S., Wyatt, E., & Webster, M. J. (2009). Decreased glutamic acid decarboxylase(67) mRNA expression in multiple brain areas of patients with schizophrenia and mood disorders. *Journal of psychiatric research*, *43*(11), 970–977.

Thornicroft, G., Tansella, M., Becker, T., Knapp, M., Leese, M., Schene, A., Vazquez-Barquero, J. L., & EPSILON Study Group (2004). The personal impact of schizophrenia in Europe. *Schizophrenia research*, *69*(2-3), 125–132.

Torres, U. S., Duran, F. L., Schaufelberger, M. S., Crippa, J. A., Louzã, M. R., Sallet, P. C., Kanegusuku, C. Y., Elkis, H., et al. (2016). Patterns of regional gray matter loss at different

stages of schizophrenia: A multisite, cross-sectional VBM study in first-episode and chronic illness. *NeuroImage. Clinical*, *12*, 1–15.

Tran TS, Rubio ME, Clem RL, Johnson D, Case L, Tessier-Lavigne M, Huganir RL, Ginty DD, Kolodkin AL (2009). Secreted semaphorins control spine distribution and morphogenesis in the postnatal CNS. *Nature*;462(7276):1065-9.

Trubetskoy V, Pardiñas AF, Qi T, Panagiotaropoulou G, Awasthi S, Bigdeli TB, Bryois J, Chen CY, et al (2022). Mapping genomic loci implicates genes and synaptic biology in schizophrenia. *Nature*;604(7906):502-508.

Tseng, K. Y., Chambers, R. A., & Lipska, B. K. (2009). The neonatal ventral hippocampal lesion as a heuristic neurodevelopmental model of schizophrenia. *Behavioural brain research*, 204(2), 295–305.

Tsubomoto, M., Kawabata, R., Zhu, X., Minabe, Y., Chen, K., Lewis, D. A., & Hashimoto, T. (2019). Expression of Transcripts Selective for GABA Neuron Subpopulations across the Cortical Visuospatial Working Memory Network in the Healthy State and Schizophrenia. *Cerebral cortex (New York, N.Y. : 1991)*, *29*(8), 3540–3550.

Uchida, T., Furukawa, T., Iwata, S., Yanagawa, Y., & Fukuda, A. (2014). Selective loss of parvalbumin-positive GABAergic interneurons in the cerebral cortex of maternally stressed Gad1-heterozygous mouse offspring. *Translational psychiatry*, *4*(3), e371

Uematsu, M., Hirai, Y., Karube, F., Ebihara, S., Kato, M., Abe, K., Obata, K., Yoshida, S., Hirabayashi, M., Yanagawa, Y., & Kawaguchi, Y. (2008). Quantitative chemical composition of cortical GABAergic neurons revealed in transgenic venus-expressing rats. *Cerebral cortex*, *18*(2), 315–330.

Ueno, H., Fujii, K., Suemitsu, S., Murakami, S., Kitamura, N., Wani, K., Aoki, S., Okamoto, M., Ishihara, T., & Takao, K. (2018). Expression of aggrecan components in perineuronal nets in the mouse cerebral cortex. *IBRO reports*, *4*, 22–37.

Ueno, H., Suemitsu, S., Murakami, S., Kitamura, N., Wani, K., Okamoto, M., Aoki, S., & Ishihara, T. (2017). Postnatal development of GABAergic interneurons and perineuronal nets in mouse temporal cortex subregions. *International journal of developmental neuroscience : the official journal of the International Society for Developmental Neuroscience*, *63*, 27–37.

Ueno, H., Suemitsu, S., Murakami, S., Kitamura, N., Wani, K., Matsumoto, Y., Okamoto, M., Aoki, S., & Ishihara, T. (2018). Juvenile stress induces behavioral change and affects perineuronal net formation in juvenile mice. *BMC neuroscience*, *19*(1), 41.

Ueno H, Suemitsu S, Murakami S, Kitamura N, Wani K, Okamoto M, Matsumoto Y, Ishihara T (2017). Region-specific impairments in parvalbumin interneurons in social isolation-reared mice. *Neuroscience*;359:196-208.

Ueno H, Suemitsu S, Okamoto M, Matsumoto Y, Ishihara T (2017). Parvalbumin neurons and perineuronal nets in the mouse prefrontal cortex. *Neuroscience*; 343:115-127.

Uhlhaas, P. J., & Singer, W. (2010). Abnormal neural oscillations and synchrony in schizophrenia. *Nature reviews. Neuroscience*, *11*(2), 100–113.

Uhlenhaut, N. H., Barish, G. D., Yu, R. T., Downes, M., Karunasiri, M., Liddle, C., Schwalie, P., Hübner, N., & Evans, R. M. (2013). Insights into negative regulation by the GR from genome-wide profiling of inflammatory cistromes. *Molecular cell*, *49*(1), 158–171.

Vaskinn A, Sundet K, Simonsen C, Hellvin T, Melle I, Andreassen OA (2011). Sex differences in neuropsychological performance and social functioning in schizophrenia and bipolar disorder. Neuropsychology.

van Os, J., & Kapur, S. (2009). Schizophrenia. *Lancet (London, England)*, *374*(9690), 635–645.

van Rijssen, T. J., van Dijk, E. H. C., Yzer, S., Ohno-Matsui, K., Keunen, J. E. E., Schlingemann, R. O., Sivaprasad, S., Querques, G., Downes, S. M., Fauser, S., Hoyng, C. B., Piccolino, F. C., Chhablani, J. K., Lai, T. Y. Y., Lotery, A. J., Larsen, M., Holz, F. G., Freund, K. B., Yannuzzi, L. A., & Boon, C. J. F. (2019). Central serous chorioretinopathy: Towards an evidence-based treatment guideline. *Progress in retinal and eye research*, 73, 100770.

van Winkel R., Stefanis N.C., Myin-Germeys I (2008). Psychosocial stress and psychosis. A review of the neurobiological mechanisms and the evidence for gene-stress interaction. *Schizophrenia Bulletin;* 34:1095–1105.

van Winkel R, van Beveren NJ, Simons C; Genetic Risk and Outcome of Psychosis (GROUP) Investigators (2011). AKT1 moderation of cannabis-induced cognitive alterations in psychotic disorder. *Neuropsychopharmacology*; 36(12):2529-37.

Varese F, Smeets F, Drukker M, Lieverse R, Lataster T, Viechtbauer W, et al (2012). Childhood adversities increase the risk of psychosis: a meta-analysis of patient-control, prospective- and cross-sectional cohort studies. *Schizophrenia Bulletin*; 38(4):661–71.

Valtcheva, N., Primorac, A., Jurisic, G., Hollmén, M., & Detmar, M. (2013). The orphan adhesion G protein-coupled receptor GPR97 regulates migration of lymphatic endothelial cells via the small GTPases RhoA and Cdc42. *The Journal of biological chemistry*, *288*(50), 35736–35748.

Vaskinn A, Sundet K, Simonsen C, Hellvin T, Melle I, Andreassen OA (2011). Sex differences in neuropsychological performance and social functioning in schizophrenia and bipolar disorder. *Neuropsychology*. Jul;25(4):499-510.

Vedunova, M., Sakharnova, T., Mitroshina, E., Perminova, M., Pimashkin, A., Zakharov, Y., Dityatev, A., & Mukhina, I. (2013). Seizure-like activity in hyaluronidase-treated dissociated hippocampal cultures. *Frontiers in cellular neuroscience*, *7*, 149.

Veldic, M., Guidotti, A., Maloku, E., Davis, J. M., & Costa, E. (2005). In psychosis, cortical interneurons overexpress DNA-methyltransferase 1. *Proceedings of the National Academy of Sciences of the United States of America*, *102*(6), 2152–2157.

Vidal, E., Bolea, R., Tortosa, R., Costa, C., Domènech, A., Monleón, E., Vargas, A., Badiola, J. J., & Pumarola, M. (2006). Assessment of calcium-binding proteins (Parvalbumin and Calbindin D-28K) and perineuronal nets in normal and scrapie-affected adult sheep brains. *Journal of virological methods*, *136*(1-2), 137–146.

Vigetti, D., Deleonibus, S., Moretto, P., Karousou, E., Viola, M., Bartolini, B., Hascall, V. C., Tammi, M., De Luca, G., & Passi, A. (2012). Role of UDP-N-acetylglucosamine (GlcNAc) and O-GlcNAcylation of hyaluronan synthase 2 in the control of chondroitin sulfate and hyaluronan synthesis. *The Journal of biological chemistry*, *287*(42), 35544–35555.

Vierling-Claassen, D., Siekmeier, P., Stufflebeam, S., & Kopell, N. (2008). Modeling GABA alterations in schizophrenia: a link between impaired inhibition and altered gamma and beta range auditory entrainment. *Journal of neurophysiology*, *99*(5), 2656–2671.

Vogel, C., & Marcotte, E. M. (2012). Insights into the regulation of protein abundance from proteomic and transcriptomic analyses. *Nature reviews. Genetics*, *13*(4), 227–232.

Voges, D., Zwickl, P., & Baumeister, W. (1999). The 26S proteasome: a molecular machine designed for controlled proteolysis. *Annual review of biochemistry*, *68*, 1015–1068.

Volk, D. W., Austin, M. C., Pierri, J. N., Sampson, A. R., & Lewis, D. A. (2000). Decreased glutamic acid decarboxylase67 messenger RNA expression in a subset of prefrontal cortical gamma-aminobutyric acid neurons in subjects with schizophrenia. *Archives of general psychiatry*, *57*(3), 237–245.

Wade, D., Harrigan, S., Edwards, J., Burgess, P. M., Whelan, G., & McGorry, P. D. (2005). Patterns and predictors of substance use disorders and daily tobacco use in first-episode psychosis. *The Australian and New Zealand journal of psychiatry*, *39*(10), 892–898.

Wager TD, Phan KL, Liberzon I, Taylor SF (2003). Valence, gender, and lateralization of functional brain anatomy in emotion: a meta-analysis of findings from neuroimaging. *Neuroimage*;19(3):513-31.

Wagg, A., Verdejo, C., & Molander, U. (2010). Review of cognitive impairment with antimuscarinic agents in elderly patients with overactive bladder. *International journal of clinical practice*, 64(9), 1279–1286.

Walker, D. J., & Spencer, K. A. (2018). GC programming of neuroimmune function. *General and comparative endocrinology*, *256*, 80–88.

Walker, J. J., Spiga, F., Gupta, R., Zhao, Z., Lightman, S. L., & Terry, J. R. (2015). Rapid intra-adrenal feedback regulation of GC synthesis. *Journal of the Royal Society, Interface*, *12*(102), 20140875.

Wang, D., Ichiyama, R. M., Zhao, R., Andrews, M. R., & Fawcett, J. W. (2011). Chondroitinase combined with rehabilitation promotes recovery of forelimb function in rats with chronic spinal cord injury. *The Journal of neuroscience : the official journal of the Society for Neuroscience*, *31*(25), 9332–9344.

Wang HX, Gao WJ (2009). Cell type-specific development of NMDA receptors in the interneurons of rat prefrontal cortex. *Neuropsychopharmacology*. Jul;34(8):2028-40

Wang X., Luo, Q., Tian, F., Cheng, B., Qiu, L., Wang, S., He, M., Wang, H., Duan, M., & Jia, Z. (2019). Brain grey-matter volume alteration in adult patients with bipolar disorder under different conditions: a voxel-based meta-analysis. *Journal of psychiatry & neuroscience, 44*(2), 89–101.

Wang Y, Ma Y, Hu J, Cheng W, Jiang H, Zhang X, Li M, Ren J, Li X (2015). Prenatal chronic mild stress induces depression-like behavior and sex-specific changes in regional glutamate receptor expression patterns in adult rats. *Neuroscience*. Aug 20;301:363-74.

Wang, T., Sinha, A. S., Akita, T., Yanagawa, Y., & Fukuda, A. (2018). Alterations of GABAergic Neuron-Associated Extracellular Matrix and Synaptic Responses in *Gad1*-Heterozygous Mice Subjected to Prenatal Stress. *Frontiers in cellular neuroscience*, *12*, 284.

Wang, Q., Zhou, Q., Zhang, S., Shao, W., Yin, Y., Li, Y., Hou, J., Zhang, X., Guo, Y., Wang, X., Gu, X., & Zhou, J. (2016). Elevated Hapln2 Expression Contributes to Protein Aggregation and Neurodegeneration in an Animal Model of Parkinson's Disease. *Frontiers in aging neuroscience*, *8*, 197.

Watanabe M. (1990). Prefrontal unit activity during associative learning in the monkey. *Experimental brain research*, *80*(2), 296–309.

Watanabe E, Fujita SC, Murakami F, Hayashi M, Matsumura M (1989). A monoclonal antibody identifies a novel epitope surrounding a subpopulation of the mammalian central neurons. Neuroscience; 29(3):645-57.

Watanabe, H., Gao, L., Sugiyama, S., Doege, K., Kimata, K., & Yamada, Y. (1995). Mouse aggrecan, a large cartilage proteoglycan: protein sequence, gene structure and promoter sequence. *The Biochemical journal*, *308*, 433–440.

Weber, P., Bartsch, U., Rasband, M. N., Czaniera, R., Lang, Y., Bluethmann, H., Margolis, R. U., Levinson, S. R., Shrager, P., Montag, D., & Schachner, M. (1999). Mice deficient for tenascin-R display alterations of the extracellular matrix and decreased axonal conduction velocities in the CNS. *The Journal of neuroscience : the official journal of the Society for Neuroscience*, *19*(11), 4245–4262.

Weikum, E. R., Knuesel, M. T., Ortlund, E. A., & Yamamoto, K. R. (2017). GR control of transcription: precision and plasticity via allostery. *Nature reviews. Molecular cell biology*, *18*(3), 159–174.

Weickert, C. S., Fung, S. J., Catts, V. S., Schofield, P. R., Allen, K. M., Moore, L. T., Newell, K. A., Pellen, D., et al. (2013). Molecular evidence of N-methyl-D-aspartate receptor hypofunction in schizophrenia. *Molecular psychiatry*, *18*(11), 1185–1192.

Wegner, F., Härtig, W., Bringmann, A., Grosche, J., Wohlfarth, K., Zuschratter, W., & Brückner, G. (2003). Diffuse perineuronal nets and modified pyramidal cells immunoreactive for glutamate and the GABA(A) receptor alpha1 subunit form a unique entity in rat cerebral cortex. *Experimental neurology*, *184*(2), 705–714.

Wegrzyn, D., Manitz, M. P., Kostka, M., Freund, N., Juckel, G., & Faissner, A. (2021). Poly I:C-induced maternal immune challenge reduces perineuronal net area and raises spontaneous network activity of hippocampal neurons in vitro. *The European journal of neuroscience*, *53*(12), 3920–3941.

Weickert, C. S., Fung, S. J., Catts, V. S., Schofield, P. R., Allen, K. M., Moore, L. T., Newell, K. A., Pellen, D., Huang, X. F., Catts, S. V., & Weickert, T. W. (2013). Molecular evidence of N-methyl-D-aspartate receptor hypofunction in schizophrenia. *Molecular psychiatry*, 18(11), 1185–1192.

Weinstock M. (2008). The long-term behavioural consequences of prenatal stress. *Neuroscience and biobehavioral reviews*, *32*(6), 1073–1086.

Weiser, M., Vega-Saenz de Miera, E., Kentros, C., Moreno, H., Franzen, L., Hillman, D., Baker, H., & Rudy, B. (1994). Differential expression of Shaw-related K+ channels in the rat central nervous system. *The Journal of neuroscience : the official journal of the Society for Neuroscience*, *14*(3 Pt 1), 949–972.

Wen, T. H., Binder, D. K., Ethell, I. M., & Razak, K. A. (2018). The Perineuronal 'Safety' Net? Perineuronal Net Abnormalities in Neurological Disorders. *Frontiers in molecular neuroscience*, *11*, 270.

Whitfield, G. K., Jurutka, P. W., Haussler, C. A., & Haussler, M. R. (1999). Steroid hormone receptors: evolution, ligands, and molecular basis of biologic function. *Journal of cellular biochemistry*, *Suppl 32-33*, 110–122.

Whitehead G, Jo J, Hogg EL, Piers T, Kim DH, Seaton G, Seok H, Bru-Mercier G, Son GH, Regan P, Hildebrandt L, Waite E, Kim BC, Kerrigan TL, Kim K, Whitcomb DJ, Collingridge GL, Lightman SL, Cho K (2013). Acute stress causes rapid synaptic insertion of Ca2+ -permeable AMPA receptors to facilitate long-term potentiation in the hippocampus. *Brain*; 136(Pt 12):3753-65.

Wiese, S., Karus, M., & Faissner, A. (2012). Astrocytes as a source for extracellular matrix molecules and cytokines. *Frontiers in pharmacology*, *3*, 120.

Wight T. N. (2018). A role for proteoglycans in vascular disease. *Matrix biology : journal of the International Society for Matrix Biology*, *71-72*, 396–420.

Wight, T. N., Kang, I., & Merrilees, M. J. (2014). Versican and the control of inflammation. *Matrix biology : journal of the International Society for Matrix Biology*, *35*, 152–161.

Wilk, S., & Orlowski, M. (1980). Cation-sensitive neutral endopeptidase: isolation and specificity of the bovine pituitary enzyme. *Journal of neurochemistry*, *35*(5), 1172–1182.

Willis, A., Pratt, J. A., & Morris, B. J. (2021). BDNF and JNK Signaling Modulate Cortical Interneuron and Perineuronal Net Development: Implications for Schizophrenia-Linked 16p11.2 Duplication Syndrome. *Schizophrenia bulletin*, *47*(3), 812–826.

Willis, A., Pratt, J. A., & Morris, B. J. (2022). Enzymatic Degradation of Cortical Perineuronal Nets Reverses GABAergic Interneuron Maturation. *Molecular neurobiology*, *59*(5), 2874–2893.

Willner K, Vasan S, Abdijadid S. Atypical Antipsychotic Agents. [Updated 2022 Nov 7]. In: StatPearls. Treasure Island (FL): StatPearls Publishing

Woo, M., Hakem, R., Furlonger, C., Hakem, A., Duncan, G. S., Sasaki, T., Bouchard, D., Lu, L., Wu, G. E., Paige, C. J., & Mak, T. W. (2003). Caspase-3 regulates cell cycle in B cells: a consequence of substrate specificity. *Nature immunology*, *4*(10), 1016–1022

Woo, T. U., Walsh, J. P., & Benes, F. M. (2004). Density of glutamic acid decarboxylase 67 messenger RNA-containing neurons that express the N-methyl-D-aspartate receptor subunit NR2A in the anterior cingulate cortex in schizophrenia and bipolar disorder. *Archives of general psychiatry*, *61*(7), 649–657.

Wood, G. K., Lipska, B. K., & Weinberger, D. R. (1997). Behavioral changes in rats with early ventral hippocampal damage vary with age at damage. *Brain research. Developmental brain research*, 101(1-2), 17–25.

Woodward, E., Rangel-Barajas, C., Ringland, A., Logrip, M. L., & Coutellier, L. (2023). Sex-Specific Timelines for Adaptations of Prefrontal Parvalbumin Neurons in Response to Stress and Changes in Anxiety- and Depressive-Like Behaviors. *eNeuro*, *10*(3), ENEURO.0300-22.2023.

Worrel, J. A., Marken, P. A., Beckman, S. E., & Ruehter, V. L. (2000). Atypical antipsychotic agents: a critical review. *American journal of health-system pharmacy : AJHP : official journal of the American Society of Health-System Pharmacists*, *57*(3), 238–255.

Wright, I. C., Ellison, Z. R., Sharma, T., Friston, K. J., Murray, R. M., & McGuire, P. K. (1999). Mapping of grey matter changes in schizophrenia. *Schizophrenia research*, *35*(1), 1–14.

Wright, I. C., Rabe-Hesketh, S., Woodruff, P. W., David, A. S., Murray, R. M., & Bullmore, E. T. (2000). Meta-analysis of regional brain volumes in schizophrenia. *The American journal of psychiatry*, *157*(1), 16–25.

Woo, T. U., Walsh, J. P., & Benes, F. M. (2004). Density of glutamic acid decarboxylase 67 messenger RNA-containing neurons that express the N-methyl-D-aspartate receptor subunit NR2A in the anterior cingulate cortex in schizophrenia and bipolar disorder. *Archives of general psychiatry*, *61*(7), 649–657.

Wu, X., & Xu, X. M. (2016). RhoA/Rho kinase in spinal cord injury. *Neural regeneration research*, *11*(1), 23–27.

Wulff, P., Ponomarenko, A. A., Bartos, M., Korotkova, T. M., Fuchs, E. C., Bähner, F., Both, M., Tort, A. B., Kopell, N. J., Wisden, W., & Monyer, H. (2009). Hippocampal theta rhythm and its coupling with gamma oscillations require fast inhibition onto parvalbumin-positive interneurons. *Proceedings of the National Academy of Sciences of the United States of America*, *106*(9), 3561–3566.

Yamada, Y., Itano, N., Hata, K., Ueda, M., & Kimata, K. (2004). Differential regulation by IL-1beta and EGF of expression of three different hyaluronan synthases in oral mucosal epithelial cells and fibroblasts and dermal fibroblasts: quantitative analysis using real-time RT-PCR. *The Journal of investigative dermatology*, *122*(3), 631–639.

Yamada J, & Jinno S (2013). Spatio-temporal differences in perineuronal net expression in the mouse hippocampus, with reference to parvalbumin. *Neuroscience*. Dec 3;253:368-79.

Yamada, J., & Jinno, S. (2017). Molecular heterogeneity of aggrecan-based perineuronal nets around five subclasses of parvalbumin-expressing neurons in the mouse hippocampus. *The Journal of comparative neurology*, *525*(5), 1234–1249.

Yamada, H., Watanabe, K., Shimonaka, M., & Yamaguchi, Y. (1994). Molecular cloning of brevican, a novel brain proteoglycan of the aggrecan/versican family. *The Journal of biological chemistry*, *269*(13), 10119–10126.

Yamada, J., Ohgomori, T., & Jinno, S. (2015). Perineuronal nets affect parvalbumin expression in GABAergic neurons of the mouse hippocampus. *The European journal of neuroscience*, *41*(3), 368–378.

Yamaguchi Y. (2000). Lecticans: organizers of the brain extracellular matrix. *Cellular and molecular life sciences : CMLS*, *57*(2), 276–289.

Yamamoto, S., Nishiyama, S., Kawamata, M., Ohba, H., Wakuda, T., Takei, N., Tsukada, H., & Domino, E. F. (2011). Muscarinic receptor occupancy and cognitive impairment: a PET study with [11C](+)3-MPB and scopolamine in conscious monkeys. *Neuropsychopharmacology: official publication of the American College of Neuropsychopharmacology*, 36(7), 1455–1465.

Yu, Z., Chen, N., Hu, D., Chen, W., Yuan, Y., Meng, S., Zhang, W., Lu, L., Han, Y., & Shi, J. (2020). Decreased Density of Perineuronal Net in Prelimbic Cortex Is Linked to Depressive-Like Behavior in Young-Aged Rats. *Frontiers in molecular neuroscience*, *13*, 4.

Yu, Z., Han, Y., Hu, D., Chen, N., Zhang, Z., Chen, W., Xue, Y., Meng, S., Lu, L., Zhang, W., & Shi, J. (2022). Neurocan regulates vulnerability to stress and the anti-depressant effect of ketamine in adolescent rats. *Molecular psychiatry*, *27*(5), 2522–2532.

Yuen, E. Y., Liu, W., Karatsoreos, I. N., Feng, J., McEwen, B. S., & Yan, Z. (2009). Acute stress enhances glutamatergic transmission in prefrontal cortex and facilitates working memory. *Proceedings of the National Academy of Sciences of the United States of America*, *106*(33), 14075–14079.

Vogt, D., Cho, K. K. A., Lee, A. T., Sohal, V. S., & Rubenstein, J. L. R. (2015). The parvalbumin/somatostatin ratio is increased in Pten mutant mice and by human PTEN ASD alleles. *Cell reports*, *11*(6), 944–956.

You, K. T., Li, L. S., Kim, N. G., Kang, H. J., Koh, K. H., Chwae, Y. J., Kim, K. M., Kim, Y. K., Park, S. M., Jang, S. K., & Kim, H. (2007). Selective translational repression of truncated proteins from frameshift mutation-derived mRNAs in tumors. *PLoS biology*, *5*(5), e109.

You, J. M., Yun, S. J., Nam, K. N., Kang, C., Won, R., & Lee, E. H. (2009). Mechanism of GC-induced oxidative stress in rat hippocampal slice cultures. *Canadian journal of physiology and pharmacology*, *87*(6), 440–447.

You, J., Hong, S. Q., Zhang, M. Y., Zhao, H. L., Liu, T. Z., Zhou, H. L., Cai, Y. Q., Xu, Z. M., Guo, Y., Jiang, X. D., & Xu, R. X. (2012). Passive immunization with tenascin-R (TN-R) polyclonal antibody promotes axonal regeneration and functional recovery after spinal cord injury in rats. *Neuroscience letters*, *525*(2), 129–134.

Yoshimura, T., Kameyama, K., Takagi, T., Ikai, A., Tokunaga, F., Koide, T., Tanahashi, N., Tamura, T., Cejka, Z., & Baumeister, W. (1993). Molecular characterization of the "26S" proteasome complex from rat liver. *Journal of structural biology*, *111*(3), 200–211.

Young AS, Niv N, Cohen AN, Kessler C, McNagny K (2010). The appropriateness of routine medication treatment for schizophrenia. *Schizophrenia Bulletin*;36(4):732-9.

Young, N. M., & Williams, R. E. (1985). Assignment of lectins specific for D-galactose or N-acetyl-D-galactosamine to two groups, based on their circular dichroism. *Canadian journal of biochemistry and cell biology = Revue canadienne de biochimie et biologie cellulaire*, *63*(4), 268–271.

Zalachoras I, Houtman R, Meijer OC (2013). Understanding stress-effects in the brain via transcriptional signal transduction pathways. *Neuroscience*;242:97-109.

Zadrożna, M., Nowak, B., Łasoń-Tyburkiewicz, M., Wolak, M., Sowa-Kućma, M., Papp, M., Ossowska, G., Pilc, A., & Nowak, G. (2011). Different pattern of changes in calcium binding proteins immunoreactivity in the medial prefrontal cortex of rats exposed to stress models of depression. *Pharmacological reports : PR*, *63*(6), 1539–1546.

Zeng, B. Y., Medhurst, A. D., Jackson, M., Rose, S., & Jenner, P. (2005). Proteasomal activity in brain differs between species and brain regions and changes with age. *Mechanisms of ageing and development*, *126*(6-7), 760–766.

Zhang, F., Gu, W., Hurles, M. E., & Lupski, J. R. (2009). Copy number variation in human health, disease, and evolution. *Annual review of genomics and human genetics*, 10, 451–481.

Zhang, N., Yan, Z., Liu, H., Yu, M., He, Y., Liu, H., Liang, C., Tu, L., Wang, L., Yin, N., Han, J., Scarcelli, N., Yang, Y., Wang, C., Zeng, T., Chen, L. L., & Xu, Y. (2021). Hypothalamic Perineuronal Nets Are Regulated by Sex and Dietary Interventions. *Frontiers in physiology*, *12*, 714104.

Zhang, J. Y., Liu, T. H., He, Y., Pan, H. Q., Zhang, W. H., Yin, X. P., Tian, X. L., Li, B. M., Wang, X. D., Holmes, A., Yuan, T. F., & Pan, B. X. (2019). Chronic Stress Remodels Synapses in an Amygdala Circuit-Specific Manner. *Biological psychiatry*, *85*(3), 189–201.

Zhang, Y., Behrens, M. M., & Lisman, J. E. (2008). Prolonged exposure to NMDAR antagonist suppresses inhibitory synaptic transmission in prefrontal cortex. *Journal of neurophysiology*, *100*(2), 959–965

Zhang, L., Bowen, T., Grennan-Jones, F., Paddon, C., Giles, P., Webber, J., Steadman, R., & Ludgate, M. (2009). Thyrotropin receptor activation increases hyaluronan production in preadipocyte fibroblasts: contributory role in hyaluronan accumulation in thyroid dysfunction. *The Journal of biological chemistry*, *284*(39), 26447–26455.

Zhang, W., Watson, C. E., Liu, C., Williams, K. J., & Werth, V. P. (2000). GCs induce a near-total suppression of hyaluronan synthase mRNA in dermal fibroblasts and in osteoblasts: a molecular mechanism contributing to organ atrophy. *The Biochemical journal*, *349*(Pt 1), 91–97.

Zhong, Y., & Bellamkonda, R. V. (2007). Dexamethasone-coated neural probes elicit attenuated inflammatory response and neuronal loss compared to uncoated neural probes. *Brain research*, *1148*, 15–27.

Zhou, X. H., Brakebusch, C., Matthies, H., Oohashi, T., Hirsch, E., Moser, M., Krug, M., Seidenbecher, C. I., Boeckers, T. M., Rauch, U., Buettner, R., Gundelfinger, E. D., & Fässler, R. (2001). Neurocan is dispensable for brain development. *Molecular and cellular biology*, *21*(17), 5970–5978.

Zimnisky, R, Chang, G, Gyertyán, I, et al (2013). Cariprazine, a dopamine D(3)-receptor-preferring partial agonist, blocks phencyclidine-induced impairments of working memory, attention set-shifting, and recognition memory in the mouse. *Psychopharmacology*; 226(1): 91–100.

Zipursky, R. B., Lambe, E. K., Kapur, S., & Mikulis, D. J. (1998). Cerebral gray matter volume deficits in first episode psychosis. *Archives of general psychiatry*, *55*(6), 540–546.

Zong, W. X., Edelstein, L. C., Chen, C., Bash, J., & Gélinas, C. (1999). The prosurvival Bcl-2 homolog Bfl-1/A1 is a direct transcriptional target of NF-kappaB that blocks TNFalpha-induced apoptosis. *Genes & development*, *13*(4), 382–387.